A Phased-Bottom-Up Approach to the Eumelanin Challenge

By

Haiyan Huang

A thesis submitted to McGill University

In partial fulfillment of the requirements for the degree of

Doctor of Philosophy

Department of Chemistry

McGill University, Montreal

June 2022

Abstract

Eumelanin is a multifunctional biopolymer that colors human skin, hair, and eyes. Its biosynthesis begins with the tyrosinase catalyzed oxidation of L-tyrosine (**Tyr**) to either 5, 6-dihydroxyindole-2-carboxylic acid (**DHICA**) or 5, 6-dihydroxyindole (**DHI**). **DHICA** and **DHI** are the last known intermediates in the biosynthetic pathway, as their spontaneous oxidation leads to complex, insoluble, and heterogeneous materials.

Decades of experimental and theoretical efforts have not yielded a structure of eumelanin, and as a result, the molecular origins of its unique physical properties, including broadband UV absorption, metal-chelation, redox-reactivity *etc*., remain unknown. Previous attempts to mimic the biosynthesis have suffered from poor regio- and chemoselectivity. Other approaches have provided well-defined structures, but access to eumelanin beyond a trimer has not been achieved. To date, there has not been a strategy developed to reveal and manipulate the redox properties of these units.

This thesis details our efforts to develop a phased bottom-up strategy that leverages the precision of C-H functionalization and transition metal-catalyzed cross-coupling to produce well-defined organic molecules possessing melanin-like properties. To this end, a bio-inspired catalytic aerobic cyclization of amino-phenols in a concise 2-stage operation was developed, creating a range of opportunities for directed C-H functionalization reactions to install a halogen or a boronic ester at each of the heterocycle‘s positions. A building-block based iterative approach to the eumelanin oligomers was established, that enabled a systematic synthesis of covalently linked **DHI**-units from a monomer to a pentamer. Oxidation of a kinetically stabilized dimer was accomplished and revealed the first insights into the tautomeric landscape of the resulting inodle-5,6-*ortho*-quinones (**IQs**). Finally, a total synthesis of a porphyrin-like tetra-indole-quinone, a protomolecule based upon thoretical studies, was developed. Current efforts are focused on the final oxidative reaction, in order to reveal the theoretically predicted oxidation pattern.

Résumé

L'eumélanines est un biopolymères multifonctionnels qui colore la peau, les cheveux et les yeux humains. Sa biosynthèse commence par l'oxydation catalysée par la tyrosinase de la L-tyrosine (**Tyr**) en acide 5,6-dihydroxyindole-2-carboxylique (**DHICA**) ou en 5,6-dihydroxyindole (**DHI**). Le **DHICA** et le **DHI** sont les derniers intermédiaires connus de la voie de biosynthèse, car leur oxydation spontanée conduit à des matériaux complexes, insolubles et hétérogènes.

Des décennies d'efforts expérimentaux et théoriques n'ont pas permis de définir la structure de l'eumélanine et, par conséquent, les origines moléculaires de ses propriétés physiques uniques, notamment une large bande d'absorption UV, la chélation de métaux, une réactivité d'oxydoréduction *etc*., restent inconnues. Ces propriétés comprennent. Les tentatives précédentes pour imiter la biosynthèse ont souffert d'une faible régio- et chimiosélectivité. D'autres approches ont fourni des structures bien définies, mais l'accès à l'eumélanine, au-delà d'un trimère, n'a pas été réalisé. À ce jour, aucune stratégie n'a été développée pour révéler et manipuler les propriétés d'oxydoréduction de ces unités.

Cette thèse décrit nos efforts pour développer une stratégie ascendante progressive qui vient tirer profit de la précision de la fonctionnalisation C-H et du couplage croisé catalysé par les métaux de transition pour produire des molécules organiques bien définies possédant des propriétés semblables à celles de la mélanine. À cette fin, une cyclisation aérobique catalytique bio-inspirée, à partir d'amino-phénols, a été développée dans une opération concise en deux étapes, créant une série d'opportunités pour des réactions de fonctionnalisation C-H dirigées afin d'installer un halogène ou un ester boronique à chacune des positions de l'hétérocycle. Une approche itérative basée sur des blocs de construction pour les oligomères d'eumélanine a été établie, ce qui a permis une synthèse systématique d'unités **DHI** liées de manière covalente d'un monomère à un pentamère. L'oxydation d'un dimère cinétiquement stabilisé a permis d'obtenir les premières informations sur l'ensemble tautomérique des inodle-5,6-*ortho*-quinones (**IQs**) résultants. Pour terminer, une synthèse totale d'un tétra-indole-quinone de type porphyrine, une protomolécule basée sur des études théoriques, a été développée. Les efforts actuels se concentrent sur la réaction oxydative finale, afin de révéler le schéma d'oxydation prédit par la théorie.

for my grandfather

Acknowledgement

Foremost, I would like to thank my supervisor, Prof. Jean-Philip Lumb, for giving me the opportunity to join your group and for providing an excellent environment in which to learn and grow. Your knowledge and passion for chemistry, along with your unique perspective and positive mindset have always been an inspiration and a motivation for me. I appreciate your constant guidance and support throughout the ups and downs of a challenging total synthesis project. Secondly, I would like to thank my committee members Prof. Gleason and Prof. Arndtsen, for the thought-provoking questions and the insightful discussions. I extend my gratitude to all the faculty members for allowing me the use of chemicals, equipment, and facilities in the department. I also acknowledge our collaborators at The Ohio State University (Prof. Bern Kohler, Lily Kinziabulatova, and Marisa Barilla) and at the University of Girona (Prof. Lluis Blancafort, Dr. Marco Bortoli, and Anju Manickoth)

I am indebted to my fellow Lumb group members, past and present, for chemistry discussions, advice, and fun time together. Thank you to: Dr. Kenneth Esguerra, Dr. Naresh Vemula, and Matt Halloran, for being great friends, offering advice, and helping me to overcome cultural and language barriers since day one; Dr. Wenbo Xu, Dr. Zheng Huang, and Ohhyeon Kwon for being great mentors and sharing chemistry knowledge generously; Luke Burke for never failing to make the lab a happier place with your sense of humour; Carlos Razziel Azpilcueta Nicolas, for offering helpful advice and allowing me to smell your amazing lunch often. Madison Carroll, for taking great care of lab jobs and the cute drawings on the fume hood sash. Wenyu Qian, for showing your wonderful cooking skills. Simon Edelmann for introducing me to the awesome Podcasts and keeping me motivated during the final stretch. Derek Meng, for bringing a good laugh to the lab by asking many questions; Jackie Wu, for being a great company during the lunch break; Dr. Tom Singleton, for kindly sharing your experience; En Zhao, for teaching me how to use HPLC patiently; Darcy Burley, for kindly laughing at my bad jokes. HyunJune Jun, for having conversations during the long NMR waiting time. I cannot forget to acknowledge the amazing melanin team members that I have had the privilege of working alongside. Thank you to Xueqing Wang, for always offering help in and out of the lab and sharing your passion for airplanes; Laura Jeliazkov, for

never hesitating to help me and being able to relate to my experience; Yiming Zhang, for being an awesome undergraduate and making the experience of mentoring you an opportunity to learn. Other members of the department are also owed tremendous gratitude for your support and advice. The past and current members of the Gleason research group (Dr. Jonathan Hughes, Dr. Sam Plamondon, Dr. Adam Elmehriki, Dr. Ryan Barrett, Dr. Josie Warnica, Donald Campbell, Ali Mansour, and Yufei Wang) have provided a supportive environment to learn and grow. I would like to thank the Perepichka research group (Dr. Yuan Fang, Dr. Afshin Dadvand, Nathan Yee, Ehsan Hamzehpoor, Ying-Hsuan Liu, Chenghao Liu, and Yuxuan Che) for your help and for providing a desk space when I needed it. I also acknowledge the chemistry discussion and support from the past and current members of the Arndtsen research group (Dr. Gerado Martin Torres, Dr. Garrison Kinney, Dr. Hyseyin Erguven, Dr. Yi Liu, Dr. Pierre-Louis Lagueux-Tremblay, Taleah Levesque, Angela Kaiser, Anthony Labelle, Jose Zgheib, Cuihan Zhou, Ming Tam, Yiyang Ma, and Meijing Jiang), the Tsantrizos' research group (Dr. Karunakar Reddy Bonepally, Yuting Feng, Ifenna Mbaezue, Kevin Lee, Beka Boutin, and Rebecca Kim), and the Li research group (Dr. Wenbo Liu, Dr. Xijie Dai, Dr. Zihang Qiu, Dr. Jianbin Li, Dr. Chenchen Li, Dr. Alejandra Dominguez, Dr. Sosthene Ung, Chia-Yu Huang, and Yiram Kim).

For the technical support and assistance, Dr. Robin Stein and Dr. Tara Sprules (McGill NMR Facility), Dr. Nadim Saade and Dr. Alexander Wahba (M.S. Facility, McGill), and Dr. Hatem Titi (Crystallographer, McGill) deserve special mentions. The project would have been impossible without your assistance in obtaining analytical data and your willingness to offer advice.

Thank you to the department's office staff for always being there to help. Special thanks to Chantal Marotte, for your incalculable assistance and advice. Thank you to Richard Rossi, Weihua Wang, and Jean-Philippe Guay, for fixing our equipment and pumps and making daily lab work possible. There are a lot of people in the department who have helped me, encouraged me, and inspired me, more than I have space for. I appreciate all the help you offered, no matter how big, thank you. Lastly, I would like to thank my family for your love and support. Thank you to my grandparents, for showing me resilience, strength, and kindness. Thank you to my parents who taught me curiosity, courage, and integrity. Your unconditional love has given me the strength to pursue any ambition in life. It's a stroke of luck to be in this family.

Contribution of Authors

During my doctoral research, all work was performed by me unless otherwise stated in the text. All manuscripts are co-authored by Dr. Jean-Philip Lumb, who acted as research supervisor.

Chapter 1:

This chapter provides an introduction to melanin, including the classification, the proposed biosynthesis, the current understanding of its structure, and an overview of the previous synthetic efforts to melanin fragments.

Chapter 2:

This chapter describes the synthesis of functionalized eumelanin monomer units which will be used in subsequent chapters (Chapter 3 and 4) to build eumelanin linear and cyclic oligomers.
In this chapter, Dr. Zheng Huang and Ohhyeon Kwon developed the reaction conditions for the biomimetic synthesis of 5,6-differenciated indole (**2-10**) and its functionalization at the C4 and C7 positions. The author performed the C2/C3 functionalization of **2-10** and optimized its C7 functionalization. The author performed all the syntheses and C2/C7 functionalization of the acetonide protected indoles.

Chapter 3:

This chapter describes an iterative assembly of functionalized **DHI** building blocks through the 2- and 7‘- position to the eumelanin pentamer. The author performed all the studeis.

Chapter 4:

This chapter describes the successful synthesis of a protected cyclic tetramer and the efforts to oxidize and sterically stabilize the deprotected cyclic tetramer. The author developed the entire synthetic route. Xueqing Wang, Yiming Zhang, and Laura Jeliazkov helped with the preparation of monomers.

Table of Contents

List of Figures

Chapter 1

Chapter 2

Chapter 3

Chapter 4

Chapter 5

List of Schemes

Chapter 1

Chapter 2

Chapter 3

Chapter 4

Chapter 5

List of Tables

Chapter 2

Chapter 3

Chapter 4

List of Abbreviations

°C	degrees Celsius
Å	angstrom
Ac	acetyl
Ac_2O	acetic anhydride
AcOH	acetic acid
atm	atmosphere
B_2Pin_2	bis(pinacolato)diboron
Bn	benzyl
Boc	*tert*-butoxycarbonyl
br	broad
Calc.	calculated
cod	1,5-dicyclooctadiene
CPME	cyclopentyl methyl ether
Cy	cyclohexyl
CyH	cyclohexane
dba	dibenzylideneacetone
DBED	*N*,*N*'-di-*tert*-butylethylenediamine
DCC	*N,N'*-dicyclohexylcarbodiimide
DDQ	2,3-dichloro-5,6-dicyano-1,4-benzoquinone
DHI	5,6-dihydroxyindole
DHICA	5,6-dihydroxyindole-2-carboxylic acid
DIPEA	*N,N*-diisopropylethylamine
DMAP	4-(dimethylamino)-pyridine
DMF	*N,N'*-dimethylformamide
DMSO	dimethyl sulfoxide
DOPA	3,4-dihydroxyphenylalanine
dppf	1,1'-bis(diphenylphosphino)ferrocene
dppp	1,3-Bis(diphenylphosphino)propane

dtbpy	4,4'-di-*tert*-butyl-2,2'-bipyridyl
equiv	equivalent(s)
Et	ethyl
EtOAc	ethyl acetate
g	gram(s)
h	hour(s)
HEPES	4-(2-hydroxyethyl)-1-piperazineethanesulfonic acid
HFIP	1,1,1,3,3,3-hexafluoroisopropanol
HMBC	heteronuclear multiple bond correlation
HRMS	high resolution mass spectrometry
HSQC	heteronuclear single quantum correlation
Hz	Hertz
hv	light
i-Pr	isopropyl
IQ	indolequinone
IR	infrared (spectroscopy)
J	coupling constant
λ	wavelength
LDA	lithium diisopropylamide
m	multiplet or milli
m	meta
m/z	mass to charge ratio
Me	methyl
MeCN	acetonitrile
MeOH	methanol
MHz	megahertz
MIDA	*N*-methyliminodiacetic acid
min	minute(s)

mol	mole(s)
MS	molecular sieves
MTBE	methyl *tert*-butyl ether
NBS	*N*-bromosuccinimide
n-BuLi	*n*-butyl lithium
NEt_3	triethylamine
NHPI	*N*-hydroxyphthalimide
NIS	*N*-iodosuccinimide
NMP	*N*-methyl-2-pyrrolidone
NMR	nuclear magnetic resonance
nOe	nuclear Overhauser effect
NOESY	nuclear Overhauser enhancement spectroscopy
o	ortho
[O]	oxidant
OAc	acetate
OTf	trifluoromethanesulfonate
p	para
Ph	phenyl
Phen	1,10-phenanthroline
PPTS	pyridinium *p*-toluenesulfonate
py/pyr	pyridine
q	quartet
QI	quinone imine
QM	quinone methide
r.t.	room temperature
R_f	retention factor
s	singlet
SPhos	2-Dicyclohexylphosphino-2',6'-dimethoxybiphenyl
t	triplet

TBAF	*tetra-n*-butylammonium fluoride
TBSCl	*tert*-butyldimethylsilyl chloride
TDAE	tetrakis(dimethylamino)ethylene
t-Bu	*tert*-butyl
t-BuLi	*tert*-butyl lithium
TESCl	triethylsilyl chloride
THF	tetrahydrofuran
TIPSCl	triisopropylsilyl chloride
TLC	thin layer chromatography
TMEDA	*N,N,N',N'*-tetramethylethylenediamine
tmphen	3,4,7,8-tetramethyl-1,10-phenanthroline
TMS	tetramethylsilane / trimethylsilyl
TMSCl	trimethylsilyl chloride
TMSOTf	Trimethylsilyl trifluoromethanesulfonate
TNM	tetranitromethane
UV/vis	ultraviolet-visible
XPhos	2-dicyclohexylphosphino-2',4',6'-triisopropylbiphenyl

Chapter 1 : Introduction

Melanin is a broad term that encompasses multi-functional biopolymers ubiquitously found in all living organisms including bacteria, fungi, plants, and animals. It is derived from the oxidative polymerization of phenols or catechols and has provided a unique source of inspiration for the design of multifunctional materials. Unlike the vast majority of natural pigments (e.g., chlorophyll and carotenoid), melanin cannot be described as a well-defined structure, and instead, proposed structures (**1-1** and **1-2**) or related oligomers (Figure 1-1) are used as hypothetical representations.

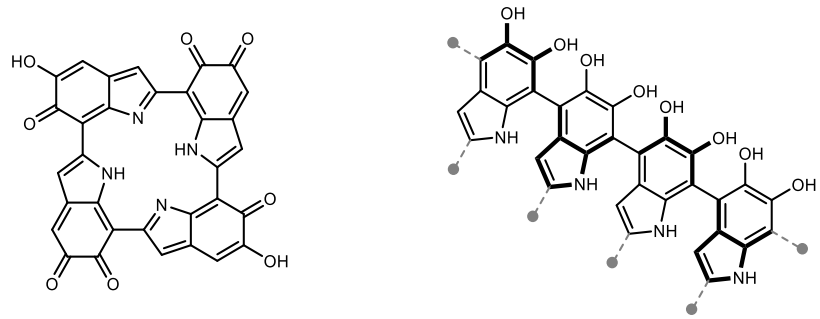

proposed cyclic structure of eumelanin (**1-1**) proposed linear structure of eumelanin (**1-2**)

Figure 1-1-1 Proposed structures of eumelanin

As a result, the molecular origins of melanin's unique physical properties remain unknown. These properties include broadband UV absorption, sub-picosecond non-radiative decay, metal-chelation, redox-reactivity, and paramagnetism.[1] Investigation of the structure-function relationships is notoriously challenging due primarily to melanin's poor solubility in most organic solvents, its amorphous character, its heterogeneity, and its close association or covalent attachment to the cellular ingredients of the biological matrix.

Many of the current technological applications seeking to use melanin-inspired materials would benefit from structure-function correlations, as would our general understanding of its role in biology. In Chapter 1, we provide a clear classification of melanin, offer an overview of the key biosynthetic studies of eumelanin and pheomelanin (the two sub-types of melanin found mainly in mammals), summarize the current understanding of eumelanin's structure, and provide an overview of synthetic efforts toward well-defined eumelanin monomers and oligomers.

1.1 Classification

The difficulties of determining the structures of melanin have not only hampered the potential design of functional materials that possess melanin-type properties, but have also resulted in a lack of general consensus on what melanin is.[2-4] Indeed, the definition of melanin is as elusive as its structure. Conventionally, any black pigment falls into the category of melanin. However, the melanin between different organisms can be very different. Furthermore, within a single organism, there can be multiple different types of melanin depending on their biosynthetic precursors and pathways. Because of the wide presence and the complexity of melanin, the first section of this thesis aims to provide a clear classification of melanin based upon the current literature.

The word 'melanin' originates from the Greek word "melanos", which means black, or dark. It is a descriptive term meant to reflect the variety of black, brown, yellow and red natural biopolymers of diverse natural and chemical compositions. The term was first introduced by Jöns Jacob Berzelius to describe the choroid coat of the eye in 1840.[3] Since then it has been used to define any black or dark brown pigment throughout the phylogenetic tree purely based on color and without any specific structural, biogenetic, or functional implication. In 1927 and 1948, key studies were performed by Raper[5] and Mason[6] respectively, in which Raper isolated 5,6-dihydroxyindole (**DHI**) and 5,6-dihydroxyindole-2-carboxylic acid (**DHICA**) from black eumelanin, and Mason proposed the original biosynthetic pathway to the polymer eumelanin (Figure 1-2). This led to a classification scheme that lasted until the 1960s that classified melanin into two categories: the black-brown eumelanin derived by the tyrosinase-catalyzed oxidation of L-tyrosine (**1-3**) via **DHI** and **DHICA** intermediates, and the yellow-reddish pheomelanin, also derived from L-tyrosine (**1-3**), but in the presence of L-cysteine (**1-8**) via benzothiazine heterocycles (**1-9**). The classification of melanin evolved further in the next few decades, as melanin was isolated from other organisms and various biosynthetic precursors besides L-tyrosine (**1-3**) were discovered. In 1955, melanin was found in nerve cells, generating a new category of neuromelanin. Neuromelanin is often mixed with both dopamine (**1-7**) and benzothiazine (**1-9**) units. Its degradation is often implicated in neurodegenerative disorders such

as Parkinson's and Alzheimer's disease [7]. In 1972, pyomelanin was first introduced by Yabuuchi and Ohyama, who described a water-soluble brown pigment produced by the sanious bacterium *Pseudomonas aeruginosais*.[8] This pigment derives from tyrosine catabolism through homogentisic acid (**HGA**)(**1-5**), and plays an important role in mitigating oxidative stress.[9,10] Alkaptomelanin is another designation for pyomelanin; however, pyomelanin is taken to refer to the pigment as produced by microbes, whereas alkaptomelanin is the pigment produced by humans. In 1976, the nitrogen-free allomelanin was discovered and traced to the polymerization of 1,8-dihydroxynaphthalene (**1-10, DHN**) and protocatechuic acid (**1-11**). Some literature classifies pyomelanin as a subgroup of allomelanin, since they are both present in microorganisms. However, in our opinion, these two categories should be distinct, due to their differing precursor molecules. In summary, melanin is classified into six categories: eumelanin, pheomelanin, neuromelanin, pyomelanin, alkaptomelanin, and allomelanin. Eumelanin, pheomelanin, neuromelanin, and alkaptomelanin are mainly found in animal tissues, whereas allomelanin and pyomelanin are mainly found in microorganisms and plants.

Of note is that the above categories pertain only to natural melanin. There are also many examples of synthetic melanins that are inspired by the biopolymers, but produced by abiotic oxidative polymerization. The recent development of synthetic eumelanins have begun to play a broader role in potentially unravelling the structure-function relationships of natural melanins. Although synthetic eumelanin has remarkably similar macroscopic properties to natural melanin, their chemical structures are likely quite different. The chemical structures of synthetic melanin are dependent on the precursor monomers (e.g., dopamine, L-DOPA, or tyrosine), reaction conditions (e.g., temperature, pH, oxidants, and reaction time), and post-synthetic procedures used to isolate and prepare samples.[11-13] Thus, synthetic melanin should not be used as a synonym to natural melanin, and data based on synthetic melanin should not be interpreted as reliably representative of natural eumelanin. A complete, molecular-level understanding of both natural and synthetic eumelanin remains elusive.

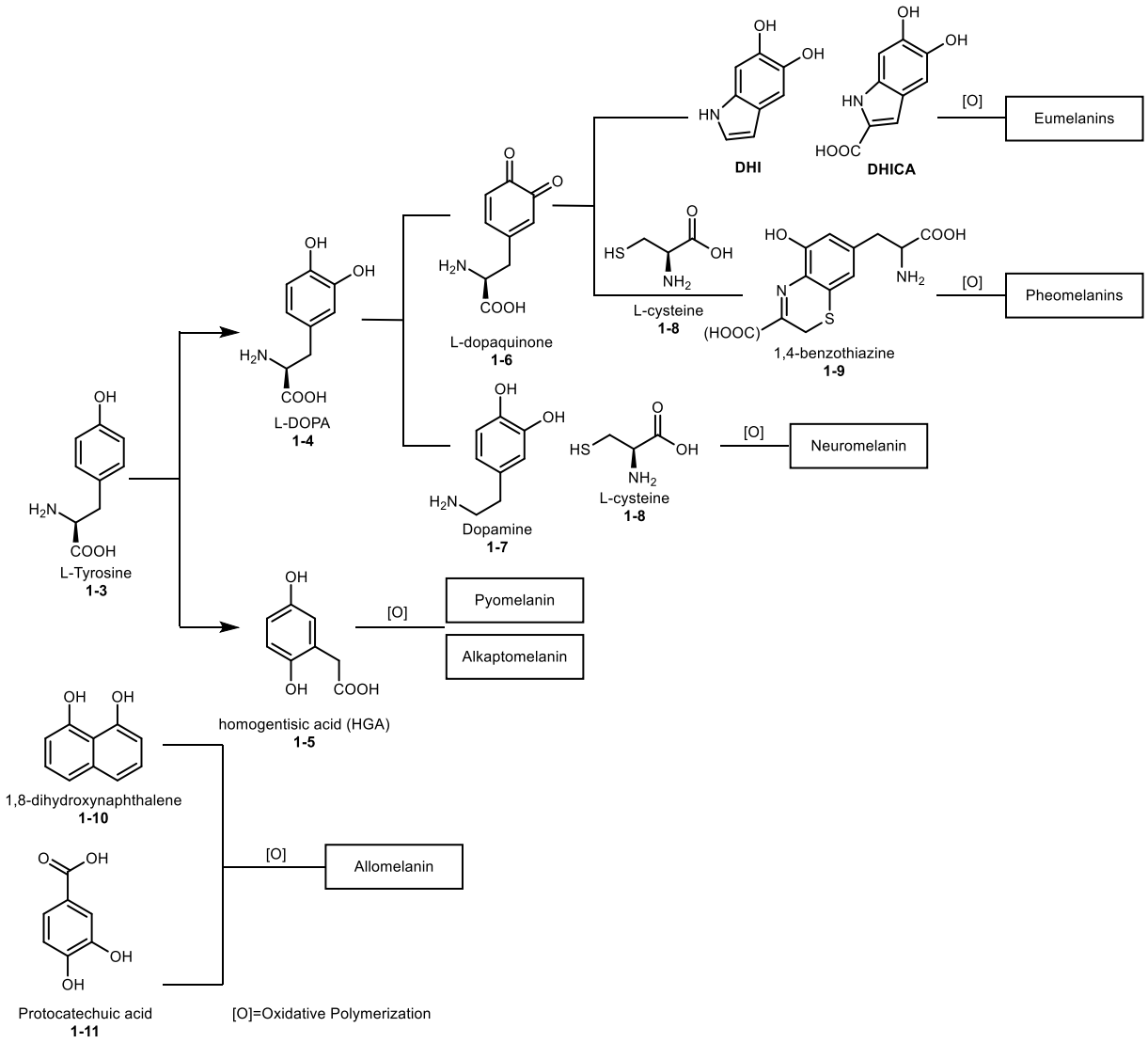

Figure 1-2 Classification of melanin

1.2 Biosynthesis of Eumelanin and Pheomelanin

Eu- and pheo-melanogenesis, the biochemical pathways responsible for melanin biosynthesis in mammals, occurs in intracellular organelles called melanosomes, which are found within star-shaped cells called melanocytes.[14, 15] These melanosomes are then subsequently transferred to surrounding epidermal cells, termed keratinocytes. We summarize here the currently accepted biosynthetic pathway and the melanogenic enzymes involved. We focus on mammalian eumelanin and pheomelanin and do not address specific aspects of the melanogenic pathway in prokaryotes or in plants.[16, 17]

1.2.1 Early Stages of Eumelanogenesis and Pheomelanogenesis

In vertebrates, eumelanins are derived from the amino acid L-tyrosine (**1-3**) by a series of enzymatic and chemical reactions that comprise the Raper-Mason biosynthetic pathway (Scheme 1-1). Three known metalloenzymes are involved in the melanogenic pathway, including tyrosinase, tyrosinase-related protein 1 (Tyrp1),[18] and tyrosinase-related protein 2 (Tyrp2), also called dopachrome tautomerase (Dct).[19, 20] Melanogenesis starts from the tyrosinase-catalyzed oxidation of L-tyrosine (**1-3**) to L-dopaquinone (**1-6**). L-dopaquinone (**1-6**) is an important branch point between eumelanin and pheomelanin (Scheme 1-1), and its fate depends on the local concentration of L-cysteine (**1-8**).

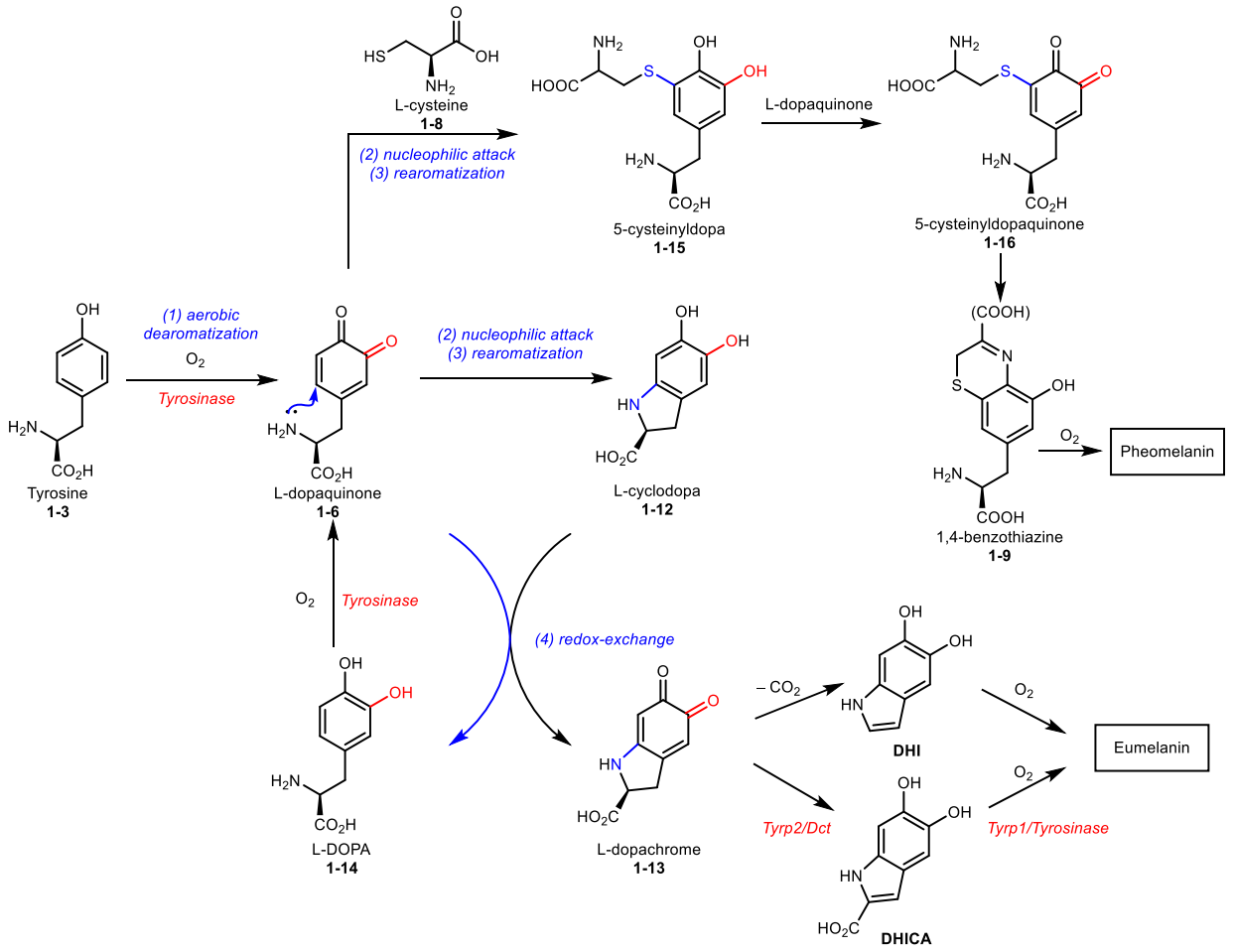

Scheme 1-1 Eumelanogenesis and Pheomelanogenesis

In the absence of sulfhydryl compounds (such as cysteine), L-dopaquinone (**1-6**) undergoes an intramolecular 1,4-addition of the amino group followed by rearomatization to yield L-cyclodopa (**1-12**). Redox exchange between L-cyclodopa (**1-12**) and L-dopaquinone (**1-6**) then gives L-dopachrome (**1-13**) and L-dopa (**1-14**). L-dopa (**1-14**) is believed to undergo tyrosinase-catalyzed oxidation back to L-dopaquinone (**1-6**). L-dopachrome (**1-13**) is a second branch point in the pathway, and can lead to the two eumelanin monomeric precursors, **DHI** and **DHICA**. Nonenzymatic decarboxylative rearrangement of L-dopachrome (**1-13**) yields **DHI** and CO_2. Alternatively, L-dopachrome (**1-13**) may be enzymatically transformed into **DHICA** (Scheme 1-1) by the action of Dct (or Tyrp2). Oxidative polymerization of **DHI** and **DHICA** then leads to eumelanin polymers. It is worth noting that oxidation is much slower for **DHICA** than it is for **DHI** because of the electron-withdrawing carboxyl group at C2 (indole numbering), thus **DHICA** oxidation *in vivo* is most likely an enzymatic reaction.[21, 22] In mice, Tyrp1 can modulate the oxidation of **DHICA**.[23] Although human Tyrp1 is unable to catalyze this transformation, human tyrosinase can oxidize **DHICA** as well as tyrosine, dopa, and DHI.[18]

Tyrosinase is the dinuclear copper-containing, membrane-bound glycoprotein located in the melanosome that is a key regulatory and rate-limiting melanogenic enzyme**.** Dct/Tyrp2 shares many structural similarities with tyrosinase, including the position and number of histidine (His) residues that are likely involved in the chelation of metal cofactors. However, the nature of the metal cofactor is different. It is widely accepted that Dct/Tyrp2 contain two zinc atoms in their active sites, as purified Dct/Tyrp2 is found to contain bound zinc ions and enzymatic activity can be reconstituted from apoenzymatic preparations exclusively by the addition of zinc, not by copper or iron ions. This is consistent with the nature of the reaction catalyzed by Dct/Tyrp2: Zn (II) is devoid of redox properties and therefore ineffective for oxidative reactions. However, it is highly efficient as a tautomerization catalyst. Accordingly, the presence of zinc ions instead of copper in the metal-binding site is considered the most important factor determining the catalytic events at the active site of Dct/Tyrp2. Tyrp1 is the most abundant glycoprotein expressed specifically in melanocytes. However, its catalytic activity remains controversial. A

recent crystal structure of a mammalian Tyrp1 reveals two zinc ions in the active site instead of copper ions, as found in tyrosinases.[24]

The biosynthesis of pheomelanin results from the addition of cysteine (**1-8**) to L-dopaquinone (**1-6**) to afford thiol adduct, 5-cysteinyldopa (**1-15**). Oxidation of 5-cysteinyldopa (**1-15**) yields the corresponding 5-cysteinyldopaquinones (**1-16**). Condensation reactions then provide 1,4-benzothiazine (**1-9**) intermediates, which would subsequently lead to the formation of pheomelanin via oxidative polymerization (Scheme 1-1).

The rate constant for all four important steps in the early phases of melanogenesis were reported based on pulse radiolysis studies (r1-r4, Scheme 1-2).[25] Pulse radiolysis is a tool to study the fates of reactive melanin precursors. The technique relies on the production of the dibromide radical anion Br_2^- due to pulse radiolysis of an N_2O-saturated aqueous buffer containing KBr. The dibromide radical anions oxidize L-dopa (**1-14**) to dopasemiquinones, which then disproportionates to L-dopaquinone (**1-6**) and L-dopa (**1-14**). Two things worth noting are that the L-dopaquinone (**1-6**) generated by pulse radiolysis might behave differently from that generated by tyrosinase and that the technique is based on the generation of exceedingly low levels of oxidized species in the presence of large amounts of the unreacted substrate, for example, low levels of L-dopaquinone (**1-6**) in the presence of large amounts of L-dopa (**1-14**).

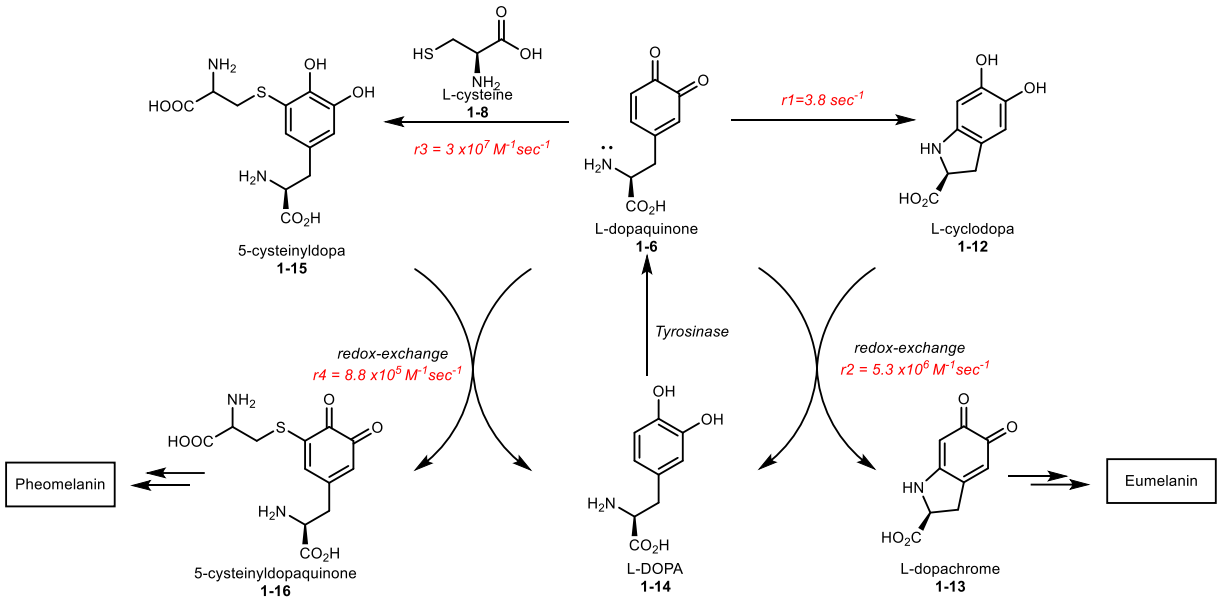

Scheme 1-2 Kinetics of early stages of eumelanogenesis and pheomelanogensis

In eumelanogenesis, the intramolecular addition of the amino group to L-cyclodapa (**1-12**) is relatively slow (r1 = 3.8 s^{-1}). However, once L-cyclodopa (**1-12**) is formed, the redox exchange to L-dopachrome (**1-13**) and L-dopa (**1-14**) is rapid (r2 = 5.3 x10^6 $M^{-1}sec^{-1}$). In contrast, the addition of L-cysteine (**1-8**) to 5-cysteinyldopa (**1-15**) proceeds quickly with a second order rate constant r3 = 3x10^7 $M^{-1}sec^{-1}$. The subsequent redox exchange to 5-cysteinyldopaquinone (**1-16**) proceeds at a slower rate of r4 = 8.8x10^5 $M^{-1}sec^{-1}$. Given the difference in rate constants r1 and r3, cysteinyldopa formation is preferred over cyclodopa formation if the cysteine concentration is above 0.13 μM. This value, however, might be pH-dependent as the rate of dopaquinone cyclization (r1) becomes 100-fold slower when the pH is reduced from 8.6 to 5.6 (Scheme 1-2).[26]

1.2.2 Biomimetic Oxidation of DHI

The Raper-Mason pathway provided insight into the initial stages of eumelanin biosynthesis (from L-tyrosine to **DHI** and **DHICA**). However, delineating the subsequent oxidative polymerization of **DHI** and **DHICA** has proven to be challenging, and as a result, our understanding of the oxidative polymerization is limited. In this section, we discuss our current understanding of the oxidative polymerization, with a focus on **DHI**. The polymerization that constitutes

pheomelogenesis is less studied, and is not the focus of our studies. Readers interested in this process are referred to reviews.[27, 28]

The biomimetic oxidation of **DHIs** has been studied extensively, and forms the backbone of our current mechanistic understanding. Biomimetic oxidation of **DHIs** encompasses both enzymatic and chemical oxidations performed *in vitro*. For example, a 2,2'-dimer **1-17** was first isolated via oxidation of **DHIs** in 1985 by Prota and co-workers.[29] In this work, mushroom tyrosinase catalyzed the aerobic oxidation of **DHI** in 4-(2-hydroxyethyl)-1-piperazineethanesulfonic acid (HEPES) buffer at pH 6.8 in the presence of $Zn(OAc)_2$ or $NiSO_4$ to produce **1-17** following a reductive workup with sodium dithionite and acetylation of the free-catechols with acetic anhydride in the presence of pyridine (Scheme 1-3).

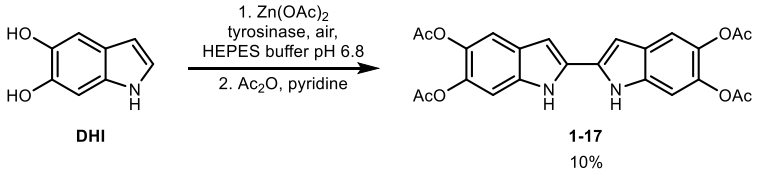

Scheme 1-3 Enzyme-catalyzed bio-inspired synthesis of 2,2'-dimer

In the absence of metals, dimers **1-18** and **1-19**, and trimers **1-20** and **1-21** were obtained. They were formed by peroxidase/H_2O_2 oxidation at physiological pH, followed by reductive work-up with sodium dithionite and then acetylation of the free-catechols.[30, 31] These two studies revealed that the oxidative coupling of **DHI** occurs predominantly through the C2, C4, and C7 positions of the indole ring (Scheme 1-4).

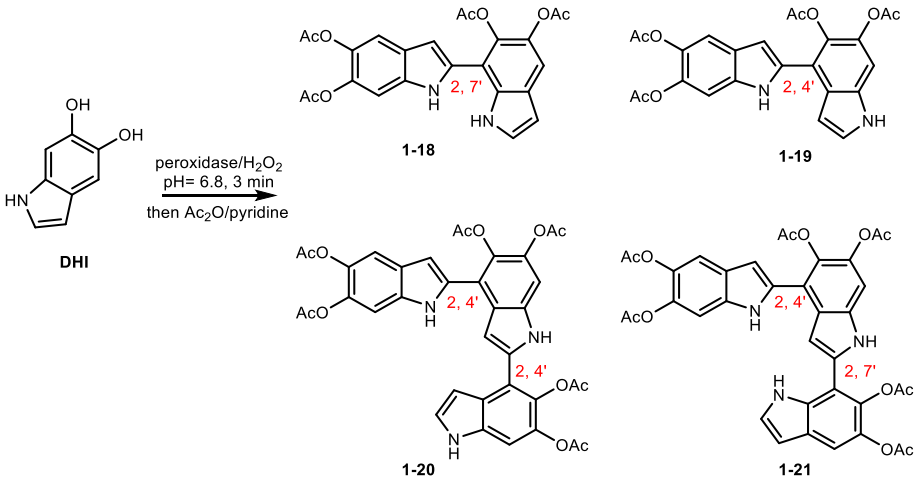

Scheme 1-4 Enzyme-catalyzed bio-inspired synthesis of dimers and trimers

Delineating the polymerization beyond a trimer stage was not achieved until 2007,[32] when d'Ischia reported the first tetramer (**1-23**) upon oxidation of the 2,4'-dimer (**1-22**) mediated by the peroxidase/H_2O_2 system in the presence of Zn^{2+} ions in β-hydroxy-4-(2-hydroxyethyl)-1-piperazinepropanesulfonic acid (HEPPSO) buffer at pH 7.4. The role of Zn^{2+} ions was suggested to enhance the formation of **1-23** over alternative oxidative coupling pathways. In the absence of Zn^{2+} ions, only a trace amount of **1-23** was obtained along with several other species that could not be elucidated. This study described the mode of polymerization at the C3 position for the first time. The yield of **1-23** was only 2%, and related oxidations have failed to provide meaningful quantities of material for further analysis (Scheme 1-5).

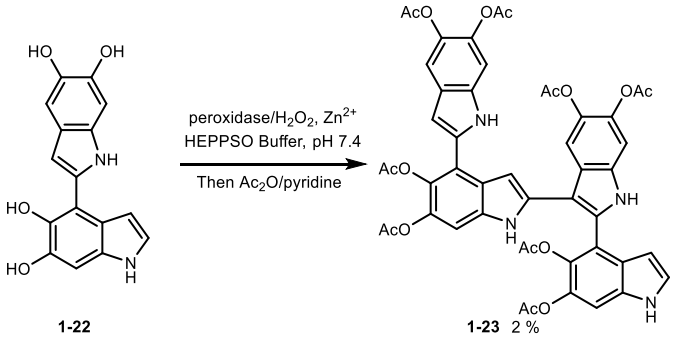

Scheme 1-5 Enzyme-catalyzed bio-inspired synthesis of tetramer from 2,4'-dimer

In subsequent years, three additional tetramers were obtained by oxidative coupling of a 2,7'-dimer (**1-24**) with the peroxidase/H_2O_2 system. The products were linked through 4,4'-(**1-26**), 2,3'-(**1-27**) and the 3,3'-(**1-25**) linkages (Scheme 1-6).[33]

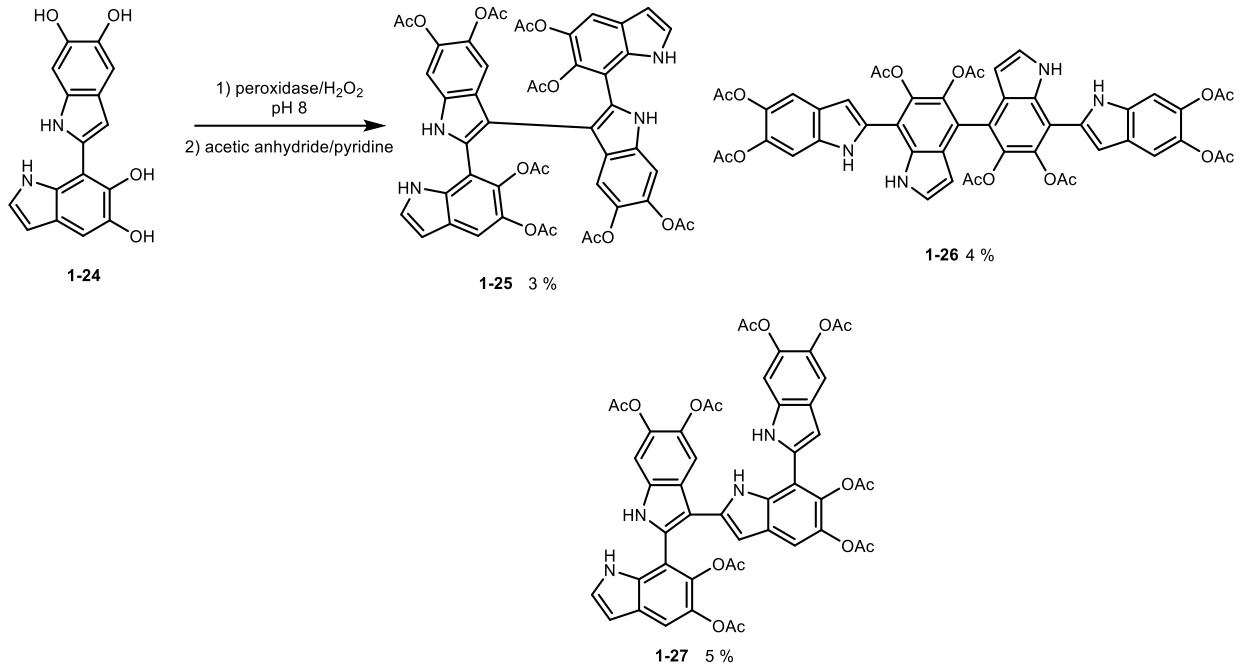

Scheme 1-6 Enzyme-catalyzed bio-inspired synthesis of tetramers from **1-24**

Isolation of a macrocyclic pentamer was reported in 2010 via biomimetic oxidation of N-methylated dimer **1-28** and trimer **1-29** with peroxidase/H_2O_2 at pH 7.4 followed by reductive work-up and acetylation of the free-catechols.[34] DFT investigation suggested that the formation of pentamer **1-31** involves the generation of quinone-methide **1-30**, featuring an inter-unit double bond followed by quinone-catechol coupling to generate the 4,4' bond (shown in red). Although the authors believe that the isolation of **1-31** support macrocyclic structures in eumelanin and contributed to the patterns of structural diversity generated during **DHI** oxidative polymerization, we believe more evidence is needed to draw such a conclusion as the N-methyl substituted indoles are not components of eumelanin (Scheme 1-7).

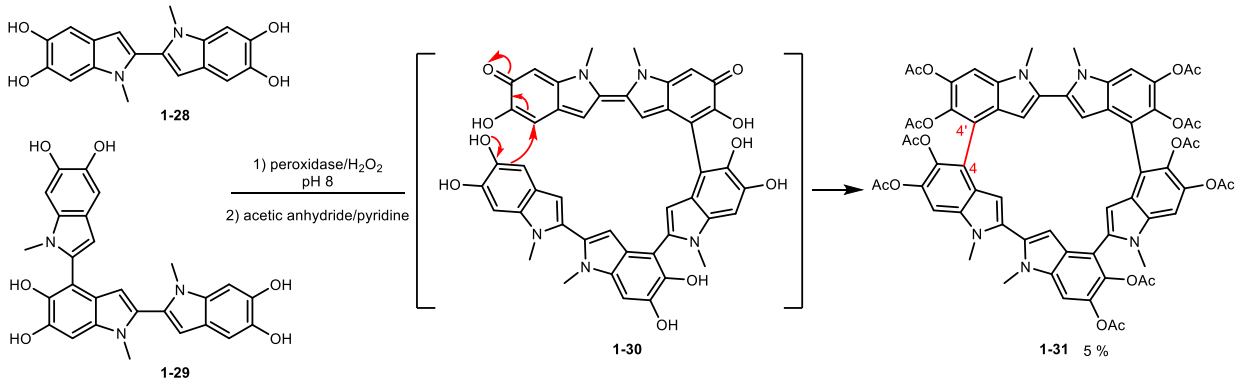

Scheme 1-7 Enzyme-catalyzed bio-inspired synthesis of a cyclic pentamer

1.2.3 Chemical Properties of DHI

Mimicry of eumelanin biosynthesis has provided black materials with physical properties that resemble natural eumelanin, and shown that the **DHI** undergoes oxidative coupling with a preference for C2, C4, and C7 positions. Nevertheless, the details of this mechanism remain unclear, and these studies have not been able to access well-defined eumelanin derivatives that display the properties of eumelanin granules. Issues of selectivity during biosynthesis may result from the promiscuous reactivity of intermediate semiquinone radicals (**SQs**) that form upon $1e^{-}|1H^{+}$ oxidation of **DHI**. The spin density of **SQ-I** is distributed across O-C6, C2, C7, and C9 when the hydrogen atom is removed from C6-OH and the spin density of **SQ-II** is distributed across O-C5, C4, and C8 when the hydrogen atom is removed from C5-OH (Scheme 1-8a, where the pink circles indicate the probability density for the unpaired electron). Two possible mechanisms for the rapid decay of **SQs** have been proposed: (1) disproportionation of **SQs** resulting in the formation of indolequinone (**IQ**), which can tautomerize to afford the quinone-methide (**QM**) and quinone-imine (**QI**) (Scheme 1-8b). Computational studies suggested that **IQ** is 2.3 kcal/mol and 6.4 kcal/mol more stable than **QM** and **QI** respectively. Dimers, with 2,7'-dimer as an example, can be formed via a catechol-quinone coupling of the resulting **DHI** and **IQ** (or its two tautomers) (Scheme 1-8c).[35] (2) Radical coupling between different possible semiquinone radicals could afford a range of oligomer intermediates, with C2, and C7 radical coupling as an example (Scheme 1-8d).

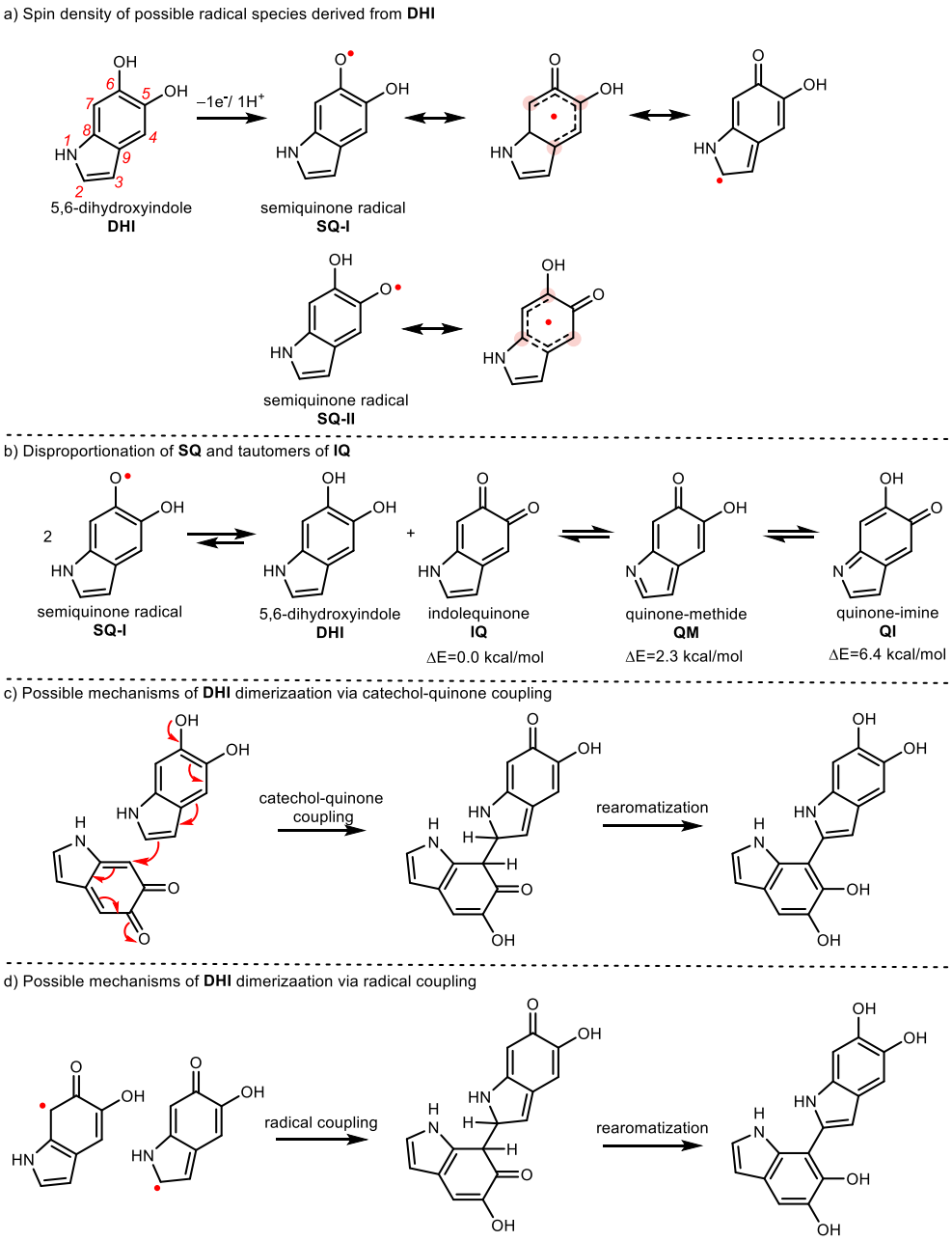

Scheme 1-8 Difficulties in direct mimicary of eumalnin biosynthesis

a) spin density of possible radical species derived from **DHI**; b) disproportionation of **SQ**, tautomers of **IQ**, and calculated relative energy of **IQ** and its tautomers; c) possible mechanism of **DHI** dimerization via catechol-quinone coupling (with 2,7'-dimer as an example); d) possible mechanism of **DHI** dimerization via radical coupling (with 2,7'-dimer as an example)

Furthermore, dimers, trimers, or oligomers. are susceptible to rapid oxidation upon their formation, further complicating the elucidation of products formed by oxidation. With dimer **1-22** as an example, a recent study, on an integrated chemical, pulse radiolytic, and quantum

chemical approach has provided insight into the structures of the transient species formed by oxidation of dimer **1-22**.[36] An unstable, two-electron oxidation **1-22** was suggested to be a quinone-methide **1-32** with a double bond between the two indole units. A possible mechanism for the formation of tetramer **1-23** consists of a nucleophilic attack of the extended quinone methide **1-32** at the 3-position by the **1-22** via the C2 position. The reactivity was rationalized based on the intrinsic structural properties of the extended quinone methide and a significant LUMO coefficient at C3 (Scheme 1-9). [36]

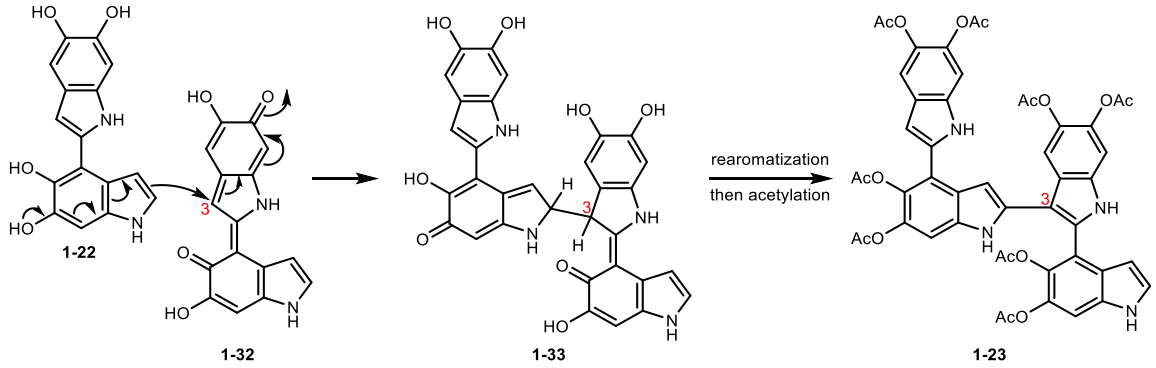

Scheme 1-9 A proposed mechanism for a tetramer formation via a bio-inspired approach

In addition to **DHI**'s marked facility for oxidation, a characteristic feature of **DHI** is its nucleophilicity at C2, versus dominant reactivity at C3 for unsubstituted indoles. This reactivity was suggested to result from the catechol moiety, pushing electron density from the C6-OH to the pyrrole ring.[37] An example that illustrated the reactivity at the C2 position of **DHI** was the reaction with 3,4-dihydroxybenzaldehyde **1-34** that led to the formation of **1-35.**[38] Whereas, indole reacted with benzaldehyde **1-36** to provide bis-indolylmethane **1-37** at the C3 position (Scheme 1-10).[39]

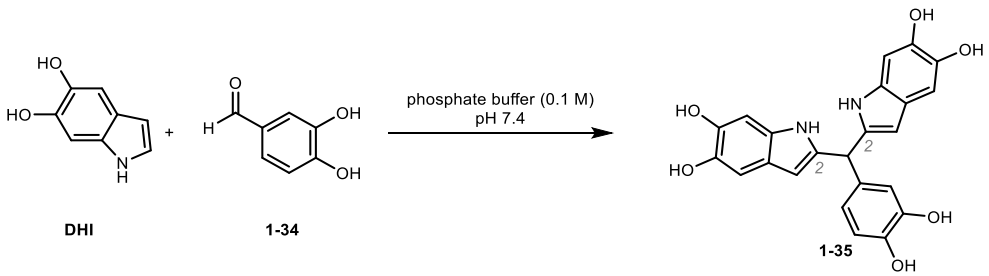

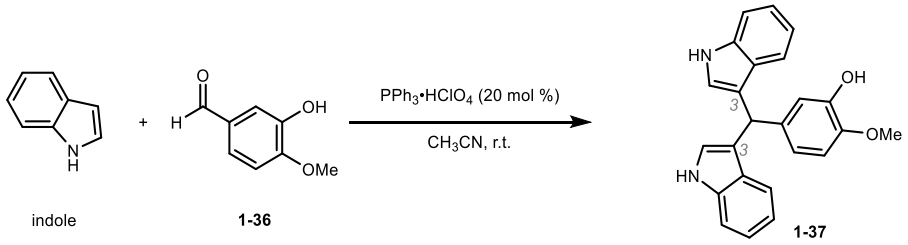

Scheme 1-10 Reactivity at the C2 position of **DHI** versus at the C3 position of indoles

1.3 Current Structure Elucidation of Eumelanin

The challenges associated with the structural elucidation of melanin have not stopped the development of theories and methods to explain the emergence of physical properties of eumelanin.

A chemical disorder model has been proposed in the early 2000s to explain melanin's characteristic broadband absorption. It was suggested that broadband absorption arises from the superposition of narrower spectra from many chromophores with distinct transition energies. These include oligomers with different lengths, and structures and in different redox states (colored Gaussians in figure 1-3a).[40]

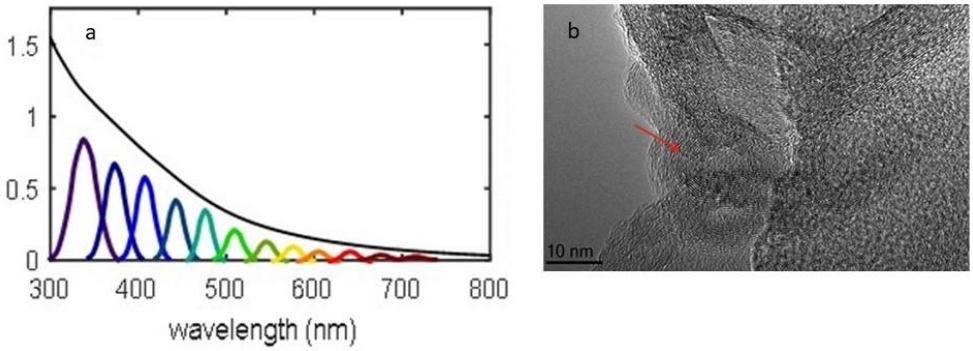

Figure 1-3 Chemical disorder model and TEM image

a) absorption spectrum of eumelanin (black curve) and narrower spectrum from different chromophores (colored Gaussians, recreated by Professor Kohler at The Ohio State University); b) High-resolution TEM images of eumelanin prepared via oxidation of dopamine (2 g/L in an aerated Tris buffer, at 50 mM and at pH 8.5, reaction time of 24 h), the red arrow indicates that the molecule aggregate and form an onion-like nanostructure composed of stacked plans arranges in concentric rings.[41]

The disorder model was soon challenged by X-ray scattering ,[42, 43] atomic force microscopy (AFM),[44] scanning tunnelling microscopy (STM) ,[45] and transmission electron microscopy (TEM) [41, 46] studies that have suggested that eumelanin is comprised of small nearly planar oligomers stacked together via π-π interactions to form graphite-like layered aggregates with an interlayer

distance of 3-4 Å. As shown in the high-resolution TEM images of eumelanin (Figure 1-3b), the molecules aggregate and form an onion-like nanostructure composed of stacked planes (indicated by the red arrow). It is hypothesized that the spectroscopic properties of molecules in these stacked environments will change, but understanding how remains unclear.[47, 48]

A single layer of the aggregates has proven to be around 15–20 Å via STM and matrix-assisted laser desorption/ionization mass spectrometry (MALDI-MS) studies detected the presence of ions with m/z values below 1500 amu,[49] which suggest that tetramer or pentamers of covalently bonded **DHI** monomers are the most probable molecules to account for the small planar oligomers proposed by these studies.

Spectroscopic and microscopic approaches toward the understanding of the structure and composition of eumelanin have offered useful information. However, questions regarding the molecular structure of the small nearly planar oligomers, and the molecular origin of their intriguing physiochemical properties remain largely unknown.

Computer modeling has greatly enhanced our understating of the above-mentioned questions in recent years. Atomistic simulation methods, such as density functional theory (DFT) and molecular dynamics (MD) simulations have served as a powerful tool to predict the physicochemical properties of eumelanin, opening the possibility to understand structure-property relationships and optimize materials to achieve desired functions. In 2006, Kaxiras proposed a structural model for the small nearly planar oligomer, which was referred to as protomolecule (Figure 1-4a). The protomolecule was proposed as a cyclic tetramer consisting of 4 basic molecular units of **DHI** and its tautomers covalently linked via the 2- and 7-positions in an arrangement containing an inner porphyrin-type ring (**1-1**). DFT calculations of the superposition of tetramers indicated broadband absorption properties compatible with the optical properties of natural eumelanins.[50,51]

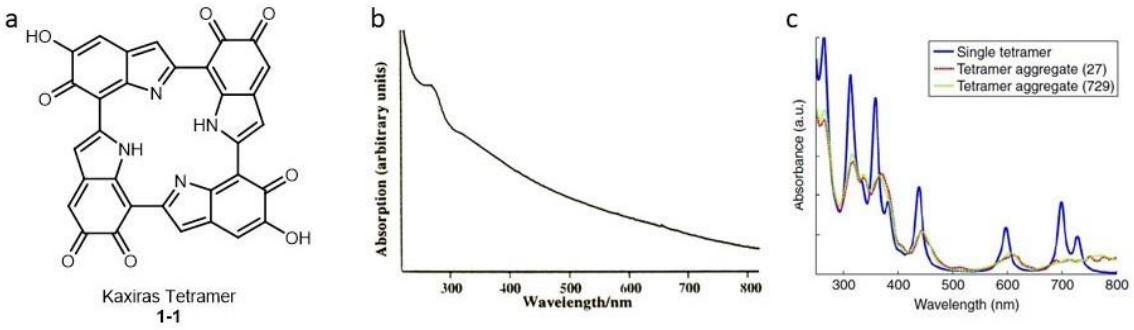

Figure 1-4 Comparison of the absorption spectra of natural eumelanin and proposed Kaxiras' tetramer

a) proposed Kaxiras' tetramer structure; b) absorption spectrum of an aqueous solution of natural eumelanin from Sepia Officinalis at room temperature; c) calculated absorption spectra of large-scale system with Kaxiras' tetramer as protomolecule (excitonic interaction was considered)

The monotonic increase of absorbance in the ultraviolet region, one of the most important spectroscopic features of eumelanin that provides an efficient photoprotective function to living organisms, was not rationalized until the tetramer model was re-subjected to a first-principles computational investigation by the Buehler group.[52]

Calculated spectra of the large-scale systems obtained from the MD simulations with a proper account of the excitonic coupling showed that although the single tetramer showed sharp absorption, the spectrum of a large aggregate of the tetramer is smooth and monotonically increasing toward the higher-energy end (Scheme 1-4c), which resembles the spectra of natural eumelanin (Scheme 1-4b). Two factors were suggested as contribute to the broadening and lowering of the absorption peak at the lower-energy portion of the spectrum. First, the excitonic interaction between stacked tetramer protomolecues is enhanced due to the short interlayer distance of 3-4 Å. Second, there is an interplay of geometry order and disorder. More specifically, the geometric order refers to the stacking of the planar eumelanin protomolecues in the secondary structure (Figure 1-5b). Geometric disorder concerns the lack of preference for the rotational degree of freedom between adjacent molecules and the random orientation between aggregates in the tertiary structure (Figure 1-5c). A snapshot of the large-scale system is shown in Figure 1-5d, where geometric order can be seen in the yellow box whereas between the ordered stacks the geometry is disordered.

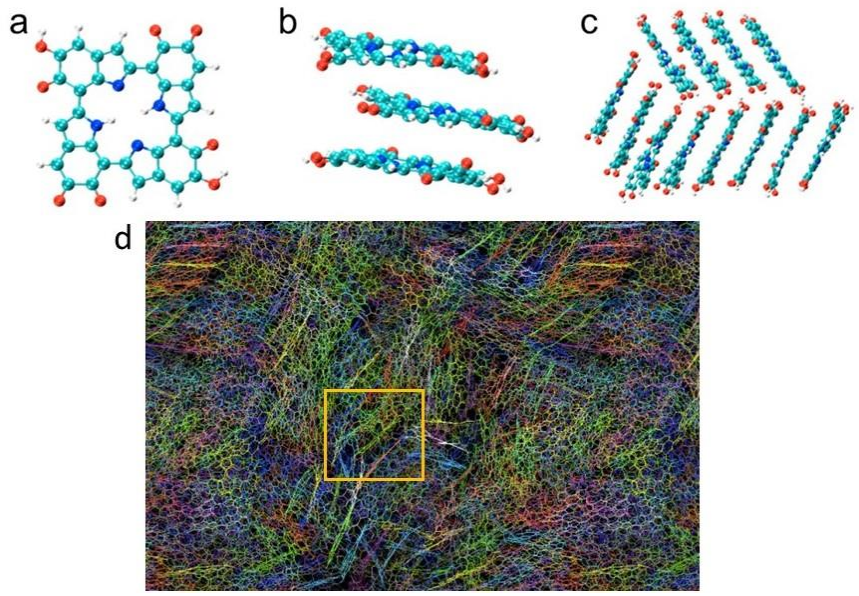

Figure 1-5 Primary, secondary, and tertiary structure of eumalnin protomolecules

a) Primary structures are protomolecules; b) Secondary structures are formed by stacked protomolecules; c) Tertiary (aggregate) structures are formed by weak noncovalent interactions between the secondary structures in random-like orientations.[53] (d) Snapshots of the large-scale systems after the MD simulation.

Collectively, the disordered aggregates resulted in a smooth spectrum in which the absorbance increases toward the higher-energy end monotonically.

Spectroscopic and computational modelling studies have offered useful insight into understanding eumelanin's structure. However, there is still a lack of direct evidence of the proposed structure and a lack of well-defined eumelanin materials within this size regime. An alternative approach to overcome these challenges is highly desirable.

1.4 Synthetic Approaches to Eumelanin Derivatives

Because of the on-going structural debate, there is a need for well-defined dimers, trimers, and higher-order oligomers of **DHI** that can shed light on the emergence of eumelanin's properties from a molecular perspective. To this end, *de novo* synthesis, where well-defined oligomers of **DHI** can be synthesized on-scale have attracted interest.

This section summarizes current efforts to synthesize **DHI** and its oligomers. In section 1.4.1, we provide an overview of **DHI** monomer syntheses. In section 1.4.2, we summarize the current

synthetic efforts related to well-defined eumelanin oligomer derivatives. To be clear, the synthetic approaches highlighted in this section are those that lead to identifiable organic structures. Although referred to as synthetic eumelanin, oxidative polymerization of dopamine, **DHI**, or dopa to different shapes of melanin will not be discussed here, as they do not provide a well-defined structure but instead, evolve to complex mixtures. Readers interested in these related materials are referred to a series of relevant review articles. [13, 54]

1.4.1 Synthesis of 5,6-dihydroxyindole Monomer

Synthetic approaches to **DHI** involve: 1) bio-inspired one-pot approaches based on oxidative coupling of biosynthetic precursors or 2) multistep approaches based on extension and refinement of conventional indole syntheses. Importantly, **DHI** undergoes facile oxidation and turns black rapidly, even in the solid-state, upon exposure to air. Thus, a suitable catechol protecting group is necessary for both manipulating the compound in different chemical transformations and storing it for a prolonged time. The most common protecting groups are acetyl and benzyl groups. Acetyl is of interest because it can be hydrolyzed *in situ* for studies of eumelanin formation and structural elucidation. Benzyl groups are favored in multistep synthetic protocols and can be cleanly removed by catalytic hydrogenolysis.

1.4.1.1 Biomimetic and Bio-inspired Approaches to monomers

Bio-inspired synthesis of **DHI** draws inspiration from the early state of melanogenesis in which oxidative cyclization yields **DHI** from tyrosine (Scheme 1-1). These approaches employ enzymes, including mushroom tyrosinase, horseradish peroxidase, or chemical oxidants such as ceric ammonium nitrate or potassium ferricyanide.

The first bio-inspired synthesis of **DHI** employing enzymes was reported by Raper and co-workers in 1927.[5] At pH 6-6.5, a solution of L-tyrosine (**1-3**) was treated with oxygen and tyrosinase. A hydrogen atmosphere was then applied, followed by the addition of a saturated solution of SO_2. Because of the instability of **DHI**, the product was methylated with dimethyl sulfate under a hydrogen atmosphere. Eventually, crystalline 5,6-dimethoxyindole (**1-38**) was obtained. The

study also showed that L-dopa (**1-14**) was transformed into **1-38** under the same conditions. Although attempted, removal of the methyl protecting groups on **DHI** were unsuccessful (Scheme 1-11).

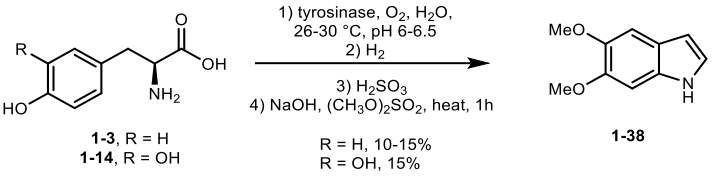

Scheme 1-11 Enzymatic oxidation of tyrosine and L-dopa to **DHI** derivative

In 1987, **DHI** derivatives were obtained via mushroom tyrosinase-catalyzed oxidation of dopamine derivatives (**1-39** to **1-42**) in air by Lim *et al.* [55] The reactions were quenched with ascorbic acid followed by acetylation with acetic anhydride. N-methyl-5,6-diacetoxyinodle **1-43**, N-isopropyl-5,6-diacetoxyindole **1-44**, and N-H derivatives **1-45** and **1-46** were obtained as products following this method. However, **1-45** and **1-46** were only obtained in low yield (Scheme 1-12).

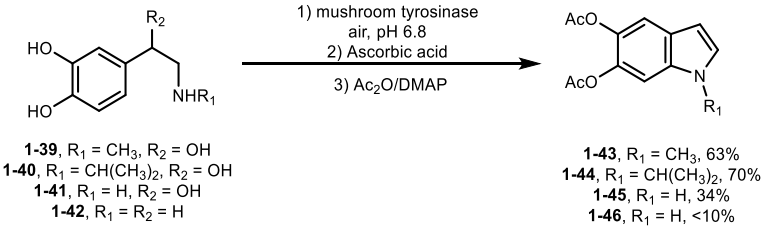

Scheme 1-12 Enzymatic oxidation of *N*-alkyl-5,6-diacetoxyindoles to **DHI** derivatives

Oxidation of L-dopa (**1-14**) with potassium ferricyanide by Harley-Mason and co-workers provided a red solution, which was assigned as L-dopachrome (**1-13**).[56, 57] Treatment of **1-13** with an excess of zinc acetate yielded **DHI**. The action of zinc ions in catalyzing the rearrangement from **1-13** to **DHI** was studied. It was suggested that a Zn complex (**1-47**) could be formed from methyl protected **1-13** and a Zn ion. Spontaneous decomposition of **1-47** could afford the corresponding indole (Scheme 1-13).

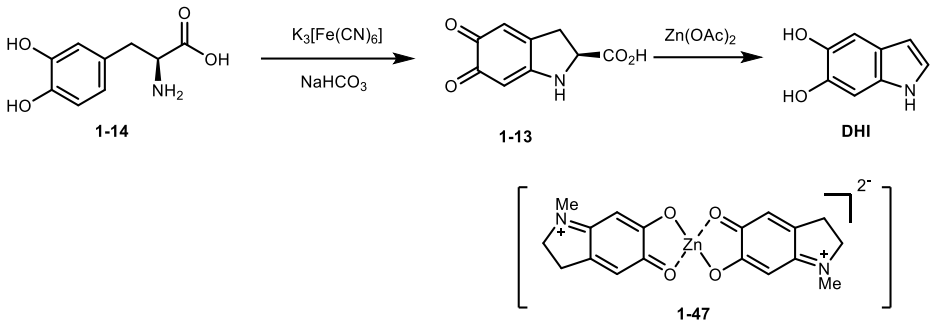

Scheme 1-13 Chemical oxidation of L-dopa to **DHI**

In 1987, milligram to sub-gram quantities of **DHI** and **DHICA** were prepared by a chemical oxidation reported by *Ito et al.*.[58] Here, L-dopachrome (**1-13**) was generated *in situ* by oxidation of L-dopa (**1-14**) with potassium ferricyanide at pH 6.5, which underwent spontaneous decarboxylation to give **DHI** in 40 % isolated yield, while treatment of dopachrome (**1-13**) in NaOH at pH 13 afforded **DHICA** in 38 % isolated yield (Scheme 1-14).

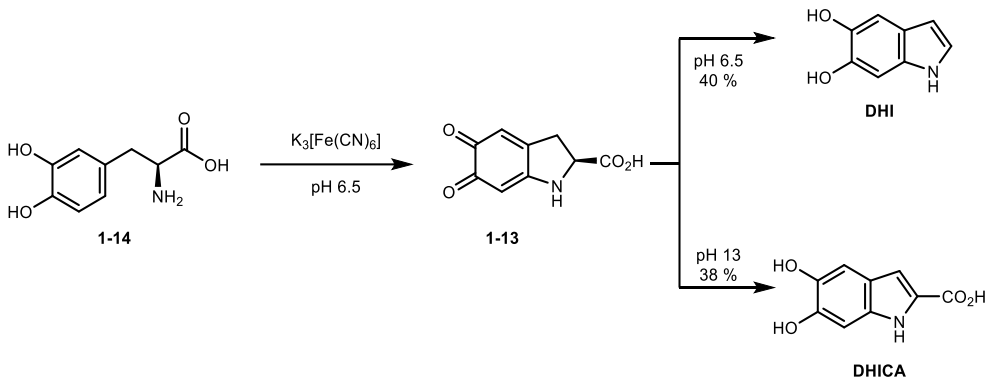

Scheme 1-14 Chemical oxidation of L-dopa to **DHI** and **DHICA**

1.4.1.2 Approach based on conventional indole syntheses

Biomimetic syntheses have been utilized for the rapid preparation of up to hundreds of milligrams of pure **DHIs**, but they have not been used on larger scales, due to a combination of factors that include limited solubility of the substrate, limited efficiency of the cyclization step, and competition with intermolecular processes that predominate at higher concentrations. These limitations have motived the development of multistep approaches based on the extension and refinement of conventional indole syntheses. The organization of this section is

based on the bonds that are constructed in the formation of the pyrrole ring. The approaches to the assembly of the pyrrole ring are represented in Figure 1-6.

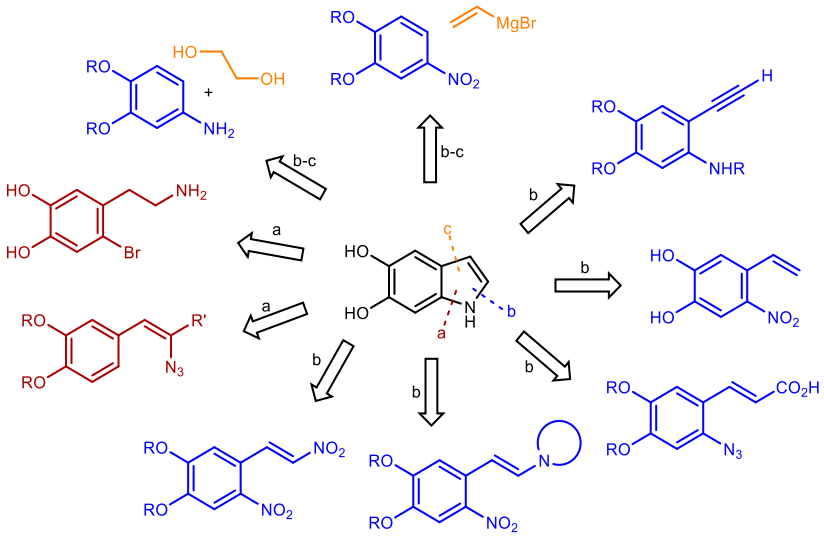

Figure 1-6 Retrosynthetic representation of the main assemblies of the pyrrole ring

1.4.1.2.1 DHI syntheses via b bond formation

The multistep approach to **DHI** based on conventional indole syntheses is exemplified by the classical reductive cyclization of 2,β-dinitrostyrene. This synthesis was pioneered by Harley-Mason,[56] Burton and Duffield,[59] and Robertson[60] in the 1940s. Several modifications were made to reductive cyclization conditions in the 1960s,[61] and 1980s.[62] The most commonly used conditions are Fe/AcOH, H_2/Pt-C, or Zn/$Na_2S_2O_4$. The benzyl protecting group is more often used compared with others because of its efficient deprotection using catalytic hydrogenation over Pd/C (Scheme 1-15).

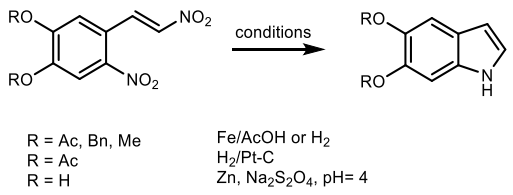

Scheme 1-15 Conditions for reductive cyclization of dinitrostyrene

In 1999, Prota and co-worders developed a gram-scale synthesis of **DHI** based on the 2, β-dinitrostyrene (**1-54**) reductive cyclization.[63] Nitrostyrene (**1-51**) was prepared by Henry condensation of benzaldehyde (**1-48**) with nitromethane. Treatment of nitrostyrene (**1-51**) with tetranitromethane (TNM) in ethanol/0.1 M $NaHCO_3$ buffer (pH=8) in the presence of Zn(II) ions afforded regioselective nitration product (**1-54**). It was suggested that Zn metal cation served as a labile OH-protecting group under mild alkaline conditions, directing nitration to the position *ortho* to the nitrovinyl group.[63] Then reductive cyclization of the resulting 2, β-dinitrostyrene (**1-54**) with $Na_2S_2O_4$ at pH 4 in the presence of Zn (II) afforded **DHI** in 52 % yield. The *in-situ* formation of ZnS_2O_4 proved to be essential for product formation. This approach was effective with benzyl or acetyl as protecting group and resulted in the corresponding product **1-57** and **1-58** in 90 % and 70 % yield, respectively (Scheme 1-16).

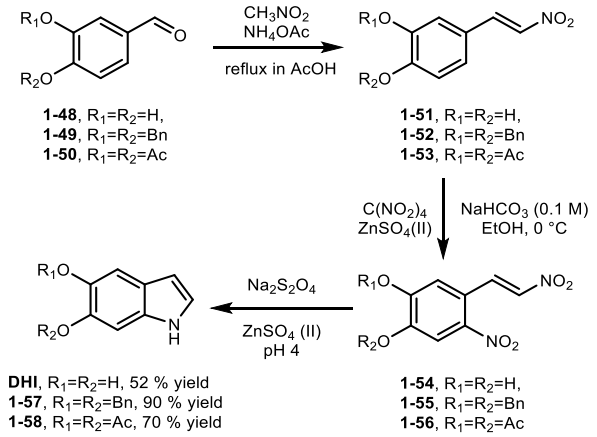

Scheme 1-16 Synthesis of DHI derivatives via reductive cyclization

In 1987, Kawase *et al*. described a modification of the Leimgruber-Batcho indole synthesis that provided access to 2,3-unsubstituted indoles.[64] The method involved a condensation of 2-nitrotoluene (**1-59**) with tripiperidinomethane (**1-60**) to afford 2-nitro-β-piperidinostyrenes (**1-61**), which underwent reductive cyclization *in situ* mediated by iron and acetic acid in the presence of silica gel. With this procedure, benzyl protected **DHI** (**1-57**) was obtained from **1-61** with a 62% yield (Scheme 1-17).

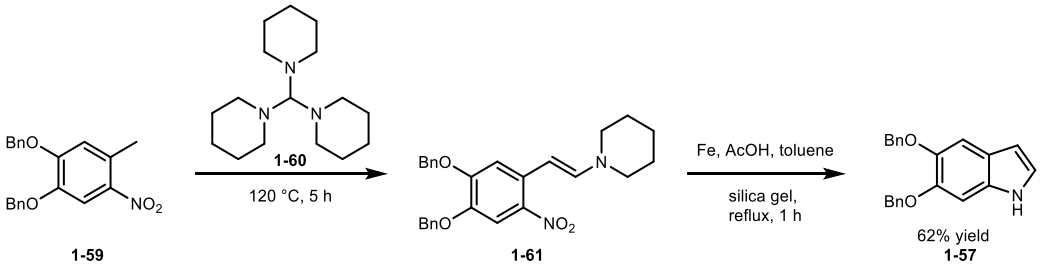

Scheme 1-17 Synthesis of **DHI** derivative via Leimgruber-Batcho indole synthesis

In 1984, Lutz and co-workers developed a cyclic carbonate ester as a storable and ready source of **DHI**.[65] The synthesis started with the formation of carbonate ester (**1-63**) by treating 3,4-methylenedioxycinnamic acid (**1-62**) with phosphorus pentachloride (PCl_5) and formic acid. Subsequent nitration with fuming nitric acid in the presence of sulfuric acid afforded **1-64**. Reduction of the nitro group with $SnCl_2$ resulted in **1-65**. Diazotization of **1-65** with $NOSO_4H$ followed by treatment with sodium azide, gave the azide intermediate **1-66**, which then underwent thermal decomposition and cyclization in the presence of copper powder to the desired product **1-67** (Scheme 1-18). Indirect evidence for the deprotection of **1-67** to **DHI** was provided by the application of a DMSO solution of **1-67** to the upper arm skin of one of the researchers. A zone of increased pigmentation developed within 5 h and reached a maximum intensity in about 12 h.

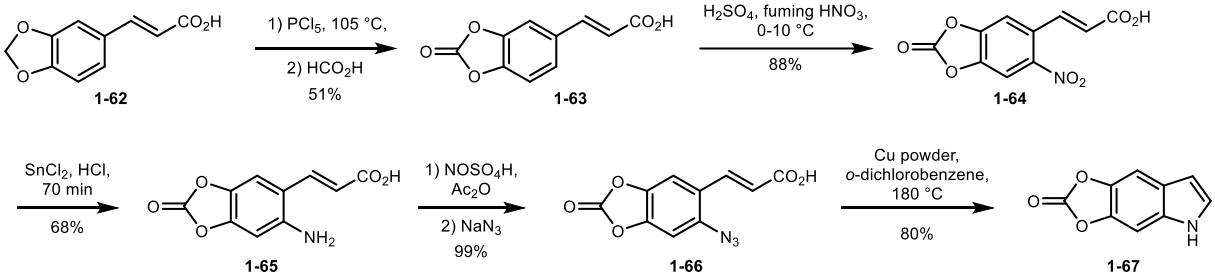

Scheme 1-18 Synthesis of cyclic carbonate ester protected **DHI** derivative

A modified Cadogan indole synthesis was developed by Huleatt *et al*. to prepare **DHI**.[66] *o*-nitrostyrene (**1-69**) was prepared via Wittig methylenation of **1-68** using *n*-butyllithium and methyltriphenylphosphonium bromide in THF at −78 °C and it could be performed on a multi-gram scale. Employing microwave heating in the subsequent cyclization step in the presence of triphenylphosphine and $MoO_2Cl_2(dmf)_2$ converted **1-69** to **1-70** in a high yield (Scheme 1-19).

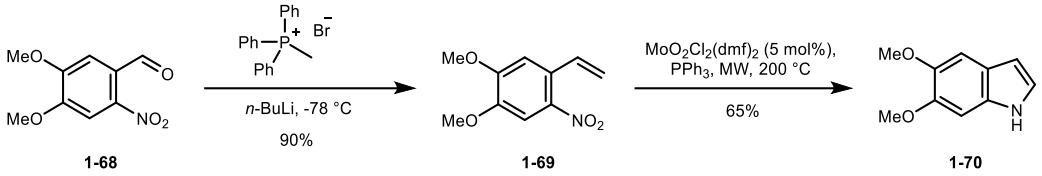

Scheme 1-19 Synthesis of **DHI** derivative via Cadogan indole synthesis

This approach was recently applied in the synthesis of 4- or 7-bromo and 4,7-dibromo derivatives of **DHI** by Chia and co-workers. [66] 5-bromovanillin (**1-71**) was methylated with Me_2SO_4 followed by nitration using Ac_2O/65% HNO_3 with H_2SO_4 to afford **1-72** in 78% yield. A Witting methylenation following the same condition mentioned above (Scheme 1-19), converted **1-72** to styrene **1-73**. Then a Cadogan type cyclization of **1-73** afforded **1-74** with triphenylphosphine and $MoO_2Cl_2(dmf)_2$ at elevated temperature. The substrate scope showed good yields on methylated-**DHI (1-70)**, 4-bromo-(**1-76**), 7-bromo-(**1-75**), and 4,7-dibromo-(**1-77**) derivatives (Scheme 1-20).

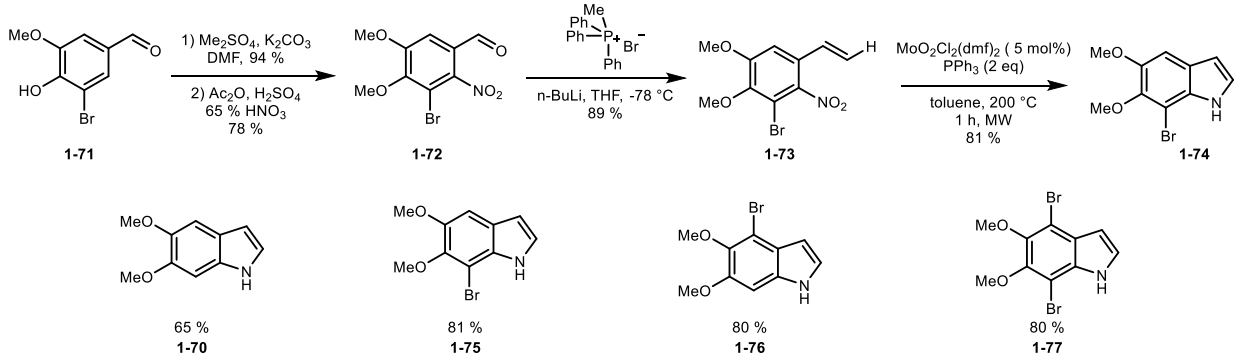

Scheme 1-20 Synthesis of bromo-indoles via Cadogan indole synthesis

More recently, an *ortho*-ethynylaniline-based strategy was developed in a synthetic effort directed toward oligomers of **DHI**. Reduction of **1-78** to the iodoaniline **1-79** was achieved with sodium dithionite in 1:1 acetone-0.1 M phosphate buffer (pH 7.4). Sonogashira coupling with trimethylsilylacetylene followed by deprotection with potassium fluoride led to the *o*-ethynylaniline **1-81**. Then direct cyclization of **1-81** yielded benzyl protected **DHI** (**1-57**) in 75% yield. This approach is compatible with both acetyl and benzyl protecting groups (Scheme 1-21).[67]

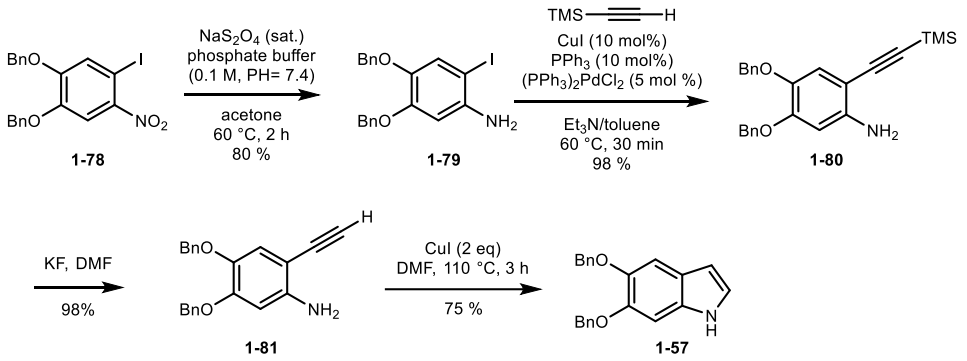

Scheme 1-21 Synthesis of **DHI** derivative via sequential Sonogashira coupling/cyclization

1.4.1.2.2 DHI syntheses via a bond formation

Synthesis of **DHI** through cyclization of 6-bromophenethylamine (**1-80**) was first reported by Harley-Mason[68] in 1952. 2-(3,4-dimethoxyphenyl)ethylamine (**1-82**) was bromated and then demethylated to produce 2-(2-bromo-4,5-dihydroxyphenyl)ethylamine (**1-83**), which was then oxidized by potassium ferricyanide to 5,6-dihydroxyindole (**DHI**). Although **DHI** was obtained in two steps, the yield was low due to the instability of the unprotected catechol in **DHI** (Scheme 1-22).

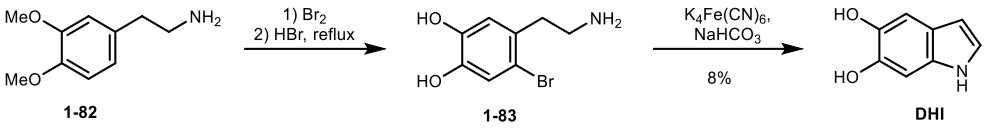

Scheme 1-22 Synthesis of **DHI** via oxidative cyclization

Another DHI derivative synthesis from ethylamine was reported.[69] 3-benzyloxy-6-bromo-4-methoxyphenethylamine (**1-85**), prepared from the corresponding 6-bromo-3,4-disubstituted benzylcyanides (**1-84**) via a sodium borohydride reduction in the presence of boron trifluoride, was treated with sodium methylsulfinylmethylide to provide 5-benzyloxy-6-methoxyindole (**1-86**) via a benzyne intermediate (Scheme 1-23).

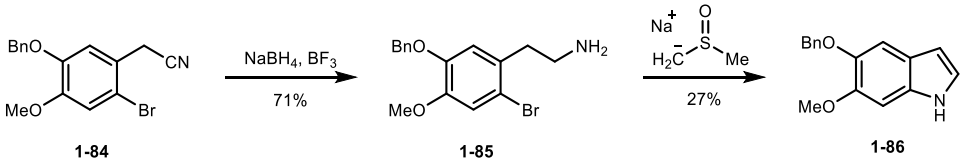

Scheme 1-23 Synthesis of **DHI** derivative via benzyne formation

Another method from Chia and co-workers to prepare bromo derivatives of **DHI** was reported based on the Hemetsberger-Knittle indole synthesis.[70] Isovanillin (**1-87**) was brominated and subsequently methylated with Me_2SO_4 to afford 2-bromoveratraldehyde (**1-88**). Knoevenagel condensation of **1-88** with methyl azidoacetate afforded bromo azidocinnamate (**1-89**), which was then converted to **1-90** via thermolysis. **1-90** was then converted to a 4-bromo derivative of **DHI** (**1-76**) via a two-step process: saponification of the methyl ester in NaOH followed by microwave mediated thermal decarboxylation in quinoline (Scheme 1-24).

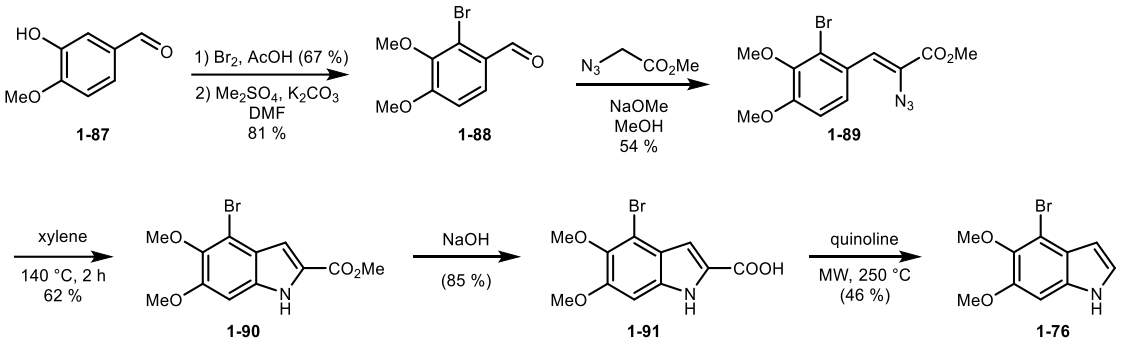

Scheme 1-24 Synthesis of bromo-indole via Hemetsberger-Knittle indole synthesis

1.4.1.2.3 DHI syntheses via c and b bonds formation

In an effort to synthesize 7-bromo and 4,7-dibromo derivatives of **DHI**, a different route was developed based on Bartoli's indole synthesis.[70] 5-nitroguaiaco (**1-92**) was brominated selectively at the C6 position with bromine to **1-93**. Subsequent methylation with Me_2SO_4 provided **1-94**, which was then treated with vinylmagnesium bromide to yield **1-75** in 66 % yield. Similarly, a selective bromination of **1-94** with NBS in a TFA/H_2SO_4 mixed solvent system afforded **1-95**, which was subjected to vinylmagnesium bromide yielded 4,7-dibromo-indole (**1-77**) in modest yield (Scheme 1-25).

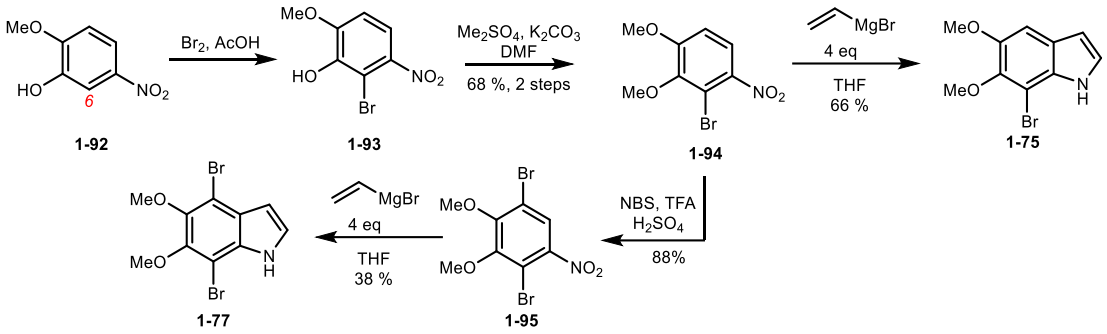

Scheme 1-25 Synthesis of bromo-indoles via Bartoli indole synthesis

The direct access to indoles from anilines was made possible through a catalyst system developed by Llabres-Campener *et al* (Scheme 1-26).[71] The pyrrole ring was constructed from dehydrogenative condensation of aniline (**1-96**) and ethylene glycol in the presence of a combination of ZnO and Pt/Al_2O_3. The proposed mechanism is presented in Scheme 1-26. Ethylene glycol was transformed into monoaldehyde (**1-97**) by Pt/Al_2O_3 in the presence of ZnO as activating agent. Condensation between aldehyde (**1-97**) and aniline (**1-96**) generated imine (**1-98**) then tautomerization led to **1-99** or **1-100**. Indole **1-70** was then formed by cyclization/elimination reactions. The reaction favored substrates with electron-donating groups and gave 5,6-dimethoxyindole (**1-70**) in 84 % yield.

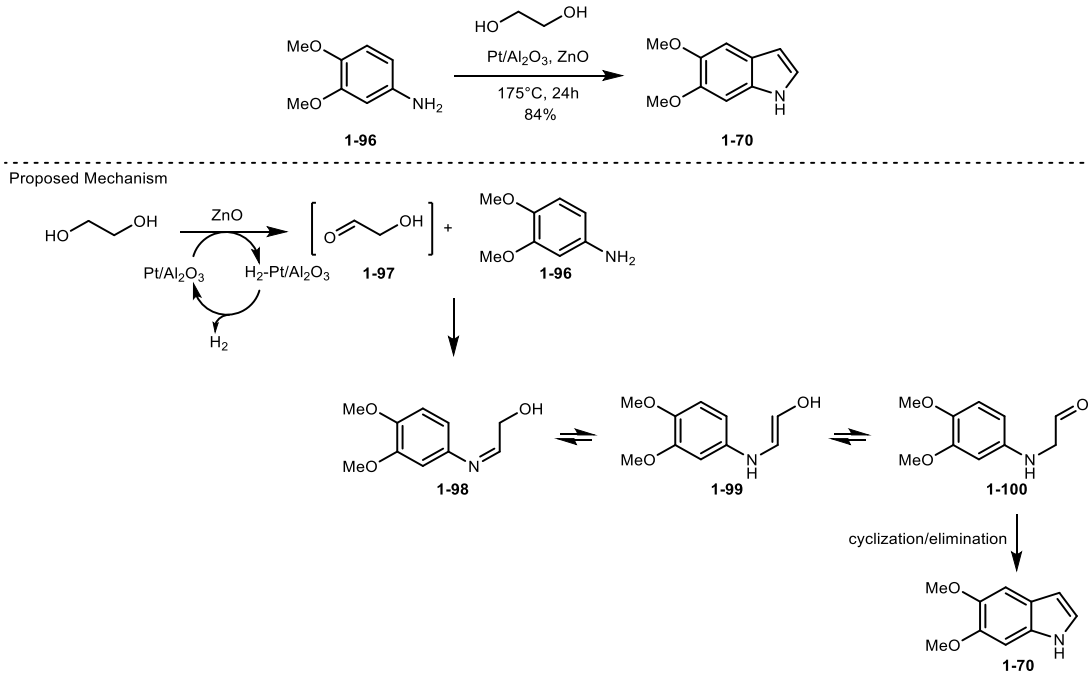

Scheme 1-26 Synthesis of DHI derivative via dehydrogenative condensation of aniline

1.4.2 Synthesis of Eumelanin Oligomers

Whereas numerous synthetic efforts have been directed to **DHI**, synthetic approaches to dimers and trimers are less-well developed. Here we summarize the available synthetic approaches published to date.

The synthesis of 3,3'-dimer (**1-105**) was developed by Baldwin and co-workers.[72] The synthesis commenced with catechol protection of 3,4-dihydroxybenzaldehyde (**1-48**) with benzyl chloride. A Henry reaction of **1-49** with nitromethane afforded **1-52**, which was converted to 2,β-dinitrostyrene **1-55** upon nitration with nitric acid in acetic acid. Reductive cyclization of **1-55** with iron powder in acetic acid provided **1-57** in 61%. Deprotonation of **1-57** with *n*-butyllithium followed by the addition of triisopropylsilyl chloride gave protected indole **1-101** in 95% yield. Iodination at the C3 position of **1-101** with I_2 and $Hg(OAc)_2$ or *N*-iodosuccinimide (NIS) gave **1-102** cleanly. The sterically demanding triisopropyl silane (TIPS) group directs iodination to C3. $Pd(PhCN)_2Cl_2$ catalyzed reductive homocoupling of **1-102** to **1-103** using tetrakis(dimethylamino)ethylene (TDAE) as a mild reductant was achieved in 68% yield. Desilylation of **1-103** with tetrabutylammonium fluoride (TBAF) afforded benzyl protected dimer (**1-104**) in 82% yield. Pd black catalyzed hydrogenation of **1-104** revealed 5,5',6,6'-tetrahydroxy-3,3'-bisindole (**1-105**) in 94% yield (Scheme 1-27).

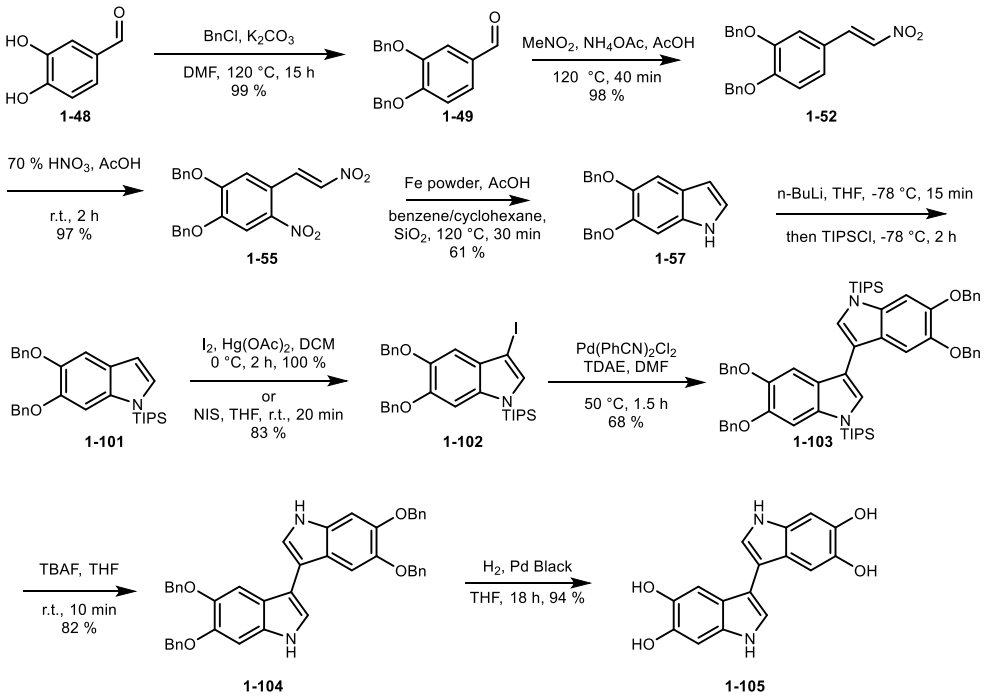

Scheme 1-27 Synthesis of 3,3'-dimer via reductive homocoupling

In 2008, Chai and co-workers demonstrated syntheses of diverse, sterically hindered biindolyl systems and, verified the feasibility of constructing protected **DHI** dimers via a one-pot Miyaura borylation and subsequent transition metal-mediated Suzuki-Miyaura cross-coupling protocol between two bromoindoles. For example, Miyaura borylation of 7-bromo indole (**1-75**) followed by Suzuki coupling with 4-bromo indole (**1-76**) catalyzed by $Pd_2(dba)_3$ with XPhos as a ligand and $K_3PO_4 \cdot H_2O$ as a base provided 4,7'-dimer (**1-106**) in 75% yield (Scheme 1-28).[73] The syntheses of bromoindole monomers was discussed in Scheme 1-20.[74]

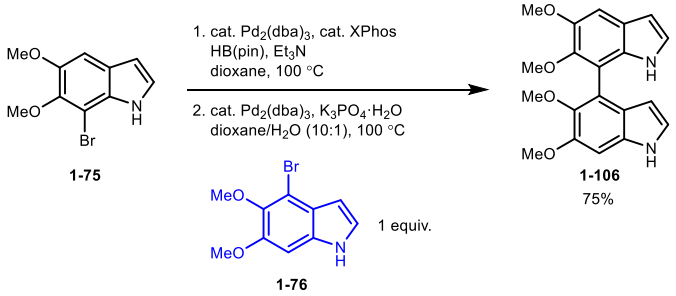

Scheme 1-28 Synthesis of 4,7'-dimer via sequential Miyaura borylation/Suzuki coupling

In 2009, the synthesis of a 2,2'-dimer (**1-108**) was reported by d'Ischia and co-workers, highlighting sequential coupling and cyclization steps involving suitably protected *o*-ethynylaniline intermediates.[67] Preparation of **1-81** was discussed in Scheme 1-21. Oxidative dimerization of **1-81** with $Cu(OAc)_2$ in pyridine resulted in **1-107**, which was subjected to a CuI mediated cyclization that afforded the 2,2'-dimer (**1-108**) via an intramolecular cyclization in satisfactory yield (Scheme 1-29).

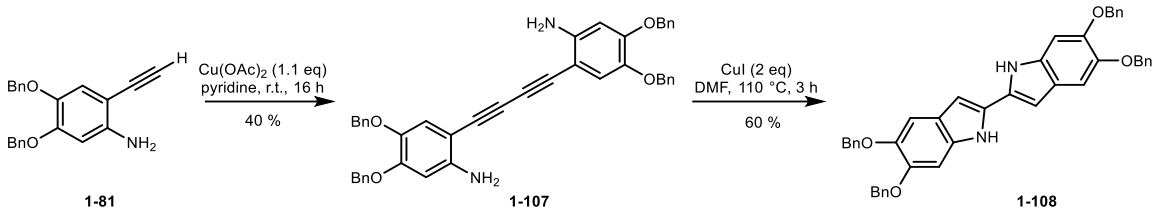

Scheme 1-29 Synthesis of 2,2'-dimer via sequential Sonogashira coupling/cyclization

The synthesis of the 2, 7'-dimer (**1-118**) was demonstrated by d'Ischa and co-workers (Scheme 1-30).[67] This synthetic approach started from the protection of catechol (**1-109**) with acetic anhydride in pyridine followed by hydrogenation of the nitro group of **1-110** using Pd/C at elevated pressures.

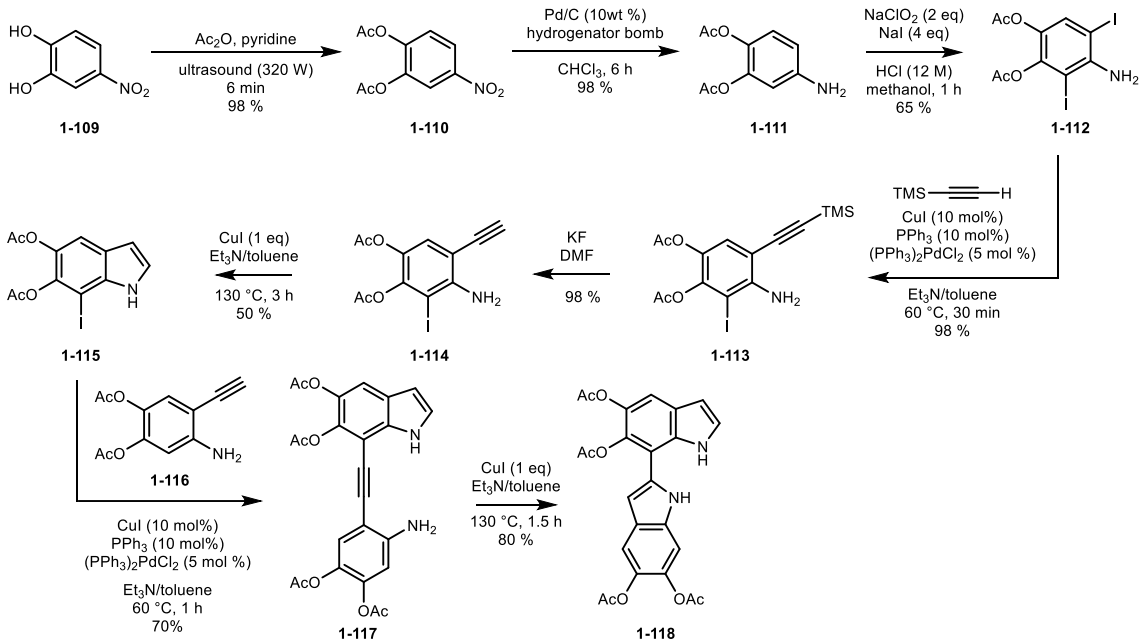

Scheme 1-30 Synthesis of 2,7'-dimer via sequential Sonogashira coupling/cyclization

Subsequent iodination of **1-111** with NaI/$NaClO_2$ yielded *o,o*-diiodoaniline (**1-112**), which is a key intermediate in the synthetic sequence. **1-113** was then obtained in a good yield following a regioselective Sonogashira coupling with trimethylsilylacetylene. Desilylation of **1-113** with potassium fluoride followed by CuI-promoted cyclization led to 7-iodoindole **1-115.** Another sequential Sonogashira coupling between **1-115** and **1-116** followed by CuI-promoted cyclization gave 2,7'-dimer (**1-118**, Scheme 1-30).

In 2010, the d'Ischai group extended this approach to the synthesis of trimer **1-124**.[75] The conversion of **1-114** to **1-124** is illustrated in Scheme 1-31. Cyclization of **1-114** to 5,6-diacetoxy-7-iodoindole (**1-115**) was efficiently carried out via an improved procedure that was based on $Cu(OAc)_2$ as a catalyst in dry CH_2Cl_2.

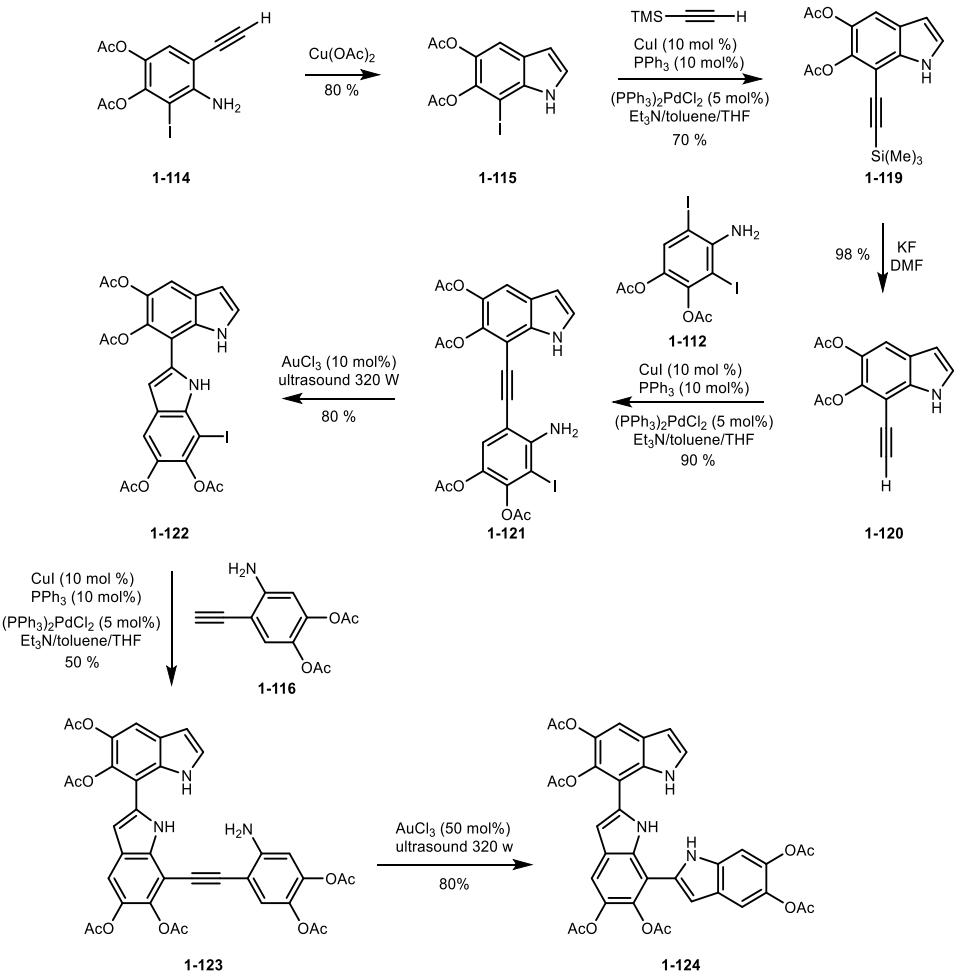

Scheme 1-31 Synthesis of 2, 7, 2', 7''-trimer via sequential Sonogashira coupling/cyclization

Sonogashira coupling of **1-115** and trimethylsilylacetylene followed by desilylation with potassium fluoride led to 5,6-diacetoxy-7-ethynylindole (**1-120**). Selective Sonogashira coupling between **1-120** and *o,o*-diiodoaniline (**1-112**) provided indolylethynylaniline (**1-121**). Then cyclization of **1-121** was carried out using $AuCl_3$ as a catalyst to afford dimer **1-122**. Finally, trimer **1-124** was obtained following another sequential Sonogashira coupling between **1-122** and **1-116** followed by $AuCl_3$-catalyzed cyclization of **1-123** (Scheme 1-31).

1.5 Conclusion

Due to the intriguing physicochemical properties, broad applications, and the elusive chemical composition of eumelanin and eumelanin-inspired material, understanding the molecular origin of its unique physicochemical properties has remained of significant importance. Eumelanin's biosynthesis begins with an oxidative cyclization of L-tyrosine to either 5, 6-dihydroxy-indole-2-carboxylic acid (**DHICA**) or 5, 6-dihydroxyindole (**DHI**) which is catalyzed by the enzyme tyrosinase. **DHI** and **DHICA** are the last known intermediates in the pathway because their spontaneous oxidation leads to complex, insoluble, heterogeneous materials.

Biomimetic oxidation of **DHI** has revealed that the prevalent mode of coupling of **DHI** is at the C2, C4, and C7 positions, however, it generates black material that only contains a low yield of well-defined materials. In addition, the detailed mechanism of **DHI/DHICA** oxidative polymerization remains a matter of debate.

A chemical disorder model, containing various oligomers with different lengths, structures and in different redox states, was proposed to explain eumelanin's characteristic broadband absorption. However, at small distances expected between eumelanin's chromophore, strong interactions are expected that will cause the transition energies of the isolated units to change, where the superposition principle does not hold.

Recent developments in spectroscopic and microscopic studies have suggested that eumelanin is comprised of small nearly planar oligomers (protomolecule) stacked together via π-π interactions to form graphite-like layered aggregates. A protomolecule, Kaxiras' cyclic tetramer,

has been proposed as a major component of eumelanin via in silico modelling by multiple research groups. This model was able to reproduce most of eumelanin's physical properties. While attractive, a lack of direct evidence of the proposed structure has motivated synthetic approaches to access well-defined eumelanin oligomers possessing eumelanin-like properties.

Syntheses of **DHI** via bio-inspired approaches have been developed, however, these approaches suffer from issues of limited efficiency in the cyclization step, and competition with intermolecular processes. Thus, approaches based on conventional indole syntheses are more commonly used. Syntheses of **DHI** oligomers, however, are less developed and have not been extended to oligomers beyond the stage of a trimer. Thus, alternative approaches to well-defined oligomers beyond trimers and a total synthesis of the Kaxiras' tetramer must be developed in order to advance our fundamental understanding of eumelanin and related materials.

1.6 Reference

1. Meredith, P.; Sarna, T., The physical and chemical properties of eumelanin. *Pigment Cell Res.* **2006,** *19* (6), 572-594.

2. Hill, H. Z., The function of melanin or six blind people examine an elephant. *Bioessays* **1992,** *14* (1), 49-56.

3. d'Ischia, M.; Wakamatsu, K.; Napolitano, A.; Briganti, S.; Garcia-Borron, J.-C.; Kovacs, D.; Meredith, P.; Pezzella, A.; Picardo, M.; Sarna, T.; Simon, J. D.; Ito, S., Melanins and melanogenesis: methods, standards, protocols. *Pigment Cell & Melanoma Research* **2013,** *26* (5), 616-633.

4. Cao, W.; Zhou, X.; McCallum, N. C.; Hu, Z.; Ni, Q. Z.; Kapoor, U.; Heil, C. M.; Cay, K. S.; Zand, T.; Mantanona, A. J.; Jayaraman, A.; Dhinojwala, A.; Deheyn, D. D.; Shawkey, M. D.; Burkart, M. D.; Rinehart, J. D.; Gianneschi, N. C., Unraveling the Structure and Function of Melanin through Synthesis. *Journal of the American Chemical Society* **2021,** *143* (7), 2622-2637.

5. Raper, H. S., The Tyrosinase-tyrosine Reaction: Production from Tyrosine of 5: 6-Dihydroxyindole and 5: 6-Dihydroxyindole-2-carboxylic Acid—the Precursors of Melanin. *Biochemical Journal* **1927,** *21* (1), 89-96.

6. Mason, H. S., The Chemistry of Melanin: III Mechanism of the Oxidation of Dihydroxyphenylalanine by Tyrosinase. *J. Biol. Chem.* **1948,** *172* (1), 83-99.

7. Martín-Bastida, A.; Lao-Kaim, N. P.; Roussakis, A. A.; Searle, G. E.; Xing, Y.; Gunn, R. N.; Schwarz, S. T.; Barker, R. A.; Auer, D. P.; Piccini, P., Relationship between neuromelanin and dopamine terminals within the Parkinson's nigrostriatal system. *Brain* **2019,** *142* (7), 2023-2036.

8. Schmaler-Ripcke, J.; Sugareva, V.; Gebhardt, P.; Winkler, R.; Kniemeyer, O.; Heinekamp, T.; Brakhage, A. A., Production of Pyomelanin, a Second Type of Melanin, via the Tyrosine Degradation Pathway in Aspergillus fumigatus. *Applied and Environmental Microbiology* **2009,** *75* (2), 493-503.

9. Au - Ketelboeter, L. M.; Au - Bardy, S. L., Methods to Inhibit Bacterial Pyomelanin Production and Determine the Corresponding Increase in Sensitivity to Oxidative Stress. *JoVE* **2015,** (102), e53105.

10. Coon, S. L.; Kotob, S.; Jarvis, B. B.; Wang, S.; Fuqua, W. C.; Weiner, R. M., Homogentisic acid is the product of MelA, which mediates melanogenesis in the marine bacterium Shewanella colwelliana D. *Applied and Environmental Microbiology* **1994,** *60* (8), 3006-3010.

11. Bernsmann, F.; Ball, V.; Addiego, F.; Ponche, A.; Michel, M.; Gracio, J. J. d. A.; Toniazzo, V.; Ruch, D., Dopamine−Melanin Film Deposition Depends on the Used Oxidant and Buffer Solution. *Langmuir* **2011,** *27* (6), 2819-2825.

12. Bernsmann, F.; Ponche, A.; Ringwald, C.; Hemmerlé, J.; Raya, J.; Bechinger, B.; Voegel, J.-C.; Schaaf, P.; Ball, V., Characterization of Dopamine−Melanin Growth on Silicon Oxide. *The Journal of Physical Chemistry C* **2009,** *113* (19), 8234-8242.

13. Liebscher, J.; Mrówczyński, R.; Scheidt, H. A.; Filip, C.; Hădade, N. D.; Turcu, R.; Bende, A.; Beck, S., Structure of Polydopamine: A Never-Ending Story? *Langmuir* **2013,** *29* (33), 10539-10548.

14. Prota, G., Chapter 2 -Melanin Producing Cells. *Melanins and Melanogenesis*, Prota, G., Ed. Academic Press: San Diego, 1992; pp 14-33.

15. Westerhof, W., The discovery of the human melanocyte. *Pigment Cell Res.* **2006,** *19* (3), 183-193.

16. Claus, H.; Decker, H., Bacterial tyrosinases. *Systematic and Applied Microbiology* **2006,** *29* (1), 3-14.

17. Mayer, A. M., Polyphenol oxidases in plants and fungi: Going places? A review. *Phytochemistry* **2006,** *67* (21), 2318-2331.

18. Olivares, C.; Jiménez-Cervantes, C.; Lozano, J. A.; Solano, F.; García-Borrón, J. C., The 5,6-dihydroxyindole-2-carboxylic acid (DHICA) oxidase activity of human tyrosinase. *The Biochemical journal* **2001,** *354* (Pt 1), 131-139.

19. Tsukamoto, K.; Jackson, I. J.; Urabe, K.; Montague, P. M.; Hearing, V. J., A second tyrosinase-related protein, TRP-2, is a melanogenic enzyme termed DOPAchrome tautomerase. *The EMBO journal* **1992,** *11* (2), 519-526.

20. Pawelek, J.; Körner, A.; Bergstrom, A.; Bologna, J., New regulators of melanin biosynthesis and the autodestruction of melanoma cells. *Nature* **1980,** *286* (5773), 617-619.

21. Jiménez-Cervantes, C.; Solano, F.; Kobayashi, T.; Urabe, K.; Hearing, V. J.; Lozano, J. A.; García-Borrón, J. C., A new enzymatic function in the melanogenic pathway. The 5,6-dihydroxyindole-2-carboxylic acid oxidase activity of tyrosinase-related protein-1 (TRP1). *J. Biol. Chem.* **1994,** *269* (27), 17993-18000.

22. Kobayashi, T.; Urabe, K.; Winder, A.; Jiménez-Cervantes, C.; Imokawa, G.; Brewington, T.; Solano, F.; García-Borrón, J. C.; Hearing, V. J., Tyrosinase related protein 1 (TRP1) functions as a DHICA oxidase in melanin biosynthesis. *The EMBO Journal* **1994,** *13* (24), 5818-5825.

23. Boissy, R. E.; Sakai, C.; Zhao, H.; Kobayashi, T.; Hearing, V. J., Human tyrosinase related protein-1 (TRP-1) does not function as a DHICA oxidase activity in contrast to murine TRP-1. *Exp. Dermatol.* **1998,** *7* (4), 198-204.

24. Lai, X.; Wichers, H. J.; Soler-Lopez, M.; Dijkstra, B. W., Structure of Human Tyrosinase Related Protein 1 Reveals a Binuclear Zinc Active Site Important for Melanogenesis. *Angew. Chem. Int. Ed.* **2017,** *56* (33), 9812-9815.

25. Ito, S.; Wakamatsu, K., Chemistry of Mixed Melanogenesis—Pivotal Roles of Dopaquinone†. *Photochemistry and Photobiology* **2008,** *84* (3), 582-592.

26. Thompson, A.; Land, E. J.; Chedekel, M. R.; Subbarao, K. V.; Truscott, T. G., A pulse radiolysis investigation of the oxidation of the melanin precursors 3,4-dihydroxyphenylalanine (dopa) and the cysteinyldopas. *Biochimica et Biophysica Acta (BBA) - General Subjects* **1985,** *843* (1), 49-57.

27. Simon, J. D.; Peles, D. N., The Red and the Black. *Acc. Chem. Res.* **2010,** *43* (11), 1452-1460.

28. Ito, S., A Chemist's View of Melanogenesis. *Pigment Cell Res.* **2003,** *16* (3), 230-236.

29. Napolitano, A.; Corradini, M. G.; Prota, G., A Reinvestigation of the Structure of Melanochrome. *Tetrahedron Lett.* **1985,** *26* (23), 2805-2808.

30. d'Ischia, M.; Napolitano, A.; Tsiakas, K.; Prota, G., New intermediates in the oxidative polymerisation of 5,6-dihydroxyindole to melanin promoted by the peroxidase/H2O2 system. *Tetrahedron* **1990,** *46* (16), 5789-5796.

31. d'Ischia, M.; Napolitano, A.; Prota, G., Peroxidase as an alternative to tyrosinase in the oxidative polymerization of 5,6-dihydroxyindoles to melanin(s). *Biochimica et Biophysica Acta (BBA) - General Subjects* **1991,** *1073* (2), 423-430.

32. Panzella, L.; Pezzella, A.; Napolitano, A.; d'Ischia, M., The First 5,6-Dihydroxyindole Tetramer by Oxidation of 5,5‘,6,6‘-Tetrahydroxy- 2,4‘-biindolyl and an Unexpected Issue of Positional Reactivity en Route to Eumelanin-Related Polymers. *Org. Lett.* **2007,** *9* (7), 1411-1414.

33. Pezzella, A.; Panzella, L.; Natangelo, A.; Arzillo, M.; Napolitano, A.; d'Ischia, M., 5,6-Dihydroxyindole Tetramers with “Anomalous” Interunit Bonding Patterns by Oxidative Coupling of 5,5‘,6,6‘-Tetrahydroxy-2,7‘-biindolyl: Emerging Complexities on the Way toward an Improved Model of Eumelanin Buildup. *J. Org. Chem.* **2007,** *72* (24), 9225-9230.

34. Arzillo, M.; Pezzella, A.; Crescenzi, O.; Napolitano, A.; Land, E. J.; Barone, V.; d’Ischia, M., Cyclic Structural Motifs in 5,6-Dihydroxyindole Polymerization Uncovered: Biomimetic Modular Buildup of a Unique Five-Membered Macrocycle. *Org. Lett.* **2010,** *12* (14), 3250-3253.

35. Okuda, H.; Wakamatsu, K.; Ito, S.; Sota, T., Possible Oxidative Polymerization Mechanism of 5,6-Dihydroxyindole from ab Initio Calculations. *The Journal of Physical Chemistry A* **2008,** *112* (44), 11213-11222.

36. Pezzella, A.; Panzella, L.; Crescenzi, O.; Napolitano, A.; Navaratman, S.; Edge, R.; Land, E. J.; Barone, V.; d'Ischia, M., Short-Lived Quinonoid Species from 5,6-Dihydroxyindole Dimers en Route to Eumelanin Polymers: Integrated Chemical, Pulse Radiolytic, and Quantum Mechanical Investigation. *Journal of the American Chemical Society* **2006,** *128* (48), 15490-15498.

37. d'Ischia, M.; Napolitano, A.; Pezzella, A., 5,6-Dihydroxyindole Chemistry: Unexplored Opportunities Beyond Eumelanin. *European Journal of Organic Chemistry* **2011,** *2011* (28), 5501-5516.

38. Manini, P.; Pezzella, A.; Panzella, L.; Napolitano, A.; d'Ischia, M., New insight into the oxidative chemistry of noradrenaline: competitive o-quinone cyclisation and chain fission routes leading to an unusual 4-[bis-(1H-5,6-dihydroxyindol-2-yl)methyl]-1,2-dihydroxybenzene derivative. *Tetrahedron* **2005,** *61* (16), 4075-4080.

39. Nagarajan, R.; Perumal, P. T., Electrophilic Substitution of Indoles Catalyzed by Triphenyl Phosphonium Perchlorate: Synthesis of 3-acetyl Indoles and Bis-indolylmethane Derivatives. *Synth. Commun.* **2002,** *32* (1), 105-109.

40. Tran, M. L.; Powell, B. J.; Meredith, P., Chemical and Structural Disorder in Eumelanins: A Possible Explanation for Broadband Absorbance. *Biophys. J.* **2006,** *90* (3), 743-752.

41. Chen, C.-T.; Ball, V.; de Almeida Gracio, J. J.; Singh, M. K.; Toniazzo, V.; Ruch, D.; Buehler, M. J., Self-Assembly of Tetramers of 5,6-Dihydroxyindole Explains the Primary Physical Properties of Eumelanin: Experiment, Simulation, and Design. *ACS Nano* **2013,** *7* (2), 1524-1532.

42. Cheng, J.; Moss, S. C.; Eisner, M.; Zschack, P., X-Ray Characterization of Melanins—I. *Pigment Cell Res.* **1994,** *7* (4), 255-262.

43. Cheng, J. I. N.; Moss, S. C.; Eisner, M., X-Ray Characterization of Melanins—II. *Pigment Cell Res.* **1994,** *7* (4), 263-273.

44. Clancy, C. M. R.; Simon, J. D., Ultrastructural Organization of Eumelanin from Sepia officinalis Measured by Atomic Force Microscopy. *Biochemistry* **2001,** *40* (44), 13353-13360.

45. Zajac, G. W.; Gallas, J. M.; Cheng, J.; Eisner, M.; Moss, S. C.; Alvarado-Swaisgood, A. E., The fundamental unit of synthetic melanin: a verification by tunneling microscopy of X-ray scattering results. *Biochimica et Biophysica Acta (BBA) - General Subjects* **1994,** *1199* (3), 271-278.

46. Watt, A. A. R.; Bothma, J. P.; Meredith, P., The supramolecular structure of melanin. *Soft Matter* **2009,** *5* (19), 3754-3760.

47. Stark, K. B.; Gallas, J. M.; Zajac, G. W.; Golab, J. T.; Gidanian, S.; McIntire, T.; Farmer, P. J., Effect of Stacking and Redox State on Optical Absorption Spectra of Melanins−Comparison of Theoretical and Experimental Results. *The Journal of Physical Chemistry B* **2005,** *109* (5), 1970-1977.

48. Kohl, F. R.; Grieco, C.; Kohler, B., Ultrafast spectral hole burning reveals the distinct chromophores in eumelanin and their common photoresponse. *Chemical Science* **2020,** *11* (5), 1248-1259.

49. Napolitano, A.; Pezzella, A.; Prota, G.; Seraglia, R.; Traldi, P., Structural Analysis of Synthetic Melanins from 5,6-Dihydroxyindole by Matrix-assisted Laser Desorption/Ionization Mass Spectrometry. *Rapid Commun. Mass Spectrom.* **1996,** *10* (4), 468-472.

50. Kaxiras, E.; Tsolakidis, A.; Zonios, G.; Meng, S., Structural Model of Eumelanin. *Phys. Rev. Lett.* **2006,** *97* (21), 218102.

51. Meng, S.; Kaxiras, E., Theoretical Models of Eumelanin Protomolecules and their Optical Properties. *Biophys. J.* **2008,** *94* (6), 2095-2105.

52. Chen, C.-T.; Chuang, C.; Cao, J.; Ball, V.; Ruch, D.; Buehler, M. J., Excitonic effects from geometric order and disorder explain broadband optical absorption in eumelanin. *Nature Communications* **2014,** *5* (1), 3859.

53. d'Ischia, M.; Napolitano, A.; Ball, V.; Chen, C.-T.; Buehler, M. J., Polydopamine and Eumelanin: From Structure–Property Relationships to a Unified Tailoring Strategy. *Acc. Chem. Res.* **2014,** *47* (12), 3541-3550.

54. Alfieri, M. L.; Micillo, R.; Panzella, L.; Crescenzi, O.; Oscurato, S. L.; Maddalena, P.; Napolitano, A.; Ball, V.; d'Ischia, M., Structural Basis of Polydopamine Film Formation: Probing 5,6-Dihydroxyindole-Based Eumelanin Type Units and the Porphyrin Issue. *ACS Applied Materials & Interfaces* **2018,** *10* (9), 7670-7680.

55. Lim, M. I.; Patil, D. G., Mushroom tyrosinase as an oxidant for the synthesis of 5,6-dihydroxyindole derivatives. *Tetrahedron Lett.* **1987,** *28* (33), 3775-8.

56. Bu'Lock, J. D.; Harley-Mason, J., 497. Melanin and its precursors. Part III. New syntheses of 5 : 6-dihydroxyindole and its derivatives. *Journal of the Chemical Society (Resumed)* **1951,** (0), 2248-2252.

57. Harley-Mason, J.; Bu'Lock, J. D., Synthesis of 5:6-Dihydroxyindole Derivatives: an Oxido-reduction Rearrangement Catalysed by Zinc Ions. *Nature* **1950,** *166* (4233), 1036-1037.

58. Wakamatsu, K.; Ito, S., Preparation of Eumelanin-Related Metabolites 5,6-Dihydroxyindole, 5,6-Dihydroxyindole-2-Carboxylic Acid, and Their O-Methyl Derivatives. *Anal. Biochem.* **1988,** *170* (2), 335-340.

59. Burton, H.; Duffield, J. A., The Melanin Problem : a Synthesis of 5 : 6-Dihydroxy-Indole and Its Derivatives. *Nature* **1948,** *161* (4097), 725-725.

60. Beer, R. J. S.; Clarke, K.; Khorana, H. G.; Robertson, A., The Melanin Problem : a Synthesis of 5 : 6-Dihydroxyindole. *Nature* **1948,** *161* (4092), 525-525.

61. Benigni, J. D.; Minnis, R. L., The syntheses of 5,6-dihydroxyindole and some of its derivatives. *J. Heterocycl. Chem.* **1965,** *2* (4), 387-392.

62. Murphy, B. P.; Schultz, T. M., Synthesis and physical properties of 5,6-dihydroxyindole. *J. Org. Chem.* **1985,** *50* (15), 2790-2791.

63. Novellino, L.; d'Ischia, M.; Prota, G., Expedient Synthesis of 5,6-Dihydroxyindole and Derivatives via an Improved Zn(II)-Assisted 2,β-Dinitrostyrene Approach. *Synthesis* **1999,** *1999* (05), 793-796.

64. Kawase, M.; Sinhababu, A. K.; Borchardt, R. T., Silica gel-assisted reductive cyclization of 2-nitro-β-piperidinostyrenes, derived from 2-nitrotoluenes, to indoles. *J. Heterocycl. Chem.* **1987,** *24* (6), 1499-501.

65. Lutz, W. B.; McNamara, C. R.; Olinger, M. R.; Schmidt, D. F.; Doster, D. E.; Fiedler, M. D., Synthesis of 5,6-carbonyldioxyindole, a melanogenic cyclic carbonate ester of 5,6-dihydroxyindole. *J. Heterocycl. Chem.* **1984,** *21* (4), 1183-8.

66. Huleatt, P. B.; Lau, J.; Chua, S.; Tan, Y. L.; Duong, H. A.; Chai, C. L. L., Concise, efficient and practical assembly of bromo-5,6-dimethoxyindole building blocks. *Tetrahedron Lett.* **2011,** *52* (12), 1339-1342.

67. Capelli, L.; Manini, P.; Pezzella, A.; Napolitano, A.; d'Ischia, M., Efficient Synthesis of 5,6-Dihydroxyindole Dimers, Key Eumelanin Building Blocks, by a Unified o-Ethynylaniline-Based Strategy for the Construction of 2-Linked Biindolyl Scaffolds. *J. Org. Chem.* **2009,** *74* (18), 7191-7194.

68. Harley-Mason, J., Melanin and its precursors. VI. Further synthesis of 5,6-dihydroxyindole and its derivatives. *J. Chem. Soc.* **1953**, 200-3.

69. Ito, K.; Tanaka, H.; Kayama, M., Studies on the syntheses of indoline derivatives from N-sulfonamides. *Chem. Pharm. Bull.* **1977,** *25* (6), 1249-55.

70. Huleatt, P. B.; Choo, S. S.; Chua, S.; Chai, C. L. L., Expedient routes to valuable bromo-5,6-dimethoxyindole building blocks. *Tetrahedron Lett.* **2008,** *49* (36), 5309-5311.

71. Llabres-Campaner, P. J.; Ballesteros-Garrido, R.; Ballesteros, R.; Abarca, B., Straight Access to Indoles from Anilines and Ethylene Glycol by Heterogeneous Acceptorless Dehydrogenative Condensation. *J. Org. Chem.* **2018,** *83* (1), 521-526.

72. Mee, S. P. H.; Lee, V.; Baldwin, J. E.; Cowley, A., Total synthesis of 5,5′,6,6′-tetrahydroxy-3,3′-biindolyl, the proposed structure of a potent antioxidant found in beetroot (Beta vulgaris). *Tetrahedron* **2004,** *60* (16), 3695-3712.

73. Duong, H. A.; Chua, S.; Huleatt, P. B.; Chai, C. L. L., Synthesis of Biindolyls via Palladium-Catalyzed Reactions. *J. Org. Chem.* **2008,** *73* (22), 9177-9180.

74. Huleatt, P. B.; Lau, J.; Chua, S.; Tan, Y. L.; Duong, H. A.; Chai, C. L. L., Concise, efficient and practical assembly of bromo-5,6-dimethoxyindole building blocks. *Tetrahedron Lett.* **2011,** *52* (12), 1339-1342.

75. Capelli, L.; Manini, P.; Pezzella, A.; d'Ischia, M., First synthetic entry to the trimer stage of 5,6-dihydroxyindole polymerization: ortho-alkynylaniline-based access to the missing 2,7′:2′,7′′-triindole. *Org. Biomol. Chem.* **2010,** *8* (19), 4243-4245.

Chapter 2 : Syntheses and Functionalization of Eumelanin Monomers

2.1 Introduction

The challenges of controlling the biomimetic oxidative polymerization of **DHI**, the lack of direct evidence of the Kaxiras tetramer (**1-1**), and the need for a strategy to access well-defined eumelanin oligomers beyond a trimer have motivated us to develop an alternative, phased-bottom-up approach to well-defined eumelanin model compounds.

The tyrosinase catalyzed biosynthesis of eumelanin by aerobic oxidation of **DHI** and **DHICA** is seemingly chaotic when placed into comparison with the iterative and enzymatically controlled growth of DNA or polypeptide strands. Although the biosynthesis of **DHI** and **DHICA** from L-tyrosine is initiated by tyrosinase, the ensuing chain growth following oxidation of **DHI** and **DHICA** is not enzymatically controlled. The coupling of these monomers is not regioselective between C2, C4 and C7 (indole numbering), and oxidative chain elongation is likely in competition with oxidative modification of the chain backbone. Finally, chain aggregation adds an additional layer of complexity by creating multi-dimensional networks of redox-active components (Figure 2-1).

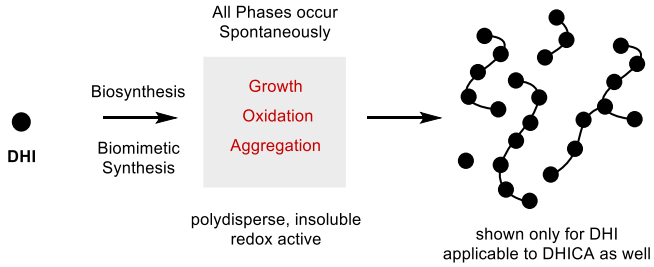

Figure 2-1 Competitive three phases of biosynthesis

We envisioned disentangling the three competitive phases of biosynthesis, namely chain-growth, chain-oxidation, and chain-aggregation when **DHI** is oxidized. More specifically, to prevent chain oxidation in the process of chain growth, we devised a *de novo* synthesis of eumelanin via a bottom-up strategy that relies on a non-biomimetic series C-H functionalization and transition metal-catalyzed cross-coupling reaction of protected 5,6-catechol derivatives to create chains with absolute control over regioselectivity and length. What is lost in efficiency is gained in selectivity (Figure 2-2).

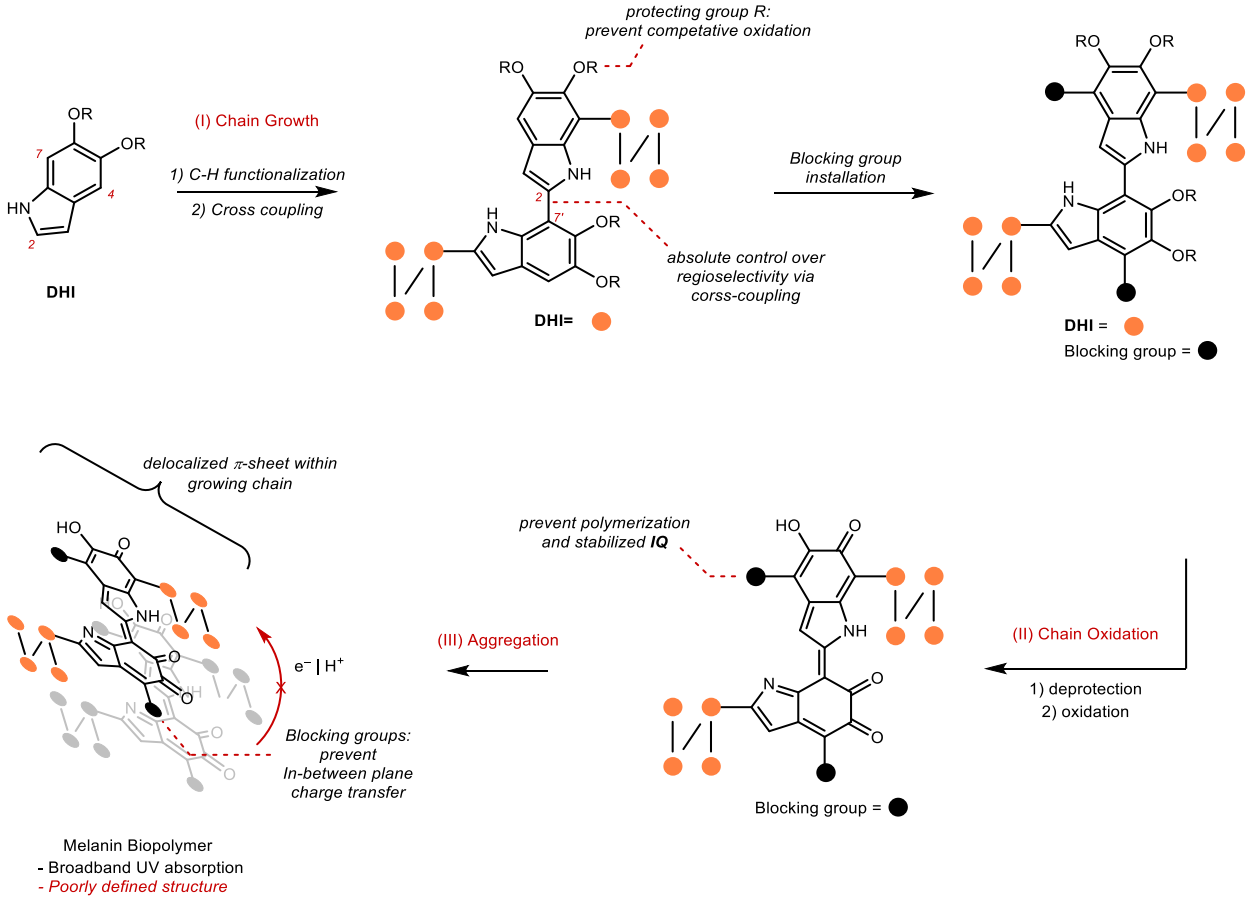

Figure 2-2 Phased-bottom-up strategy to the eumelanin challenge

To decouple chain growth when studying chain oxidation, we proposed installing "blocking groups" at each of the potential sites of chain growth. While 5,6-*ortho*-inodolequinone (**IQ**),[1] oxidized dimer units,[2] or oxidized cyclic tetramer[3, 4] have been implicated as potential intermediates in the process of oxidizing **DHI** to eumelanin pigment, isolation of any of these intermediates has never been achieved, presumably due to their instability and spontaneous polymerization to higher-order subunits of eumelanin. Indeed, all previously isolated eumelanin model compounds are at the catechol oxidation state.[5, 6] The blocking groups would not only prevent polymerization during chain oxidation but also stabilize the oxidized eumelanin derivatives without excessive perturbation of their electronic structure (Figure 2-2). Steric stabilization by 3,5-di-*tert*-butyl groups has demonstrated efficacy in stabilizing catechols and *ortho*-quinones (**OQ**) (e.g. 3,5-di-*t*Bu-**OQ** is stable and commercially available, whereas **OQ** decays rapidly at room temperature), and Jones has shown that the lifetime of 2,3-

naphthoquinone (**2-2**) can be lengthened by incorporating *ortho*-tolyl substituents at C1 and C4 (Scheme 2-1a).[7] Nevertheless, blocking groups have rarely been used to stabilize **IQ** or its higher-order oligomers. One exception was reported by Prota and co-workers in 1996, describing a transient species ($T_{1/2}$ ~5 min) following the oxidation of 2, 3-dimethyl-**DHI** (**2-3**) that was tentatively assigned as 2,3-dimethyl-**IQ** (**2-4**) based upon *in situ* ^{1}H-NMR spectroscopy (Scheme 2-1b).[8]

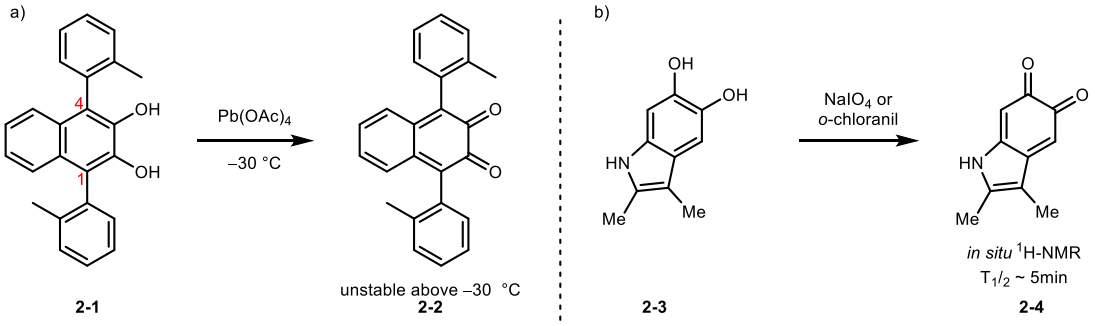

Scheme 2-1 Blocking group stabilization of a) naphthoquinone b) 2,3-methyl-**IQ**

Furthermore, calculations indicate that eumelanin tends to planarize and form aggregates by π-stacking. Short distances between stacked chromophores could lead to orbital-orbital overlap and charge transfer in-between planes, with the possibility of creating covalent bonds and potentially insoluble macromolecules.[4, 9, 10] Therefore, we hypothesized that our blocking group strategy would decouple chain-oxidation from chain-aggregation by providing steric stabilization between eumelanin π-sheets (Figure 2-2).

The successful implementation of our phased-bottom-up strategy required a concise synthesis of polyfunctional indoles with complementary functional handles at sites of chain growth, a technique to extend these building blocks into well-defined chains, and a strategy to install blocking groups and then reveal and manipulate the redox-active polycatechols. Collectively, these form the basis of this thesis.

Outline of Thesis: Our efforts to address these challenges are divided into Chapters 2-4, which provide a phased-bottom-up approach to different eumelanin derivatives with well-defined structures and high purity. In Chapter 2, we will describe the synthesis of 5,6-dihydroxyindole (**DHI**) monomers on synthetically useful scales with differentiated protecting groups on the C5,

C6-catechol, and the subsequent C-H functionalization at C2, C3, C4 and C7 (indole numbering). In Chapter 3, we will focus on chain growth that leverages regioselective C-H functionalization and transition metal-catalyzed cross-coupling to create chains with absolute control over connectivity and length. These efforts culminate in the successful development of a bottom-up iterative synthesis of **DHI**-oligomers up to the stage of a pentamer. In Chapter 4, we detail our attempts to synthesize the Kaxiras cyclic tetramer (**1-1**), a porphyrin-like tetra-indole-quinone, via a macrocyclization of its linear precursor. In addition, we will discuss our efforts to oxidize the cyclic tetramer (**1-1**) and a 2,7'-dimer with blocking groups in order to reveal the theoretically predicted oxidation pattern. Finally, in Chapter 5, we provide conclusions and future directions for the continuation of this research program (Figure 2-3).

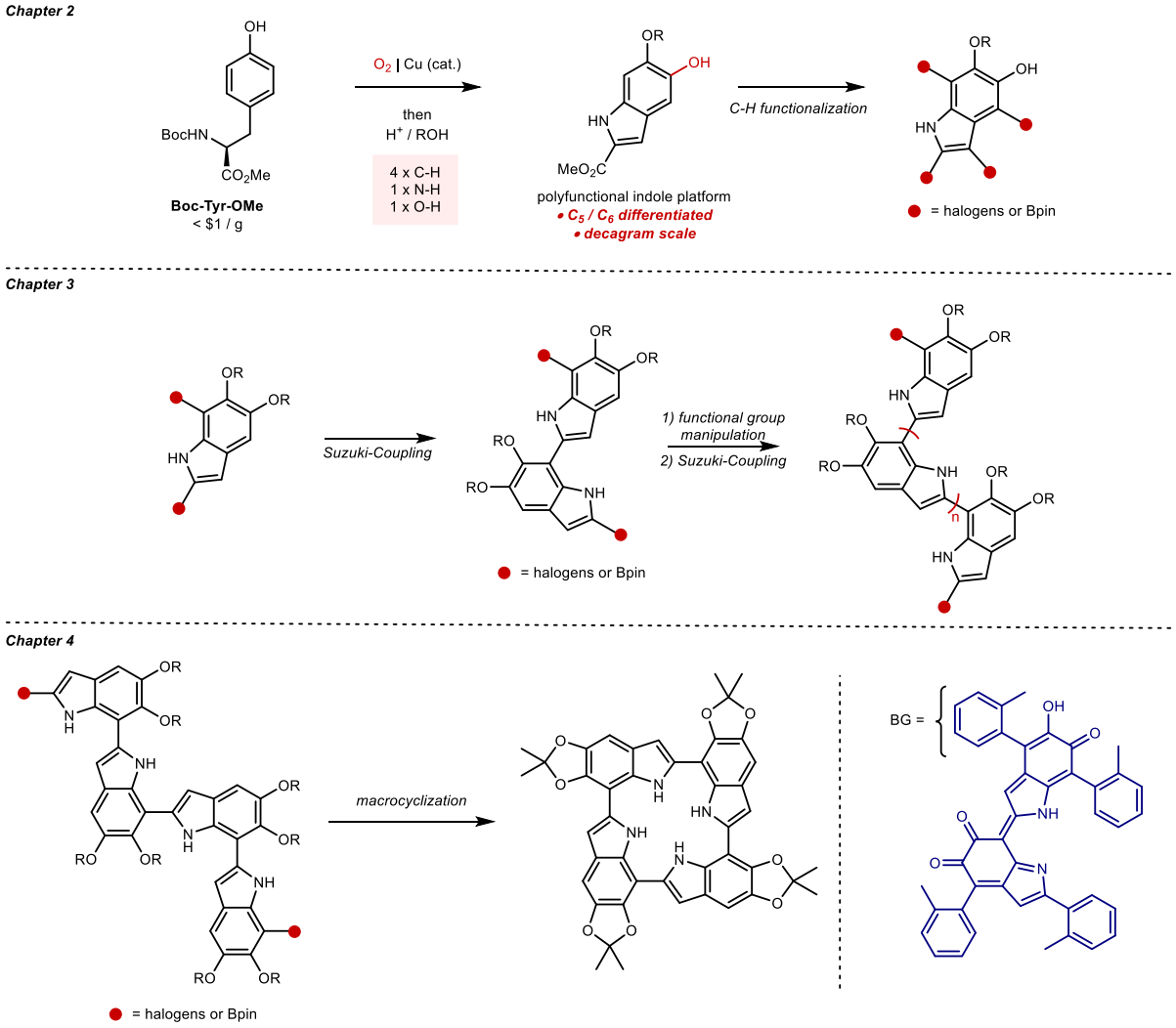

Figure 2-3 Overview of Chapters 2-4

2.2 Bio-inspired Synthesis of Indole Building Blocks:

To investigate our phased-bottom-up approach to eumelanin, we required a gram-scale synthesis of 5,6-dihydroxyindole (**DHI**) and its derivatives that could be used in subsequent cross-coupling reactions for chain growth. We first turned our attention to the biosynthesis of **DHI** and **DHICA** from L-tyrosine (**1-3**) via oxidative cyclization of the corresponding aminophenols, as described in Chapter 1, Scheme 1-1. Biosynthesis provides a highly efficient approach to indoles compared with multistep synthetic approaches based on conventional indole syntheses. Efforts to mimic the early stage of melanogenesis to produce **DHI** and **DHICA** have been reported by Ito and co-workers from L-DOPA (**1-14**) (see Chapter 1, Scheme 1-14).[11] This transformation is limited to milligram quantities and requires the relatively expensive starting material L-DOPA (969 USD/100g). A direct cyclization of L-tyrosine (**1-3**) would offer a more attractive approach to **DHI** and **DHICA** derivatives (L-tyrosine, 99 USD/100g).

At the time of our early studies, the only related examples were oxidative cyclization of tyrosine derivatives to 6-hydroxy-indoline **2-7** using hypervalent iodine from Wipf [12] and Canesi [13] (Scheme 2-2). The limitation of current methodologies and our interests in eumelanin motivated us to develop an efficient, biomimetic synthesis of **DHI** and **DHICA** from L-tyrosine derivatives.

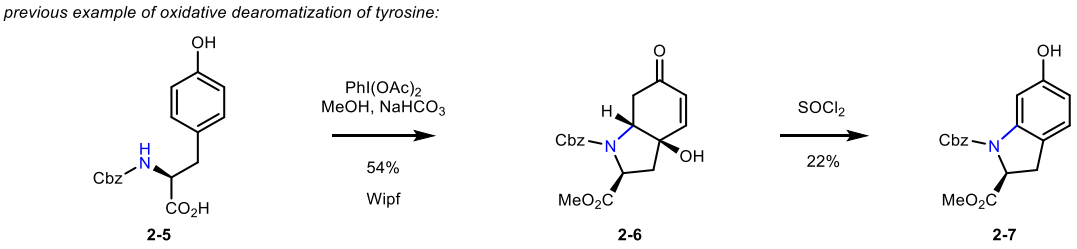

Scheme 2-2 Previous example of oxidative dearomatization of a tyrosine derivative

To this end, we considered our previously developed Cu-catalyzed aerobic oxygenation of phenols to *ortho*-quinones[14] and whether they could be applied to the oxygenative homo-coupling of **2-8** to produce *ortho*-quinone **2-9**. While bioinspired, this process is nevertheless distinct from the 4 e^- | 2 H^+ oxidation catalyzed by tyrosinase, and instead, it undergoes a net 6 e^- | 4 H^+ oxidation process to **2-9**. Notably, **2-9** is at the same oxidation state as both **DHI** and

DHICA (Scheme 2-3), suggesting that a subsequent cyclization to produce these sensitive materials could be conducted under redox neutral conditions. The compartmentalization of the oxidation and the cyclization phases would, in principle, circumvent redox-exchange between catechols and *ortho*-quinones,[15] and produce **DHI** and **DHICA** under non-oxidizing conditions.

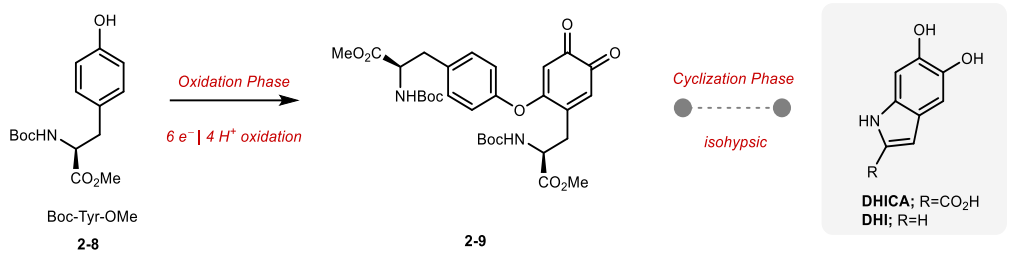

Scheme 2-3 Bio-inspired aerobic oxidation of Boc-Try-OMe

To evaluate our hypothesis, we investigated reaction conditions for the synthesis of homo-coupled *ortho*-quinone (**2-9**) from Boc-Tyr-OMe (**2-8**) under previously developed conditions in our group composed of 4 mol% $[Cu^{I}(CH_3CN)_4](PF_6)$ (abbreviated as $CuPF_6$) and 5 mol% *N,N'*-di-*tert*-butylethylenediamine (DBED) under 1 atm of pure O_2. [14]

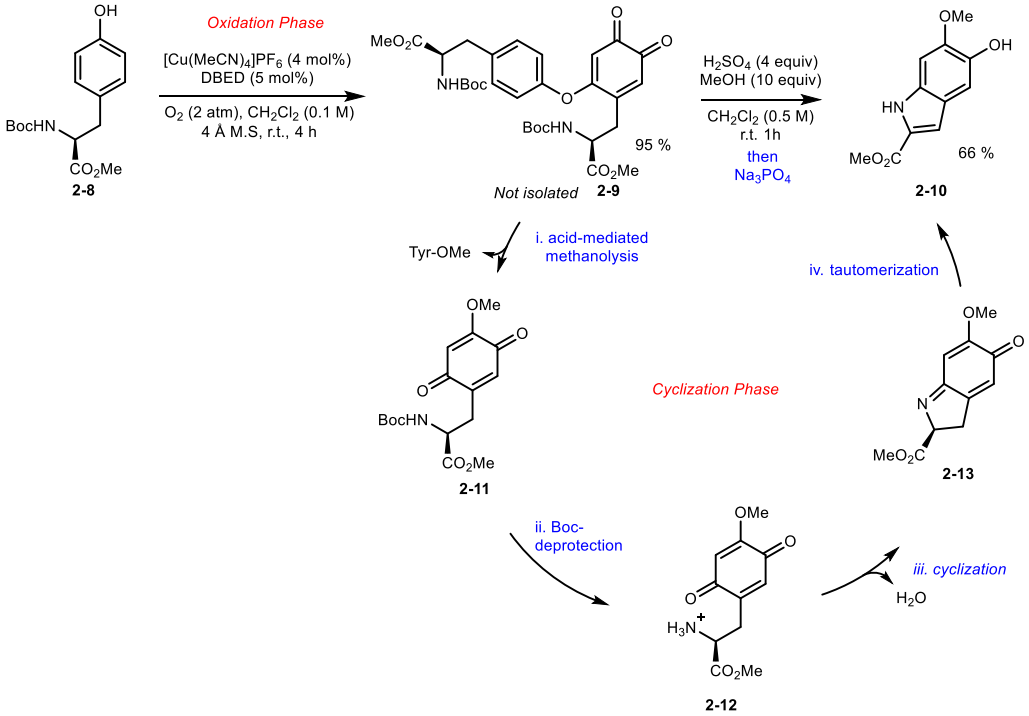

Scheme 2-4 Bio-inspired synthesis of indole from **2-8**

To our delight, **2-9** was obtained in 95 % NMR yield. Subsequent acid-mediated methanolysis followed by cyclization converted **2-9** to indole **2-10** in 66 % yield on a 1 mmol scale (Scheme 2-4). Mechanistically, **2-9** was first converted to **2-11** by exposure to sulfuric acid (H_2SO_4) and MeOH in CH_2Cl_2. Boc deprotection of **2-11** in the presence of H_2SO_4 liberated the ammonium salt **2-12**. Next, cyclization of **2-12** upon adjustment of the pH with saturated aqueous Na_3PO_4 afforded **2-13**, which was converted into indole **2-10** (*Reaction optimizations were conducted by Dr. Zheng Huang and Mr. Ohhyeon Kwon*).

I joined the project with the goal of scaling up this 2-stage operation to 200 mmol scale. To this end, treatment of phenol **2-8** with $CuPF_6$ (4 mol%) and DBED (5 mol%) under O_2 (1 atm) in CH_2Cl_2 in the presence of 4 Å molecular sieves, followed by acidic, aqueous work-up afforded quinone **2-9** as a crude mixture. The key to the setup was to seal a 2L round bottom flask with two septas on top of each other, and to fasten them to the flask with Cu-wire (Figure 2-4). The subsequent open-flask acid-mediated cyclization proceeded smoothly upon treatment of the quinone mixture **2-9** with H_2SO_4 (concentrated, 4 eq.) and MeOH (10 eq.) in CH_2Cl_2 then followed by cyclization upon neutralization with saturated aqueous Na_3PO_4, which produced 12g of **2-10** in a concise 2-stage operation. Collectively, we have prepared more than 100 g of **2-10**, which is a benchtop stable solid. In addition, Boc-Tyr-OMe (**2-8**) can be recovered via *in situ* Boc-protection of **2-14**. This 2-stage approach to indole (**2-10**) does not require sophisticated glassware, the catalyst components are commercially available and inexpensive, and it was completed within hours at room temperature.

Overall, the process functionalizes 4 C-H bonds, 1 N-H bond and the O-H bond of methanol to convert an inexpensive amino-phenol building block into an indole with a methyl ester at C2, a free phenol at C5, and an aryl ether at C6. Importantly, whereas the C2 and C3 positions are inherently nucleophilic, and the C4 and C7 positions are accessible by directing groups, the C5 and C6 positions of indoles are remote, and difficult to differentiate.[16] Our method allows the synthesis of 5,6-differentiated indoles, creating a range of opportunities for directed C-H functionalization reactions to install a halogen or a boronic ester at each of the heterocycle‘s remaining positions (C2, C3, C4, and C7).

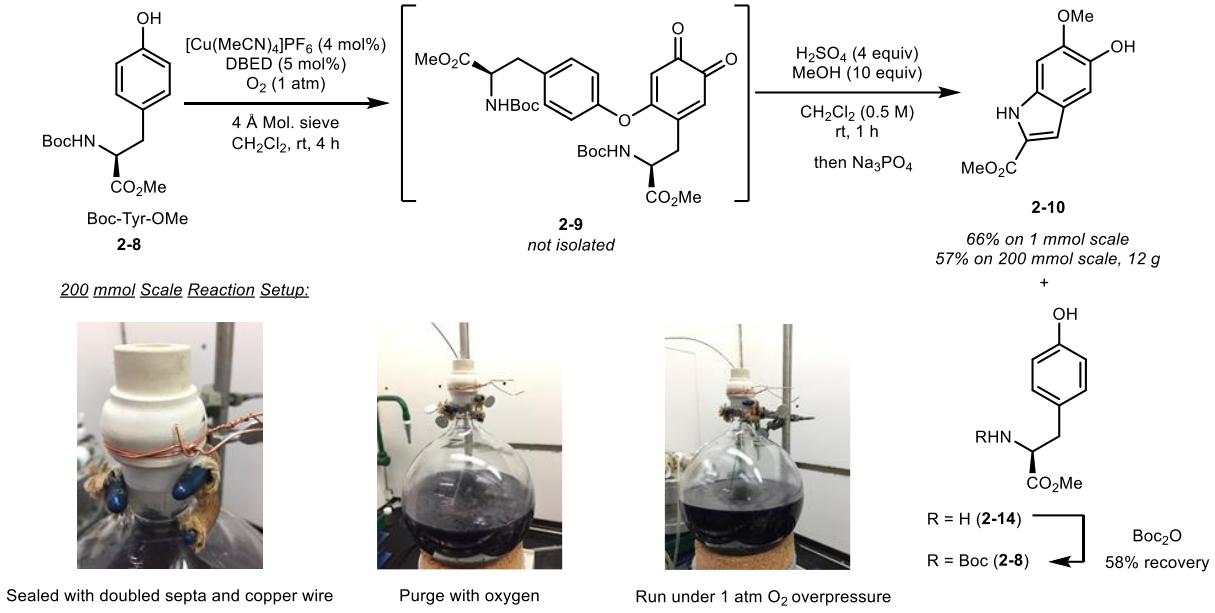

Figure 2-4 Large-scale bio-inspired synthesis of indole from **2-8**

2.3 Polyfunctionalization of 5,6-differentiated Indoles

To create eumelanin chains with absolute control over regioselectivity and length, we set out to investigate suitable conditions for installing functional handles at each of the remaining positions of the indoles (C2, C3, C4, and C7). The types of functional handles we were interested in were boronic esters and halogens as they could undergo transition metal-catalyzed Suzuki-Miyaura coupling to form carbon-carbon bonds with high precision.

2.3.1 Decarboxylative Borylation and Protonation

To synthesize the boronic ester at C2, we initially considered converting the methyl ester to the corresponding carboxylic acid at C2, before exploiting the carboxylic acid as a functional handle for the regiospecific decarboxylative borylation. Decarboxylative borylation on indoles have been demonstrated by Glorius [17] and Fu [18]. In Glorius's work, redox-active ester **2-16a** was converted to indolyl boronate ester **2-17a** under transition metal-free photoinduced conditions with Cs_2CO_3 and B_2Pin_2 in the presence of pyridine (Scheme 2-5a). In Fu's work, an isonicotinate ester catalyzed decarboxylative borylation was reported. NHPI-ester **2-16b** was converted to indolyl boronate ester **2-17b** with isonicotinate *tert*-butyl ester and B_2Pin_2 in $PhCF_3$ at 100 °C (Scheme 2-5b).

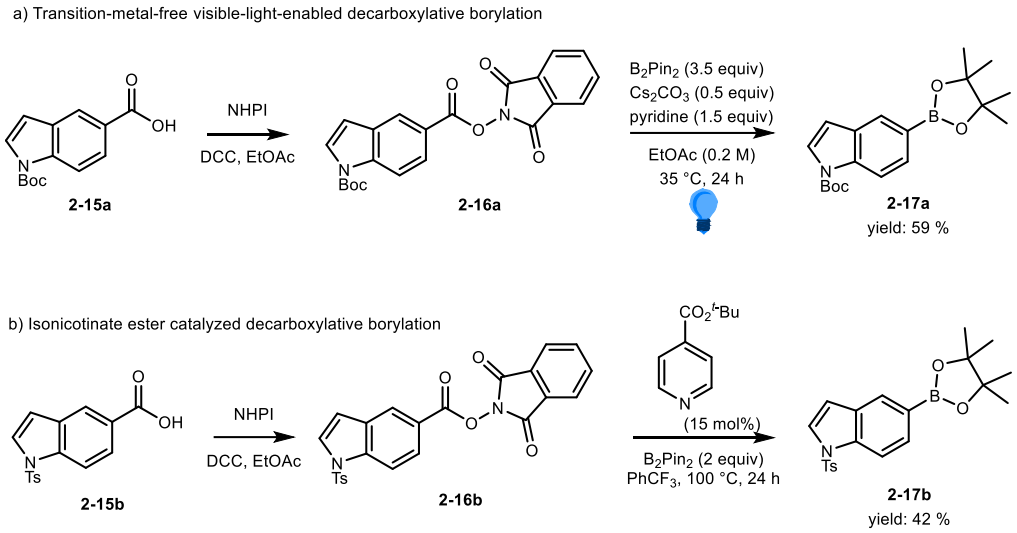

Scheme 2-5 Literature examples of decarboxylative borylation

Implementation of the above-mentioned decarboxylative borylation conditions to our substrate **2-19,** however, proved to be ineffective. **2-19** was obtained via protection of the C5 phenol of **2-10** as a TIPS silyl ether followed by saponification with $LiOH{\cdot}H_2O$ in a mixture of H_2O and THF (Scheme 2-6).

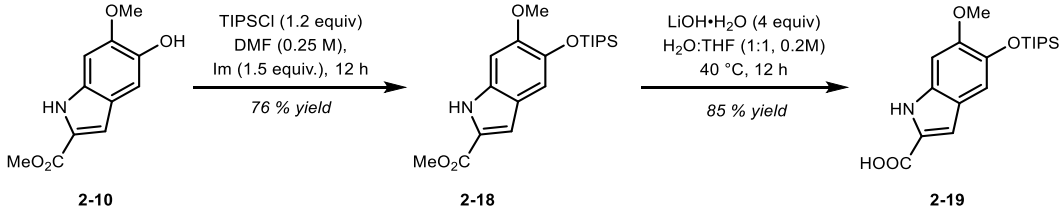

Scheme 2-6 Protection of phenol and saponification

With **2-19** in hand, redox-active ester **2-20** was obtained via coupling of **2-19** and *N*-hydroxyphthalimide (NHPI). Treatment of **2-20** with isonicotinate *tert*-butyl ester (20 mol %) and B_2Pin_2 (2 equiv) in different solvents ($PhCF_3$ or EtOAc) at different reaction times (3 h or 16 h) at 100 °C resulted in less than 5 % conversion of **2-20** and the desired product **2-21** was not observed (Scheme 2-7).

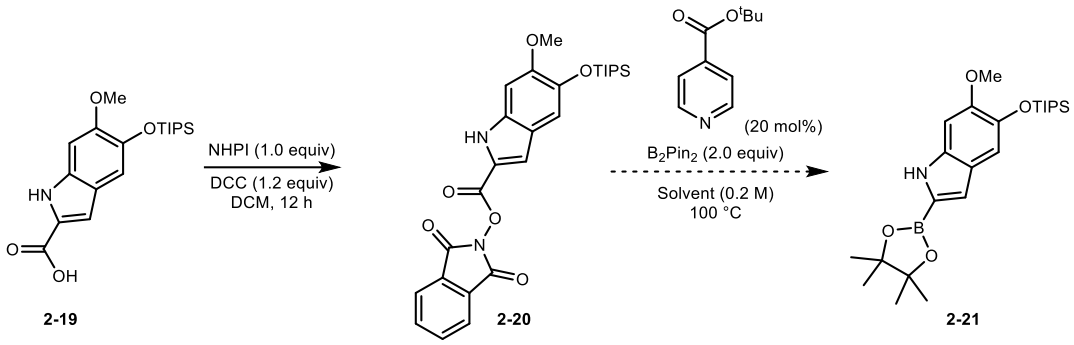

Scheme 2-7 Isonicotinate tert-butyl ester catalyzed decarboxylative borylation

Subjecting **2-20** to Glorius's condition with B_2Pin_2 (3.5 equiv), Cs_2CO_3 (0.5 equiv), and pyridine in EtOAc at room temperature under blue LED, unfortunately, led to a low conversion of **2-20** even with extended reaction time and elevated reaction temperature (Scheme 2-8).

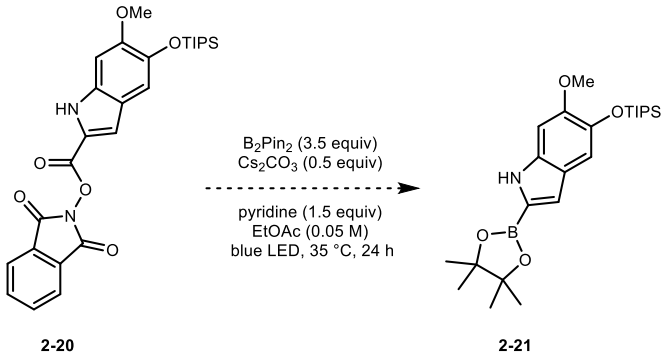

Scheme 2-8 Photoinduced decarboxylative borylation

The challenges of C2-decarboxylative borylation prompted us to consider an alternative approach to C2-borylation, namely protodecarboxylation and then C-H borylation at the C2 position. To this end, we evaluated conditions to remove the carboxylic acid on **2-19** or **2-22**. Treatment of **2-22** with Ag_2CO_3 (10 mol %) at 120 °C (entry 1),[19] led to complete consumption of **2-22** without any discernable products. Similarly, conditions composed of Cu_2O and 1,10-phenanthroline (Phen) in a mixture of *N*-methyl-2-pyrrolidone (NMP) and quinoline resulted in no desired product (entry 2).[20] Considering the possible thermal instability of **2-22**, we then evaluated various conditions on substrate **2-19**, where the C5-phenol was protected as a triisopropyl silyl ether. Although the Cu_2O and Phen conditions failed to provide any product with **2-19** (entry 3), decarboxylation with Cu-carboxylate (**2-24**) in quinoline afforded **2-23** in 85 % yield

(entry 4). [21] Taking a closer look at the potential mechanism,[22] we anticipated the reaction would proceed similarly with other Cu complexes, for example, Cu-carboxylate (**2-25**) or $Cu(OAc)_2 \cdot H_2O$. When subjecting **2-19** to 10 mol % **2-25** (entry 5) or 10 mol % $Cu(OAc)_2 \cdot H_2O$ (entry 6), 83 % and 80 % **2-23** were obtained separately. For the simplicity of operation, we proceeded with $Cu(OAc)_2 \cdot H_2O$ in our synthesis. This reaction can be performed on a gram scale (Table 2-1).

Table 2-1 Condition optimization for protodecarboxylation

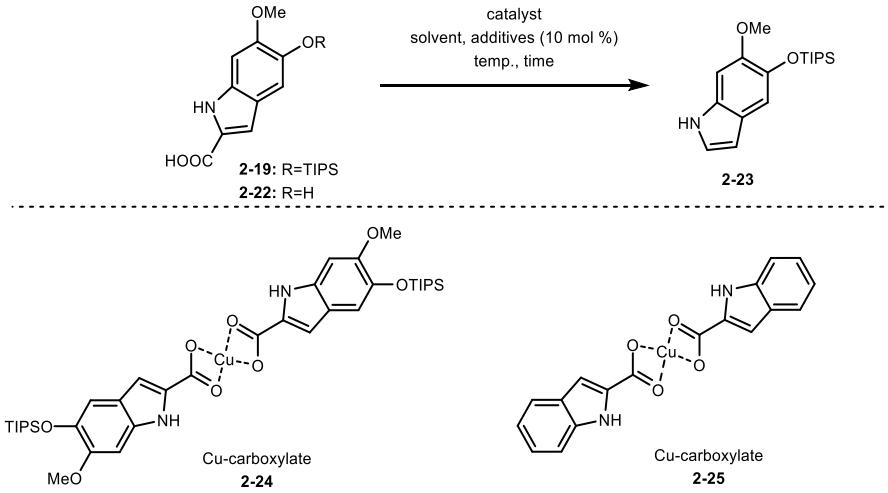

Entry	Substrate	Catalyst	Solvent	Temp (°C)	Time (h)	Additives	Yield (%)
1	**2-22**	Ag_2CO_3 (10 mol%)	DMSO (0.2 M)	120	16	NA	0--
2	**2-22**	Cu_2O (5 mol%)	NMP/quinoline (3:1, 0.5 M)	170	16	Phen	0
3	**2-19**	Cu_2O (5 mol%)	NMP/quinoline (3:1, 0.5 M)	170	16	Phen	0
4[a]	**2-19**	**2-24**	Quinoline (0.12 M)	215	4.5	NA	85
5[a]	**2-19**	**2-25**	Quinoline (0.12 M)	215	4.5	NA	83
6	**2-19**	$Cu(OAc)_2 \cdot H_2O$	Quinoline (0.2 M)	215	4.5	NA	80

a) Cu-carboxylate was made by adding $CuSO_4$ in H_2O to the mixture of carboxylic acid and Na_2CO_3 at 75 °C.

2.3.2 C-H Borylation of 5,6-differentiated Indoles

With decagrams of **2-10** and grams of **2-23** in hand, we investigated conditions for the C-H borylation at each of the remaining positions on the indole core, with the goal of leveraging the innate reactivity of indole, or the directing abilities of the N-H and C5-OH groups. For example, the Ir-catalyzed borylation is selective for C2 to **2-21** when subjecting **2-23** to previously described conditions for C-2 borylation of unsubstituted indole,[23, 24] consisting of $[Ir(COD)(OMe)]_2$ (1.5 mol %), dtbpy (3.0 mol %), and B_2Pin_2 (1.0 equiv), in THF for 1 h. Installing a bulky Boc protecting group on the indole nitrogen (**2-26**) was found to direct the C-H borylation selectively to the C3 position of **2-27** in 80 % yield.[25] Borylation at the C7 position of C2-substituted **2-28** with the C5-OH protected as a TBS ether proceeded smoothly to **2-29** in 84 % yield (Scheme 2-9a).[26] To borylate at C4, silyl ether **2-30** was obtained from the C5-phenol to employ Hartwig's silyl-directed *ortho*-borylation conditions,[27] which provided **2-31** in 93% yield in the presence of the free N-H indole (Scheme 2-9b, C4 borylation was done by Dr. Zheng Huang)

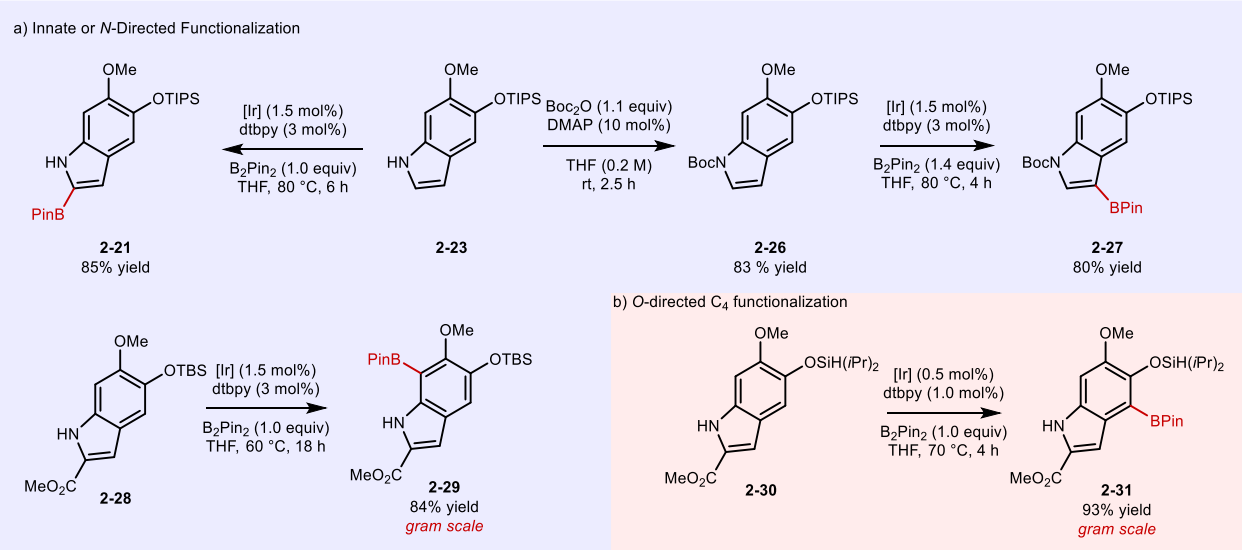

Scheme 2-9 C-H borylation Conditions

$[Ir]=[Ir(COD)(OMe)]_2$

2.3.3 Halogenation of 5,6-differentiated Indoles

Halogenation reactions to install complimentary cross-coupling handles at each of the positions on indoles **2-10** and **2-23** were then explored. For C2 halogenation, we initially considered a direct decarboxylative iodination (I_2, K_3PO_4 in MeCN at 100°C) that was reported by Larrosa and co-

workers. [28, 29] Subjecting **2-19** to I_2, K_3PO_4 in MeCN at 100°C, however, only resulted in a low yield of **2-32** with complete consumption of **2-19.** Protection of the indole nitrogen proved to be critical to the regioselectivity of this reaction as 29 % of C2-iodo indole **2-35** could be obtained along with 61 % **2-36** when indole nitrogen was methylated as **2-34** (Scheme 2-10). However, considering the low yield of **2-35** and the difficulties of removing methyl groups, we did not pursue this reaction further.

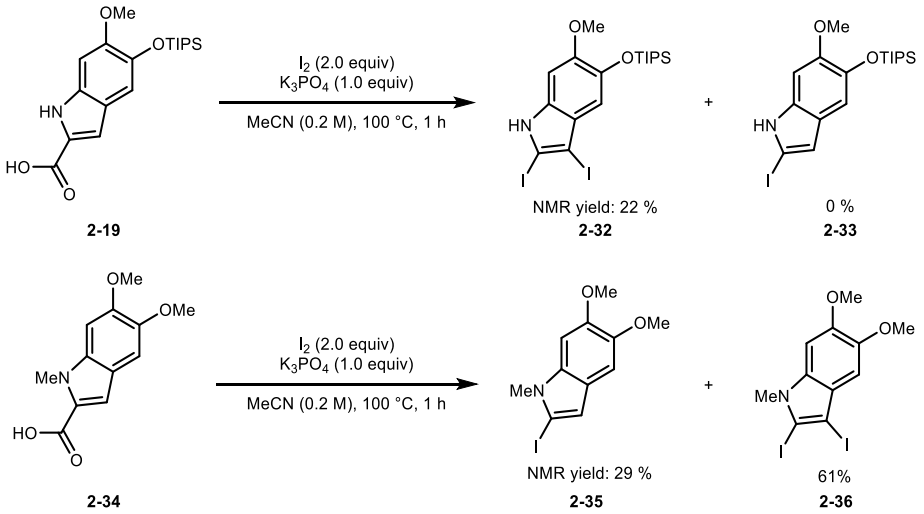

Scheme 2-10 Decarboxylative iodination

Alternatively, C2-halogenation could be accomplished via halodeborylation with CuI (10 mol %), 1,10-phenanthroline (Phen, 20 mol %), and KI (1.5 equiv) in MeOH/H_2O (9:1, 0.05 M),[30] which converted **2-21** to **2-33** in 56 % yield. The C7-iodide **2-37** was readily prepared via iodination of **2-29** with Cu_2O (10 mol%), NH_4OH (28 wt% aq., 2.5 equiv), NaI (2 equiv), in MeOH under an atmosphere of O_2 (balloon) at room temperature.[31] Bromination was selective for C4 when the C5-OH group was free and the nitrogen was protected with a Boc-group (see **2-39**, Scheme 2-11), but it was selective for C3 when the nitrogen was free and the C5-OH was protected as the silyl ether (see **2-40**, Scheme 2-11) (*C4 and C3 bromination were done by Dr. Zheng Huang*).

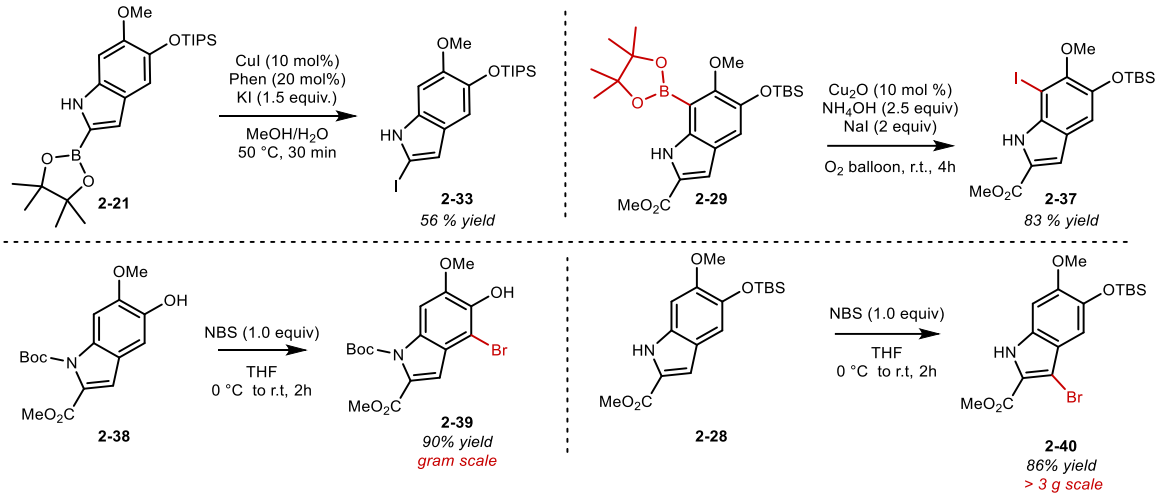

Scheme 2-11 Halogenation at C2, C7, C4, and C3 positions

In summary, we have described an efficient large-scale synthesis of indole **2-10** inspired by the biosynthesis of eumelanin. We have addressed the challenge of C5/C6 differentiation with a uniquely efficient and bio-inspired cyclization of phenethylamino-phenols. The resulting indoles allow us to direct C-H functionalization at each of the heterocycle's remaining positions with complete regiocontrol. Given the power of modern cross-coupling technologies and the prevalence of indoles, these building blocks should serve as attractive starting materials for a range of applications.

2.4 Synthesis of Acetonide Protected Indole

Although the bio-inspired synthesis of indole **2-10** provided an efficient approach to decagrams of indole building blocks and C-H functionalizations at each of the remaining positions have proven to be successful, installing functional handles at the C2 position on **2-10** required decarboxylation under harsh conditions. This created potential challenges for late-stage manipulation of sensitive substrates.

Therefore, we turned our attention to an alternative synthesis of a C2-unsubstituted indole core (**2-45**) based upon the Leimgruber-Batcho indole synthesis.[32] Our synthesis of **2-45** commenced with acetonide protection of 4-methyl-catechol (**2-41**) with 2,2-dimethoxypropane (DMP). The crude mixture of **2-42** was then subjected to nitration using fuming nitric acid in acetic acid, which

resulted in **2-43** in 83 % yield. Condensation of **2-43** with *N,N*-dimethylformamide dimethyl acetal mediated by pyrrolidine provided enamine **2-44**. Finally, indole **2-45** was obtained in 70 % yield via a Raney-Nickel reductive cyclization of **2-44.** This 4-step sequence only required one chromatographic purification, following the last step, and it could be conducted on a decagram scale to provide 10 g of **2-45** in a single pass (Scheme 2-12).

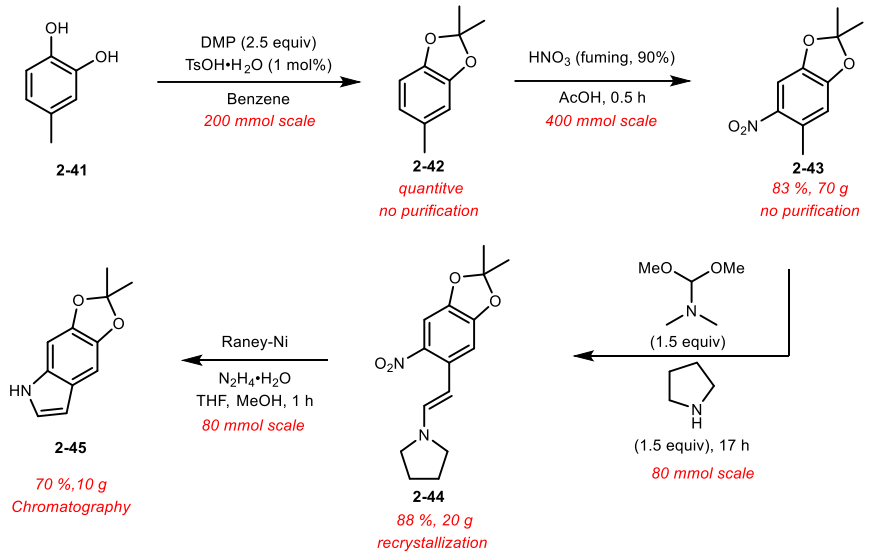

Scheme 2-12 Modified Leimgruber-Batcho indole synthesis

2.5 Polyfunctioanzliation of Acetonide Protected Indoles

To create eumelanin chains with indole **2-45**, we investigated conditions to functionalize **2-45** according to our previous success in functionalizing **2-10**. We focused on the C2 and C7 positions, since this linkage has a long history in the eumelanin literature as a hypothetical site for chain growth. More importantly, it is the desired linkage in the Kaxiras cyclic tetramer.

2.5.1 C-H Borylation of Acetonide Protected Indoles

Our investigation of the C-H borylation of **2-45** evaluated the effects of solvent, temperature, equivalents of B_2Pin_2 and concentration in order to determine if the C2 and C7 positions could be functionalized selectively. Beginning with the [Ir(COD)OMe]$_2$-dtbpy catalyst in THF at room temperature, we observed the formation of **2-46** in 46 % yield with the incomplete conversion of **2-45** (entry 1). Extending reaction time from 2 h to 4 h, afforded both **2-46** and **2-47** in a 1:1 ratio (entry 2). Because starting material **2-45** and products **2-46** and **2-47** are inseparable by column

chromatography, we aimed to find conditions that could provide **2-46** selectively, while also consuming all of **2-45** (Table 2-2).

In an attempt to suppress the formation of **2-47**, we investigated a lower temperature, but, unfortunately, no conversion of **2-45** was observed after 4 h at 0 °C (entry 3). When the solvent was changed to dioxane, we observed that the formation of **2-47** was lower, but this also led to a lower conversion of **2-45** (entry 4). Borylation can be carried out in the presence of an excess of the substrate to B_2Pin_2 to avoid multiple borylations of arenes.[24] To this end, reducing the amount of B_2Pin_2 from 1 equivalent to 0.5 equivalent, although preventing multiple borylations, unfortunately resulted also in a lower conversion of **2-45** (entry 5). At this point, we are still not able to isolate **2-46** in high purity (Table 2-2).

When the solvent was changed to cyclohexane, the reaction delivered a 74 % yield of **2-47** at room temperature (entry 6). It has been demonstrated that borylation reactions are accelerated in nonpolar solvents, such as hexanes, but slowed in a more coordinating solvent. [33] A higher yield of **2-47** and complete conversion of **2-45** was achieved at elevated temperatures in cyclohexane (entry 7). These conditions remain effective on the gram scale, and grams of **2-47** can be obtained in pure form following column chromatography (Table 2-2).

Table 2-2 Condition optimization for C-H borylation

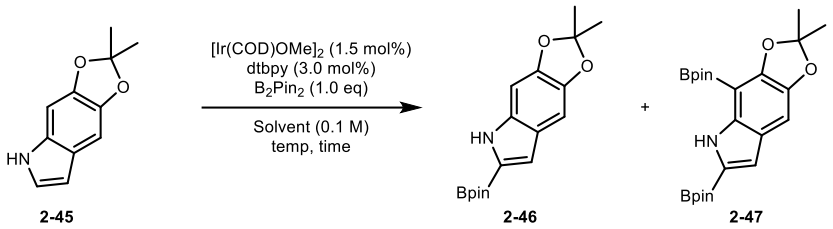

Entry	Solvent	Time (h)	Temp (°C)	B_2Pin_2 (equiv)	Conversion (%)	Yield [a] **2-46/2-47**
1	THF	2	rt	1	65	46/0
2	THF	4	rt	1	90	40/41
3	THF	4	0	1	10	0/0
4	Dioxane	4	rt	1	82	58/16
5	Dioxane	4	rt	0.5	15	13/0
6	CyH	4	rt	1	80	5/74
7	CyH	1	50	2	100	0/[82] [b]

a) Yields were determined by NMR with hexamethylbenzene as the internal standard.
b) Isolated yield in brackets.

Because borylation at C2 is faster than borylation at C7, it is not possible to selectively install a boron group at C7 via direct C-H borylation of **2-45**. Thus, directing groups on the indole nitrogen are usually employed to control regioselectivity to favor C7 over C2. Inspired by Shi [34] and Ingleson,[35] we explored a metal-free directed C-H borylation at the C7 position with a pivaloyl directing group on the indole nitrogen. The regioselectivity was proposed to come from the formation of an intermediate **2-49**, where the boron in BBr_3 coordinates to the carbonyl oxygen to form a six-membered ring with the C7 carbon on indole. Protection of the indole nitrogen of **2-45** with pivaloyl chloride proceeded smoothly to afford **2-48** in 88 % yield. Unfortunately, no discernable products were obtained when **2-48** was subjected to the BBr_3 conditions (Scheme 2-13).

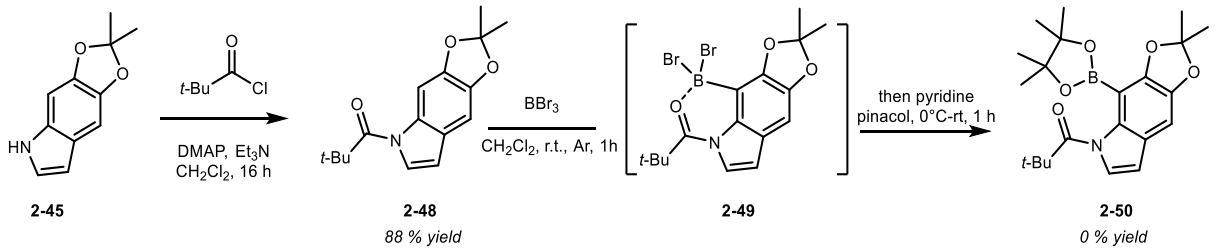

Scheme 2-13 pivaloyl directed C7 borylation

Although site-selective C-H borylation can be efficiently achieved with the assistance of other directing groups, most of them are difficult to remove or modify, thus limiting the practical application of this methodology. To address this issue, we anticipated installing a silyl blocking group at C2 of indole **2-45**, with the goal of using the indole nitrogen to subsequently direct borylation to C7 selectively.[26, 36]

To test our hypothesis, we investigated transition-metal-catalyzed carbon-hydrogen (C-H) silylation conditions, using iridium complexes in the presence of excess hydrogen acceptors without directing/protecting group on the indole nitrogen, as developed by Falck[24] and Takai[25] independently. The desired product **2-51a** was obtained in 10 % yield when 2-norbornene was used as a hydrogen acceptor (entry 1). Changing the hydrogen acceptor to 3,3-dimethyl-1-butene did not improve the yield of **2-51a**. (Table 2-3).

Table 2-3 Direct C-H silylation of **2-45**

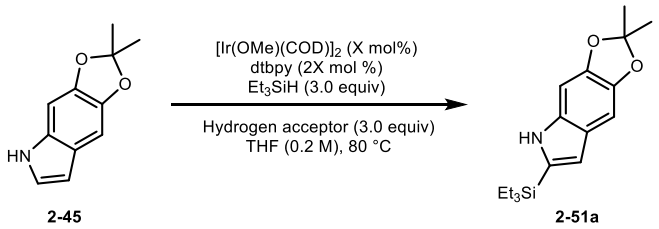

2-45 **2-51a**

Entry	Hydrogen acceptors	$[Ir(OMe)(COD)]_2$ (mol %)	dtbpy (mol %)	Conversion (%)	Yield (%)
1		5.0	10.0	81	18
2		2.5	5.0	70	8

To obtain a better yield of **2-51a**, an alternative method via a potassium *tert*-butoxide catalyzed direct silylation of aromatic heterocycles with hydrosilanes that was developed by Stoltz, Grubbs and co-workers[37] was also attempted. Although C2 silylation has been demonstrated successfully on *N*-substituted indoles in their work (Scheme 2-14a), this condition proved to be ineffective on our substrate. The reaction proceeded with less than 10 % conversion of **2-52** and the desired product **2-51b** was not observed (Scheme 2-14b).

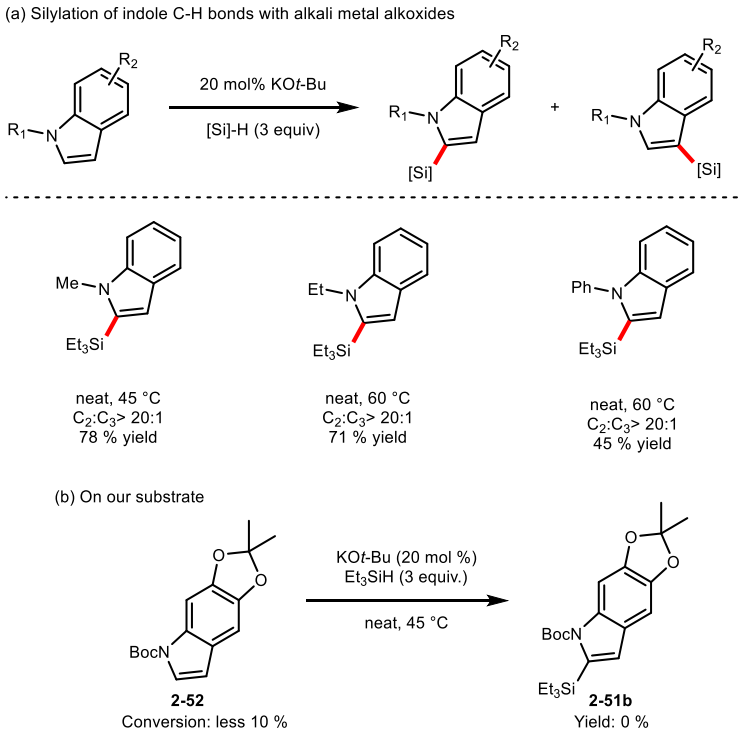

Scheme 2-14 Potassium *tert*-butoxide catalyzed direct silylation

The challenge of direct C-H silylation prompted us to consider another approach to install the silyl group at the C2 position. Snieckus and co-workers have demonstrated that a carbonyl-directed lithiation can be used to activate the C2 position, and that the resulting lithium anion can be trapped by a suitable silicon electrophile. For example, directed *ortho* metalation (DoM) to C2 has been accomplished with Boc, SO_2Ph, $CONR_2$ (R=Et, *i*-Pr, Ph, pyrrolidinyl) groups on nitrogen. Considering the feasibility of installing and removing a *tert*-butyloxycarbonyl (Boc) group and its tolerance to downstream transformations, we chose the Boc group as an indole nitrogen protecting group. Boc protection of **2-45** afforded **2-52** in 90 % yield. Subsequent C2 lithiation via directed DoM using lithium diisopropylamide (LDA) in THF at −78 °C afforded **2-53** in situ, which was then treated with trimethylsilyl chloride (TMSCl) to afford **2-54** following work-up (Scheme 2-15). Notably, LDA outperformed other lithium bases, including *n*-BuLi, *s*-BuLi, and *s*-BuLi with TMEDA.

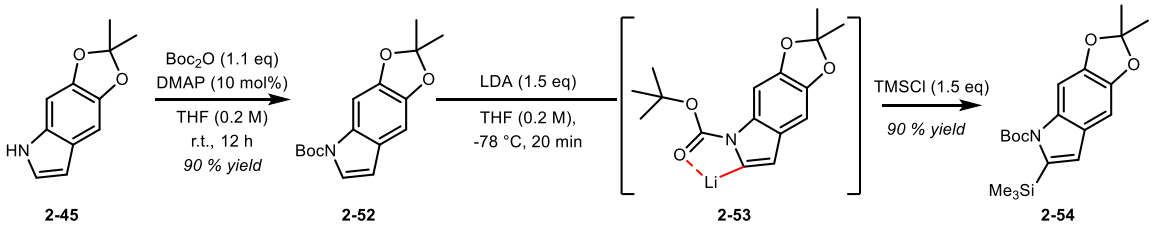

Scheme 2-15 Directed ortho metalation/silylation

With decagrams of **2-54** in hand, we considered two pathways for the C-B bond construction at the C7 position. In pathway A, we envisioned the carbonyl of the Boc group and the oxygen at C6 of the indole directing lithiation to the C7 position, as shown in intermediate **2-55**, which would then be treated with a boron electrophile to afford **2-56a** (Scheme 2-16, Pathway A). In pathway B, we anticipated an N-Boc deprotection to **2-57** followed by a N-H directed C-7 borylation sequence would generate **2-56b** (Scheme 2-16, Pathway B).

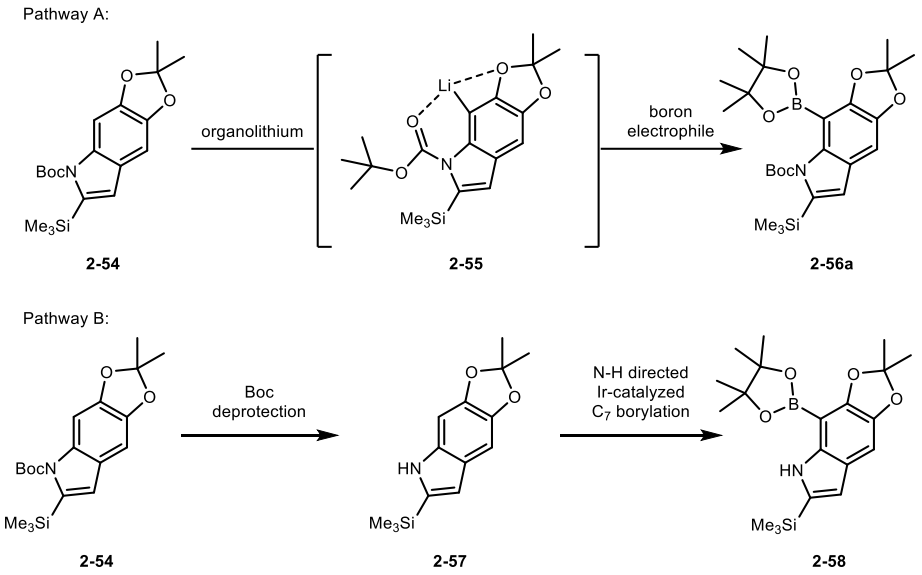

Scheme 2-16 two pathways to C7-borylation

To probe the feasibility of pathway A, we subjected **2-54** to organolithium reagents at −78 °C, followed by the addition of electrophiles. The addition of isopropoxy tetramethyl dioxaborolane as a boron electrophile afforded a low conversion of **2-54** and a low yield of **2-56a** (entry 1), which was not sufficient to confirm the regioselectivity of lithiation/borylation.

Table 2-4 Directed metalation/C7-borylation

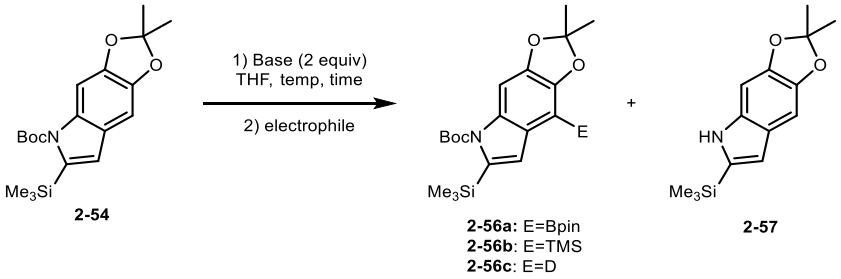

Entry	Electrophile (equiv)	Base	Time (h)	Temp (° C)	Conversion (%)	Yield [b] **2-56/2-57** (%)
1	Isopropoxy tetramethyl dioxaborolane (2.0)	LDA	1	−78	30	8/0
2	TMSCl (1.5)	LDA	7	0	73	70/0
3 [a]	MeOD (excess)	*s*-BuLi	7	−78 to 0	36	22/12

a) Deuterium incorporation was observed for proton at C4 position (6.82 ppm).

b) Yields were determined by NMR with hexamethylbenzene as the internal standard.

Luckily, we observed the formation of 70 % bis-silylated **2-56b** when changing the electrophile to TMSCl (entry 2). When using MeOD as an electrophile, we observed 22 % deuterium incorporation for the proton with a resonance at 6.82 ppm along with 12 % **2-57** (entry 3, Table 2-4). **2-56b** and **2-56c** provided enough material to confirm the regioselectivity of lithiation of **2-54.**

To our surprise, 2D NMR analysis showed that silylation occurred at C4 instead of C7. The key signal is a nOe between the Boc *t-butyl* proton (H_C) and the C7 proton H_B at 7.43 ppm in structure **2-59**. This should not be seen if the silylation was on the C7 position as structure **2-56b** (Figure 2-5).

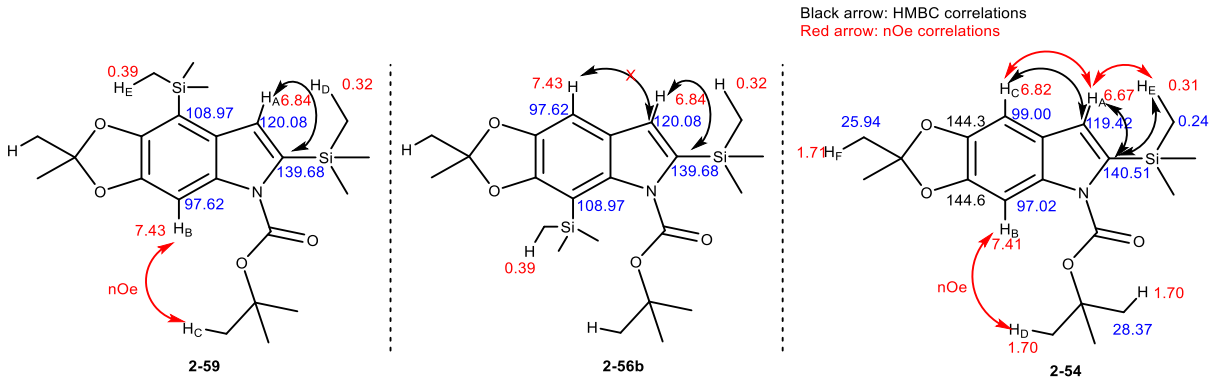

Figure 2-5 NMR analysis of lithiation regioselectivity

In addition, HMBC signals for **2-54** showed that the proton at 0.31 ppm (H_E) correlates with the C2 carbon at 140.51 ppm, which only sees aromatic proton H_A at 6.67 ppm. This confirms the C3 proton is at 6.67 ppm. Based on HSQC signals, the C3 proton H_A (6.67 ppm) is on the C3 carbon at 119.42 ppm, which correlates with the proton at 6.82 ppm. In addition, 1D nOe showed a correlation between the C3 proton H_A and a proton at 6.82 ppm. Moreover, proton H_D on Boc (1.70 ppm) sees proton H_B at 7.41 ppm but not the proton at 6.82 ppm (Figure 2-5). Collectively, this confirms the proton at 6.82 ppm is indeed the C4 proton H_C and lithiation on **2-54** occurred at the C4 position instead of C7. Pathway A was, therefore, proved to be ineffective to access C7-functionalized indoles.

To study the viability of pathway B, we examined conditions for the removal of the Boc group (Table 2-5). Heating a neat sample of **2-54** to 180 °C [38, 39] did not result in the formation of **2-57** (entry 1). Absorbing **2-54** onto silica gel followed by gentle heating under reduced pressure[40] led to 90 % **2-45**, in which Boc deprotection and protodesilyation occurred simultaneously (entry 2). Treatment of **2-54** with TMSOTf and 2,6-lutidine at different temperatures[41] resulted in no conversion of **2-54** (entries 3 and 4). When **2-54** was heated to 140 °C in xylenes,[42] a 15 % conversion of **2-54** and 10 % of **2-57** was obtained (entry 5). Finally, we observed a 57 % yield of **2-57** when **2-54** was warmed to 140 ° in DMF for 5 h.[43] Extended reaction time led to a higher yield of protodesilylation **2-45**. Although the yield of **2-57** is only 57%, the mass balance is 92 %. The remaining **2-54** can be recovered and treated to the reaction condition again to obtain a higher yield of **2-57**.

Table 2-5 Condition optimization for Boc deprotection

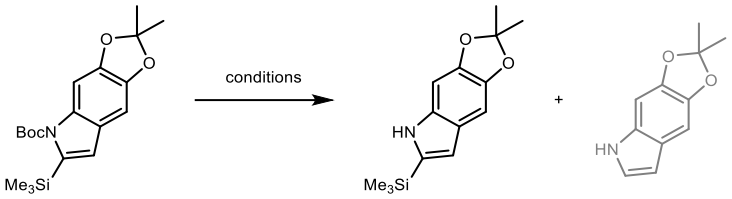

2-54 **2-57** **2-45**

Entry	Condition	Temp (°C)	Time	Conversion (%)	Yield (%) **2-57**/**2-45**
1	neat	180	10 min	0	0/0
2	Silica gel, vacuum	50	12 h	100	0/90
3	TMSOTf, 2,6-lutidine	−5 to 0	6	0	0/0
4	TMSOTf, 2,6-lutidine	r.t. to 40	8	0	0/0
5	Xylene (0.05 M)	140	4.5 h	15	10/0
6	DMF (0.2 M)	140	5 h	65	57/3

With **2-57** in hand, we then explored N-H directed C7 borylation. Solvent effects were evaluated and are summarized in Table 2-6. Using cyclopentyl methyl ether (CPME) as a solvent, the reaction proceeded with 60 % conversion of **2-57** and afforded **2-58** in 56 % yield (entry 1). Extending the reaction time to 4 h led to a 95 % conversion of **2-57** and a 70 % yield of **2-58** (entry 2). Further extending the reaction time to 14 h, however, resulted in a 34 % yield of **2-58**. This is due presumably to over-borylation at both C4 and C7 positions in prolonged reaction times (entry 3). When the reaction was performed in THF (entry 4) or in methyl tert-butyl ether (MTBE) (entry

5), we did not observe an improvement of the yield of **2-58** within 1 h. To our delight, when the reaction was performed in cyclohexane, it proceeded smoothly to **2-58** with an 83 % yield (entry 6).

Table 2-6 Condition optimization for N-H directed C7 borylation

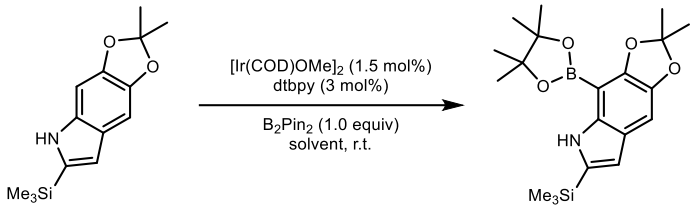

2-57 **2-58**

Entry	Solvent	Conversion (%)	Time (h)	Yield (%)
1	CPME	60	1	56
2	CPME	95	4	70
3	CPME	78	14	34
4	THF	67	1	46
5	MTBE	85	1	58
6	CyH	100	1	83

2.5.2 Halogenation of Acetonide Protected Indoles

Halogenations at the C2 and C7 positions of indole **2-45** were then explored. For C7 halogenation, we have demonstrated that the C7-iodide **2-37** was readily prepared by iodination of **2-29** with Cu_2O (10 mol%), NH_4OH (28 wt% aq., 2.5 equiv), and NaI (2 equiv) in MeOH under an O_2 balloon at room temperature (Scheme 2-17).[31] However, implementing these conditions on monomer **2-58** failed to provide a consistent yield of **2-60** when running the reaction on a larger scale. The reaction provided 72 % **2-60** on 0.2 mmol, but the yield dropped to 40 % on 1 mmol.

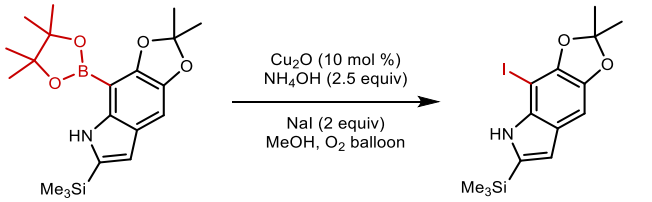

2-58 **2-60**

scale: 0.2 mmol, yield: 72 %
scale: 1.0 mmol, yield: 40 %

Scheme 2-17 Cu_2O-catalyzed C7-iodination

To address this issue, we turned our attention to CuI-catalyzed halogenation of aryl boronates developed by Hartwig and co-workers.[30] Our optimization of the C-7 borylation of **2-58** evaluated the effects of ligands, O_2 concentration, addition sequence, and reaction time (Table 2-7).

Treatment of **2-58** with CuI (10 mol%), phenanthroline (Phen, 20 mol %), and KI in the air led to a 58 % yield of **2-60** along with an 11% yield of by-product **2-57**, which forms by concomitant protodeborylation (entry 1). At an applied pressure of 50 bar O_2, selectivity for **2-60** increased to 75 % (entry 2). Premixing catalyst, ligand, KI, and solvent before slow addition of **2-58** led to slight decreases in the observed yields of both **2-60** and **2-57**. The reaction conducted with other bidentate nitrogen ligands resulted in either decreased yields of **2-62** and increased yields of **2-57** (entries 6-7), or no production of **2-60** (entries 5 and 8). A notable exception was the performance of 3,4,7,8-tetramethyl-1,10-phenanthroline (tmphen) (entry 4), which led to the formation of **2-60** in 73 % yield. Performing this reaction with tmphen as a ligand on a larger scale, however, led to a lower yield of **2-60** (entry 9). In contrast, reactions with Phen afforded consistently high yields of **2-60** on larger scales up to 1 gram (entry 10)(Table 2-7).

Table 2-7 Condition optimization for C7-iododeborylation

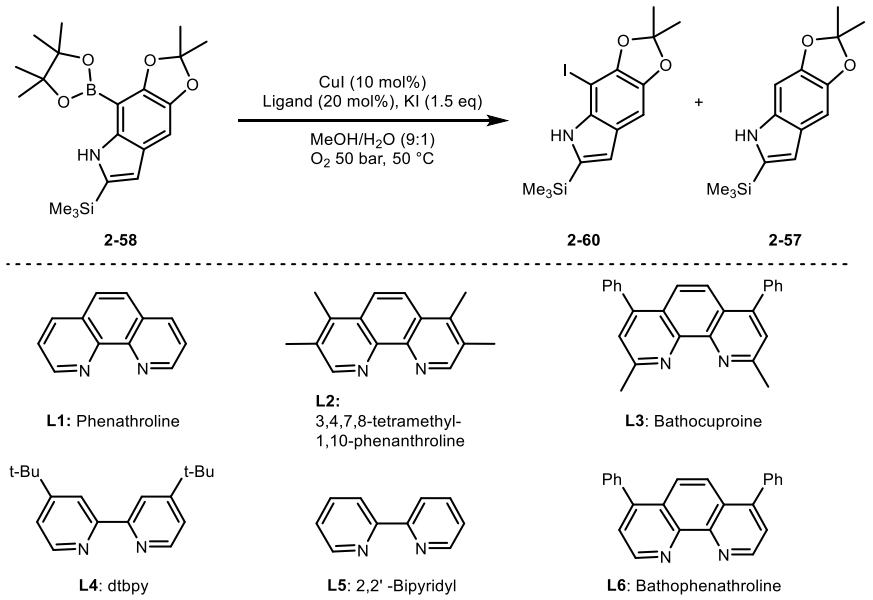

Entry	Ligand	Scale (mmol)	Concentration (M)	Conversion (%)	Time (min)	Yield [a] **2-60/2-57** (%)
1[b]	L1	0.2	0.05	100	60	58/25
2	L1	0.2	0.05	100	35	75/12
3[c]	L1	0.2	0.05	100	35	69/10
4	L2	0.2	0.05	100	40	73/8
5	L3	0.2	0.05	28	60	0/0
6	L4	0.2	0.05	100	30	54/29
7	L5	0.1	0.05	100	30	64/20
8	L6	0.1	0.05	33	30	0/13
9	L2	1.0	0.1	100	30	60/6
10	L1	4.0	0.1	100	60	71/5

a) Yields were determined by NMR with hexamethylbenzene as an internal standard.

b) Entry 1: the reaction was running under air instead of O_2

c) Entry 3: Addition of catalyst, ligand, KI and solvent first. Then dropwise substrate in MeOH into the reaction. For all the other entries, the addition of all the solid reagents first then followed by the addition of solvent.

In addition to C7-iodination, we also attempted the bromination and chlorination of **2-58** under conditions that were developed by Hartwig and co-workers[44] that employ stoichiometric amounts of $CuBr_2$/$CuCl_2$. Treatment of **2-58** with $CuBr_2$ (3 equiv) in MeOH and H_2O at 80 °C for 1 h resulted in 20 % of **2-61**. When changing the halogenation reagent to $CuCl_2$ (3 equiv), **2-58** was converted to **2-62** in 47 % yield (Scheme 2-18). We did not pursue this transformation further as bromination and chlorination were lower in yield compared with iodination, and the silyl groups at the C2 positions were lost in both cases.

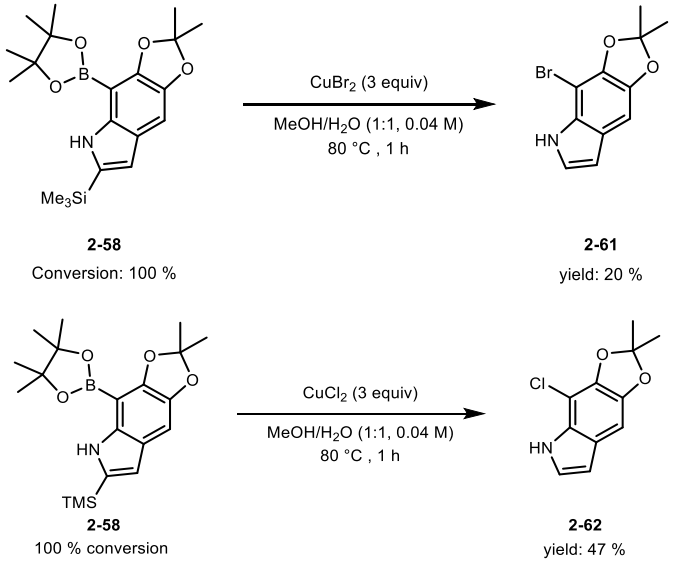

Scheme 2-18 Bromination and chlorination of **2-58**

For C2 halogenation, applying the optimized iododeborylation conditions (20 mol % CuI, 40 mol % Phen, 10 equiv KI, and O_2) to **2-47** resulted in 35 % 2,7-bisiodoindole **2-63**. We did not observe selective C2 iodination **2-65**, and the byproduct was tentatively identified as C2-protodeborylation **2-64** (Scheme 2-19).

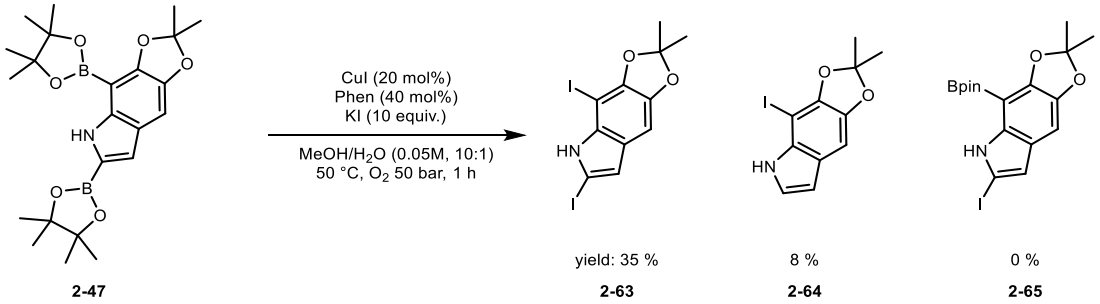

Scheme 2-19 Selective iododeborylation attempts

All attempts to purify reaction mixtures containing **2-63** were unsuccessful. While encouraging, we did not pursue the synthesis of **2-63** from **2-47** further, since the downstream Suzuki-coupling with **2-58** soon proved to be ineffective (see Chapter 4, Section 4.2, Table 4-1).

To address the issue of C2-selective iodination, we investigated two alternative approaches, including the iododesilylation approach and the directed metalation/iodination approach. Firstly, we explored iododesilylation conditions (Table 2-8). Treatment of **2-57** with ICl and $AgBF_4$ in DCM and MeOH for 2 h resulted in complete consumption of **2-57**. However, we did not observe any discernible products (entry 1). Changing the substrate to Boc-protected **2-54**, we observed the formation of 13 % of **2-67** under the same conditions as entry 1 (entry 2). Treatment of **2-54** with NIS in CH_2Cl_2 for an hour afforded **2-67** in 3 %. To our delight, extending the reaction time from 1 h to 23 h using NIS afforded **2-67** in 46 % yield.

Table 2-8 iododesilylation condition

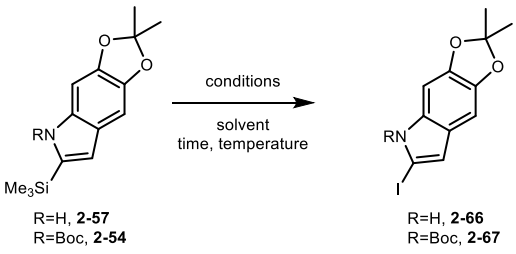

Entry	R	Conditions	Time (h)	Conversion (%)	Yield [a] (%)
1	H	ICl (1.3 equiv), $AgBF_4$ (1.1 equiv) CH_2Cl_2:MeOH (1:1, 0.1 M), 0 °C to r.t. 2 h	2	100	0
2	Boc	ICl (1.3 equiv), $AgBF_4$ (1.1 equiv) CH_2Cl_2:MeOH (1:1, 0.1 M), 0 °C to r.t., 2 h	2	100	13
3	Boc	NIS (1.2 equiv), CH_2Cl_2 (0.14 M), 0°C	1	23	3
4	Boc	NIS (1.2 equiv), CH_2Cl_2 (0.14 M), 0°C to r.t	23	80	46

a) Yields were determined by NMR with hexamethylbenzene as an internal standard.

Alternatively, we investigated the directed metalation/iodination approach to synthesize C2-iodoindole (Table 2-9). Subjecting **2-52** to a mixture of *s*-BuLi/TMEDA at −78 °C for 1 h followed by the addition of 1,2-diiodoethane afforded a 38 % yield of **2-67** after gradually warming the reaction mixture to room temperature over 6 h (entry 1). Increasing the number of equivalents of *s*-BuLi, TMEDA, 1,2-diiodoethane, as well as the reaction time (17 h), led to increased consumption of **2-52** to 85 %, but led to a lower yield of **2-67** in 23 % yield (entry 2). When performing the reaction at a lower temperature (−78 to −41 °C) and shorter reaction time (5 h), we obtained a 51% yield of **2-67** cleanly (entry 3). Similarly, the reaction provided a 56 % yield of **2-67** when TMEDA was omitted (entry 4). When changing the base to LDA, to our delight, 75 % of **2-67** was obtained cleanly at −78 °C (entry 5). Increasing the equivalent of LDA, and 1,2-diiodoethane led to a lower yield of **2-67** although the conversion of **2-52** was improved to 95 % (entry 6).

Table 2-9 Condition optimization for C2 metalation/iodination

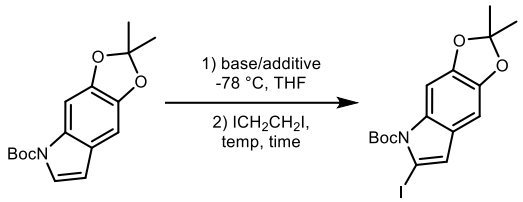

2-52 **2-67**

Entry	Base (equiv)	TMEDA (equiv)	ICH_2CH_2I (equiv)	Time (h)	Temp (°C)	Consumption of **2-52** (%)	Yield [a] of **2-67** (%)
1	*s*-BuLi (1.5)	1.5	3.0	6	−78 to rt	55	38
2	*s*-BuLi (2.5)	2.5	5.0	17	−78 to rt	85	23
3	*s*-BuLi (2.5)	2.5	5.0	5	−78 to −41	57	51
4	*s*-BuLi (2.5)	0	5.0	1	−78	76	56
5	LDA (1.5)	0	2.0	1	−78	78	75
6	LDA (2.0)	0	5.0	1	−78	95	65

a) Yields were determined by NMR with hexamethylbenzene as an internal standard.

2.6 Conclusion

In summary, we have developed a concise synthesis of polyfunctional indoles with complementary functional handles at sites of chain growth. The bio-inspired synthesis of indole from inexpensive aminophenols provided a concise decagram scale synthesis of indole building block **2-10**. Modified Leimgruber-Batcho indole synthesis afforded decagram quantities of C2-unsubstituted indole **2-45**. Collectively, these two building blocks (**2-10** and **2-45**) allowed for C-H functionalization reactions to install halogens or boronic esters at each of the heterocycles' remaining positions (C2, C3, C4 and C7).

Relying on the innate reactivity of indole, as well as the directing abilities of the N-H and the C5-OH, we have demonstrated successful regioselective borylation (Scheme 2-20).

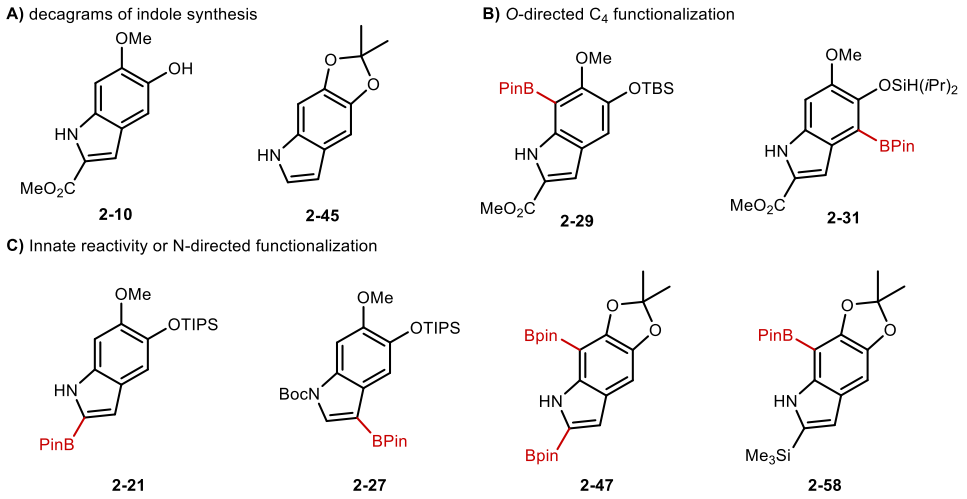

Scheme 2-20 Decagram indoles and borylated indole building blocks

Halogenation via halodeborylation, NBS bromination, or directed *ortho* metalation/iodination provided a library of indole building blocks with halogen functional handles (Scheme 2-21). This collection of functionalized building blocks creates a range of opportunities for Suzuki-coupling reactions to extend monomers into well-defined chains.

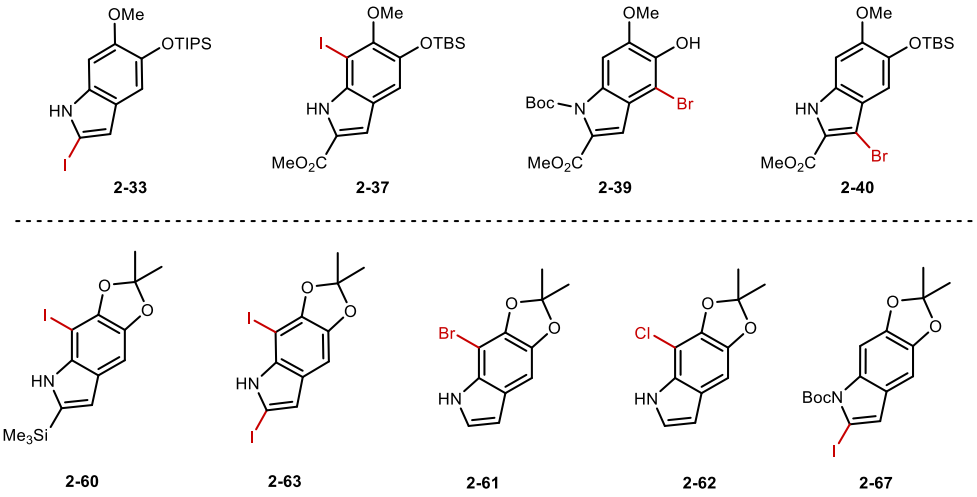

Scheme 2-21 Halogenated indole building blocks

2.7 Experimental Section

Materials and Methodologies:

Chemicals and solvents were purchased from Sigma Aldrich, Alfa Aesar, Strem Chemicals, TCI or Oakwood, and used as received without further purification. $[Cu(CH_3CN)_4](PF_6)$ (99.99%) was purchased from Sigma Aldrich, and stored under an inert atmosphere. Sulfuric acid (95-98 wt%) was purchased either from Sigma Aldrich (99.99% pure) or ACP chemical (lab grade), and no substantiate difference in performance was observed. Solvents were dried and purified using a PureSolv MD 7 (from Innovative Technology) or MB SPS 800 (from MBraun). We have not observed differences in the reaction outcome using either of these solvent purifiers. Cyclohexane was distilled over CaH_2 under N_2. Molecular sieves (4 Å, powdered and "activated") were purchased from Sigma Aldrich and were flame-dried with a torch in the reaction vessel under vacuum prior to use.

Proton nuclear magnetic resonance (^{1}H NMR) spectra were acquired using Varian Mercury 400 MHz, Varian Inova QANUC 500 MHz, Varian VNMRS 500 MHz, Bruker AVIIIHD 500 MHz, or Bruker AVIIIHD 400 MHz spectrometers. Chemical shifts (δ) are reported in parts per million (ppm) and are calibrated to the residual solvent peak. Coupling constants (*J*) are reported in Hz. Multiplicities are reported using the following abbreviations: *s* = singlet; *brs*=broad singlet; *d* = doublet; *t* = triplet; *q* = quartet; *m* = multiplet (range of multiplet is given). Carbon nuclear magnetic resonance (^{13}C NMR) spectra were acquired using Varian VNMRS 125 MHz, Bruker AVIIIHD 125 MHz, or Bruker AVIIIHD 101 MHz spectrometers. Chemical shifts (δ) are reported in parts per million (ppm) and are calibrated to the residual solvent peak. High resolution mass spectra (HRMS) were recorded using a Bruker maXis Impact TOF mass spectrometer. Fourier-transform infrared (FT-IR) spectra were recorded on an alpha Bruker FT-IR spectrometer. Analytical thin-layer chromatography was performed on pre-coated 250 mm layer thickness silica gel 60 F_{254} plates (EMD Chemicals Inc.). Visualization was performed by ultraviolet light and/or by staining with potassium permanganate or cerium molybdate. Purifications by column chromatography were performed using either a Biotage Isolera™ One or standard column chromatography using silica gel (40-63 µm, 230-400 mesh).

General Procedures

General Procedure A: Ir-catalyzed Borylation of Indoles. A flame-dried Schlenk tube equipped with a Teflon-coated stir bar was charged with the starting indole (1.0 equiv), B_2pin_2 (1.0 – 2.0 equiv), 4,4'-di-*tert*-butyl-2,2'-bipyridyl (dtbpy, 1.0 – 6.0 mol%), and $[Ir(COD)(OMe)]_2$ (0.5 – 3.0 mol%). The Schlenk tube was evacuated and backfilled with N_2 (this process was repeated three times), then dry, degassed solvent (THF, cyclohexane, dioxane, CPME or MTBE) was added under a positive pressure of N_2. The tube was sealed and heated to the indicated temperature in a pre-heated oil bath. After the indicated time, the tube was cooled to ambient temperature, and the reaction mixture was transferred to a round-bottom flask. The resulting mixture was concentrated *in vacuo* and then purified by silica gel column chromatography using the indicated solvent system as eluent to afford the desired product.

Compound 2-10

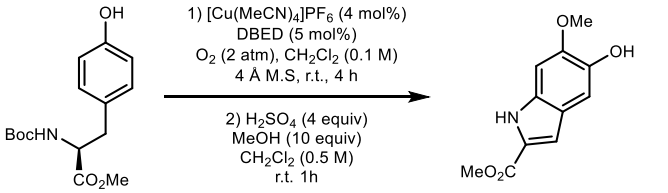

Procedure: A flame-dried, 25 mL Radley tube equipped with 4Å molecular sieves (200 mg), a Teflon-coated stir bar and a rubber septum was charged with $[Cu(CH_3CN)_4](PF_6)$ (14.9 mg, 0.04 mmol, 4 mol%) and **2-8** (295.3 mg, 1.0 mmol, 1.0 equiv). The reaction vessel was then evacuated and backfilled with N_2 (this process was repeated three times), prior to the addition of *N*,*N*'-di-*tert*-butylethylenediamine (DBED, 10.8 μL, 0.05 mmol, 5 mol%) and dry, degassed CH_2Cl_2 (10 mL, 0.1 M). The rubber septum was then rapidly removed and replaced with a Radley cap, which was connected to a tank of O_2 and pressurized to 1 atm. Under a constant pressure of O_2 (1 atm), the reaction was vented 3 times for 10 s to remove N_2. The reaction mixture was then stirred at ambient temperature for 4h, depressurized by opening to the atmosphere and quenched by the addition of $NaHSO_4$ (20 mL, 10% by weight aqueous solution). The phases were then separated, and the aqueous phase was extracted with CH_2Cl_2 (3 × 20 mL). The combined organic fractions

were then dried over $MgSO_4$, filtered, and concentrated *in vacuo* to afford a blood-red residue, which was transferred to a 50 mL round-bottom flask. A Teflon-coated stir bar was then added followed by the addition of dry CH_2Cl_2 (1 mL) and dry MeOH (202.3 µL, 5.0 mmol, 10.0 equiv). Upon dissolution of the reaction mixture with stirring, concentrated H_2SO_4 (95-98 wt%, 112.2 µL, 2.0 mmol, 4.0 equiv) was added dropwise under air. Rapid gas evolvement was observed within 2 min, and the resulting biphasic mixture was stirred at room temperature for 1h. Excess acid was then neutralized by the addition of a saturated aqueous solution of Na_3PO_4 (5 mL), and the reaction mixture was then stirred for an additional 10 min. The resulting mixture was then extracted with EtOAc (3 × 20 mL). The combined organic fractions were dried over $MgSO_4$, filtered and concentrated *in vacuo*. The crude reaction mixture was purified by silica gel column chromatography (30 % EtOAc in hexanes) to afford **2-10** (73.0 mg, 0.33 mmol) as an off-white solid in a 66 % yield.

Characterization:

$\mathbf{R_f}$ = (EtOAc/hexanes 3:7): 0.33; **IR** (neat) v = 3311, 1671, 1639, 1529, 1509, 1444, 1386, 1311, 1256, 1219, 1195, 1146 cm^{-1}; **^{1}H NMR** (500 MHz, $CDCl_3$) δ 8.68 (br. s, 1H), 7.13 (s, 1H), 7.08 (dd, *J* = 2.0, 0.6 Hz, 1H), 6.83 (s, 1H), 5.52 (s, 1H), 3.96 (s, 3H), 3.91 (s, 3H); **^{13}C NMR** (126 MHz, $CDCl_3$) δ 162.4, 147.8, 142.2, 131.9, 126.1, 121.3, 108.8, 105.2, 93.1, 56.2, 51.9; **HRMS**: Calcd. for $C_{11}H_{11}NO_4$ $[M-H]^-$ = 220.0615 m/z, found = 220.0608 m/z.

Procedure for large-scale synthesis: A flame-dried, 2 L round-bottom flask equipped with 4Å molecular sieves (40 g), a Teflon-coated stir bar and a rubber septum was charged with $[Cu(CH_3CN)_4](PF_6)$ (2.98 g, 8.0 mmol, 4 mol%) and **2-8** (200 mmol, 59.07 g, 1.0 equiv). ACS grade CH_2Cl_2 (1 L, measured by graduated cylinder) was then added under air, followed by the addition of *N*,*N*'-di-*tert*-butylethylenediamine (DBED, 2.16 mL, 10.0 mmol, 5 mol%) via a syringe. The resulting deep purple mixture was then capped with a rubber septum. Another rubber septum was then put on top of the flask, and affixed to the flask using copper wire (see Figure 2-4 for the reaction set-up). The reaction flask was connected to a tank of O_2 via a long needle and then purged for 5min with O_2 (0.2 atm) before pressurizing to 1.0 atm. The reaction mixture was then stirred under O_2 (1 atm) at ambient temperature for 4h, depressurized by opening to the atmosphere and filtered through a pad of celite. The filtrate was quenched by the addition of

$NaHSO_4$ (200 mL, 10% by weight aqueous solution). The phases were then separated, and the aqueous phase was extracted with CH_2Cl_2 (3 $\times$ 200 mL). The combined organic fractions were then dried over $MgSO_4$, filtered, and concentrated *in vacuo* in a 2 L round-bottom flask to afford a blood-red residue which was dissolved in ACS grade CH_2Cl_2 (200 mL) and HPLC grade MeOH (40.5 mL, 1.0 mol, 10.0 equiv). Concentrated H_2SO_4 (95-98 wt%, 22.4 mL, 400 mmol, 4.0 equiv) was then added to the reaction flaks dropwise under air over 10 min. Rapid gas evolvement was observed for the first 2 min, and the resulting biphasic mixture was stirred at room temperature for an additional 1h. The excess acid was neutralized by the addition of a saturated aqueous solution of Na_3PO_4 (1 L) dropwise over 30 min, and stirred for an additional 10 min. The resulting mixture was then acidified to pH = 2 with HCl (6 M, 7 mL), and extracted with EtOAc (3 $\times$ 500 mL). The combined organic fractions were then dried over $MgSO_4$, filtered through a plug of silica gel, and concentrated *in vacuo*. The crude reaction mixture was precipitated by the addition of EtOAc/hexanes (1:1, 200 mL). Material remaining in the mother liquor was purified by silica gel column chromatography (25 % to 50 % EtOAc in hexanes). This material was combined with the solid obtained by precipitation to afford **2-10** (12.6 g, 57 mmol, 57%) as a tan solid. ^{1}H-NMR of this material suggests a purity of at least 95%. However, the slightly colored impurity can be removed by recrystallization from EtOAc/hexanes to afford a white crystalline solid.

Recovery of Boc-Tyr-OMe (2-8): The aqueous layer was basified to pH = 8 using 30% NaOH. EtOAc (200 mL) was then added, followed by Boc_2O (26.2 g, 120 mmol, 0.6 equiv). After stirring at room temperature for 12 h, the reaction mixture was poured into a separatory funnel, and extracted with EtOAc (3 $\times$ 500 mL). The combined organic fractions were dried over Na_2SO_4, filtered and concentrated *in vacuo*. The crude product was purified by flash chromatography on silica gel using hexanes:EtOAc (3:1 to 1:1) as eluent to afford **2-8** (17.0 g, 57.6 mmol) as a pale-yellow solid in 58 % yield.

Compound 2-18

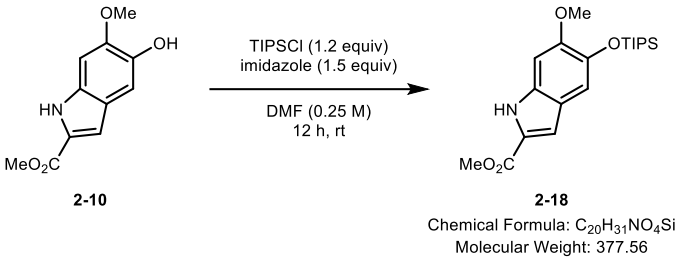

2-10 **2-18**

Chemical Formula: $C_{20}H_{31}NO_4Si$
Molecular Weight: 377.56

Procedure: A 250 mL flame-dried, round-bottom flask, equipped with a Teflon-coated stir bar and a rubber septum, was charged with **2-10** (4.42 g, 20 mmol, 1 equiv) and imidazole (2.04 g, 30 mmol, 1.5 equiv) followed by the addition of DMF (80 mL, 0.25 M). To the resulting reaction mixture was added triisopropylsilyl chloride (4.62 g, 24 mmol, 1.2 equiv). The resulting homogeneous reaction mixture was then stirred at ambient temperature for 12 h and then quenched with HCl (50 mL, 1M). The resulting heterogeneous, biphasic reaction mixture was then extracted with EtOAc (100 mL x 3). The combined organic phases were washed with water (200 mL x 3), brine (100 mL x 2) then dried over Na_2SO_4, filtered, and concentrated *in vacuo*. The resulting residue was purified by silica gel column chromatography (25% EtOAc in hexanes) to afford **2-18** as a white solid (5.7 g, 15.1 mmol) in a 76% yield.

Characterization:

$\mathbf{R_f}$ = (EtOAc/hexane 1:1): 0.77; **IR** (neat) v = 3322, 2943, 2865, 1680, 1523, 1248, 1213, 1152, 906 cm^{-1}; **^{1}H NMR** (400 MHz, $CDCl_3$) δ 8.82 (br. s, 1H), 7.08 (s, 1H), 7.06 (d, *J* = 1.3 Hz, 1H), 6.78 (d, *J* = 0.8 Hz, 1H), 3.91 (s, 3H), 3.84 (s, 3H), 1.33-1.21 (m, 3H), 1.10 (d, *J* = 7.4 Hz, 18H); **^{13}C NMR** (126 MHz, $CDCl_3$) δ 162.4, 152.2, 142.3, 120.9, 125.7, 120.9, 111.4, 108.9, 93.8, 55.6, 51.9, 18.1, 13.0; **HRMS**: Calcd. for $C_{20}H_{31}NO_4Si$ $[M+Na]^+$ = 400.1915 m/z, found = 400.1910 m/z.

Compound 2-19

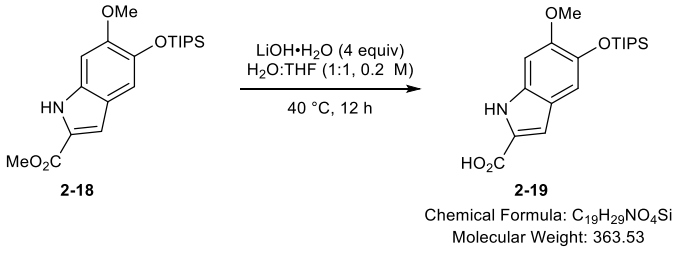

2-18 **2-19**

Chemical Formula: $C_{19}H_{29}NO_4Si$
Molecular Weight: 363.53

Procedure: A 50 mL flame-dried, round-bottom flask, equipped with a Teflon-coated stir bar and a rubber septum, was charged with **2-18** (1.9 g, 5.0 mmol, 1.0 equiv). To the reaction flask was

added THF (12.5 mL, 0.2 M).and $LiOH \cdot H_2O$ (0.84 g, 20 mmol, 4.0 equiv.) in H_2O (12.5 mL, 0.2 M). The resulting reaction mixture was then stirred at 40 °C for 12 h before acidified with HCl (2 M, 50 mL). The resulting mixture was then extracted with EtOAc (50 mL x 3). The combined organic phases were dried over Na_2SO_4, filtered, and concentrated *in vacuo*. This resulting crude reaction mixture was then purified by silica gel column chromatography (25% EtOAc in hexanes to 16% MeOH in EtOAc) to afford **2-19** as a white solid (1.5 g, 4.25 mmol) in 85 % yield.

Characterization:

R_f = (methanol/EtOAc 1:5): 0.43; **IR** (neat) v = 3150, 2940, 2863, 1716, 1685, 1527, 1206, 1180, 1152, 1015, 915 cm^{-1}; **^{1}H NMR** (500 MHz, Acetone-d_6) δ 10.53 (brs, 1H), 7.13 (s, 1H), 7.05 (dd, *J* = 2.2, 0.9 Hz, 1H), 7.03 (s, 1H), 3.86 (s, 3H), 1.35 – 1.24 (m, 3H), 1.11 (d, *J* = 7.4 Hz, 18H); **^{13}C NMR** (101 MHz, Acetone-d_6) δ 162.8, 152.4, 142.7, 134.5, 127.4, 121.7, 111.6, 108.9, 95.1, 55.8, 18.4, 13.6; **HRMS**: Calcd. for $C_{19}H_{29}NO_4Si$ $[M+Na]^+$ = 386.1758 m/z, found = 386.1776 m/z.

Compound 2-20:

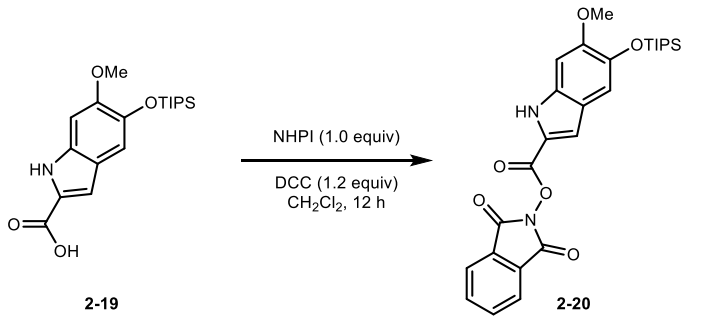

2-19 **2-20**

Chemical Formula: $C_{27}H_{32}N_2O_6Si$
Molecular Weight: 508.65

Procedure: A 10 mL round-bottom flask, equipped with a Teflon-coated stir bar and a rubber septum, was charged with carboxylic acid **2-19** (181.76 mg, 0.5 mmol, 1.0 equiv) and *N*-hydroxyphthalimide (81.57 mg, 0.5 mmol, 1.0 equiv). The reaction flask was then evacuated and backfilled with N_2 (this process was repeated three times), prior to the addition of a solution of *N, N'*-dicyclohexylcarbodiimide (123.80 mg, 0.6 mmol, 1.1 equiv) in dry, degassed CH_2Cl_2 (5 ml, 0.1 M). The reaction mixture was then stirred at ambient temperature for 12 h and then the white precipitate formed was filtered off and the filtrate was concentrated *in vacuo*. The crude reaction mixture was purified by silica gel column chromatography (25 % EtOAc in hexanes) to afford **2-20** (78.84 mg, 0.155 mmol) as a light-yellow solid in 31 % yield.

Characterization:

R_f = (EtOAc/hexanes 1:3): 0.37; **^{1}H NMR** (500 MHz, $CDCl_3$) δ 8.93 (brs, 1H), 7.95 – 7.87 (m, 2H), 7.84 – 7.76 (m, 2H), 7.37-7.34 (m, 1H), 7.10-7.09 (m, 1H), 6.79 (s, 1H), 3.86 (s, 3H), 1.35 – 1.22 (m, 3H), 1.11 (d, *J* = 7.4 Hz, 18H).; **^{13}C NMR** (126 MHz, $CDCl_3$) δ 162.37, 157.89, 153.56, 142.95, 134.91, 134.64, 134.60, 129.15, 124.15, 120.82, 119.62, 113.03, 111.33, 93.54, 55.61, 18.07, 12.94.; **HRMS**: Calcd. for $C_{27}H_{31}N_2O_6Si$ $[M-H]^+$ = 507.19569 m/z, found =507.19584 m/z.

Compound 2-22:

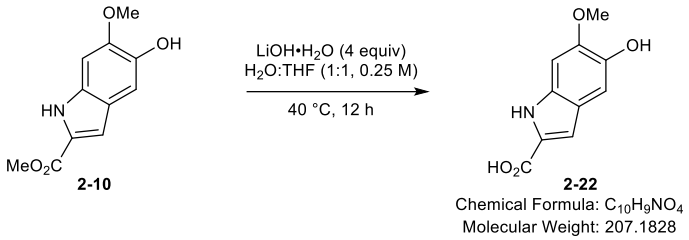

Procedure: A flame-dried, round-bottom flask, equipped with a Teflon-coated stir bar and a rubber septum, was charged with **2-10** (2.21 g, 10 mmol, 1.0 equiv.) and $LiOH{\cdot}H_2O$ (1.68 g, 40 mmol, 4.0 equiv). The flask was evacuated and backfilled with N_2 (this process was repeated for 3 times), prior to the addition of dry and degassed THF (20 mL) and H_2O (20 mL). The resulting mixture was stirred at 40 ^oC for 12 h and then acidified with HCl (2 M, 50 mL) followed by extraction with EtOAc (3 x 50 mL). The combined organic phases were then dried over Na_2SO_4, filtered through a plug of silica gel (washed with EtOAc:MeOH, 100 mL, 10:1), and concentrated *in vacuo* to afford **2-22** (2.16 g, 9.3 mmol) as a tan solid in 93 % yield.

Characterization:

R_f = (EtOAc/MeOH 5:1): 0.51; **^{1}H NMR** (500 MHz, acetone-d^6) δ 10.46 (br. s, 1H), 7.19 (brs, 1H), 7.05 – 6.85 (m, 3H), 3.89 (s, 3H); **^{13}C NMR** (126 MHz, acetone-d^6) δ 163.0, 149.3, 143.8, 133.4, 127.1, 122.0, 108.7, 105.7, 94.7, 56.2. The characterization data matches previous reports.[45]

Compound 2-23

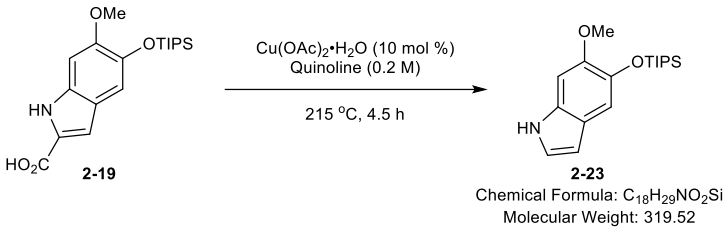

Procedure: A 50 mL Schlenk tube, equipped with a Teflon-coated stir bar and a glass stopper, was charged with carboxylic acid **2-19** (1.83 g, 5.0 mmol, 1.0 equiv) and $Cu(OAc)_2 \cdot H_2O$ (99.83 mg, 0.5 mmol, 10 mol%). The tube was evacuated and backfilled with N_2 (this process was repeated for 3 times), followed by the addition of quinoline (25 mL, 0.2 M) under a positive pressure of N_2. The resulting mixture was then stirred at 215 °C for 4.5 h and then cooled down to ambient temperature and quenched with HCl (100 mL, 1M). The resulting mixture was then extracted with EtOAc (100 mL x 3). The combined organic layers were then dried over $MgSO_4$, filtered, and concentrated *in vacuo*. The crude mixture was then purified by silica gel column chromatography (25 % EtOAc in hexanes) to afford **2-23** (1.28 g, 4.0 mmol) as a off-white solid in 80 % yield.

Characterization:

$\mathbf{R_f}$ = (EtOAc/hexanes 1:3): 0.32; **IR** (neat) v = 3409, 3384, 2943, 2866, 1473, 1318, 1296, 1214, 1132, 882 cm^{-1}; **^{1}H NMR** (500 MHz, $CDCl_3$) δ 7.91 (brs, 1H), 7.09 (s, 1H), 7.04 (dd, *J* = 2.9, 2.5 Hz, 1H), 6.83 (s, 1H), 6.38 (t, *J* = 2.2 Hz, 1H), 3.82 (s, 3H), 1.33 – 1.24 (m, 3H), 1.11 (d, *J* = 7.4 Hz, 18H); **^{13}C NMR** (126 MHz, $CDCl_3$) δ 149.0, 141.2, 131.0, 122.8, 121.1, 110.6, 102.3, 94.8, 56.0, 18.2, 13.0; **HRMS**: Calcd. for $C_{18}H_{29}NO_2Si$ $[M+Na]^+$ = 342.1860 m/z, found =342.1876 m/z.

Compound 2-21

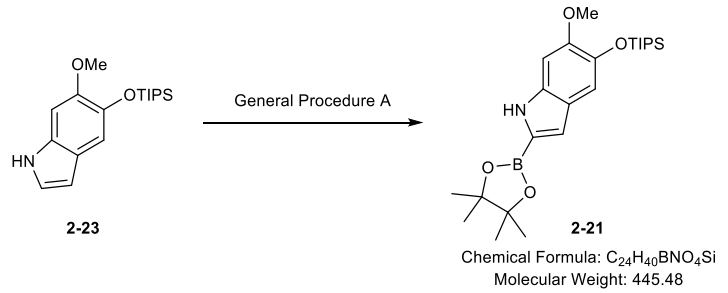

Procedure: The reaction was carried out according to the General Procedure A, the reaction was performed in THF at 80 °C for 2 h.

Amounts of Reagents:

2-23 (159.8 mg, 0.5 mmol, 1.0 equiv)

$[Ir(OMe)(COD)]_2$ (4.9 mg, 0.0075 mmol, 1.5 mol%)

dtbpy (8.1 mg, 0.015 mmol, 3.0 mol%)

B_2pin_2 (126.9 mg, 0.5 mmol, 1.0 equiv)

THF (1.5 mL, 0.3 M)

Purification: 10 % EtOAc in hexanes.

Yield of Product:

2-21: 189.3 mg, 0.425 mmol, 85 %, off-white solid.

Characterization:

$\mathbf{R_f}$ = (EtOAc/hexanes, 1:9) 0.38; **IR** (neat) v = 3357, 2976, 2944, 2865, 1533, 1371, 1288, 1258, 1219, 1139, 918 cm^{-1}; **^{1}H NMR** (500 MHz, $CDCl_3$) δ 8.36 (brs, 1 H), 7.08 (s, 1 H), 6.95 (d, *J* = 1.2 Hz, 1H), 6.77 (s, 1 H), 3.82 (s, 3 H), 1.34 (s, 12 H), 1.30- 1.23 (m, 3 H), 1.10 (d, *J*= 7.2 Hz, 18 H); **^{13}C NMR** (126 MHz, $CDCl_3$) δ 150.6, 141.3, 133.9, 132.0, 121.5, 113.6, 110.7, 93.7, 83.9, 55.6, 24.8, 18.0, 12.9; **HRMS**: Calcd. for $C_{24}H_{40}BNO_4Si$ $[M+Na]^+$ = 468.2712 m/z, found = 468.2760 m/z.

Compound 2-21b

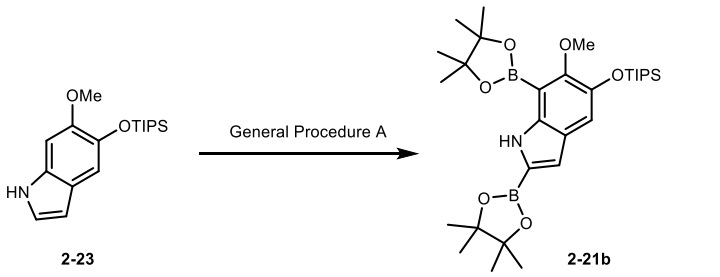

Procedure: The reaction was carried out according to the General Procedure A, the reaction was performed in THF at 80 °C for 23 h.

Amounts of Reagents:

2-23 (159.8 mg, 0.5 mmol, 1.0 equiv)

$[Ir(OMe)(COD)]_2$ (4.9 mg, 0.0075 mmol, 1.5 mol%)

dtbpy (8.1 mg, 0.015 mmol, 3.0 mol%)

B_2pin_2 (253.9 mg, 1.0 mmol, 2.0 equiv)

THF (1.5 mL, 0.3 M)

Purification: 5 % EtOAc in hexanes.

Yield of Product:

2-21b: 234.3 mg, 0.41 mmol, 82 %, off-white solid.

Characterization:

R_f = (EtOAc/hexanes, 1:9) 0.53; **^{1}H NMR** (400 MHz, $CDCl_3$) δ 9.43 (brs, 1H), 7.20 (s, 1H), 6.94 (d, *J* = 2.2 Hz, 1H), 3.83 (s, 3H), 1.42 (s, 12H), 1.35 (s, 12H), 1.34 – 1.24 (m, 3H), 1.11 (d, *J* = 7.4 Hz, 18H).

Compound 2-26

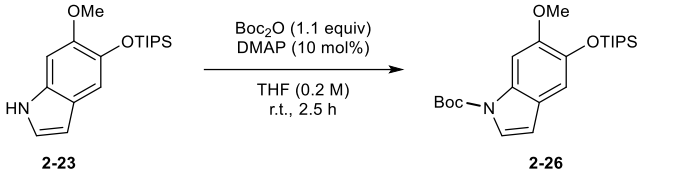

2-23 **2-26**

Chemical Formula: $C_{23}H_{37}NO_4Si$
Molecular Weight: 419.64

Procedure: A 10 mL flame-dried, round-bottom flask, equipped with a Teflon-coated stir bar and a rubber septum, was charged with **2-23** (131.0 mg, 0.41 mmol, 1 equiv), DMAP (5.0 mg, 0.45 mmol, 10 mol %), and Boc_2O (98.2 mg, 0.45 mmol, 1.1 equiv). The flask was evacuated and backfilled with N_2 (this process was repeated for 3 times), followed by the addition of dry, degassed THF (2.0 mL, 0.20 M). The resulting homogeneous reaction mixture was stirred at ambient temperature for 2.5 h and then concentrated *in vacuo*. The crude mixture was purified by silica gel column chromatography (20 % EtOAc in hexanes) to afford **2-26** as yellow oil (142.7 mg, 0.34 mmol) in 83% yield.

Characterization:

R_f = (EtOAc/hexanes, 1:3) 0.69 ; **IR** (neat) ν = 2943, 2866, 1731, 1480, 1455, 1378, 1298, 1216, 1129 cm^{-1}; **^{1}H NMR** (400 MHz, $CDCl_3$) δ 7.71 (brs, 1H), 7.42 (s, 1H), 7.01 (s, 1H), 6.40 (d, *J* = 3.7 Hz, 1H), 3.87 (s, 3H), 1.66 (s, 9H), 1.34 – 1.22 (m, 3H), 1.11 (d, *J* = 7.3 Hz, 18H); **^{13}C NMR** (101 MHz, $CDCl_3$) δ 150.0, 149.7, 142.6, 130.3, 124.3, 123.4, 111.2, 107.1, 99.3, 83.2, 55.7, 28.3, 18.1, 13.0; **HRMS**: Calcd. for $C_{23}H_{37}NO_4Si$ $[M+Na]^+$ = 442.2400 m/z, found = 442.2384 m/z.

Compound 2-27

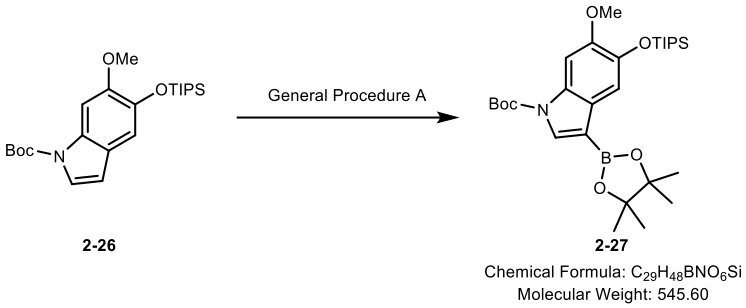

Procedure: The reaction was carried out according to the General Procedure A, the reaction was performed in THF at 80 °C for 4 h.

Amounts of Reagents:

2-26 (209.8 mg, 0.5 mmol, 1.0 equiv)

$[Ir(OMe)(COD)]_2$ (5.0 mg, 0.0075 mmol, 1.5 mol%)

dtbpy (4.0 mg, 0.015 mmol, 3.0 mol%)

B_2pin_2 (177.76 mg, 0.7 mmol, 1.4 equiv)

THF (1.5 mL, 0.3 M)

Purification: 10 % EtOAc in hexanes.

Yield of Product:

2-27: 218.24 mg, 0.40 mmol, 80 %, yellow oil.

Characterization:

R_f = (EtOAc/hexanes, 1:9) 0.45; **IR** (neat) v = 2976, 2943, 2867, 1736, 1554, 1479, 1309, 1120 cm^{-1}; **^{1}H NMR** (400 MHz, $cdcl_3$) δ 7.83 (s, 1H), 7.70(s, 1H), 7.53 (s, 1H), 3.88 (2, 3H), 1.64(s, 9H), 1.35 (s, 12 H), 1.32-1.25 (m, 3H), 1.13 (d, 18H); **^{13}C NMR** (101 MHz, $CDCl_3$) δ 149.7, 149.6, 142.6, 133.2, 131.0, 126.6, 112.9, 99.0, 83.5, 83.3, 56.0, 28.4, 25.1, 18.1, 12.9; **HRMS**: Calcd. for $C_{29}H_{48}BNO_6Si$ $[M+Na]^+$ = 568.3240 m/z, found = 568.3236 m/z.

Compound 2-28

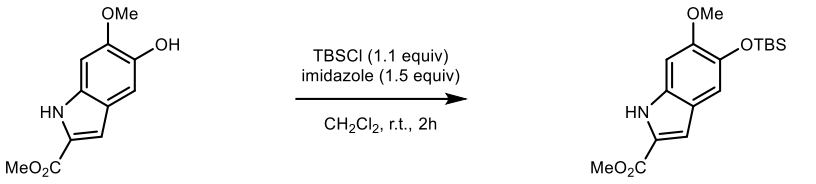

2-10 **2-28**
Chemical Formula: $C_{17}H_{25}NO_4Si$
Molecular Weight: 335.4702

Procedure: A 250 mL flame-dried round-bottom flask equipped with a Teflon-coated stir bar and a rubber septum was charged with **2-10** (6.64 g, 30 mmol, 1.0 equiv), TBSCl (4.97 g, 33 mmol, 1.1 equiv), and imidazole (3.06 g, 45 mmol, 1.5 equiv). The reaction flask was then evacuated and backfilled with N_2 (this process was repeated for 3 times), prior to the addition of dry, degassed CH_2Cl_2 (150 mL). After being stirred at room temperature for 2h, the reaction mixture was quenched with HCl (150 mL, 1M) and then extracted with CH_2Cl_2 (150 mL x 3). The combined organic layers were then dried over $MgSO_4$, filtered and concentrated *in vacuo*. The crude reaction mixture was purified by silica gel column chromatography (25 % EtOAC in hexanes) to afford **2-28** (8.04 g, 24 mmol) as a white solid in 80 % yield.

Characterization:

R_f = (EtOAc/hexanes, 1:4) 0.18; **IR** (neat) ν = 3341, 2926, 2854, 1679, 1634, 1520, 1496, 1470, 1458, 1442, 1416, 1362, 1268, 1243, 1228, 1211, 1152 cm^{-1}; **^{1}H NMR** (500 MHz, $CDCl_3$) δ 8.83 (s, 1 H), 7.08 (s, 1 H), 7.07 (dd, *J* = 2.1 Hz, 0.9 Hz, 1H), 6.80 (d, *J* = 0.9 Hz, 1H), 3.92 (s, 3 H), 3.85 (s, 3 H), 1.02 (s, 9 H), 0.16 (s, 6 H); **^{13}C NMR** (126 MHz, $CDCl_3$) δ 162.5, 152.1, 141.8, 133.1, 125.8, 121.0, 112.1, 108.8, 93.8, 55.6, 51.9, 25.9, 18.6, 4.6; **HRMS**: Calcd. for $C_{17}H_{25}NNaO_4Si$ $[M+Na]^+$ = 358.1445 m/z, found 358.1443 m/z.

Compound 2-29

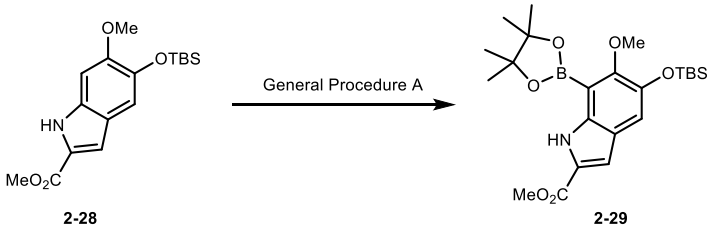

2-28 **2-29**
Chemical Formula: $C_{23}H_{36}BNO_6Si$
Molecular Weight: 461.4370

Procedure: The reaction was carried out according to the General Procedure A, the reaction was performed in THF at 60 °C for 18 h.

Amounts of Reagents:

2-28 (1.68 g, 5.0 mmol, 1.0 equiv)

$[Ir(OMe)(COD)]_2$ (49.7 mg, 0.075 mmol, 1.5 mol%)

dtbpy (40.3 mg, 0.15 mmol, 3.0 mol%)

B_2pin_2 (1.78 g, 7.0 mmol, 1.4 equiv)

THF (15 mL, 0.3 M)

Purification: 10 % EtOAc in hexanes.

Yield of Product:

2-29: 1.94 g, 4.20 mmol, 84%, off-white solid.

Characterization:

$\mathbf{R_f}$ = (EtOAc/hexane, 1:4) 0.45; **IR** (neat) ν = 3441, 2929, 2856, 1711, 1581, 1532, 1437, 1423, 1404, 1372, 1350, 1298, 1232, 1167, 1142, 1026 cm^{-1}; **^{1}H NMR** (500 MHz, $CDCl_3$) δ 9.79 (s, 1 H), 7.24 (s, 1 H), 7.07 (d, *J* = 2.4 Hz, 1 H), 3.93 (s, 3 H), 3.84 (s, 3 H), 1.42 (s, 12 H), 1.05 (s, 9 H), 0.21 (s, 6 H); **^{13}C NMR** (126 MHz, $CDCl_3$) δ 162.4, 158.2, 144.6, 137.8, 126.9, 123.2, 115.9, 107.7, 104.9, 83.7, 62.0, 51.8, 25.9, 25.0, 18.3, -4.5; **HRMS**: Calcd. for $C_{23}H_{36}BNNaO_6Si$ $[M+Na]^+$ = 484.22933 m/z, found 484.22972 m/z.

Compound 2-32:

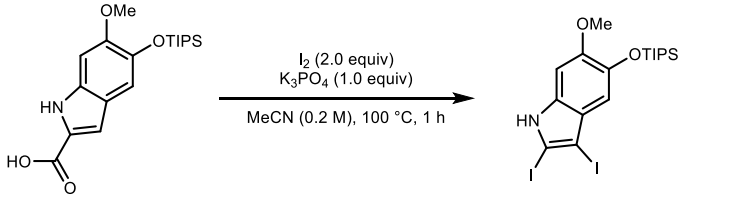

2-19 **2-32**

Chemical Formula: $C_{18}H_{27}I_2NO_2Si$
Molecular Weight: 571.31

Procedure: A 2 mL flame-dried, microwave vial, equipped with a Teflon-coated stir bar and a rubber septum, was charged with **2-19** (36.3 mg, 0.1 mmol, 1.0 equiv), I_2 (50.7 mg, 0.2 mmol, 2.0 equiv), and anhydrous K_3PO_4 (21.3 mg, 0.1 mmol, 1.0 equiv). The flask was then evacuated and

backfilled with N_2 (this process was repeated for 3 times) before the addition of dry, degassed MeCN (0.5 mL, 0.2 M). The resulting mixture was then stirred at 100 °C for 1 h under a positive pressure of N_2 before quenching with an aqueous solution of $Na_2S_2O_8$ (3 mL, 15 % by weight) and a saturated aqueous solution of Na_2CO_3 (3 mL). The aqueous phase was then extracted with EtOAc (10 mL x 3). The combined organic fractions were washed with brine (20 mL), dried over $MgSO_4$, filtered and concentrated *in vacuo*. The resulting crude mixture was purified by silica gel column chromatography (10 % EtOAc in hexanes) to afford **2-32** as a yellow solid (11.4 mg, 0.02 mmol) in 20 % yield.

Characterization:

R_f = (EtOAc/hexanes, 1:3) 0.61; **^{1}H NMR** (500 MHz, $CDCl_3$) δ 8.12 (s, 1H), 6.82 (s, 1H), 6.76 (s, 1H), 3.82 (s, 3H), 1.33 – 1.22 (m, 3H), 1.11 (d, *J* = 7.4 Hz, 18H).; **HRMS**: Calcd. for $C_{18}H_{27}I_2NNaO_2Si$ $[M+Na]^+$ = 593.9793 m/z, found = 593.9788 m/z.

Compound 2-34:

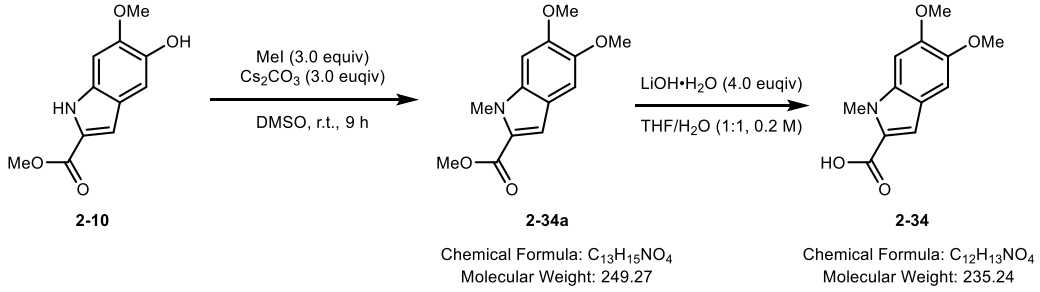

2-10 **2-34a** **2-34**

Chemical Formula: $C_{13}H_{15}NO_4$
Molecular Weight: 249.27

Chemical Formula: $C_{12}H_{13}NO_4$
Molecular Weight: 235.24

Procedure to 2-34a: A 50 mL flame-dried, round-bottom flask, equipped with a Teflon-coated stir bar and a rubber septum, was charged with **2-10** (1.1 g, 5.0 mmol, 1.0 equiv), and Cs_2CO_3 (4.9 g, 15.0 mmol, 3.0 equiv). The flask was then evacuated and backfilled with N_2 (this process was repeated for 3 times) before the addition of dry, degassed DMSO (10 mL, 0.5M). The resulting mixture was then stirred at ambient temperature for 9 h under a positive pressure of N_2 and then quenched with a saturated aqueous solution of NH_4Cl (20 mL). The aqueous phase was extracted with EtOAc for three times (3 x 20 mL). The combined organic fractions were washed with brine (20 mL), dried over $MgSO_4$, filtered and concentrated *in vacuo*. The crude mixture was purified by silica gel column chromatography (25 % EtOAc in hexanes) to afford **2-34a** as a white solid (0.92 g, 3.7 mmol) in 74 % yield.

Characterization of 2-34a:

R_f = (EtOAc/hexanes, 1:3) 0.25; **^{1}H NMR** (500 MHz, $CDCl_3$) δ 7.18 (d, *J* = 0.8 Hz, 1H), 7.03 (s, 1H), 6.76 (s, 1H), 4.04 (s, 3H), 3.98 (s, 3H), 3.93 (s, 3H), 3.88 (s, 3H).

Procedure to 2-34: A 50 mL round-bottom flask, equipped with a Teflon-coated stir bar and a rubber septum, was charged with **2-34a** (0.92 g, 3.7 mmol, 1.0 equiv) and THF (10 mL, 0.2 M). To the resulting mixture was added $LiOH{\cdot}H_2O$ (0.62 g, 14.8 mmol, 4.0 equiv.) in H_2O (10 mL, 0.2 M). The resulting reaction mixture was then stirred at 65 °C for 12 h before adding HCl (50 mL, 2M) and H_2O (100 mL). The resulting white precipitate was then filtered and afforded **2-34** as white solid (0.98 g, 4.2 mmol) in 89 % yield.

Characterization of 2-34:

R_f = (EtOAc/hexanes, 1:1): 0.20; **^{1}H NMR** (500 MHz, Acetone-d_6) δ 7.19 (s, 1H), 7.12 (s, 1H), 7.05 (s, 1H), 4.03 (s, 3H), 3.91 (s, 3H), 3.83 (s, 3H).

Compound 2-35 and 2-36:

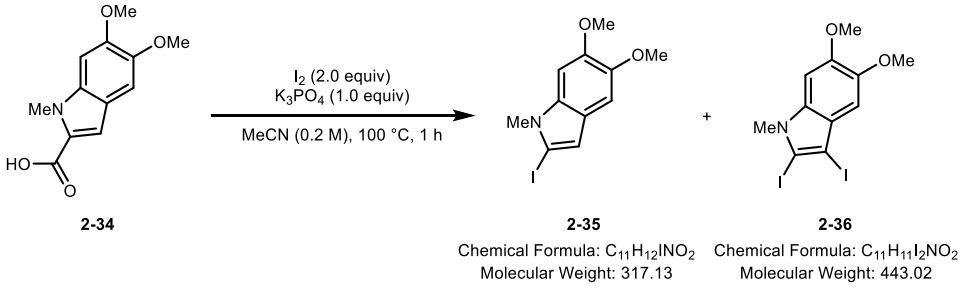

2-34

2-35
Chemical Formula: $C_{11}H_{12}INO_2$
Molecular Weight: 317.13

2-36
Chemical Formula: $C_{11}H_{11}I_2NO_2$
Molecular Weight: 443.02

Procedure: A 2 mL flame-dried, microwave vial, equipped with a Teflon-coated stir bar and a rubber septum, was charged with **2-34** (23.5 mg, 0.1 mmol, 1.0 equiv), I_2 (50.7 mg, 0.2 mmol, 2.0 equiv), and anhydrous K_3PO_4 (21.3 mg, 0.1 mmol, 1.0 equiv). The flask was then evacuated and backfilled with N_2 (this process was repeated for 3 times) before the addition of dry, degassed MeCN (0.5 mL, 0.2 M). The resulting mixture was then stirred at 100 °C for 1 h under a positive pressure of N_2 and then quenched with an aqueous solution of $Na_2S_2O_8$ (3 mL, 15 % by weight) and a saturated aqueous solution of Na_2CO_3 (3 mL). The aqueous phase was extracted with EtOAc (3 x 10 mL). The combined organic fractions were then washed with brine (5 mL), dried over $MgSO_4$, filtered, and concentrated *in vacuo*. The crude reaction mixture was then purified by silica

gel column chromatography (10 % EtOAc in hexanes) to afford **2-35** as a yellow solid (7.3 mg, 0.023 mmol) in 23 % yield and **2-36** as a yellow solid (26.1 mg, 0.059 mmol) in 59 % yield.

Characterization of 2-35:

R_f = (EtOAc/hexanes, 1:9) 0.50; **^{1}H NMR** (500 MHz, $CDCl_3$) δ 6.98 (s, 1H), 6.78 (s, 1H), 6.65 (d, *J* = 0.8 Hz, 1H), 3.95 (s, 3H), 3.91 (s, 3H), 3.71 (s, 3H).; **HRMS**: Calcd. for $C_{11}H_{12}INNaO_2$ $[M+Na]^+$ = 339.9805 m/z, found = 339.9804 m/z

Characterization of 2-36:

R_f = (EtOAc/hexanes, 1:9) 0.41; **^{1}H NMR** (400 MHz, $CDCl_3$) δ 6.82 (s, 1H), 6.77 (s, 1H), 3.96 (s, 3H), 3.96 (s, 3H), 3.83 (s, 3H).; **^{13}C NMR** (126 MHz, $CDCl_3$) δ 147.95, 146.19, 132.35, 124.78, 102.89, 93.47, 91.58, 70.46, 56.52, 56.48, 36.43.; **HRMS**: Calcd. for $C_{11}H_{11}I_2NNaO_2$ $[M+Na]^+$ = 465.8771 m/z, found = 465.8764 m/z.

Compound 2-33:

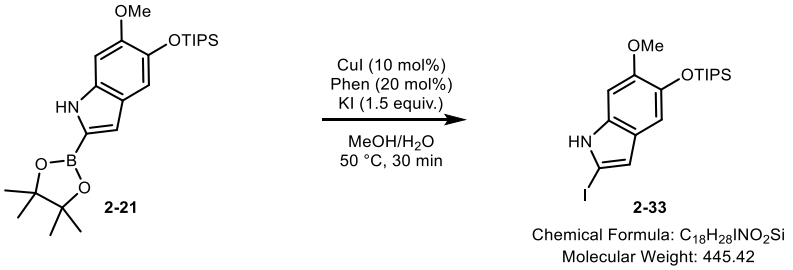

Procedure: A 10 mL round-bottom flask equipped with a Teflon-coated stir bar and a rubber septum was charged with **2-21** (238.31 mg, 0.53 mmol, 1.0 equiv), CuI (10.09 mg, 0.053 mmol, 10 mol%), 1,10-phenanthroline (Phen, 19.10 mg, 0.106 mmol, 20 mol%), KI (131.14 mg, 0.79 mmol, 1.5 equiv), and MeOH/H_2O (9mL/1mL, 0.05 M, 9:1). The rubber septum was then connected to a tank of O_2, pressurized to 50 kpa, and was vented 3 times for 10 s each time. Under a constant pressure of O_2 (50 kpa), the reaction mixture was then stirred at 50 ^oC for 0.5 h before depressurizing by opening to the atmosphere and concentrated *in vacuo*. The resulting wine-red residue was then diluted and extracted with EtOAc (3 x 30 mL). The combined organic fractions were washed with brine (20 mL), dried over $MgSO_4$, filtered and concentrated *in vacuo*. The crude mixture was purified by silica gel column chromatography (10 % EtOAc in hexanes) to afford **2-33** as a white solid (132.20 mg, 0.30 mmol) in 56 % yield.

Characterization:

R_f = (EtOAc/hexanes, 1:9) 0.31; **^{1}H NMR** (500 MHz, $CDCl_3$) δ 7.83 (s, 1H), 7.00 (s, 1H), 6.76 (s, 1H), 6.52 (s, 1H), 3.80 (s, 3H), 1.27 (m, 3H), 1.10 (d, *J* = 7.5 Hz, 18H).; **^{13}C NMR** (126 MHz, $CDCl_3$) δ 148.98, 141.25, 133.96, 122.90, 112.13, 109.19, 93.85, 70.68, 55.82, 17.99, 12.84.; **HRMS**: Calcd. for $C_{18}H_{27}INO_2Si$ $[M-H]^+$ = 444.08612 m/z, found = 444.08556 m/z.

Compound 2-37

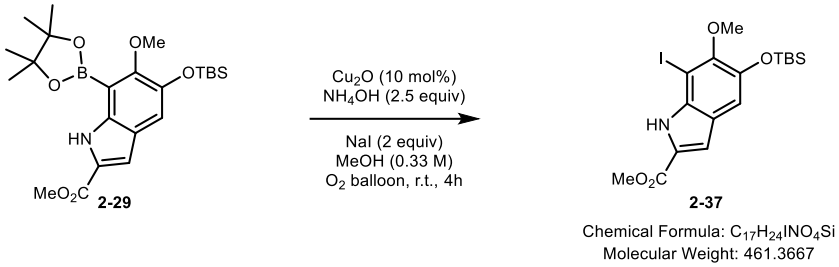

Procedure: A 100 mL round-bottom flask equipped with a Teflon-coated stir bar was charged with Cu_2O (71.6 mg, 0.5 mmol, 10 mol%) and a concentrated solution of ammonium hydroxide (1.78 mL, 12.5 mmol, 2.5 equiv). The resulting mixture was stirred under air for 30 min to dissolve the red Cu_2O and generate a blue-purple solution. **2-29** (5 mmol, 2.31 g, 1.0 equiv), NaI (1.50 g, 10 mmol, 2.0 equiv), and MeOH (15 mL) were then added to the blue-purple solution The flask was then capped with a rubber septum and purged with O_2 for 5 min, prior to stirring at ambient temperature for 4h with an oxygen balloon. It was then concentrated *in vacuo*, diluted with a mixture of brine (25 mL) and water (25 mL) and extracted with EtOAc (3 × 50 mL). The combined organic layers were dried over $MgSO_4$, filtered and concentrated *in vacuo*. The crude mixture was purified by silica gel column chromatography (20 % EtOAc in hexanes) to afford **2-37** (1.92 g, 4.2 mmol) as a white solid in 83 % yield.

Characterization:

R_f = (EtOAc/hexanes, 1:5) 0.44; **IR** (neat) v = 3238, 2928, 2856, 1693, 1557, 1519, 1441, 1361, 1273, 1235, 1145 cm^{-1}; **^{1}H NMR** (500 MHz, $CDCl_3$) δ 8.71 (br. s, 1H), 7.21 (d, *J* = 2.2 Hz, 1H), 7.07 (s, 1H), 3.93 (s, 3H), 3.85 (s, 3H), 1.04 (s, 9H), 0.20 (s, 6H); **^{13}C NMR** (126 MHz, $CDCl_3$) δ 161.9, 151.6, 144.5, 135.1, 127.6, 123.1, 112.5, 109.6, 73.6, 60.8, 52.1, 25.8, 18.4, -4.5; **HRMS**: Calcd. for $C_{17}H_{24}INO_4Si$ $[M+Na]^+$ = 484.0412 m/z, found = 484.0402 m/z.

Compound 2-37b

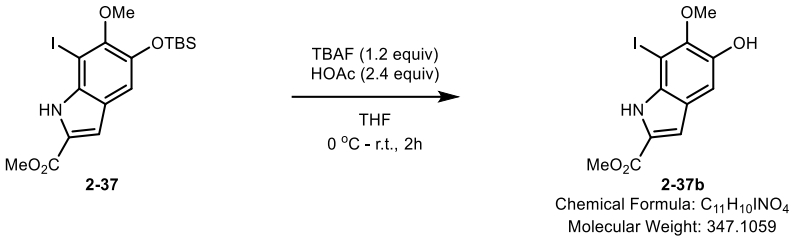

Procedure: A 250 mL flame-dried round-bottom flask equipped with a Teflon-coated stir bar and a rubber septum was charged with **2-37** (5.4 mmol, 2.47 g, 1.0 equiv). The reaction falsk was evacuated and backfilled with N_2 (this process was repeated for 3 times), prior to the addition of dry, degassed THF (80 mL, 0.06 M). The resulting mixture was then cooled to 0 °C in an ice bath, and a solution of tetrabutylammonium fluoride trihydrate (TBAF, 2.02 g, 6.4 mmol, 1.2 equiv) and HOAc (732.0 µL, 12.8 mmol, 2.4 equiv) in THF (20 mL) was added dropwise to the flask via a syringe. The resulting reaction mixture was warmed to room temperature and stirred for 2h. It was then concentrated to *a* 20 mL final volume *in vacuo*, diluted with a saturated aqueous solution of $NaHCO_3$ (50 mL), and extracted with EtOAc (3 × 50 mL). The combined organic layers were then dried over $MgSO_4$, filtered, and concentrated *in vacuo*. The crude reaction mixture was purified by silica gel column chromatography (40 % EtOAc in hexanes) to afford **2-37b** (1.76 g, 5.1 mmol) as a white solid in 94 % yield.

Characterization:

R_f = (EtOAc/hexanes, 1:2) 0.40; **IR** (neat) v = 3333, 2940, 1696, 1560, 1519, 1507, 1456, 1439, 1419, 1362, 1313, 1289, 1236, 1219, 1192, 1156, 1141 cm^{-1}; **^{1}H NMR** (500 MHz, $CDCl_3$) δ 8.68 (br. s, 1H), 7.23 (d, *J* = 2.2 Hz, 1H), 7.17 (s, 1H), 5.48 (br. s, 1H), 3.945 (s, 3H), 3.938 (s, 3H); **^{13}C NMR** (126 MHz, $CDCl_3$) δ 162.0, 147.8, 144.7, 134.4, 127.9, 123.8, 109.6, 106.9, 71.5, 61.9, 52.2; **HRMS**: Calcd. for $C_{11}H_{10}INO_4$ $[M-H]^-$ = 345.9582 m/z, found = 345.9575 m/z.

Compound 2-42:

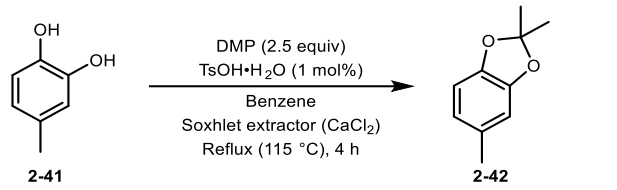

2-41 **2-42**

Chemical Formula: $C_{10}H_{12}O_2$
Molecular Weight: 164.20

Procedure: A 1L flame-dried, round-bottom flask, equipped with a Teflon-coated stir bar, a Soxhelt extractor, and a rubber septum was charged with **2-41** (24.8 g, 200 mmol, 1 equiv.), *p*-toluenesulfonic acid monohydrate (380.4 mg, 2 mmol, 1 mol% equiv.), and benzene (200 mL, 1.0 M). To this reaction mixture was added 2,2-dimethoxypropane (61.5 mL, 500 mmol, 2.5 equiv.), under a positive pressure of N_2. The reaction mixture was then heated to reflux (at 115 °C) with a Soxhelt extractor ($CaCl_2$, 58 g) for 4 h. The reaction mixture was then cooled to ambient temperature, filtered on a pad of Celite, and washed with EtOAc. Upon concentrating the filtrate *in vacuo*, the resulting crude mixture **2-4** (31.5 g, 192 mmol, 96 %) was obtained as a brown oil and was used without further purification. The compound can be easily purified via vacuum distillation at 80 °C to obtain a light-yellow oil (27.9 g, 170 mmol, 85 %).

Characterization:

$\mathbf{R_f}$ = (hexanes) 0.5; **^{1}H-NMR** (400 MHz, CD_3Cl_3): δ (ppm) = 6.63–6.56 (m, 3H), 2.27 (s, 3 H), 1.66 (s, 6H). The analytical data was consistent with the literature.[46]

Compound 2-43:

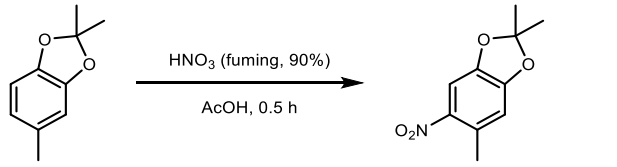

2-42 **2-43**

Chemical Formula: $C_{10}H_{11}NO_4$
Molecular Weight: 209.20

Procedure: A 2L round-bottom flask, equipped with a Teflon-coated stir bar was charged with **2-42** (65.7 g, 400 mmol, 1.0 equiv.) and acetic acid (450 mL). To this solution was added fuming HNO_3 (35 mL) in acetic acid (100 mL) dropwise over 30 min at 0 °C. The resulting mixture was stirred at ambient temperature for 30 min before pouring into a beaker containing ice. The

resulting precipitate was collected by vacuum filtration and washed with water to afford **2-43** (70 g, 400 mmol) as a yellow solid in 83 % yield. This solid and was used without further purification.

Characterization: $\mathbf{R_f}$ = (DCM/hexanes, 1:9) 0.48; **^{1}H-NMR** (DMSO-d, 500MHz): δ =7.54 (s, 1 H), 6.98 (s, 1 H), 2.46 (s, 3 H), 1.70 (s, 6 H). The analytical data was consistent with the literature.[32]

Compound 2-44:

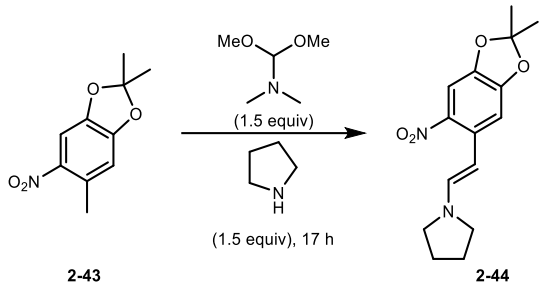

Procedure: The synthesis of **2-44** was performed by making modifications to the method of Leimgruber *et al.*[47] A flame-dried, 250 mL round-bottom flask equipped with a Teflon-coated stir bar was charged with **2-43** (16.7 g, 80 mmol, 1.0 equiv), pyrrolidine (10.0 mL, 120 mmol, 1.5 equiv.), and *N,N*'-dimethylformamide dimethyl acetal (16.0 mL, 120 mmol, 1.5 equiv). The resulting homogenous solution was heated at reflux (110 °C) for 17 hr under a positive pressure of N_2 and then allowed to cool to room temperature. The resulting mixture was then dilute and extracted with EtOAc (150 mL x 3) and washed with water (150 mL x 3). The phases were then separated, and the organic layer was washed with brine (100 mL x 3), dried over $MgSO_4$ then concentrated *in vacuo*. The resulting blood red residue was then dissolved in CH_2Cl_2 (15 mL) and MeOH (70 mL) and cooled to −20 °C. Filtration of the resulting mixture afforded **2-44** (18.8 g, 64.9 mmol) as a red needle crystal Upon concentrating the filtrate *in vacuo*, the resulting residue was recrystallized from MeOH (50 mL) at −20 °C to afford **2-44** (1.6 g, 5.5 mmol) as a red solid. In total, this afforded **2-44** (20.4 g, 70.4 mmol) in 88 % yield.

Characterization: $\mathbf{R_f}$ = (EtOAc/hexanes, 1:4) 0.60; **^{1}H-NMR** (DMSO-d, 500MHz): δ 7.60 (d, *J* = 13.4 Hz, 1H), 7.35 (s, 1H), 7.13 (s, 1H), 6.00 (d, *J* = 13.4 Hz, 1H), 3.27 (t, *J* = 6.3 Hz, 4H), 1.93 – 1.85 (m, 4H), 1.66 (s, 6H). The analytical data was consistent with the literature.[32]

Compound 2-45:

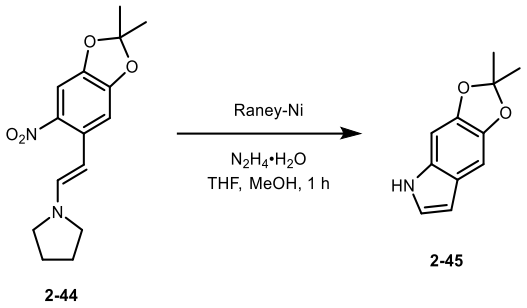

2-44 **2-45**

Procedure: The synthesis of **2-45** was performed by making modifications to the method of Leimgruber *et al.*[47] A 3-neck round-bottom flask equipped with a Teflon-coated stir bar, a reflux condenser was charged with Raney-Nickel (5 g), THF (138 mL, 0.5 M), MeOH (138 mL, 0.5 M), and **2-44** (20.3 g, 70 mmol, 1.0 equiv). To the resulting solution was added $N_2H_4 \cdot H_2O$ (N_2H_4 64-65 %, 5.0 mL, 1.5 equiv.) dropwise over 5 min. Additional $N_2H_4 \cdot H_2O$ (5.0 mL, 1.5 equiv) was added after 30 min. The resulting reaction mixture was stirred at 46 °C for 2 h and then allowed to cool to room temperature followed by filtration through a pad of Celite. Upon concentrating the filtrate *in vacuo*, the resulting crude mixture was purified using silica gel column chromatography (10 % EtOAc in hexanes) to afford **2-45** as a light brown solid (9.4 g, 50 mmol) in 71 % yield.

Characterization:

R_f =(EtOAc/hexanes, 1:9) 0.37; **^{1}H NMR** (500 MHz, $CDCl_3$): δ 7.97 (brs, 1H), 7.05 (dd, *J* = 3.2, 2.4 Hz, 1H), 6.91 (t, *J* = 0.6 Hz, 1H), 6.76 (t, *J* = 0.7 Hz, 1H), 6.41 (ddd, *J* = 3.1, 2.1, 0.9 Hz, 1H), 1.69 (s, 7H). The analytical data was consistent with the literature.[32]

Compound 2-47:

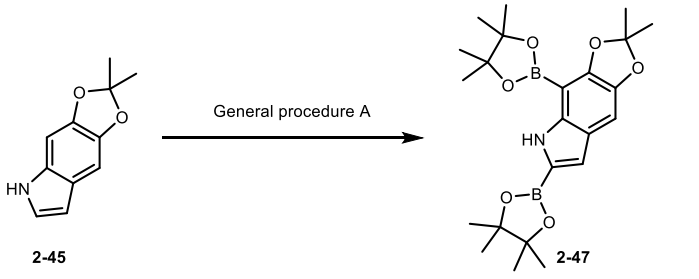

2-45 **2-47**

Chemical Formula: $C_{23}H_{33}B_2NO_6$
Molecular Weight: 441.14

Procedure: The reaction was carried out according to the General Procedure A and was performed in cyclohexane at 50 °C for 1 h.

Amounts of Reagents:

2-45 (1.9 g, 10 mmol, 1.0 equiv)

$[Ir(OMe)(COD)]_2$ (99.4 mg, 0.15 mmol, 1.5 mol%)

dtbpy (80.5 mg, 0.3 mmol, 3.0 mol%)

B_2pin_2 (5.1 g, 20.0 mmol, 2.0 equiv)

Cyclohexanes (30 mL)

Purification: 10 % EtOAc in hexanes.

Yield of Product:

2-47: 3.6 g, 8.2 mmol, 82%, white solid.

Characterization:

$\mathbf{R_f}$ = (hexanes/EtOAc, 9:1) 0.35; **IR** (neat) v = 3455, 2978, 2940, 1524, 1444, 1377, 1311, 1259, 1136, 1062, 991, 696, 852, 695, 668, 544 cm^{-1}; **^{1}H NMR** (500 MHz, $CDCl_3$) δ 9.37 (brs, 1H), 6.97 (s, 1H), 6.94 (d, *J* = 2.3 Hz, 1H), 1.70 (s, 6H), 1.41 (s, 12H), 1.35 (s, 12H); **^{13}C NMR** (126 MHz, cdcl$_3$) δ 153.20, 143.16, 138.37, 120.87, 117.45, 113.81, 102.34, 83.78, 83.75, 26.09, 25.09, 24.95.; **HRMS**: Calcd. for $C_{23}H_{34}O_6NB_2$ $[M+H]^+$ = 442.25668 m/z, found 442.25669 m/z.

Compound 2-48:

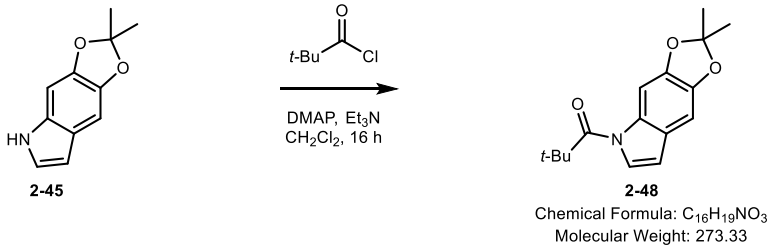

2-45

2-48

Chemical Formula: $C_{16}H_{19}NO_3$

Molecular Weight: 273.33

Procedure: A 5 mL flame-dried, round-bottom flask, equipped with a Teflon-coated stir bar and a rubber septum, was charged with **2-45** (37.84 mg, 0.2 mmol, 1 equiv) and DMAP (2.44 mg, 0.02 mmol, 0.1 equiv). The reaction flask was evacuated and backfilled with N_2 (this process was repeated for 3 times) before the addition of pivaloyl chloride (28.9 mg, 0.24 mmol, 1.2 equiv) and dry, degassed CH_2Cl_2 (0.6 mL, 0.3 M). The resulting homogeneous reaction mixture was stirred at ambient temperature for 16 h and then concentrated *in vacuo*. The resulting crude reaction mixture was purified by silica gel column chromatography (5 % EtOAc in hexanes) to afford **2-48** as a colorless oil (48.1 mg, 0.18 mmol) in 88 % yield.

Characterization:

R_f = (EtOAc/hexanes, 1:9) 0.6; **^{1}H NMR** (400 MHz, $CDCl_3$) δ 7.99 (s, 1H), 7.58 (d, *J* = 3.8 Hz, 1H), 6.83 (s, 1H), 6.47 (d, *J* = 3.8 Hz, 3H), 1.69 (s, 6H), 1.50 (s, 9H).

Compound 2-51a:

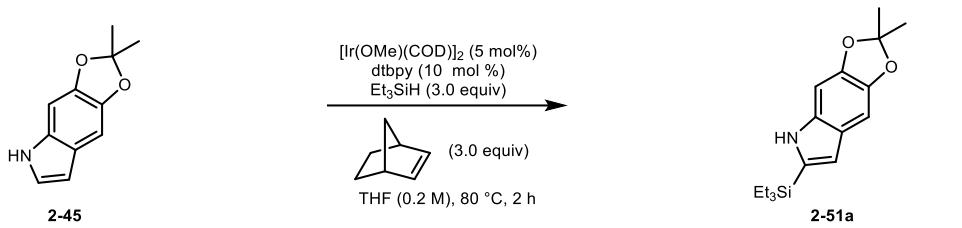

2-45 **2-51a**

Chemical Formula: $C_{17}H_{25}NO_2Si$
Molecular Weight: 303.48

Procedure: A 10 mL flame-dried Schlenk tube equipped with a Teflon-coated stir bar and a glass stopper was charged with the **2-45** (37.8 mg, 0.2 mmol, 1.0 equiv),dtbpy (5.4 mg, 0.02 mmol, 10 mol%), and $[Ir(COD)(OMe)]_2$ (6.6 mg, 0.01 mmol, 5 mol%). The Schlenk tube was evacuated and backfilled with N_2 (this process was repeated three times) and then 2-borbornene (56.5 mg, 0.6 mmol, 3 equiv) and dry, degassed THF (1 mL, 0.2 M) was added under a positive pressure of N_2. After stirring for 5 min, triethylsilane (69.7 mg, 0.6 mmol, 3 euqiv) was added dropwise under a positive pressure of N_2. The resulting reaction mixture was heated at 80 °C for 2 h before cooling to ambient temperature and concentrated *in vacuo*. The crude reaction mixture was then purified by silica gel column chromatography to afford **2-51a** (10.9 mg, 0.036 mmol) as a yellow oil in 18 % yield.

Characterization:

R_f = (EtOAc/hexanes, 1:9) 0.5; **^{1}H NMR** (500 MHz, $CDCl_3$) δ 7.92 (s, 1H), 6.89 (s, 1H), 6.76 (s, 1H), 6.59 (d, *J* = 3.0 Hz, 1H), 1.68 (s, 6H), 1.01 (t, *J* = 7.8 Hz, 9H), 0.80 (q, *J* = 8.2 Hz, 6H).; **^{13}C NMR** (126 MHz, $CDCl_3$) δ 145.55, 143.31, 133.74, 133.56, 122.30, 117.21, 112.53, 98.46, 91.37, 25.90, 7.62, 3.80.

Compound 2-52:

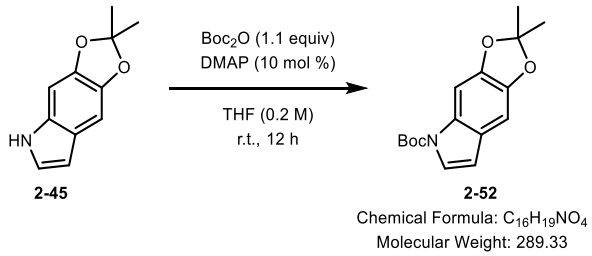

Procedure: A 500 mL flame-dried, round-bottom flask, equipped with a Teflon-coated stir bar and a rubber septum, was charged with **2-45** (9.5 g, 50.0 mmol, 1 equiv), DMAP (610.9 mg, 5.0 mmol, 0.1 equiv), Boc_2O (12.0 g, 55.0 mmol, 1.1 equiv), and THF (250 mL, 0.20 M). The resulting homogeneous reaction mixture was then stirred at ambient temperature for 12 h before concentrated *in vacuo*. The crude reaction mixture was then purified by silica gel column chromatography (5 % EtOAc in hexanes) to afford **2-52** as a white solid (13.02 g, 45.0 mmol) in 90 % yield.

Characterization:

R_f = (EtOAc/hexanes, 1:9) 0.65; **IR** (neat) v = 3154, 3120, 2982, 2935, 1729, 1471, 1392, 1292, 1137, 998, 867, 835, 769, 752 cm^{-1}; **^{1}H NMR** (400 MHz, $CDCl_3$) δ 7.57 (brs, 1H), 7.44 (d, *J* = 3.7 Hz, 1H), 6.83 (s, 1H), 6.42 (dd, *J* = 3.7, 0.7 Hz, 1H), 1.69 (s, 6H), 1.67 (s, 9H). **^{13}C NMR** (126 MHz, $CDCl_3$) δ 149.92, 146.20, 144.51, 129.87, 124.32, 117.87, 107.47, 99.57, 96.85, 83.64, 28.34, 25.91.; **HRMS**: Calcd. For $C_{16}H_{19}O_4NNa$ $[M+Na]^+$ =312.12063 m/z, found =312.12031 m/z.

Compound 2-54:

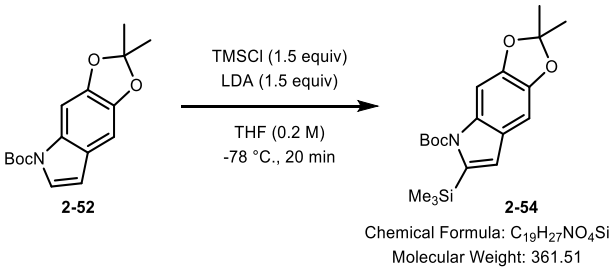

Procedure: A 500 mL flame-dried, round-bottom flask, equipped with a Teflon-coated stir bar and a rubber septum, was charged with **2-52** (10.7 g, 37.0 mmol, 1 equiv). The flask was then evacuated and backfilled with N_2 (this process was repeated for 3 times) before the addition of dry, degassed THF (185 mL, 0.2 M). To the resulting homogeneous mixture was added TMSCl (7.0 mL, 55.5 mmol, 1.5 equiv), and LDA (27.8 mL, 55.5 mmol, 1.5 equiv, 2.0 M in THF) dropwise at

−78 °C in a dry ice/acetone bath under a positive pressure of N_2. The resulting mixture was then stirred at −78 °C for 20 min prior to quenching with a saturated aqueous solution of NH_4Cl (20 mL). The resulting mixture was then extracted with EtOAc (50 mL x 3). The combined organic fractions were washed with brine (50 mL), dried over $MgSO_4$, filtered and concentrated *in vacuo*. The crude mixture was then purified by silica gel column chromatography (5 % EtOAc in hexanes) to afford **2-54** as a white solid (12.5 g, 34.8 mmol) in 94 % yield.

Characterization:

R_f = (EtOAc/hexanes, 1:9) 0.69; **IR** (neat) v = 2979, 2903, 1726, 1472, 1382, 1326, 1203, 1159,1150, 1129, 1027, 904, 842, 768, 632 cm^{-1}; **^{1}H NMR** (500 MHz, $CDCl_3$) δ 7.41 (s, 1H), 6.80 (s, 1H), 6.68 (s, 1H), 1.69 (s, 6H), 1.69 (s, 9H), 0.31 (s, 9H). **^{13}C NMR** (126 MHz, $CDCl_3$) δ 151.15, 146.47, 144.33, 140.46, 132.53, 124.85, 119.38, 117.94, 99.07, 97.09, 83.90, 28.36, 25.90, 0.21.; **HRMS**: Calcd. for $C_{19}H_{27}O_4NNaSi$ $[M+Na]^+$ =384.16016 m/z, found =384.15958 m/z.

Compound 2-57:

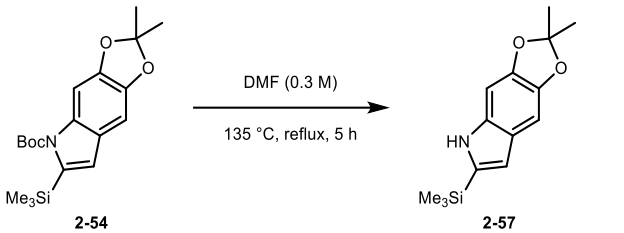

2-54 **2-57**

Chemical Formula: $C_{14}H_{19}NO_2Si$
Molecular Weight: 261.40

Procedure: A flame-dried, 250 mL round-bottom flask equipped with a Teflon-coated stir bar and a rubber septum was charged with **2-54** (3.9 g, 10.0 mmol, 1 equiv) and DMF (36 mL, 0.3 M). The resulting homogenous mixture was heated at reflux (135 °C) under a positive pressure of N_2 and then allowed to cool to ambient temperature after 5 h. The resulting mixture was then extracted with EtOAc (50 mL x 3). The combined organic fractions were washed with H_2O (30 mL x 3) and brine (20 mL x 3), dried over $MgSO_4$, filtered, and concentrated *in vacuo*. The crude reaction mixture was then recrystallized with toluene (13 mL) at 65 °C and then cooled down to −20 °C. Filtration then afforded **2-57** as a white crystal (2.4 g, 9.2 mmol) in 84 % yield.

Characterization: **R_f** = (hexanes/EtOAc, 9:1) 0.53; **IR** (neat) v = 3409, 2985, 2957, 1504, 1451, 1384, 1230, 1153, 1103, 982, 948, 872, 835, 780, 752, 659, 627 wcm^{-1}; **^{1}H NMR** (500 MHz, $CDCl_3$) δ 7.93

(brs, 1H), 6.88 (t, *J* = 0.7 Hz, 1H), 6.76 (t, *J* = 0.7 Hz, 1H), 6.58 (dd, *J* = 2.2, 1.0 Hz, 1H), 1.68 (s, 6H), 0.31 (s, 9H).; **^{13}C NMR** (126 MHz, $CDCl_3$) δ 145.65, 143.40, 136.29, 133.75, 122.33, 117.22, 111.55, 98.56, 91.40, 25.86, -0.84.; **HRMS**: Calcd. for $C_{14}H_{19}NNaO_2Si$ $[M+Na]^+$ = 284.1077 m/z, found = 284.1081 m/z.

Compound 2-58:

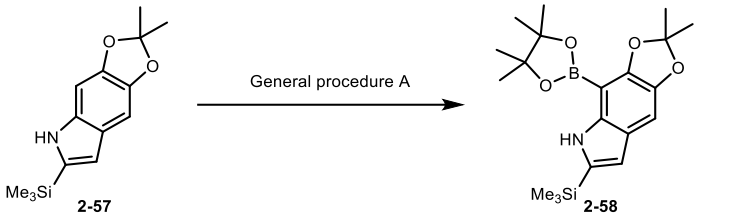

Procedure: The reaction was carried out according to the General Procedure A and was performed in cyclohexanes at room temperature for 40 min.

Amounts of Reagents:

2-57 (2.6 g, 10 mmol, 1.0 equiv)

$[Ir(OMe)(COD)]_2$ (99.43 mg, 0.15 mmol, 1.5 mol%)

dtbpy (80.52 mg, 0.30 mmol, 3.0 mol%)

B_2pin_2 (2.5 g, 10 mmol, 1.0 equiv)

Cyclohexanes (25 mL, 0.4M),

Purification: 10% EtOAc in hexanes.

Yield of Product

2-58: 3.2 g, 8.3 mmol, 83 %, white solid.

Characterization:

R_f = (EtOAc/hexanes, 1:9) 0.50; **IR** (neat) v = 3441, 2982, 2954, 1613, 1452, 1385, 1289, 1194, 1137, 1104, 1061, 991, 836, 754, 667, 628 cm^{-1}; **^{1}H NMR** (500 MHz, $CDCl_3$) δ 9.24 (brs, 1H), 6.98 (s, 1H), 6.56 (d, *J* = 2.3 Hz, 1H), 1.70 (s, 6H), 1.40 (s, 12H), 0.32 (s, 9H).; **^{13}C NMR** (126 MHz, $CDCl_3$) δ 151.78, 142.87, 138.35, 135.34, 121.11, 117.30, 110.54, 102.04, 83.71, 26.00, 25.13, -0.88.; **HRMS**: Calcd. For $C_{20}H_{31}O_4NBSi$ $[M+H]^+$ =388.21099 m/z, found =388.21015 m/z.

Compound 2-60:

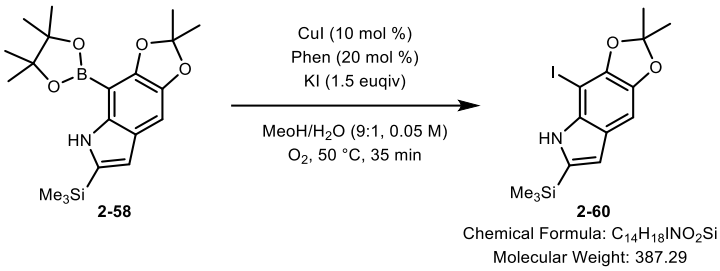

Procedure: A 50 mL round-bottom flask equipped with a Teflon-coated stir bar and a rubber septum was charged with **2-58** (774.72 mg, 2 mmol, 1 equiv), CuI (38.09 mg, 0.2 mmol, 10 mol%), phenanthroline (72.08 mg, 0.4 mmol, 20 mol%), KI (498.0 mg, 3 mmol, 1.5 equiv), and MeOH/H_2O (36 mL/4 mL, 0.05 M, 9:1). The rubber septum was then connected to a tank of O_2, pressurized to 50 kpa, and was vented 3 times for 10 s each time. Under a constant pressure of O_2 (50 kpa), the reaction mixture was then stirred at 50 ^oC for 35 min before depressurizing by opening to the atmosphere and concentrated *in vacuo* to afford a wine-red residue. The resulting mixture was then extracted with EtOAc (50 mL x 3). The phases were separated, and the organic factions were washed with brine (30 mL), dried over $MgSO_4$, filtered, and concentrated *in vacuo*. The resulting crude mixture was purified by silica gel column chromatography (5 % EtOAc in hexanes) to afford **2-60** as a white solid (549.9 mg, 1.42 mmol) in 71 % yield.

Characterization:

$\mathbf{R_f}$ = (EtOAc/hexanes, 1:9) 0.64; **IR** (neat) v = 3367, 2954, 1460, 1310, 1247, 1210, 1190, 1153, 1103, 985, 945, 923, 836, 731 cm^{-1}; **^{1}H NMR** (500 MHz, $CDCl_3$) δ 7.90 (brs, 1H), 6.82 (d, *J* = 0.7 Hz, 1H), 6.73 (d, *J* = 2.3 Hz, 1H), 1.73 (s, 6H), 0.34 (s, 9H).; **^{13}C NMR** (126 MHz, cdcl$_3$) δ 147.09, 142.52, 136.65, 135.27, 121.90, 117.82, 113.06, 98.76, 53.86, 25.97, -0.87.; **HRMS**: Calcd. for $C_{14}H_{19}O_2NISi$ $[M+H]^+$ = 388.02242 m/z, found = 388.02305 m/z.

Compound 2-61:

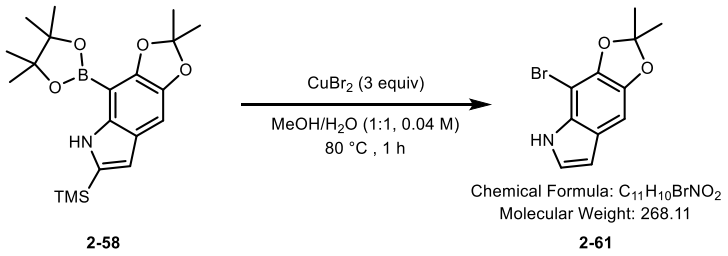

Procedure: A 10 mL flame-dried, round-bottom flask, equipped with a Teflon-coated stir bar and a rubber septum, was charged with **2-58** (77.5 mg, 0.2 mmol, 1 equiv). The reaction flask was then evacuated and backfilled with N_2 (this process was repeated for 3 times) before the addition of MeOH (2.5 mL, 0.08 M) and $CuBr_2$ (134.0 mg, 0.6 mmol, 3 equiv) in H_2O (2.5 mL). The resulting reaction mixture was stirred at 80 °C for 1 h and then opened to the air and concentrated *in vacuo*. The resulting residue was then diluted and extracted with EtOAc (30 mL x 3). The combined organic fractions were washed with brine (20 mL), dried over $MgSO_4$, filtered and concentrated *in vacuo*. The crude mixture was then purified by silica gel column chromatography (10 % EtOAc in hexanes) to afford **2-61** as a yellow solid (10.7 mg, 0.04 mmol) in 20 % yield.

Characterization: $\mathbf{R_f}$ = (EtOAc/hexanes, 1:9) 0.65; **^{1}H NMR** (500 MHz, $CDCl_3$) δ 8.13 (brs, 1H), 7.10 (dd, *J* = 3.1, 2.4 Hz, 1H), 6.87 (d, *J* = 0.7 Hz, 1H), 6.48 (dd, *J* = 3.1, 2.2 Hz, 1H), 1.74 (s, 6H).; **HRMS**: Calcd. for $C_{14}H_{19}O_2NISi$ $[M+H]^+$ = 388.02242 m/z, found = 388.02305 m/z.

Compound 2-62:

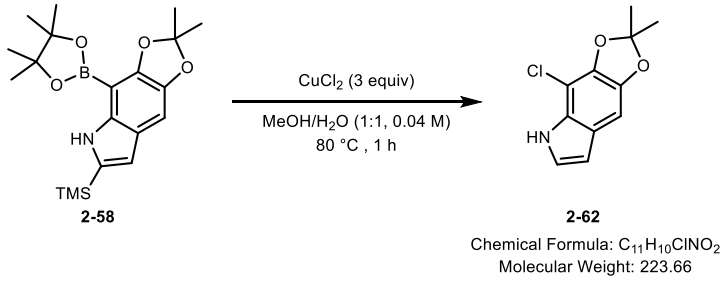

Procedure: A 5 mL flame-dried, round-bottom flask, equipped with a Teflon-coated stir bar and a rubber septum, was charged with **2-58** (38.7 mg, 0.1 mmol, 1 equiv). The flask was then evacuated and backfilled with N_2 (this process was repeated for 3 times) before the addition of MeOH (1.25 mL, 0.08 M) and $CuCl_2$ (40.3 mg, 0.3 mmol, 3 equiv) in H_2O (1.25 mL). The resulting reaction mixture was stirred at 80 °C for 1 h and then opened to the air and concentrated *in*

vacuo. The resulting residue was then diluted and extracted with EtOAc (10 mL x 3). The combined organic fractions were washed with brine (10 mL) and dried over $MgSO_4$, filtered and concentrated *in vacuo*. The crude mixture was purified by silica gel column chromatography (10 % EtOAc in hexanes) to afford **2-62** as a yellow solid (10.5 mg, 0.05 mmol) in 47 % yield.

Characterization:

R_f = (EtOAc/hexanes, 1:9) 0.65; **^{1}H NMR** (500 MHz, $CDCl_3$) δ 8.17 (brs, 1H), 7.10 (dd, *J* = 3.1, 2.4 Hz, 1H), 6.85 (d, *J* = 0.7 Hz, 1H), 6.44 (dd, *J* = 3.1, 2.2 Hz, 1H), 1.74 (s, 6H).

Compound 2-63:

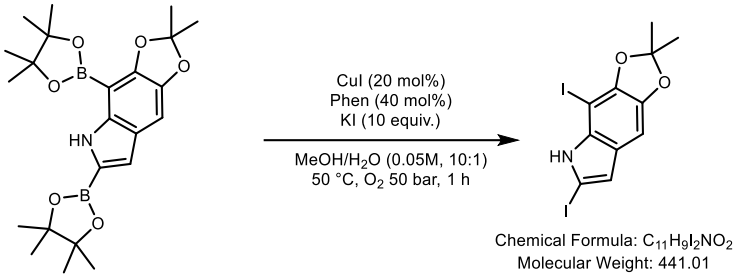

Procedure: A 10 mL round-bottom flask equipped with a Teflon-coated stir bar and a rubber septum was charged with **2-47** (44.14 mg, 0.1 mmol, 1.0 equiv), CuI (1.9 mg, 0.01 mmol, 10 mol%), 1,10-phenanthroline (Phen, 3.6 mg, 0.02 mmol, 20 mol%), KI (166.0 mg, 1.0 mmol, 10 equiv), and MeOH/H_2O (1.8 mL/0.2 mL, 0.05 M, 9:1). The rubber septum was then connected to a tank of O_2, pressurized to 50 kpa, and was vented 3 times for 10 s each time. Under a constant pressure of O_2 (50 kpa), the reaction mixture was then stirred at 50 ^oC for 1 h before depressurizing by opening to the atmosphere and concentrated *in vacuo* to afford a wine-red residue. The resulting residue was then diluted and extracted with EtOAc (30 mL x 3). The combined organic fractions were washed with brine (10 mL) and dried over $MgSO_4$, filtered and concentrated *in vacuo*. The resulting crude mixture was purified by silica gel column chromatography (10 % EtOAc in hexanes) to afford **2-63** as a yellow solid (15.4 mg, 0.035 mmol) in 35 % yield.

Characterization:

R_f = (EtOAc/hexanes, 1:9) 0.35; **^{1}H NMR** (400 MHz, $CDCl_3$) δ 7.91 (s, 1H), 6.75 (d, *J* = 0.6 Hz, 1H), 6.68 (d, *J* = 2.2 Hz, 1H), 1.72 (s, 6H).; **HRMS**: Calcd. for $C_{11}H_9I_2NNaO_2$ $[M+Na]^+$ = 463.8615 m/z, found = 463.2413 m/z.

Compound 2-67:

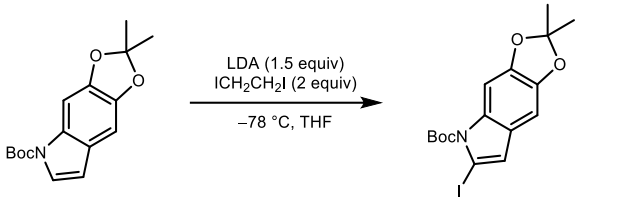

2-52 **2-67**

Chemical Formula: $C_{16}H_{18}INO_4$
Molecular Weight: 415.23

Procedure: A 5 mL flame-dried, round-bottom flask, equipped with a Teflon-coated stir bar and a rubber septum, was charged with **2-52** (28.93 mg, 0.1 mmol, 1 equiv). The flask was then evacuated and backfilled with N_2 (this process was repeated for 3 times) before the addition of dry, degassed THF (1 mL, 0.1 M). To the resulting homogeneous reaction solution was added LDA (0.075 mL, 0.15 mmol, 1.5 equiv, 2.0 M in THF) dropwise at −78 °C in a dry ice/acetone bath under a positive pressure of N_2. The resulting reaction mixture was then stirred at −78 °C for 1 h prior to the addition of 1,2-diiodoethane (56.3 mg, 0.2 mmol, 2 equiv). After stirring at −78 °C for additional 30 min, the reaction mixture was quenched by the addition of a saturated aqueous solution of NH_4Cl (5 mL). The resulting mixture was then extracted with EtOAc (20 mL x 3). The combined organic fractions were then washed with brine (20 mL), dried over $MgSO_4$, filtered and concentrated *in vacuo*. The resulting crude mixture was purified by silica gel column chromatography (30 % CH_2Cl_2 in hexanes) to afford **2-67** as a yellow oil (29.1 mg, 0.07 mmol) in 70 % yield.

Characterization:

R_f = (CH_2Cl_2/hexanes, 3:7) 0.30; **^{1}H NMR** (400 MHz, $CDCl_3$) δ 7.54 (s, 1H), 6.81 (s, 1H), 6.73 (s, 1H), 1.70 (s, 9H), 1.68 (s, 6H).; **^{13}C NMR** (126 MHz, $CDCl_3$) δ 149.36, 146.39, 144.50, 132.40, 125.07, 121.93, 118.11, 98.03, 97.28, 85.31, 70.04, 28.45, 25.93.; **HRMS**: Calcd. for $C_{16}H_{18}INNaO_4$ $[M+Na]^+$ =438.0173 m/z, found =438.0163 m/z.

2.8 Reference

1. Mostert, A. B., Melanin, the What, the Why and the How: An Introductory Review for Materials Scientists Interested in Flexible and Versatile Polymers. *Polymers* **2021,** *13* (10).

2. Napolitano, A.; Corradini, M. G.; Prota, G., A Reinvestigation of the Structure of Melanochrome. *Tetrahedron Letters* **1985,** *26* (23), 2805-2808.

3. Kim, Y. J.; Khetan, A.; Wu, W.; Chun, S.-E.; Viswanathan, V.; Whitacre, J. F.; Bettinger, C. J., Evidence of Porphyrin-Like Structures in Natural Melanin Pigments Using Electrochemical Fingerprinting. *Advanced Materials* **2016,** *28* (16), 3173-3180.

4. Chen, C. T.; Chuang, C.; Cao, J.; Ball, V.; Ruch, D.; Buehler, M. J., Excitonic effects from geometric order and disorder explain broadband optical absorption in eumelanin. *Nature Communication* **2014,** *5*, 3859.

5. Panzella, L.; Pezzella, A.; Napolitano, A.; d'Ischia, M., The First 5,6-Dihydroxyindole Tetramer by Oxidation of 5,5‘,6,6‘-Tetrahydroxy-2,4‘-biindolyl and an Unexpected Issue of Positional Reactivity en Route to Eumelanin-Related Polymers. *Organic Letters* **2007,** *9* (7), 1411-1414.

6. d'Ischia, M.; Napolitano, A.; Tsiakas, K.; Prota, G., New intermediates in the oxidative polymerisation of 5,6-dihydroxyindole to melanin promoted by the peroxidase/H_2O_2 system. *Tetrahedron* **1990,** *46* (16), 5789-5796.

7. Jones, D. W.; Pomfret, A., 1,4-Di-o-toly-2,3-naphthoquinone. *Journal of the Chemical Society, Perkin Transactions 1* **1991,** (1), 13-18.

8. Napolitano, A.; Pezzella, A.; d'Ischia, M.; Prota, G., The first characterisation of a transient 5,6-indolequinone. *Tetrahedron Letters* **1996,** *37* (24), 4241-4242.

9. Chen, C.-T.; Martin-Martinez, F. J.; Jung, G. S.; Buehler, M. J., Polydopamine and eumelanin molecular structures investigated with ab initio calculations. *Chemical Science* **2017,** *8* (2), 1631-1641.

10. Meng, S.; Kaxiras, E., Theoretical Models of Eumelanin Protomolecules and their Optical Properties. *Biophysical Journal* **2008,** *94* (6), 2095-2105.

11. Wakamatsu, K.; Ito, S., Preparation of Eumelanin-Related Metabolites 5,6-Dihydroxyindole, 5,6-Dihydroxyindole-2-Carboxylic Acid, and Their O-Methyl Derivatives. *Anal Biochem* **1988,** *170* (2), 335-340.

12. Wipf, P.; Kim, Y. T., Studies on the Synthesis of Stemona Alkaloids-Stereoselective Preparation of the Hydroindole Ring-System by Oxidative Cyclization of Tyrosine. *Tetrahedron Letters* **1992,** *33* (38), 5477-5480.

13. L'Homme, C.; Menard, M. A.; Canesi, S., Synthesis of the erythrina alkaloid erysotramidine. *The Journal of Organic Chemistry* **2014,** *79* (17), 8481-8485.

14. Esguerra, K. V. N.; Fall, Y.; Lumb, J.-P., A Biomimetic Catalytic Aerobic Functionalization of Phenols. *Angewandte Chemie International Edition* **2014,** *53* (23), 5877-5881.

15. Huang, Z.; Askari, M. S.; Esguerra, K. V. N.; Dai, T.-Y.; Kwon, O.; Ottenwaelder, X.; Lumb, J.-P., A bio-inspired synthesis of oxindoles by catalytic aerobic dual C–H functionalization of phenols. *Chemical Science* **2016,** *7* (1), 358-369.

16. Leitch, J. A.; Bhonoah, Y.; Frost, C. G., Beyond C2 and C3: Transition-Metal-Catalyzed C–H Functionalization of Indole. *Acs Catalysis* **2017,** *7* (9), 5618-5627.

17. Candish, L.; Teders, M.; Glorius, F., Transition-Metal-Free, Visible-Light-Enabled Decarboxylative Borylation of Aryl N-Hydroxyphthalimide Esters. *Journal of the American Chemical Society* **2017,** *139* (22), 7440-7443.

18. Cheng, W. M.; Shang, R.;Zhao, B.; Xing, W. L.; Fu, Y., Isonicotinate Ester Catalyzed Decarboxylative Borylation of (Hetero)Aryl and Alkenyl Carboxylic Acids through N-Hydroxyphthalimide Esters. *Organic Letters* **2017,** *19* (16), 4291-4294.

19. Cornella, J.; Sanchez, C.; Banawa, D.; Larrosa, I., Silver-catalysed protodecarboxylation of ortho-substituted benzoic acids. *Chem Commun (Camb)* **2009,** (46), 7176-8.

20. Gooßen, L. J.; Thiel, W. R.; Rodríguez, N.; Linder, C.; Melzer, B., Copper-Catalyzed Protodecarboxylation of Aromatic Carboxylic Acids. *Advanced Synthesis & Catalysis* **2007,** *349* (14-15), 2241-2246.

21. Piers, E.; Haarstad, V. B.; Cushley, R. J.; Brown, R. K., The Synthesis of Mercaptoindoles. *Canadian Journal of Chemistry* **1962,** *40* (3), 511-517.

22. Cohen, T.; Schambach, R. A., Copper-quinoline decarboxylation. *Journal of the American Chemical Society* **1970,** *92* (10), 3189-3190.

23. Ishiyama, T.; Takagi, J.; Hartwig, J. F.; Miyaura, N., A Stoichiometric Aromatic C□H Borylation Catalyzed by Iridium(I)/2,2′-Bipyridine Complexes at Room Temperature. *Angewandte Chemie International Edition* **2002,** *41* (16), 3056-3058.

24. Takagi, J.; Sato, K.; Hartwig, J. F.; Ishiyama, T.; Miyaura, N., Iridium-catalyzed C–H coupling reaction of heteroaromatic compounds with bis(pinacolato)diboron: regioselective synthesis of heteroarylboronates. *Tetrahedron Letters* **2002,** *43* (32), 5649-5651.

25. Kallepalli, V. A.; Shi, F.; Paul, S.; Onyeozili, E. N.; Maleczka, R. E., Jr.; Smith, M. R., 3rd, Boc groups as protectors and directors for Ir-catalyzed C-H borylation of heterocycles. *The Journal of Organic Chemistry* **2009,** *74* (23), 9199-201.

26. Paul, S.; Chotana, G. A.; Holmes, D.; Reichle, R. C.; Maleczka, R. E., Jr.; Smith, M. R., 3rd, Ir-catalyzed functionalization of 2-substituted indoles at the 7-position: nitrogen-directed aromatic borylation. *Journal of the American Chemical Society* **2006,** *128* (49), 15552-3.

27. Boebel, T. A.; Hartwig, J. F., Silyl-directed, iridium-catalyzed ortho-borylation of arenes. A one-pot ortho-borylation of phenols, arylamines, and alkylarenes. *Journal of the American Chemical Society* **2008,** *130* (24), 7534-5.

28. Perry, G. J. P.; Quibell, J. M.; Panigrahi, A.; Larrosa, I., Transition-Metal-Free Decarboxylative Iodination: New Routes for Decarboxylative Oxidative Cross-Couplings. *Journal of the American Chemical Society* **2017,** *139* (33), 11527-11536.

29. Quibell, J. M.; Perry, G. J. P.; Cannas, D. M.; Larrosa, I., Transition-metal-free decarboxylative bromination of aromatic carboxylic acids. *Chemical Science* **2018,** *9* (15), 3860-3865.

30. Partridge, B. M.; Hartwig, J. F., Sterically Controlled Iodination of Arenes via Iridium-Catalyzed C–H Borylation. *Organic Letters* **2013,** *15* (1), 140-143.

31. Loach, R. P.; Fenton, O. S.; Amaike, K.; Siegel, D. S.; Ozkal, E.; Movassaghi, M., C7-derivatization of C3-alkylindoles including tryptophans and tryptamines. *J Org Chem* **2014,** *79* (22), 11254-63.

32. E. Zembower, D.; Xie, Y.; Koohang, A.; J. Kuffel, M.; M. Ames, M.; Zhou, Y.; Mishra, R.; Aye Mar, A.; T. Flavin, M.; Xu, Z.-Q., Methylenedioxy- and Ethylenedioxy-Fused Indolocarbazoles: Potent Human Topoisomerase I Inhibitors and Antitumor Agents. *Anti-Cancer Agents in Medicinal Chemistry* **2012,** *12* (9), 1117-1131.

33. Pagni, R., Solvents and Solvent Effects in Organic Chemistry, Third Edition (Christian Reichardt). *Journal of Chemical Education* **2005,** *82* (3), 382.

34. Lv, J.; Chen, X.; Xue, X.-S.; Zhao, B.; Liang, Y.; Wang, M.; Jin, L.; Yuan, Y.; Han, Y.; Zhao, Y.; Lu, Y.; Zhao, J.; Sun, W.-Y.; Houk, K. N.; Shi, Z., Metal-free directed sp2-C–H borylation. *Nature* **2019,** *575* (7782), 336-340.

35. Iqbal, S. A.; Cid, J.; Procter, R. J.; Uzelac, M.; Yuan, K.; Ingleson, M. J., Acyl-Directed ortho-Borylation of Anilines and C7 Borylation of Indoles using just BBr3. *Angewandte Chemie International Edition* **2019,** *58* (43), 15381-15385.

36. Hartung, C. G.; Fecher, A.; Chapell, B.; Snieckus, V., Directed ortho Metalation Approach to C-7-Substituted Indoles. Suzuki−Miyaura Cross Coupling and the Synthesis of Pyrrolophenanthridone Alkaloids. *Organic Letters* **2003,** *5* (11), 1899-1902.

37. Toutov, A. A.; Liu, W.-B.; Betz, K. N.; Fedorov, A.; Stoltz, B. M.; Grubbs, R. H., Silylation of C–H bonds in aromatic heterocycles by an Earth-abundant metal catalyst. *Nature* **2015,** *518*, 80.

38. Rawal, V. H.; Cava, M. P., Thermolytic removal of t-butyloxycarbonyl (BOC) protecting group on indoles and pyrroles. *Tetrahedron Letters* **1985,** *26* (50), 6141-6142.

39. Baran, P. S.; Shenvi, R. A.; Mitsos, C. A., A Remarkable Ring Contraction En Route to the Chartelline Alkaloids. *Angewandte Chemie International Edition* **2005,** *44* (24), 3714-3717.

40. apelqvist, T.; Wensbo, D., Selective removal of the N-BOC protective group using silica gel at low pressure. *Tetrahedron Letters* **1996,** *37* (9), 1471-1472.

41. Zhang, A. J.; Russell, D. H.; Zhu, J. P.; Burgess, K., A method for removal of N-BOC protecting groups from substrates on TFA-sensitive resins. *Tetrahedron Letters* **1998,** *39* (41), 7439-7442.

42. Pinkerton, D. M.; Banwell, M. G.; Willis, A. C., Total syntheses of tambjamines C, E, F, G, H, I and J, BE-18591, and a related alkaloid from the marine bacterium Pseudoalteromonas tunicata. *Organic Letters* **2007,** *9* (24), 5127-30.

43. Beck, E. M.; Hatley, R.; Gaunt, M. J., Synthesis of rhazinicine by a metal-catalyzed C-H bond functionalization strategy. *Angewandte Chemie International Edition* **2008,** *47* (16), 3004-7.

44. Murphy, J. M.; Liao, X.; Hartwig, J. F., Meta Halogenation of 1,3-Disubstituted Arenes via Iridium-Catalyzed Arene Borylation. *Journal of the American Chemical Society* **2007,** *129* (50), 15434-15435.

45. Tichenor, M. S.; Trzupek, J. D.; Kastrinsky, D. B.; Shiga, F.; Hwang, I.; Boger, D. L., Asymmetric Total Synthesis of (+)- and ent-(−)-Yatakemycin and Duocarmycin SA: Evaluation of

Yatakemycin Key Partial Structures and Its Unnatural Enantiomer. *Journal of the American Chemical Society* **2006,** *128* (49), 15683-15696.

46. Leibig, D.; Müller, A. H. E.; Frey, H., Anionic Polymerization of Vinylcatechol Derivatives: Reversal of the Monomer Gradient Directed by the Position of the Catechol Moiety in the Copolymerization with Styrene. *Macromolecules* **2016,** *49* (13), 4792-4801.

47. Batcho, A. D.; Leimgruber, W., Indoles from 2-Methylnitrobenzenes by Condensation with Formamide Acetals Followed by Reduction: 4-Benzyloxyindole, *Org. Synth*. **1985**, *63*, 214

Chapter 3 : Eumelanin Chain Growth

3.1 Introduction

Previous efforts to synthesize eumelanin from **DHI** or **DHICA** relying upon biomimetic oxidation in which chain-growth, chain-oxidation and chain-aggregation occur in competition resulted in complex mixtures with low yields and limited synthetic value.[1-3] Further insights into the structure of the oligomeric species generated during the oxidative polymerization of **DHI** have been hindered by the marked complexity of the reaction mixtures and poor isolated yields. The availability of a collection of **DHI** oligomers of variable molecular size is therefore pivotal for future advances in the structural characterization of eumelanin biopolymers. The current state-of-the-art to access eumelanin derivatives with high purity is restricted to chains of up to three **DHI** units (Chapter 1, Scheme 1-31).[4, 5]

Eliminating this synthesis bottleneck thus represents both a major challenge and an extraordinary opportunity for eumelanin chemistry. In Chapter 3, we develop a complementary approach that compartmentalizes C-C bond formation (chain growth) from chain-oxidation and chain-aggregation. More specifically, we devise a bottom-up, iterative strategy that leverages the precision of C-H functionalization and transition metal-catalyzed cross-coupling.

Iterative building block assembly has been successfully demonstrated in the preparation of polypeptides[6] and oligonucleotides[7], which have given rise to automated synthesizers and revolutionized the field of synthetic biology, therapeutics, drug discovery *etc*. There are also examples of iterative synthetic platforms that have been applied to small-molecule synthesis, as described by the groups of Aggarwal,[8, 9, 10] Crudden,[11] Burke[12] and others[13-15]. For example, iterative cross-coupling that sequentially assembles bifunctional *N*-methyliminodiacetic acid (MIDA) boronate has been demonstrated and automated for the syntheses of more than 10 natural small molecules, such as crocacin C and ratanhine, by Burke and co-workers (Scheme 3-1).[12, 16, 17] These iterative cycles relied on bifunctional MIDA boronate building blocks. MIDA ligands attenuate the reactivity of boronic acid in cross-coupling reactions thus preventing

undesired oligomerization. Subsequent deprotection of MIDA then enables another round of Suzuki-coupling, and eventually, to the iterative and automated synthesis of complex targets.

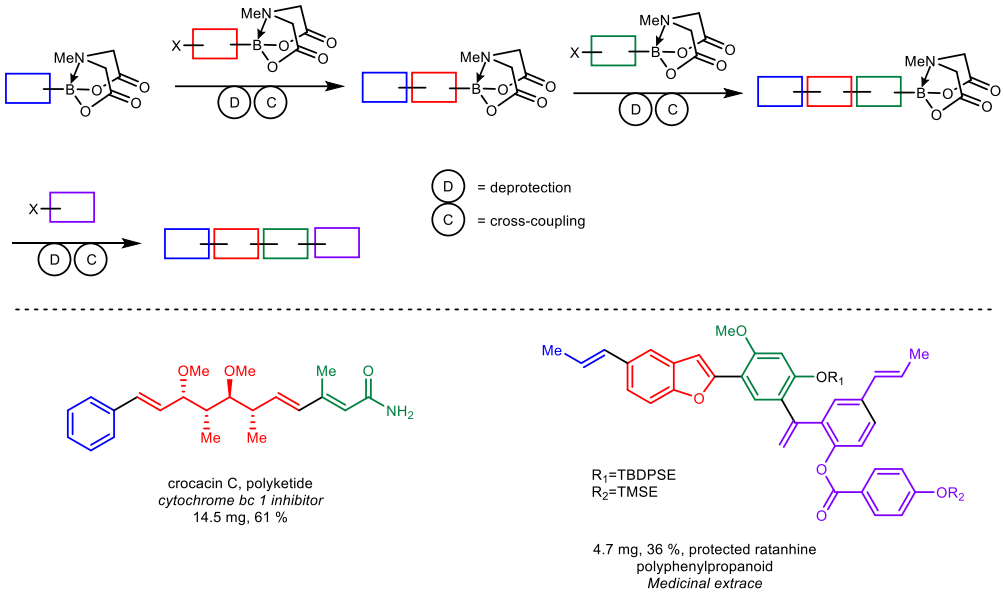

Scheme 3-1 Iterative cross coupling of bifunctional MIDA boronate

Beyond natural products, iterative assembly methods have also enabled the synthesis of oligomeric materials. For example, a convergent iterative synthesis has been developed by Moore and co-workers for the synthesis of phenylacetylene oligomers **3-6** (Scheme 3-2).[18, 19]

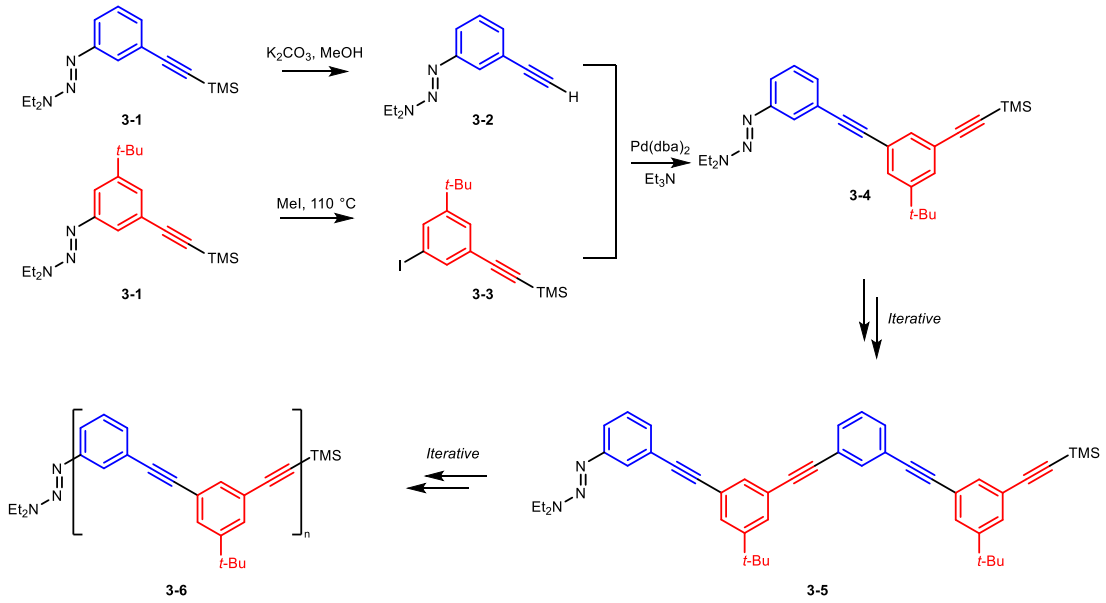

Scheme 3-2 Iterative synthesis of phenylacetylene oligomers

The bifunctional building block can be selectively activated in two different ways: a dialkyltriazene (**3-1**) can be converted to an iodide (**3-3**) with methyl iodide or a TMS protecting group can be removed to reveal a reactive terminal alkyne (**3-2**). Sonogashira coupling of **3-2** and **3-3** afford intermediate **3-4**, which contains a dialkyltriazene moiety and a protected alkyne moiety. Repeating this process using **3-4** enables rapid exponential molecular growth to **3-5** then **3-6** (Scheme 3-2).

Eumelanin presents an ideal example for iterative building block assembly, as it incorporates common repeat motifs, namely **DHI** and **DHICA**. However, an iterative strategy has never been demonstrated for eumelanin synthesis. In Chapter 3, we describe an iterative synthesis of a eumelanin dimer, trimer, tetramer, and pentamer through an iterative sequence of Suzuki-cross coupling, desilylation, and selective borylation (Scheme 3-3).

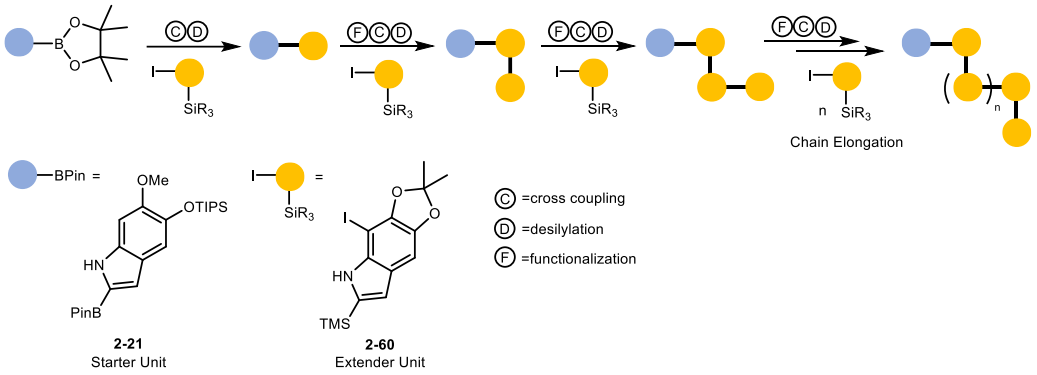

Scheme 3-3 This work: Iterative synthesis of eumelanin oligomer derivatives

We focus on the interative assembly of functionalized **DHI** building blocks through the 2- and 7'-positions, as this particular linkage has a long history in the melanin literature as a hypothetical site for chain-growth.[20, 21] Key to our iterative-chain-growth (ICG) strategy is the design of monomer **2-60**, bearing a silyl group at C2 and a halogen at C7. This design was crucial for chain elongation since the C2 silyl group blocked reactivity at C3 during cross coupling, but could be removed under mildly acidic conditions to allow for a sequential round of chain extension by selective borylation at C2.

Collectively, this advance forms the basis of Chapter 3. In Section 3.2, we detail conditions for carbon-carbon bond formation between C2 and C7' positions to form dimers. In section 3.3, we

describe our efforts to functionalize the C2 or C7 positions of the dimers. In Section 3.4, we demonstrate the synthesis of eumelanin chains up to a pentamer employing our generalized, robust iterative-chain-growth (ICG) strategy (Scheme 3-4).

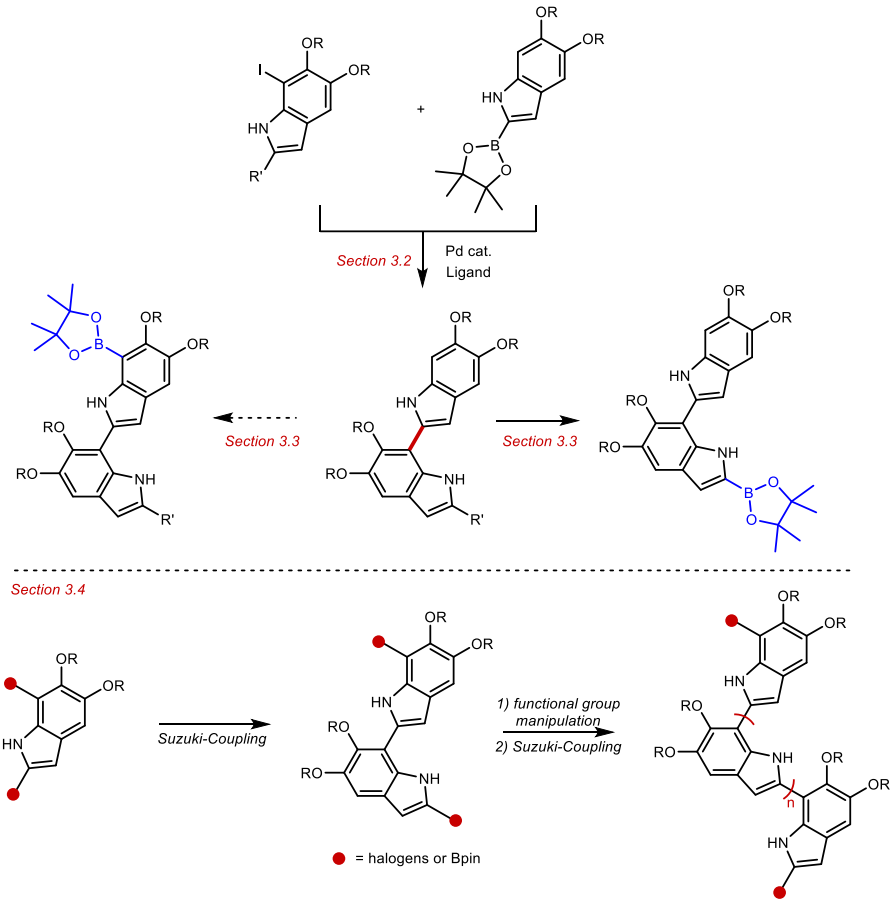

Scheme 3-4 Outline for Chapter 3

3.2 Synthesis of 2,7'-dimers

Having developed efficient syntheses of the necessary monomer building blocks (Chapter 2), we turned our attention toward their coupling. We began by examining well-established Suzuki-coupling conditions that have been previously used in C2 or C7 cross-coupling reactions of indole heterocycles.

Suzuki-Miyaura coupling (SMC) reactions have been extensively explored over the past two decades,[22, 23] and they provide mild conditions for creating biaryl bonds with good functional group tolerance. Nevertheless, nitrogen-containing heterocycles with free N-H groups present persistent challenges due to rapid protodeborylation under typical SMC reaction conditions at

elevated temperatures,[24, 25] and the potential for N-Pd complexes to form under basic conditions.[26] In the early 2000s, Buchwald and co-workers developed several highly efficient dialkylbiaryl phosphine ligands for the Pd-catalyzed SMC reaction of heteroaryl halides and heteroaryl boronic acids or esters (Table 3-1).[24, 27, 28]

Table 3-1 Suzuki-Coupling of indole or pyrrole heterocycles with dialkylbiaryl phophine ligands

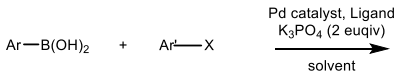

Entry	Boronic Acid	Aryl halide	Catalyst	Ligand	solvent/temperature	Yield (%)
1	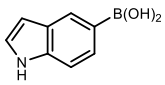 **3-7**	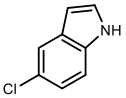 **3-8**	Pd_2dba_3	XPhos	n-butanol, 100 °C	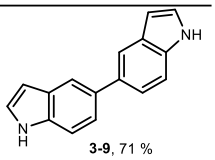 **3-9**, 71 %
2	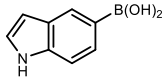 **3-7**	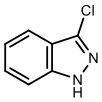 **3-10**	SPhos-Pd-G_2	NA	dioxane/H_2O, 100 °C	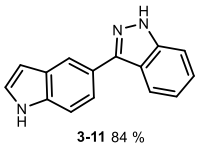 **3-11** 84 %
3	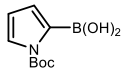 **3-12**	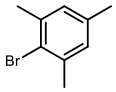 **3-13**	$Pd(OAc)_2$	SPhos	n-butanol, 100 °C	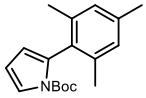 **3-14,** 89 %
4	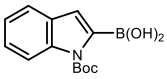 **3-15**	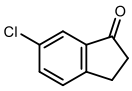 **3-16**	XPhos-Pd-G_2	NA	THF/aq.0.5 M K_3PO_4, 40°C	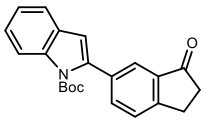 **3-17**, 88 %

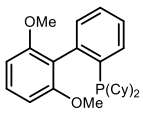
SPhos

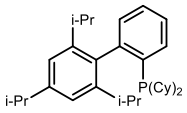
XPhos

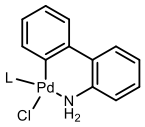
L=XPhos, XPhos-Pd-G2
L=SPhos, SPhos-Pd-G2

In their work, treatment of N-H indoles **3-7** and **3-8** with Pd_2dba_3 and XPhos afforded the cross-coupled product **3-9** in 71 % at 100 °C (entry 1). The use of the SPhos-Pd-G2 pre-catalyst delivered the cross-coupled product **3-11** in an 84 % yield after SMC reaction between **3-7** and 3-chloroindazole **3-10** (entry 2). Using SPhos (entry 3) or XPhos-Pd-G2 (entry 4) as a ligand, N-Boc-protected pyrroles (**3-12**) and indoles with a boronic acid at C2 (**3-13**), which are known to be

susceptible to protodeborylation, also provided good yields in the coupling with aryl bromide **3-13** or chloride **3-16** (Table 3-1).

In addition, Chai and co-workers have demonstrated the synthesis of dimers via a one-pot Miyaura borylation and subsequent transition metal-mediated Suzuki-Miyaura cross-coupling protocol between two bromoindoles (Chapter 1, Scheme 1-28). Following the same strategy, a collection of biindolyls were also obtained in their work, which include 4,4'- (**3-18**), 4,7'- (**3-20**), and 7,7'-(**3-19**) dimers (Scheme 3-5).[29]

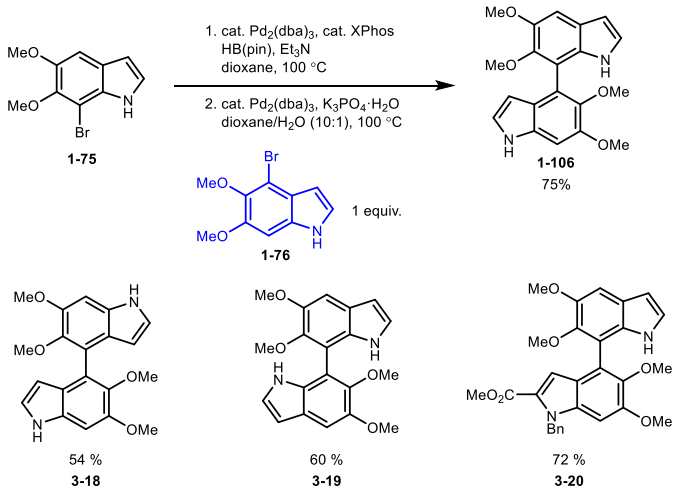

Scheme 3-5 One-pot Miyaura borylation and Suzuki-Miyaura coupling to biindoles

With these precedents in mind, we investigated SMC conditions between monomers **2-37** and **2-21** (Table 3-2). With the X-Phos-Pd-G3 precatalyst (5 mol %), K_3PO_4 (2.1 equiv.) in THF and H_2O (2.8:1) at ambient temperature, the desired dimer **3-21** was obtained in 36 % yield (entry 1). Similarly, the use of the SPhos-Pd-G3 precatalyst led to a 26 % yield of **3-21** (entry 2)**.** With $Pd(OAc)_2$ (5 mol %) and XPhos (5.5 mol%), the yield of **3-21** was improved to 68 % (entry 3). Switching the ligand to SPhos further improved the yield of **3-21** to 80 % (entry 4). Over the course of our optimization studies, we discovered that H_2O was required for a successful reaction; too little water led to a decreased yield of **3-21** (entry 5).[30] The effect of H_2O is consistent with previous studies by Denmark and Hartwig,[31, 32] in which transmetalation proved to be occurring between an aryl-Pd(II)-OH complex and a neutral boronic acid in the intermolecular Suzuki coupling. To drive the reaction closer to complete conversion, extended reaction times and

elevated temperatures were applied to the conditions composed of $Pd(OAc)_2$ (5 mol %) and SPhos (5.5 mol %). To our delight, complete conversions of both **2-37** and **2-21** were attained and the yield of **3-21** was increased to 88 % (entry 6).

Table 3-2 Optimization of reaction conditions for Suzuki Coupling between **2-37** and **2-21**

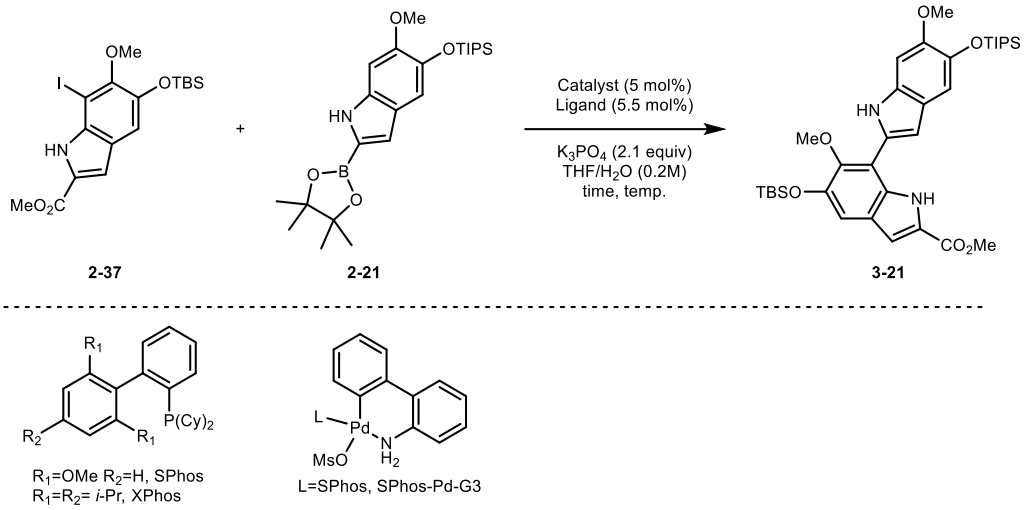

Entry	Catalyst	Ligand	Time (h)	Temp (°C)	THF/H_2O	Conversion **2-37**/**2-21** (%)	Yield [a] (%)
1	XPhos-Pd-G3	NA	1	r.t.	2.8/1	49/43	36
2	Sphos-Pd-G3	NA	1	r.t.	2.8/1	29/65	26
3	$Pd(OAc)_2$	XPhos	1	r.t.	2.8/1	70/84	68
4	$Pd(OAc)_2$	SPhos	1	r.t.	2.8/1	81/84	80
5	$Pd(OAc)_2$	SPhos	1	r.t.	10/1	67/73	50
6	$Pd(OAc)_2$	SPhos	3	65	2.8/1	100/100	88

c) Yields were determined by NMR with hexamethylbenzene as the internal standard.

Purification of **3-21**, however, was challenging because it was inseparable from impurities by column chromatography. At ambient temperature, as mentioned above, the reaction proceeded with an incomplete conversion. Major impurities, in this case, were the unreacted substrates **2-37** and **2-21**. At elevated temperature, when the complete conversion was achieved, other impurities that were not identifiable but close in polarity with **3-21** were observed. As a workaround, **2-37b** was exploited as an alternative 7-iodide coupling partner. The difference in R_f value between **3-22** and the remaining substrate is then greater than it was between **3-21**, which makes purification and isolation of **3-22** significantly easier.

The optimization studies of Suzuki coupling between **2-37b** and **2-21** are summarized in Table 3-3. Treatment of **2-37b** and **2-21** with $Pd(OAc)_2$ as the catalyst and SPhos as the ligand at ambient temperature afforded 82 % and 80 % conversion of **2-37b** and **2-21** respectively. However, the yield of **3-22** was only 38 % (entry 1). Employing SPhos-Pd-G3 precatalyst (entry 2) or a bulkier ligand XPhos (entry 3) proved to be ineffective as well. Gratifyingly, when elevating the reaction temperatures to 65 °C under $Pd(OAc)_2$ and SPhos conditions, we obtained **3-22** in 61 % yield (entry 4). Extending the reaction time to 2 h delivered **3-22** in 65 % yield with no observable byproducts and thus was suitable for purification by column chromatography (entry 5).

Table 3-3 Optimization of reaction conditions for Suzuki coupling between **2-37b** and **2-21**

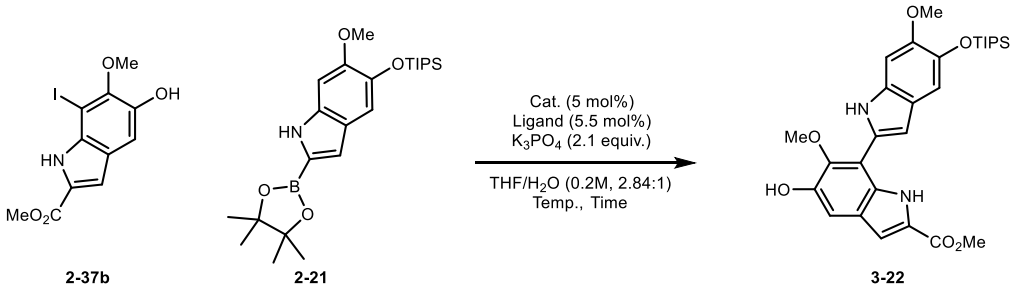

Entry	Catalyst	Ligand	Time (h)	Temp (°C)	Conversion **2-37b**/**2-21** (%)	Yield [a] (%)
1	$Pd(OAc)_2$	SPhos	4	r.t.	82/80	38
2	SPhos-Pd-G_3	NA	4	r.t.	47/30	12
3	$Pd(OAc)_2$	XPhos	4	r.t.	79/77	35
4	$Pd(OAc)_2$	SPhos	1	65	80/93	61
5	$Pd(OAc)_2$	SPhos	2	65	80/97	65

a) Yields were determined by NMR with hexamethylbenzene as an internal standard

3.3 Functionalization at the C2 and C7 Positions on Dimers

To extend dimers to higher-order oligomers, we investigated conditions to grow chains along the C7 position and the C2 position separately. In section 3.2.1, we detail our efforts to install a functional handle at the C7 position of the dimers. In section 3.2.2, we describe selective C2 functionalization of the dimers.

3.3.1 Efforts Toward C7 borylation on Dimers

With the previous success of N-H directed C7 borylation on monomers **2-28** (Chapter 2, Scheme 2-9), we attempted to implement the same borylation strategy to dimer **3-21**. Our enthusiasm

for this strategy, however, was quickly diminished, as all attempts to borylate the C7 position on dimers produced none of the desired product.

For example, with dimer **3-21**, attempted borylation under Ir-catalyzed conditions proceeded with less than 5 % conversion and no desired product **3-23** was detected (Scheme 3-6). We hypothesized that the challenges of functionalizing at the C7 position stemmed from 1) the deactivation of the Ir catalyst via coordination with both of the indole nitrogens (**3-21a**, Scheme 3-7) or 2) the increased steric hindrance from the C5-TBS and C6-methyl substituents (**3-21b**, Scheme 3-7) that might prevent hydrogen bonding between the hydrogen on the indole nitrogen and an oxygen atom of a B-Pin on Ir, as has been proposed in the literature (**3-25**, Scheme 3-7).[33]

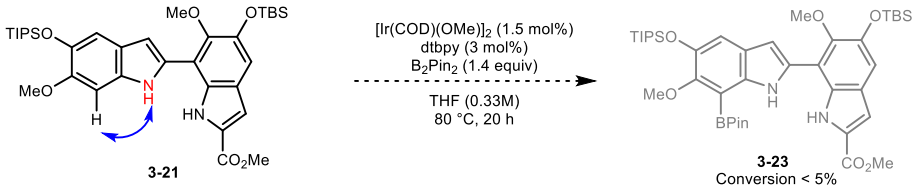

Scheme 3-6 Attempted C7 Borylation of Dimers **3-21**

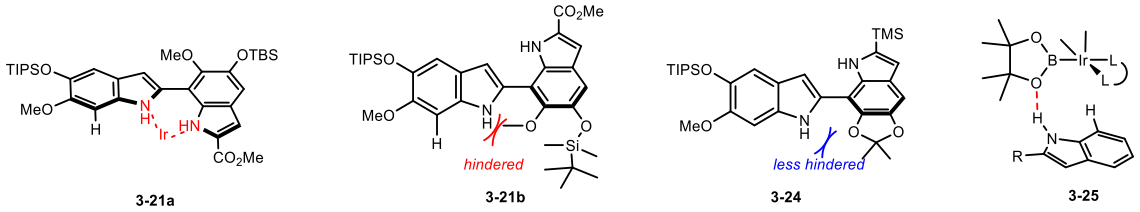

Scheme 3-7 Proposed solutions for C7 borylation on dimer

To test our first hypothesis, the N-Boc, N'-H dimer **3-26** was prepared to disrupt the potential deactivation of the Ir-catalyst by two indole nitrogens. However, the N-H directed borylation of **3-26** proceeded with low conversion and the desired product **3-27** was not observed (Scheme 3-8).

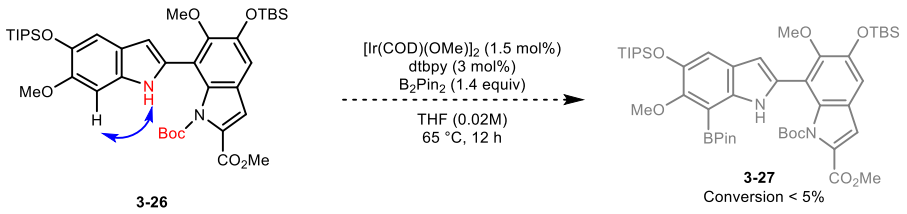

Scheme 3-8 Attempted C7 Borylation of dimer **3-26**

To test our second hypothesis, dimer **3-24** was chosen as the substrate. **3-24** was synthesized via Suzuki-coupling reaction between **2-21** and **2-60** under our optimized conditions, namely 5 mol % $Pd(OAc)_2$, 5.5 mol % SPhos, 2.1 eq. K_3PO_4, in THF/H_2O (4:1) at room temperature for 1 hour, which resulted in **3-24** in a yield of 82 % (Scheme 3-9).

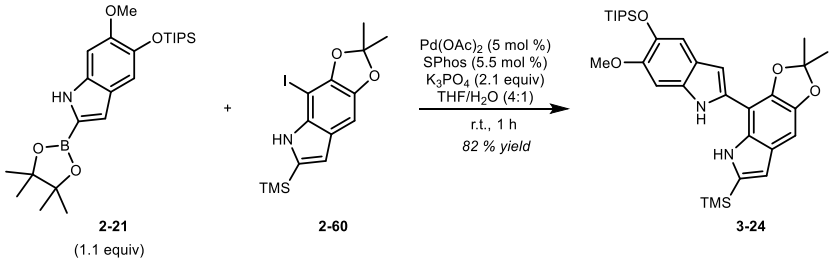

Scheme 3-9 Suzuki coupling to dimer **3-24**

Compared with methyl and TBS protecting groups on **3-21b**, the acetonide group in **3-24** is smaller (Scheme 3-7) and was anticipated to impose less steric hindrance on the N-H, thus enabling the hydrogen bonding between the hydrogen on the indole nitrogen and an oxygen atom of a B-Pin on Ir. We surveyed different ligands, dtbpy and tmphen (entries 1 and 2), a smaller borylation reagent, B_2Cat_2 (entry 3), and a non-coordinating solvent, cyclohexane (entry 4), however, all attempts failed to produce the desired C7-functionalized dimer **3-28**. It became clear that direct C7-borylation on the dimer would not be feasible in our hands (Table 3-4).

Table 3-4 Attempted C7 Borylation of dimer **3-24**

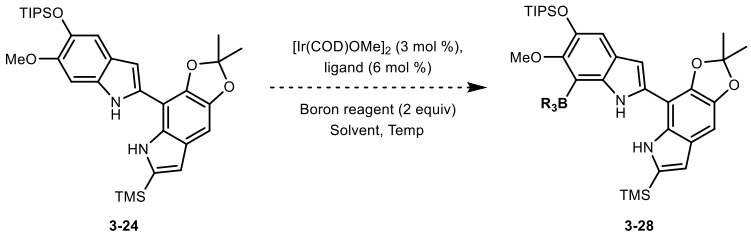

Entry	Solvent	Boron reagent	Ligand	Conversion (%)	Time (h)	Temp. (°C)	Yield (%)
1	THF (0.05 M)	B_2pin_2	dtbpy	<5	4	60	0
2	THF (0.05 M)	B_2pin_2	tmphen	<5	4	60	0
3	THF (0.05 M)	B_2cat_2 (4 equiv)	dtbpy	80	4	80	0
4	CyH (0.05 M)	B_2cat_2 (4 equiv)	dtbpy	100	4	80	0

Entry 3 and 4: After stirring at 80 °C for 4 h, the reaction was quenched by addition of Et_3N and pinacol (6 equiv) at ambient temperature.

3.3.2 Functionalizing at the C2 position of dimers

With the challenges of functionalizing the C7 position on dimers clearly illustrated, we turned our attention to installing a functional handle on the C2 positions of dimers in hopes of growing the chain along the C2 direction.

To this end, we envisioned that a similar protodecarboxylation strategy of **2-19** (Chapter 2, Table 2-1) would unmask the C2 position on **3-22** for subsequent installation of the required functional handle for iterative chain extension. As a starting point, we investigated protodecarboxylation conditions for **3-29**, which was prepared via a two-step sequence including protection of the free phenol with triisopropylsilyl chloride (TIPSCl) followed by saponification of the C2 carboxylate (Scheme 3-10).

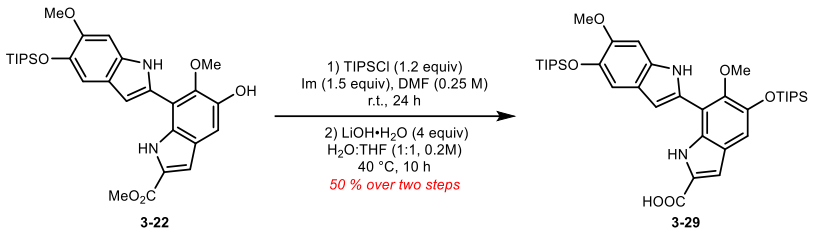

Scheme 3-10 Preparation of **3-29**

Unfortunately, attempts to protodecarboxylate at the C2 position on dimer **3-29** proved to be challenging. Applying the same conditions that yielded grams of protodecarboxylated monomer **2-23** only led to the decomposition of **3-29** (entry 1). Shortening the reaction time to 1 h also led to decomposition of **3-29** (entry 2). After only 10 min, 50 % of substrate **3-29** could be recovered, but no desired product **3-30** was detected (Table 3-5).

Table 3-5 Attempted C2 protodecarboxylation of **3-29**

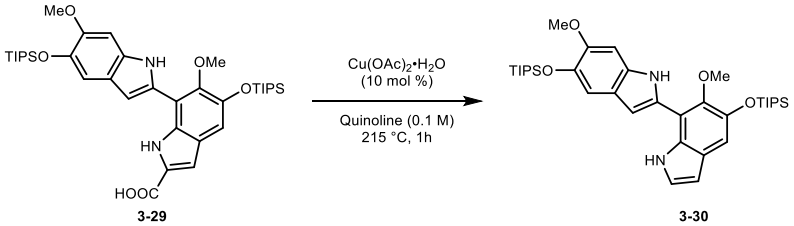

Entry	Time	Conversion (%)	Yield (%)
1	4.5 h	100	0
2	1 h	100	0
3	10 min	50	0

Due to the challenge of protodecarboxylation on **3-29**, we considered an alternative strategy in which a more labile functional group would be used at C2 in place of the carboxylic acid. In this context, the utility of the trimethylsilyl (TMS) group at the C2 position of indole to mask reactivity at both C2 and C3 has been reported.[33, 34] Moreover, Smith and co-workers have demonstrated that the TMS group can be readily removed by treatment with *tetra*-*n*-butylammonium fluoride (TBAF) in the presence of a boronic ester, which allowed access to C7-borylated indoles **3-33** (Scheme 3-11).

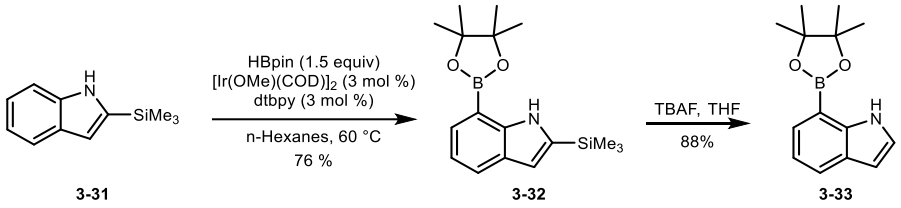

Scheme 3-11 C7 borylation of indole via silylation/desilylation

In an effort to access C7-substituted indoles, Sneikus and co-workers developed a sequential C2-metalation/silylation, C7-metalation and electrophile trapping using an amide directing group on N1. The group subsequently showed that the C2-TMS of **3-35** was readily cleaved under the conditions of Suzuki-Miyaura coupling, underscoring its lability (Scheme 3-12).

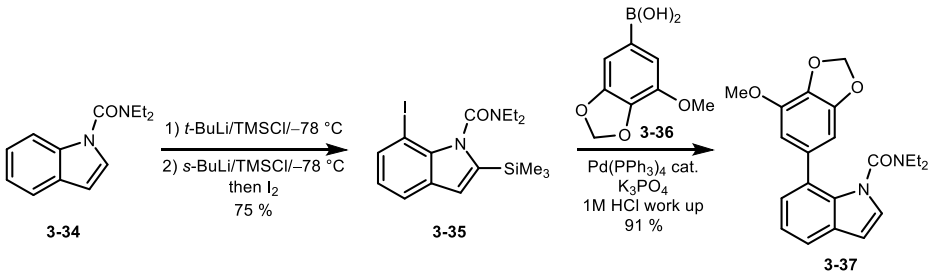

Scheme 3-12 C7 iodination of indole via directed metalation/silylation/desilylation

With this literature precedent, we examined protodesilylation on dimer **3-24** (Table 3-6). Unfortunately, neither the conditions by Smith[12], employing TBAF, or milder conditions employing KHF_2 in MeOH[35] yielded any desired product. **3-24** was nearly completely consumed to unidentifiable products upon exposure to TBAF (entry 1). Treatment of **3-24** with KHF_2 led to no consumption of the **3-24** within 5 h (entry 2). To our delight, pyridinium *p*-toluenesulfonate

(PPTS) in MeOH converted **3-24** to **3-38** in consistently high yields (89-97 %) even on gram scale (entries 3-5).

Table 3-6 Optimization of reaction conditions for C2-desilylation

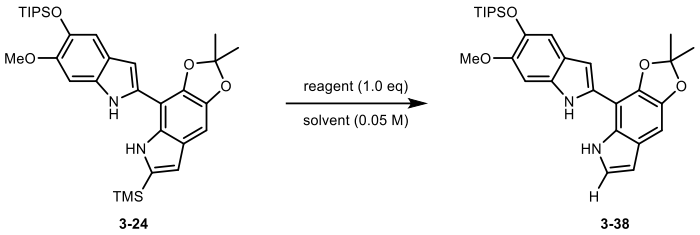

3-24 **3-38**

Entry	Reagent	Solvent	Conversion (%)	Time (h)	Yield (%)
1	TBAF	THF	90	7	0
2	KHF_2	MeOH	0	5	0
3	PPTS	MeOH	100	2	96
4	PPTS	MeOH	100	2	89
5[a]	PPTS	MeOH	100	2	97

a) Entry 5 was performed on 2 mmol scale.

With **3-38** in hand, we investigated the borylation at the C2 position of **3-38**, and were pleased to obtain a 94 % yield of **3-39** under our standard conditions, composed of $[Ir(OMe)(COD)]_2$ (3.0 mol %), dtbpy (6.0 mol %), and B_2Pin_2 (1equiv) for 1 h at 60 °C (Scheme 3-13). Controlling the reaction time and the number of equivalents of B_2Pin_2 is critically important to the selective borylation at C2. Extending the reaction time or increasing the equivalents of B_2Pin_2 resulted in over-borylation.

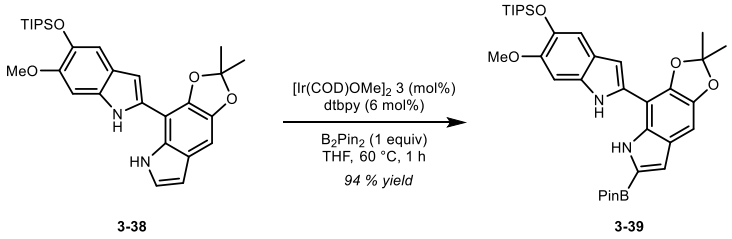

3-38 **3-39**

Scheme 3-13 Selective C2-borylation of dimer **3-38**

In summary, we have demonstrated an efficient sequence to couple the monomer units to form a dimer, and then to functionalize the dimer at the desired site of chain growth. This iterative sequence is composed of an efficient Suzuki-coupling of a starter unit **2-21** bearing a boronic

ester at C2 and an extender unit **2-60** containing an iodide at the C7 position and a trimethylsilyl group at C2. Protodesilylation under mildly acidic conditions unmasks the C2 position to **3-38**, and a selective C2 borylation to **3-39** sets the stage for further chain growth (Scheme 3-14).

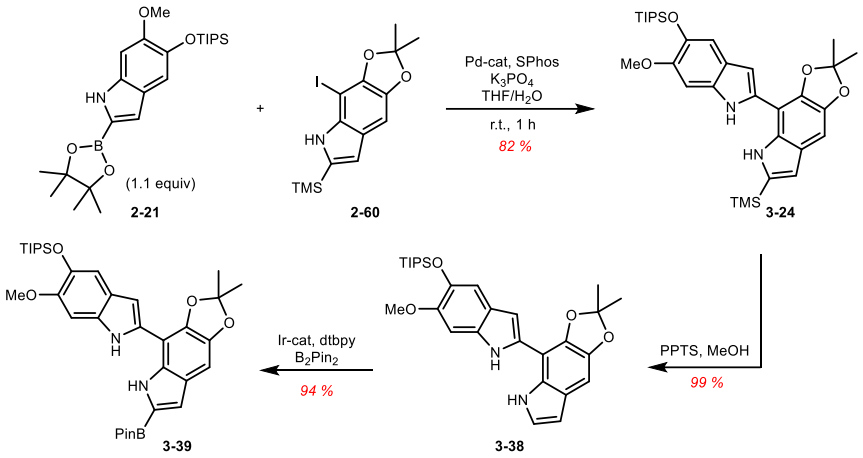

Scheme 3-14 Summary scheme of the cross-coupling, desilylation, borylation sequence

3.4 Iterative Eumelanin Chain Growth

To perform an iterative chain growth that could access higher-order eumelanin oligomers, we tested the generality of our sequence by synthesizing a trimer, a tetramer, and a pentamer of **DHI** units.

We began our synthesis by targeting trimer **3-41**. Suzuki-coupling between **3-39** and **2-60** provided trimer **3-40** in an 86 % yield when the reaction was performed at 60 °C for 1.5 h. Desilyation was found to be highly effective at the trimer stage under PPTS/MeOH condition as well, resulting in trimer **3-41** in 84 % yield (Scheme 3-15).

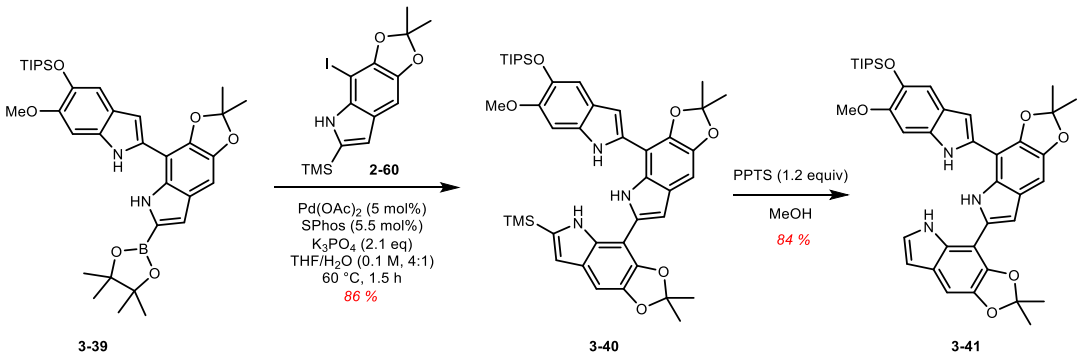

Scheme 3-15 Iterative synthesis to trimer **3-41**

With **3-41** in hand, we then focused on applying the iterative synthesis sequence to tetramer **3-44**. Remarkably, borylation on the C2 position of **3-41** proceeded smoothly under our previously optimized Ir-catalyzed borylation conditions and provided **3-42** in an 83 % yield. Elongating the chain by one unit of **2-60** via Suzuki-coupling afforded **3-43**. However, we observed protodeborylation byproduct **3-41** that was inseparable **3-43** by column chromatography. Thus, desilylation was carried out on the crude reaction mixture and to afford **3-44** in a 58 % yield over two steps after purification (Scheme 3-16).

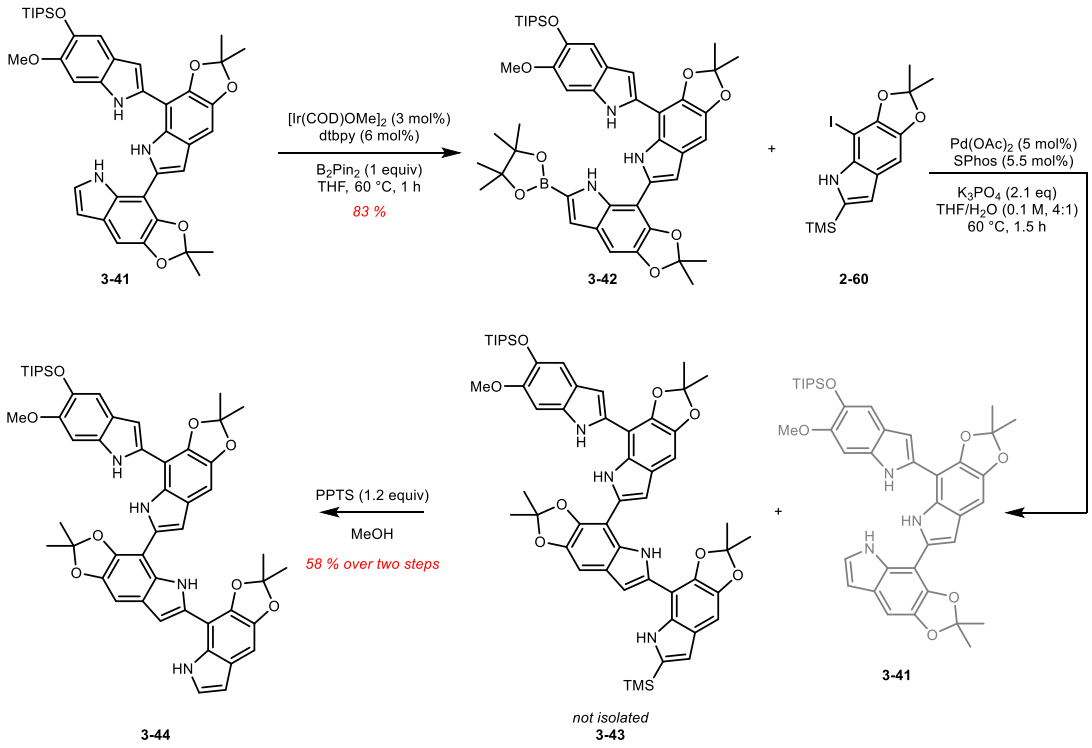

Scheme 3-16 Iterative synthesis to tetramer **3-44**

A final sequence of borylation, cross coupling, and desilylation were explored in order to access linear pentamer **3-47**. The selective C2-borylation on tetramer **3-44** is slower than it was on dimer **3-38** and trimer **3-41**. Ir-catalyzed borylation afforded **3-45** in 70 % yield after 6 h. We obtained **3-46** in 68 % yield along with 10 % protodeborylation of **3-45** in the subsequent cross coupling with **2-60.** Small amount of desilylation of **3-46** was observed upon standing in $CDCl_3$ for 5-6 h. We suspected that this reactivity was due to trace amounts of HCl generated in $CDCl_3$ over time. The reaction mixture was then subjected to PPTS in MeOH directly and afforded **3-47** in a 60 %

yield over two steps. This completed the first synthesis of an eumelanin pentamer (Scheme 3-17).

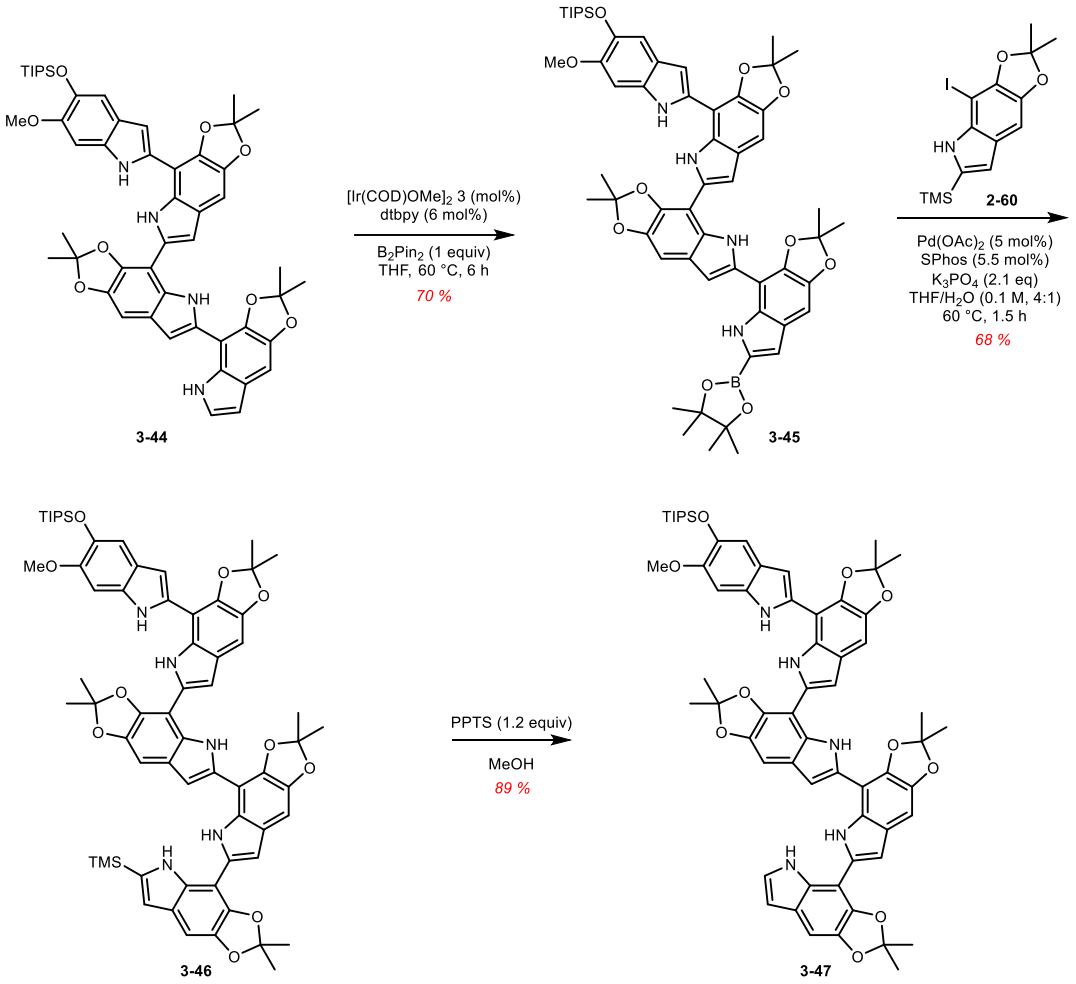

Scheme 3-17 Iterative synthesis to pentamer **3-47**

UV/vis absorption spectra of monomer (**2-23**), dimer (**3-38**), trimer (**3-41**), tetramer (**3-44**), and pentamer (**3-47**) were measured (Figure 3-1). A red shift from monomer to oligomers was observed. No obvious red shift was shown from trimer to pentamer. As expected, the absorption spectra did not present a broad band absorption, which proves that our efforts of decoupling oxidation from chain growth have been effective. Further studies are ongoing in collaboration with the Kohler lab. (*Spectroscopic data was from Lily Kinziabulatova at the Kohler lab, The Ohio State University*).

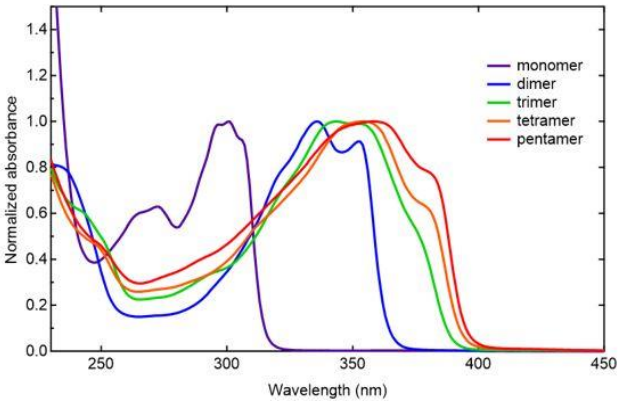

Figure 3-1 UV/vis absorption spectra of monomer to pentamer

3.5 Conclusion

In summary, our iterative-chain-growth approach provides a general and simplified strategy for higher order eumelanin oligomers with absolute control over regioselectivity and length. It provides several advantages over existing synthetic methods that could only provide chains of up to three **DHI** units, or longer oligomers as complex mixtures with low yield and limited synthetic value.[3, 37, 38] Capitalizing on these advances, and the inherent modularity of eumelanin, we envision that a generalized strategy based on **DHI** building blocks and iterative chain growth will allow for an efficient, flexible, and eventually, fully automated, access to eumelanin biopolymers.

3.6 Experimental Section

Materials and Methodologies:

Chemicals and solvents were purchased from Sigma Aldrich, Alfa Aesar, Strem Chemicals, TCI or Oakwood Chemicals. Chemicals were used as received without further purification. Solvents were dried and purified using a PureSolv MD 7 (from Innovative Technology) or MB SPS 800 (from MBraun). Cyclohexane and quinoline were distilled over CaH_2 under a positive pressure of N_2. $[Ir(COD)(OMe)]_2$ was purchased from Sigma Aldrich, and stored inside of a MBraun Labmaster glove box (<1 ppm O_2 and H_2O) filled with a dry N_2 atmosphere at −20 °C. Unless otherwise noted, reactions were performed in flame-dried glassware under a positive pressure of N_2 using standard synthetic organic, inert atmosphere techniques.

Proton nuclear magnetic resonance (^{1}H NMR) spectra were acquired using Varian Mercury 400 MHz, Varian Inova QANUC 500 MHz, Varian VNMRS 500 MHz, Bruker AVIIIHD 500 MHz, or Bruker AVIIIHD 400 MHz spectrometers. Chemical shifts (δ) are reported in parts per million (ppm) and are calibrated to the residual solvent peak. Coupling constants (*J*) are reported in Hz. Multiplicities are reported using the following abbreviations: *s* = singlet; *brs*=broad singlet; *d* = doublet; *t* = triplet; *q* = quartet; *m* = multiplet (range of multiplet is given). Carbon nuclear magnetic resonance (^{13}C NMR) spectra were acquired using Varian VNMRS 125 MHz, Bruker AVIIIHD 125 MHz, or Bruker AVIIIHD 101 MHz spectrometers. Chemical shifts (δ) are reported in parts per million (ppm) and are calibrated to the residual solvent peak. High resolution mass spectra (HRMS) were recorded using a Bruker maXis Impact TOF mass spectrometer. Fourier-transform infrared (FT-IR) spectra were recorded on an alpha Bruker FT-IR spectrometer. Analytical thin-layer chromatography was performed on pre-coated 250 mm layer thickness silica gel 60 F_{254} plates (EMD Chemicals Inc.). Visualization was performed by ultraviolet light and/or by staining with potassium permanganate or cerium molybdate. Purifications by column chromatography were performed using either a Biotage Isolera™ One or standard column chromatography using silica gel (40-63 µm, 230-400 mesh).

General Procedures

General Procedure A: Suzuki-Miyaura Coupling of Indoles A flame-dried Schlenk tube equipped

with a Teflon-coated stir bar and a glass stopper was charged with iodoindole (1.0 equiv), indole boronic acid pinacol ester (1.0-1.2 equiv), Pd-catalyst (5 mol %), ligand (5.5 mol %) and base (2.1 equiv). The Schlenk tube was evacuated and backfilled with N_2 (this process was repeated three times) prior to the addition of degassed dry solvent under a positive pressure of N_2, followed by the addition of degassed deionized H_2O. The tube was sealed and heated to the indicated temperature in a pre-heated oil bath. After the indicated time, the reaction was cooled to ambient temperature and quenched by the addition of a saturated aqueous solution of NH_4Cl to afford a neutral reaction mixture with a pH=7. The phases were then separated, and the aqueous phase was extracted with EtOAc. The combined organic fractions were then washed with brine then dried over $MgSO_4$, filtered, and concentrated *in vacuo*. The resulting residue was purified by silica gel column chromatography using the indicated solvent system as eluent to afford the desired product.

General Procedure B: Ir-catalyzed Borylation of Indoles In an inert atmosphere glove box, a flamed-dried vial equipped with a Teflon-coated stir bar was charged with indole (1.0 equiv) and dry degassed solvent (THF or cyclohexane). In another three flamed-dried vials, B_2pin_2 (1.0–2.0 equiv), dtbpy (3.0–14.0 mol%), and $[Ir(COD)(OMe)]_2$ (1.5–7.0 mol%) were dissolved in dry, degassed solvent separately The solution of B_2Pin_2 was then added to the solution of $[Ir(COD)OMe]_2$. To this resulting mixture was added the solution of dtbpy. The resulting mixture was stirred in the glovebox for 0.5 h at ambient temperature before adding to the solution of indole. The reaction vial was sealed and heated to the indicated temperature in a pre-heated oil bath outside of the glove box. After the indicated time, the reaction was cooled to ambient temperature, and transferred to a round-bottom flask. The resulting reaction mixture was concentrated *in vacuo* and purified by silica gel column chromatography using the indicated solvent system as eluent to afford the desired product.

General Procedure C: Desilylation of Indoles A flame-dried round bottom flask, equipped with a Teflon coated stir bar, was charged with the starting indole (1.0 equiv) and pyridinium *p*-toluenesulfonate (PPTS, 1.0-1.2 equiv). The flask was evacuated and backfilled with N_2 (this process was repeated three times) before the addition of dry, degassed solvent (MeOH or MeOH/THF) under a positive pressure of N_2. The resulting reaction mixture was then stirred at

ambient temperature for the indicated time, as monitored by thin-layer chromatography (TLC). After the addition of H_2O and EtOAc, the aqueous layer was extracted with EtOAc. The combined organic layers were then washed with brine, dried over $MgSO_4$, and concentrated *in vacuo*. The crude reaction mixture was purified by silica gel column chromatography using the indicated solvent system as eluent to afford the desired product.

Compound 3-21

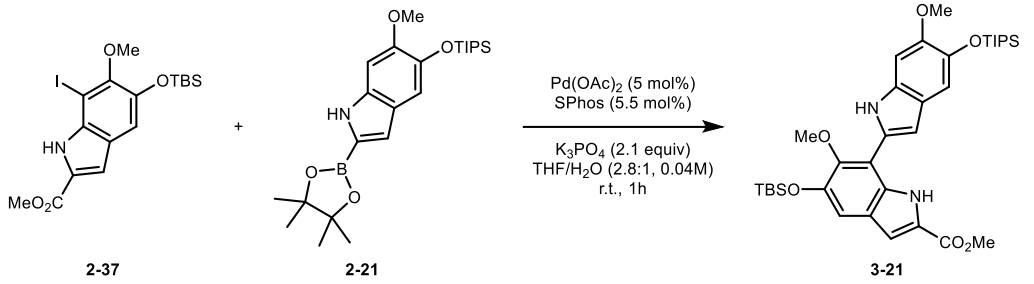

Procedure: The reaction was carried out according to the General Procedure A, the reaction was performed in THF/H_2O (2.8:1, 0.04 M) at ambient temperature for 1 h.

Amounts of Reagents:

2-37 (46.14 mg, 0.1 mmol, 1.0 equiv)

2-21 (44.55 mg, 0.1 mmol, 1.0 equiv)

$Pd(OAc)_2$ (1.12 mg, 0.005 mmol, 5 mol%)

SPhos (2.26 mg, 0.0055 mmol, 5.5 mol %)

K_3PO_4 (44.58 mg, 0.21 mmol, 2.1 equiv)

THF (2.5 mL), H_2O (0.8 mL)

Purification: 10 % EtOAc in hexanes.

Yield of Product:

3-21: NMR yield (hexamethylbenzene as an internal standard): 80 %

Isolated yield: 32.65 mg, 0.05 mmol, 50 %, off-white solid.

Characterization:

$\mathbf{R_f}$ = (EtOAc/hexanes, 1:9) 0.43; **^{1}H NMR** (500 MHz, $CDCl_3$) δ 9.29 (s, 1H), 9.23 (s, 1H), 7.17 (s, 1H),

7.12 (d, *J* = 2.1 Hz, 1H), 7.07 (d, *J* = 0.6 Hz, 1H), 6.92 (s, 1H), 6.79 (dd, *J* = 2.1, 0.8 Hz, 1H), 3.94 (s, 3H), 3.88 (s, 3H), 3.74 (s, 3H), 1.38 – 1.28 (m, 3H), 1.15 (d, *J* = 7.4 Hz, 18H), 1.07 (s, 9H), 0.25 (s, 6H); **HRMS**: Calcd. for $C_{35}H_{52}N_2NaO_6Si_2$ $[M+Na]^+$ = 675.3256 m/z, found = 675.3250 m/z.

Compound 3-22

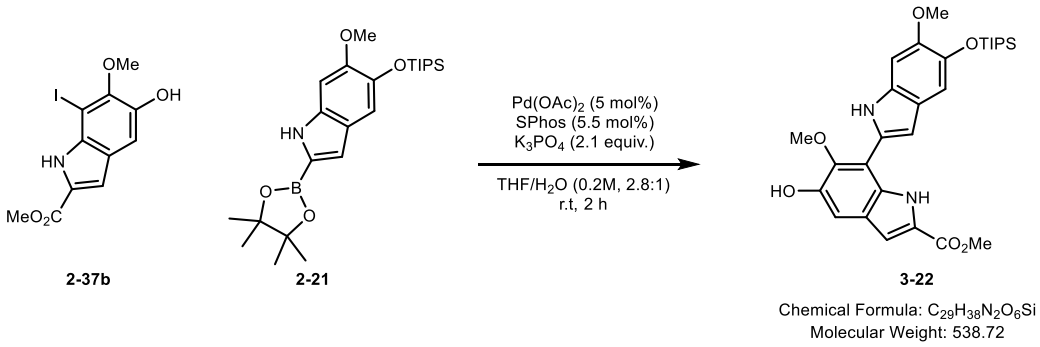

Procedure: The reaction was carried out according to the General Procedure A, the reaction was performed in THF/H_2O (2.8:1, 0.2 M) at ambient temperature for 2 h.

Amounts of Reagents:

2-37b (694.22 mg, 2.0 mmol, 1.0 equiv)

2-21 (890.96 mg, 2.0 mmol, 1.0 equiv)

$Pd(OAc)_2$ (22.45 mg, 0.1 mmol, 5 mol%)

SPhos (45.16 mg, 0.11 mmol, 5.5 mol %)

K_3PO_4 (891.53 mg, 4.2 mmol, 2.1 equiv)

THF (10.0 mL), H_2O (3.5 mL)

Purification: 10 % to 20 % EtOAc in hexanes.

Yield of Product:

3-22: 668.01 mg, 1,24 mmol, 62 %, white solid.

Characterization:

R_f = (EtOAc/hexanes, 1:3) 0.24; **^{1}H NMR** (500 MHz, $CDCl_3$) δ 9.16 (s, 1H), 8.85 (s, 1H), 7.18 (s, 2H), 7.14 (d, *J* = 2.1 Hz, 1H), 6.92 (s, 1H), 6.79 (d, *J* = 2.1 Hz, 1H), 5.60 (s, 1H), 3.94 (s, 3H), 3.89 (s, 3H), 3.66 (s, 3H), 1.32-1.38 (m, 3H), 1.16 (d, *J* = 7.5 Hz, 18H); **^{13}C NMR** (101 MHz, $CDCl_3$) δ 162.21, 149.85, 144.68, 143.46, 141.67, 131.69, 130.02, 128.53, 127.97, 124.52, 121.57, 110.31, 109.99,

108.87, 105.30, 102.21, 94.43, 61.62, 56.00, 52.14, 18.18, 13.01.; **HRMS**: Calcd. for $C_{29}H_{38}N_2NaO_6Si$ $[M+Na]^+$ = 561.2391 m/z, found = 561.2384 m/z.

Compound 3-26a:

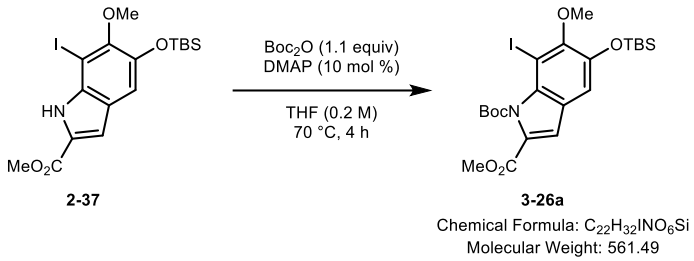

2-37 **3-26a**

Chemical Formula: $C_{22}H_{32}INO_6Si$
Molecular Weight: 561.49

Procedure: A 10 mL flame-dried, round-bottom flask, equipped with a Teflon-coated stir bar and a rubber septum, was charged with **2-37** (230.7 mg, 0.5 mmol, 1.0 equiv), DMAP (6.1 mg, 0.05 mmol, 0.1 equiv), Boc_2O (120.04 mg, 0.55 mmol, 1.1 equiv), and THF (2.5 mL, 0.20 M). The resulting homogeneous reaction mixture was then stirred at 70° for 4 h and then concentrated *in vacuo*. The resulting crude reaction mixture was purified by silica gel column chromatography (10 % EtOAc in hexanes) to afford **3-26a** as a yellow oil (137.6 mg, 0.25 mmol) in 49 % yield.

Characterization:

R_f = (EtOAc/hexanes, 1:3) 0.42; **^{1}H NMR** (500 MHz, $CDCl_3$) δ 7.11 (s, 1H), 7.04 (s, 1H), 3.89 (s, 3H), 3.83 (s, 3H), 1.72 (s, 9H), 1.03 (s, 9H), 0.19 (s, 6H).

Compound 3-26:

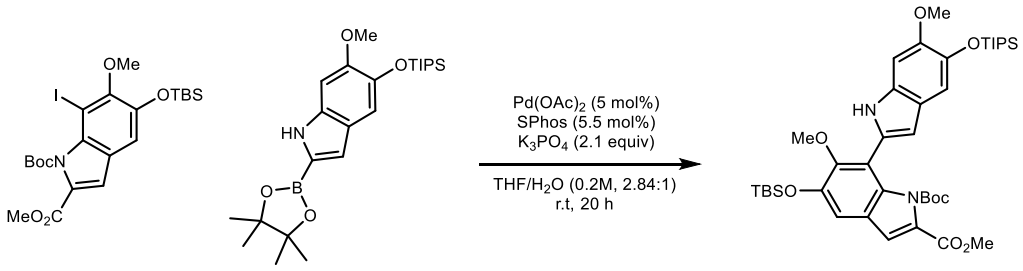

3-26a **2-21** **3-26**

Chemical Formula: $C_{40}H_{60}N_2O_8Si_2$
Molecular Weight: 753.10

Procedure: The reaction was carried out according to the General Procedure A, the reaction was performed in THF/H_2O (2.8:1, 0.2 M) at ambient temperature for 20 h.

Amounts of Reagents:

3-26a (61.7 mg, 0.11 mmol, 1.0 equiv)

2-21 (49.0 mg, 0.11 mmol, 1.0 equiv)

$Pd(OAc)_2$ (1.23 mg, 0.0055 mmol, 5 mol%)

SPhos (2.50 mg, 0.0061 mmol, 5.5 mol %)

K_3PO_4 (49.0 mg, 0.23 mmol, 2.1 equiv)

THF (2.2 mL), H_2O (0.44 mL)

Purification: 10 % EtOAc in hexanes.

Yield of Product:

3-26: 22.6 mg, 0.03 mmol, 27 %, yellow solid.

Characterization:

$\mathbf{R_f}$ = (EtOAc/Hexanes, 1:9) 0.5; **^{1}H NMR** (500 MHz, $CDCl_3$) δ 8.59 (brs, 1H), 7.86 (s, 1H), 7.12 – 7.09 (m, 2H), 7.05 (s, 1H), 6.54 (s, 1H), 3.93 (s, 3H), 3.88 (s, 3H), 3.64 (s, 3H), 1.35 – 1.26 (m, 3H), 1.14 (dd, *J* = 7.5, 1.4 Hz, 18H), 1.09 (s, 9H), 1.04 (s, 9H), 0.25 (s, 3H), 0.23 (s, 3H).

Compound 3-24:

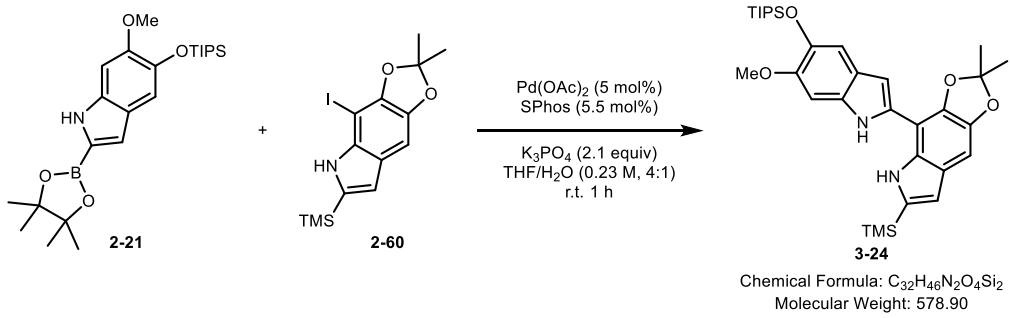

Procedure: The reaction was carried out according to the General Procedure A, the reaction was performed in THF/H_2O at ambient temperature for 1 h.

Amounts of Reagents:

2-21 (446.10 mg, 1.0 mmol, 1.1 equiv)

2-60 (348.56 mg, 0.9 mmol, 1.0 equiv)

$Pd(OAc)_2$ (10.10 mg, 0.045 mmol, 5 mol%)

SPhos (22.58 mg, 0.049 mmol, 5.5 mol %)

K_3PO_4 (401.19 mg, 1.89 mmol, 2.1 equiv)

THF (4.0 mL), H_2O (1.0 mL)

Purification: 5 % to 10 % EtOAc in hexanes.

Yield of Product:

3-24: 428.38 mg, 0.74 mmol, 82 %, light yellow solid.

Characterization:

$\mathbf{R_f}$ = (EtOAc/hexane, 1:9): 0.46; **IR** (neat) v = 3450, 2950, 2870, 1480, 1300, 1160, 835, 677, 440 cm^{-1}; **^{1}H NMR** (500 MHz, $CDCl_3$) δ 9.03 (brs, 1H), 8.51 (s, 1H), 7.17 (s, 1H), 6.96 (s, 1H), 6.89 (s, 1H), 6.71 (dd, *J* = 2.2, 0.8 Hz, 1H), 6.66 (d, *J* = 2.1 Hz, 1H), 3.89 (s, 3H), 1.78 (s, 6H), 1.40 – 1.27 (m, 3H), 1.15 (d, *J* = 7.4 Hz, 18H), 0.38 (s, 9H); 13C NMR (101 MHz, CDCl3) δ 149.50, 143.21, 141.50, 141.10, 137.02, 131.10, 130.69, 130.64, 123.20, 121.76, 118.04, 112.18, 110.13, 99.74, 99.67, 98.03, 94.51, 55.97, 26.16, 18.19, 13.03, -0.76; **HRMS**: Calcd. for $C_{32}H_{46}N_2O_4Si_2$ $[M+H]^+$ = 579.3069 m/z, found =579.3064 m/z.

Compound 3-29a

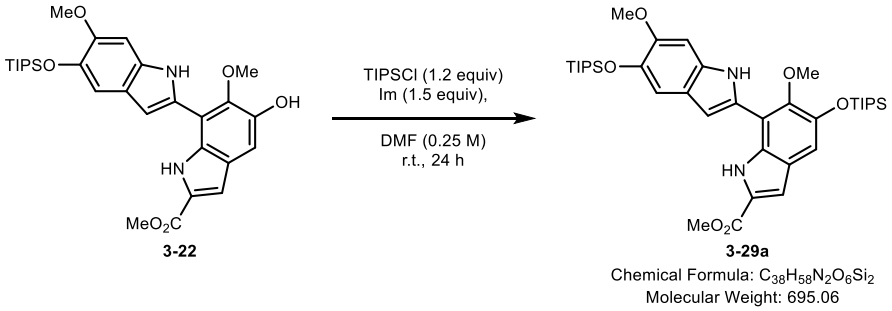

Procedure: A 10 mL flame-dried, round-bottom flask, equipped with a Teflon-coated stir bar and a rubber septum, was charged with **3-22** (269.36 mg, 0.5 mmol, 1 equiv), imidazole (51.06 mg, 0.6 mmol, 1.5 equiv), and DMF (2.0 mL, 0.25 M). To the resulting mixture was added tri-isopropylsilyl chloride (115.27 mg, 0.13 mL, 1.2 equiv.). The resulting homogeneous reaction mixture was then stirred at ambient temperature for 24 h and then quenched with HCl (50 mL, 1M). The resulting heterogeneous, biphasic mixture was then extracted with EtOAc (3 x 20 mL). The combined organic phases were washed with water (100 mL), brine (100 mL), and then dried over Na_2SO_4, filtered, and concentrated *in vacuo*. The resulting crude mixture was then purified

by silica gel column chromatography (10 % EtOAc in hexanes) to afford **3-29a** as an off-white solid (310 mg, 0.45 mmol) in 89 % yield.

Characterization:

$\mathbf{R_f}$ = (EtOAc/hexanes, 1:3): 0.74; **^{1}H NMR** (500 MHz, $CDCl_3$) δ 9.36 (d, *J* = 2.1 Hz, 1H), 9.26 (d, *J* = 2.2 Hz, 1H), 7.19 (s, 1H), 7.14 (d, *J* = 2.1 Hz, 1H), 7.09 (s, 1H), 6.93 (s, 1H), 6.81 (d, *J* = f2.1 Hz, 1H), 3.94 (s, 3H), 3.89 (s, 3H), 3.77 (s, 3H), 1.43 – 1.32 (m, 6H), 1.18 (d, *J* = 3.5 Hz, 18H), 1.17 (d, *J* = 3.5 Hz, 18H).; **^{13}C NMR** (126 MHz, $CDCl_3$) δ 162.24, 149.60, 147.36, 145.40, 141.44, 131.42, 130.37, 129.97, 127.58, 124.12, 121.51, 111.19, 110.21, 110.16, 108.88, 101.52, 94.48, 61.12, 55.96, 52.03, 18.19, 18.16, 18.15, 17.81, 12.99, 12.42.; **HRMS**: Calcd. for $C_{38}H_{57}N_2O_6Si_2$ $[M-H]^+$ = 693.37606 m/z, found = 693.37467 m/z.

Compound 3-29

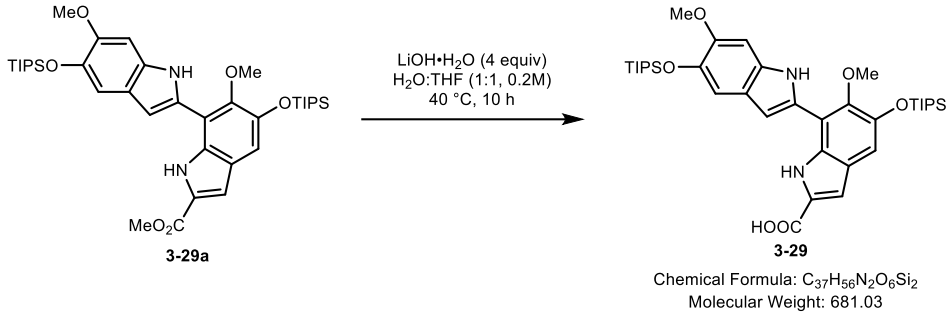

Procedure: A 10 mL round-bottom flask, equipped with a Teflon-coated stir bar and a rubber septum, was charged with **3-29a** (173.77 mg, 0.25 mmol, 1.0 equiv) and THF (0.6 mL). To the resulting mixture was added $LiOH{\cdot}H_2O$ (42 mg, 1.0 mmol, 4.0 equiv) in H_2O (0.6 mL). The resulting mixture was then stirred at 40 °C for 10 h and then acidified with HCl (2 M, 10 mL). The resulting mixture was then extracted with EtOAc (3 x 20 mL). The combined organic phases were then dried over Na_2SO_4, filtered, and concentrated *in vacuo*. The crude mixture was purified by silica gel column chromatography (25 % EtOAc in hexanes to 10 % MeOH in EtOAc) to afford **3-29** as a tan solid (95.34 mg, 0.14 mmol) in 56 % yield.

Characterization:

$\mathbf{R_f}$ = (MeOH/EtOAc, 1:9): 0.53; **^{1}H NMR** (500 MHz, $CDCl_3$) δ 9.37 (s, 1H), 9.26 (s, 1H), 7.27 (s, 1H), 7.18 (s, 1H), 7.10 (s, 1H), 6.92 (s, 1H), 6.80 (s, 1H), 3.88 (s, 3H), 3.78 (s, 3H), 1.44 – 1.31 (m, 6H),

1.17 (m, 36H).; **^{1}H NMR** (500 MHz, Acetone) δ 10.33 (s, 1H), 9.75 (s, 1H), 7.22 (s, 1H), 7.16 (s, 3H), 6.89 (d, *J* = 2.2 Hz, 1H), 3.86 (s, 3H), 3.72 (s, 3H), 1.41 (m, 3H), 1.36 – 1.28 (m, 3H), 1.18 (d, *J* = 7.6 Hz, 18H), 1.15 (d, *J* = 7.4 Hz, 18H).; **^{13}C NMR** (126 MHz, Acetone) δ 149.87, 148.34, 145.98, 141.69, 133.20, 131.63, 130.42, 124.96, 122.63, 112.69, 110.95, 110.56, 109.36, 102.76, 95.74, 61.18, 55.93, 18.45, 18.43, 13.66, 13.61.; **HRMS**: Calcd. for $C_{37}H_{55}N_2O_6Si_2$ $[M-H]^+$ = 679.36041 m/z, found = 679.35727 m/z.

Compound 3-38

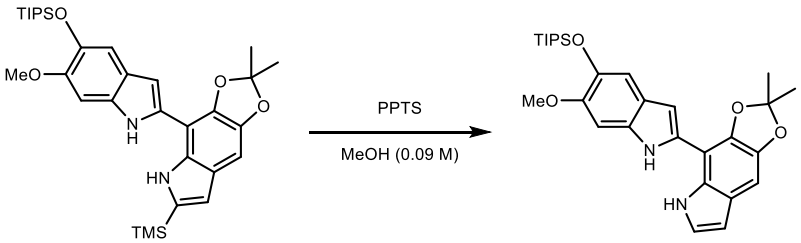

3-24 **3-38**

Procedure: The reaction was carried out according to the General Procedure C, the reaction was performed in MeOH at ambient temperature for 3 h.

Amounts of Reagents:

3-24 (528.5 mg, 0.91 mmol, 1.0 equiv)

PPTS (228.7 mg, 0.91 mmol, 1.0 equiv)

MeOH (10.0 mL)

Purification: 10 % EtOAc in hexanes.

Yield of Product:

3-38: 456.05 mg, 0.90 mmol, 99 %, off-white solid.

Characterization:

R_f = (EtOAc/hexanes, 1:9) 0.34; **IR** (neat) v = 3444, 2939, 2863, 1479, 1299, 1186, 987, 852, 676, 414 cm^{-1}; **^{1}H NMR** (500 MHz, $CDCl_3$) δ 8.99 (s, 1H), 8.60 (s, 1H), 7.16 (t, *J* = 2.8 Hz, 1H), 7.13 (s, 1H), 6.95 (s, 1H), 6.92 (s, 1H), 6.74 (d, *J* = 2.1 Hz, 1H), 6.49 (dd, *J* = 3.2, 2.1 Hz, 1H), 3.88 (s, 3H), 1.79 (s, 6H), 1.32 (sep, *J* = 6.9 Hz, 3H), 1.14 (d, *J* = 7.5 Hz, 18H). **^{13}C NMR** (126 MHz, $CDCl_3$) δ 149.49, 143.20, 141.47, 140.74, 131.13, 130.45, 127.53, 122.95, 122.20, 121.81, 117.99, 110.14, 103.48, 99.98,

98.43, 94.56, 56.00, 26.18, 18.16, 18.16, 13.01; **HRMS**: Calcd. for $C_{29}H_{38}N_2O_4Si$ [M-H]$^+$ = 505.2528 m/z, found = 505.2536 m/z.

Compound 3-39

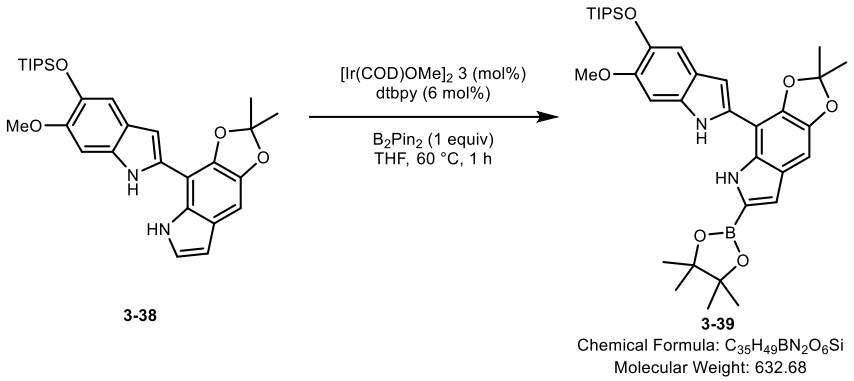

3-38

3-39

Chemical Formula: $C_{35}H_{49}BN_2O_6Si$

Molecular Weight: 632.68

Procedure: The reaction was carried out according to the General Procedure B, the reaction was performed in THF at 60 °C for 1 h.

Amounts of Reagents:

3-38 (456.05 mg, 0.9 mmol, 1.0 equiv)

$[Ir(OMe)(COD)]_2$ (17.89 mg, 0.027 mmol, 3.0 mol%)

dtbpy (14.49 mg, 0.054 mmol, 6.0 mol%)

B_2pin_2 (228.54 mg, 0.9 mmol, 1.0 equiv)

THF (18 mL, 0.05 M)

Purification: 10% EtOAc in hexanes.

Yield of Product:

3-39: 540.9 mg, 0.85 mmol, 94%, white solid.

Characterization:

R_f = (EtOAc/hexanes, 8:2) 0.54; **IR** (neat) v = 3446, 2940, 2863, 1525, 1479, 1259, 1218, 1135, 852, 680 cm^{-1}; **^{1}H NMR** (500 MHz, $CDCl_3$) δ 8.98 (s, 1H), 8.90 (s, 1H), 7.18 (s, 1H), 7.04 (d, *J* = 2.1 Hz, 1H), 6.94 (s, 1H), 6.89 (s, 1H), 6.82 (d, *J* = 2.2Hz, 1H), 3.88 (s, 4H), 1.78 (s, 6H), 1.38 (s, 12H), 1.36 – 1.28 (m, 3H), 1.14 (d, *J* = 7.4 Hz, 18H); **^{13}C NMR** (126 MHz, $CDCl_3$) δ 149.43, 143.50, 142.21, 141.36, 131.20, 130.82, 130.09, 122.98, 121.82, 118.17, 115.02, 110.22, 100.57, 100.56, 99.80, 98.38, 94.45, 84.15, 55.87, 26.16, 24.90, 18.15, 12.99; **HRMS**: Calcd. for $C_{35}H_{48}N_2O_6BSi$ [M-H]$^+$ =

631.3380 m/z, found = 631.3393 m/z.

Compound 3-40:

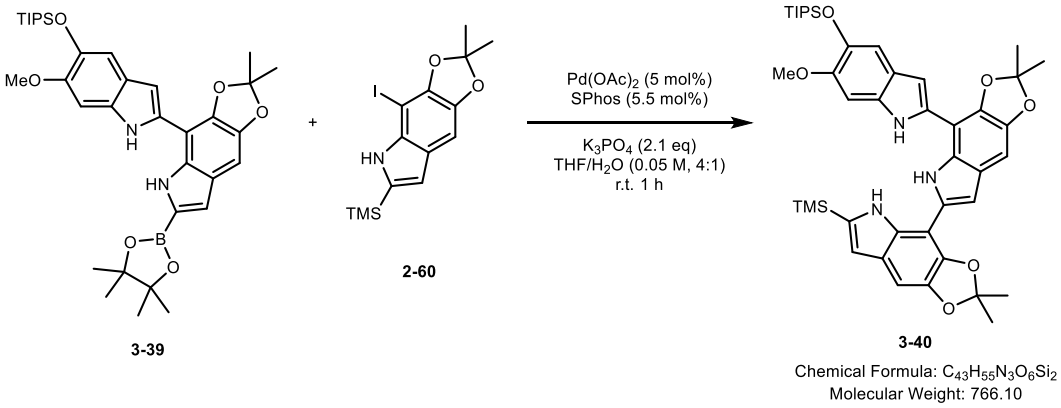

Procedure: The reaction was carried out according to the General Procedure A, the reaction was performed in THF/H_2O at ambient temperature for 1 h.

Amounts of Reagents:

3-39 (537.78 mg, 0.85 mmol, 1.1 equiv)

2-60 (298.21 mg, 0.77 mmol, 1.0 equiv)

$Pd(OAc)_2$ (8.53 mg, 0.038 mmol, 5 mol%)

SPhos (17.24 mg, 0.042 mmol, 5.5 mol %)

K_3PO_4 (343.88 mg, 1.62 mmol, 2.1 equiv)

THF (15.0 mL), H_2O (3.7 mL)

Purification: 5 % to 10 % EtOAc in hexanes.

Yield of Product:

3-40: 509.5 mg, 0.66 mmol, 86 %, light yellow solid.

Characterization:

$\mathbf{R_f}$ = (EtOAc/hexanes, 1:9) 0.33; **IR** (neat) v = 3452, 2940, 2863, 1479, 1446, 1303, 1197, 985, 835, 754, 659, 406 cm^{-1}; **^{1}H NMR** (400 MHz, $CDCl_3$) δ 10.00 (s, 1H), 9.06 (s, 1H), 8.48 (s, 1H), 7.12 (s, 1H), 7.00 (s, 1H), 6.98 (s, 1H), 6.92 (s, 1H), 6.85 (d, *J* = 2.1 Hz, 1H), 6.78 (d, *J* = 2.3 Hz, 1H), 6.69 (d, *J* = 2.1 Hz, 1H), 3.90 (s, 3H), 1.85 (s, 6H), 1.83 (s, 6H), 1.36 – 1.27 (m, 3H), 1.15 (dd, *J* = 7.2 Hz, 18H), 0.40 (s, 9H); **^{13}C NMR** (101 MHz, $CDCl_3$) δ 149.57, 143.50, 143.33, 141.54, 141.14, 140.73, 137.17,

131.11, 130.74, 130.52, 130.45, 127.54, 123.42, 122.87, 121.94, 118.20, 118.15, 112.30, 109.97, 100.33, 99.77, 99.66, 99.60, 98.23, 97.94, 94.69, 56.09, 26.21, 26.08, 18.13, 12.97, -0.76. **HRMS**: Calcd. for $C_{43}H_{55}N_2NaO_6Si_2$ $[M+Na]^+$ = 788.3522 m/z, found = 788.3510 m/z.

Compound 3-41:

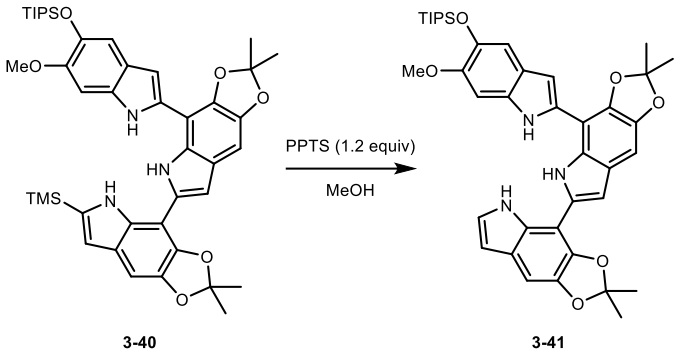

Procedure: The reaction was carried out according to the General Procedure C, the reaction was performed in MeOH at ambient temperature for 3 h.

Amounts of Reagents:

3-40 (509.5 mg, 0.66 mmol, 1.0 equiv)

PPTS (199.03 mg, 0.79 mmol, 1.2 equiv)

MeOH (13.0 mL, 0.05 M)

Purification: 10 % EtOAc in hexanes.

Yield of Product:

3-41: 384.71 mg, 0.55 mmol, 84 %, off-white solid.

Characterization:

$\mathbf{R_f}$ = (EtOAc/hexanes, 2:8) 0.2; **IR** (neat) v = 3450, 2939, 2863, 1446, 1301, 1197, 985, 883, 852, 661, 435 cm^{-1}; **^{1}H NMR** (500 MHz, $CDCl_3$) δ 10.05 (s, 1H), 9.04 (s, 1H), 8.57 (s, 1H), 7.20 (dd, *J* = 3.1, 2.4 Hz, 1H), 7.12 (s, 1H), 6.98 (s, 1H), 6.95 (s, 1H), 6.94 (s, 1H), 6.84 (dd, *J* = 3.1, 2.3f Hz, 1H), 6.80 (d, *J* = 2.3 Hz, 1H), 6.52 (dd, *J* = 3.1, 2.0 Hz, 1H), 3.89 f(s, 3H), 1.85 (s, 6H), 1.82 (s, 6H), 1.28-1.35 (m, 3H), 1.15 (d, *J* = 7.4 Hz, 18H); **^{13}C NMR** (126 MHz, cdcl3) δ 149.55, 143.45, 143.28, 141.54, 140.73, 140.71, 131.11, 130.55, 130.53, 127.47, 127.21, 123.13, 122.84, 122.44, 121.97, 118.19,

118.09, 109.97, 103.61, 100.26, 99.92, 99.78, 99.61, 98.62, 97.89, 94.70, 56.09, 26.21, 26.11, 18.13, 12.98.; **HRMS**: Calcd. for $C_{40}H_{48}N_3O_6$ $[M+H]^+$ = 694.33069 m/z, found = 394.32955 m/z.

Compound 3-42:

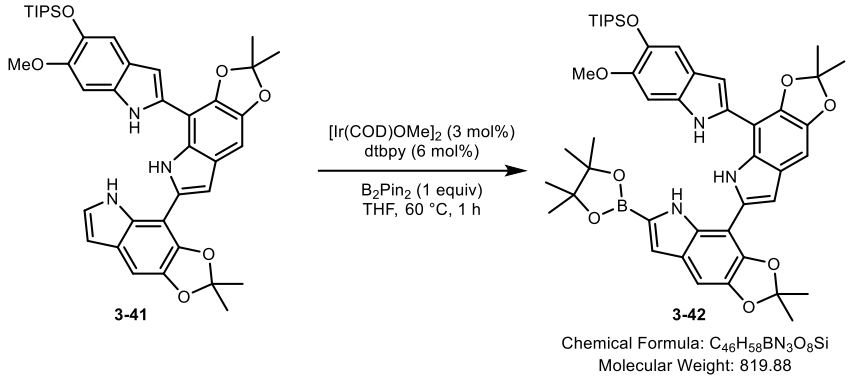

Procedure: The reaction was carried out according to the General Procedure B, the reaction was performed in THF at 60 °C for 1 h.

Amounts of Reagents:

3-41 (353.8 mg, 0.5 mmol, 1.0 equiv)

$[Ir(OMe)(COD)]_2$ (10.14 mg, 0.015 mmol, 3.0 mol%)

dtbpy (8.21 mg, 0.03 mmol, 6.0 mol%)

B_2pin_2 (129.5 mg, 0.5 mmol, 1.0 equiv)

THF (10 mL, 0.05 M)

Purification: 20% EtOAc in hexanes.

Yield of Product:

3-42: 350.2 mg, 0.43 mmol, 83 %, off-white solid.

Characterization:

$\mathbf{R_f}$ = (EtOAc/hexanes, 1:4) 0.39; **IR** (neat) v = 3453, 2935, 2863, 1299, 1261, 1216, 1197, 1135, 852, 661, 464 cm^{-1}; **^{1}H NMR**(400 MHz, $CDCl_3$) δ 10.03 (s, 1H), 9.04 (s, 1H), 8.87 (s, 1H), 7.11 (s, 1H), 7.07 (d, *J* = 2.1 Hz, 1H), 7.00 (s, 1H), 6.98 (s, 1H), 6.93 (s, 1H), 6.90 (d, *J* = 2.2 Hz, 1H), 6.84 (d, 1H), 3.89 (s, 3H), 1.85 (s, 6H), 1.83 (s, 6H), 1.39 (s, 12H), 1.36 – 1.27 (m, 3H), 1.14 (d, *J* = 7.3 Hz, 18H); **^{13}C NMR** (101 MHz, $CDCl_3$) δ 149.53, 143.57, 143.43, 142.12, 141.52, 140.73, 131.11, 130.56, 130.42, 130.34, 127.53, 123.20, 122.86, 121.96, 118.30, 118.17, 114.96, 109.96, 100.69, 99.75,

99.69, 99.57, 98.65, 98.01, 94.69, 84.20, 56.08, 26.22, 26.16, 24.97, 18.13, 12.97.; **HRMS**: Calcd. for $C_{46}H_{57}N_3O_8BSi$ $[M-H]^+$ = 818.40135 m/z, found = 818.40014 m/z.

Compound 3-43:

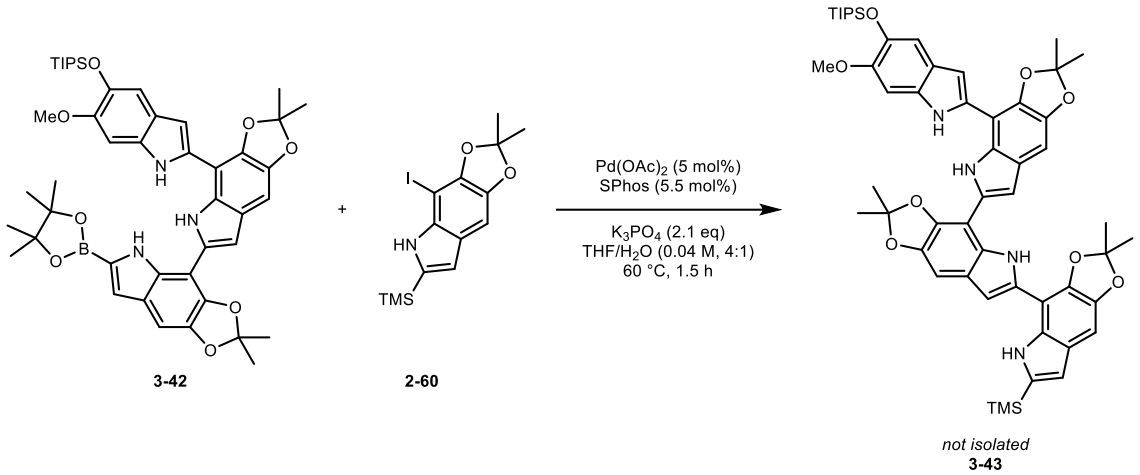

Procedure: The reaction was carried out according to the General Procedure A, the reaction was performed in THF/H_2O at 60 °C for 1.5 h.

Amounts of Reagents:

3-42 (352.5 mg, 0.43 mmol, 1.1 equiv)

2-60 (151.0 mg, 0.39 mmol, 1.0 equiv)

$Pd(OAc)_2$ (4.38 mg, 0.019 mmol, 5 mol %)

SPhos (8.81 mg, 0.042 mmol, 5.5 mol %)

K_3PO_4 (173.9 mg, 0.82 mmol, 2.1 equiv)

THF (8.0 mL), H_2O (2.0 mL)

Purification: 10 % EtOAc in hexanes.

Yield of Product:

3-43: 69 % (NMR yield calculated using hexamethylbenzene as an internal standard), light yellow solid.

Characterization:

R_f = (EtOAc/hexanes, 1:9) 0.30; **^{1}H NMR** (500 MHz, $CDCl_3$) δ 10.12 (s, 1H), 9.95 (s, 1H), 9.06 (s, 1H), 8.50 (s, 1H), 7.14 (s, 1H), 7.03 (s, 1H), 6.99 (s, 1H), 6.93 (s, 1H), 6.93 (s, 1H), 6.87-6.88 (m, 2H),

6.81 (d, *J* = 2.1 Hz, 1H), 6.70 (d, *J* = 2.1 Hz, 1H), 3.91 (s, 3H), 1.90 (s, 6H), 1.87 (s, 6H), 1.84 (s, 6H), 1.37 – 1.29 (m, 3H), 1.16 (d, *J* = 7.4 Hz, 18H), 0.40 (s, 9H).

Compound 3-44:

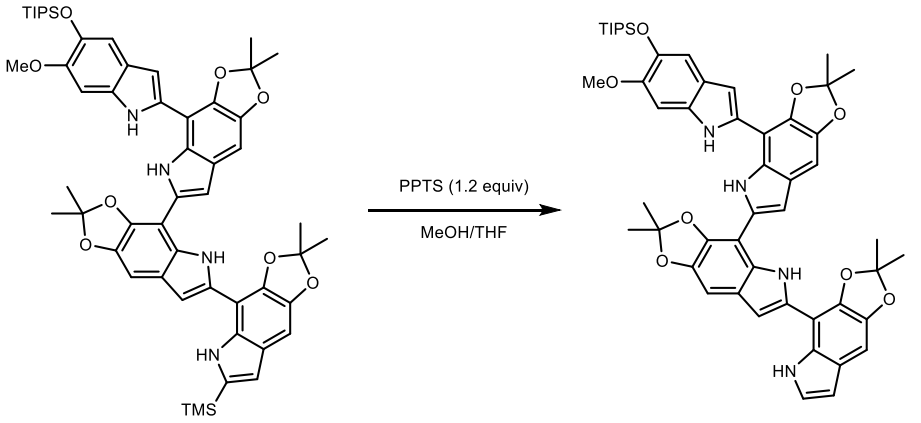

3-43 **3-44**

Chemical Formula: $C_{51}H_{56}N_4O_8Si$
Molecular Weight: 881.11

Procedure: The reaction was carried out according to the General Procedure C, the reaction was performed in MeOH and THF at ambient temperature for 6 h.

Amounts of Reagents:

3-43 (390.0 mg, 0.40 mmol, 1.0 equiv)

PPTS (120.6 mg, 0.48 mmol, 1.2 equiv)

MeOH (10 mL), THF (2 mL)

Purification: 10 % EtOAc in hexanes.

Yield of Product:

3-44: 206.18 mg, 0.23 mmol, 60 % over two steps, off-white solid.

Characterization:

$\mathbf{R_f}$ = (EtOAc/hexanes, 1:9) 0.23; **IR** (neat) v = 34550, 2937, 2863, 1446, 1303, 1199, 1170, 983, 850, 754, 661, 435 cm^{-1}; **^{1}H NMR** (500 MHz, $CDCl_3$) δ 10.11 (s, 1H), 10.00 (s, 1H), 9.05 (s, 1H), 8.59 (s, 1H), 7.20 (dd, 3.2, 2.2 Hz 1H), 7.13 (s, 1H), 6.99 (m, 2H), 6.96 (s, 1H), 6.92 (s, 1H), 6.87-6.88 (m, 2H), 6.83 (d, *J* = 2.2 Hz, 1H), 6.52 (dd, *J* = 3.2, 2.1 Hz, 1H), 3.90 (s, 3H), 1.89 (s, 6H), 1.87 (s, 6H),

1.83 (s, 6H), 1.36 – 1.29 (m, 3H), 1.15 (d, *J* = 7.4 Hz, 18H); **^{13}C NMR** (126 MHz, $CDCl_3$) δ 149.60, 143.52, 143.28, 141.57, 140.78, 140.74, 140.72, 131.13, 130.77, 130.64, 130.49, 127.47, 127.24, 127.13, 123.15, 123.10, 122.96, 122.47, 121.97, 118.29, 118.16, 109.98, 103.64, 100.42, 100.00, 99.85, 99.71, 99.59, 98.70, 98.07, 97.66, 94.70, 56.09, 26.24, 26.15, 18.14, 12.98; **HRMS**: Calcd. for $C_{51}H_{55}N_4O_8Si$ $[M-H]^+$ = 879.37946 m/z, found = 879.37924 m/z.

Compound 3-45:

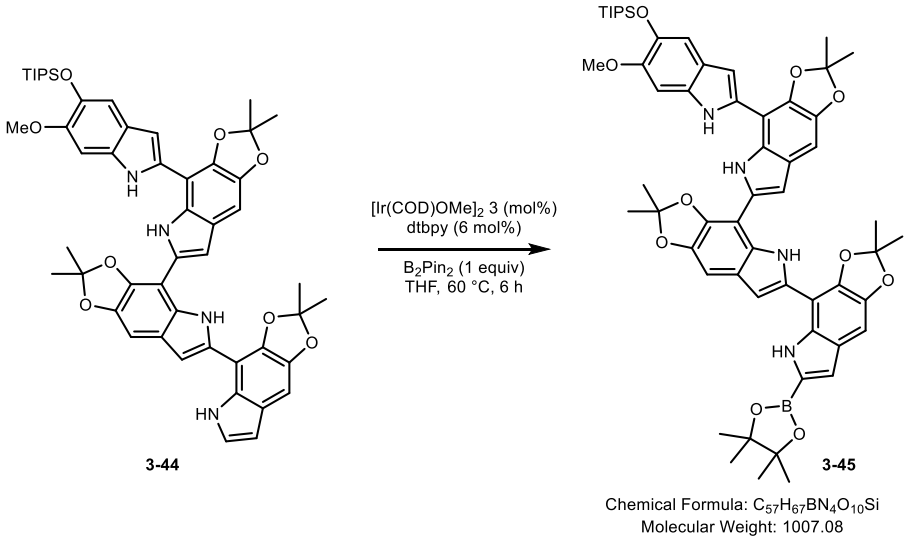

Procedure: The reaction was carried out according to the General Procedure B, the reaction was performed in THF at 60 °C for 6 h.

Amounts of Reagents:

3-44 (72.2 mg, 0.08 mmol, 1.0 equiv)

$[Ir(OMe)(COD)]_2$ (1.59 mg, 0.0024 mmol, 3.0 mol%)

dtbpy (1.29 mg, 0.0048 mmol, 6.0 mol%)

B_2pin_2 (20.32 mg, 0.08 mmol, 1.0 equiv)

THF (1.6 mL, 0.05 M)

Purification: 20% EtOAc in hexanes.

Yield of Product:

3-45: 55.8 mg, 0.055 mmol, 70 %, white solid.

Characterization:

R_f = (EtOAc/hexanes, 1:4) 0.43; **IR** (neat) v = 3446, 2962, 2861, 1303, 1259, 1014, 854, 796, 663, 435 cm^{-1}; **^{1}H NMR** (500 MHz, $CDCl_3$) δ 10.12 (brs, 1H), 9.98 (brs, 1H), 9.06 (brs, 1H), 8.91 (brs, 1H), 7.13 (s, 1H), 7.08 (d, *J* = 2.0 Hz, 1H), 7.05 (s, 1H), 6.99 (s, 1H), 6.95 – 6.93 (m, 2H), 6.92 (s, 1H), 6.89 – 6.87 (m, 2H), 3.90 (s, 3H), 1.90 (s, 6H), 1.88 (s, 6H), 1.84 (s, 6H), 1.40 (s, 12H), 1.36 – 1.29 (m, 3H), 1.16 (d, *J* = 7.4 Hz, 18H); **^{13}C NMR** (126 MHz, $CDCl_3$) δ 149.58, 143.56, 143.51, 143.49, 142.14, 141.56, 140.76, 140.72, 131.14, 130.68, 130.55, 130.49, 130.44, 127.47, 127.18, 123.24, 123.12, 122.97, 121.98, 118.36, 118.27, 118.25, 115.02, 109.97, 100.87, 99.97, 99.86, 99.71, 99.67, 99.54, 98.72, 98.20, 97.65, 94.71, 84.21, 56.08, 26.28, 26.22, 26.15, 24.97, 18.13, 12.98, 1.18.; **HRMS**: Calcd. for $C_{57}H_{68}N_4O_{10}BSi$ $[M+H]^+$ = 1007.47923 m/z, found = 1007.47881 m/z.

Compound 3-46:

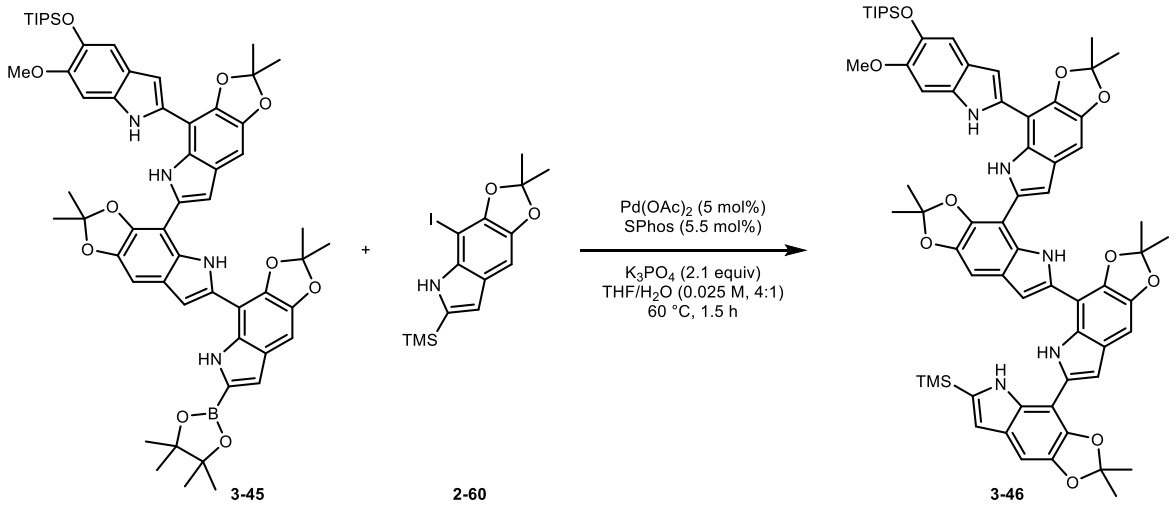

Procedure: The reaction was carried out according to the General Procedure A, the reaction was performed in THF/H_2O at 60 °C for 1.5 h.

Amounts of Reagents:

3-45 (55.8 mg, 0.055 mmol, 1.1 equiv)

2-60 (19.4 mg, 0.05 mmol, 1.0 equiv)

$Pd(OAc)_2$ (0.56 mg, 0.0025 mmol, 5 mol %)

SPhos (1.13 mg, 0.00275 mmol, 5.5 mol %)

K_3PO_4 (22.3 mg, 0.11 mmol, 2.1 equiv)

THF (2.0 mL), H_2O (0.5 mL)

Purification: 10 % to 20 % EtOAc in hexanes.

Yield of Product:

3-46: 39.2 mg, 0.034 mmol, 68 %, light yellow solid.

Characterization:

R_f = (EtOAc/hexanes, 1:4) 0.47; **^{1}H NMR** (500 MHz, $CDCl_3$) δ 10.13 (d, *J* = 2.2 Hz, 1H), 10.07 (d, *J* = 2.3 Hz, 1H), 9.97 (d, *J* = 2.2 Hz, 1H), 9.06 (d, *J* = 2.2 Hz, 1H), 8.50 (brs, 1H), 7.14 (s, 1H), 7.04 (s, 1H), 7.00 (s, 1H), 6.96 (s, 1H), 6.94 (m, 2H), 6.92 (d, *J* = 2.2 Hz, 2H), 6.89 (d, *J* = 2.1 Hz, 1H), 6.82 (d, *J* = 2.2 Hz, 1H), 6.70 (d, *J* = 2.1 Hz, 1H), 3.91 (s, 3H), 1.91 (s, 6H), 1.90 (s, 6H), 1.87 (s, 6H), 1.84 (s, 6H), 1.37 – 1.29 (m, 3H), 1.16 (d, *J* = 7.5 Hz, 18H), 0.40 (s, 9H).; **^{13}C NMR** (101 MHz, $CDCl_3$) δ 149.61, 143.59, 143.55, 143.32, 141.58, 141.16, 140.81, 140.78, 140.75, 137.21, 131.14, 130.97, 130.84, 130.59, 130.47, 127.50, 127.20, 127.12, 123.46, 123.21, 123.14, 122.97, 121.96, 118.38, 118.36, 118.31, 118.22, 112.33, 109.98, 100.45, 100.14, 100.08, 99.86, 99.73, 99.69, 99.59, 99.56, 98.33, 98.20, 97.84, 97.67, 94.70, 56.08, 26.26, 26.24, 26.21, 26.17, 18.14, 12.98, -0.76.; **HRMS**: Calcd. for $C_{65}H_{73}N_5NaO_{10}Si_2$ $[M+Na]^+$ = 1162.4788 m/z, found = 1162.4802 m/z.

Compound 3-47:

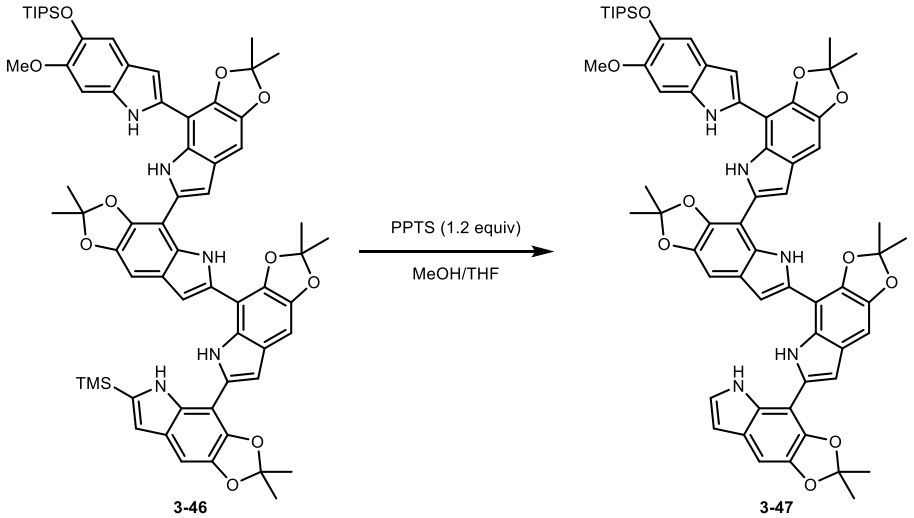

Procedure: The reaction was carried out according to the General Procedure C, the reaction was

performed in MeOH and THF at ambient temperature for 6 h.

Amounts of Reagents:

3-46 (39.2 mg, 0.034 mmol, 1.0 equiv)

PPTS (10.3 mg, 0.041mmol, 1.2 equiv)

MeOH (2.0 mL), THF (0.2 mL)

Purification: 20 % EtOAc in hexanes.

Yield of Product:

3-47: 206.18 mg, 0.03 mmol, 89 %, off-white solid.

Characterization:

$\mathbf{R_f}$ = (EtOAc/hexanes, 1:4) 0.14; **IR** (neat) v = 3444, 2935, 2863, 1446, 1303, 1199, 1170, 983, 852, 755, 663, cm^{-1}; **^{1}H NMR** (500 MHz, $CDCl_3$) δ 10.12 (d, *J* = 2.2 Hz, 1H), 10.08 (d, *J* = 2.2 Hz, z1H), 10.01 (d, *J* = 2.0 Hz, 1H), 9.06 (d, *J* = 2.1 Hz, 1H), 8.59 (brs, 1H), 7.21 (dd, *J* = 3.1, 2.4 Hz, 1H), 7.14 (s, 1H), 6.99 (s, 2H), 6.96 (s, 2H), 6.94 (s, 1H), 6.91 (m, 2H), 6.88 (d, *J* = 2.1 Hz, 1H), 6.84 (d, *J* = 2.2 Hz, 1H), 6.53 (dd, *J* = 3.1, 2.1 Hz, 1H), 3.90 (s, 3H), 1.91 (s, 6H), 1.90 (s, 6H), 1.88 (s, 6H), 1.84 (s, 6H), 1.37 – 1.28 (m, 3H), 1.16 (d, *J* = 7.4 Hz, 18H).; **^{13}C NMR** (201 MHz, $CDCl_3$) δ 149.61, 143.59, 143.55, 143.51, 143.28, 141.58, 140.81, 140.77, 140.75, 131.14, 130.86, 130.79, 130.60, 130.47, 127.50, 127.24, 127.15, 127.12, 123.22, 123.15, 123.13, 122.97, 122.48, 121.97, 118.38, 118.35, 118.31, 118.17, 109.98, 103.64, 100.43, 100.14, 100.08, 99.88, 99.86, 99.73, 99.69, 99.55, 98.71, 98.15, 97.84, 97.67, 94.70, 56.09, 26.27, 26.26, 26.24, 26.17, 18.14, 12.99.; **HRMS**: Calcd. for $C_{62}H_{65}N_5NaO_{10}Si$ $[M+Na]^+$ = 1090.4393 m/z, found = 1090.4346 m/z.

3.7 References

1. d'Ischia, M.; Wakamatsu, K.; Napolitano, A.; Briganti, S.; Garcia-Borron, J.-C.; Kovacs, D.; Meredith, P.; Pezzella, A.; Picardo, M.; Sarna, T.; Simon, J. D.; Ito, S., Melanins and melanogenesis: methods, standards, protocols. *Pigment Cell & Melanoma Research* **2013,** *26* (5), 616-633.

2. d'Ischia, M.; Napolitano, A.; Pezzella, A., 5,6-Dihydroxyindole Chemistry: Unexplored Opportunities Beyond Eumelanin. *European Journal of Organic Chemistry* **2011,** *2011* (28), 5501-5516.

3. Panzella, L.; Pezzella, A.; Napolitano, A.; d'Ischia, M., The First 5,6-Dihydroxyindole Tetramer by Oxidation of 5,5‘,6,6‘-Tetrahydroxy- 2,4‘-biindolyl and an Unexpected Issue of Positional Reactivity en Route to Eumelanin-Related Polymers. *Organic Letters* **2007,** *9* (7), 1411-1414.

4. Capelli, L.; Manini, P.; Pezzella, A.; Napolitano, A.; d’Ischia, M., Efficient Synthesis of 5,6-Dihydroxyindole Dimers, Key Eumelanin Building Blocks, by a Unified o-Ethynylaniline-Based Strategy for the Construction of 2-Linked Biindolyl Scaffolds. *The Journal of Organic Chemistry* **2009,** *74* (18), 7191-7194.

5. Capelli, L.; Manini, P.; Pezzella, A.; d'Ischia, M., First synthetic entry to the trimer stage of 5,6-dihydroxyindole polymerization: ortho-alkynylaniline-based access to the missing 2,7′:2′,7′′-triindole. *Organic & Biomolecular Chemistry* **2010,** *8* (19), 4243-4245.

6. Merrifield, R. B., Automated Synthesis of Peptides. *Science* **1965,** *150* (3693), 178-185.

7. Caruthers, M. H., Gene Synthesis Machines: DNA Chemistry and Its Uses. *Science* **1985,** *230* (4723), 281-285.

8. Balieu, S.; Hallett, G. E.; Burns, M.; Bootwicha, T.; Studley, J.; Aggarwal, V. K., Toward Ideality: The Synthesis of (+)-Kalkitoxin and (+)-Hydroxyphthioceranic Acid by Assembly-Line Synthesis. *Journal of the American Chemical Society* **2015,** *137* (13), 4398-4403.

9. Fiorito, D.; Keskin, S.; Bateman, J. M.; George, M.; Noble, A.; Aggarwal, V. K., Stereocontrolled Total Synthesis of Bastimolide B Using Iterative Homologation of Boronic Esters. *Journal of the American Chemical Society* **2022**.

10. Burns, M.; Essafi, S.; Bame, J. R.; Bull, S. P.; Webster, M. P.; Balieu, S.; Dale, J. W.; Butts, C. P.; Harvey, J. N.; Aggarwal, V. K., Assembly-line synthesis of organic molecules with tailored shapes. *Nature* **2014,** *513* (7517), 183-8.

11. Crudden, C. M.; Ziebenhaus, C.; Rygus, J. P.; Ghozati, K.; Unsworth, P. J.; Nambo, M.; Voth, S.; Hutchinson, M.; Laberge, V. S.; Maekawa, Y.; Imao, D., Iterative protecting group-free cross-coupling leading to chiral multiply arylated structures. *Nat. Commun.* **2016,** *7*, 11065.

12. Li, J.; Ballmer, S. G.; Gillis, E. P.; Fujii, S.; Schmidt, M. J.; Palazzolo, A. M.; Lehmann, J. W.; Morehouse, G. F.; Burke, M. D., Synthesis of many different types of organic small molecules using one automated process. *Science* **2015,** *347* (6227), 1221-6.

13. Negishi, E.-i.; Liou, S.-Y.; Xu, C.; Huo, S., A Novel, Highly Selective, and General Methodology for the Synthesis of 1,5-Diene-Containing Oligoisoprenoids of All Possible Geometrical Combinations Exemplified by an Iterative and Convergent Synthesis of Coenzyme Q10. *Organic Letters* **2002,** *4* (2), 261-264.

14. Nicolaou, K. C.; Daines, R. A.; Chakraborty, T. K.; Ogawa, Y., Total synthesis of amphoteronolide B and amphotericin B. 2. Total synthesis of amphoteronolide B. *Journal of the American Chemical Society* **1988,** *110* (14), 4685-4696.

15. Suzuki, A.; Sasaki, M.; Nakagishi, T.; Ueda, T.; Hoshiya, N.; Uenishi, J. i., Construction of Iterative Tetrahydrofuran Ring Units and Total Synthesis of (+)-Goniocin. *Organic Letters* **2016,** *18* (9), 2248-2251.

16. Gillis, E. P.; Burke, M. D., A simple and modular strategy for small molecule synthesis: iterative Suzuki-Miyaura coupling of B-protected haloboronic acid building blocks. *Journal of the American Chemical Society* **2007,** *129* (21), 6716-7.

17. Woerly, E. M.; Roy, J.; Burke, M. D., Synthesis of most polyene natural product motifs using just 12 building blocks and one coupling reaction. *Nature Chemistry* **2014,** *6*, 484.

18. Zhang, J.; Moore, J. S.; Xu, Z.; Aguirre, R. A., Nanoarchitectures. 1. Controlled synthesis of phenylacetylene sequences. *Journal of the American Chemical Society* **1992,** *114* (6), 2273-2274.

19. Moore, J. S., Shape-Persistent Molecular Architectures of Nanoscale Dimension. *Accounts of Chemical Research* **1997,** *30* (10), 402-413.

20. d'Ischia, M.; Napolitano, A.; Tsiakas, K.; Prota, G., New intermediates in the oxidative polymerisation of 5,6-dihydroxyindole to melanin promoted by the peroxidase/H_2O_2 system. *Tetrahedron* **1990,** *46* (16), 5789-5796.

21. d'Ischia, M.; Napolitano, A.; Prota, G., Peroxidase as an alternative to tyrosinase in the oxidative polymerization of 5,6-dihydroxyindoles to melanin(s). *Biochimica et Biophysica Acta (BBA) - General Subjects* **1991,** *1073* (2), 423-430.

22. Miyaura, N.; Suzuki, A., Palladium-Catalyzed Cross-Coupling Reactions of Organoboron Compounds. *Chemical Reviews* **1995,** *95* (7), 2457-2483.

23. Martin, R.; Buchwald, S. L., Palladium-catalyzed Suzuki-Miyaura cross-coupling reactions employing dialkylbiaryl phosphine ligands. *Acc. Chem. Res.* **2008,** *41* (11), 1461-73.

24. Kinzel, T.; Zhang, Y.; Buchwald, S. L., A new palladium precatalyst allows for the fast Suzuki-Miyaura coupling reactions of unstable polyfluorophenyl and 2-heteroaryl boronic acids. *Journal of the American Chemical Society* **2010,** *132* (40), 14073-5.

25. Lennox, A. J. J.; Lloyd-Jones, G. C., The Slow-Release Strategy in Suzuki–Miyaura Coupling. *Israel Journal of Chemistry* **2010,** *50* (5-6), 664-674.

26. Düfert, M. A.; Billingsley, K. L.; Buchwald, S. L., Suzuki-Miyaura Cross-Coupling of Unprotected, Nitrogen-Rich Heterocycles: Substrate Scope and Mechanistic Investigation. *Journal of the American Chemical Society* **2013,** *135* (34), 12877-12885.

27. Billingsley, K. L.; Anderson, K. W.; Buchwald, S. L., A Highly Active Catalyst for Suzuki–Miyaura Cross-Coupling Reactions of Heteroaryl Compounds. *Angewandte Chemie International Edition* **2006,** *45* (21), 3484-3488.

28. Billingsley, K.; Buchwald, S. L., Highly Efficient Monophosphine-Based Catalyst for the Palladium-Catalyzed Suzuki−Miyaura Reaction of Heteroaryl Halides and Heteroaryl Boronic Acids and Esters. *Journal of the American Chemical Society* **2007,** *129* (11), 3358-3366.

29. Duong, H. A.; Chua, S.; Huleatt, P. B.; Chai, C. L. L., Synthesis of Biindolyls via Palladium-Catalyzed Reactions. *The Journal of Organic Chemistry* **2008,** *73* (22), 9177-9180.

30. Kuivila, H. G.; Jr., J. F. R.; Mangravite, J. A., Electrophilic Displacement Reactions: XV. Kinetics and Mechanism of the Base-catalyzed Protodeboronation of Areneboronic Acids. *Canadian Journal of Chemistry* **1963,** *41* (12), 3081-3090.

31. Thomas, A. A.; Denmark, S. E., Pre-transmetalation intermediates in the Suzuki-Miyaura reaction revealed: The missing link. *Science* **2016,** *352* (6283), 329.

32. Carrow, B. P.; Hartwig, J. F., Distinguishing Between Pathways for Transmetalation in Suzuki−Miyaura Reactions. *Journal of the American Chemical Society* **2011,** *133* (7), 2116-2119.

33. Paul, S.; Chotana, G. A.; Holmes, D.; Reichle, R. C.; Maleczka, R. E., Jr.; Smith, M. R., 3rd, Ir-catalyzed functionalization of 2-substituted indoles at the 7-position: nitrogen-directed aromatic borylation. *J Am Chem Soc* **2006,** *128* (49), 15552-3.

34. Hartung, C. G.; Fecher, A.; Chapell, B.; Snieckus, V., Directed ortho Metalation Approach to C-7-Substituted Indoles. Suzuki−Miyaura Cross Coupling and the Synthesis of Pyrrolophenanthridone Alkaloids. *Organic Letters* **2003,** *5* (11), 1899-1902.

35. Lakshman, M. K.; Tine, F. A.; Khandaker, T. A.; Basava, V.; Agyemang, N. B.; Benavidez, M. S. A.; Gasi, M.; Guerrera, L.; Zajc, B., KHF2, a mild and selective desilylating agent for phenol t-butyldimethylsilyl (TBDMS) ethers. *Synlett* **2017,** *28* (3), 381-385.

36. Hartmann, O.; Kalesse, M., The Total Synthesis of (−)-Aurafuron A. *Organic Letters* **2012,** *14* (12), 3064-3067.

37. Pezzella, A.; Panzella, L.; Natangelo, A.; Arzillo, M.; Napolitano, A.; d'Ischia, M., 5,6-Dihydroxyindole Tetramers with “Anomalous” Interunit Bonding Patterns by Oxidative Coupling of 5,5‘,6,6‘-Tetrahydroxy-2,7‘-biindolyl: Emerging Complexities on the Way toward an Improved Model of Eumelanin Buildup. *The Journal of Organic Chemistry* **2007,** *72* (24), 9225-9230.

38. Arzillo, M.; Pezzella, A.; Crescenzi, O.; Napolitano, A.; Land, E. J.; Barone, V.; d’Ischia, M., Cyclic Structural Motifs in 5,6-Dihydroxyindole Polymerization Uncovered: Biomimetic Modular Buildup of a Unique Five-Membered Macrocycle. *Organic Letters* **2010,** *12* (14), 3250-3253.

Chapter 4 : Total Synthesis of Kaxiras' Cyclic Tetramer

Despite the absence of a well-defined structure, decades of spectroscopic and theoretical studies analyzing natural and synthetic eumelanin support a structure consisting of small planar units held together by π-stacking interactions to form graphite-like layered aggregates (Chapter 1, Section 1.3). While none of these planar molecules has been isolated from natural samples, a principal contender based upon theoretical studies, is the porphyrin-like tetra-indole-quinone (**1-1**) that is commonly referred to as the Kaxiras' tetramer (Figure 4-1). Several studies based upon computer modelling have suggested that **1-1** could reproduce certain features of eumelanin's optical properties if aggregated into small ensembles.[1-4] Intrigued by its fascinating structure and potential relevance to eumelanin, we initiated a project with the aim of completing the first total synthesis of **1-1**.

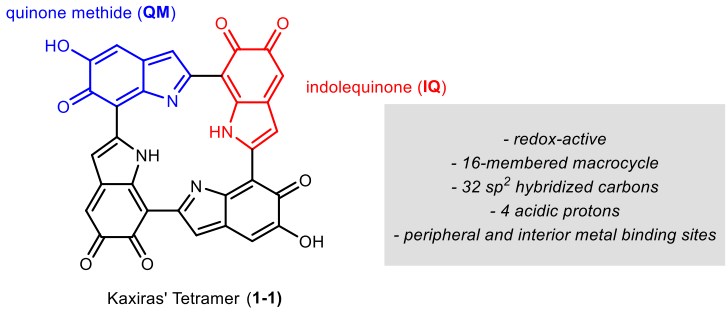

Figure 4-1 Structural features of Kaxiras' tetramer

4.1 Retrosynthesis

Kaxiras' tetramer (**1-1**) contains several structural features that make it a challenging synthetic target. **1-1** is composed of a highly functionalized 16-membered macrocyclic structure that includes 32 sp^2 hybridized carbons, it has 4 acidic protons and metal biding sites at both the periphery of the ring and the porphyrin-like interior. **1-1** is likely redox-active and could exist in multiple tautomeric forms (indolequinone and quinone methide). Although calculations show that the quinone methide (**QM**) tautomer is energetically favored in Kaxiras' tetramer, the effects of placing these units within a macrocycle is unclear, and likely influenced by the steric repulsion of the H atoms projecting towards the interior portion of the ring. These features, along with its potential relevance to eumelanin make **1-1** an interesting target for total synthesis.

Presented in Schemes 4-1, 4-2, and 4-4 are our retrosynthetic analyses of **1-1**. We first simplified **1-1** to the fully reduced, tetra-catechol (**4-1**). In the forward synthesis, Kaxiras and co-workers calculated that the formation of tetra-oxidized **1-1** is energetically favored.[5] **4-1** could be simplified to a protected derivative **4-2**. Because catechols are easily oxidized, acidic and capable of chelating metals, we chose to mask them as the corresponding acetonides until the late stages of the synthesis (Scheme 4-1). **4-2** was subsequently simplified by two complementary strategies.

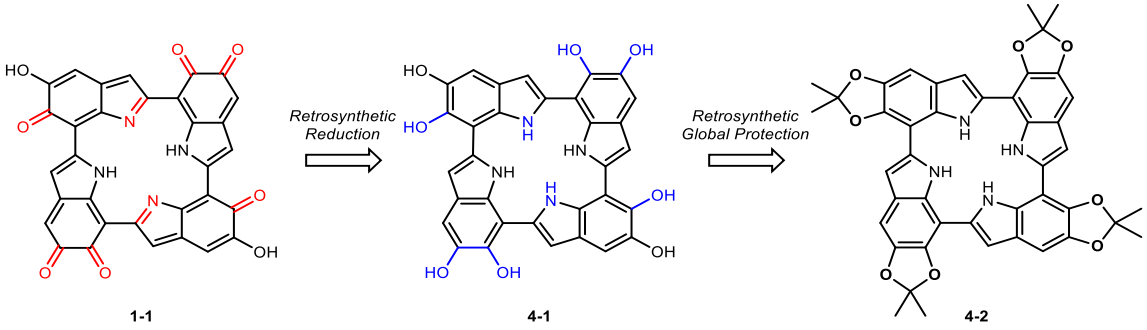

Scheme 4-1 Retrosynthetic analysis of Kaxiras' tetramer

Retrosynthetic strategy A attempted to capitalize on the C_4 symmetry of **4-2** by disconnecting two of the C2-C7 bonds to create two identical fragments **4-3**. In the forward direction, we anticipated a dimerization/macrocyclization cascade as a means of forming the 16-membered ring (Scheme 4-2).

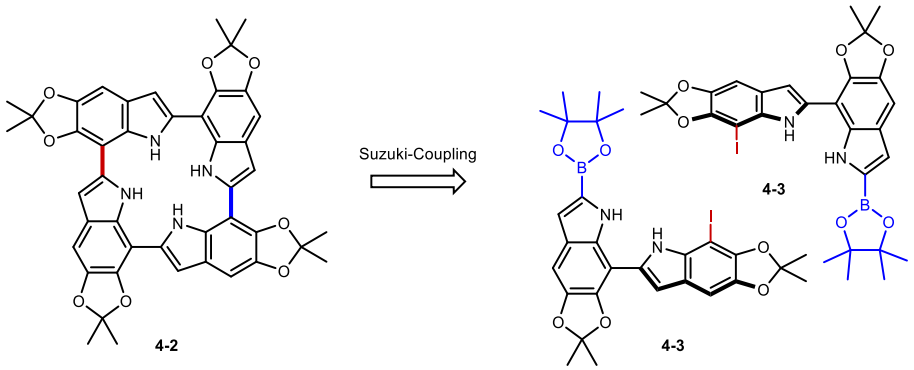

Scheme 4-2 Retrosynthetic analysis of Kaxiras' tetramer: Strategy A

The only related example of such a transformation was reported by Shinokubo and co-workers.[6] In their work, a tetra-indole macrocycle (**4-5**) consisting of repeating indole subunits was synthesized via a convergent dimerization of **4-4** upon treatment with $Pd_2dba_3{\cdot}CHCl_3$ and Buchwald's biphenylphosphine ligand SPhos. Attempts to synthesize **4-5** through tetramerization

of 2-boryl-7-iodoindole via Suzuki–Miyaura cross-coupling failed and afforded only a complex mixture (Scheme 4-3).

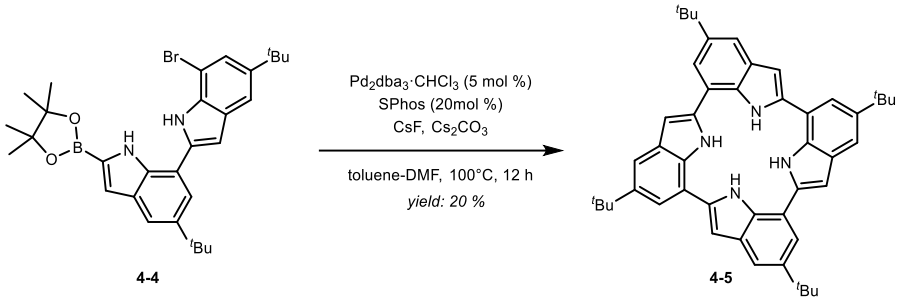

Scheme 4-3 Synthesis of tetra-indole macrocycle

Alternatively, in Retrosynthetic strategy B, we considered an approach where a single carbon-carbon bond cleavage of **4-2** would lead to linear tetramers **4-6** or **4-7**. In the forward synthesis, macrocyclization would hinge on an intramolecular Suzuki-Coupling from **4-6** or an oxidative coupling from diboronic ester **4-7**. **4-6** and **4-7** could arise from convergent couplings of two dimer units **4-8** with **4-10** or **4-9** with **4-10**, which was envisioned to come from functionalization of the parent indole monomeric units (Scheme 4-4).

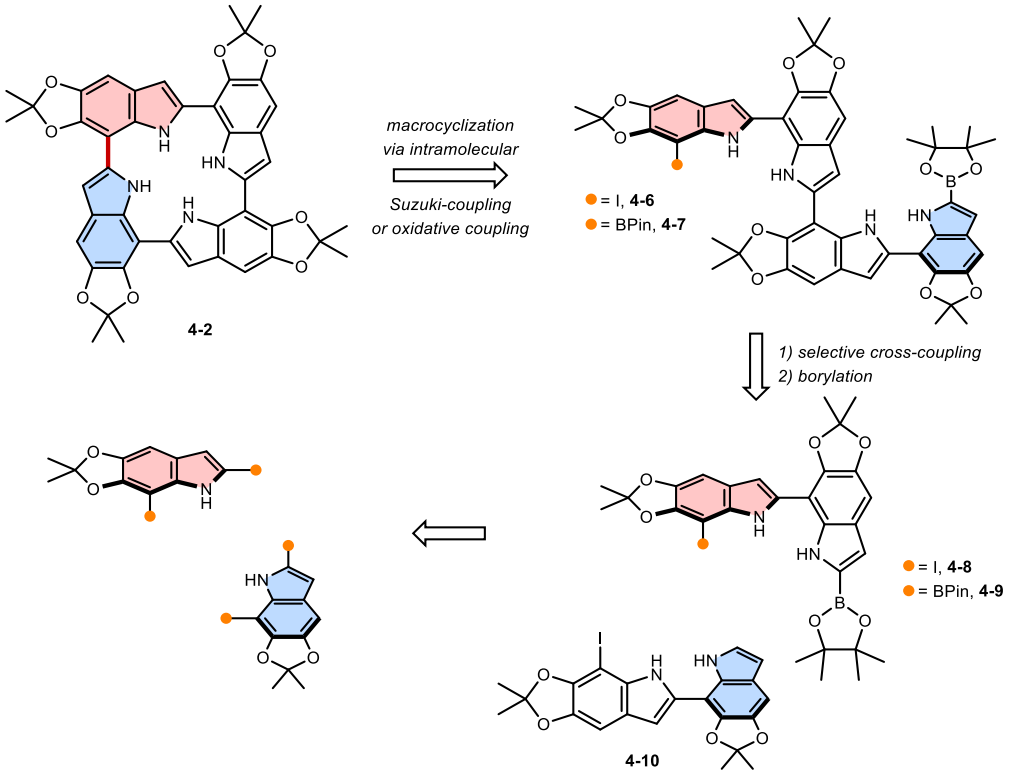

Scheme 4-4 Retrosynthetic analysis of Kaxiras' tetramer: Strategy B

Current synthetic methods toward efficient macrocycle formation with a high content of sp^2 hybridized carbon atoms are limited and remain as a synthetic challenge. Macrocyclization entails an entropic loss, and must address issues of inter- vs intra- molecular reactivity.[7, 8]

In 2017, Jasti and co-workers demonstrated a mild oxidative boronic ester homocoupling reaction for the synthesis of strained and conformationally restricted macrocycles with $Pd(PPh_3)_2Cl_2$ and KF under air in THF/H_2O. Boric acid was used as a sacrificial boron source to mitigate the decomposition pathway of the boronic esters to their corresponding phenols, a common reaction product of boronic acids and esters in the presence of hydrogen peroxide. This methodology proved to be effective for the synthesis of strained alkynes (**4-11**), acerogenin E macrocyclic precursor (**4-12**), and strained polyparaphenylenes (**4-13**, Scheme 4-5).[9]

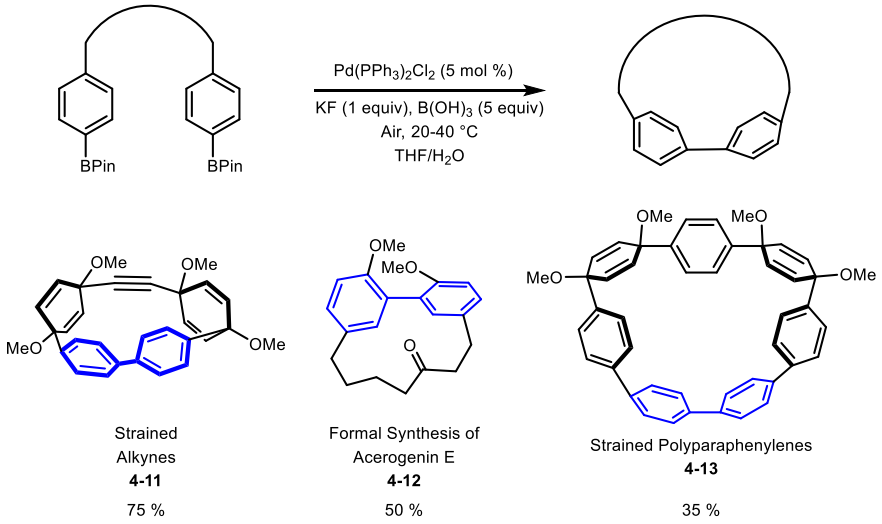

Scheme 4-5 Synthesis of strained and conformationally restricted macrocycles

In 2018, Schindler and co-workers reported a scalable synthesis of mycocyclosin,[10] a diketopiperazine natural product that was first synthesized by Hutton and co-worker.[11] The macrocyclization step in constructing the highly strained bicyclic framework provided **4-17** in high yield on gram-scale with $Pd(dppf)Cl_2{\cdot}CH_2Cl_2$, B_2Pin_2, K_2CO_3, and air (Scheme 4-6). In the key step of constructing the highly strained bicyclic framework, they proposed two complementary mechanistic regimes. In the first pathway, a Miyaura borylation of the bis-iodide (**4-14**) led to **4-15**, which undergoes an intramolecular Suzuki-Miyaura cross coupling. Alternatively, two

consecutive borylations of **4-14** could provide **4-16**, which formed **4-17** under Pd(II)-catalyzed intramolecular oxidative coupling conditions.

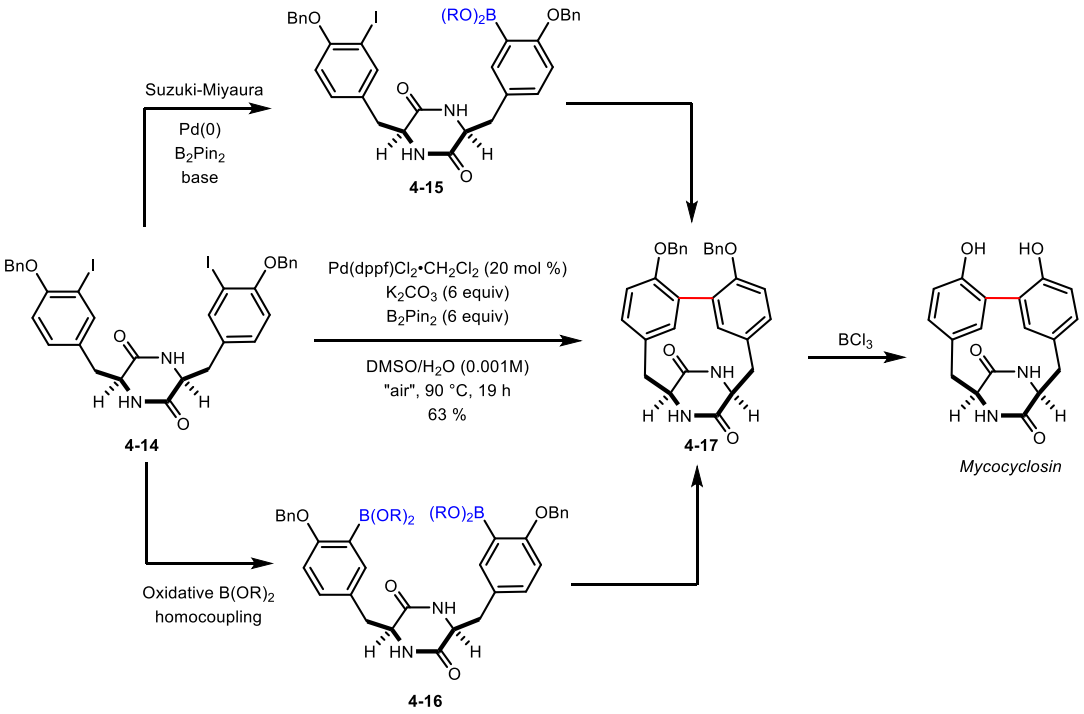

Scheme 4-6 Synthesis of Mycocyclosin

In our early stages of planning, we recognized that the stability of **1-1** could be a potential complication of its synthesis. In particular, we were concerned about the possibility of polymerization through the C4 positions (indole numbering), given the possibility of radical character at these positions (Figure 4-2).

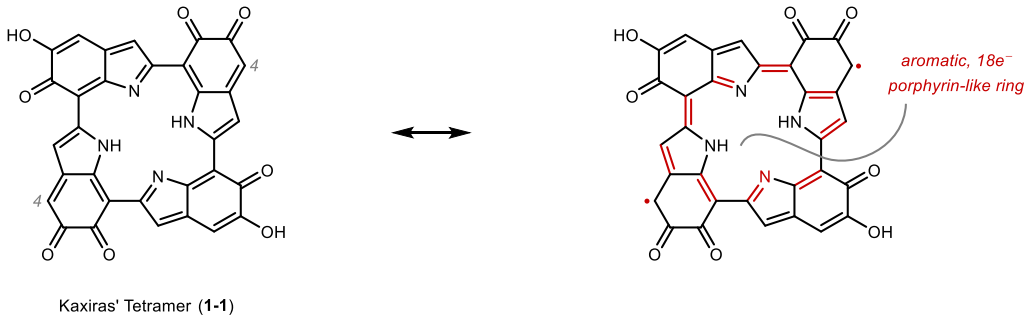

Figure 4-2 Radical character at C4 positions of **1-1**

Furthermore, calculations indicate that **1-1** is a planar molecule that could form aggregates by π-stacking interactions.[4] Therefore, we hypothesized that our blocking group strategy would decouple chain-oxidation from chain-growth and chain-aggregation by providing steric stabilization to **1-1** without perturbation of the quinone's π-system. Retrosynthetically, blocked Kaxiras' tetramer (**4-18**) could arise from **4-19** via global deprotection then oxidation. We identified **4-20** as a precursor to **4-19** via global Suzuki-coupling with blocking groups (e.g. 2-iodotoluene). **4-20** was envisioned to come from a global borylation of **4-2** (Scheme 4-7).

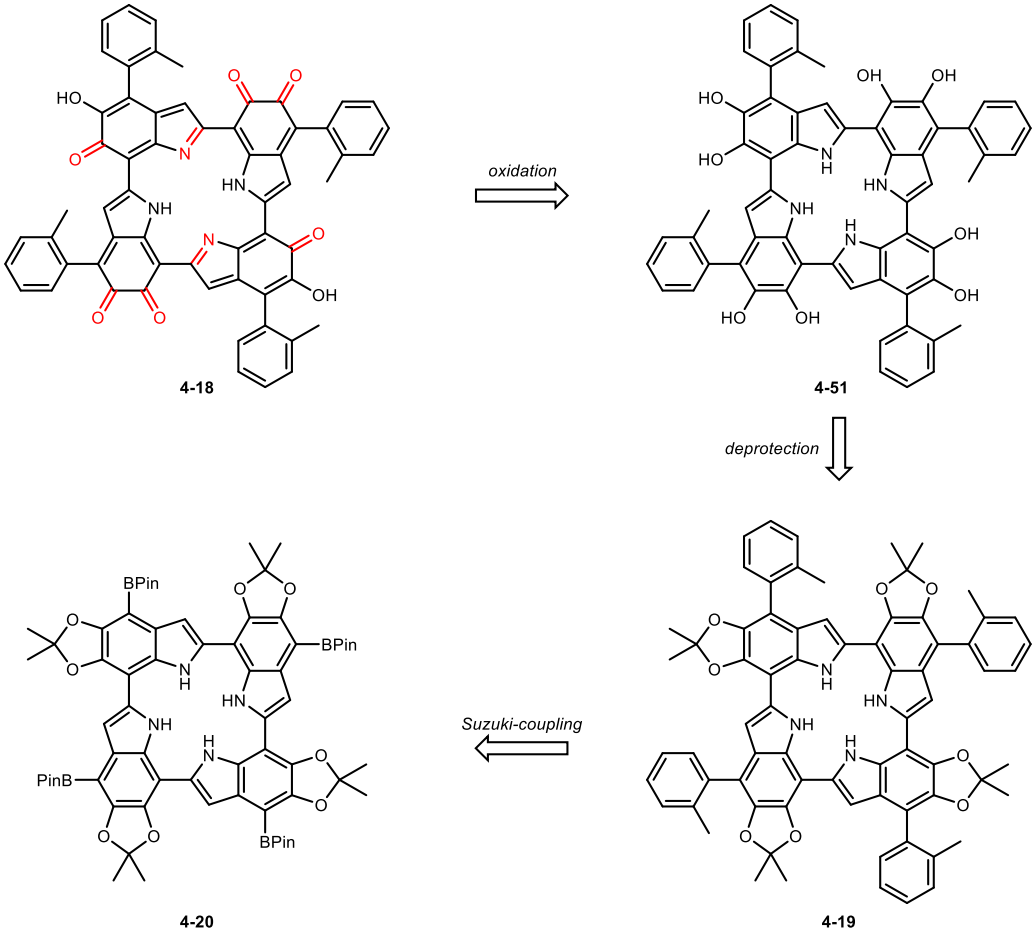

Scheme 4-7 Retrosynthetic analysis of blocked Kaxiras' tetramer

<u>Outline of Chapter 4</u>: In Chapter 4, we describe our efforts in executing the planed total synthesis of Kaxiras' cyclic tetramer **1-1**. In Section 4.2, we focus on solving the issue of selective functionalization at the C7 positions of dimers. In Section 4.3, we discuss the synthesis of the reduced Kaxiras cyclic tetramer (**4-2**) via dimerization/macrocyclization from bis-functionalized

dimer (**4-3**). In section 4.3, we illustrate the synthesis of **4-2** via an intramolecular macrocyclization from diboronic ester (**4-7**). Finally, in section 4.5, capitalizing on our blocking group strategy, we describe our success in obtaining a dimer at quinone oxidation state that possess eumelanin-like physical properties and our success in synthesizing an oxidized cyclic tetramer.

4.2 C7 Functionalization on Dimers

Critical to the success of our approaches to the Kaxiras tetramer was our ability to access precursors **4-3** and **4-6**/**4-7**, which requires functional handles on the C7 positions of the dimer and tetramers. Having previously experienced difficulties when attempting the C-H borylation of dimers **3-21**, **3-26**, and **3-24** (Chapter 3, Section 3.3.1), we required an alternative approach to address this challenge.

During our initial investigation of biaryl bond formation via Suzuki-coupling (Chapter 3, Section 3.2), we also discovered that the cross coupling between **2-58** and **2-66** or **2-33** proceeded with a modest yield of dimers **4-21** and **3-24** (Scheme 4-8).

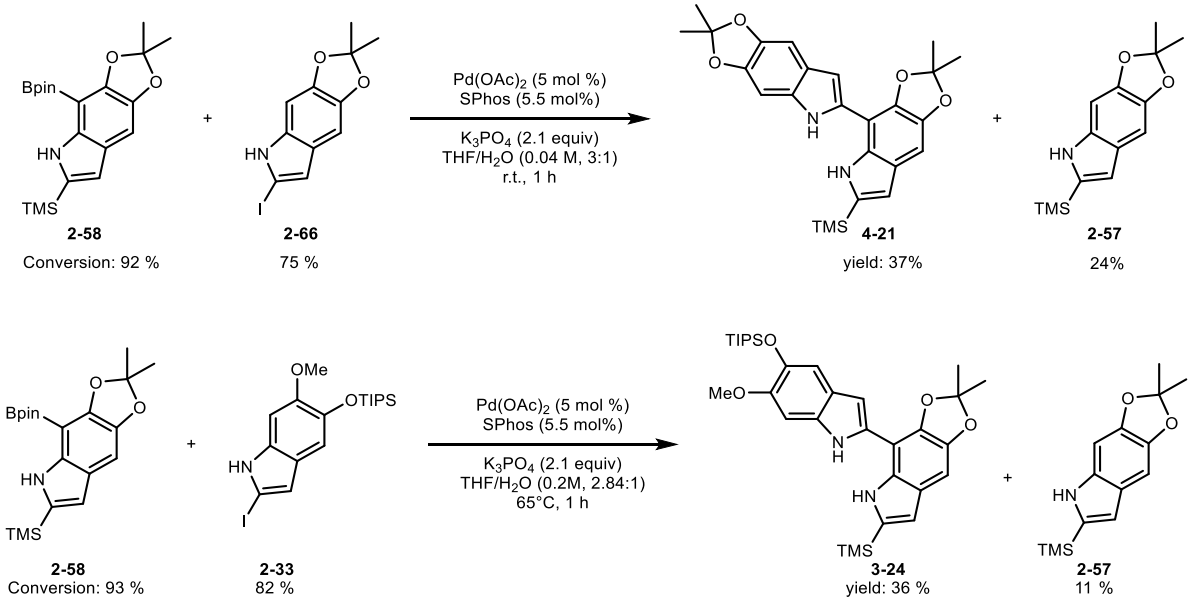

Scheme 4-8 Suzuki coupling of 2-iodo-indoles and 7-Bpin-indoles

Inspired by these results, we anticipated that a selective cross coupling between **2-58** and **2-63** could provide the desired C7-iodo dimers. Selective Suzuki-coupling reactions have been demonstrated via judicious site-selective introduction of different types of halogens into a substrate, as demonstrated in the elegant synthesis of Dragmacidin D by Stoltz, Garg, and Sarpong.[13] For polyhalogenated heteroaromatics containing a single type of halogen, the site-selectivity is dictated by intrinsic polarities of the ring carbons.[14]

Our attempts to selectively construct the 2,7'-bond by regioselective cross-coupling, unfortunately, proved to be ineffective. Significant protodeborylation of **2-58** occurred under the reaction conditions at ambient temperature within 30 min (entry 1). Elevated temperatures, extended reaction times, and reduced solvent/H_2O ratio led to complete conversion of **2-58**, yet only protodeborylation byproduct **2-57** was observed (entries 2 and 3).

Table 4-1 Condition optimization to 7-iodo-dimer

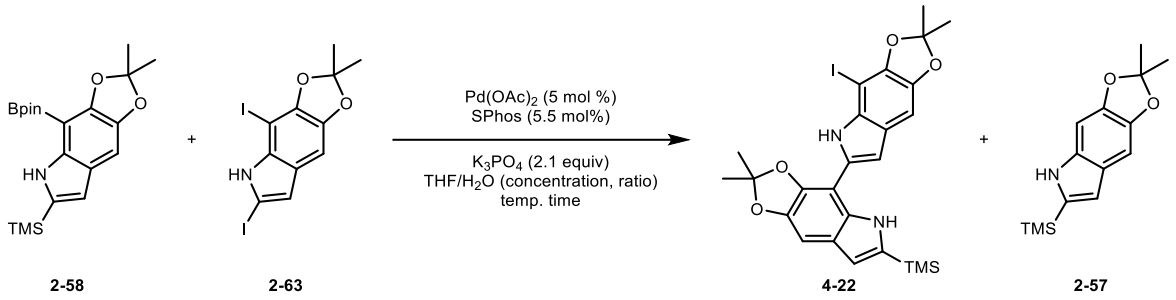

2-58 **2-63** **4-22** **2-57**

Entry	**2-58** (equiv)	**2-63** (equiv)	Temp (° C)	Time (min)	Con. (M)	Ratio THF/H_2O	Conversion **2-58/2-63** (%)	Yield **4-22/2-57** (%)
1	1.1	1.0	r.t.	30	0.15	2.81/1	64/37	0/34
2	1.0	1.1	60	40	0.08	4.86/1	100/26	0/65
3	1.1	1.0	rt	60	0.05	2.81/1	100/58	0/90

4.2.1 Installation of Boronic Ester at the C7 Position on Dimers

We then envisioned that a selective C2 cross-coupling between **2-37** and **2-21b** could be a possible alternative as the electronic requirement for Suzuki coupling matches with the polarity of the indoles. Despite the literature precedent for site-selective Suzuki-coupling with polyhalogenated heteroaromatics containing a single type of halogen, examples of selective Suzuki-coupling in polyborylated heteroaromatics, to the best of our knowledge, is unknown. To investigate the site selective Suzuki-coupling, the cross-coupling reaction between **2-21b** and **2-**

37 was explored. The cross-coupling reactions occurred selectively at the C2 position of **2-21b** and afforded **4-23** in 56 % yield, determined by ^{1}H-NMR using hexamethylbenzene as an internal standard (Scheme 4-9).

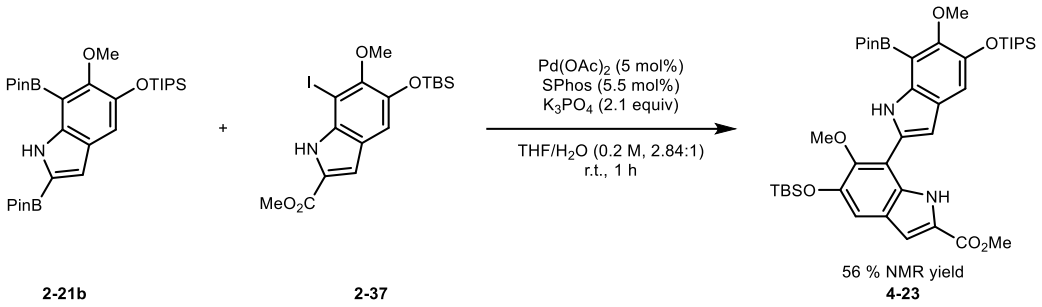

Scheme 4-9 Cross-coupling to 7-Bpin-dimer

To confirm the C2, C7'-connectivity of **4-23**, selective deprotection of the TBS group was necessary to obtain analytically pure dimers. This was due to the similar R_f values of **4-23** and the remaining substrates and byproducts. Selective removal of the TBS group proceeded smoothly using potassium bifluoride (KHF_2) in THF/MeOH to **4-24** in 50 % yield (Scheme 4-10).

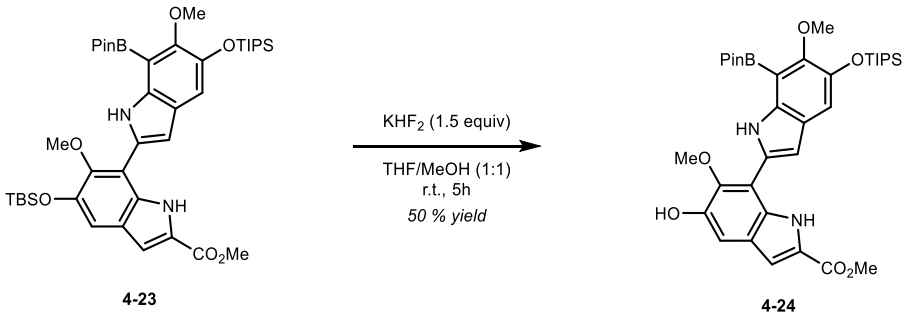

Scheme 4-10 Selective deprotection of TBS group

The structural elucidation of **4-24** was conducted by 1D and 2D NMR spectroscopy. The key signal in distinguishing the formation of a 2,7'- versus a 7,7'- carbon-carbon bond connectivity was the presence of a nOe correlation between H_F and H_B (Figure 4-3, red arrow). If the cross coupling had occurred between positions 7 and 7' to form compound **4-24b**, there would not be a correlation between H_F and H_B.

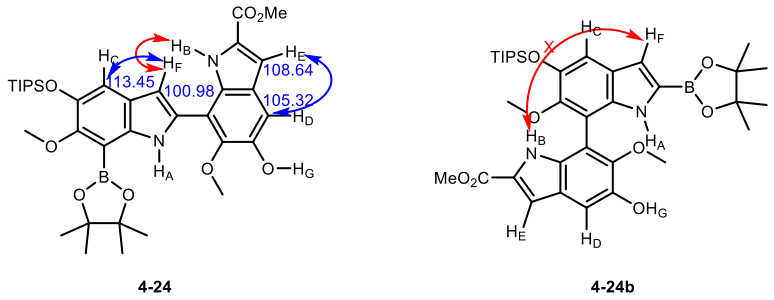

Figure 4-3 Key 2D NMR correlation (red=nOe correlations, blue=HMBC correlations)

Despite our success in synthesizing **4-23**, chain extension at C2 remained a challenge as the methyl ester was difficult to remove for subsequent functionalization at the C2 position. As we illustrated in Chapter 3, Section 3.3.2, we had previously addressed this issue by incorporating a silyl group at C2. Therefore, we turned our attention to the selective coupling of **2-47** and **2-60** and were delighted to find that under similar conditions (THF/H_2O=4:1, ambient temperature, 1 h), cross coupling of **2-47** and **2-60** provided the C7-borylated dimer **4-25** in 70 % yield. Further attempts to optimize the reaction by changing the phosphine ligand to XPhos or Xantphos (entries 2 and 4), or the Pd precatalyst to either SPhos-Pd-G2 (entry 3) or $Pd_2(dba)_3$ source (entry 5) failed to provide **4-25** in higher yields. Small amounts of trimer **4-26** were obtained in yields ranging from 3-8 % (Table 4-2).

Table 4-2 Selected condition optimization of selective Suzuki-coupling

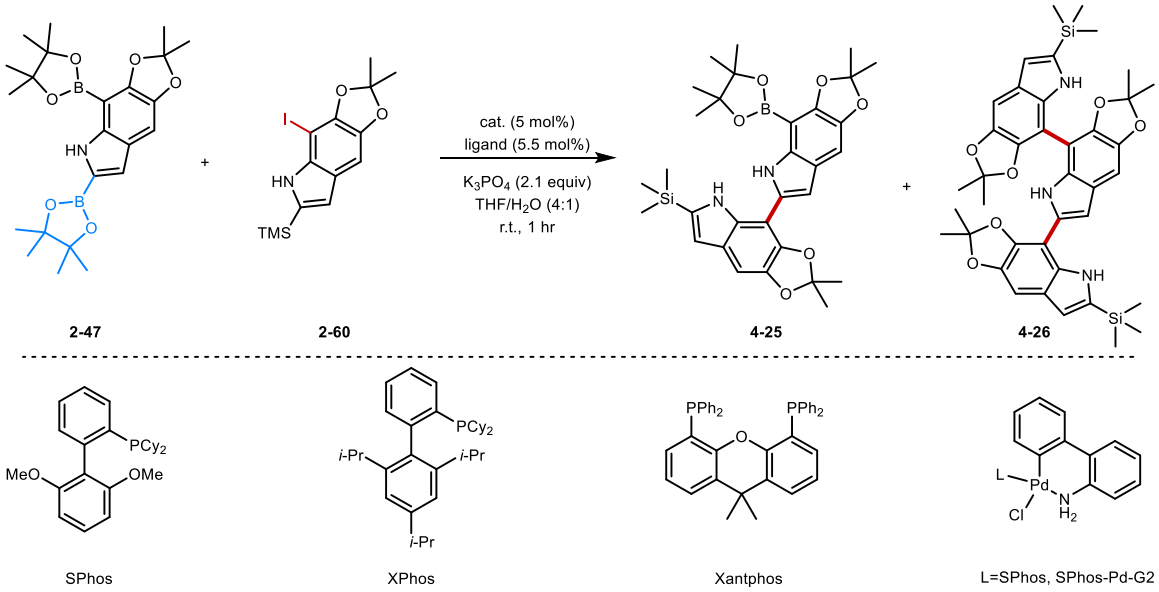

Entry	Catalyst	Ligand	Ligand (mol %)	Conversion **2-47**/**2-60** (%)	Yield of **4-25** (%)
1	$Pd(OAc)_2$	SPhos	5.5	100/78	70
2	$Pd(OAc)_2$	XPhos	5.5	100/75	44
3	SPhos-Pd-G2	SPhos	5.0	100/88	43
4	$Pd(OAc)_2$	Xantphos	5.5	90/80	26
5	$Pd_2(dba)_3$	SPhos	11.0	83/65	31

The structural elucidation of **4-25** was conducted by 1D and 2D NMR spectroscopy. The key nOe correlation between H_F and H_B was also observed, as it was for **4-24**. Desilylation of **4-25** under our previously developed conditions (PPTS, MeOH) delivered **4-27** in 80 % yield. Single crystals of **4-27** were obtained and confirmed the C2, C7' connectivity unambiguously (Scheme 4-11).

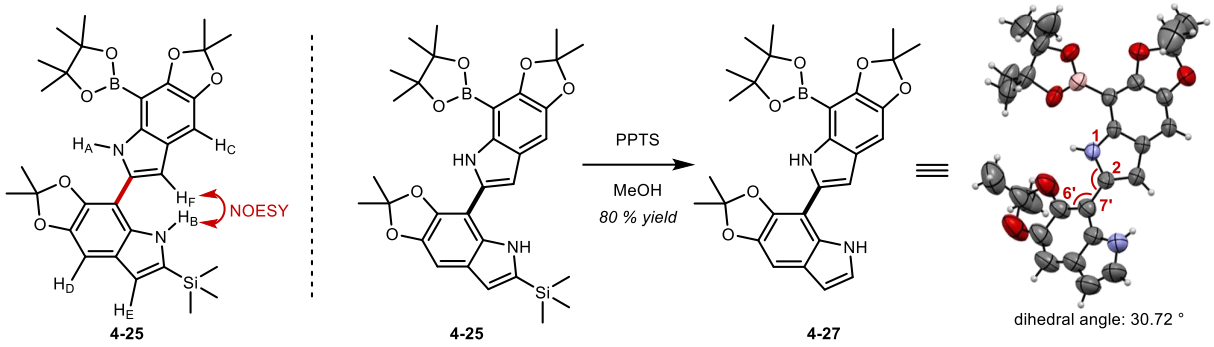

Scheme 4-11 Desilylation and structure confirmation of 2,7'-bond connectivity

4.2.2 Halodeborylation at C7 Position on Dimer

Having established an efficient synthesis of dimers bearing the C7-boronic ester (**4-25** and **4-27**), we turned our attention to developing suitable conditions for conversion of the boronic esters to halogens, which would allow for chain growth with monomers or dimers bearing the C2-boronic ester.

With compound **4-25** in hand, we attempted to oxidize the Bpin substituent at C7 to the corresponding iodide, using our previously developed conditions (see Chapter 2, Table 2-7). Using CuI, phenanthroline (Phen) and KI provided the desired product **4-28**, but only in 3 % yield. We suspected that under the oxidizing conditions, dimer **4-28** was oxidized to **4-28a**, featuring a double bond between two monomeric units. We hypothesize that the formation of an oxide **4-29a** in the presence of O_2, subsequent nucleophilic addition of the oxide to the C3 position

afforded a purple compound **4-29** in 3 % yield**.** Alternatively, the C7' position in **4-29a** was susceptible to nucleophilic addition upon oxidation. In this case, the addition of methanol led to a yellow compound **4-30** in 20 % yield (Scheme 4-12). The structures of compounds **4-29** and **4-30** are not confirmed at this time, but rather, are based upon ^{1}H-NMR and HRMS.

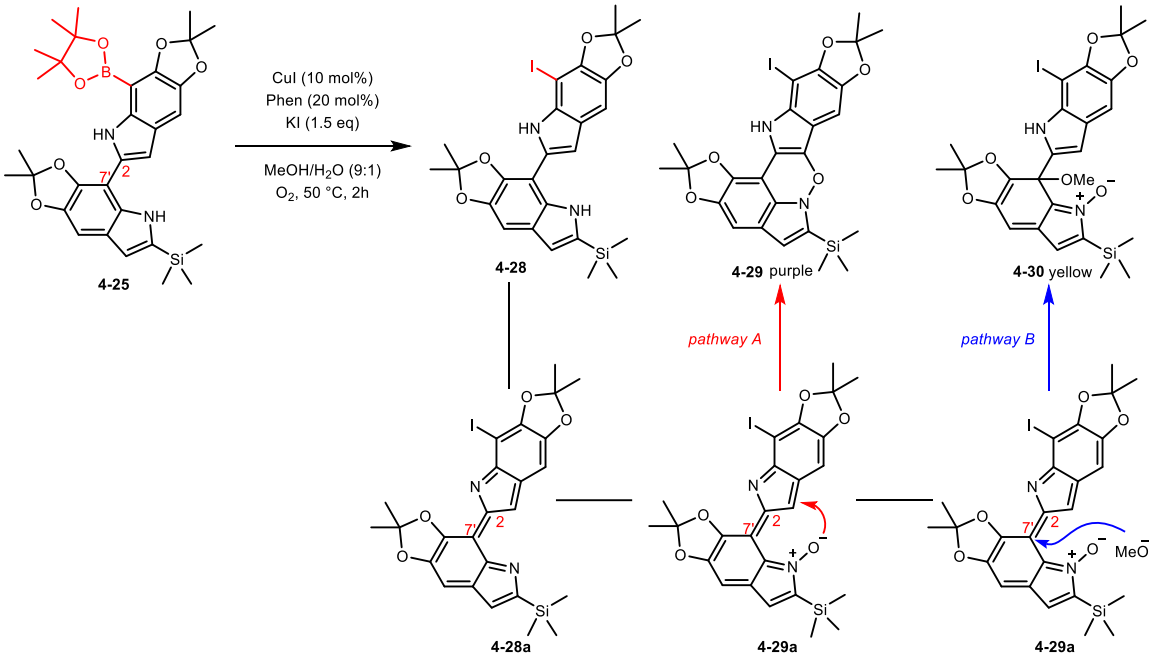

Scheme 4-12 Proposed reaction pathways to the byproduct formation in halodeborylation reaction

Given our inability to oxidize the C7-boronic ester to the corresponding iodide, we anticipated that careful tuning of the electronic properties of **4-25** could help to slow the undesired pathways. Specifically, we planned to install an electron-withdrawing group on the nitrogen atoms to make the dimer less susceptible to oxidation and to facilitate the iodination reaction. To this end, we first examined Boc as a protecting group, and to our delight, Boc protection with an excess amount of Boc_2O (10 equiv) and DMAP (50 mol %) delivered compound **4-31** with a single Boc group on the nitrogen atom of indole A in 45 % yield (Table 3-3). Regioselectivity was determined by 2D NMR, HMBC spectrum indicated a correlation of H_H to the C2 carbon in indole B (136.00 ppm). The carbon signal at 136.00 ppm correlates to a nitrogen proton, which can be seen by the C3 carbon (111.73 ppm) of indole B. We proposed that the regioselectivity arose from differences in the steric environment between the two nitrogen atoms. More specifically, the nitrogen atom of indole B is likely shielded by the TMS group at C2, leaving the nitrogen atom of indole A more

accessible for Boc-protection. Attempts to protect both nitrogen atoms with Boc groups was unsuccessful, and instead, cyclic urea **4-32** (entry 1) was isolated as the major product in 13 % yield. Decreasing the amount of Boc_2O from 10 to 5 equivalents improved the yield of **4-31** and decreased the yield of **4-32** (entry 2). At ambient temperature and with extended reaction time, the reaction proceeded smoothly to **4-31** in 77 % yield on gram scale (entry 3).

Table 4-3 Selected conditions for Boc protection of dimer **4-25**

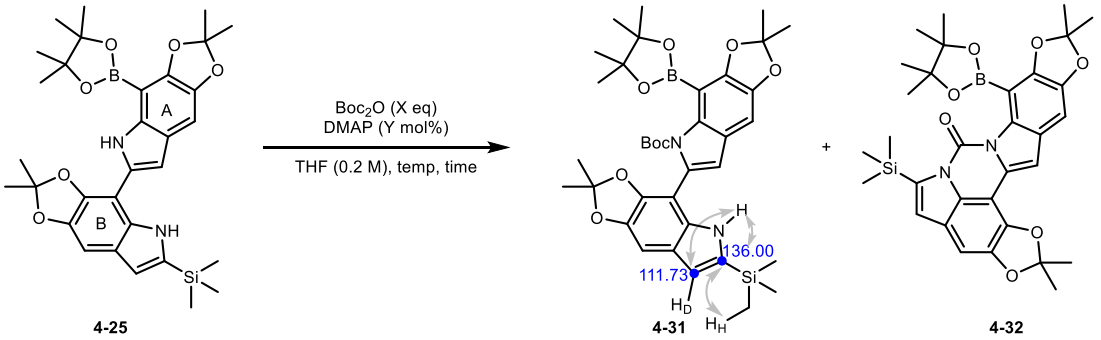

Entry	Boc_2O (equiv)	DMAP (mol%)	Temp (°C)	Time (h)	Conversion (%)	Yield **4-31/4-32** (%)
1	10	50	40	2	98	45/13
2	5	50	40	2	100	75/5
3	5	50	r.t.	12	100	77/2

Having attained **4-31** in high yields, we next examined possible conditions for iodination at C7 (Table 4-4). Gratifyingly, the reaction was found to proceed smoothly to **4-33** in 51 % yield with CuI, Phen in MeOH and H_2O (entry 1). Increasing the catalyst loading to 20 mol % failed to improve the yield of **4-33** (entry 2). The efficiency of the reaction was increased by switching the ligand to 3,4,7,8-tetramethyl-1,10-phenanthroline (tmphen) and increasing the catalyst loading to 15 mol %; this resulted in a 68 % yield of **4-33** (entry 3). Including THF to improve the solubility of the reaction mixture afforded higher yields of **4-33** (entries 4 and 5). This reaction could be conducted on gram-scale and afforded a consistent yield of **4-33** in 81 % (entry 5).

Table 4-4 Condition optimization for iododeborylation of **4-31**

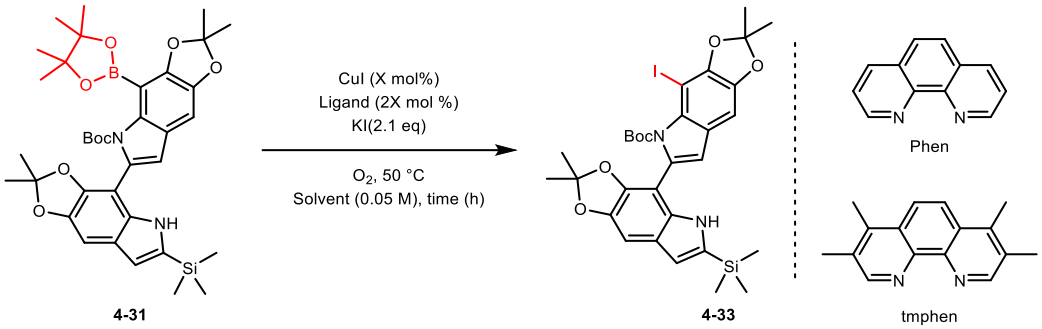

4-31 4-33

Entry	CuI (mol%)	Ligand	Solvent	Time (h)	Conversion (%)	Yield (%)
1	10	Phen	MeOH/H_2O	1	93	51
2	20	Phen	MeOH/H_2O	2	100	50
3	15	tmphen	MeOH/H_2O	2	100	68
4	15	tmphen	THF/MeOH/ H_2O	1.5	100	78
5	15	tmphen	THF/MeOH/ H_2O	2	100	81

Alternative halogenation reagents were also investigated. For example, a bromodeborylation was attempted with a stoichiometric amount of $CuBr_2$, using reaction conditions that have been reported by Hartwig and co-workers.[15] This, however, only resulted in complete consumption of **4-31** with only trace amounts of desilylation byproduct **4-35** (entry 1). Shortening the reaction time (entry 2), decreasing the amount of oxidant (entry 3), or lowering the reaction temperature (entry 4) failed afford **4-34** (Table 4-5).

Table 4-5 Conditions for bromodeboryaltion of **4-31**

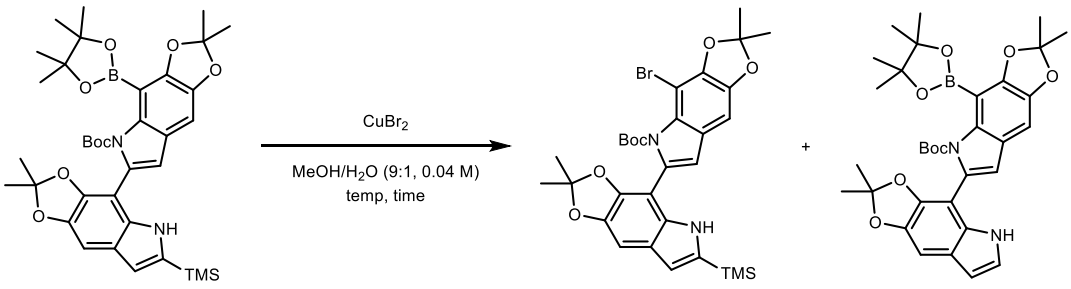

4-31 4-34 4-35

Entry	$CuBr_2$ (equiv)	Time (min)	Temp (°C)	Conversion (%)	Yield of **4-34** (%)
1	3.0	60	50	100	0
2	3.0	20	50	100	0
3	1.5	20	50	100	0
4	3.0	30	r.t.	100	0

4.3 Synthesis of Kaxiras' Cyclic Tetramer via an Intermolecular Dimerization Macrocyclization Cascade

4.3.1 Synthesis of bis-functionalized Dimer

In order to pursue Retrosynthetic Plan A (Scheme 4-2), we required a bis-functionalized dimer **4-3**. To this end, we first explored conditions to remove the Boc group of **4-33**. Under conditions previously developed in Chapter 2 (Table 2-5), deprotection of **4-33** returned only a 40 % yield of **4-36** (entry 1),[16] whereas thermolysis failed to remove the Boc group and instead resulted in decomposition of **4-33** (entry 2).[17] Treatment of **4-33** with TMSOTf (4 equiv) and triethylamine (4 equiv), under conditions developed by Burgess,[18, 19] led to only a low yield of **4-10** (entry 3). Another approach to deprotect the Boc group via addition-elimination with 3-methoxypropylamine proved to be ineffective for our substrate (entry 4).[20] To our delight, treatment of **4-33** in hexafluoro-2-propanol (HFIP) provided **4-37** and **4-10** in 40 % and 58 % yield respectively at 50 °C. By increasing the temperature to 70 °C, the yield of **4-10** was increased to 86 % (Table 4-6).

Table 4-6 Condition optimization for deprotection of **4-33**

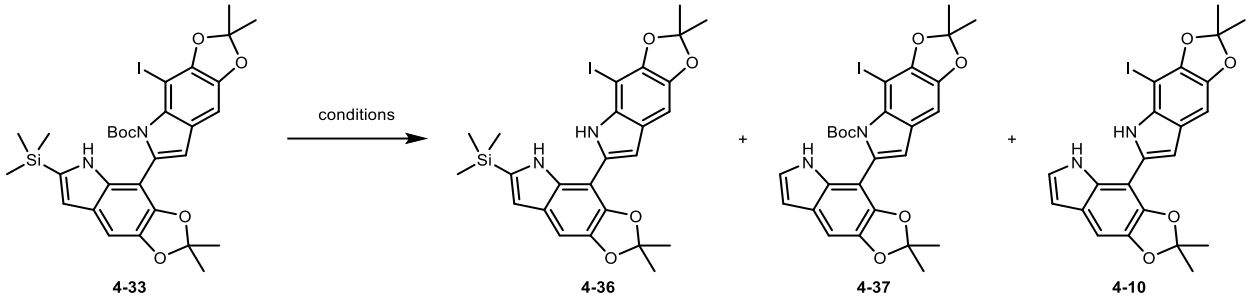

Entry	Condition	Solvent	Temp (°C)	Time (h)	Conversion (%)	Yield **4-36/4-37/4-10** (%)
1	DMF	NA	135	6	80	40/0/2
2	thermal	NA	180	2	50	0/0/0
3	TMSOTf, Et_3N	DCM	0 to r.t.	14.5	100	0/0/10
4	3-Methoxypropylamine	THF	50	13	0	0/0/0
5	HFIP	NA	50	10	100	0/40/58
6	HFIP	NA	70	10	100	0/0/86

With **4-10** in hand, we investigated its selective borylation at C2 in the presence of the C7'-idodie. Gratifyingly, borylation occurred in 70 % yield with careful control over the equivalents of B_2Pin_2 and reaction time. The structure of **4-3** was confirmed unambiguously by X-ray diffraction

analysis (Scheme 4-13). This set the stage for a convergent intermolecular Suzuki-coupling/macrocyclization to cyclic tetramer **4-2**.

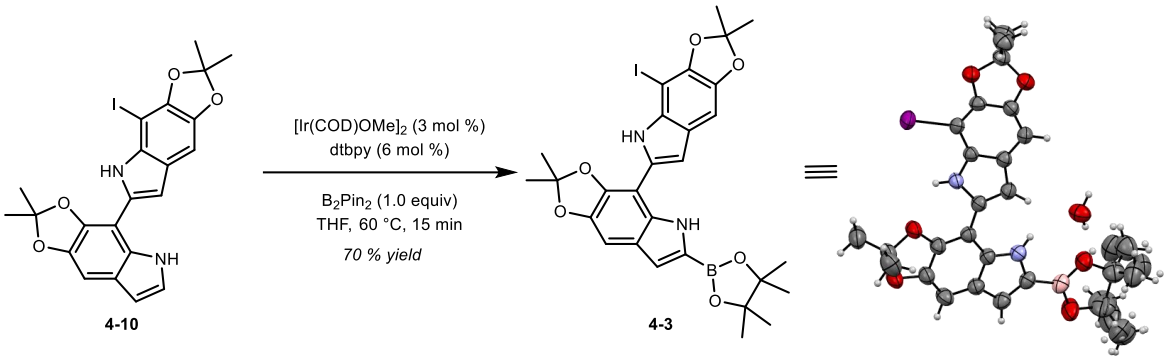

Scheme 4-13 Borylation to bis-functionalized dimer **4-3**

4.3.2 Synthesis of Cyclic Tetramer via an Intermolecular Dimerization

Having established a gram-scale synthesis of **4-3**, we explored our previously optimized conditions for Suzuki-coupling, with the hope of synthesizing cyclic tetramer **4-2** via a dimer-dimer coupling/macrocyclization cascade (Table 4-7). Disappointingly, treatment of **4-3** under our standard conditions, consisting of $Pd(OAc)_2$, SPhos, and K_3PO_4 in THF/H_2O, only resulted in protodeborylation to **4-10** (entry 1). Similarly, increasing catalyst loading or elevating reaction temperature proved to be ineffective (entries 2-3). Interestingly, switching the Pd catalyst to Buchwald's SPhos-Pd-G2 pre-catalyst afforded the **4-2** in 5 % yield with **4-10** and carbazole as the only two identifiable byproducts (entry 4). Carbazole is a byproduct of the SPhos-Pd-G2 precatalyst that releases the nitrogen heterocycle after reductive elimination. Efforts to optimize this reaction by adding supporting ligand (SPhos) (entry 5), switching to different catalysts (SPhos-Pd-G4) (entry 6), or different bases (Cs_2CO_3, DIPEA) led to no improvement (entries 7-8). Moreover, the byproduct carbazole from SPhos-Pd-G2 was inseparable with **4-2** by column chromatography, which created difficulties in obtaining purified materials.

Table 4-7 Condition optimization for dimerization/macrocyclization of **4-3**

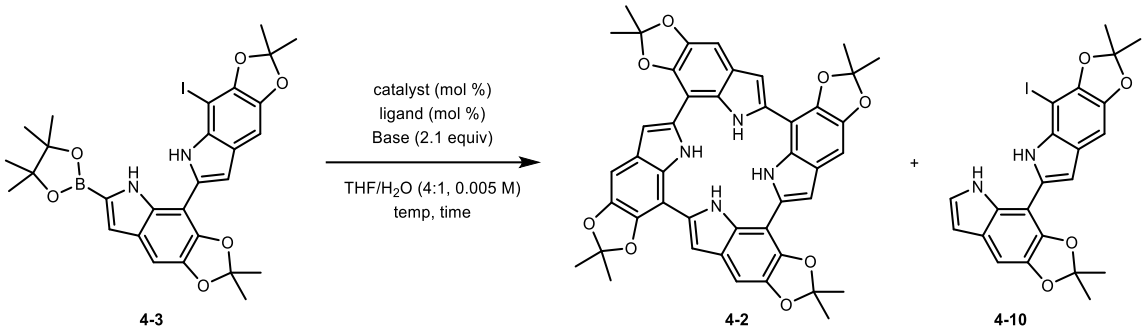

Entry	Catalyst	Cat. (mol%)	Ligand	Ligand (mol%)	Base	Time (h)	Temp (℃)	Conversion (%)	Yield [a] **4-2/4-10** (%)
1	$Pd(OAc)_2$	5	SPhos	5.5	K_3PO_4	2	r.t.	100	0/M
2	$Pd(OAc)_2$	10	SPhos	20	K_3PO_4	1	r.t.	100	0/M
3	$Pd(OAc)_2$	5	SPhos	5.5	K_3PO_4	1.5	60	100	0/M
4	SPhos-Pd-G2	5	NA	NA	K_3PO_4	1	60	100	5/2
5	SPhos-Pd-G2	5	SPhos	5	K_3PO_4	1	r.t.	40	0/3
6	SPhos-Pd-G4	5	SPhos	5	K_3PO_4	1	r.t.	100	0/0
7	SPhos-Pd-G2	5	NA	NA	Cs_2CO_3	0.5	60	100	0/M
8	SPhos-Pd-G2	5	NA	NA	DIPEA	0.5	60	100	0/M

a) M indicated the only product identified.

When **4-3** was subjected to reaction conditions initially reported by Shinokubo,[6] we observed complete consumption of **4-3** after 2 h but no evidence of **4-2** (entry 1). However, shortening the reaction time to 0.5 h resulted in the **4-2** in 5 % yield (entry 2). This result suggests that **4-2** is not stable to the reaction conditions. Therefore, the reaction was stopped after only 20 min, before complete consumption of **4-3**. However, this only led to a diminished yield of **4-2** (entry 3). An identical yield of **4-2** was obtained when the catalyst loading was increased to 10 mol % (entry 4). Given the results in entry 1-3, we anticipated a lower reaction temperature could slow down the potential decomposition of **4-2**, yet only protodeborylation product **4-10** was obtained at 80 ˚C (entry 5). With the initial observation of the formation of **4-2**, we began to probe various parameters to optimize the reaction conditions. Ligand effects were investigated with different

monodentate and bidentate phosphine ligands (PCy_3, PPh_3, XPhos, dppf, dppp). None of them provided any amount of **4-2**, and instead returned **4-10** as the product of protodeborylation (entries 6-10). Solvent effects were investigated next, including 2-Me-THF, MeCN, toluene, THF, but these changes did not lead to an improvement in yield (entries 11-13) (Table 4-8).

Table 4-8 Condition optimization for dimerization/macrocyclization of 4-3

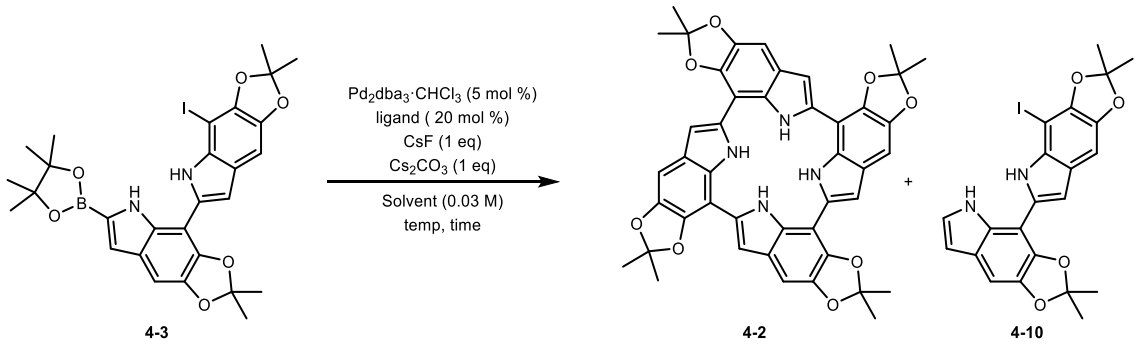

Entry	Ligand	H_2O (equiv)	Solvent	Time (h)	Temp (°C)	Consumption (%)	Yield (%)
1	SPhos	NA	DMF/Tol	2.0	100	100	0/0
2	SPhos	NA	DMF/Tol	0.5	100	100	5/0
3	SPhos	NA	DMF/Tol	0.3	100	95	3/0
4[a]	SPhos	NA	DMF/Tol	0.5	100	100	5/0
5	SPhos	NA	DMF/Tol	0.5	80	100	0/M
6	PCy_3	NA	DMF/Tol	0.5	100	90	0/M
7	PPh_3	NA	DMF/Tol	0.5	100	90	0/M
8	XPhos	NA	DMF/Tol	0.5	100	90	0
9	dppf	NA	DMF/Tol	0.5	100	40	0
10	dppp	NA	DMF/Tol	0.5	100	40	0
11	SPhos	NA	THF	0.5	80	65	0/13
12	SPhos	NA	2-Me-THF	0.5	80	43	0/8
13	SPhos	NA	MeCN/Tol	0.5	80	100	3/0
14	SPhos	0.025	DMF/Tol	0.5	100	100	7/0
15	SPhos	0.4	DMF/Tol	0.5	100	100	10/0
16	SPhos	1.0	DMF/Tol	0.5	100	100	1/0
17[b]	SPhos	0.4	DMF/Tol	0.5	100	100	10/0

a) Entry 4: catalyst loading was increased to 10 mol %, ligand was increased to 20 mol %.
b) Entry 17: reaction was performed in a Biotage microwave reactor.

Inspired by Denmark's mechanistic insight into the Suzuki−Miyaura transmetalation step and our previous studies on Suzuki-coupling to afford dimers, we hypothesized that H_2O may play a critical role in facilitating the biaryl coupling. Based on this analysis, we evaluated the effect of

H_2O. While addition of small amounts of H_2O provided a similar yield of **4-2** as entry 2 (entry 14), increasing the amount of H_2O to 0.4 equivalents proved to be beneficial and allowed for the isolation of **4-2** in 10 % yield (entry 15). In contrast, the reaction resulted in only 1 % of 4-2 when only 1 equivalent of H_2O was used (entry 16). Performing the reaction in a microwave reactor proved to be equally effective but led to no improvement in yields (entry 17)(Table 4-8).

4.4 Synthesis of Kaxiras' Cyclic Tetramer via Intramolecular Macrocyclization

4.4.1 Towards Linear Tetramer with C7-iodide

In order to pursue Retrosynthetic Plan B (Scheme 4-4), in which the Kaxiras' tetramer is constructed via an intramolecular Suzuki-couping, we required linear tetramer **4-38**. To this end, we considered two distinct pathways for the formation of **4-38**. In pathway A, a selective cross coupling between **4-3** and **4-10** could afford the C7-iodo tetramer **4-38** (Scheme 4-14).

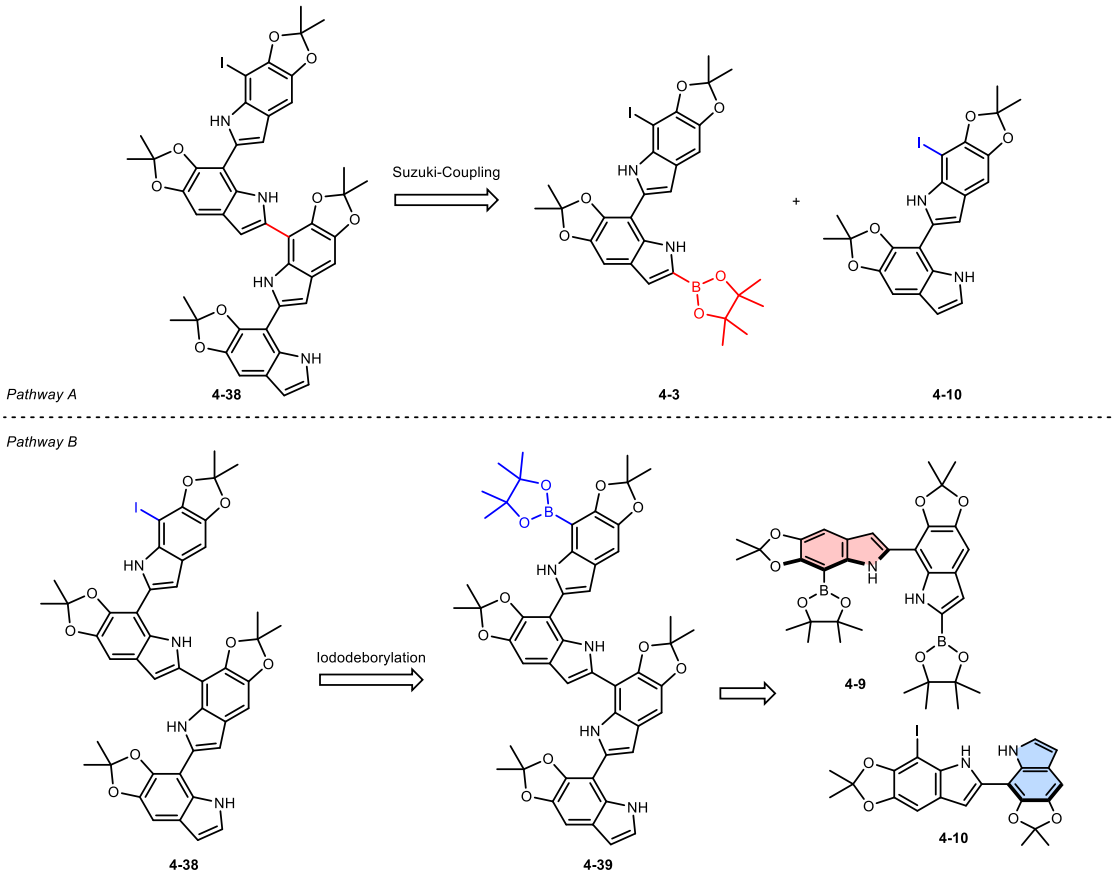

Scheme 4-14 Retrosynthetic plans for **4-38**

In pathway B, **4-38** could arise from a halodeborylation of **4-39**, which could be derived from a selective cross coupling of **4-9** and **4-10** (Scheme 4-14).

To test the feasibility of pathway A, we examined the cross-coupling reaction of **4-3** and **4-10**. With $Pd(OAc)_2$ and SPhos, the reaction afforded only 13 % of **4-38** with protodeboryaltion as the major byproduct (entry 1). Increasing the equivalents of **4-3** to compensate the substrate lost in the side reaction via protodeborylation resulted in an even lower yield of **4-38** (entry 2). Switching the catalyst to a SPhos-Pd-G2 precatalyst led to complete consumption of **4-3** but only protodeborylation of **4-3** was observed (entry 3). Decreasing the amount of H_2O failed to improve the yield as well (entry 4) (Table 4-9).

Table 4-9 Selected conditions for Suzuki-coupling of **4-3** and **4-10**

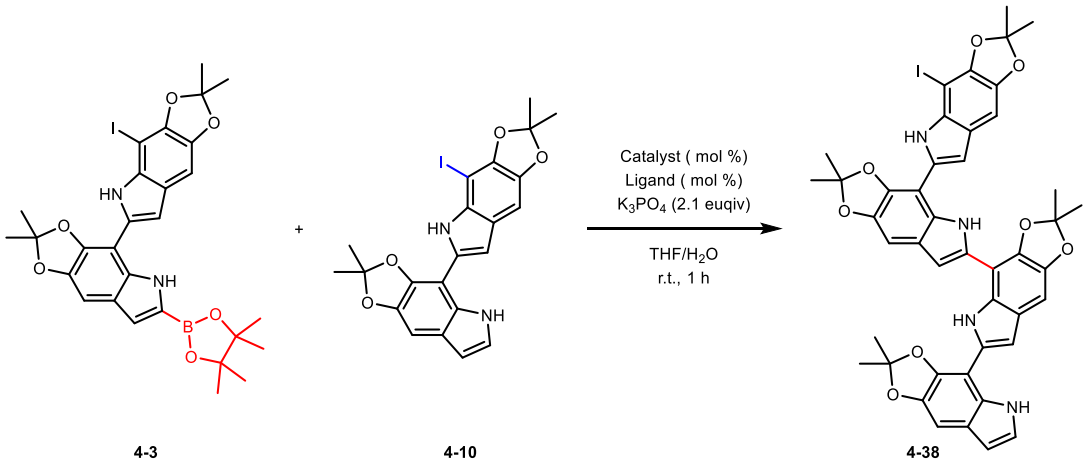

4-3 + **4-10** → **4-38**

Entry	Bpin (equiv)	Cat.	Cat. (mol%)	Ligand	Ligand (mol%)	THF/H_2O	Conversion of **4-3** (%)	Yield (%)
1	1.2	$Pd(OAc)_2$	5	SPhos	5.5	4/1	100	13
2	2.0	$Pd(OAc)_2$	5	SPhos	5.5	4/1	70	8
3	1.2	SPhos-Pd-G2	5	SPhos	5	4/1	100	0
4	1.2	$Pd(OAc)_2$	5	SPhos	5.5	15/1	100	0

To evaluate pathway B, we turned our attention to the synthesis of tetramer **4-38**, which was anticipated to arise from a selective cross coupling of **4-9** and **4-10.** First, we investigated the synthesis of bis-borylated dimer **4-9**. In the process of the synthesis, we noticed differences in reactivity between the batches of **4-27** in the borylation step. Thus, we investigated two methods in parallel to purify **4-27** (Method A and B). In Method A, chromatography was performed to purify **4-27**, and afforded material that was a light-yellow solid of high purity (determined by ^{1}H-

NMR in $CDCl_3$) (referred to as **4-27a**). Method B involved recrystallization of **4-27** from $CHCl_3$ at 70 °C, followed by filtration and washing with cold hexanes, and afforded material as a white solid of high purity (determined by ^{1}H-NMR in $CDCl_3$) (referred to as **4-27b**).

With dimer **4-27** in hand, conditions for selective C2 borylation were explored. As a starting point, treatment of **4-27a** under our standard borylation conditions resulted in minimal conversion, even with increased catalyst loading (entry 1-3). In contrast, when **4-27b** was treated with $[Ir(OMe)(COD)]_2$ (7.5 mol %), dtbpy (15 mol %), we obtained a 62 % of **4-9**, with potential over-borylation as a side reaction (entry 4). To minimize the potential over-borylation, the reaction time and catalyst loading were decreased. However, this resulted in a decreased yield of **4-9** and increased yield of byproducts (entry 5). The inconsistency in the yield led us to investigate factors that govern the reproducibility and reactivity of the borylation other than batches of **4-27** (Table 4-10).

Table 4-10 Condition optimization for selective borylation of **4-27**

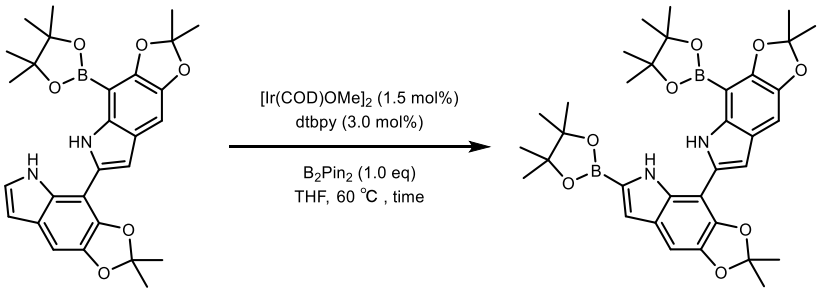

4-27 **4-9**

Entry	Ir (mol %)	dtbpy (mol %)	Time (h)	Substrate	Conversion (%)	Yield of **4-9** (%)
1	1.5	3.0	13	**4-27a**	5	0
2	3.0	6.0	13	**4-27a**	5	0
3	7.5	15	5	**4-27a**	5	0
4	7.5	15	13	**4-27b**	70	62
5	3.0	6.0	2	**4-27b**	100	53
6 [a]	3	6.0	0.2	**4-27b**	100	70

a) Pre-activated Ir/dtbpy/B_2Pin_2 complex was made before the addition of substrate.

There have been extensive studies on active species in Ir-catalyzed borylation and the effect of activating the Ir-catalyst prior to the addition of substrates.[21] Inspired by these reports, we prepared a pre-activated Ir/dtbpy/B_2Pin_2 complex before addition of the substrate. Specifically,

a solution of B_2Pin_2 was added to a solution of $[Ir(COD)OMe]_2$ followed by the addition of dtbpy. The solution was stirred in the glovebox for 0.5 h before addition of the substrate. We were pleased to find that a consistent yield was finally achieved at 70 % on gram scale within 10 min (entry 6) (Table 4-10).

Next, we investigated the Suzuki coupling between **4-9** and **4-10**, and were pleased to find that it proceeded selectively to the coupled linear tetramer **4-39** in 67 % yield. The reaction can be performed on gram-scale, and the product was purified by trituration with cold hexanes/$CHCl_3$ (Scheme 4-15).

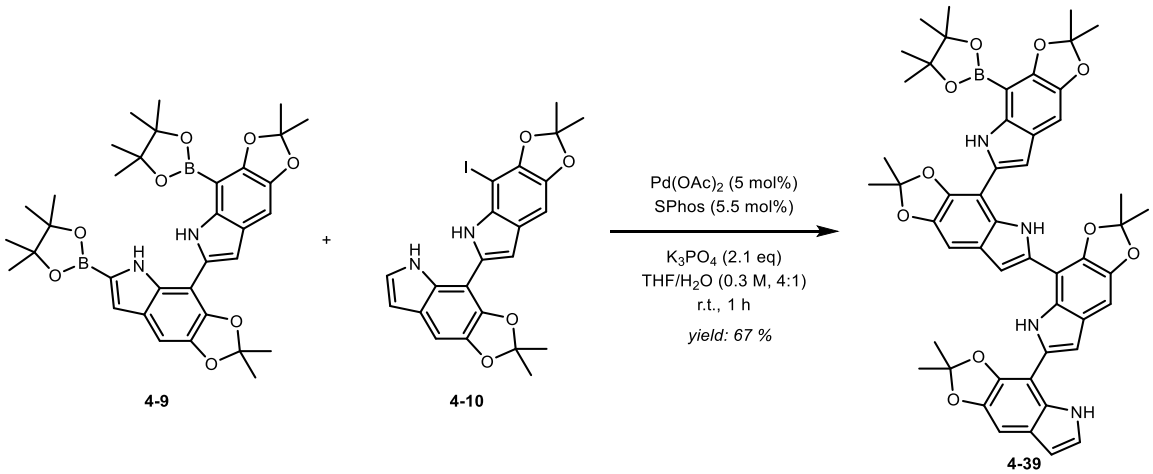

Scheme 4-15 Selective Suzuki-coupling of **4-9** and **4-10**

With **4-39** in hand, conversion of **4-39** to **4-38** under halodeborylation conditions were investigated. Only 12 % of **4-38** was obtained on small scale using CuI (15 mol%) and tmphen (30 mol%) after 15 min (entry 1). Extending the reaction time to 30 min improved the yield of **4-38** to 21 % (entry 2). Further extension of the reaction time, however, proved to be inefficient with both tmphen and dtbpy as ligands; and no other discernable products could be isolated except **4-38** (entries 3-4). When the reaction was conducted on a larger scale the yield of **4-38** was substantially decreased (entry 5) (Table 4-11).

Table 4-11 Condition optimization for iododeborylation of **4-39**

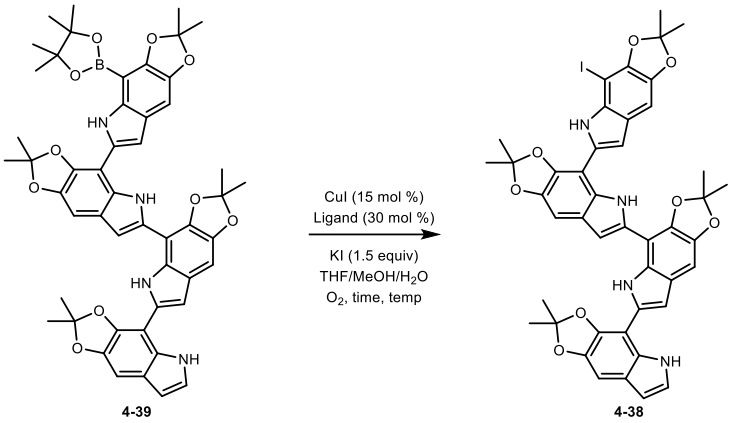

Entry	Scale (mmol)	Ligand	Time	Temp (°C)	Conversion (%)	Yield (%)
1	0.02	tmphen	15 min	50	59	12
2	0.02	tmphen	30 min	50	62	21
3	0.02	tmphen	1 h	50	65	20
4	0.05	dtbpy	1 h	40	68	17
5	0.15	tmphen	1 h	50	70	6

With small amounts of **4-38** in hand, we applied our borylation conditions with the aim of producing **4-6**. Unfortunately, in several attempts to convert **4-38** to **4-6**, only minimal consumption of **4-38** was observed with no formation of the desired product (Scheme 4-16).

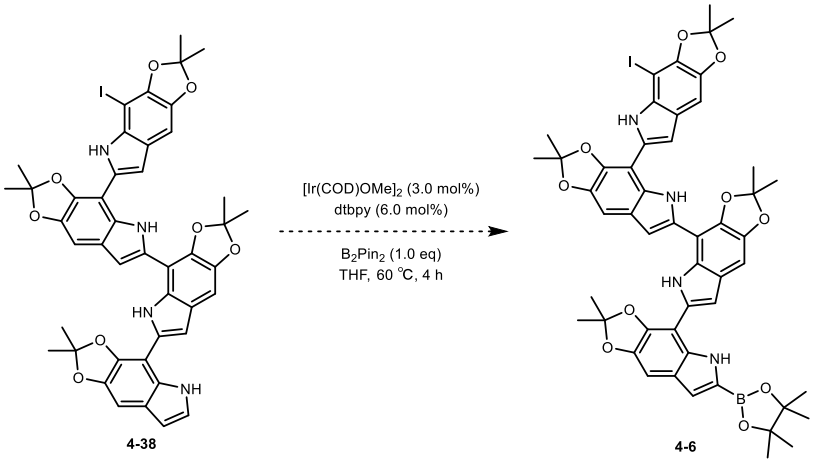

Scheme 4-16 Attempted C-H borylation of **4-38**

4.4.2 Synthesis of 2,7'''-borylated Linear Tetramer

In an attempt to overcome the challenges to access **4-6**, we devised an alternative linear precursor **4-7** in which both the C2 and C7 positions were borylated (Scheme 4-4). The success of this strategy for the synthesis of **4-2** would hinge on our ability to form a carbon-carbon between C2 and C7''' via an oxidative intramolecular macrocyclization.

With **4-39** in hand, we examined its borylation at C2 using our conditions of pre-activating the Ir catalyst. Under these conditions, the borylation of **4-39** proceeded smoothly in 73 % yield on gram-scale to afford **4-7**. Careful control of reaction time is required. Extended reaction time resulted in a mixture of **4-7** and over-borylated byproducts at various C4 positions that are not separatable by chromatography (Scheme 4-17).

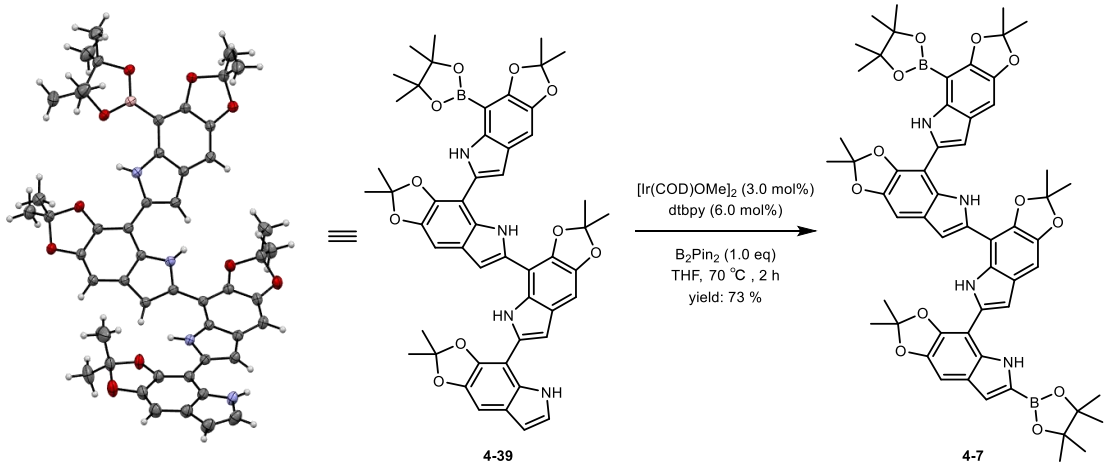

Scheme -4-17 Selective borylation of linear tetramer **4-39**

4.4.3 Synthesis of Cyclic Tetramer via Oxidative Intramolecular Macrocyclization

Inspired by conditions originally described by Jasti and co-workers,[9, 22, 23] we investigated the macrocyclization of **4-7** using $PdCl_2(PPh_3)_2$, KF and $B(OH)_3$ at different reaction times and temperatures in THF and H_2O. Unfortunately, in each of these cases, **4-7** was completely consumed without evidence of **4-2** (entries 1-3).

Next, we turned to conditions reported by Schindler and co-workers,[10] consisting of $Pd(dppf)Cl_2{\cdot}CH_2Cl_2$ (20 mol %) and K_2CO_3 (equiv) in DMSO and H_2O. After 5 min, air was added to

the reaction mixture by syringe (5 mL), resulting in the formation of **4-2** in 5 % yield after an additional 0.5 h reaction time (entry 4). Extending the reaction time to 12 h led to no observed product, consistent with our previous observation that **4-2** is not stable to the reaction conditions (entry 5). Efforts to perform the macrocyclization with lower amounts of base or in the absence of base, led to lower yields or the absence of product (entries 6 and 7) (Table 4-12).

Despite the low yield of **4-2**, the reactions proceeded with complete conversion of **4-7** within 0.5 h, and there were no isolable byproducts other than baseline impurities. Therefore, we questioned whether the low yield was due to competitive intermolecular reactions producing oligomeric/polymeric species. Recognizing that increased dilution could improve selectivity for intramolecular cyclization over intermolecular oligomerization,[8] we performed the reaction at high dilution, and were pleased to observe an improvement in the yield of **4-2** to 20 % (entry 8).

Table 4-12 Condition optimization for macrocyclization of **4-7**

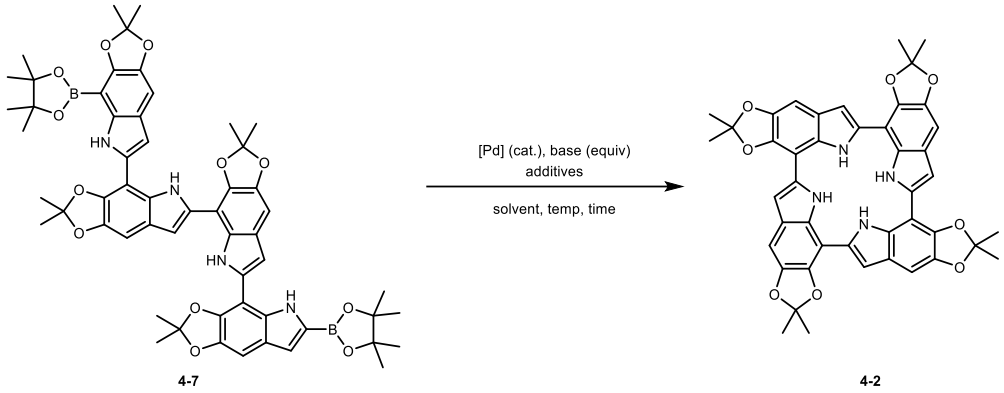

4-7 **4-2**

Entry	Catalyst	Base (equiv)	Additives	Solvent	Concen. (M)	Temp (°C)	Time (h)	Yield (%)
1	$PdCl_2(PPh_3)_2$	KF (1)	$B(OH)_3$	THF/H_2O	0.001	r.t	22	0
2	$PdCl_2(PPh_3)_2$	KF (20)	$B(OH)_3$	THF/H_2O	0.001	40	1	0
3	$PdCl_2(PPh_3)_2$	KF (1)	$B(OH)_3$	THF/H_2O	0.001	40	0.5	0
4	Pd(dppf)Cl_2·CH_2Cl_2	K_2CO_3 (6)	Air	DMSO/H_2O	0.001	90	0.5	5
5	Pd(dppf)Cl_2·CH_2Cl_2	K_2CO_3 (6)	Air	DMSO/H_2O	0.001	90	12	0
6	Pd(dppf)Cl_2·CH_2Cl_2	K_2CO_3 (0)	Air	DMSO/H_2O	0.001	90	0.5	0
7	Pd(dppf)Cl_2·CH_2Cl_2	K_2CO_3 (2)	Air	DMSO/H_2O	0.001	90	0.5	2
8	Pd(dppf)Cl_2·CH_2Cl_2	K_2CO_3 (6)	Air	DMSO/H_2O	0.0005	90	0.6	20

4.5 Chain Oxidation

Having established a reliable route to **4-2**, we turned our attention to the removal of the acetonide protecting groups. As a point of departure, we evaluated strongly acidic conditions, previously reported to remove acetonide protecting groups from catechols, but unfortunately, when applied to **4-2**, these conditions led to the formation of an insoluble black precipitate and all efforts to isolate a product from the mixture were unsuccessful (Scheme 4-18). This observation could result from the instability of **4-1** and **1-1** upon removal of the protecting groups as described in Section 4.1. Thus, we envisioned to obtain oxidized cyclic tetramer by installing a blocking group at C4 to prevent potential chain growth that would complicate the desired oxidation. As a starting point, we pursued a model study on blocked dimers to seek feasible conditions for both deprotection and oxidation.

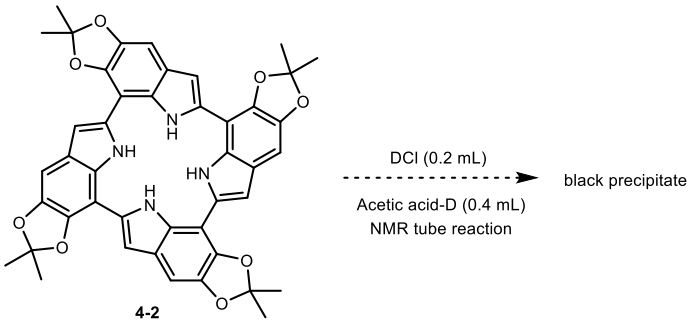

Scheme 4-18 Attempted deprotection of **4-2**

4.5.1 Oxidation of Blocked Dimers

To test our hypothesis of steric shielding, we focused our efforts on obtaining a well-defined oxidized dimer, which was expected to serve as a model substrate to the cyclic tetramer. To this end, we first investigated conditions to install blocking groups on **4-27**. We have shown in Section 4.4.1 that a selective borylation of **4-27** afforded **4-9** in high yield (Table 4-10). When increasing reaction time, temperature, and equivalents of B_2Pin_2, the tetra-boronic ester **4-9b** was obtained in 68 % yield (Scheme 4-19).

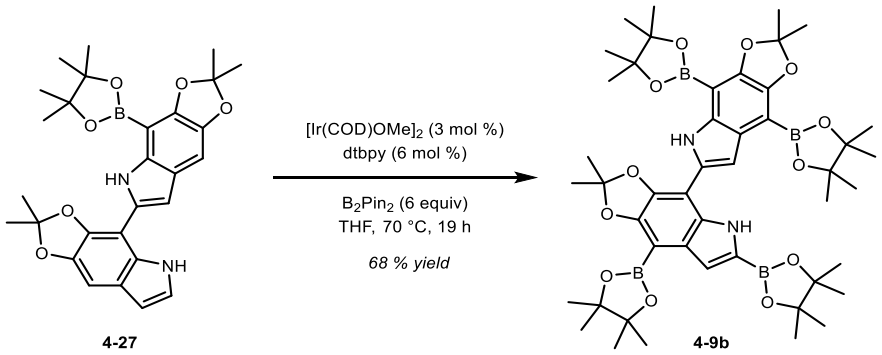

Scheme 4-19 Over-borylation of **4-27**

With **4-9b** in hand, a Suzuki-Miyaura coupling with 2-Iodotoluene proceeded smoothly under our previously optimized conditions ($Pd(OAc)_2$, SPhos, THF/H_2O) to afford 56 % **4-40** in 56 % yield (Scheme 4-20).

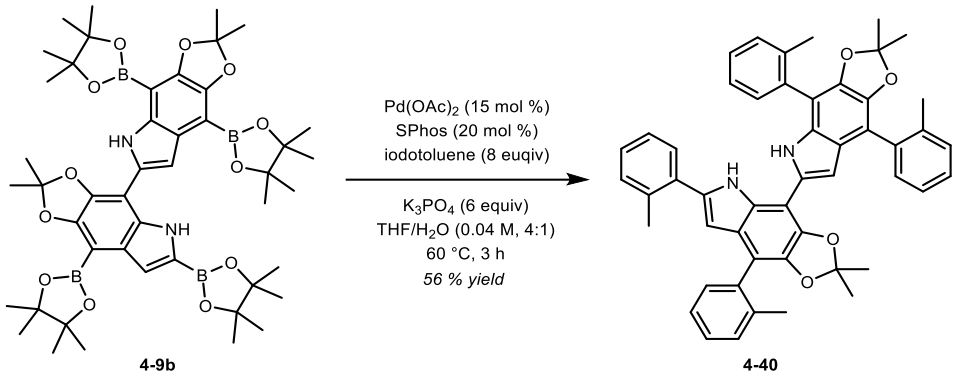

Scheme 4-20 Suzuki coupling to fully blocked dimer **4-40**

Various acetonide deprotection conditions were then explored. Strong acidic condition (6 M HCl /AcOH) proved to be ineffective on **4-40** (entry 1). We believed that this result reflects the poor solubility of **4-40** in acetic acid. Changing the solvent to MeCN resulted in low conversion of **4-40** and generated mono-deprotected **4-41** in 8 % yield (entry 2). Extending the reaction time and temperature led to a better conversion of **4-40** and provided **4-41** and **4-42** in 28 % and 29 % yield respectively (entry 3). Interestingly, treatment of unblocked dimer **4-27** to the same condition in entry 3, led to rapid decomposition of **4-27** without any discernable products. Although complete conversion of **4-40** was achieved after 12 h, lower yields of **4-41** and **4-42** were observed (entry 4). This is presumably due to the instability of both products under acid conditions at elevated temperatures. To improve the yield, we evaluated reducing conditions with ethane-1,2-dithiol, $AlCl_3$ in $MeNO_2$ at −40 °C and obtained **4-41** in 68 % yield (entry 5). Interestingly, **4-42** was not

obtained under these conditions, even at elevated temperature and extended reaction time (entries 6-8) (Table 4-13).

Table 4-13 Condition optimization for acetonide deprotection of **4-40**

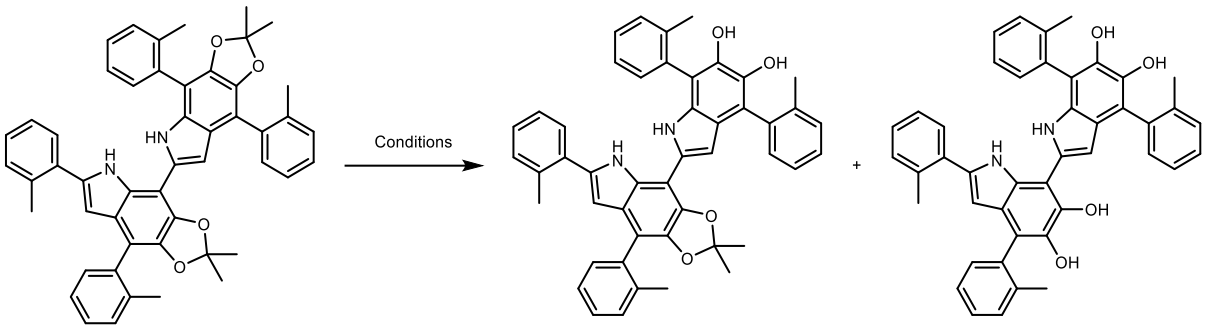

4-40 **4-41** **4-42**

Entry	Condition	Time (h)	Conversion (%)	Yield of **4-41**/**4-42** (%)
1	HCl (6 M)/AcOH (2:1, 0.02 M), 40 °C	4	0	0/0
2	HCl (con.), MeCN/Ethylene glycol (2:1, 0.009 M), 40 °C	4	10	8/0
3	HCl (con.), MeCN/Ethylene glycol (2:1, 0.009 M), 60 °C	7	60	28/29
4	HCl (con.), MeCN/Ethylene glycol (2:1, 0.009 M), 60 °C	12	100	17/18
5	Ethane-1,2-dithiol (20 equiv), $AlCl_3$ (17 equiv), $MeNO_2$, −40 °C	2	95	68/0
6	Ethane-1,2-dithiol (20 equiv), $AlCl_3$ (17 equiv), $MeNO_2$, 0 °C	1	100	69/0
7	Ethane-1,2-dithiol (20 equiv), $AlCl_3$ (17 equiv), $MeNO_2$, 0 °C to r.t	1 to 17	100	-- [a]/0
8	Ethane-1,2-dithiol (20 equiv), $AlCl_3$ (17 equiv), $MeNO_2$, 0 °C to r.t. to 40 °C	1 to 17 to 4	100	-- [a]/0

a) **4-41** was the only product; isolations were not performed. Formation of **4-42** was not observed.

Re-subjecting **4-41** to acetonide deprotection conditions (ethane-1,2-dithiol, $AlCl_3$ in $MeNO_2$) resulted in a minimal conversion of **4-41** and no **4-42** was observed. Treating **4-41** with HCl in MeCN afforded fully deprotected **4-42** in 25 % yield (Table 4-14). While the yield of **4-42** was not ideal, these experiments provided enough **4-42** and a high yield of **4-41** to study their oxidation reactions.

Table 4-14 Conditions for acetonide deprotection of **4-41**

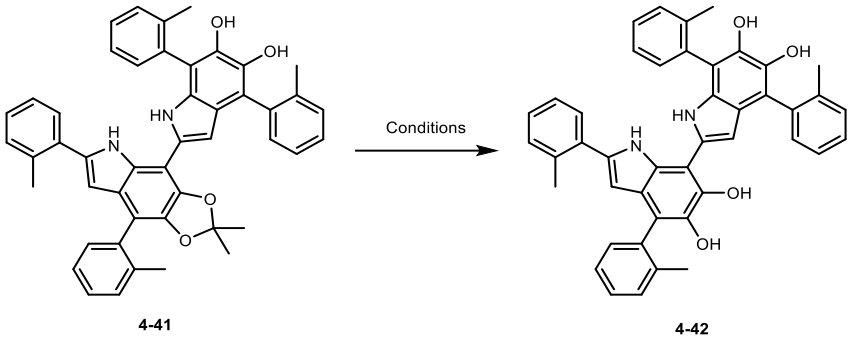

Entry	Conditions	Time (h)	Conversion (%)	Yield (%)
1	Ethane-1,2-dithiol (20 equiv), $AlCl_3$ (17 equiv), $MeNO_2$, 0 °C	4	5	0
2	HCl (con.), MeCN/Ethylene glycol (2:1, 0.009 M), 60 °C	4	70	25

Gratifyingly, the oxidation of **4-41** and **4-42** with $NaIO_4$ in a mixture of acetone and H_2O afforded oxidized dimers **4-44** and **4-43** respectively in high purity. This marks the first synthesis of a well-defined eumelanin dimer at the quinone oxidation state. Steric stabilization utilizes aryl groups at C2, C4 and C7 to prevent C-C bond formation, while enforcing a twist about the biaryl bond that ensures minimal perturbation of quinone's π-system (Scheme 4-21).

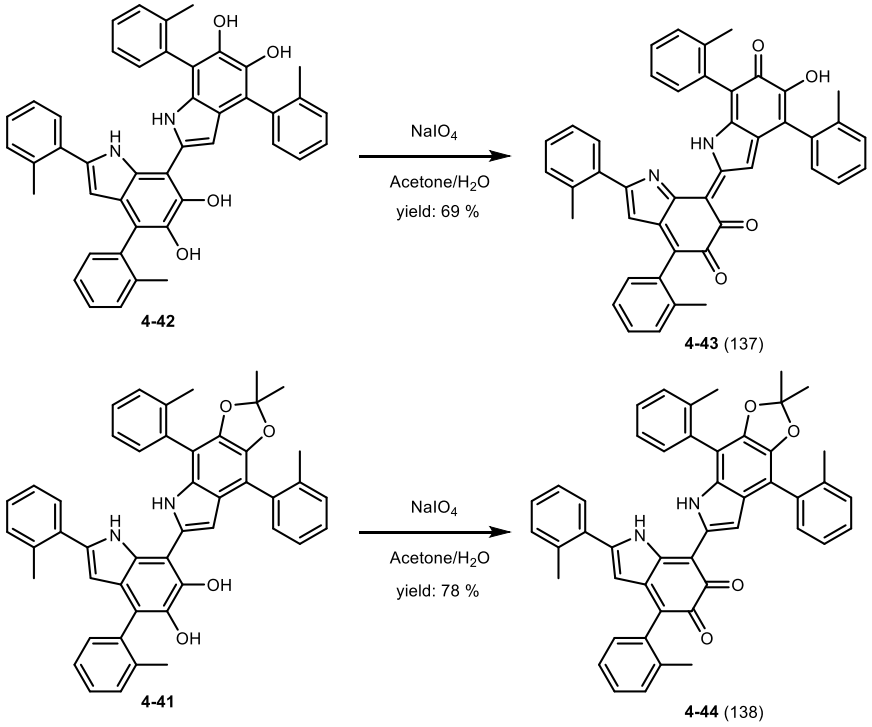

Scheme 4-21 Oxidation of **4-42** and **4-41** to oxidized dimers

This sterically stabilized eumelanin dimer exhibits characteristic properties of eumelanin, including broadband absorption and an ultrafast excited state deactivation with the signal going to zero around 120 ps (Figure 4-4). Further studies are ongoing in collaboration with the Kohler lab. (*Spectroscopic data was from Lily Kinziabulatova at the Kohler lab, Ohio State University*).

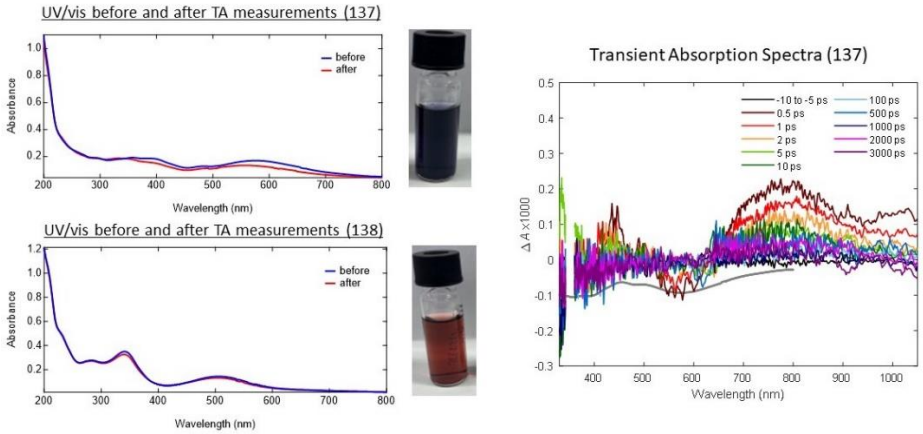

Figure 4-4 UV/Vis Spectrum of **4-43** (137) and **4-44** (138, left)**;** transient absorption spectra of **4-43** (137, right)

Dimer **4-43** has multiple tautomeric forms with differing relative energies. In collaboration with Professor Lluis Blancafort and co-workers at the University of Girona, we have examined the relative energies of these tautomers, which shows that structures with interfragment double bonds are more stable than structures with a single carbon-carbon bond between oxidized units. It potentially reflects that an extended π-system could be more stable, which is in good agreement with previous calculations on relative energies of tautomers of dimers.[24-26] Structure confirmations of **4-43** and **4-44** are ongoing in our lab (Figure 4-5). We tentatively assigned **4-43** as **4-43a** as only one N-H proton was observed according to ^{1}H NMR and it should be favoured compared with **4-43b**, **4-43d**, and **4-43f** according to the calculated relative energy.

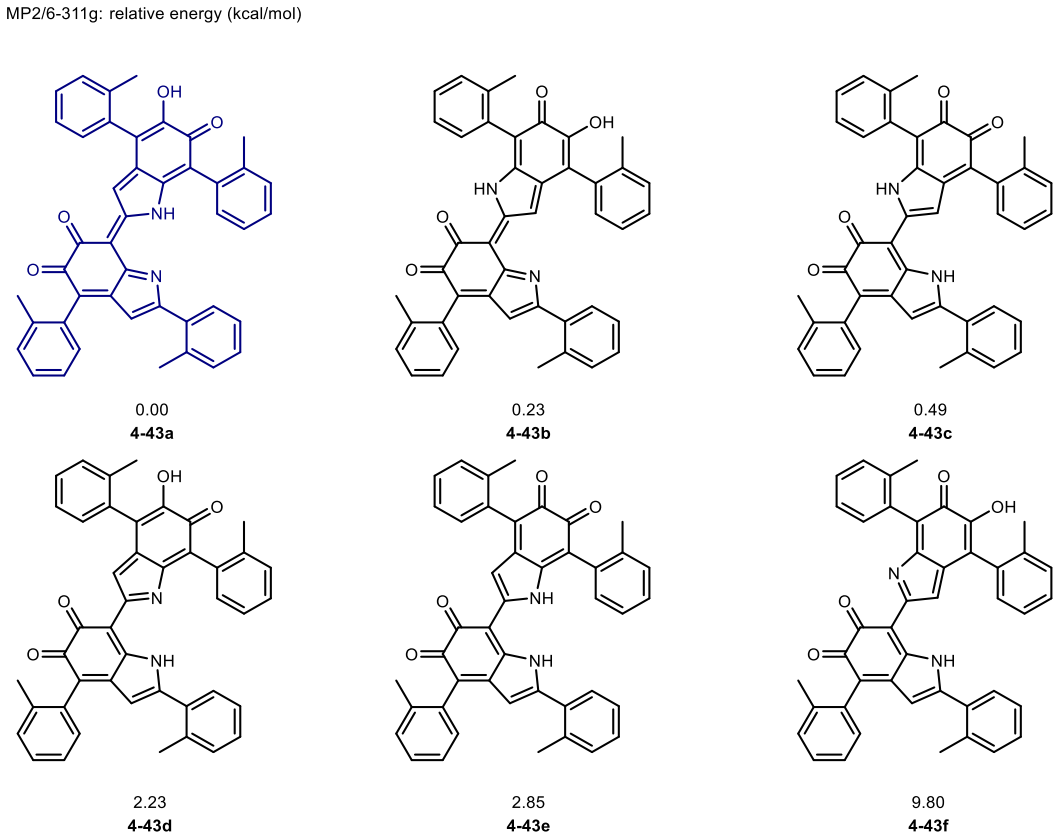

Figure 4-5 Calculated relative energies of tautomers of **4-43**

4.5.2 Oxidation of Blocked Cyclic Tetramer

Encouraged by the results on the oxidized dimers **4-43** and **4-44**, we set out to install the blocking groups on cyclic tetramer **4-2**. To our delight, **4-19** was obtained in 36 % yield, over a two-step sequence consisting of Ir-catalyzed borylation at each of the C4 positions, followed by Pd-catalyzed Suzuki-Miyaura coupling with 2-iodotoluene under our standard conditions (Scheme 4-22).

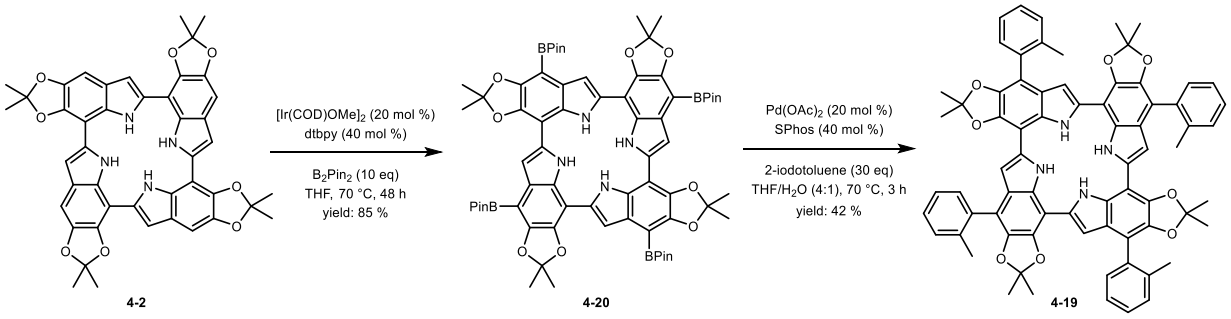

Scheme 4-22 Synthesis of fully blocked tetramer **4-19**

With **4-19** in hand, we returned to its deprotection and oxidation. Unfortunately, attempts to remove the acetonides of **4-19** proved to be challenging. Exposure of **4-19** to concentrated HCl returned a complex mixture consisting of **4-45**, **4-46**, and **4-57** at different oxidation states, as determined by HRMS following column chromatography. Oxidation of catechol to *ortho*-quinone in air during the process of purification is not surprising, especially given the electron rich nature of **4-19**. For clarity, we show the oxidized tetramers as their iodolequinone tautomers, but at this stage we are not able to confirm which tautomeric form is present (Scheme 4-23).

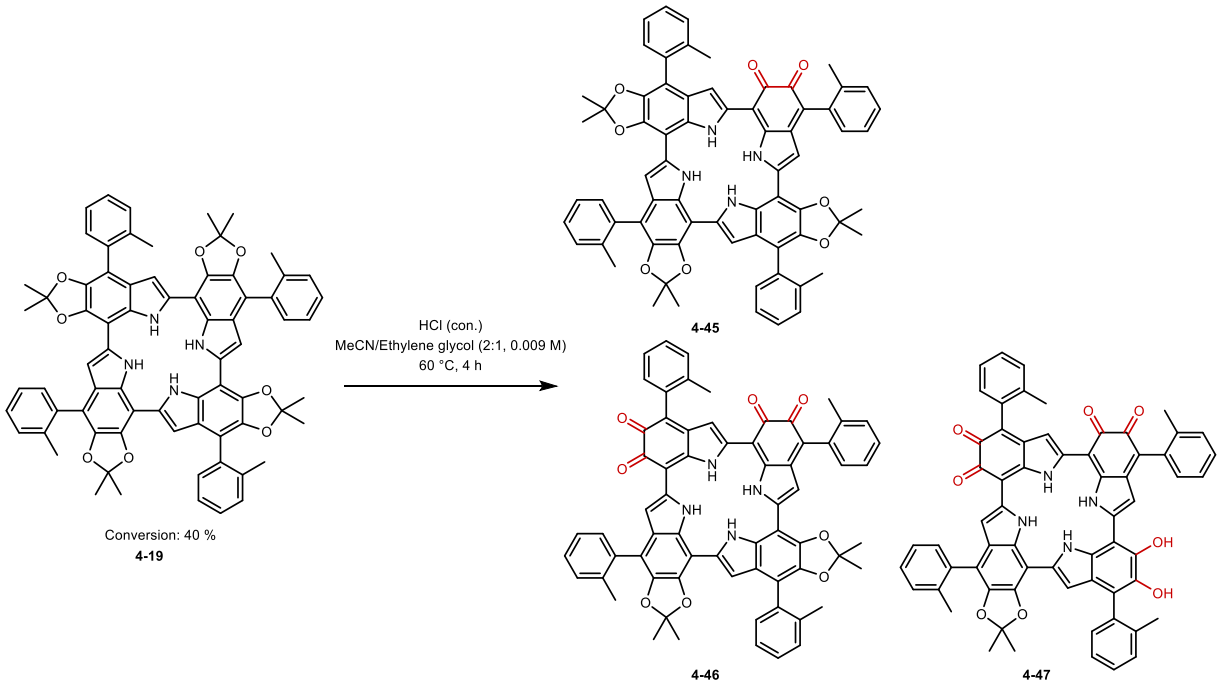

Scheme 4-23 Deprotection and oxidation of **4-19** under acidic condition

Deprotection of the reduced cyclic tetramer with ethane-1,2-dithiol was also attempted. Given the rapid oxidation of catechols, we subjected the crude reaction mixture to analysis by LCMS and were pleased to detect the mass correspond to the fully deprotected cyclic tetramer **4-48**. Efforts to purify the product by chromatography appeared to form tris-oxidized product **4-49** according to LCMS. Unfortunately, all attempts to confirm the structure of **4-49** were complicated by its decomposition (Scheme 4-24).

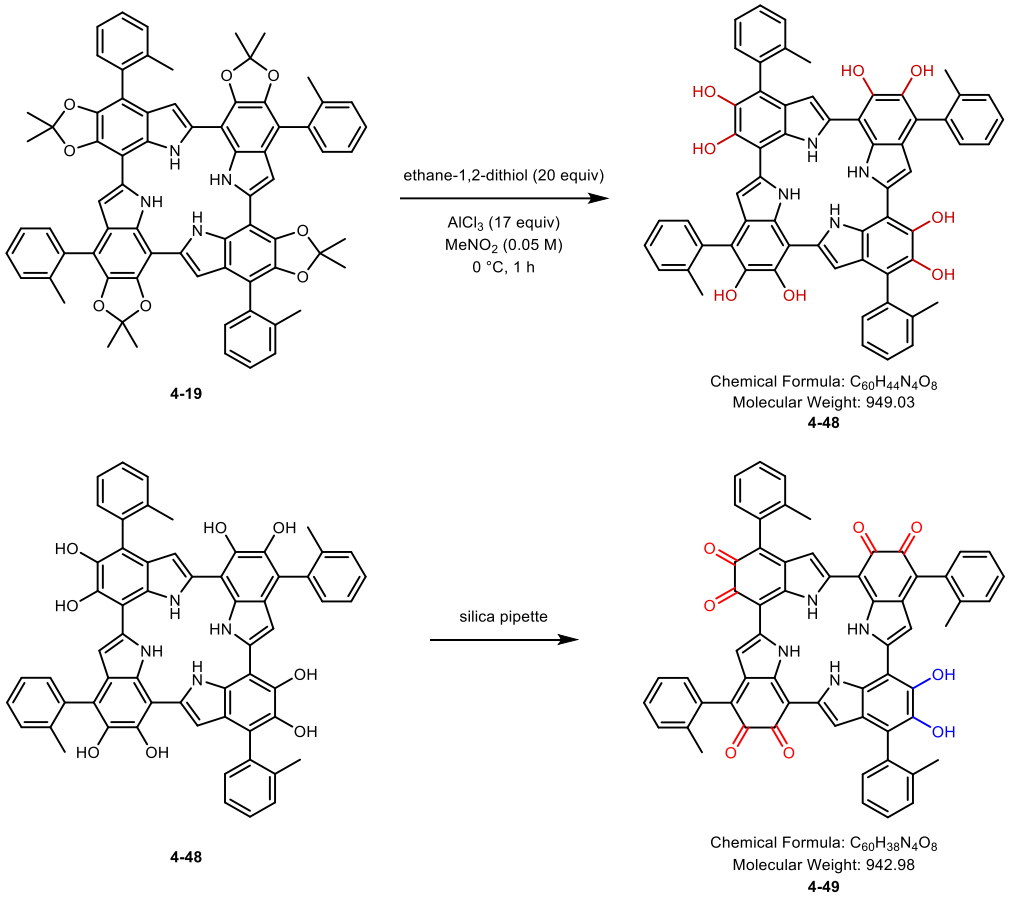

Scheme 4-24 Deprotection and oxidation of **4-19** under reductive condition

4.6 Conclusion

In summary, we have developed two complementary strategies to the first total synthesis of a 16-membered cyclic tetramer **4-2**. The first employs a Pd-catalyzed intermolecular dimerization/macrocyclization of **4-3**, and the second employs an intramolecular oxidative macrocyclization from bis-borinate **4-7**. Both approaches relied on our success of installing functional handles on the C7 positions of the dimer and tetramers. Capitalizing on our blocking group strategy, we demonstrated the first synthesis of well-defined eumelanin dimers (**4-43** and **4-44**) at the quinone oxidation state that possess eumelanin-like physical properties and the first synthesis of an oxidized cyclic tetramer (**4-49**). A gram scale supply of **4-7** is advancing our efforts towards the fully oxidized **4-18**. These efforts have provided the first cyclic tetramer relevant to **1-1** and promises to shed light on the relevance of these structures to eumelanin biopolymers.

4.7 Experimental Section

4.7.1 Materials and Methodologies:

Chemicals and solvents were purchased from Sigma Aldrich, Alfa Aesar, Strem Chemicals, TCI or Oakwood Chemicals. Chemicals were used as received without further purification. Solvents were dried and purified using a PureSolv MD 7 (from Innovative Technology) or MB SPS 800 (from MBraun). Cyclohexane was distilled over CaH_2 under N_2. $[Ir(COD)(OMe)]_2$ and $Pd_2dba_3{\cdot}CHCl_3$ were purchased from Sigma Aldrich, and stored inside of a MBraun Labmaster glove box (<1 ppm O_2 and H_2O) filled with a dry N_2 atmosphere at −20 °C. Unless otherwise noted, reactions were performed in flame-dried glassware under a positive pressure of N_2 using standard synthetic organic, inert atmosphere techniques.

Proton nuclear magnetic resonance (^{1}H NMR) spectra were acquired using Varian Mercury 400 MHz, Varian Inova QANUC 500 MHz, Varian VNMRS 500 MHz, Bruker AVIIIHD 500 MHz, or Bruker AVIIIHD 400 MHz spectrometers. Chemical shifts (δ) are reported in parts per million (ppm) and are calibrated to the residual solvent peak. Coupling constants (*J*) are reported in Hz. Multiplicities are reported using the following abbreviations: *s* = singlet; *brs*=broad singlet; *d* = doublet; *t* = triplet; *q* = quartet; *m* = multiplet (range of multiplet is given). Carbon nuclear magnetic resonance (^{13}C NMR) spectra were acquired using Varian VNMRS 125 MHz, Bruker AVIIIHD 125 MHz, or Bruker AVIIIHD 101 MHz spectrometers. Chemical shifts (δ) are reported in parts per million (ppm) and are calibrated to the residual solvent peak. High resolution mass spectra (HRMS) were recorded using a Bruker maXis Impact TOF mass spectrometer. Fourier-transform infrared (FT-IR) spectra were recorded on an alpha Bruker FT-IR spectrometer. Analytical thin-layer chromatography was performed on pre-coated 250 mm layer thickness silica gel 60 F_{254} plates (EMD Chemicals Inc.). Visualization was performed by ultraviolet light and/or by staining with potassium permanganate or cerium molybdate. Purifications by column chromatography were performed using either a Biotage Isolera™ One or standard column chromatography using silica gel (40-63 μm, 230-400 mesh).

General Procedures

General Procedure A: Suzuki-Miyaura Coupling of Indoles A flame-dried Schlenk tube equipped

with a Teflon-coated stir bar and a glass stopper was charged with iodoindole (1.0 equiv), indole boronic acid pinacol ester (1.0-1.2 equiv), Pd-catalyst (5-10 mol %), ligand (5.5-26 mol %) and base (1.0-6.0 equiv). The Schlenk tube was evacuated and backfilled with N_2 (this process was repeated three times) prior to the addition of degassed dry solvent under a positive pressure of N_2, followed by the addition of degassed deionized H_2O. The tube was sealed and heated to the indicated temperature in a pre-heated oil bath. After the indicated time, the reaction was cooled to ambient temperature and quenched by the addition of a saturated aqueous solution of NH_4Cl to afford a neutral reaction mixture with a pH=7. The phases were then separated, and the aqueous phase was extracted with EtOAc. The combined organic fractions were then washed with brine then dried over $MgSO_4$, filtered, and concentrated *in vacuo*. The resulting residue was purified by silica gel column chromatography using the indicated solvent system as eluent to afford the desired product.

General Procedure B: Ir-catalyzed Borylation of Indoles In an inert atmosphere glove box, a flamed-dried vial equipped with a Teflon-coated stir bar was charged with indole (1.0 equiv) and dry degassed solvent (THF or cyclohexane). In another three flamed-dried vials, B_2pin_2 (1.0–2.0 equiv), dtbpy (3.0–14.0 mol%), and $[Ir(COD)(OMe)]_2$ (1.5–7.0 mol%) were dissolved in dry, degassed solvent separately The solution of B_2Pin_2 was then added to the solution of $[Ir(COD)OMe]_2$. To this resulting mixture was added the solution of dtbpy. The resulting mixture was stirred in the glovebox for 0.5 h at ambient temperature before adding to the solution of indole. The reaction vial was sealed and heated to the indicated temperature in a pre-heated oil bath outside of the glove box. After the indicated time, the reaction was cooled to ambient temperature, and transferred to a round-bottom flask. The resulting reaction mixture was concentrated *in vacuo* and purified by silica gel column chromatography using the indicated solvent system as eluent to afford the desired product.

Compound 4-21:

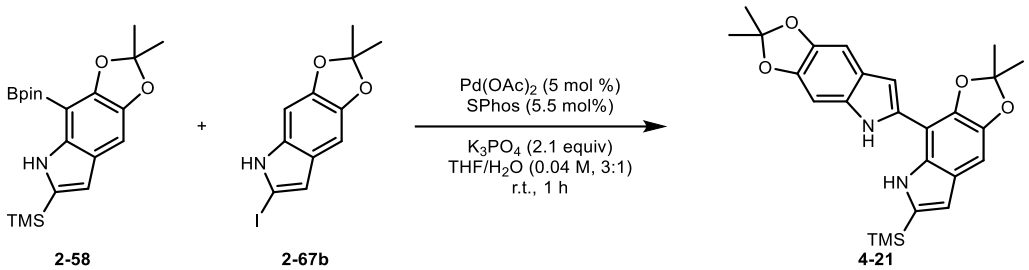

Procedure: The reaction was carried out according to the General Procedure A, the reaction was performed in THF/H_2O (3:1, 0.05 M) at ambient temperature for 1 h.

Amounts of Reagents:

2-58 (23.24 mg, 0.06 mmol, 1.0 equiv)

2-67b (18.90 mg, 0.06 mmol, 1.0 equiv)

$Pd(OAc)_2$ (0.67 mg, 0.003 mmol, 5 mol%)

SPhos (1.35 mg, 0.0033 mmol, 5.5 mol%)

K_3PO_4 (26.75 mg, 0.126 mmol, 2.1 equiv)

THF (1.2 mL), H_2O (0.4 mL)

Purification: 10 % EtOAc in hexanes.

Yield of Product:

4-21: 9.9 mg, 0.02 mmol, 37 %, light yellow solid.

Characterization:

$\mathbf{R_f}$ = (EtOAc/hexanes, 1:9) 0.35; **^{1}H NMR** (400 MHz, $CDCl_3$) δ 9.03 (s, 1H), 8.48 (s, 1H), 7.00 (s, 1H), 6.88 (s, 1H), 6.86 (s, 1H), 6.74 (dd, *J* = 2.3, 0.9 Hz, 1H), 6.66 (d, *J* = 2.1 Hz, 1H), 1.78 (s, 6H), 1.73 (s, 6H), 0.37 (s, 9H).; **HRMS**: Calcd. for $C_{25}H_{28}N_2NaO_{14}Si$ $[M+Na]^+$ = 471.1711 m/z, found = 471.1703 m/z.

Compound 4-23:

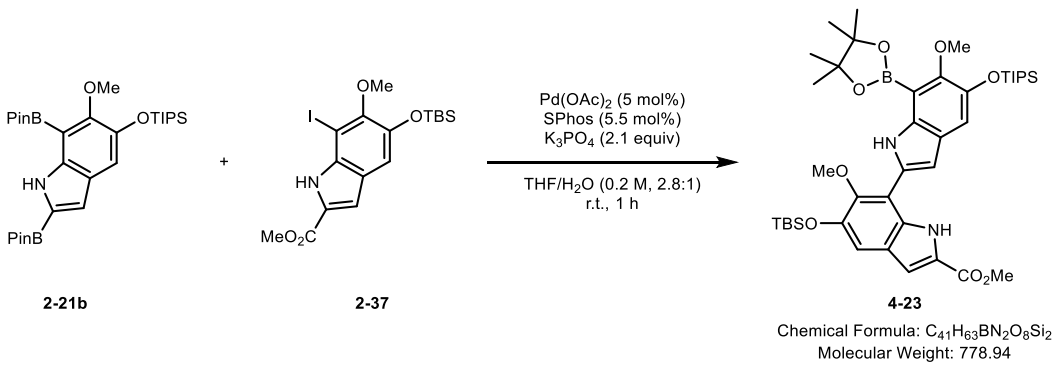

Procedure: The reaction was carried out according to the General Procedure A, the reaction was performed in THF/H_2O at ambient temperature for 1 h.

Amounts of Reagents:

2-21b (113.3 mg, 0.2 mmol, 1.0 equiv)

2-37 (92.3 mg, 0.2 mmol, 1.0 equiv)

$Pd(OAc)_2$ (2.25 mg, 0.01 mmol, 5 mol%)

SPhos (4.52 mg, 0.011 mmol, 5.5 mol %)

K_3PO_4 (89.2 mg, 0.42 mmol, 2.1 euqiv)

THF (1.0 mL), H_2O (0.35 mL)

Purification: 5 % to 10 % EtOAc in hexanes.

Yield of Product:

4-23: 62.3 mg, 0.08 mmol, 40 %, light yellow solid.

Characterization:

$\mathbf{R_f}$ = (EtOAc/hexanes 1:9): 0.54; ^{1}**H NMR** (500 MHz, $CDCl_3$) δ 10.65 (s, 1H), 9.27 (s, 1H), 7.30 (s, 1H), 7.13 (d, *J* = 2.1 Hz, 1H), 7.10 (s, 1H), 6.80 (d, *J* = 2.3 Hz, 1H), 3.95 (s, 3H), 3.89 (s, 3H), 3.78 (s, 3H), 1.43 (s, 12H), 1.42 – 1.38 (m, 3H), 1.18 (d, *J* = 7.4 Hz, 18H), 1.07 (s, 9H), 0.25 (s, 6H).; **HRMS**: Calcd. for $C_{41}H_{63}BN_2NaO_8Si_2$ $[M+Na]^+$ = 801.4108 m/z, found =801.4127 m/z.

Compound 4-24:

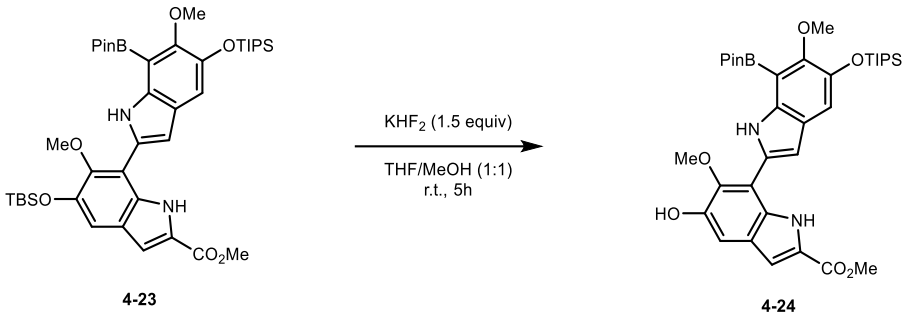

4-23 **4-24**

Procedure: A 10 mL flame-dried round-bottom flask equipped with a Teflon-coated stir bar and a rubber septum was charged with **4-23** (0.08 mmol, 62.32 mg, 1.0 equiv, contain small amount of impurity). The reaction flask was evacuated and backfilled with N_2 (this process was repeated for 3 times) prior to the addition of dry degassed THF (0.4 mL) and MeOH (0.4 mL). The resulting reaction mixture was stirred at ambient temperature for 5 h and then concentrated *in vacuo.* The crude mixture was purified by silica gel column chromatography (10% EtOAc in hexanes) to afford **4-24** (26.59 mg, 0.04 mmol, 50 %) as a white solid.

Characterization:

R_f = (EtOAc/hexanes, 1:9) 0.29; **^{1}H NMR** (500 MHz, $CDCl_3$) δ 10.24 (s, 1H), 9.21 (s, 1H), 7.31 (s, 1H), 7.14 (d, *J* = 2.0 Hz, 1H), 6.81 (d, *J* = 2.2 Hz, 1H), 5.72 (s, 1H), 3.94 (s, 3H), 3.89 (s, 3H), 3.71 (s, 3H), 1.43 (s, 12H), 1.38-1.41 (m, 3H), 1.18 (d, *J* = 7.5 Hz, 18H).; **^{13}C NMR** (126 MHz, CDCl3) δ 171.30, 162.24, 155.27, 144.89, 144.44, 143.76, 136.73, 129.98, 129.89, 127.96, 124.56, 123.81, 113.57, 110.03, 108.85, 105.29, 101.17, 83.59, 62.26, 61.70, 60.54, 52.12, 25.14, 21.20, 18.30, 14.34, 13.04.

Compound 4-25 and 4-26:

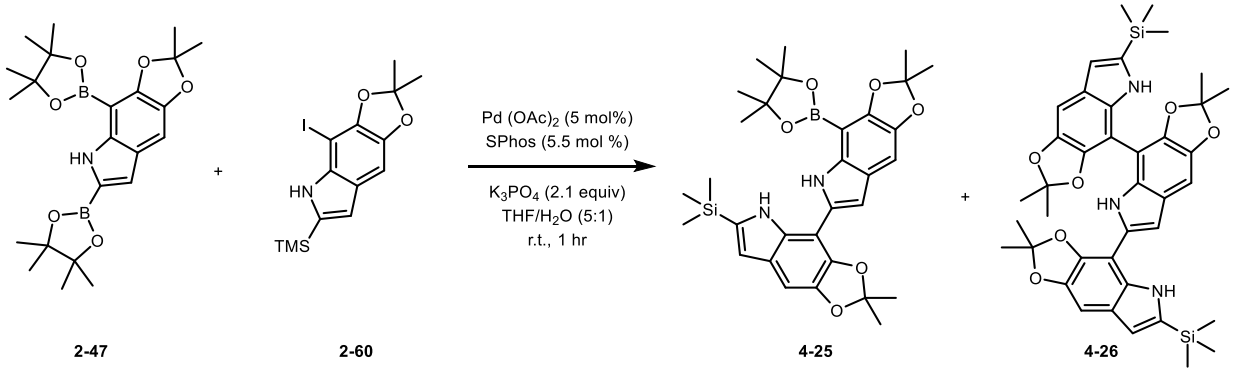

2-47 **2-60** **4-25** **4-26**

Chemical Formula: $C_{31}H_{39}BN_2O_6Si$
Molecular Weight: 574.56

Chemical Formula: $C_{39}H_{45}N_3O_6Si_2$
Molecular Weight: 707.97

Procedure: The reaction was carried out according to the General Procedure A, the reaction was performed in THF/H_2O at ambient temperature for 1 h.

Amounts of Reagents:

2-47 (2.43 g, 5.5 mmol, 1.1 euqiv)

2-60 (1.94 g, 5.0 mmol, 1.0 euqiv)

$Pd(OAc)_2$ (56.12 mg, 0.25 mmol, 5 mol%)

SPhos (112.89 mg, 0.27 mmol, 5.5 mol %)

K_3PO_4 (2.23 g, 10.5 mmol, 2.1 euqiv)

THF (25.0 mL), H_2O (5.0 mL)

Purification: 5 % to 10 % EtOAc in hexanes.

Yields of Products:

4-25: 2.01 g, 3.50 mmol, 70 %, light orange solid.

4-26: 176.9 mg, 0.25 mmol, 5 %, light yellow solid

Characterization for 4-25:

R_f = (EtOAc/hexanes, 1:9) 0.34; **IR** (neat) v = 3430, 2980, 1447, 1282, 1197, 1166, 936, 834, 752, 667 cm^{-1}; **^{1}H NMR** (500 MHz, $CDCl_3$) δ 10.09 (brs, 1H), 8.51 (brs, 1H), 7.09 (s, 1H), 6.88 (s, 1H), 6.73 (d, *J* = 2.4 Hz, 1H), 6.66 (d, *J* = 2.1 Hz, 1H), 1.80 (s, 6H), 1.75 (s, 6H), 1.43 (s, 12H), 0.37 (s, 9H). **^{13}C NMR** (126 MHz, $CDCl_3$) δ 151.78, 143.29, 143.08, 141.18, 136.80, 135.54, 130.86, 129.50, 123.01, 120.90, 117.64, 117.40, 112.13, 101.85, 99.95, 99.85, 97.70, 83.70, 26.20, 26.05, 25.20, -0.78.; **HRMS**: Calcd. for $C_{31}H_{39}BN_2NaO_6Si$ $[M+Na]^+$ = 597.2563 m/z, found = 597.2581 m/z.

Characterization for 4-26:

R_f = (EtOAc/hexanes, 1:9) 0.43; **^{1}H NMR** (500 MHz, $CDCl_3$) δ 8.91 (s, 1H), 8.55 (s, 1H), 8.23 (s, 1H), 7.13 (s, 1H), 7.04 (s, 1H), 6.86 (s, 1H), 6.84 (d, *J* = 2.2 Hz, 1H), 6.71 (d, *J* = 2.1 Hz, 1H), 6.66 (d, *J* = 2.1 Hz, 1H), 1.88 (s, 3H), 1.71 (s, 3H), 1.68 (s, 3H), 1.67 (s, 3H), 1.60 (s, 3H), 1.53 (s, 3H), 0.36 (s, 9H), 0.30 (s, 9H).; **HRMS**: Calcd. for $C_{39}H_{45}N_3NaO_6Si_2$ $[M+Na]^+$ = 730.2739 m/z, found = 730.2740 m/z.

Compound 4-27:

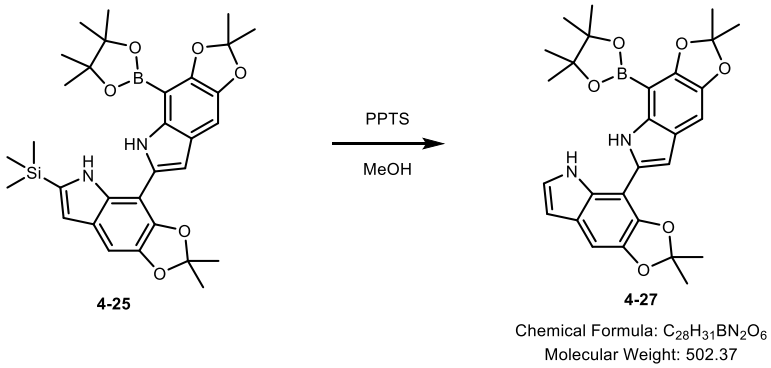

Procedure: A 25 mL flame-dried, round-bottom flask, equipped with a Teflon-coated stir bar and a rubber septum, was charged with **4-25** (1.26 g, 2.2 mmol, 1.0 equiv) and pyridinium *p*-toluenesulfonate (PPTS, 653.4 mg, 2.6 mmol, 1.1 equiv). The flask was evacuated and backfilled with N_2 (this process was repeated three times) before the addition of dry, degassed MeOH (11 mL, 0.20 M) under a positive pressure of N_2. The resulting homogeneous mixture was then stirred at room temperature for 1 h. After the addition of H_2O (30 mL) and EtOAc (30 mL), the aqueous layer was extracted with EtOAc (3 x 20 mL). The combined organic layers were washed with brine (20 mL), dried over $MgSO_4$, and concentrated *in vacuo.* The crude mixture was purified following two methods. In method A, the crude reaction mixture was purified by silica gel column chromatography (10 % EtOAc in hexanes) to afford **4-27** as a light-yellow solid (0.88 g, 1.76 mmol) in 80 % yield. In method B, the crude reaction mixture was purified via recrystallization from $CHCl_3$ (3 mL) at 70 °C to afford **4-27** as a white solid (0.77 g, 1.54 mmol) in 70 % yield.

Characterization:

R_f = (EtOAc/hexanes, 1:9) 0.22; **IR** (neat) v = 3430, 3388, 2980, 1610, 1449, 1374, 1299, 1170, 1137, 685, 848, 751, 665, 579 cm^{-1}; **^{1}H NMR** (400 MHz, $CDCl_3$) δ 10.10 (brs, 1H), 8.62 (brs, 1H), 7.15 (dd, 3.3, 2,4 Hz, 1H), 7.03 (d, *J* = 0.7 Hz, 1H), 6.90 (s, 1H), 6.74 (d, *J* = 2.2 Hz, 1H), 6.48 (dd, *J* = 3.2, 2.1 Hz, 1H), 1.80 (s, 6H), 1.73 (s, 6H), 1.42 (s, 12H). **^{13}C NMR** (126 MHz, $cdcl_3$) δ 151.74, 143.25, 143.02, 140.77, 135.52, 129.42, 127.60, 122.87, 122.06, 120.97, 117.59, 117.44, 103.38, 101.86, 100.29, 100.06, 100.04, 98.06, 83.73, 26.25, 26.05, 25.21.; **HRMS**: Calcd. for $C_{28}H_{31}N_2O_6B$ $[M]^+$ = 502.22697 m/z, found = 502.22792 m/z.

Compound 4-31 and 4-32:

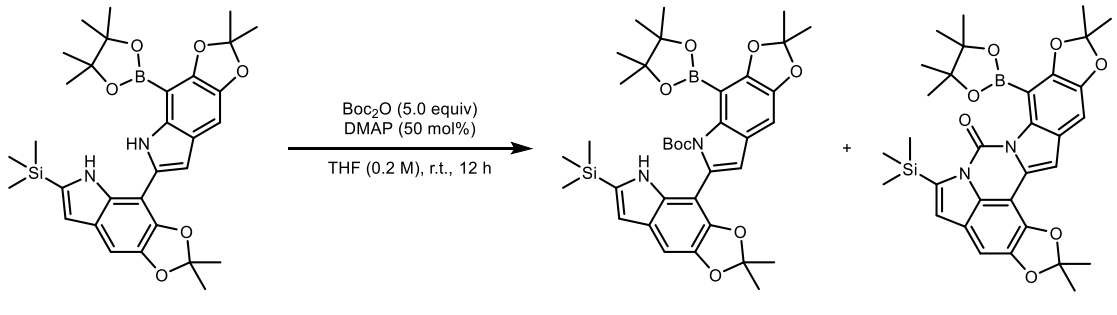

4-25

4-31
Chemical Formula: $C_{36}H_{47}BN_2O_8Si$
Molecular Weight: 674.67

4-32
Chemical Formula: $C_{32}H_{37}BN_2O_7Si$
Molecular Weight: 600.55

Procedure: A 50 mL flame-dried, round-bottom flask, equipped with a Teflon-coated stir bar and a rubber septum, was charged with **4-25** (2.33 g, 4.0 mmol, 1.0 equiv), DMAP (244.34 mg, 2.0 mmol, 50 mol %), Boc_2O (4.40 g, 20.0 mmol, 5.0 equiv), and THF (20 mL, 0.20 M). The resulting homogeneous reaction mixture was then stirred at ambient temperature for 12 h and then concentrated *in vacuo*. The crude reaction mixture was then purified by silica gel column chromatography (5 % EtOAc in hexanes) to afford **4-31** as a yellow solid (2.08 g, 3.08 mmol) in 77 % yield and **4-32** as a yellow solid (48 mg, 0.08 mmol) in 2 % yield.

Characterization of 4-31:

$\mathbf{R_f}$ = (EtOAc/ hexanes, 1:9) 0.42; **IR** (neat) v = 3464, 2977, 1707, 1368, 1304, 1203, 1154, 1094, 1012, 837, 752 cm^{-1}; **^{1}H NMR** (400 MHz, $CDCl_3$) δ 8.02 (brs, 1H), 6.85 (s, 2H), 6.61 (s, 1H), 6.56 (d, *J* = 2.2 Hz, 1H), 1.70 (s, 3H), 1.68 (s, 6H), 1.66 (s, 3H), 1.43 (s, 12H), 0.95 (s, 9H), 0.26 (s, 9H). **^{13}C NMR** (101 MHz, $CDCl_3$) δ 151.36, 150.33, 144.19, 143.22, 142.87, 136.00, 133.72, 128.15, 122.72, 121.58, 117.50, 117.40, 112.81, 111.74, 101.44, 100.19, 97.96, 83.70, 83.41, 27.27, 26.03, 26.00, 25.52, 25.48, -0.78.; **HRMS**: Calcd. for $C_{36}H_{47}N_2BNaO_8Si$ $[M+Na]^+$ = 697.3087 m/z, found = 697.3098 m/z.

Characterization of 4-32:

$\mathbf{R_f}$ = (EtOAc/ hexanes, 1:9) 0.68; **^{1}H NMR** (500 MHz, $CDCl_3$) δ 7.02 (s, 1H), 6.95 (s, 1H), 6.86 (s, 1H), 6.85 (s, 1H), 1.80 (s, 6H), 1.71 (s, 6H), 1.49 (s, 12H), 0.46 (s, 9H).; **^{13}C NMR** (126 MHz, $CDCl_3$) δ 150.12, 146.36, 146.18, 144.59, 140.09, 138.72, 130.00, 128.97, 128.26, 124.49, 121.25, 120.59,

120.15, 117.76, 105.09, 99.85, 98.98, 97.20, 84.13, 26.23, 26.02, 25.73, -0.06.; **HRMS**: Calcd. for $C_{32}H_{37}N_2NaO_7Si$ $[M+Na]^+$ = 623.2355 m/z, found = 623.2353 m/z.

Compound 4-33:

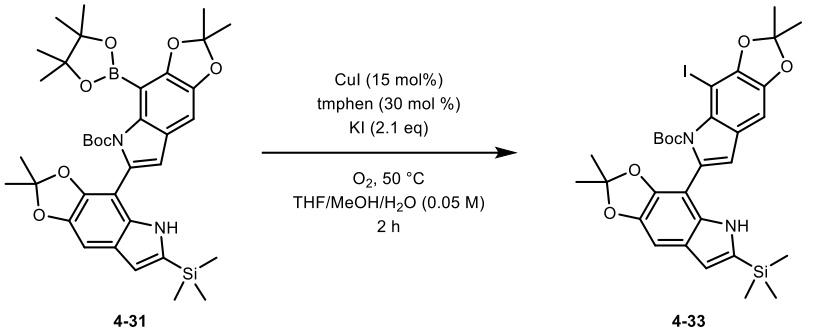

Procedure: A 100 mL round-bottom flask equipped with a Teflon-coated stir bar and rubber a septum was charged with **4-31** (1.68 g, 2.5 mmol, 1.0 equiv), CuI (70.47 mg, 0.37 mmol, 15 mol%), tmphen (177.24 mg, 0.75 mmol, 30 mol%), KI (620.84 mg, 3.75 mmol, 1.5 equiv), and THF/MeOH/H_2O (25 mL/20 mL/5 mL, 0.05 M, 5:4:1). The rubber septum was then connected to a tank of O_2, pressurized to 50 kpa, and was vented 3 times for 10 s each time. Under a constant pressure of O_2 (50 kpa), the reaction mixture was then stirred at 50 ^oC for 2 h before depressurizing by opening to the atmosphere and concentrated *in vacuo* The resulting wine-red residue was then diluted and extracted with EtOAc (3 x 30 mL). The combined organic fractions were washed with brine (20 mL), dried over $MgSO_4$, filtered and concentrated *in vacuo*. The crude reaction mixture was purified using silica gel column chromatography (5 % EtOAc in hexanes) to afford **4-33** as a grey solid (1.35 g, 2.0 mmol) in 81 %.

Characterization:

$\mathbf{R_f}$ = (EtOAc/ hexanes, 1:9) 0.48; **IR** (neat) v = 3463, 2982, 1742, 1442, 1368, 1304, 1199, 1146, 1088, 992, 836, 749 cm^{-1}; **^{1}H NMR** (500 MHz, $CDCl_3$) δ 7.87 (s, 1H), 6.92 (d, *J* = 0.6 Hz, 1H), 6.87 (s, 1H), 6.58 (s, 1H), 6.57 (d, *J* = 2.2 Hz, 1H), 1.75 (d, *J* = 5.5 Hz, 6H), 1.68 (s, 3H), 1.64 (s, 3H), 0.98 (s, 19H), 0.25 (s, 9H).; **^{13}C NMR** (126 MHz, $CDCl_3$) δ 149.31, 148.87, 144.29, 143.11, 143.04, 136.25, 134.17, 133.16, 130.56, 125.84, 121.48, 117.92, 117.76, 111.63, 109.91, 99.65, 98.92, 98.84,

83.82, 57.81, 27.08, 26.08, 26.06, 25.93, 25.92, -0.87.; **HRMS**: Calcd. for $C_{30}H_{35}IN_2NaO_6Si$ $[M+Na]^+$ = 674.1201 m/z, found = 697.1194 m/z.

Compound 4-10:

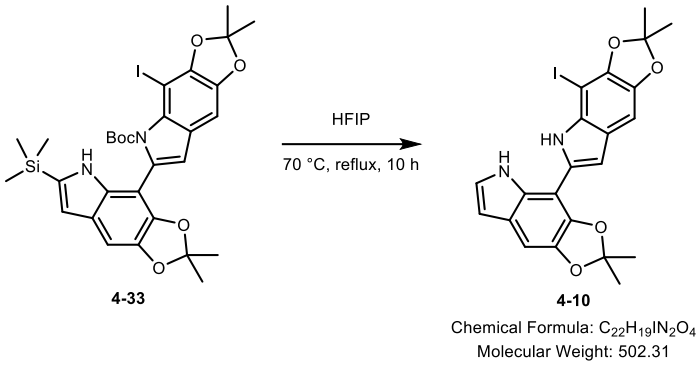

Procedure: A flame-dried, 25 mL round-bottom flask, equipped with a Teflon-coated stir bar and a rubber septum, was charged with **4-33** (1.35 g, 2 mmol, 1.0 equiv) and 1,1,1,3,3,3-Hexafluoro-2-propanol (HFIP, 10 mL, 0.2 M). The resulting homogeneous solution was heated to reflux (70 °C) and stirred for 10 h then cooled to ambient temperature and concentrated *in vacuo*. The crude reaction mixture was purified using silica gel column chromatography (10 % EtOAc in hexanes) to afford **4-10** as a bright yellow solid (0.85 g, 1.7 mmol) in 86 %.

Characterization:

R_f = (EtOAc/ hexanes, 1:9) 0.29; **IR** (neat) v = 3425, 2986, 1446, 1375, 1300, 1200, 1167, 982, 869, 829, 725 cm^{-1}; **^{1}H NMR** (500 MHz, $CDCl_3$) δ 9.22 (s, 1H), 8.54 (s, 1H), 7.16 (dd, *J* = 3.2, 2.3 Hz, 1H), 6.94 (s, 1H), 6.89 (s, 2H), 6.50 (dd, *J* = 3.2, 2.0 Hz, 1H), 1.81 (s, 6H), 1.76 (s, 6H).; **^{13}C NMR** (126 MHz, $CDCl_3$) δ 146.97, 143.29, 142.69, 140.95, 132.59, 130.31, 127.30, 123.03, 122.30, 121.54, 118.21, 117.94, 103.64, 101.54, 99.46, 98.77, 98.70, 53.92, 26.14, 26.03.; **HRMS**: Calcd. for $C_{22}H_{19}IN_2NaO_4$ $[M+Na]^+$ = 525.0282 m/z, found = 525.0263 m/z.

Compound 4-37:

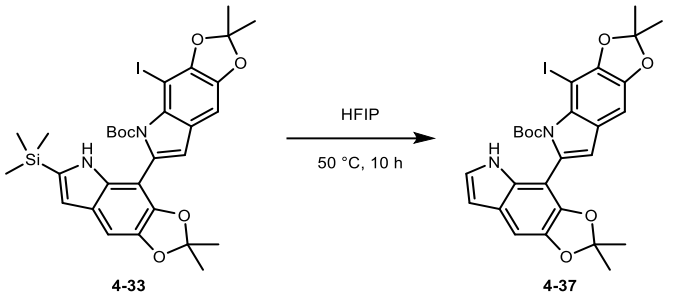

Procedure: A flame-dried, 10 mL round-bottom flask, equipped with a Teflon-coated stir bar and a rubber septum, was charged with **4-33** (13.49 mg, 0.02 mmol, 1.0 equiv) and 1,1,1,3,3,3-Hexafluoro-2-propanol (HFIP, 1 mL, 0.02 M). The resulting homogeneous solution was heated to reflux (50 °C) and stirred for 10 h then cooled to ambient temperature and concentrated *in vacuo*. The crude reaction mixture was purified using silica gel column chromatography (10 % EtOAc in hexanes) to afford **4-37** as a yellow oil (4.82 mg, 0.008 mmol) in 40 %.

Characterization:

$\mathbf{R_f}$ = (EtOAc/ hexanes, 1:9) 0.39; **^{1}H NMR** (500 MHz, $CDCl_3$) δ 8.02 (s, 1H), 6.98 (t, *J* = 2.8 Hz, 1H), 6.96 (s, 1H), 6.85 (s, 1H), 6.57 (s, 1H), 6.41 (dd, *J* = 3.1, 2.2 Hz, 1H), 1.76-1.74 (m, 6H), 1.68-1.64 (m, 6H), 1.02 (s, 9H).; **HRMS**: Calcd. for $C_{27}H_{27}IN_2NaO_6$ $[M+Na]^+$ = 625.0806 m/z, found = 625.0790 m/z.

Compound 4-3:

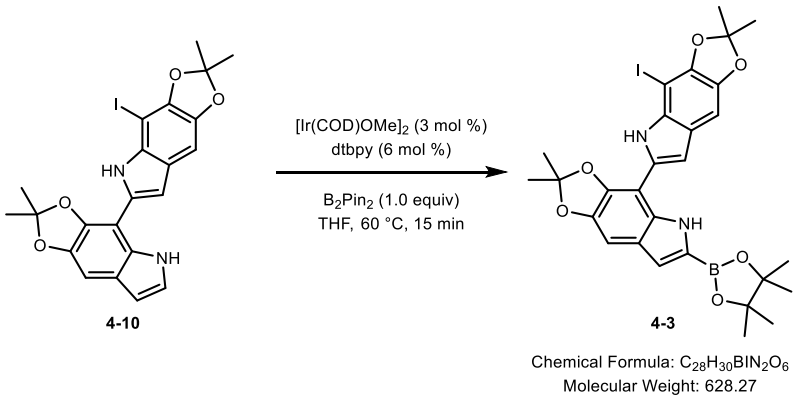

Procedure: The reaction was carried out according to the General Procedure B and was performed in THF at 60 °C for 15 min

Amounts of Reagents:

4-10 (1.0 g, 2.0 mmol, 1.0 equiv)

$[Ir(OMe)(COD)]_2$ (39.76 mg, 0.06 mmol, 3.0 mol%)

dtbpy (32.20 mg, 0.12 mmol, 6.0 mol%)

B_2pin_2 (507.88 mg, 2.0 mmol, 1.0 equiv)

THF (10 mL, 0.2 M)

Purification: 10 % EtOAc in hexanes.

Yield of Product:

4-3: 0.88 g, 1.4 mmol, 70 %, off-white solid.

Characterization:

R_f = (EtOAc/hexanes, 1:9) 0.20; **IR** (neat) v = 3432, 2979, 1524, 1465, 1449, 1374, 1298, 1260, 1212, 1166, 1136, 985, 968, 851, 692 cm^{-1}; **^{1}H NMR** (500 MHz, $CDCl_3$) δ 9.21 (s, 1H), 8.82 (s, 1H), 7.05 (d, *J* = 2.1 Hz, 1H), 6.97 (d, *J* = 2.4 Hz, 1H), 6.94 (s, 1H), 6.91 (s, 1H), 1.81 (s, 6H), 1.76 (s, 6H), 1.38 (s, 12H).; **^{13}C NMR** (126 MHz, $CDCl_3$) δ 146.96, 143.57, 142.67, 142.35, 132.60, 130.49, 130.08, 123.07, 121.53, 118.43, 117.91, 114.99, 101.89, 99.22, 98.81, 98.79, 84.19, 53.88, 26.18, 26.03, 24.96.; **HRMS**: Calcd. for $C_{28}H_{30}BIN_2NaO_6$ $[M+Na]^+$ = 651.1134 m/z, found = 651.1130 m/z.

Compound 4-38 (from cross-coupling):

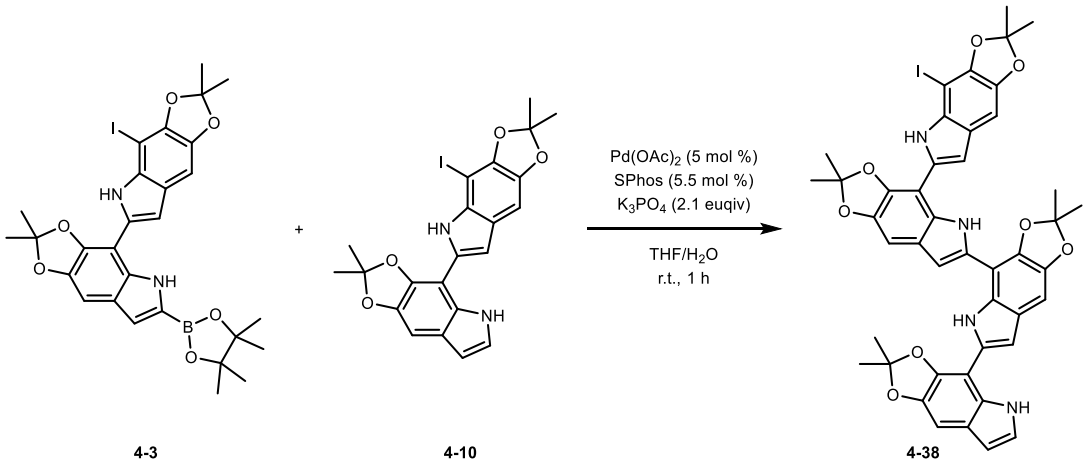

4-3 4-10 4-38

Chemical Formula: $C_{44}H_{37}IN_4O_8$
Molecular Weight: 876.70

Procedure: The reaction was carried out according to the General Procedure A, the reaction was performed in THF/H_2O (4:1, 0.05 M) at ambient temperature for 1 h.

Amounts of Reagents:

4-3 (37.70 mg, 0.06 mmol, 1.2 equiv)

4-10 (25.11 mg, 0.05 mmol, 1.0 equiv)

$Pd(OAc)_2$ (0.56 mg, 0.0025 mmol, 5 mol%)

SPhos (1.13 mg, 0.00275 mmol, 5.5 mol%)

K_3PO_4 (22.29 mg, 0.105 mmol, 2.1 equiv)

THF (1.0 mL), H_2O (0.25 mL)

Purification: 10 % EtOAc in hexanes.

Yield of Product:

4-38: 5.7 mg, 0.006 mmol, 13 %, yellow solid.

Compound 4-38 (from iododeborylation):

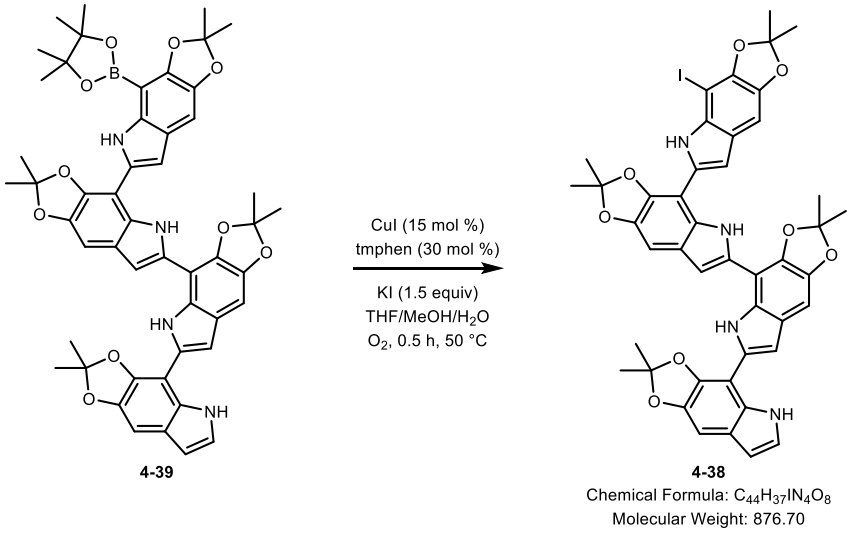

Procedure: A 10 mL round-bottom flask equipped with a Teflon-coated stir bar and a rubber septum was charged with **4-39** (43.84 mg, 0.05 mmol, 1.0 equiv), CuI (1.43 mg, 0.0075 mmol, 15 mol%), tmphen (4.03 mg, 0.015 mmol, 30 mol%), KI (12.45 mg, 0.075 mmol, 1.5 equiv), and THF/MeOH/H_2O (0.5 mL/0.4 mL/0.1 mL, 0.05 M, 5:4:1). The rubber septum was then connected to a tank of O_2, pressurized to 50 kpa, and was vented 3 times for 10 s each time. Under a constant pressure of O_2 (50 kpa), the reaction mixture was then stirred at 50 ^oC for 0.5 h before depressurizing by opening to the atmosphere and concentrated *in vacuo* The resulting wine-red

residue was then diluted and extracted with EtOAc (3 x 30 mL). The combined organic fractions were washed with brine (20 mL), dried over $MgSO_4$, filtered and concentrated *in vacuo*. The resulting crude mixture was then purified using silica gel column chromatography (10 % EtOAc in hexanes) to afford **4-38** as a yellow solid (9.2 mg, 0.0105 mmol) in 21 %.

Characterization:

R_f = (EtOAc/hexanes, 1:9) 0.31; **^{1}H NMR** (500 MHz, $CDCl_3$) δ 9.99 (s, 1H), 9.98 (s, 1H), 9.29 (s, 1H), 8.58 (s, 1H), 7.20 (dd, *J* = 3.1, 2.2 Hz, 1H), 6.99 (d, *J* = 2.4 Hz, 1H), 6.98 (s, 1H), 6.96 (s, 1H), 6.94 (s, 1H), 6.89 (d, *J* = 2.3 Hz, 1H), 6.87 (d, *J* = 0.6 Hz, 1H), 6.83 (d, *J* = 2.2 Hz, 1H), 6.52 (dd, *J* = 3.2, 2.3 Hz, 1H), 1.88 (s, 6H), 1.87 (s, 6H), 1.85 (s, 6H), 1.77 (s, 6H).; **HRMS**: Calcd. for $C_{44}H_{37}N_4NaO_8$ $[M+Na]^+$ = 899.1548 m/z, found = 899.1545 m/z.

Compound 4-9:

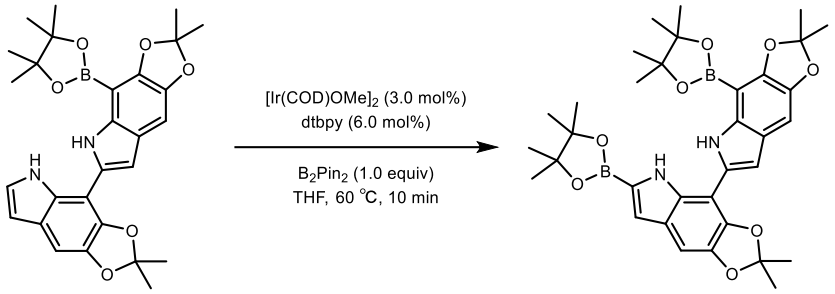

Procedure: The reaction was carried out according to the General Procedure B and was performed in THF at 60 °C for 10 min.

Amounts of Reagents:

4-27 (1.06 g, 2.12 mmol, 1.0 equiv)

$[Ir(OMe)(COD)]_2$ (39.77 mg, 0.06 mmol, 3.0 mol%)

dtbpy (32.21 mg, 0.12 mmol, 6.0 mol%)

B_2pin_2 (538.25 mg, 2.12 mmol, 1.0 equiv)

THF (10 mL, 0.2 M)

Purification: 15 % EtOAc in hexanes.

Yield of Product:

4-9: 932.4 mg, 1.5 mmol, 70 %, yellow solid.

Characterization:

R_f = (EtOAc/hexanes, 1:4) 0.40; **IR** (neat) v = 3430, 2980, 1530, 1450, 1370, 1260, 1210, 1170, 1140, 970, 852, 756, 692, 667 cm^{-1}; **^{1}H NMR** (500 MHz, $CDCl_3$) δ 10.07 (s, 1H), 8.91 (s, 1H), 7.09 (s, 1H), 7.04 (d, *J* = 2.1 Hz, 1H), 6.88 (s, 1H), 6.84 (d, *J* = 2.4 Hz, 1H), 1.80 (s, 6H), 1.74 (s, 6H), 1.43 (s, 12H), 1.37 (s, 12H).; **^{13}C NMR** (101 MHz, $CDCl_3$) δ 151.75, 143.60, 143.02, 135.60, 130.88, 129.15, 122.84, 120.97, 117.82, 117.39, 114.87, 101.95, 100.53, 100.05, 98.06, 84.11, 83.71, 26.29, 26.07, 25.21, 24.96.; **HRMS**: Calcd. for $C_{34}H_{42}B_2N_2NaO_8$ $[M+Na]^+$ = 651.3019 m/z, found = 651.3059 m/z.

Compound 4-39

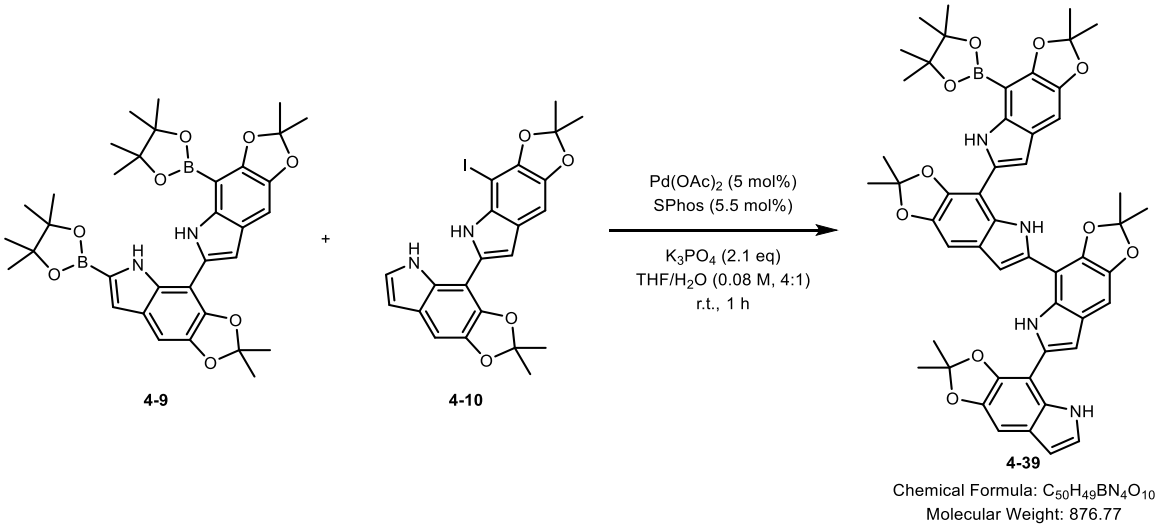

4-9 **4-10** **4-39**

Chemical Formula: $C_{50}H_{49}BN_4O_{10}$
Molecular Weight: 876.77

Procedure: The reaction was carried out according to the General Procedure A, the reaction was performed in THF/H_2O (4:1, 0.08 M) at ambient temperature for 1 h.

Amounts of Reagents:

4-9 (917.37 mg, 1.46 mmol, 1.1 equiv)

4-10 (663.05 mg, 1.32 mmol, 1.0 equiv)

$Pd(OAc)_2$ (14.82 mg, 0.06 mmol, 5 mol%)

SPhos (29.80 mg, 0.07 mmol, 5.5 mol%)

K_3PO_4 (589.60 mg, 2.77 mmol, 2.1 equiv)

THF (16.0 mL), H_2O (4.0 mL)

Purification: The crude mixture was precipitate with CH_2Cl_2 (3 ml) and hexanes (20 mL) followed by vacuum filtrations.

Yield of Product:

4-39: 771 mg, 0.88 mmol, 67 %, off-white solid.

Characterization:

R_f = (EtOAc/hexanes, 1:4) 0.26; **IR** (neat) v = 3472, 3428, 2978, 1447, 1374, 1304, 1199, 1170, 1138, 981, 851, 753 cm^{-1}; **^{1}H NMR** (400 MHz, $CDCl_3$) δ 10.23 (brs, 1H), 10.08 (brs, 1H), 10.02 (brs, 1H), 8.65 (s, 1H), 7.20 (dd, *J* = 3.1, 2.4 Hz, 1H), 7.04 (s, 1H), 6.97 (s, 1H), 6.96 (s, 1H), 6.92 (s, 1H), 6.89 (m, 2H), 6.85 (d, *J* = 2.2 Hz, 1H), 6.52 (dd, *J* = 3.2, 2.0 Hz, 1H), 1.88 (s, 12H), 1.86 (s, 6H), 1.75 (s, 6H), 1.45 (s, 12H).; **^{13}C NMR** (101 MHz, $CDCl_3$) δ 151.85, 143.56, 143.51, 143.26, 143.12, 140.80, 140.72, 135.50, 130.70, 130.52, 129.51, 127.49, 127.22, 127.15, 123.17, 123.06, 122.87, 122.46, 121.10, 118.30, 118.14, 117.86, 117.58, 103.58, 101.59, 100.49, 100.04, 100.01, 99.92, 99.65, 99.61, 98.64, 97.99, 97.30, 83.77, 26.31, 26.25, 26.09, 25.24; **HRMS**: Calcd. for $C_{50}H_{49}BN_4NaO_{10}$ $[M+Na]^+$ = 899.3434 m/z, found = 899.3408 m/z.

Compound 4-7:

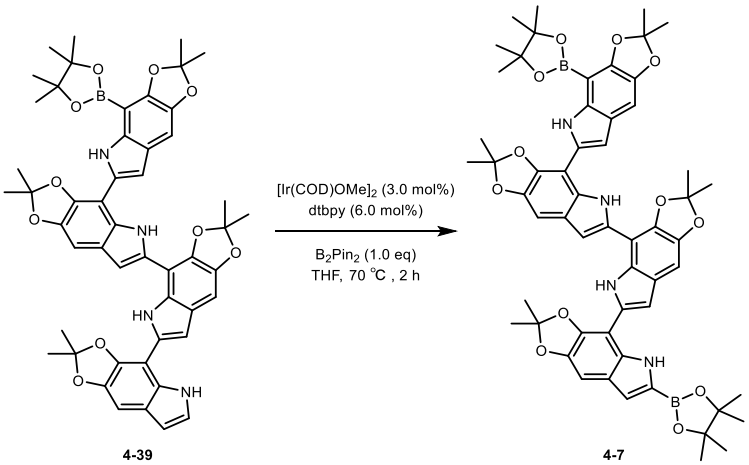

Procedure: The reaction was carried out according to the General Procedure B and was performed in THF at 70 °C for 2 h.

Amounts of Reagents:

4-39 (1.21 g, 1.38 mmol, 1.0 equiv)

$[Ir(OMe)(COD)]_2$ (26.51 mg, 0.04 mmol, 3.0 mol%)

dtbpy (21.47 mg, 0.08 mmol, 6.0 mol%)

B_2pin_2 (350.44 mg, 1.38 mmol, 1.0 equiv)

THF (17 mL, 0.08 M)

Purification: 20% EtOAc in hexanes.

Yield of Product:

4-7: 1.0 g, 1.0 mmol, 73 %, off-white solid.

Characterization:

$\mathbf{R_f}$ = (EtOAc/hexanes, 4:1) 0.25; **IR** (neat) v = 3462, 3429, 2979, 2935, 1514, 1384, 1372, 1339, 1213, 1171, 1138, 983, 853, 755, 667, 460 cm^{-1}; **^{1}H NMR** (500 MHz, $CDCl_3$) δ 10.22 (brs, 1H), 10.08 (brs, 1H), 9.98 (brs, 1H), 8.90 (brs, 1H), 7.07 (d, *J* = 2.1 Hz, 1H), 7.03-7.03 (m, 2H), 6.94 – 6.92 (m, 2H), 6.91 (s, 1H), 6.88-6.88 (m, 2H), 1.89 (s, 6H), 1.87 (s, 6H), 1.85 (s, 6H), 1.75 (s, 6H), 1.45 (s, 12H), 1.39 (s, 12H).; **^{13}C NMR** (126 MHz, $CDCl_3$) δ 151.86, 143.57, 143.56, 143.51, 143.12, 142.14, 140.79, 140.74, 135.51, 130.56, 130.50, 130.43, 129.51, 127.49, 127.21, 123.23, 123.08, 122.88, 121.10, 118.36, 118.28, 117.85, 117.54, 114.98, 101.57, 100.86, 100.05, 99.99, 99.69, 99.66, 99.59, 98.68, 98.10, 97.28, 84.21, 83.74, 26.31, 26.29, 26.26, 26.10, 25.24, 24.98.; **HRMS**: Calcd. for $C_{56}H_{61}O_{12}N_4B_2$ $[M+H]^+$ = 1003.44666 m/z, found = 1003.44838 m/z.

Compound 4-2 (from 4-3):

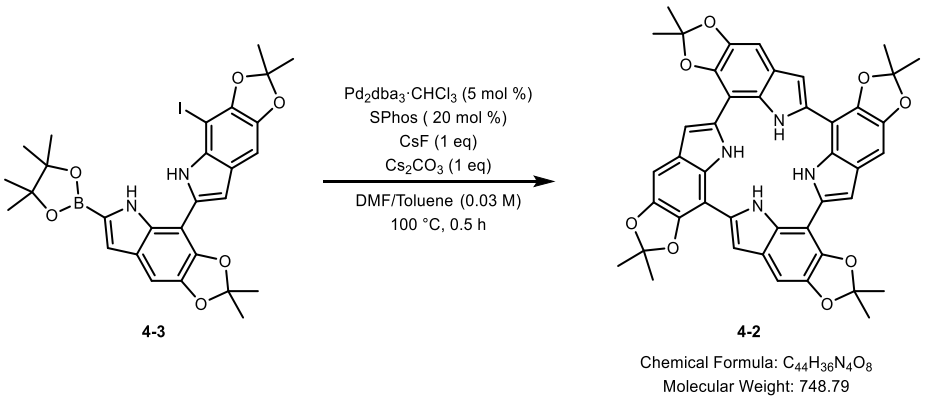

Procedure: In an inert atmosphere glove box, a flamed-dried vial equipped with a Teflon-coated stir bar was charged with **4-3** (25.14 mg, 0.04 mmol, 1.0 equiv), $Pd_2dba_3{\cdot}CHCl_3$ (2.08 mg, 0.002

mmol, 5 mol %), SPhos (3.28 mg, 0.008 mmol, 20 mol %), CsF (6.08 mg, 0.04 mmol, 1.0 equiv), and Cs_2CO_3 (13.04 mg, 0.04 mmol, 1.0 equiv). To the vial were added dry degassed toluene (0.6 mL) and DMF (0.6 mL). The vial was then sealed and taken out of glove box. Degassed deionized H_2O (0.28 mL, 0.4 equiv) was then added to the reaction vial under a positive pressure of N_2 before heating to 100 °C for 0.5 h. After cooling to ambient temperature, the reaction mixture was diluted with EtOAc (10 mL) and washed with H_2O (10 mL) and brine (5 mL). The phases were then separated, and the aqueous phase was extracted with EtOAc (3 × 20 mL). The combined organic fractions were then dried over $MgSO_4$, filtered, and concentrated *in vacuo*. The resulting crude reaction mixture was purified by preparative Thin Layer Chromatography (TLC) on silica gel (10 % EtOAc in hexanes) to afford **4-2** as a yellow solid (3 mg, 0.004 mmol) in 10 % yield.

Compound 4-2 (from 4-7):

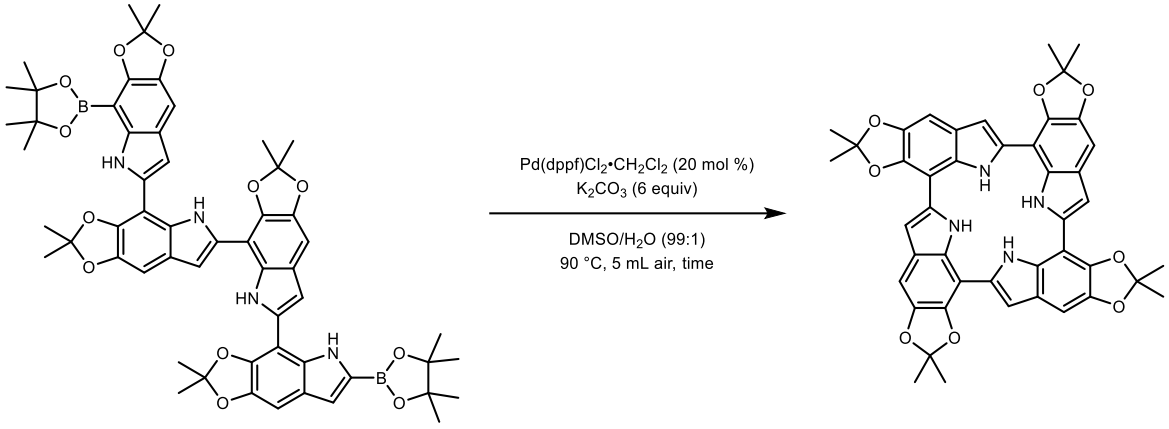

4-7 **4-2**

Chemical Formula: $C_{44}H_{36}N_4O_8$
Molecular Weight: 748.79

Procedure: A flamed-dried, 250 mL round bottom flask equipped with a Teflon-coated stir bar and a rubber septum was charged with **4-7** (50.14 mg, 0.05 mmol, 1.0 equiv), $Pd(dppf)_2Cl_2{\cdot}CH_2Cl_2$ (8.17 mg, 0.01 mmol, 20 mol%), and K_2CO_3 (41.46 mg, 0.3 mmol, 6 equiv). The flask was then evacuated and backfilled with N_2 (this process was repeated three times), prior to the addition of DMSO/H_2O (99 mL/1 mL, 0.0005 M) via cannula addition under N_2. The resulting mixture was then heated at 90 °C with vigorous stirring for 5 min followed by the addition of 5 mL of air via a syringe. The reaction was kept stirring for another 25 min. The reaction was then cooled down to room temperature and poured into a separatory funnel containing aqueous HCl (1N, 10 mL) and H_2O (50 mL). The mixture was then extracted with EtOAc (20 mL × 3) and the combined

organic layers were washed with H_2O (20 mL x 3), and brine (10 mL x 2). The organic layer was then separated and dried over Na_2SO_4 and concentrated *in vacuo* to afford the crude reaction mixture, which was purified using silica gel column chromatography (EtOAc/hexanes, 1:9) to afford **4-2** in a 20 % yield as a yellow solid (7.5 mg, 0.01 mmol).

Characterization:

R_f = (EtOAc/hexanes, 1:9) 0.30; **^{1}H NMR** (800 MHz, $CDCl_3$) δ 9.03 (s, 4H), 6.97 (d, *J* = 1.7 Hz, 4H), 6.89 (s, 4H), 1.76 (s, 24H).; **^{1}H NMR** (500 MHz, CD_3CN) δ 9.85 (s, 4H), 6.94 (s, 4H), 6.84 (d, *J* = 1.8 Hz, 4H), 1.75 (s, 24H).; **^{13}C NMR** (201 MHz, $CDCl_3$) δ 144.36, 142.24, 131.16, 129.33, 124.09, 118.10, 106.82, 100.64, 98.24, 26.12.; **HRMS**: Calcd. for $C_{44}H_{36}O_8N_4Na$ $[M+Na]^+$ = 771.2425 m/z, found = 771.2429 m/z.

Compound 4-9b:

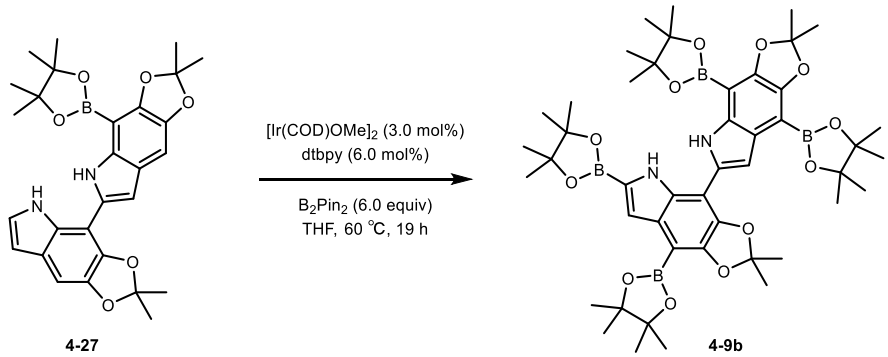

Procedure: The reaction was carried out according to the General Procedure B and was performed in THF at 60 °C for 19 h.

Amounts of Reagents:

4-27 (100.47 mg, 0.2 mmol, 1.0 equiv)

$[Ir(OMe)(COD)]_2$ (3.96 mg, 0.006 mmol, 3.0 mol%)

dtbpy (3.24 mg, 0.012 mmol, 6.0 mol%)

B_2pin_2 (304.72 mg, 1.2 mmol, 6.0 equiv)

THF (4 mL, 0.05 M)

Purification: 30 % EtOAc in hexanes.

Yield of Product:

4-9b: 123.2 mg, 0.14 mmol, 68 %, yellow solid.

Characterization:

R_f = (EtOAc/hexanes, 3:7) 0.24; **IR** (neat) v = 3425, 2979, 1519, 1371, 1218, 1220, 1139, 1010, 968, 850, 667 cm^{-1}; **^{1}H NMR** (500 MHz, $CDCl_3$) δ 10.18 (s, 1H), 9.12 (s, 1H), 7.53 (d, *J* = 2.1 Hz, 1H), 7.42 (d, *J* = 2.5 Hz, 1H), 1.82 (s, 6H), 1.74 (s, 6H), 1.46 (s, 12H), 1.42 (s, 12H), 1.39 (s, 12H), 1.36 (s, 12H).; **HRMS**: Calcd. for $C_{46}H_{65}B_4N_2O_{12}$ $[M+H]^+$ = 881.49042 m/z, found = 881.49135 m/z.

Compound 4-40:

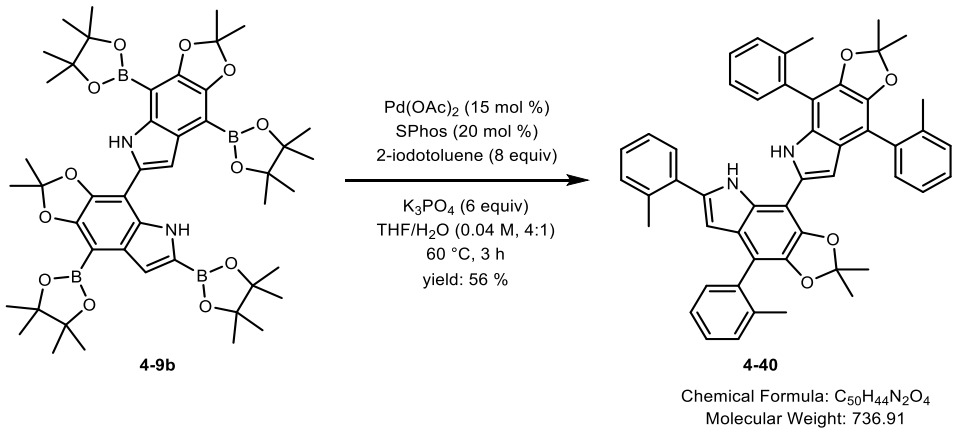

Procedure: The reaction was carried out according to the General Procedure A, the reaction was performed in THF/H_2O (4:1, 0.05 M) at 60 °C for 3 h.

Amounts of Reagents:

4-9b (70.42 mg, 0.08 mmol, 1.0 equiv)

2-iodotoluene (139.54 mg, 0.64 mmol, 8.0 equiv)

$Pd(OAc)_2$ (2.69 mg, 0.012 mmol, 15 mol%)

SPhos (6.57 mg, 0.016 mmol, 20 mol%)

K_3PO_4 (102.09 mg, 0.48 mmol, 6.0 equiv)

THF (1.6 mL), H_2O (0.4 mL)

Purification: 10 % EtOAc in hexanes.

Yield of Product:

4-40: 33.1 mg, 0.04 mmol, 56 %, yellow solid.

Characterization:

R_f = (EtOAc/hexanes, 1:9) 0.5; **^{1}H NMR** (500 MHz, $CDCl_3$) δ 9.12-9.16 (m, 1H), 8.49 (brs, 1H), 7.63-7.65 (m, 1H), 7.56-7.58 (m, 1H), 7.21-7.45 (m, 14H), 6.56-6.60 (m, 1H), 6.29-6.30 (m, 1H), 2.42-2.43 (m, 6H), 2.39-2.40 (m, 3H), 2.28-2.30 (m, 3H), 1.64-1.75 (m, 12H); **HRMS**: Calcd. for $C_{50}H_{43}N_2O_4$ $[M-H]^+$ = 735.32283 m/z, found = 735.32489 m/z.

Compound 4-41 and 4-42:

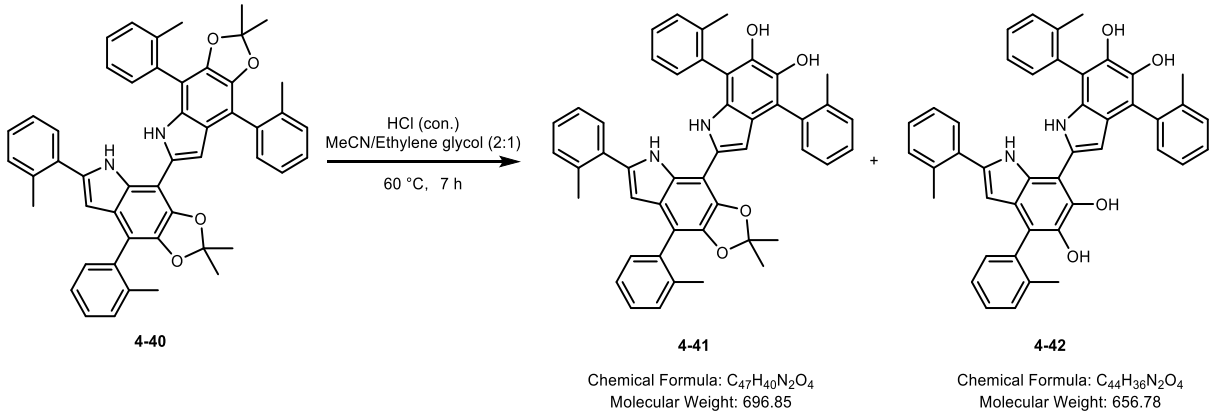

Procedure: A 5 mL flame-dried, round-bottom flask, equipped with a Teflon-coated stir bar and a rubber septum, was charged with **4-40** (10.8 mg, 0.015 mmol, 1.0 equiv). The flask was evacuated and backfilled with N_2 (this process was repeated three times) prior to the addition of dry degassed acetonitrile under a positive pressure of N_2. To the homogeneous solution was added HCl (0.1 mL, concentrated) and ethylene glycol (0.3 mL). The resulting reaction mixture was then stirred at 60 °C for 7 h before cooling to ambient temperature and quenched with the addition of a saturated aqueous solution of $NaHCO_3$ (1 mL). The phases were then separated, and the aqueous phase was extracted with EtOAc (3 × 10 mL). The combined organic fractions were then washed with brine (10 mL), dried over $MgSO_4$, filtered, and concentrated *in vacuo*. The crude mixture was then purified using silica gel column chromatography (25% to 30 % EtOAc in hexanes) to afford **4-41** as a purple solid (3 mg, 0.004 mmol) in 28 % yield and **4-42** as a dark blue solid (2.9 mg, 0.004) in 29 % yield.

Compound 4-41:

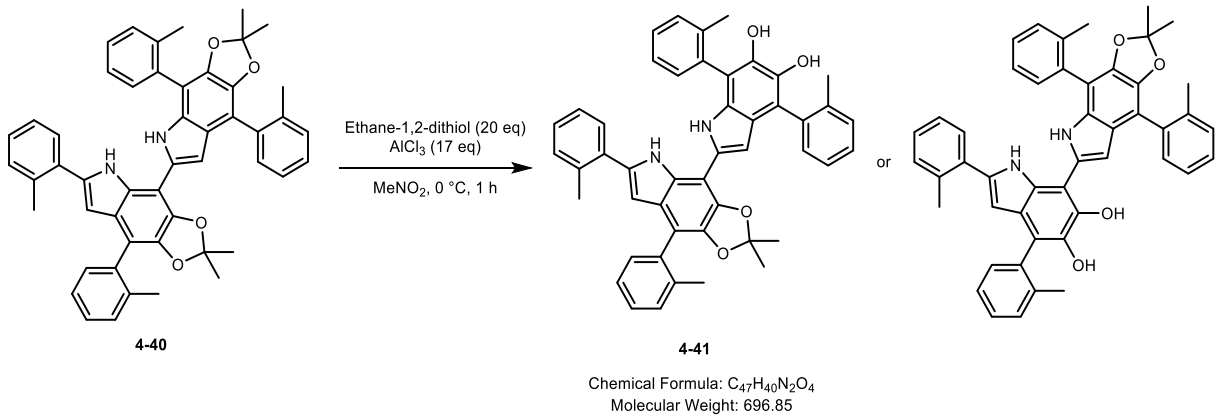

Procedure: A 5 mL flame-dried, round-bottom flask, equipped with a Teflon-coated stir bar and a rubber septum, was charged with **4-40** (25.42 mg, 0.034 mmol, 1.0 equiv). The flask was evacuated and backfilled with N_2 (this process was repeated three times) prior to the addition of $MeNO_2$ (0.35 mL) under a positive pressure of N_2. To this solution was added ethane-1,2-dithiol (64.0 mg, 0.68 mmol, 20 equiv) and $AlCl_3$ (80.0 mg, 0.6 mmol, 17 equiv) in $MeNO_2$ (0.35 mL) at 0 °C. The resulting reaction mixture was stirred at for 0 °C 1 h before the addition of a saturated aqueous solution of potassium sodium tartrate (5 mL), H_2O (5 mL), and EtOAc (10 mL). The resulting mixture was stirred at ambient temperature for 30 min. The phases were then separated, and the aqueous phase was extracted with EtOAc (3 × 10 mL). The combined organic fractions were then washed with brine (5 mL), dried over $MgSO_4$, filtered, and concentrated *in vacuo*. The resulting crude mixture was purified using silica gel column chromatography (30 % EtOAc in hexanes) to afford **4-41** as a light-yellow solid (16.4 mg, 0.023 mmol) in 69 % yield.

Characterization of 4-41:

R_f = (EtOAc/hexanes, 3:7) 0.4; **^{1}H NMR** (400 MHz, $CDCl_3$) δ 8.88 (s, 1H), 8.44 (s, 1H), 7.15-7.60 (m, 16H), 6.39 (s, 1H), 6.27 (s, 1H), 5.46 (s, 1H), 4.98 (s, 1H), 2.39 (s, 3H), 2.35 (s, 3H), 2.30 (m, 3H), 2.27 (m, 3H), 1.66 – 1.59 (m, 6H).; **HRMS**: Calcd. for $C_{47}H_{40}N_2NaO_4$ $[M+Na]^+$ = 719.2880 m/z, found = 719.2887 m/z.

Characterization of 4-42:

R_f = (EtOAc/hexanes, 3:7) 0.3; **^{1}H NMR** (400 MHz, $CDCl_3$) δ 9.07 (s, 1H), 8.50 (s, 1H), 7.21-7.40 (mf, 16H), 6.48 (s, 1H), 6.11 (s, 1H), 5.96 (s, 1H), 5.37 (s, 1H), 5.00 (s, 1H), 4.76 (s, 1H), 2.41 – 2.25 (m, 12H).; **HRMS**: Calcd. for $C_{44}H_{36}N_2NaO_4Si$ $[M+Na]^+$ = 679.2567 m/z, found = 679.2573 m/z.

Compound 4-43:

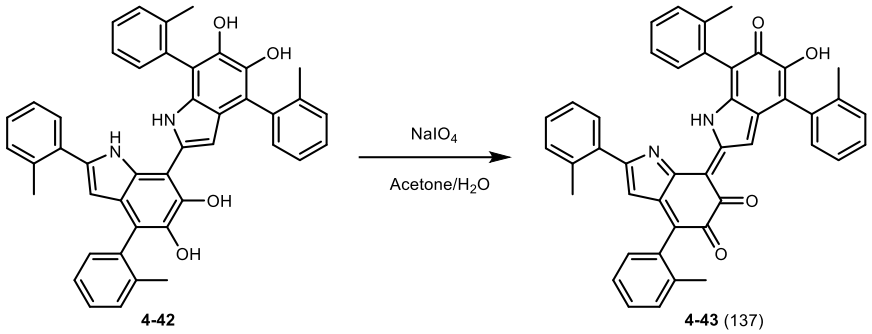

Procedure: A 5 mL flame-dried, round-bottom flask, equipped with a Teflon-coated stir bar and a rubber septum, was charged with **4-42** (2.9 mg, 0.0044 mmol, 1.0 equiv) and $NaIO_4$ (4.1 mg, 0.019 mmol, 4.4 equiv). The flask was evacuated and backfilled with N_2 (this process was repeated three times) prior to the addition of acetone (1 mL) and H_2O (0.2 mL) under a positive pressure of N_2. The resulting mixture was stirred at ambient temperature for 0.5 h before adding H_2O (2 mL) and EtOAc (2 mL). The phases were then separated, and the aqueous phase was extracted with EtOAc (3 $\times$ 10 mL). The combined organic fractions were then washed with brine (2 mL), dried over $MgSO_4$, filtered, and concentrated *in vacuo*. The resulting crude mixture was purified using silica gel column chromatography (30 % EtOAc in hexanes) to afford **4-43** as a dark-blue solid (2 mg, 0.003 mmol) in 69 % yield.

Characterization:

$\mathbf{R_f}$ = (EtOAc/hexanes, 1:4) 0.2; **^{1}H NMR** (500 MHz, acetone) δ 11.40 (s, 1H), 7.51 (m, 1H), 7.47 – 7.24 (m, 16H), 6.20 (s, 1H), 2.37 (s, 3H), 2.30 (s, 3H), 2.28 (s, 3H), 2.20 (s, 3H).; **HRMS**: Calcd. for $C_{44}H_{32}N_2NaO_4$ $[M+Na]^+$ = 675.2254 m/z, found = 675.2275 m/z.

Compound 4-44:

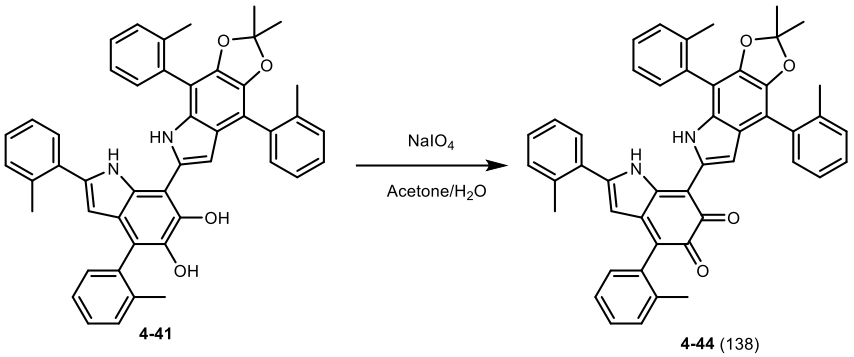

Procedure: A 5 mL flame-dried, round-bottom flask, equipped with a Teflon-coated stir bar and a rubber septum, was charged with **4-41** (3.0 mg, 0.0043 mmol, 1.0 equiv) and $NaIO_4$ (2.0 mg, 0.009 mmol, 2.2 equiv). The flask was evacuated and backfilled with N_2 (this process was repeated three times) prior to the addition of acetone (1 mL) and H_2O (0.2 mL) under a positive pressure of N_2. The resulting mixture was stirred at ambient temperature for 1 h before adding H_2O (2 mL) and EtOAc (2 mL). The phases were then separated, and the aqueous phase was extracted with EtOAc (3 $\times$ 10 mL). The combined organic fractions were then washed with brine (2 mL), dried over $MgSO_4$, filtered, and concentrated *in vacuo.* The crude reaction mixture was purified using silica gel column chromatography (20 % EtOAcin hexanes) to afford **4-44** as a pink-purple solid (2.3 mg, 0.003 mmol) in 78 % yield.

Characterization:

R_f = (EtOAc/hexanes, 1:4) 0.5; **^{1}H NMR(500 MHz, acetone)** δ 11.19 (s, 1H), 8.32 (s, 1H), 7.44 – 7.12 (m, 16H), 6.76 (dd, *J* = 2.7, 1.9 Hz, 1H), 6.26 (m, 1H), 2.42 (d, *J* = 4.4 Hz, 3H), 2.33 (d, *J* = 2.9 Hz, 3H), 2.27 (d, *J* = 5.0 Hz, 3H), 2.17 (s, 3H), 1.67 (m, 6H).; **HRMS**: Calcd. for $C_{47}H_{38}N_2NaO_4$ $[M+Na]^+$ = 717.2724 m/z, found = 717.2718 m/z.

Compound 4-20:

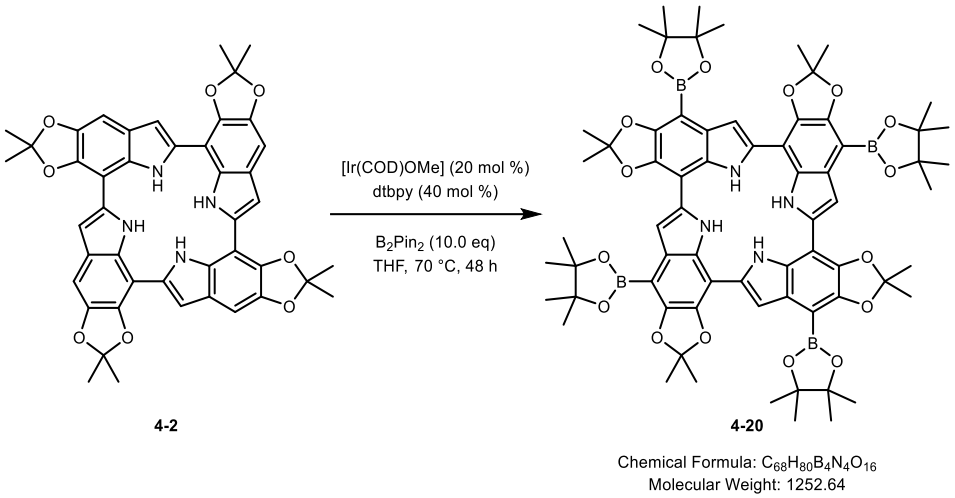

Procedure: The reaction was carried out according to the General Procedure B and was performed in THF at 70 °C for 48 h.

Amounts of Reagents:

4-2 (13.0 mg, 0.017 mmol, 1.0 equiv)

$[Ir(OMe)(COD)]_2$ (4.51 mg, 0.0068 mmol, 40 mol%)

dtbpy (3.65 mg, 0.0136 mmol, 80 mol%)

B_2pin_2 (43.17 mg, 0.17 mmol, 10.0 equiv)

THF (1.6 mL, 0.01 M)

Purification: 25 % EtOAc in hexanes.

Yield of Product:

4-20: 18.1 mg, 0.014 mmol, 85 %, yellow solid.

Characterization:

$\mathbf{R_f}$ = (EtOAc/hexanes, 3:7) 0.37; **^{1}H NMR** (800 MHz, $CDCl_3$) δ 8.99 (brs, 4H), 7.64 (d, *J* = 1.7 Hz, 4H), 1.79 (s, 24H), 1.43 (s, 48H).; **^{13}C NMR** (201 MHz, $CDCl_3$) δ 150.88, 141.74, 131.37, 129.05, 128.63, 117.83, 110.52, 103.45, 83.41, 29.85, 26.35, 25.20, 25.18, 25.01, 24.74, 1.18.; **HRMS**: Calcd. for $C_{68}H_{81}B_4N_4O_{16}$ $[M+H]^+$ = 1253.60143 m/z, found = 1253.60541 m/z.

Compound 4-19:

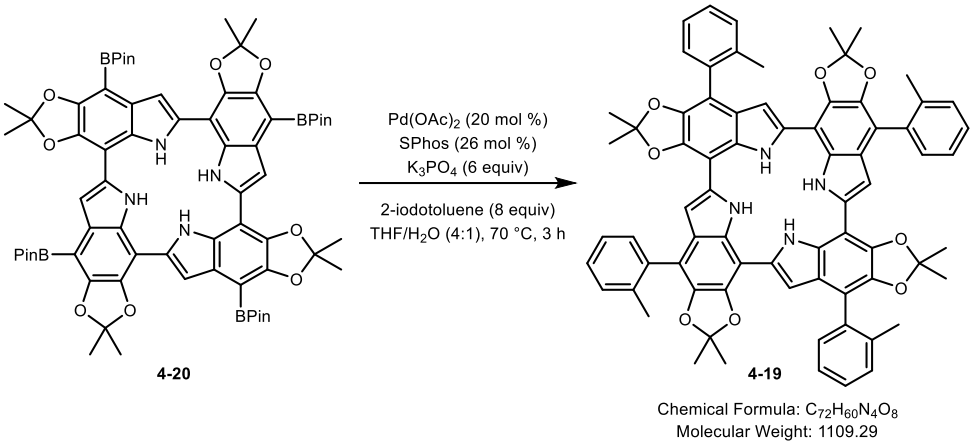

Procedure: The reaction was carried out according to the General Procedure A, the reaction was performed in THF/H_2O (4:1, 0.01 M) at 70 °C for 3 h.

Amounts of Reagents:

4-20 (25.0 mg, 0.02 mmol, 1.0 equiv)

2-iodotoluene (34.9 mg, 0.16 mmol, 8.0 equiv)

$Pd(OAc)_2$ (0.89 mg, 0.004 mmol, 20 mol%)

SPhos (2.13 mg, 0.0052 mmol, 26 mol%)

K_3PO_4 (25.47 mg, 0.12 mmol, 6.0 equiv)

THF (1.6 mL), H_2O (0.4 mL)

Purification: 10 % EtOAc in hexanes.

Yield of Product:

4-19: 9.3 mg, 0.008 mmol, 42 %, light brown solid.

Characterization:

$\mathbf{R_f}$ = (EtOAc/hexanes, 1:4) 0.56; **^{1}H NMR** (500 MHz, $CDCl_3$) δ 9.08 (s, 4H), 7.47-7.50 (m, 4H), 7.32 – 7.39 (m, 12H), 6.69-6.70 (m, 4H), 2.32-2.35 (m, 12H), 1.66-1.70 (m, 24H).; **HRMS**: Calcd. for $C_{72}H_{61}N_4O_8$ $[M+H]^+$ = 1109.44839 m/z, found = 1109.44850 m/z.

4.7.2 Crystallographic Data

Crystal data and structure refinement for 4-27	
Empirical formula	$C_{28}H_{31}BN_2O_6$
Formula weight	502.36
Temperature/K	298(2)
Crystal system	monoclinic
Space group	$P2_1/c$
a/Å	10.1772(4)
b/Å	9.5720(3)
c/Å	31.1050(12)
α/°	90
β/°	95.862(3)
γ/°	90
Volume/Å^3	3014.28(19)
Z	4
ρ_{calc}g/cm^3	1.107
μ/mm^{-1}	0.630
F(000)	1064.0
Crystal size/mm^3	0.430 × 0.110 × 0.090
Radiation	CuKα (λ = 1.54178)
2Θ range for data collection/°	9.672 to 144.36
Index ranges	-12 ≤ h ≤ 12, -8 ≤ k ≤ 11, -38 ≤ l ≤ 38
Reflections collected	29404
Independent reflections	5924 [R_{int} = 0.2022, R_{sigma} = 0.1040]
Data/restraints/parameters	5924/12/343
Goodness-of-fit on F^2	1.047
Final R indexes [I>=2σ (I)]	R_1 = 0.0798, wR_2 = 0.2184
Final R indexes [all data]	R_1 = 0.1261, wR_2 = 0.2738
Largest diff. peak/hole / e Å^{-3}	0.35/-0.23

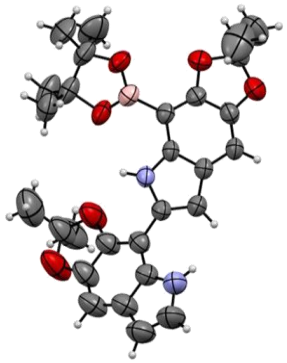

Crystal data and structure refinement for 4-3	
Empirical formula	$C_{56}H_{62}B_2I_2N_4O_{13}$
Formula weight	1274.51
Temperature/K	298(2)
Crystal system	orthorhombic
Space group	Pbcn
a/Å	24.4609(6)
b/Å	9.1408(2)
c/Å	26.2087(6)
α/°	90
β/°	90
γ/°	90
Volume/Å^3	5860.1(2)
Z	4
ρ_{calc}g/cm^3	1.445
μ/mm^{-1}	8.956
F(000)	2584.0
Crystal size/mm^3	0.243 × 0.233 × 0.051
Radiation	CuKα (λ = 1.54178)
2Θ range for data collection/°	6.744 to 144.614
Index ranges	-30 ≤ h ≤ 30, -8 ≤ k ≤ 11, -32 ≤ l ≤ 32
Reflections collected	113477
Independent reflections	5787 [R_{int} = 0.1075, R_{sigma} = 0.0320]
Data/restraints/parameters	5787/60/403
Goodness-of-fit on F^2	1.051
Final R indexes [I>=2σ (I)]	R_1 = 0.0455, wR_2 = 0.1078
Final R indexes [all data]	R_1 = 0.0739, wR_2 = 0.1380
Largest diff. peak/hole / e Å^{-3}	0.76/-0.89

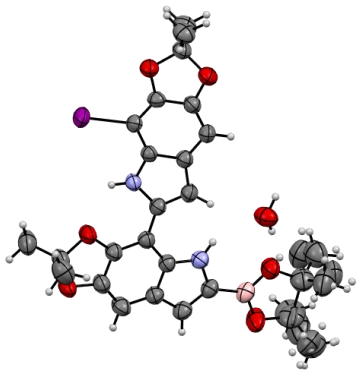

Table 1 Crystal data and structure refinement for 4-39

Empirical formula	$C_{52}H_{51}BCl_6N_4O_{10}$
Formula weight	1115.47
Temperature/K	100(2)
Crystal system	monoclinic
Space group	$P2_1/n$
a/Å	14.393(2)
b/Å	20.348(3)
c/Å	19.121(3)
α/°	90
β/°	107.996(5)
γ/°	90
Volume/Å^3	5326.0(14)
Z	4
ρ_{calc}g/cm^3	1.391
μ/mm^{-1}	3.449
F(000)	2312.0
Crystal size/mm^3	0.221 × 0.178 × 0.156
Radiation	CuKα (λ = 1.54178)
2Θ range for data collection/°	6.518 to 146.042
Index ranges	-11 ≤ h ≤ 17, -25 ≤ k ≤ 25, -23 ≤ l ≤ 23
Reflections collected	89757
Independent reflections	10560 [R_{int} = 0.0823, R_{sigma} = 0.0460]
Data/restraints/parameters	10560/0/690
Goodness-of-fit on F^2	1.037
Final R indexes [I>=2σ (I)]	R_1 = 0.0617, wR_2 = 0.1673
Final R indexes [all data]	R_1 = 0.0720, wR_2 = 0.1807
Largest diff. peak/hole / e Å^{-3}	0.74/-0.74

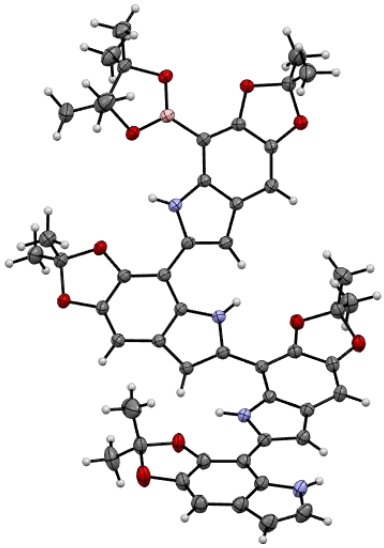

4.8 Reference

1. Kaxiras, E.; Tsolakidis, A.; Zonios, G.; Meng, S., Structural Model of Eumelanin. *Physical Review Letters* **2006,** *97* (21), 218102.

2. Meng, S.; Kaxiras, E., Theoretical Models of Eumelanin Protomolecules and their Optical Properties. *Biophysical Journal* **2008,** *94* (6), 2095-2105.

3. Chen, C.-T.; Ball, V.; de Almeida Gracio, J. J.; Singh, M. K.; Toniazzo, V.; Ruch, D.; Buehler, M. J., Self-Assembly of Tetramers of 5,6-Dihydroxyindole Explains the Primary Physical Properties of Eumelanin: Experiment, Simulation, and Design. *ACS Nano* **2013,** *7* (2), 1524-1532.

4. Chen, C. T.; Chuang, C.; Cao, J.; Ball, V.; Ruch, D.; Buehler, M. J., Excitonic effects from geometric order and disorder explain broadband optical absorption in eumelanin. *Nat. Commun.* **2014,** *5*, 3859.

5. Kaxiras, E.; Tsolakidis, A.; Zonios, G.; Meng, S., Structural model of eumelanin. *Phys. Rev. Lett.* **2006,** *97* (21), 218102.

6. Nakamura, S.; Hiroto, S.; Shinokubo, H., Synthesis and oxidation of cyclic tetraindole. *Chemical Science* **2012,** *3* (2), 524-527.

7. Gulder, T.; Baran, P. S., Strained cyclophane natural products: Macrocyclization at its limits. *Natural Product Reports* **2012,** *29* (8), 899-934.

8. Martí-Centelles, V.; Pandey, M. D.; Burguete, M. I.; Luis, S. V., Macrocyclization Reactions: The Importance of Conformational, Configurational, and Template-Induced Preorganization. *Chemical Reviews* **2015,** *115* (16), 8736-8834.

9. Darzi, E. R.; White, B. M.; Loventhal, L. K.; Zakharov, L. N.; Jasti, R., An Operationally Simple and Mild Oxidative Homocoupling of Aryl Boronic Esters To Access Conformationally Constrained Macrocycles. *Journal of the American Chemical Society* **2017,** *139* (8), 3106-3114.

10. Zhu, X.; McAtee, C. C.; Schindler, C. S., Scalable Synthesis of Mycocyclosin. *Organic Letters* **2018,** *20* (10), 2862-2866.

11. Cochrane, J. R.; White, J. M.; Wille, U.; Hutton, C. A., Total Synthesis of Mycocyclosin. *Organic Letters* **2012,** *14* (9), 2402-2405.

12. Chen, C.-T.; Martin-Martinez, F. J.; Jung, G. S.; Buehler, M. J., Polydopamine and eumelanin molecular structures investigated with ab initio calculations. *Chemical Science* **2017,** *8* (2), 1631-1641.

13. Garg, N. K.; Sarpong, R.; Stoltz, B. M., The First Total Synthesis of Dragmacidin D. *Journal of the American Chemical Society* **2002,** *124* (44), 13179-13184.

14. Almond-Thynne, J.; Blakemore, D. C.; Pryde, D. C.; Spivey, A. C., Site-selective Suzuki–Miyaura coupling of heteroaryl halides – understanding the trends for pharmaceutically important classes. *Chemical Science* **2017,** *8* (1), 40-62.

15. Murphy, J. M.; Liao, X.; Hartwig, J. F., Meta Halogenation of 1,3-Disubstituted Arenes via Iridium-Catalyzed Arene Borylation. *Journal of the American Chemical Society* **2007,** *129* (50), 15434-15435.

16. Beck, E. M.; Hatley, R.; Gaunt, M. J., Synthesis of rhazinicine by a metal-catalyzed C-H bond functionalization strategy. *Angewandte Chemie International Edition* **2008,** *47* (16), 3004-7.

17. Rawal, V. H.; Cava, M. P., Thermolytic removal of t-butyloxycarbonyl (BOC) protecting group on indoles and pyrroles. *Tetrahedron Letters* **1985,** *26* (50), 6141-6142.

18. Zhang, A. J.; Russell, D. H.; Zhu, J. P.; Burgess, K., A method for removal of N-BOC protecting groups from substrates on TFA-sensitive resins. *Tetrahedron Letters* **1998,** *39* (41), 7439-7442.

19. Pandey, S. K.; Guttormsen, Y.; Haug, B. E.; Hedberg, C.; Bayer, A., A Concise Total Synthesis of Breitfussin A and B. *Organic Letters* **2015,** *17* (1), 122-125.

20. Gulledge, Z. Z.; Carrick, J. D., Deprotection of N-tert-Butoxycarbonyl (Boc) Protected Functionalized Heteroarenes via Addition–Elimination with 3-Methoxypropylamine. *European Journal of Organic Chemistry* **2020,** *2020* (12), 1817-1822.

21. Preshlock, S. M.; Ghaffari, B.; Maligres, P. E.; Krska, S. W.; Maleczka, R. E.; Smith, M. R., High-Throughput Optimization of Ir-Catalyzed C–H Borylation: A Tutorial for Practical Applications. *Journal of the American Chemical Society* **2013,** *135* (20), 7572-7582.

22. Evans, P. J.; Darzi, E. R.; Jasti, R., Efficient room-temperature synthesis of a highly strained carbon nanohoop fragment of buckminsterfullerene. *Nature Chemistry* **2014,** *6* (5), 404-408.

23. Golder, M. R.; Jasti, R., Syntheses of the Smallest Carbon Nanohoops and the Emergence of Unique Physical Phenomena. *Accounts of Chemical Research* **2015,** *48* (3), 557-566.

24. Wang, J.; Blancafort, L., Stability and Optical Absorption of a Comprehensive Virtual Library of Minimal Eumelanin Oligomer Models. *Angewandte Chemie International Edition* **2021,** *60* (34), 18800-18809.

25. Pezzella, A.; Panzella, L.; Crescenzi, O.; Napolitano, A.; Navaratman, S.; Edge, R.; Land, E. J.; Barone, V.; d'Ischia, M., Short-Lived Quinonoid Species from 5,6-Dihydroxyindole Dimers en Route to Eumelanin Polymers: Integrated Chemical, Pulse Radiolytic, and Quantum Mechanical Investigation. *Journal of the American Chemical Society* **2006,** *128* (48), 15490-15498.

26. Okuda, H.; Wakamatsu, K.; Ito, S.; Sota, T., Possible Oxidative Polymerization Mechanism of 5,6-Dihydroxyindole from ab Initio Calculations. *The Journal of Physical Chemistry A* **2008,** *112* (44), 11213-11222.

Chapter 5 : Summary and Future Directions

5.1 Summary of Thesis

Despite decades of experimental and theoretical efforts, melanin cannot be described as a well-defined structure. As a result, the molecular origins of melanin's unique physical properties, such as broadband UV absorption, remained unknown. Current biomimetic syntheses of eumelanin produce black materials that have similar macroscopic properties to natural melanin, but have failed to provide well-defined materials suitable for structural characterization. This is because of chain-growth, chain-oxidation and chain-aggregation occur in competition upon oxidation of **DHI** or L-dopa (**1-14**). To address these limitations, we have devised a phased, bottom-up approach that disentangles these three competitive phases of biosynthesis.

In Chapter 2, we developed a biomimetic, catalytic aerobic cyclization of inexpensive and commercially available amino-phenols in a concise 2-stage operation. This process can be operated on scales of up to 200 mmol to produce 10 g of indole **2-10** in a single pass. Polyfunctionalized indoles with boronic ester or halogen at each of the heterocycle's remaining positions were successfully synthesized, creating a range of opportunities to extend these building blocks into well-defined chains. In Chapter 3, we described an iterative bottom-up strategy for higher-order eumelanin oligomer synthesis with absolute control over regioselectivity and chain length. This iterative cycle includes a highly efficient three-step sequence (Suzuki-coupling, desilylation, and borylation) and provided a simplified strategy for a linear pentamer with only two monomer building blocks, a starter unit (**2-26**) and an extender unit (**2-62**). In Chapter 4, we detailed our effort toward the first total synthesis of Kaxiras' cyclic tetramer (**4-2**) via an oxidative macrocyclization. Oxidation of the cyclic tetramer was observed by LCMS, but isolation and complete structural characterization was complicated by instability. We believe that the key to accessing Kaxiras' tetramer will be the installation of blocking groups that can stabilize the cyclic tetramer by preventing staking and chain growth. In addition, we synthesized and oxidized a eumelanin 2,7'-dimer (**4-43**) with blocking groups at 2, 4, and 7 positions, and discovered that this molecule exhibits broadband UV-vis absorption resembling eumelanin (Scheme 5-1).

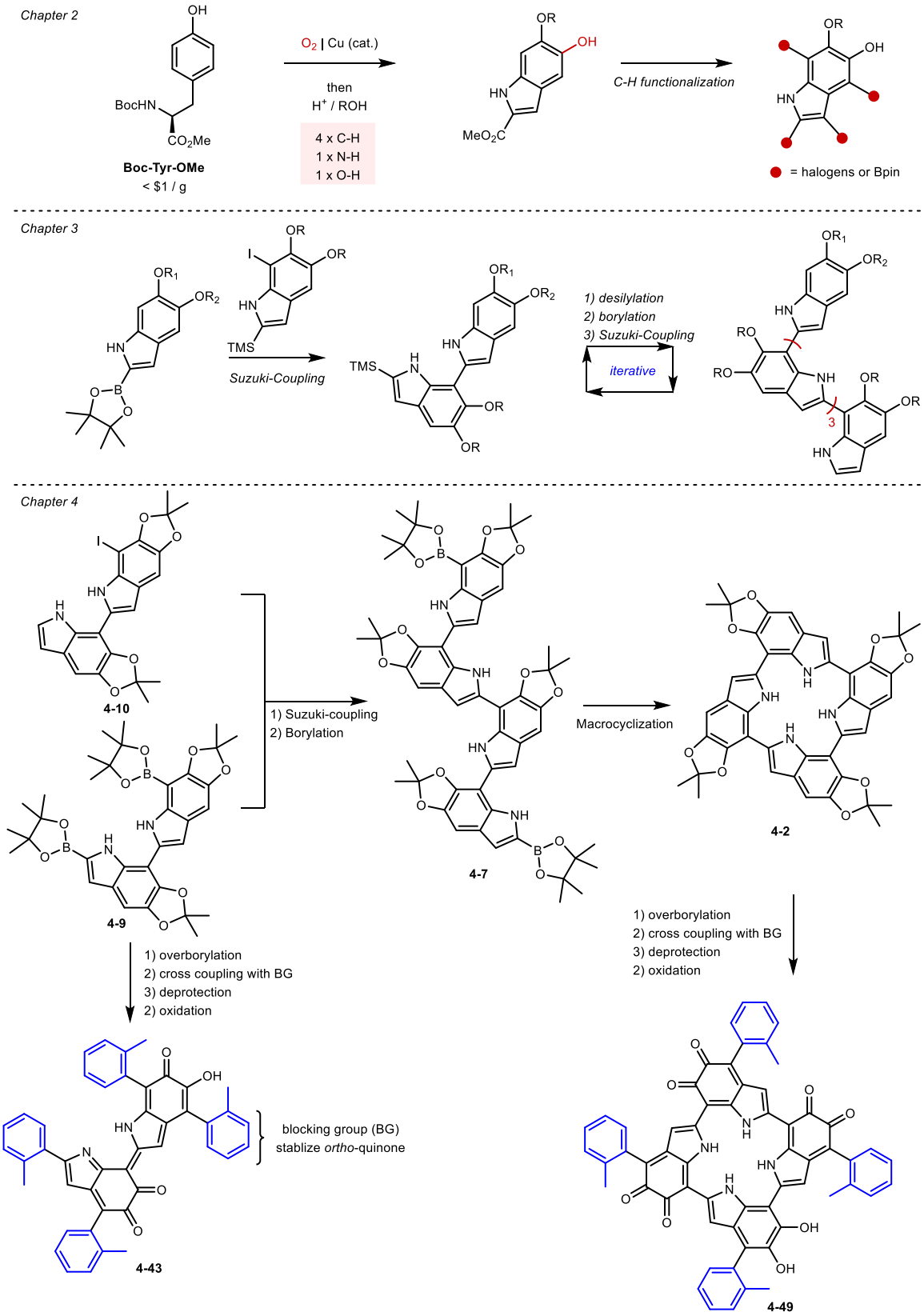

Scheme 5-1 phased-bottom-up approach to eumelanin challenge

5.2 Future Directions

5.2.1 Stabilized Cyclic Tetramer

In Chapter 4, we detected the formation of oxidized cyclic tetramer **4-49** with *ortho*-toluene as a blocking group at the C4 positions by LC-MS, however, the **4-49** was not stable for a prolonged time. We proposed that the observed instability could stem from π-stacking and then aggregation of the cyclic tetramers to insoluble materials. To address this issue, we anticipate increasing stability by installing bulkier blocking groups (Scheme 5-2). The *n*-butyl, *tert*-butyl, and methyl groups in **5-1**, **5-2**, and **5-3** could increase the distance and prevent stacking between layers of cyclic tetramers. **5-4** should also provide steric stabilization to oxidized cyclic tetramer, however, it could be more challenging to install via Suzuki-coupling due to the steric hindrance.

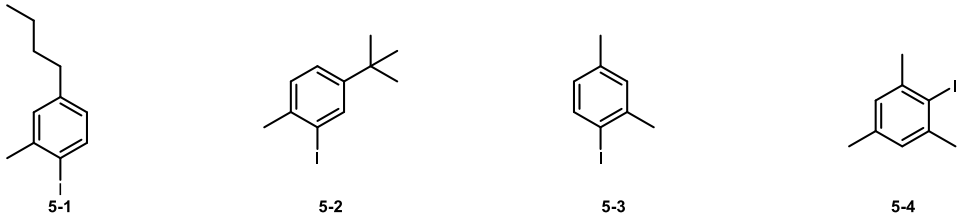

Scheme 5-2 Potential blocking groups

5.2.2 Oxidized Oligomers

In addition to oxidized dimers, trimer and tetramer could also be obtained. Synthesis of well-defined oxidized trimer and tetramer combined with their spectroscopic studies would facilitate our understanding of eumelanin oligomeric architecture, polymerization mechanism and supramolecular aggregation. Oxidized dimers **4-43** and **4-44** have been synthesized via C-H functionalization, cross-coupling reactions, and our blocking group strategy, outlined in Chapter 4. Notably, these dimers exhibit broadband absorption that resembles the spectrum of natural eumelanin. With oxidized tetramer **5-8** as an example, here we propose its synthesis based on our iterative chain growth and blocking group strategy (Scheme 5-3). The successful synthesis of **5-8** would provide insight into the effect of chain length on eumelanin's physical properties at the quinone oxidation state. By comparing the physical properties of linear tetramer (**5-8**) and cyclic tetramer (**4-18**), the effect of of the structural cyclization could be studied. [1]

During our optimization of borylation on the C2 position of linear tetramer **4-39**, we observed a small amount of over-borylated byproduct when the reaction was left for an extended reaction time. Over-borylation of all the remaining C2 and C4 positions could be obtained by extending the reaction time and increasing the equivalence of B_2Pin_2, which would provide **5-5** (Scheme 5-3)

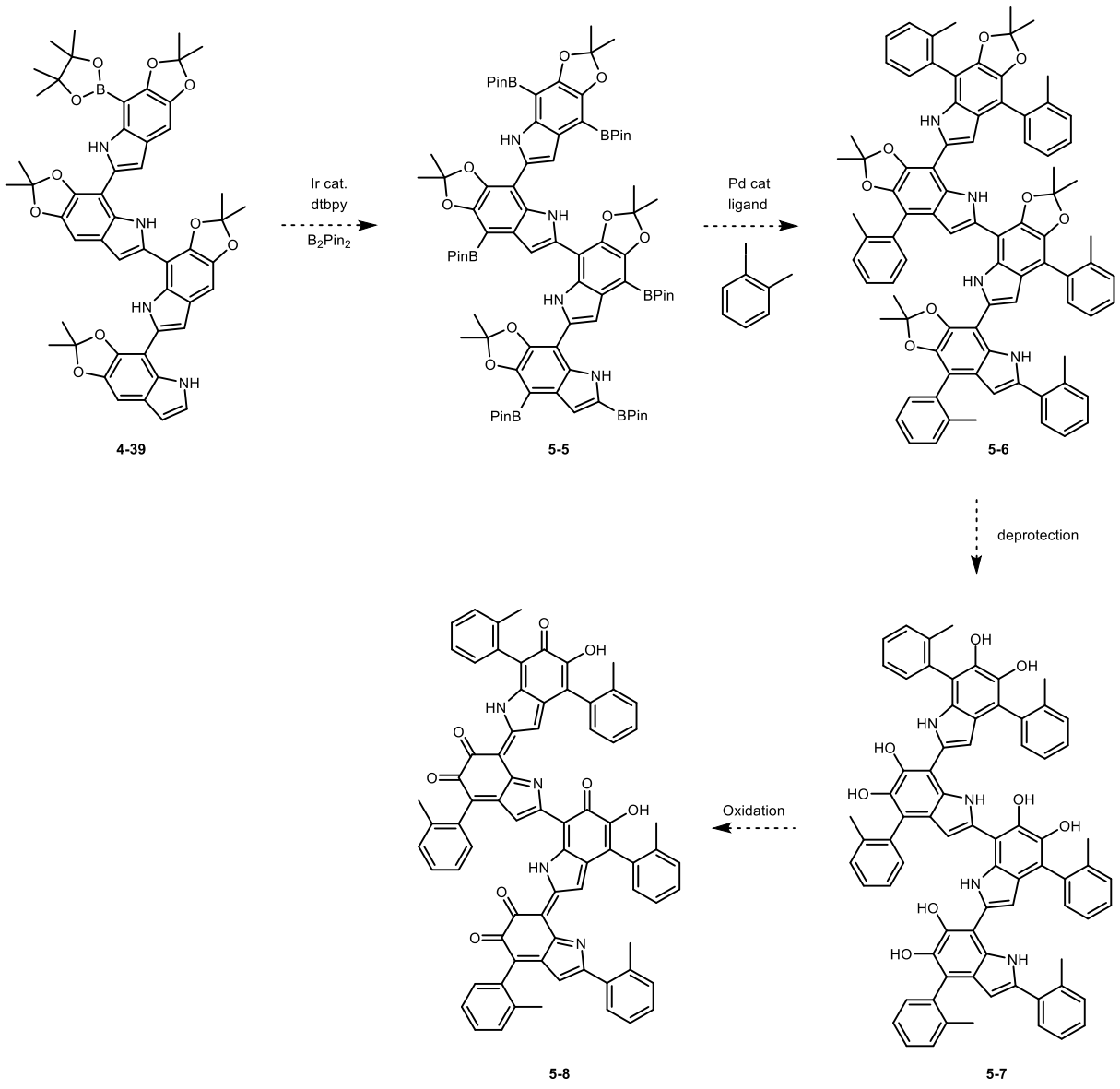

Scheme 5-3 Proposed synthesis of oxidized linear tetramer

Subsequent Suzuki-coupling between **5-5** and 2-iodotoluene would generate **5-6**. *Ortho*-toluene serves as a blocking group that could prevent polymerization at C2 and C4 positions in the process

of oxidation. Removing the acetonide groups could afford **5-7**, which would be converted to **5-8** or its tautomers upon oxidation (Scheme 5-3).

Based on our absorption spectra of oxidized dimers, we anticipate a broadband absorption resembles the spectrum of natural eumelanin. We hope that comparing the ground state and excited state spectroscopic data on oxidized monomer, dimer, trimer, tetramer, and pentamer systematically would offer further insight into the molecular origin of eumelanin's intriguing physical properties.

5.2.3 Use 2,7'-Eumelanin Dimers as Potential BODIPY Dyes

4,4-Difluoro-4-bora-3a,4a-diaza-*s*-indacene (BODIPY) dyes are widely used as fluorescent labels for proteins and DNA. They are strongly UV-absorbing small molecules that emit sharp fluorescence bands with high fluorescent quantum yields. In addition, they are easily modified synthetically, which enables tuning of their fluorescence properties. However, few BODIPY dyes emit at 800 nm or above. Near-infrared (NIR, 650-900 nm) light is beneficial for imaging living cells and animals as it penetrates deeply into tissues without significant damage to biological samples and prevents the interference from background auto-fluorescence of biological samples in living systems.[2-4] Therefore, synthesis of BODIPY-type dyes with emission above 800 nm that could be used more effectively for imaging in living cells is highly desirable. Synthetic modifications of BODIPYs to obtain red shift fluorescence emission have been demonstrated via installing conjugated systems at the 2/6 positions (**5-11**), [5] the 3/5 position (**5-12** and **5-13**), [6, 7] or by fusing aromatic units with the pyrroles to form a rigid fused ring system (**5-14**, Figure 5-1). [8, 9]

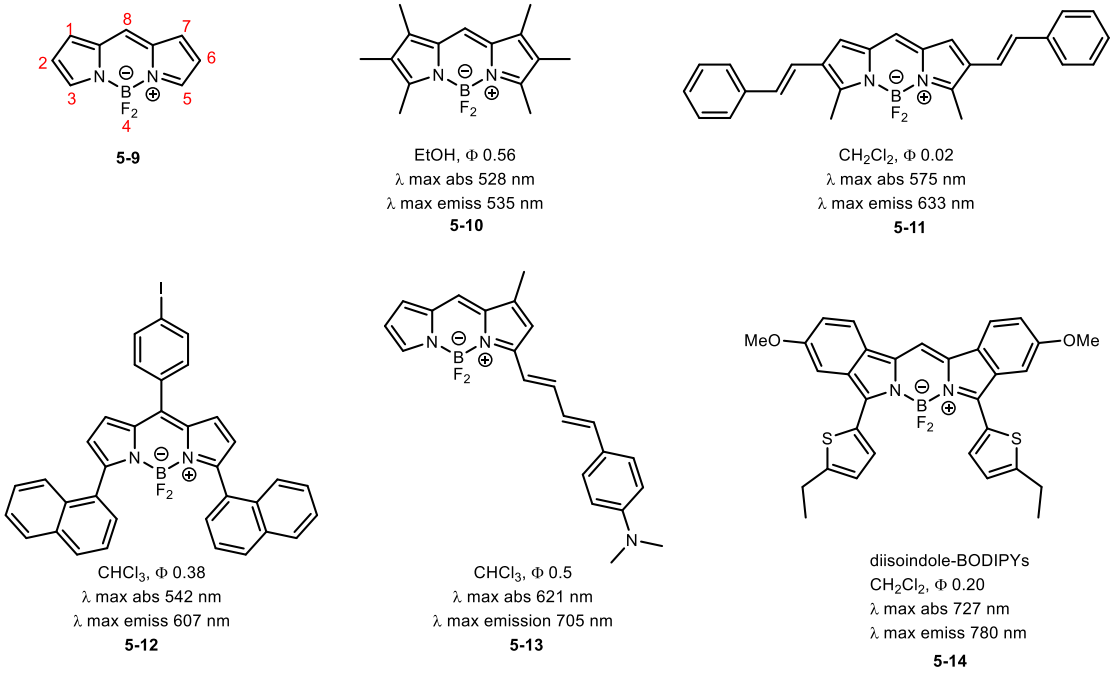

Figure 5-1 modification of BODIPY dyes

The structural similarities between BODIPYs and our 2,7'-dimers suggest that a new class of BODIPY type dyes that emit above 800 nm could be obtained (**5-15**). We reason that our dimer provides π-extension via a benzo-fused ring at the 2 and 3 positions (BODIPY numbering, **5-9**). Structural modification at the 5-position to further extend the π system could be achieved as we have demonstrated successful borylation, silylation or cross-coupling with heterocycles at this position. Thus, it is reasonable to anticipate π-extension at C5, such as **5-16** and **5-17** could be obtained via Suzuki coupling with aryl halides or vinyl halides (Figure 5-2).

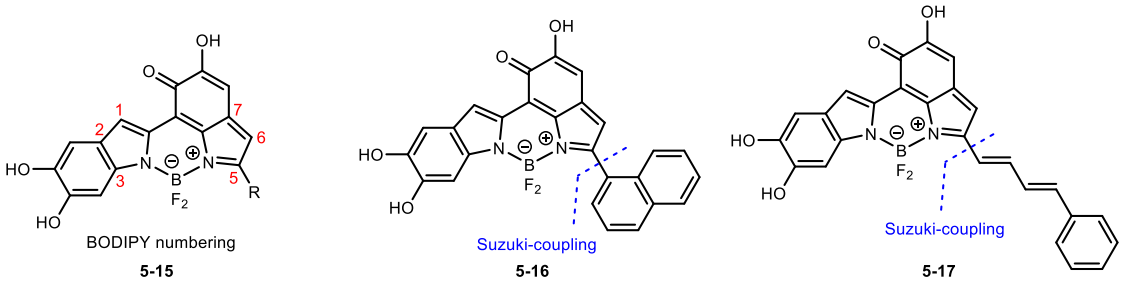

Figure 5-2 Proposed eumelanin dimer based BODIPY dyes

A derivative of **5-15** could be obtained from **4-41** via oxidation with DDQ or *p*-chloranil to **5-18**. BF_2-chelation of **5-18** using $BF_3{\cdot}Et_2O$ could afford a BODIPY dye **5-19** (Scheme 5-4).

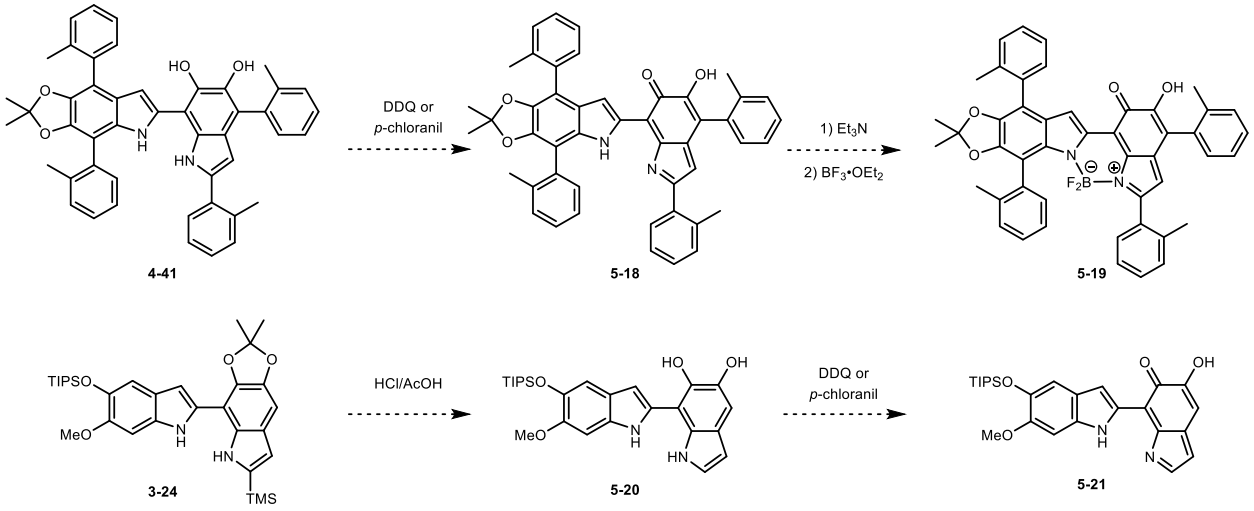

Scheme 5-4 Proposed synthesis of BODIPY dyes with eumelanin dimer

Alternatively, we could capitalize on our different protecting group strategies for the 5,6-catechols. We have described the synthesis of dimer **3-24**, where the indole 5,6-catechols were differently protected. Selective deprotection of the acetonide with HCl/AcOH could afford **5-20**. Subsequent selective oxidation could provide **5-21**, which would then form a BODIPY dye upon treatment with $BF_3{\cdot}Et_2O$ (Scheme 5-4).

5.2.4 DHICA Oligomer

Eumelanin biosynthesis begins with an oxidative cyclization of L-tyrosine (**Tyr**) to either 5, 6-dihydroxy-indole-2-carboxylic acid (**DHICA**) or 5, 6-dihydroxyindole (**DHI**) that is catalyzed by the enzyme tyrosinase. Similar to the synthetic limitation of **DHI** oligomers, a well-defined **DHICA** oligomer synthesis has not been disclosed. Biomimetic oxidation of **DHICA** results in a complex mixture with low-synthetic value. The fundamental understanding of the oxidative polymerization of **DHICA** and the access to well-defined **DHICA** oligomers could play a pivotal role in fully unravelling the structure of eumelanins.

In contrast to **DHI** oxidative polymerization where the mode of polymerization was mainly through 2, 4, and 7 positions, **DHICA** oxidatively polymerizes mainly through the 4,4'-(**5-22**), 4,7'-(**5-23**), and 7,7'-(**5-24**) positions (Figure 5-3).[10] The difference in the mode of polymerization is a function of the 2-carboxylic acid group that hinders nucleophilic addition by withdrawing the electron density from the pyrrole ring system. A presumptive isolation of tetramer **5-25** from the

tapetum lucidum of catfish was reported in 1974,[11] however, a definitive structural confirmation was not achieved due to the difficulties of isolation and purification. Our group is interested in **DHICA** oligomers, and believe that the bottom-up synthetic strategy developed in this thesis could make it possible to obtain well-defined tetramer **5-25**, which would provide more insight into the structure of eumelanin.

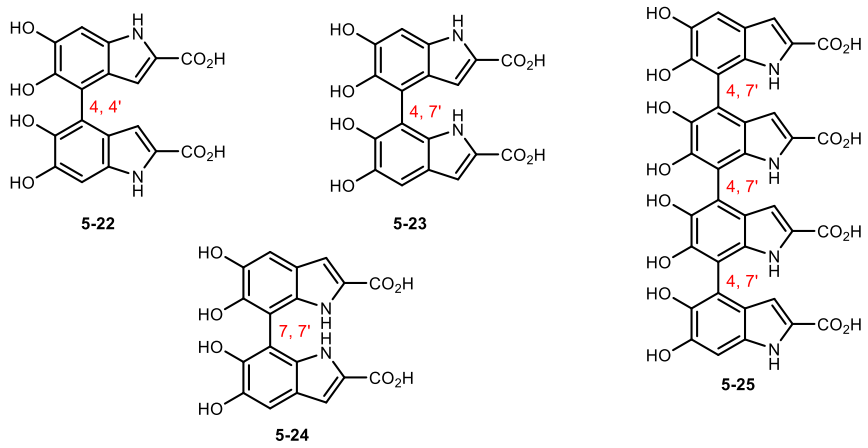

Figure 5-3 Oligomers isolate from oxidation of **DHICA**

During the course of our studies, we developed a decagram bio-inspired indole synthesis with a methyl ester at C2 (**2-10**) and demonstrated successful C4 and C7 functionalization (Chapter 2, Scheme 2-9 and 2-11). Based on this success, we propose here that tetramer **5-25** could be obtained synthetically via an iterative approach. We have demonstrated the syntheses of **2-29** and **2-39** in Chapter 2. Deprotection of the Boc group of **2-39** could afford **5-26**. Cross-coupling between **2-30** and **5-26** would provide a 4,7'-dimer **5-27**. As we have demonstrated in Chapter 2, Ir-catalyzed borylation goes preferentially to the C7 position when C2 is occupied. Thus, it is reasonable to predict that a selective borylation at the C7 position of dimer **5-27** could generate **5-28**, which would then undergo another Suzuki-coupling with **5-26** to form trimer **5-29**. A final iterative cycle including borylation and Suzuki-coupling could afford **5-25** following deprotection and saponification (Scheme 5-5).

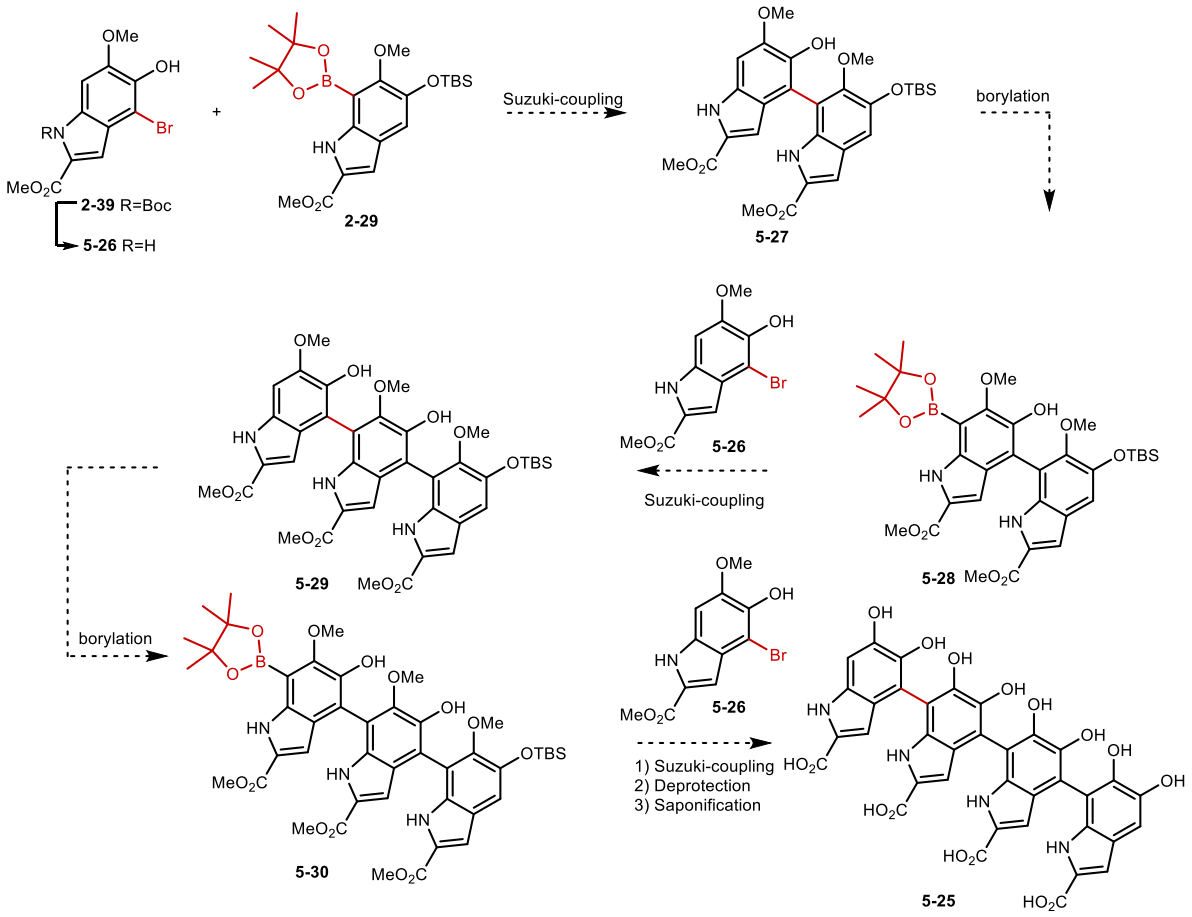

Scheme 5-5 Proposed synthesis of DHICA linear tetramer

There are two major challenges associated with **DHICA** oligomer synthesis. Firstly, unlike DHI oligomers that can adopt a more planar conformation within the molecular units connected through the C2 positions, **DHICA** oligomers contain atropisomeric interunit bonds, generating several stereoisomers for a single regioisomer. Secondly, the formation of the 4,7' bond is more sterically hindered than the formation of the 2,7' bond, which might create some challenges during the synthesis.

5.3 Reference

1. Izumi, S.; Higginbotham, H. F.; Nyga, A.; Stachelek, P.; Tohnai, N.; Silva, P. d.; Data, P.; Takeda, Y.; Minakata, S., Thermally Activated Delayed Fluorescent Donor–Acceptor–Donor–Acceptor π-Conjugated Macrocycle for Organic Light-Emitting Diodes. *Journal of the American Chemical Society* **2020,** *142* (3), 1482-1491.

2. Xiang, H.; Cheng, J.; Ma, X.; Zhou, X.; Chruma, J. J., Near-infrared phosphorescence: materials and applications. *Chemical Society Reviews* **2013,** *42* (14), 6128-6185.

3. Piatkevich, K. D.; Subach, F. V.; Verkhusha, V. V., Engineering of bacterial phytochromes for near-infrared imaging, sensing, and light-control in mammals. *Chemical Society Reviews* **2013,** *42* (8), 3441-3452.

4. Chernov, K. G.; Redchuk, T. A.; Omelina, E. S.; Verkhusha, V. V., Near-Infrared Fluorescent Proteins, Biosensors, and Optogenetic Tools Engineered from Phytochromes. *Chemical Reviews* **2017,** *117* (9), 6423-6446.

5. Gai, L.; Mack, J.; Lu, H.; Yamada, H.; Kuzuhara, D.; Lai, G.; Li, Z.; Shen, Z., New 2,6-Distyryl-Substituted BODIPY Isomers: Synthesis, Photophysical Properties, and Theoretical Calculations. *Chemistry – A European Journal* **2014,** *20* (4), 1091-1102.

6. Verwilst, P.; Kim, H.-R.; Seo, J.; Sohn, N.-W.; Cha, S.-Y.; Kim, Y.; Maeng, S.; Shin, J.-W.; Kwak, J. H.; Kang, C.; Kim, J. S., Rational Design of in Vivo Tau Tangle-Selective Near-Infrared Fluorophores: Expanding the BODIPY Universe. *Journal of the American Chemical Society* **2017,** *139* (38), 13393-13403.

7. Burghart, A.; Kim, H.; Welch, M. B.; Thoresen, L. H.; Reibenspies, J.; Burgess, K.; Bergström, F.; Johansson, L. B. Å., 3,5-Diaryl-4,4-difluoro-4-bora-3a,4a-diaza-s-indacene (BODIPY) Dyes: Synthesis, Spectroscopic, Electrochemical, and Structural Properties. *The Journal of Organic Chemistry* **1999,** *64* (21), 7813-7819.

8. Jean-Gérard, L.; Vasseur, W.; Scherninski, F.; Andrioletti, B., Recent advances in the synthesis of [a]-benzo-fused BODIPY fluorophores. *Chemical Communications* **2018,** *54* (92), 12914-12929.

9. Ulrich, G.; Goeb, S.; De Nicola, A.; Retailleau, P.; Ziessel, R., Synthesis of Bisisoindolomethene Dyes Bearing Anisole or Ethylthiophene Residues for Red and Near-IR Fluorescence. *Synlett* **2007,** *2007* (10), 1517-1520.

10. Pezzella, A.; Napolitano, A.; dIschia, M.; Prota, G., Oxidative polymerisation of 5,6-dihydroxyindole-2-carboxylic acid to melanin: A new insight. *Tetrahedron* **1996,** *52* (23), 7913-7920.

11. Ito, S.; Nicol, J. A. C., Isolation of oligomers of 5,6-dihydroxyindole-2-carboxylic acid from the eye of the catfish. *Biochemical Journal* **1974,** *143* (1), 207-217.

Appendix:

^{1}H and ^{13}C NMR Spectra Relevant to **Chapter 2**

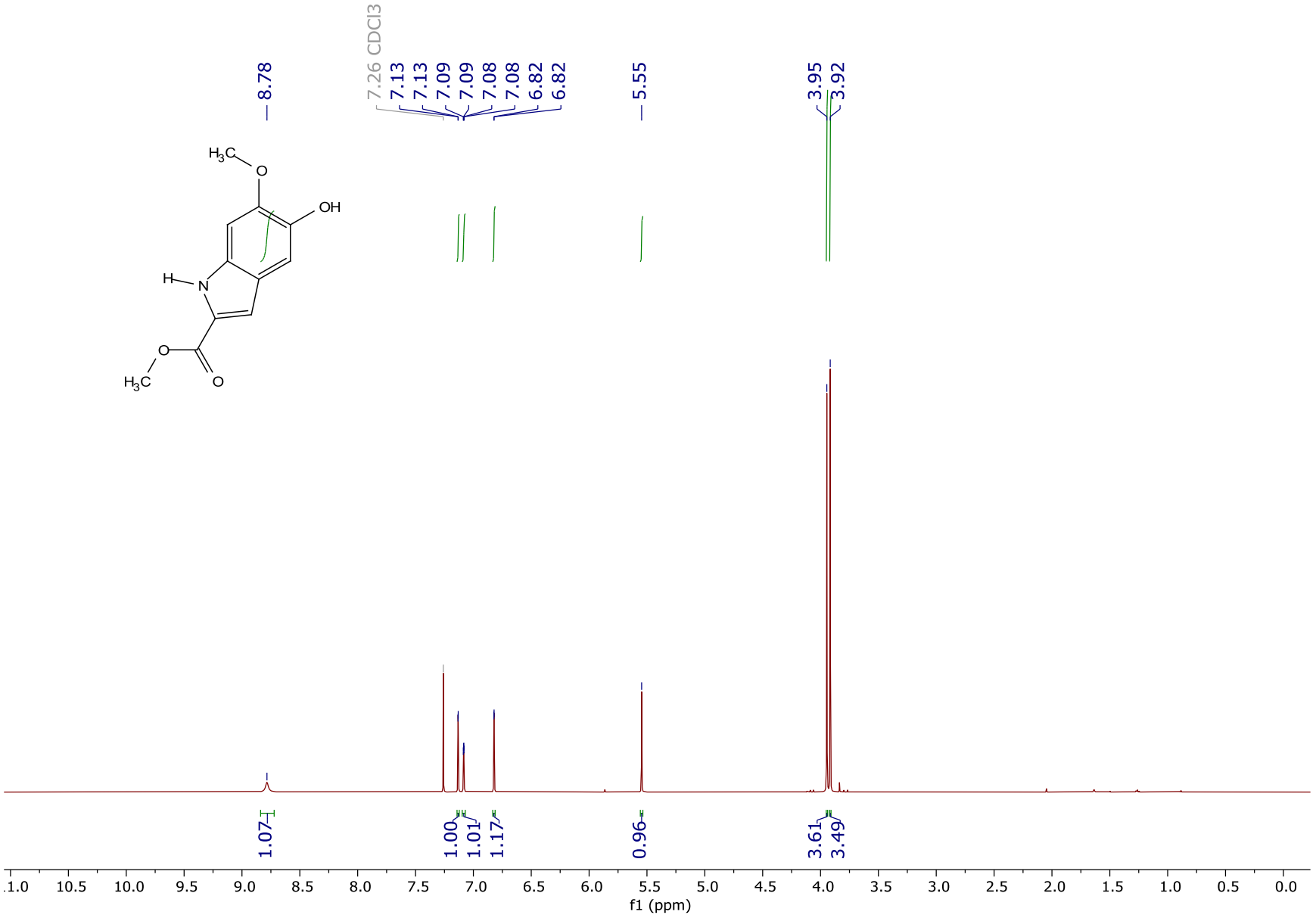
8.78
7.26 CDCl3
7.13
7.13
7.09
7.09
7.08
7.08
6.82
6.82
5.55
3.95
3.92
H3C
O
OH
H
N
O
H3C
O
1.07
1.00
1.01
1.17
0.96
3.61
3.49
f1 (ppm)

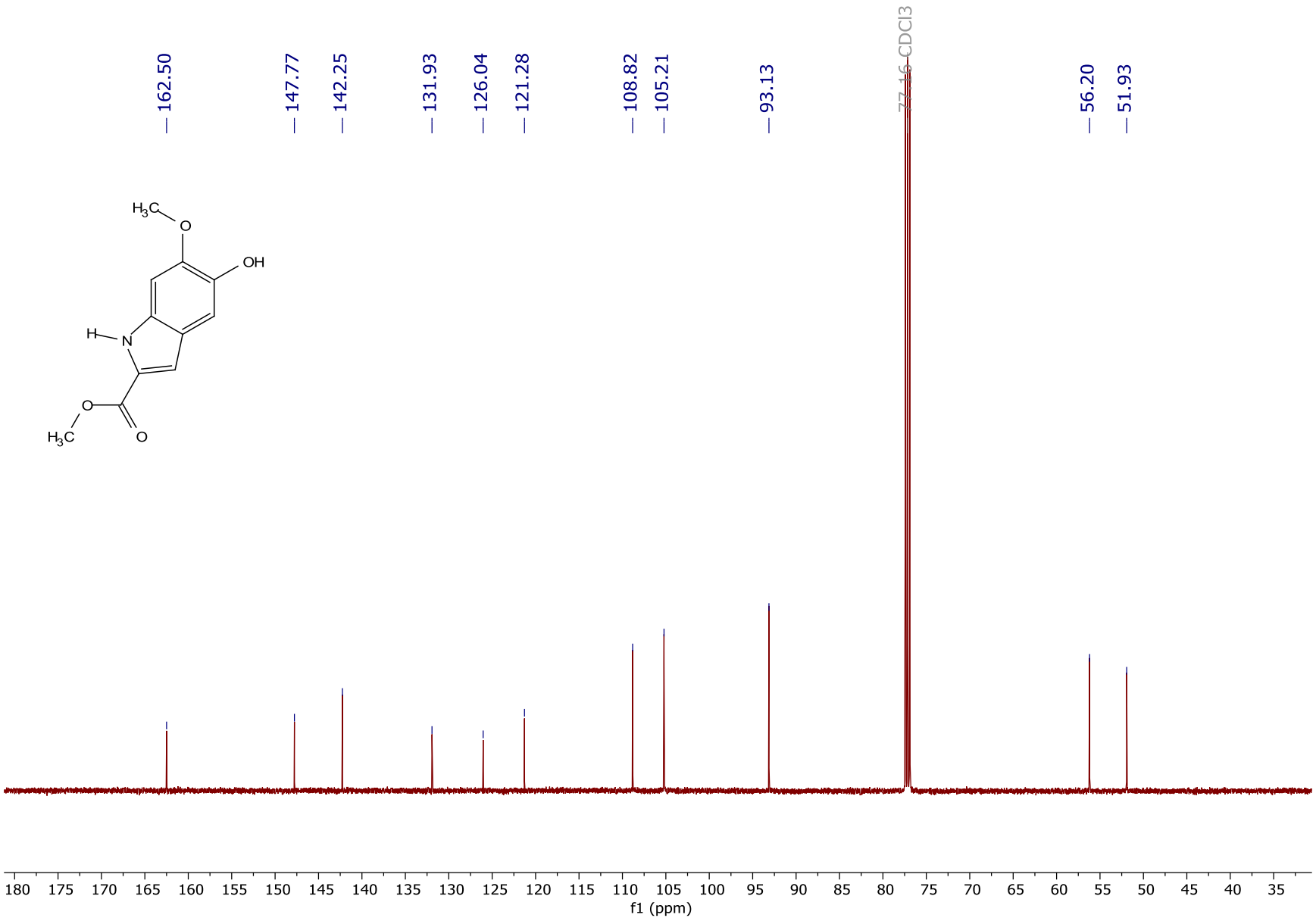
162.50
147.77
142.25
131.93
126.04
121.28
108.82
105.21
93.13
77.16 CDCl3
56.20
51.93
H3C
O
OH
H
N
O
H3C
O
180 175 170 165 160 155 150 145 140 135 130 125 120 115 110 105 100 95 90 85 80 75 70 65 60 55 50 45 40 35
f1 (ppm)

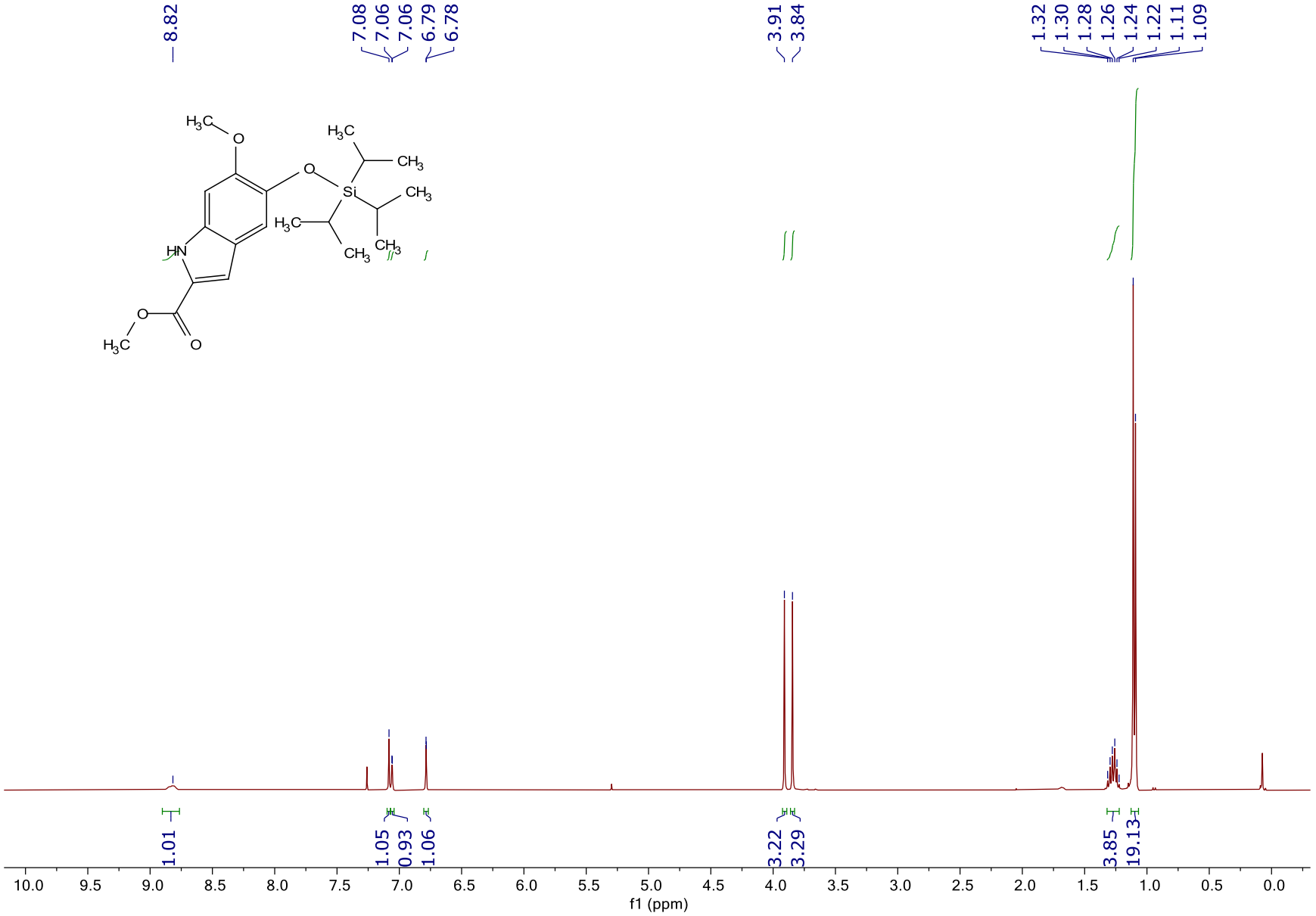
8.82
7.08
7.06
7.06
6.79
6.78
3.91
3.84
1.32
1.30
1.28
1.26
1.24
1.22
1.11
1.09
H3C
O
O
Si
CH3
H3C
CH3
H3C
CH3
CH3
HN
O
H3C
O
1.01
1.05
0.93
1.06
3.22
3.29
3.85
19.13
10.0
9.5
9.0
8.5
8.0
7.5
7.0
6.5
6.0
5.5
5.0
4.5
4.0
3.5
3.0
2.5
2.0
1.5
1.0
0.5
0.0
f1 (ppm)

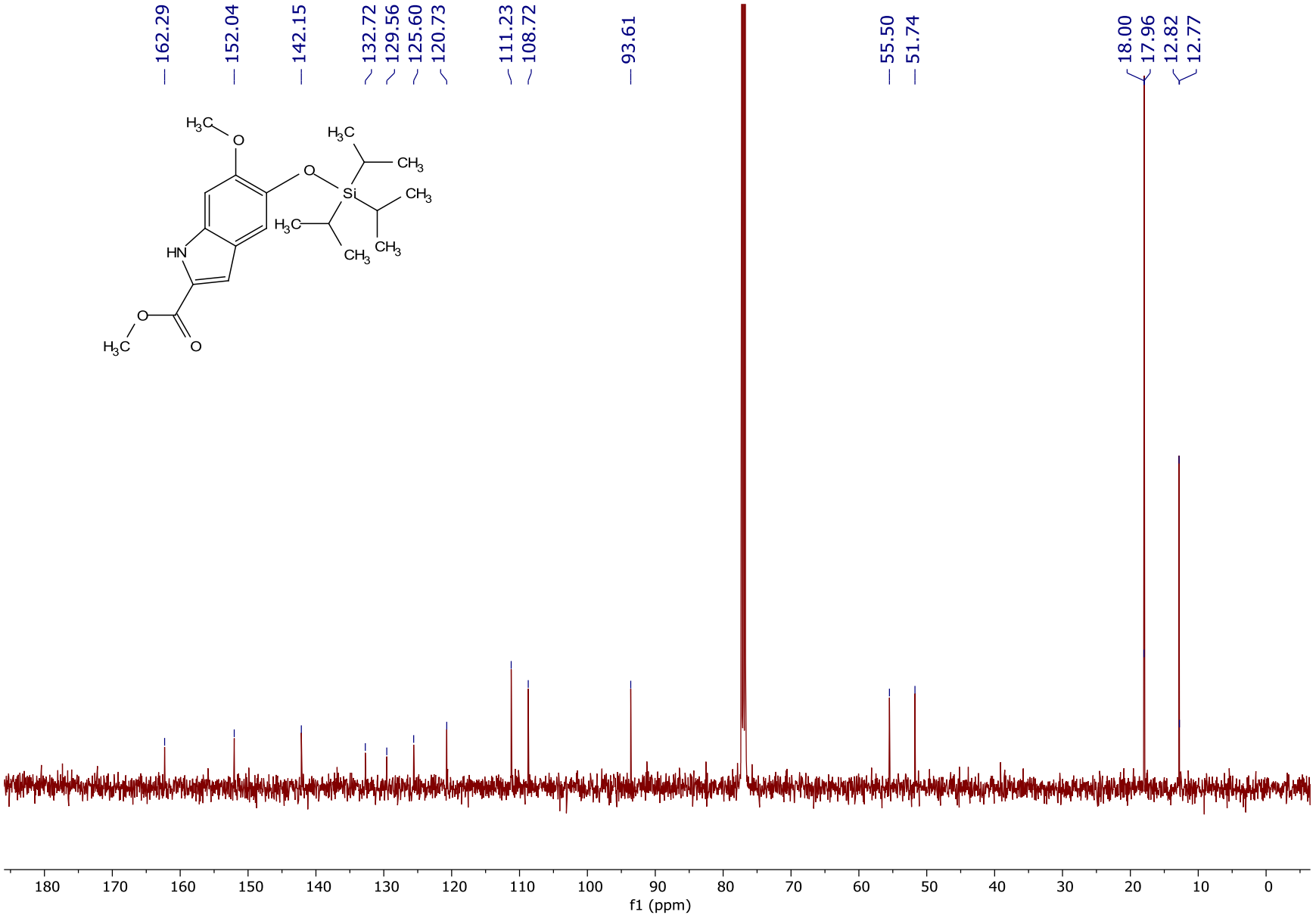
162.29
152.04
142.15
132.72
129.56
125.60
120.73
111.23
108.72
93.61
55.50
51.74
18.00
17.96
12.82
12.77
H3C
O
O
Si
H3C
CH3
CH3
H3C
CH3
CH3
HN
O
H3C
O
180
170
160
150
140
130
120
110
100
90
80
70
60
50
40
30
20
10
0
f1 (ppm)

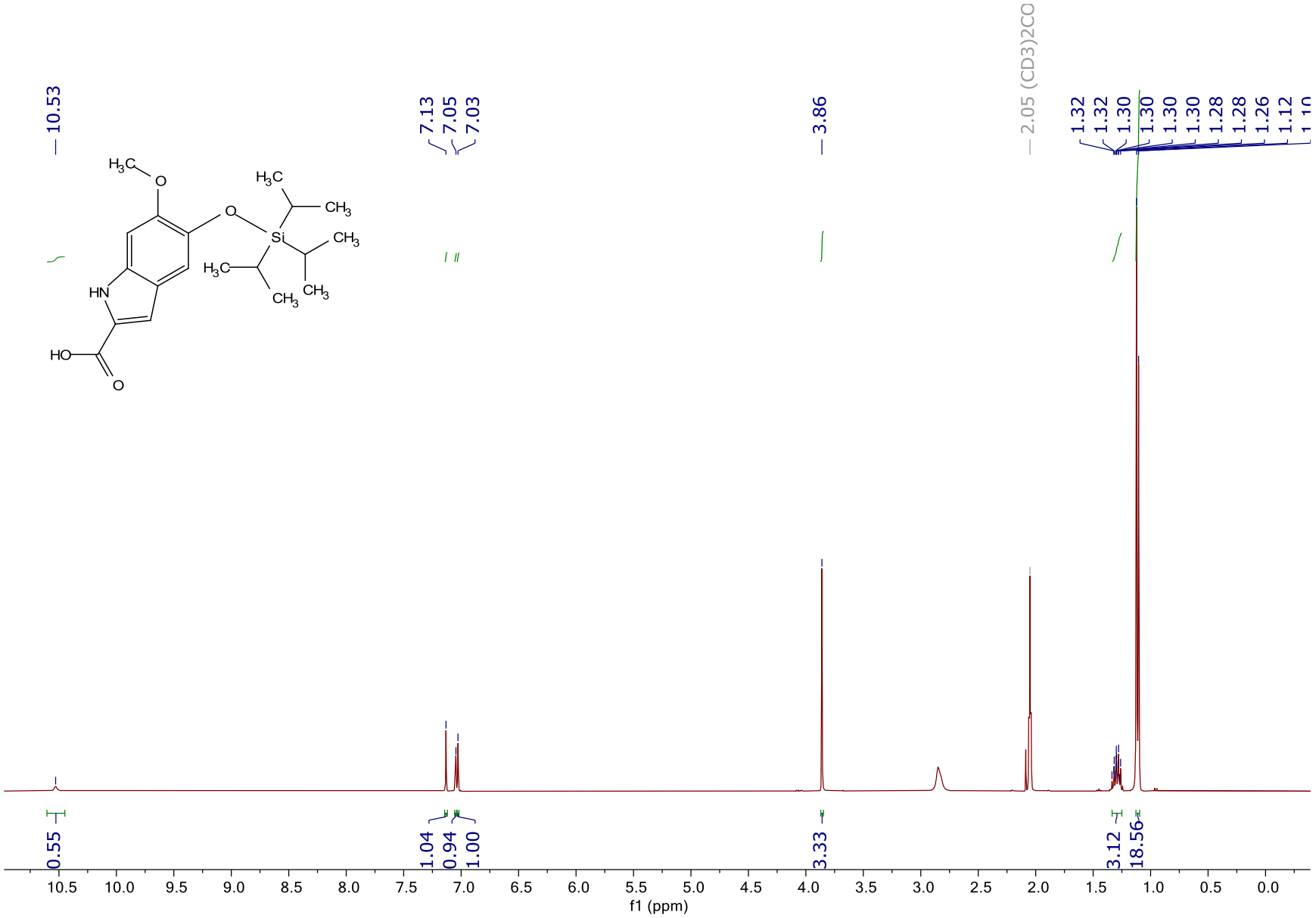
10.53
7.13
7.05
7.03
3.86
2.05 (CD3)2CO
1.32
1.32
1.30
1.30
1.30
1.30
1.28
1.28
1.26
1.12
0.55
1.04
0.94
1.00
3.33
3.12
18.56
f1 (ppm)

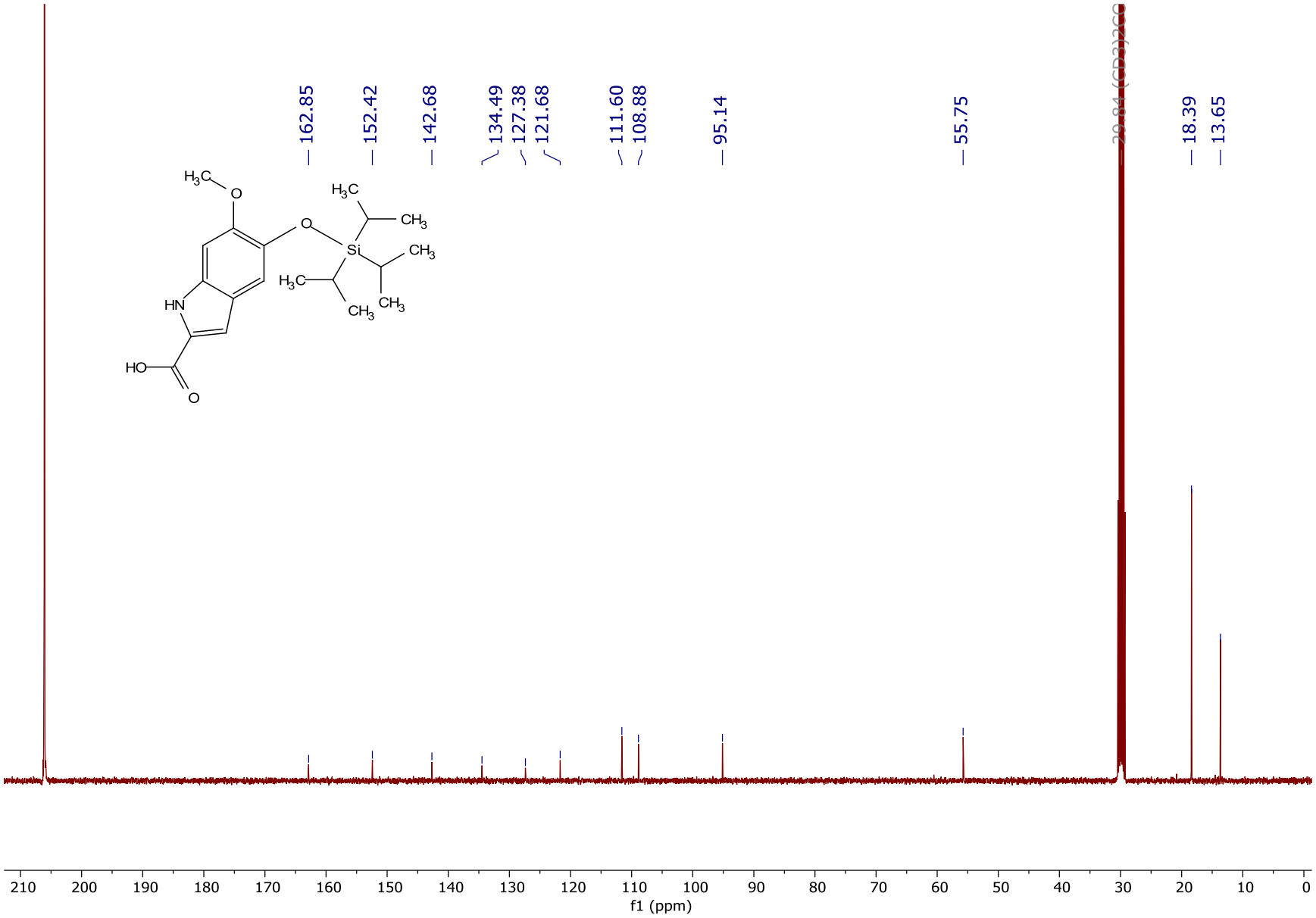
162.85
152.42
142.68
134.49
127.38
121.68
111.60
108.88
95.14
55.75
29.84
18.39
13.65
H3C
O
O
Si
CH3
HN
HO
O
210 200 190 180 170 160 150 140 130 120 110 100 90 80 70 60 50 40 30 20 10 0
f1 (ppm)

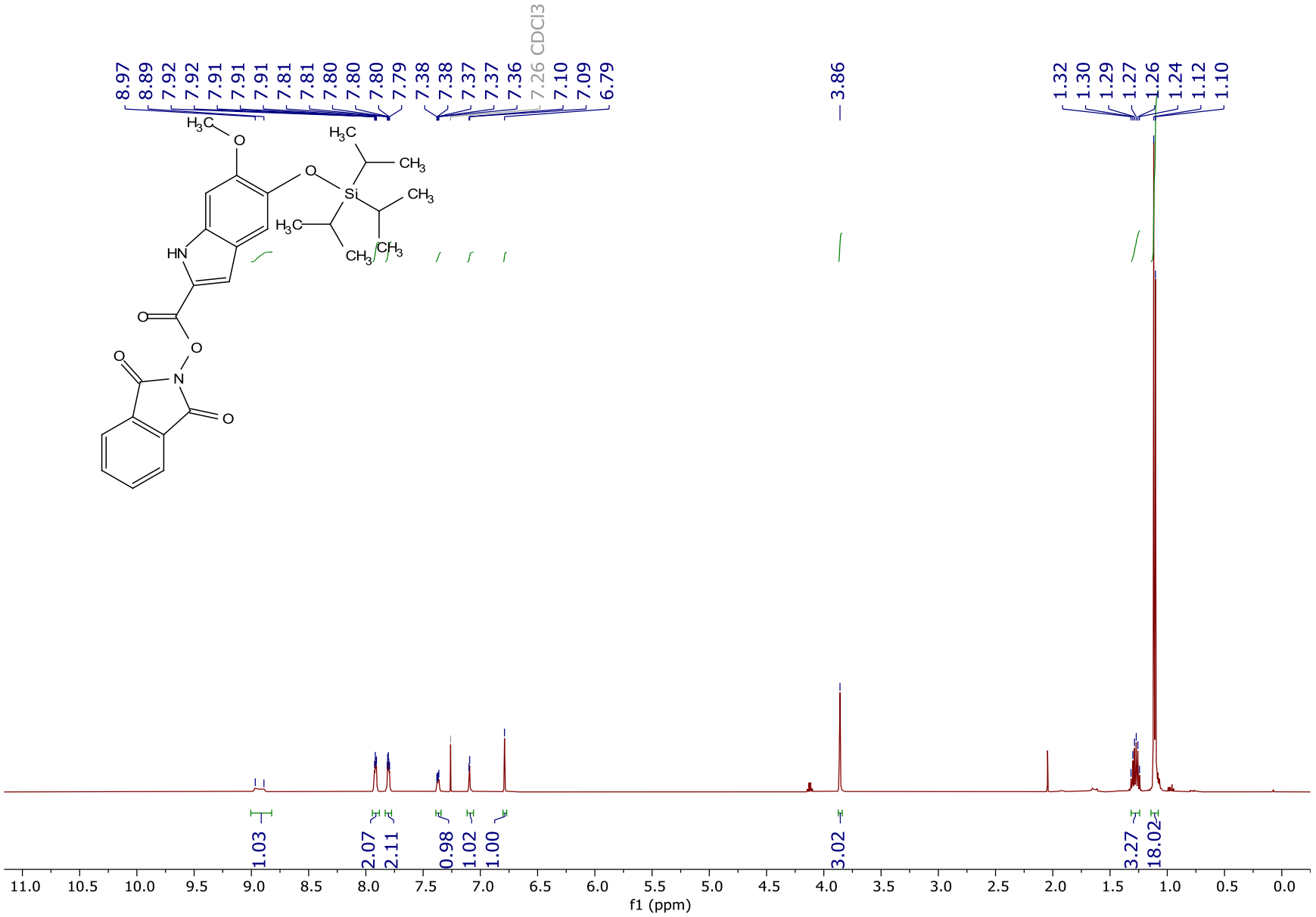
8.97
8.89
7.92
7.92
7.91
7.91
7.91
7.81
7.81
7.80
7.80
7.80
7.79
7.38
7.38
7.37
7.37
7.36
7.26 CDCl3
7.10
7.09
6.79
3.86
1.32
1.30
1.29
1.27
1.26
1.24
1.12
1.10
1.03
2.07
2.11
0.98
1.02
1.00
3.02
3.27
18.02
f1 (ppm)

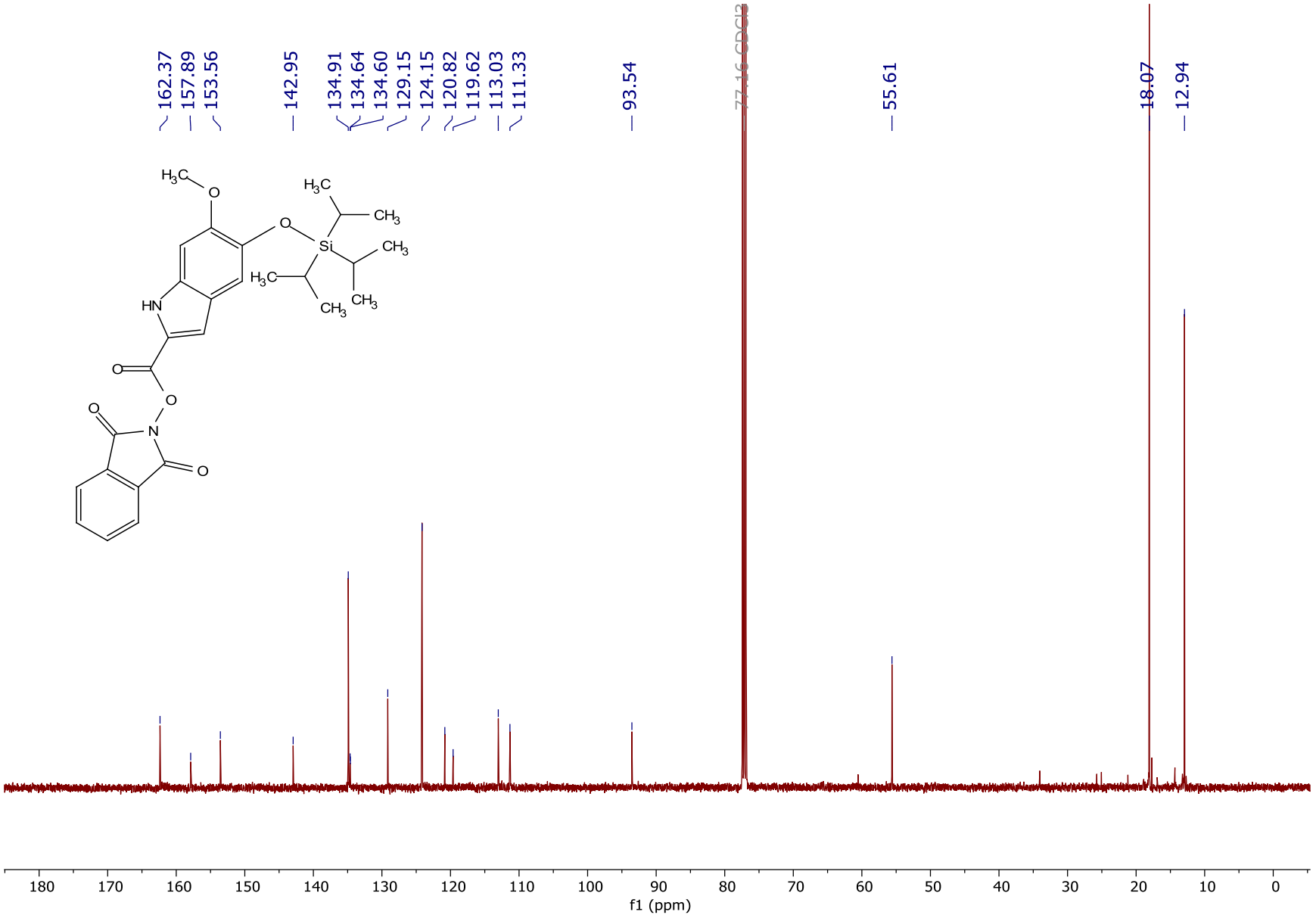
162.37
157.89
153.56
142.95
134.91
134.64
134.60
129.15
124.15
120.82
119.62
113.03
111.33
93.54
77.16 CDCl3
55.61
18.07
12.94
H3C
O
O
Si
CH3
H3C
CH3
CH3
H3C
CH3
HN
O
O
O
N
O
180
170
160
150
140
130
120
110
100
90
80
70
60
50
40
30
20
10
0
f1 (ppm)

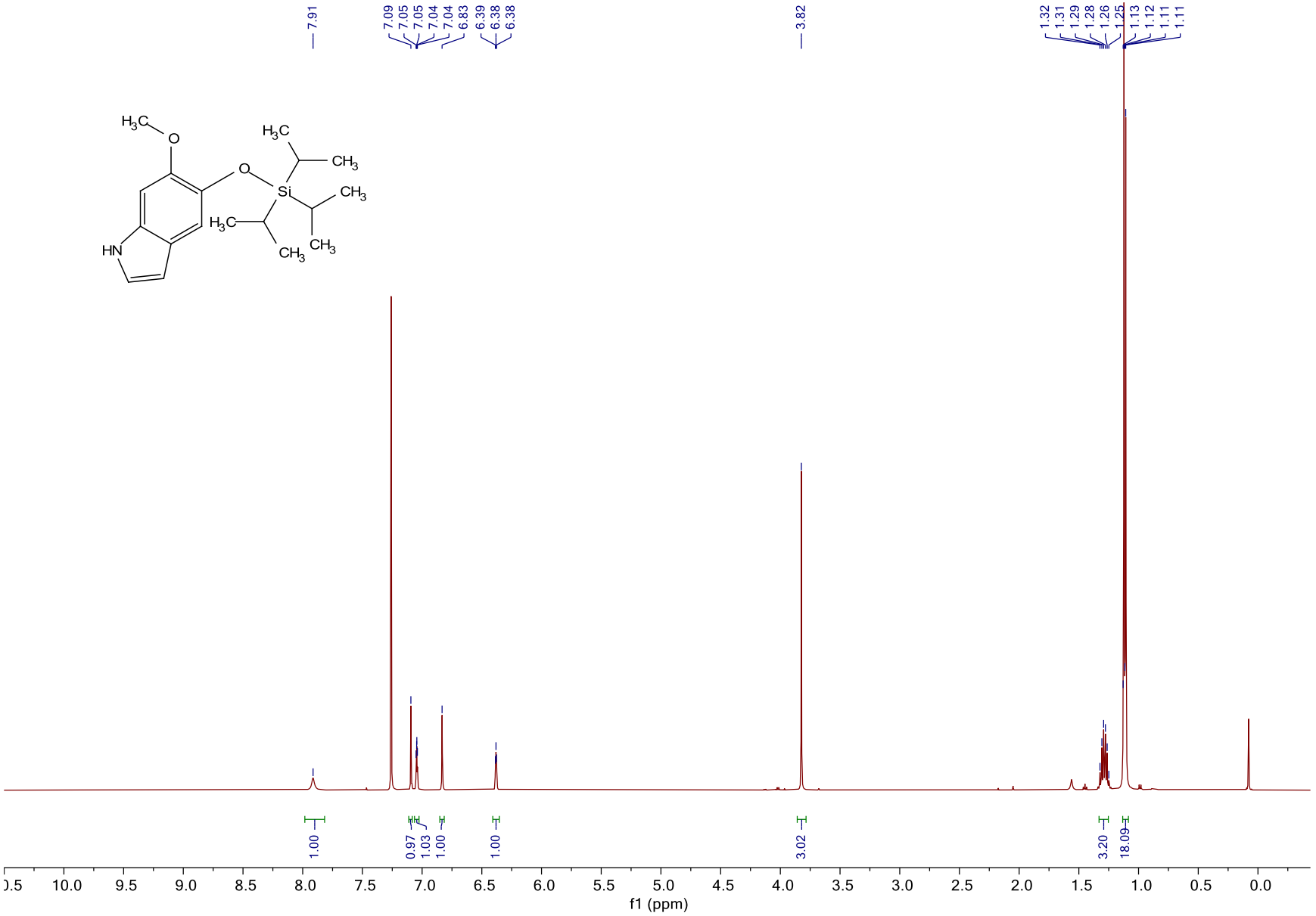
7.91
7.09
7.05
7.05
7.04
7.04
6.83
6.39
6.38
6.38
3.82
1.32
1.31
1.29
1.28
1.26
1.25
1.13
1.12
1.11
1.11
H3C
O
H3C
CH3
O
Si
CH3
H3C
CH3
CH3
HN
1.00
0.97
1.03
1.00
1.00
3.02
3.20
18.09
f1 (ppm)

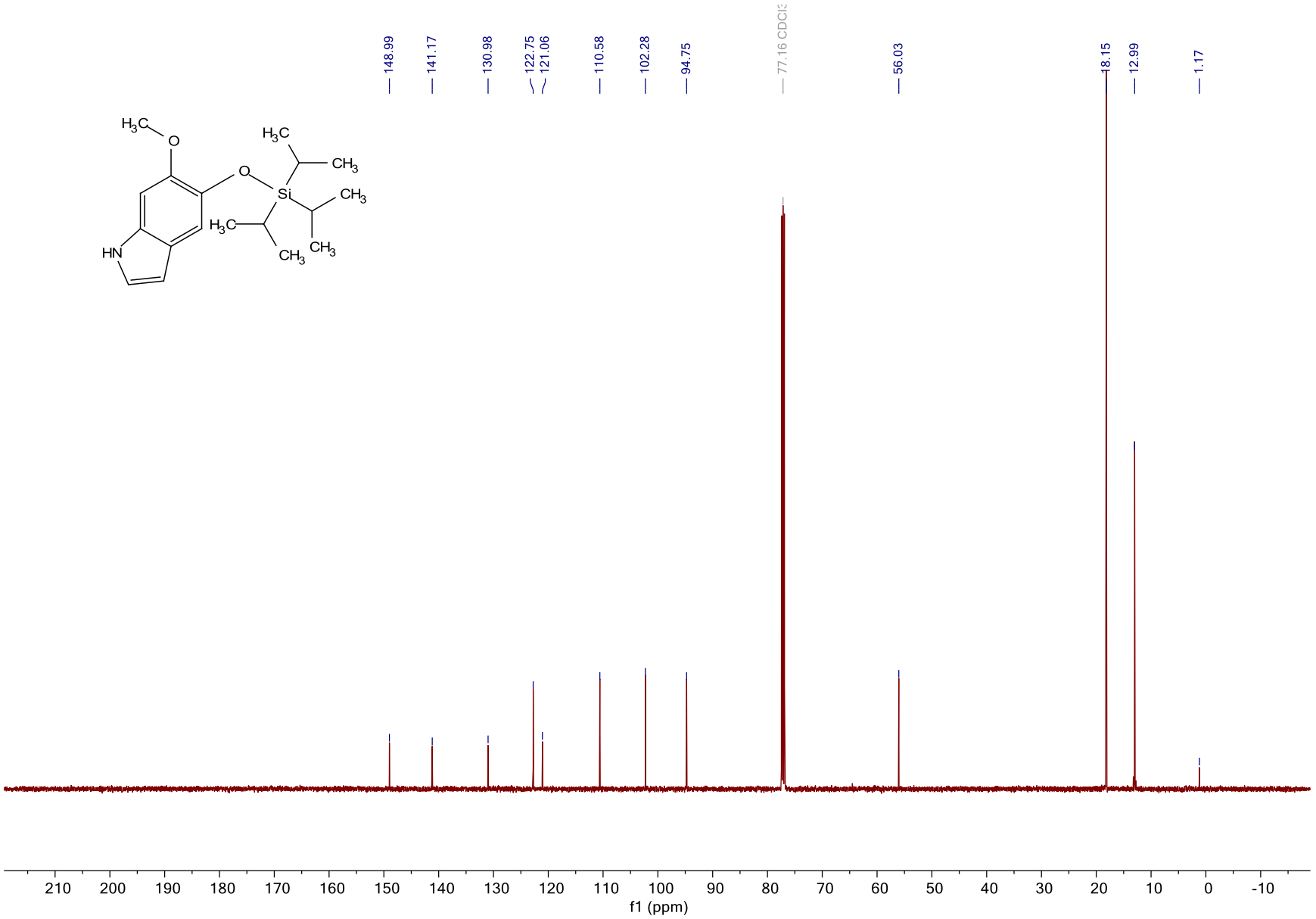
148.99
141.17
130.98
122.75
121.06
110.58
102.28
94.75
77.16 CDCl3
56.03
18.15
12.99
1.17
H3C
O
O
Si
H3C
CH3
CH3
H3C
CH3
CH3
HN
210 200 190 180 170 160 150 140 130 120 110 100 90 80 70 60 50 40 30 20 10 0 -10
f1 (ppm)

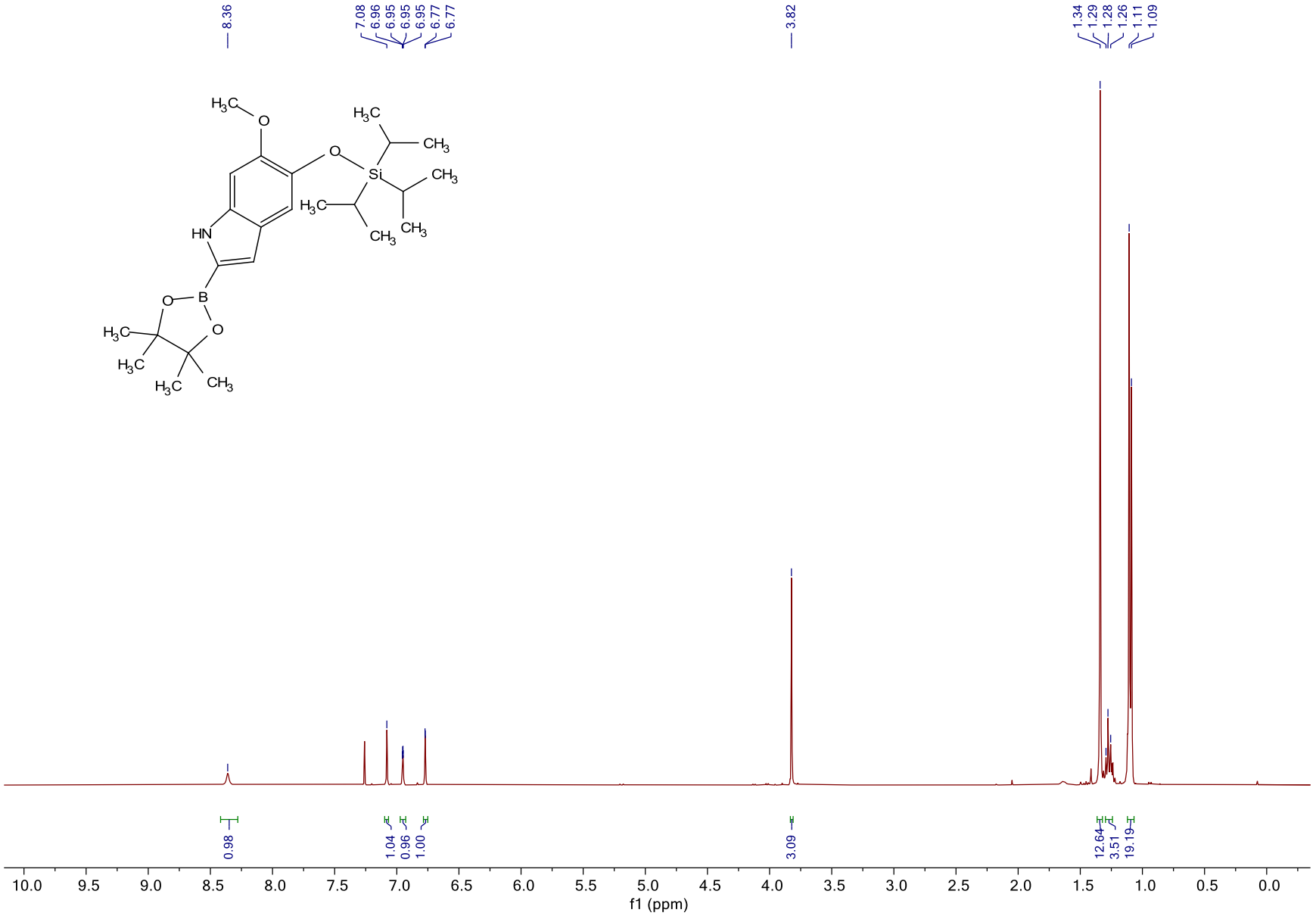
8.36
7.08
6.96
6.95
6.95
6.95
6.77
6.77
3.82
1.34
1.29
1.28
1.26
1.11
1.09
0.98
1.04
0.96
1.00
3.09
12.64
3.51
19.19
f1 (ppm)

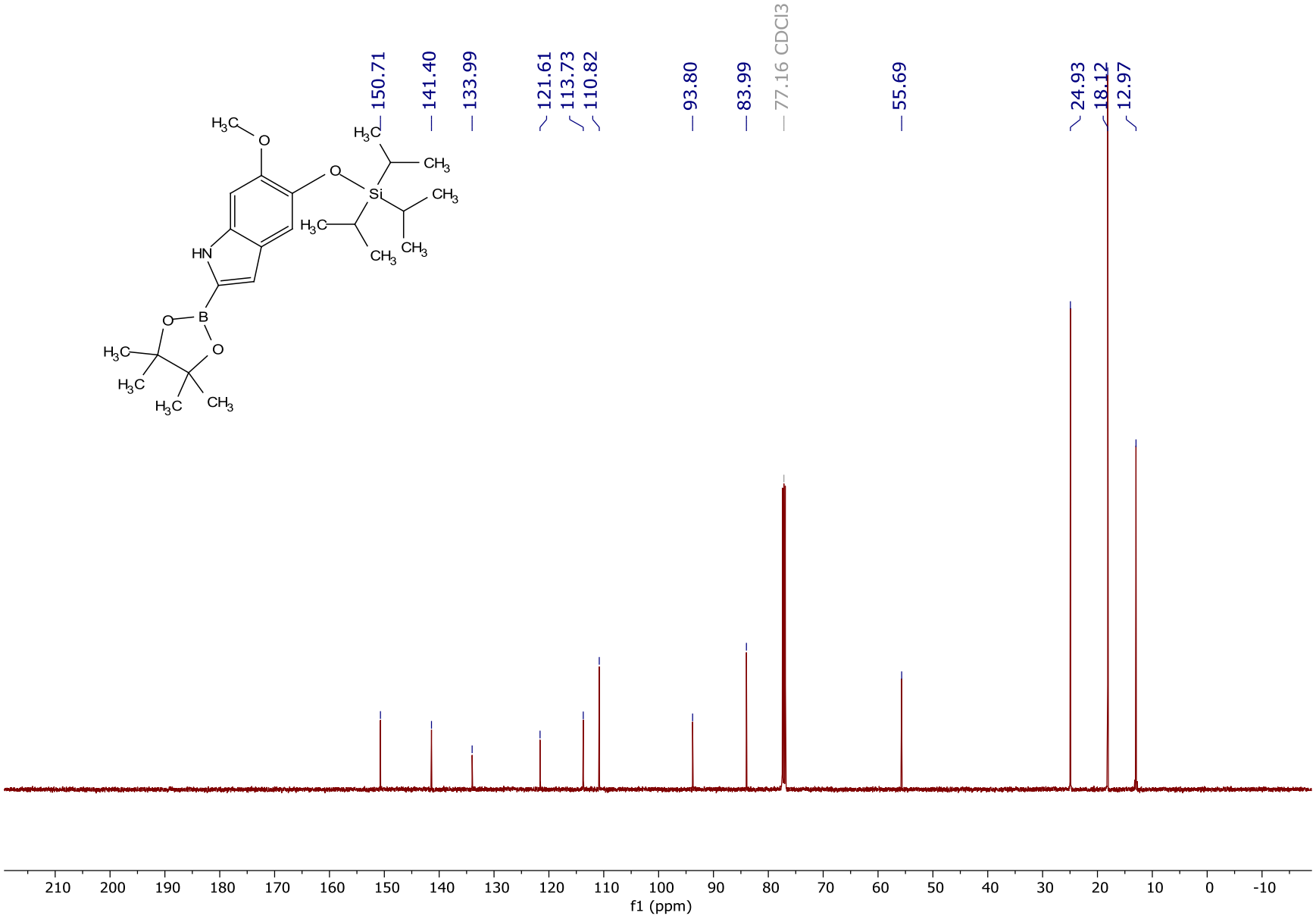
150.71
141.40
133.99
121.61
113.73
110.82
93.80
83.99
77.16 CDCl3
55.69
24.93
18.12
12.97
f1 (ppm)

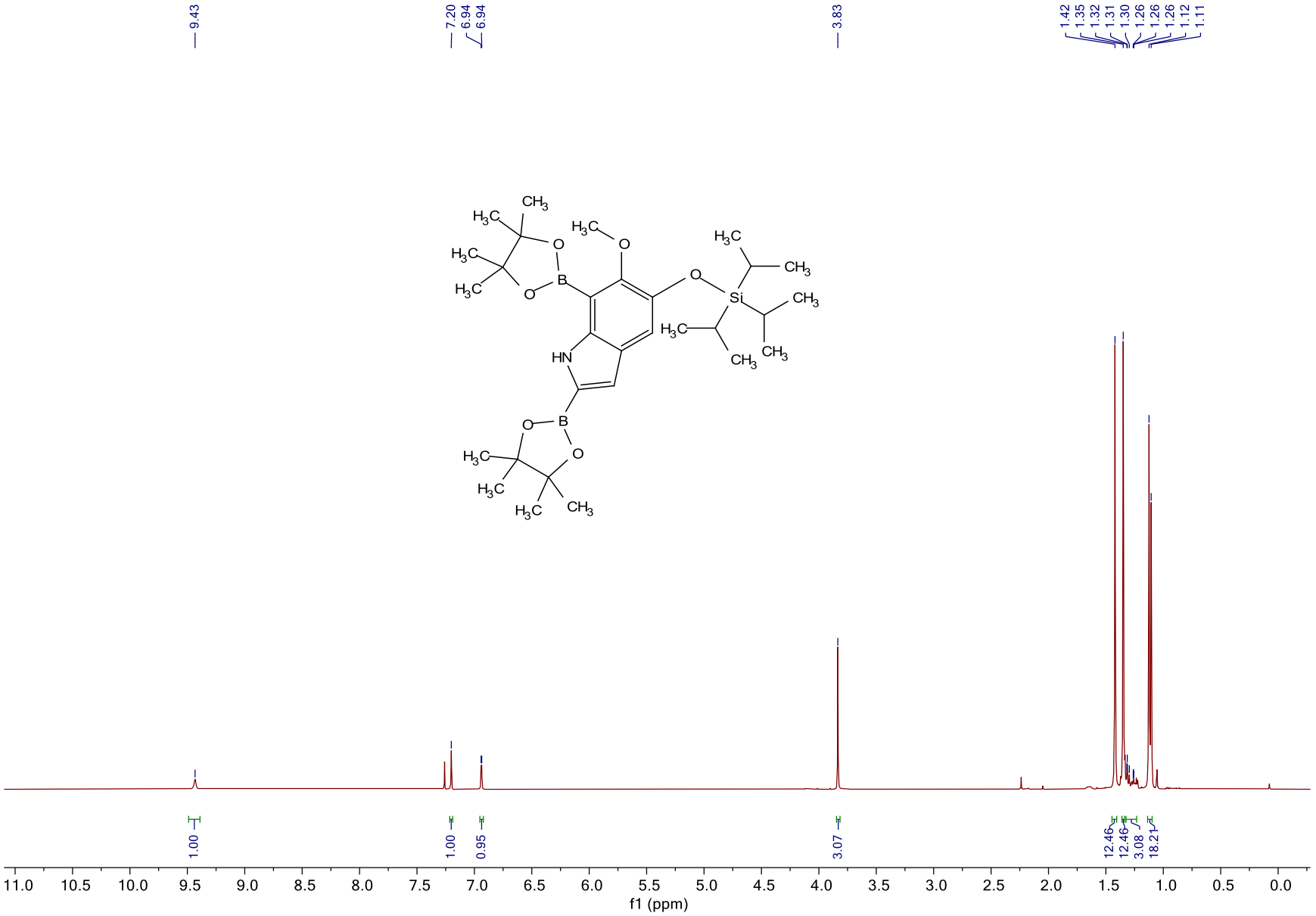
9.43
7.20
6.94
6.94
3.83
1.42
1.35
1.32
1.31
1.30
1.26
1.26
1.26
1.12
1.11
1.00
1.00
0.95
3.07
12.46
12.46
3.08
18.21
11.0
10.5
10.0
9.5
9.0
8.5
8.0
7.5
7.0
6.5
6.0
5.5
5.0
4.5
4.0
3.5
3.0
2.5
2.0
1.5
1.0
0.5
0.0
f1 (ppm)

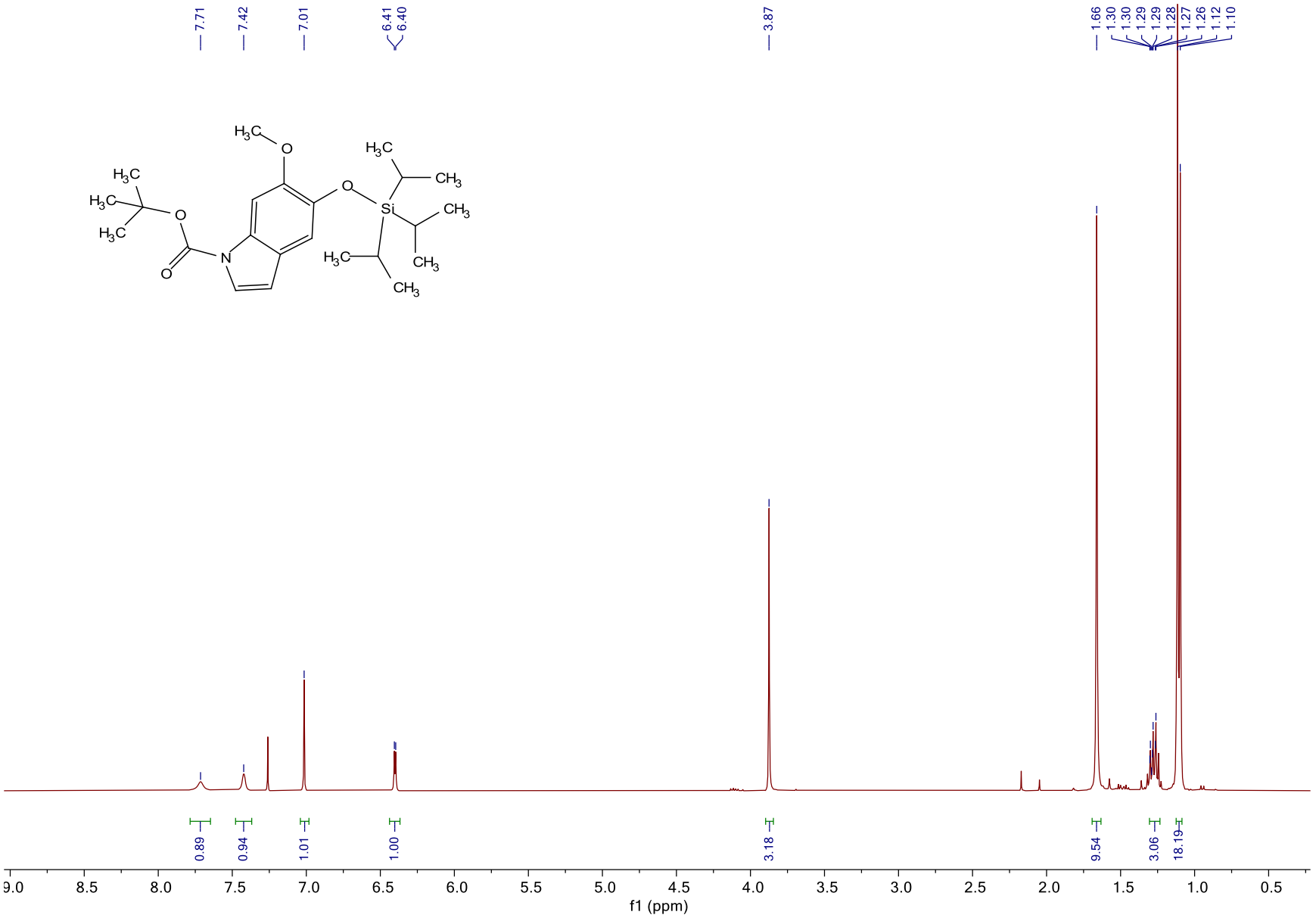
7.71
7.42
7.01
6.41
6.40
3.87
1.66
1.30
1.30
1.29
1.29
1.28
1.27
1.26
1.12
1.10
0.89
0.94
1.01
1.00
3.18
9.54
3.06
18.19
f1 (ppm)

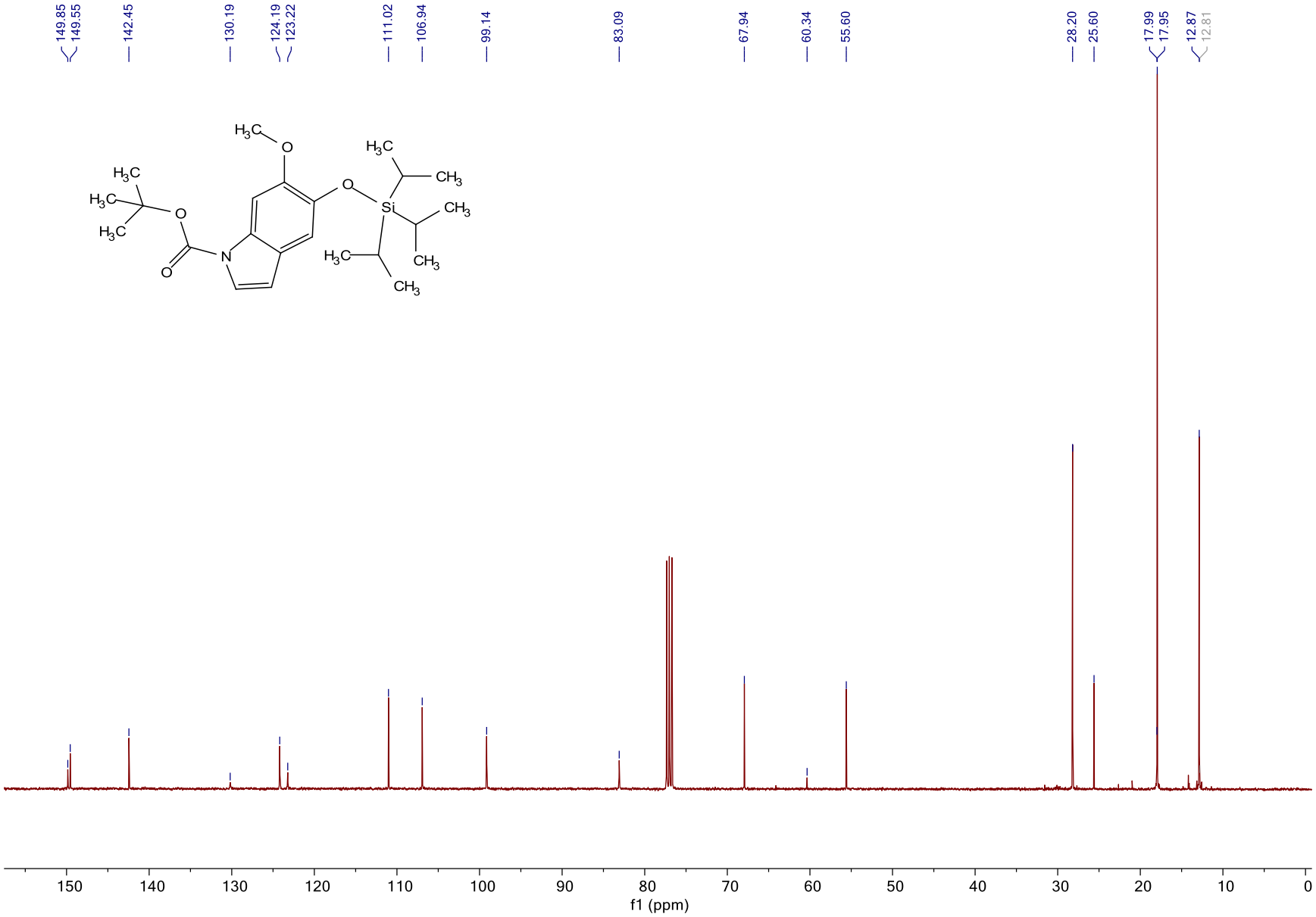
149.85
149.55
142.45
130.19
124.19
123.22
111.02
106.94
99.14
83.09
67.94
60.34
55.60
28.20
25.60
17.99
17.95
12.87
12.81
H3C
O
H3C
CH3
O
Si
CH3
H3C
CH3
H3C
O
H3C
O
N
CH3
150
140
130
120
110
100
90
80
70
60
50
40
30
20
10
0
f1 (ppm)

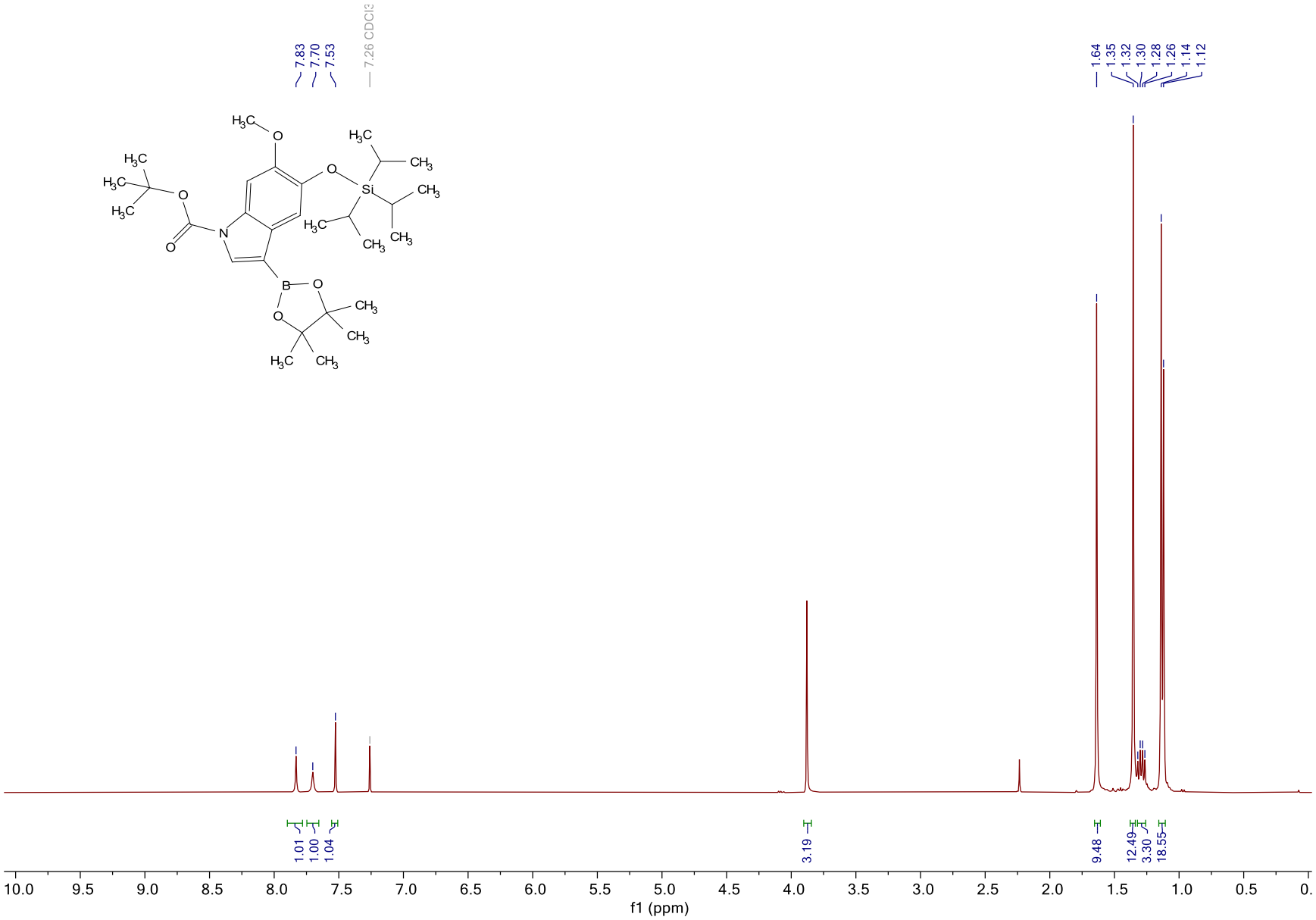
7.83
7.70
7.53
7.26 CDCl3
1.64
1.35
1.32
1.30
1.28
1.26
1.14
1.12
1.01
1.00
1.04
3.19
9.48
12.49
3.30
18.55
f1 (ppm)

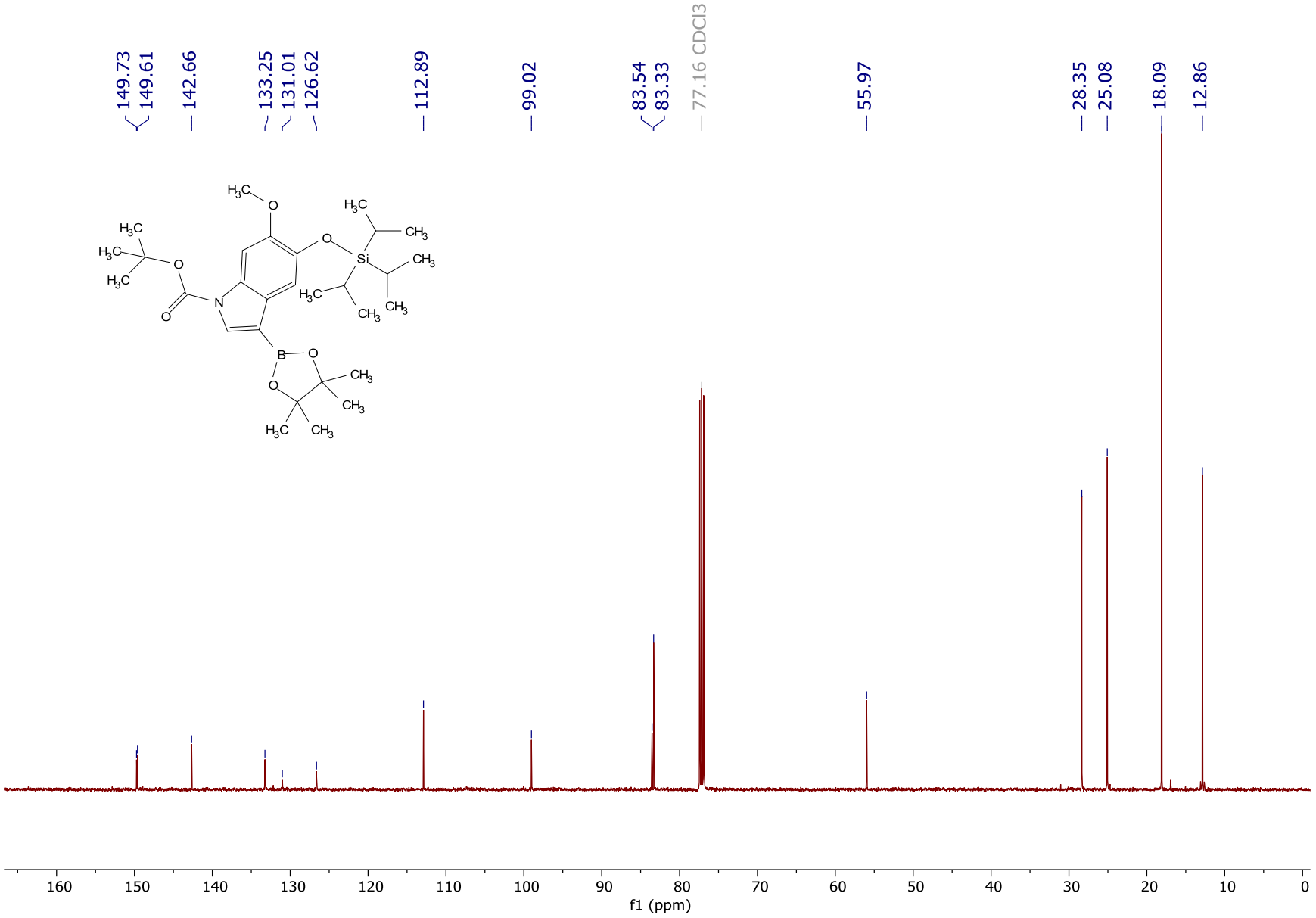
149.73
149.61
142.66
133.25
131.01
126.62
112.89
99.02
83.54
83.33
77.16 CDCl3
55.97
28.35
25.08
18.09
12.86
160
150
140
130
120
110
100
90
80
70
60
50
40
30
20
10
0
f1 (ppm)

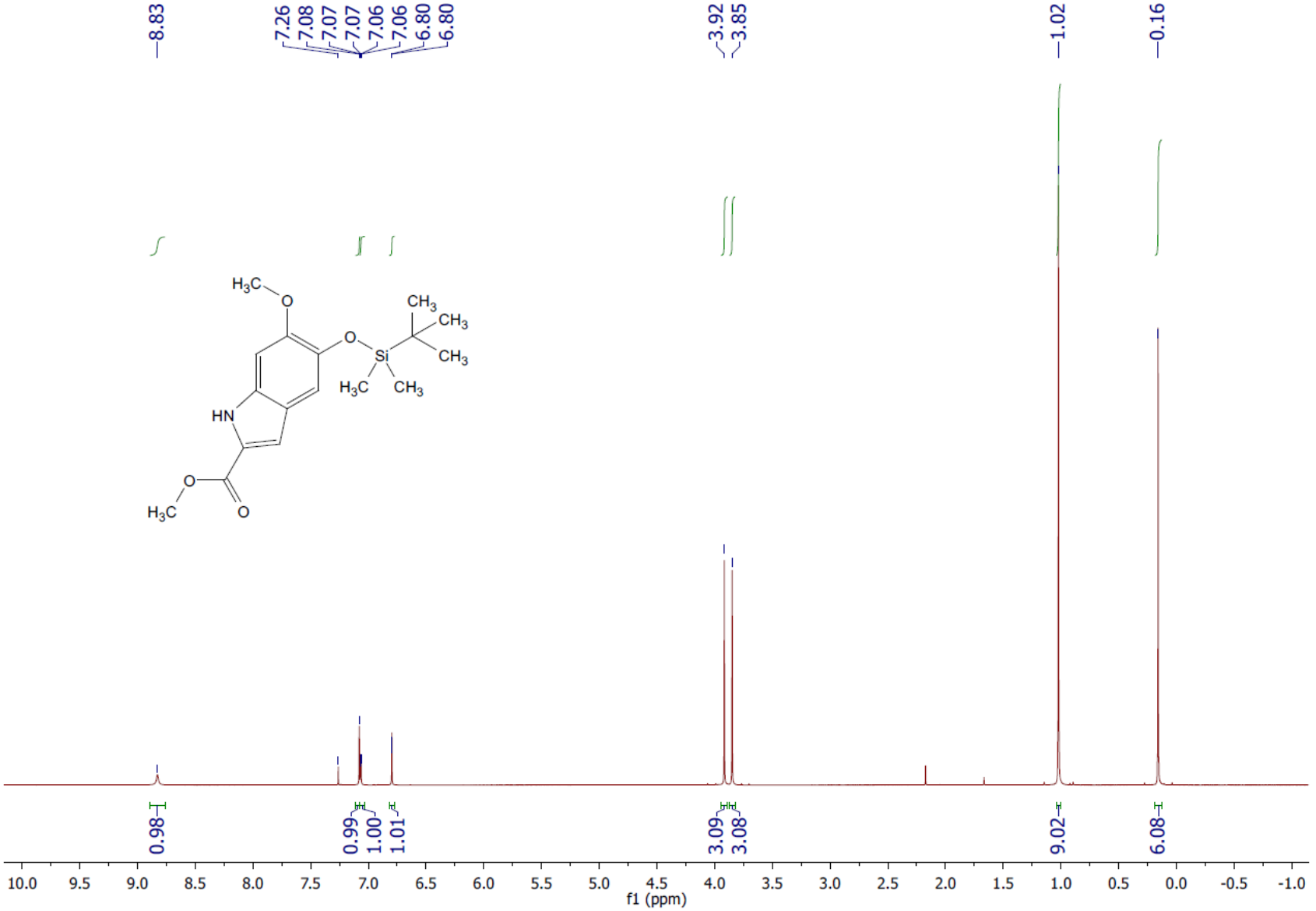
8.83
7.26
7.08
7.07
7.07
7.06
7.06
6.80
6.80
3.92
3.85
1.02
0.16
H3C
O
CH3
CH3
CH3
O
Si
H3C
CH3
HN
O
H3C
O
0.98
0.99
1.00
1.01
3.09
3.08
9.02
6.08
10.0
9.5
9.0
8.5
8.0
7.5
7.0
6.5
6.0
5.5
5.0
4.5
4.0
3.5
3.0
2.5
2.0
1.5
1.0
0.5
0.0
-0.5
-1.0
f1 (ppm)

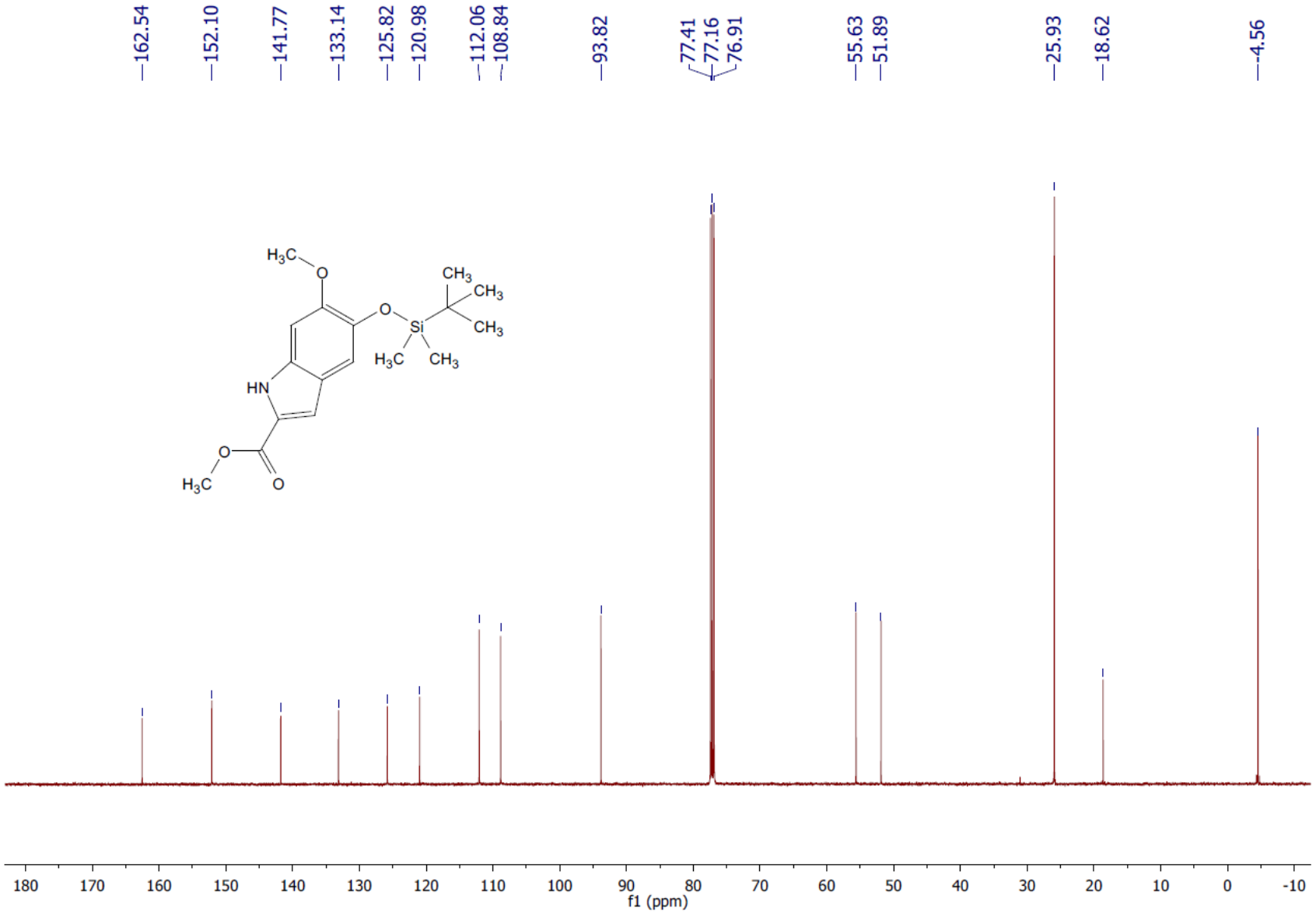
162.54
152.10
141.77
133.14
125.82
120.98
112.06
108.84
93.82
77.41
77.16
76.91
55.63
51.89
25.93
18.62
-4.56
H3C
O
CH3
CH3
CH3
O
Si
H3C
CH3
HN
O
H3C
O
180
170
160
150
140
130
120
110
100
90
80
70
60
50
40
30
20
10
0
-10
f1 (ppm)

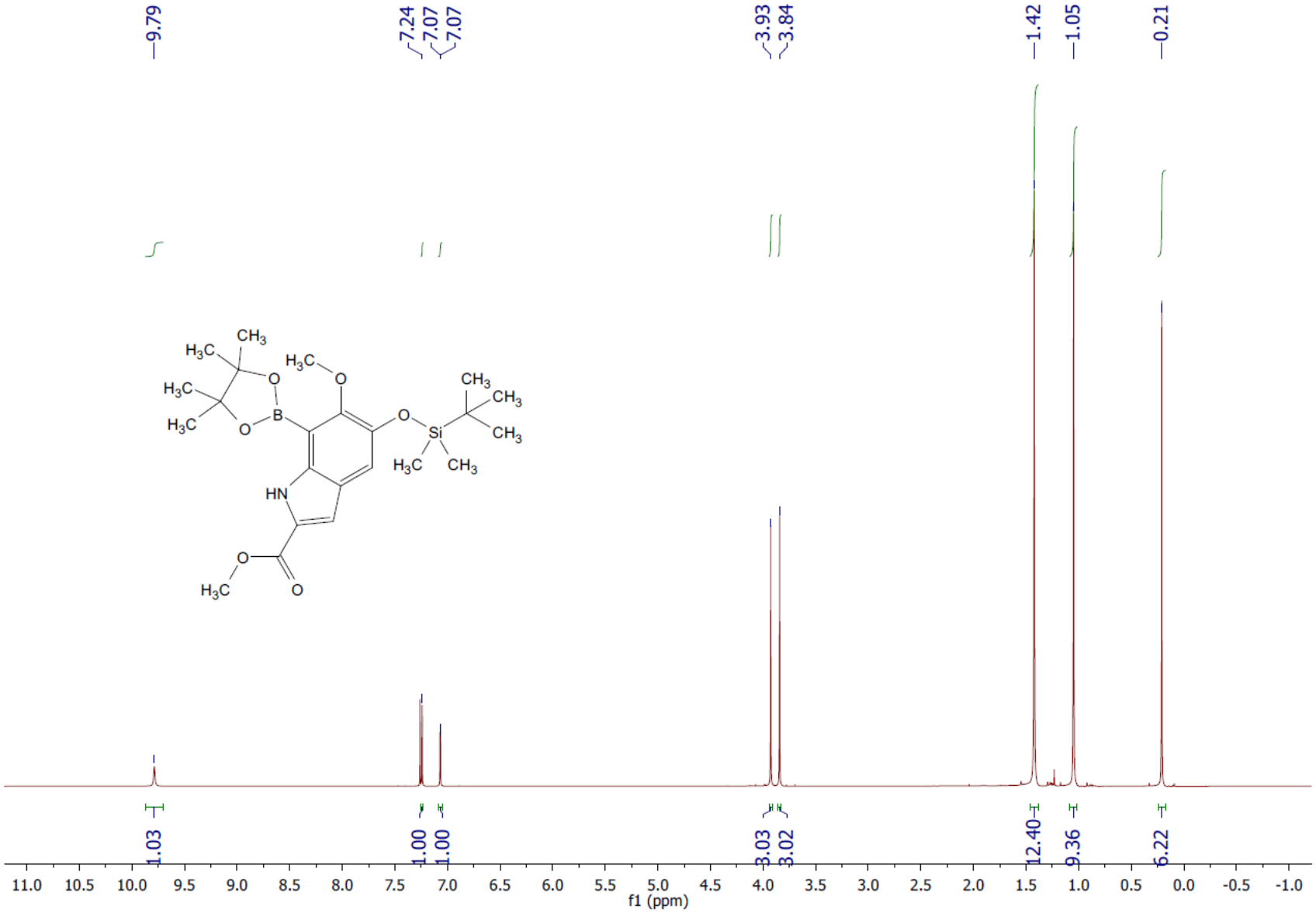
9.79
7.24
7.07
7.07
3.93
3.84
1.42
1.05
0.21
1.03
1.00
1.00
3.03
3.02
12.40
9.36
6.22
f1 (ppm)

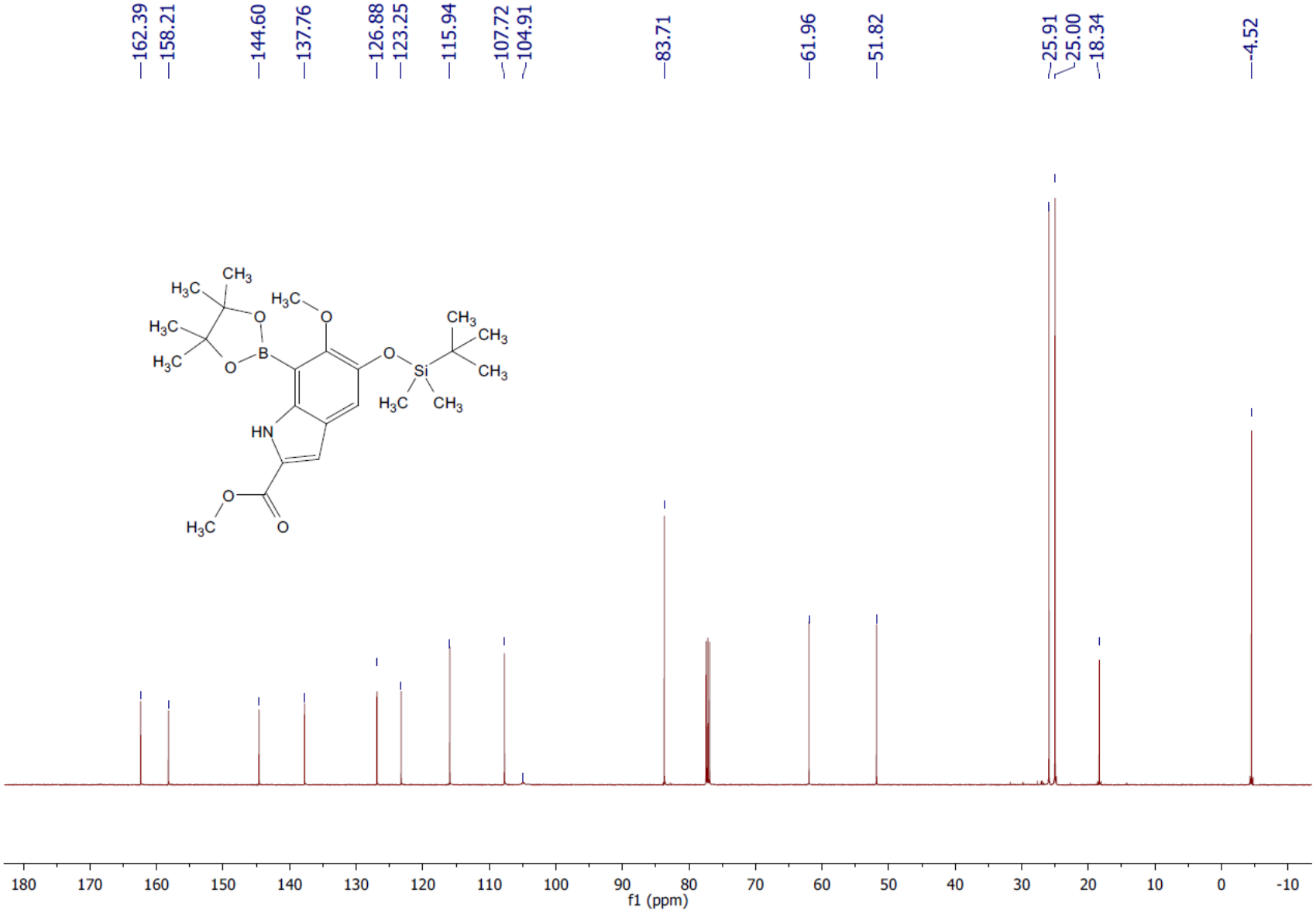
162.39
158.21
144.60
137.76
126.88
123.25
115.94
107.72
104.91
83.71
61.96
51.82
25.91
25.00
18.34
-4.52
H3C
CH3
O
B
Si
HN
180
170
160
150
140
130
120
110
100
90
80
70
60
50
40
30
20
10
0
-10
f1 (ppm)

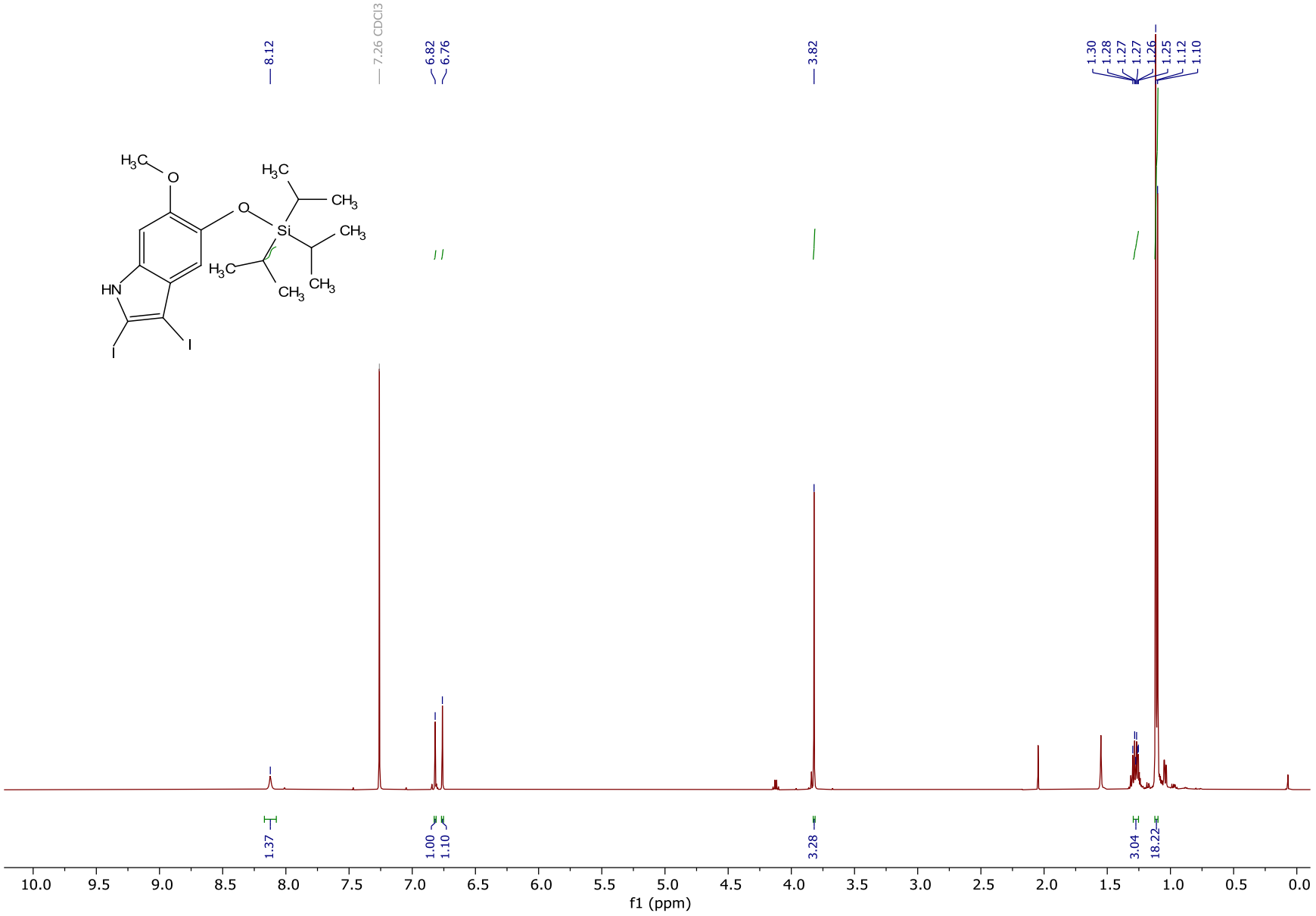
8.12
7.26 CDCl3
6.82
6.76
3.82
1.30
1.28
1.27
1.26
1.25
1.12
1.10
H3C
O
O
Si
CH3
H3C
CH3
H3C
CH3
CH3
HN
I
I
1.37
1.00
1.10
3.28
3.04
18.22
10.0 9.5 9.0 8.5 8.0 7.5 7.0 6.5 6.0 5.5 5.0 4.5 4.0 3.5 3.0 2.5 2.0 1.5 1.0 0.5 0.0
f1 (ppm)

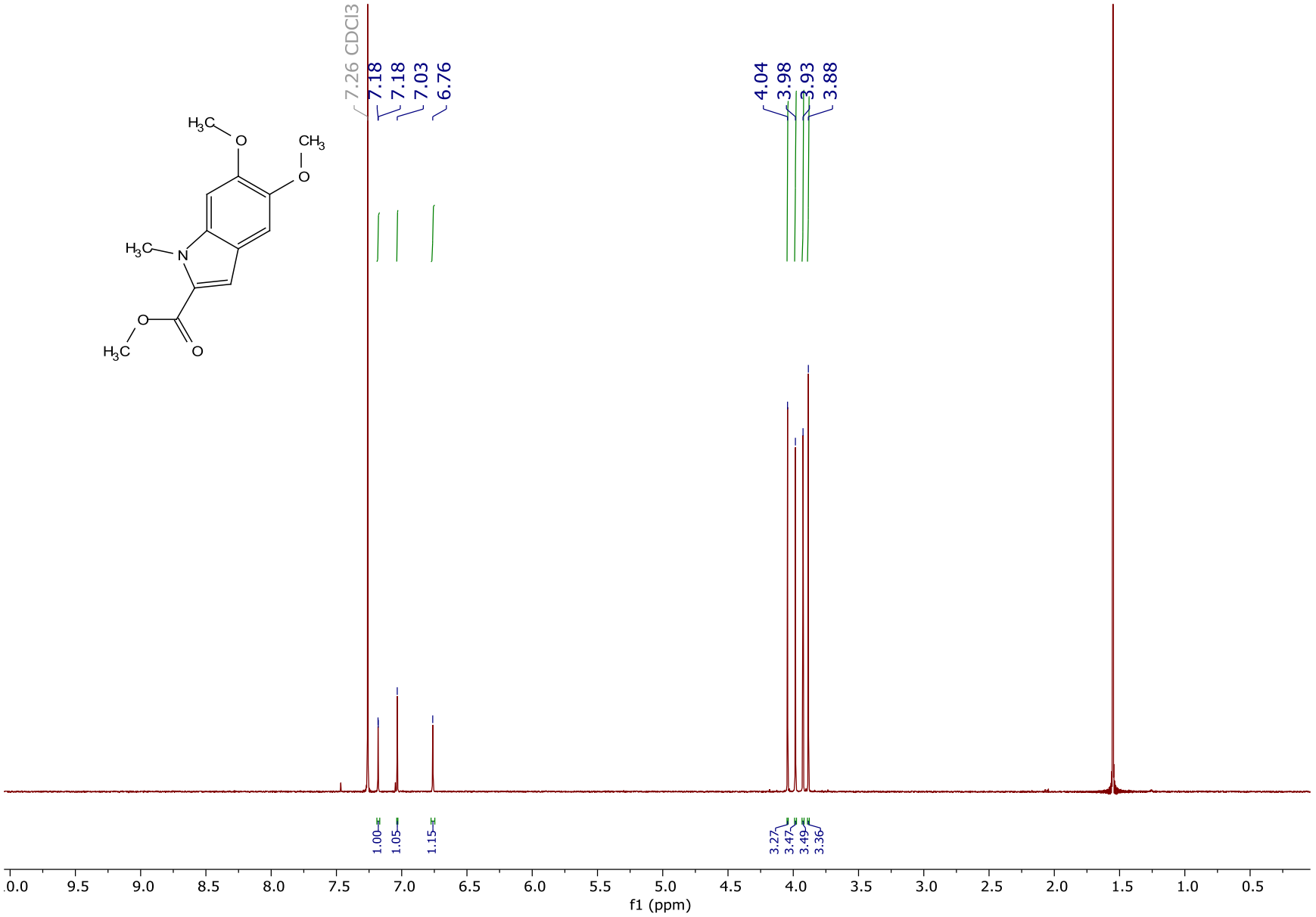
7.26 CDCl3
7.18
7.18
7.03
6.76
4.04
3.98
3.93
3.88
1.00
1.05
1.15
3.27
3.47
3.49
3.36
f1 (ppm)

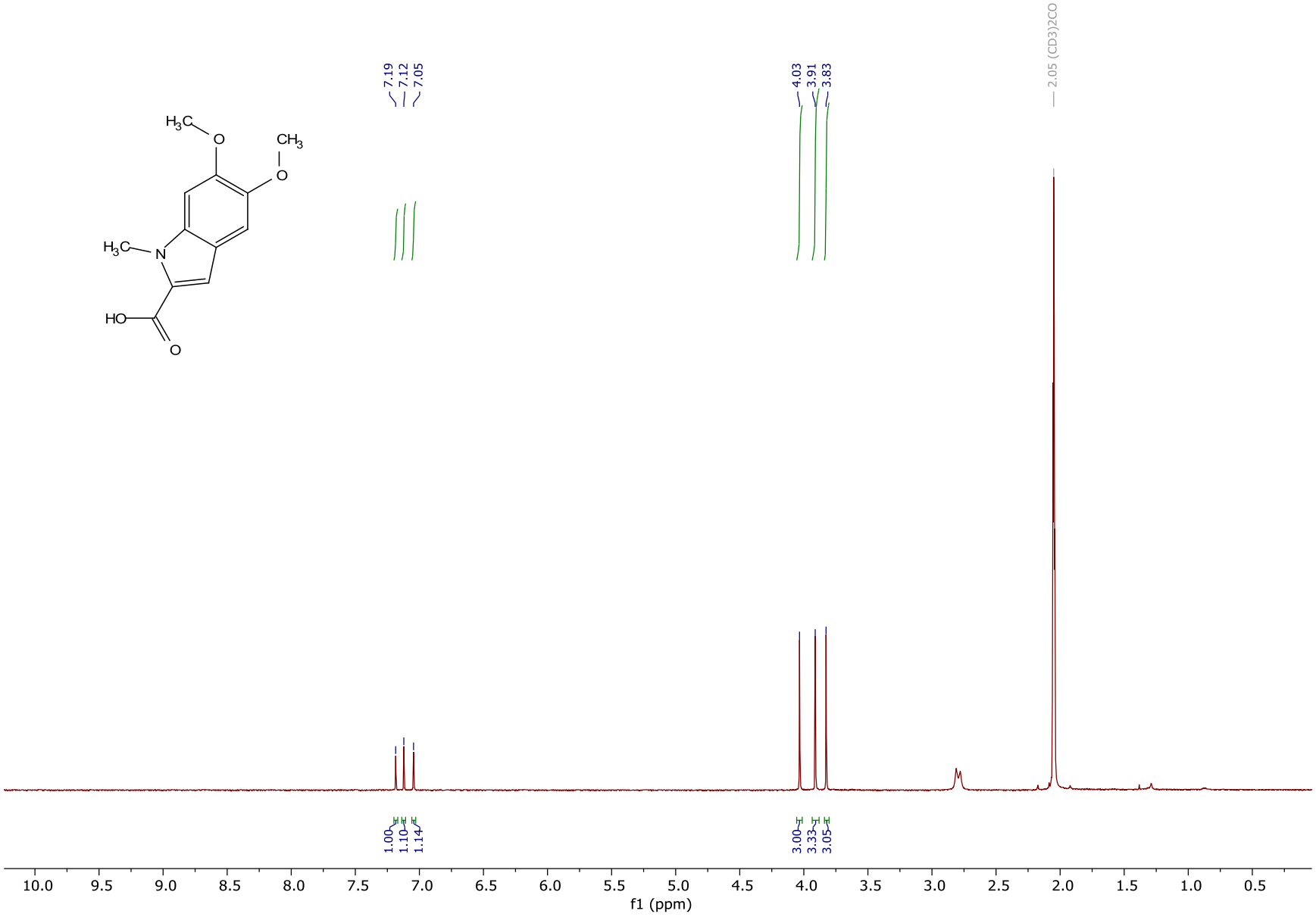
7.19
7.12
7.05
4.03
3.91
3.83
2.05 (CD3)2CO
1.00
1.10
1.14
3.00
3.33
3.05
10.0
9.5
9.0
8.5
8.0
7.5
7.0
6.5
6.0
5.5
5.0
4.5
4.0
3.5
3.0
2.5
2.0
1.5
1.0
0.5
f1 (ppm)

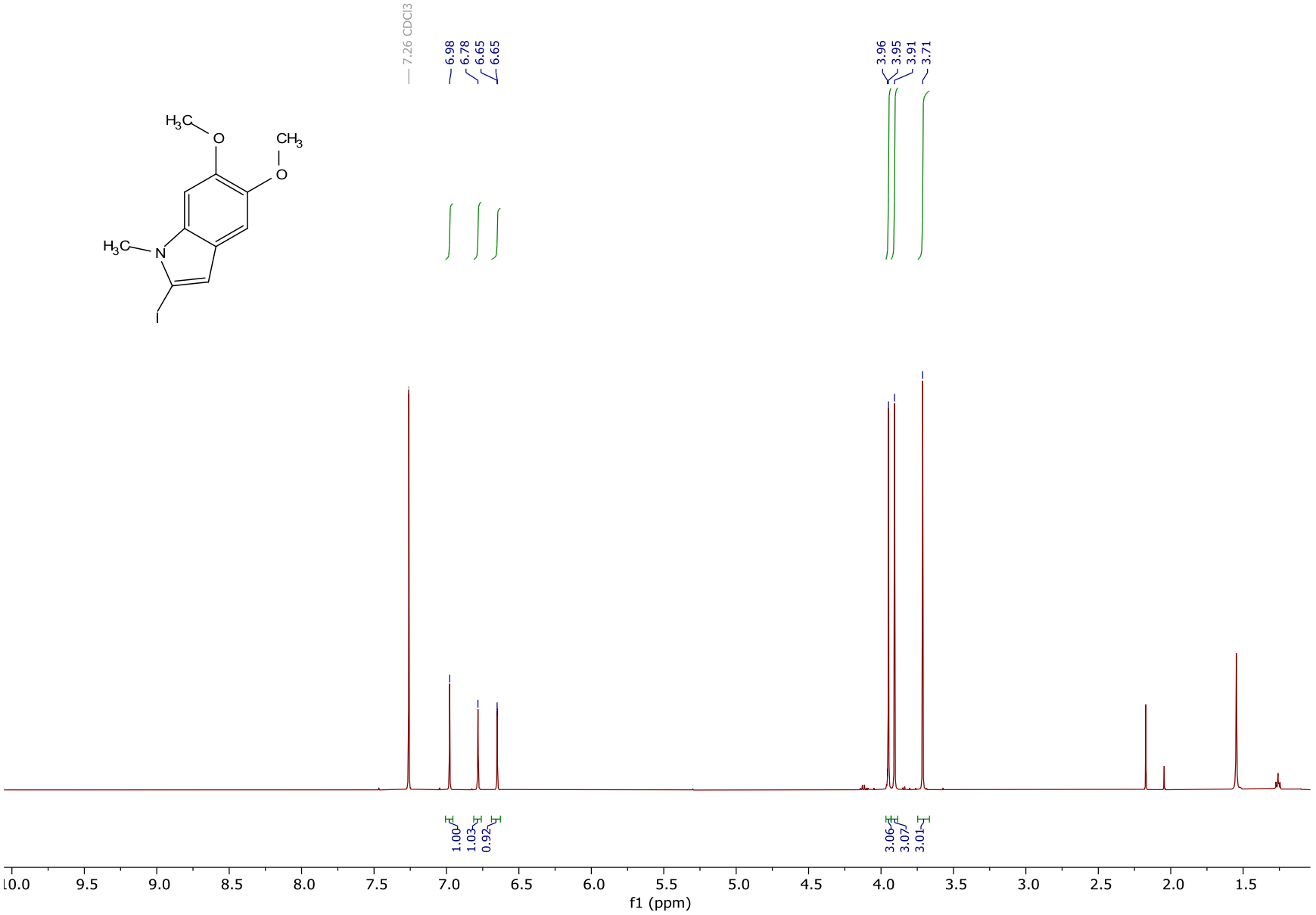
7.26 CDCl3
6.98
6.78
6.65
6.65
3.96
3.95
3.91
3.71
1.00
1.03
0.92
3.06
3.07
3.01
f1 (ppm)

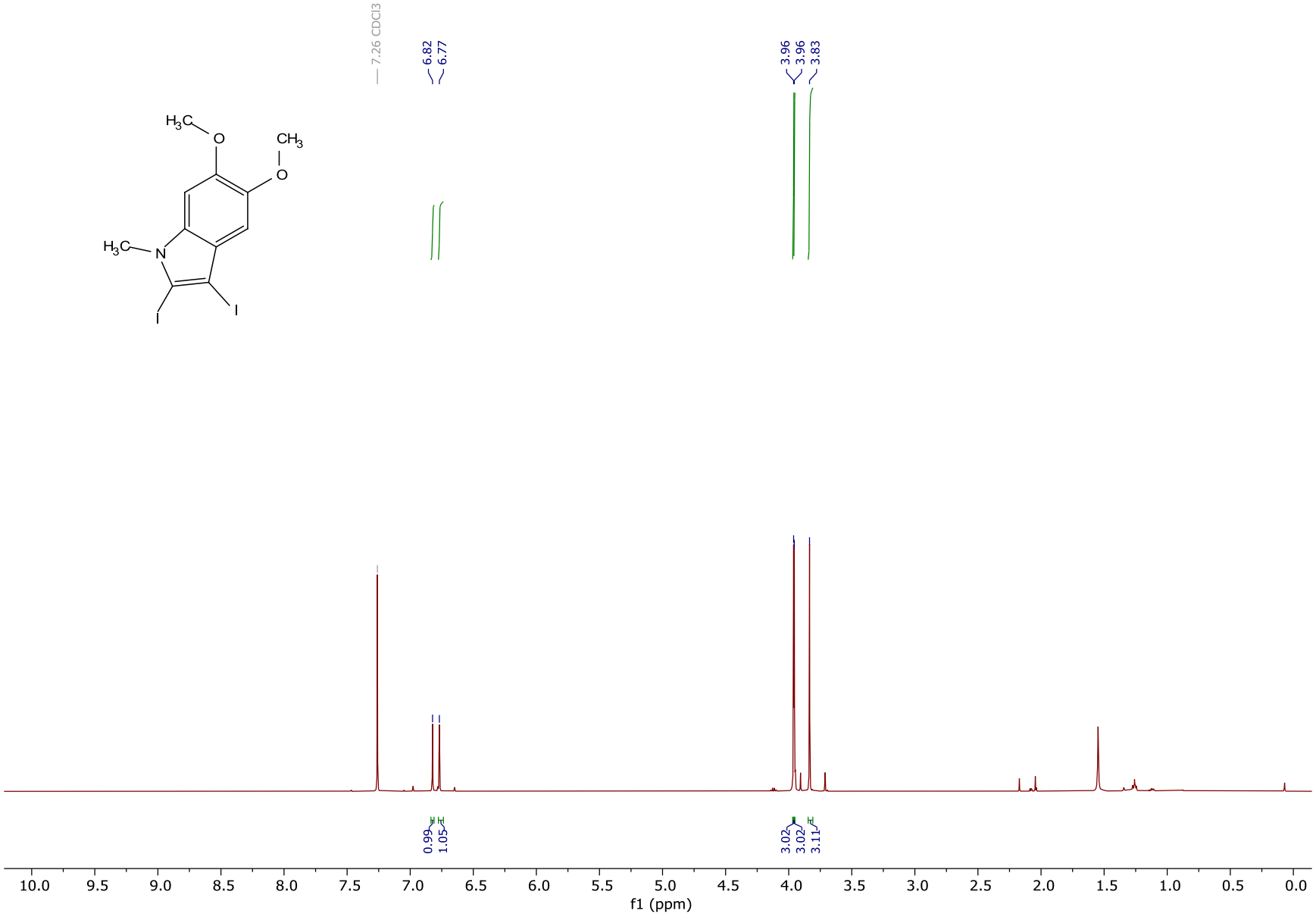
7.26 CDCl3
6.82
6.77
3.96
3.96
3.83
H3C
O
CH3
O
H3C
N
I
I
0.99
1.05
3.02
3.02
3.11
10.0
9.5
9.0
8.5
8.0
7.5
7.0
6.5
6.0
5.5
5.0
4.5
4.0
3.5
3.0
2.5
2.0
1.5
1.0
0.5
0.0
f1 (ppm)

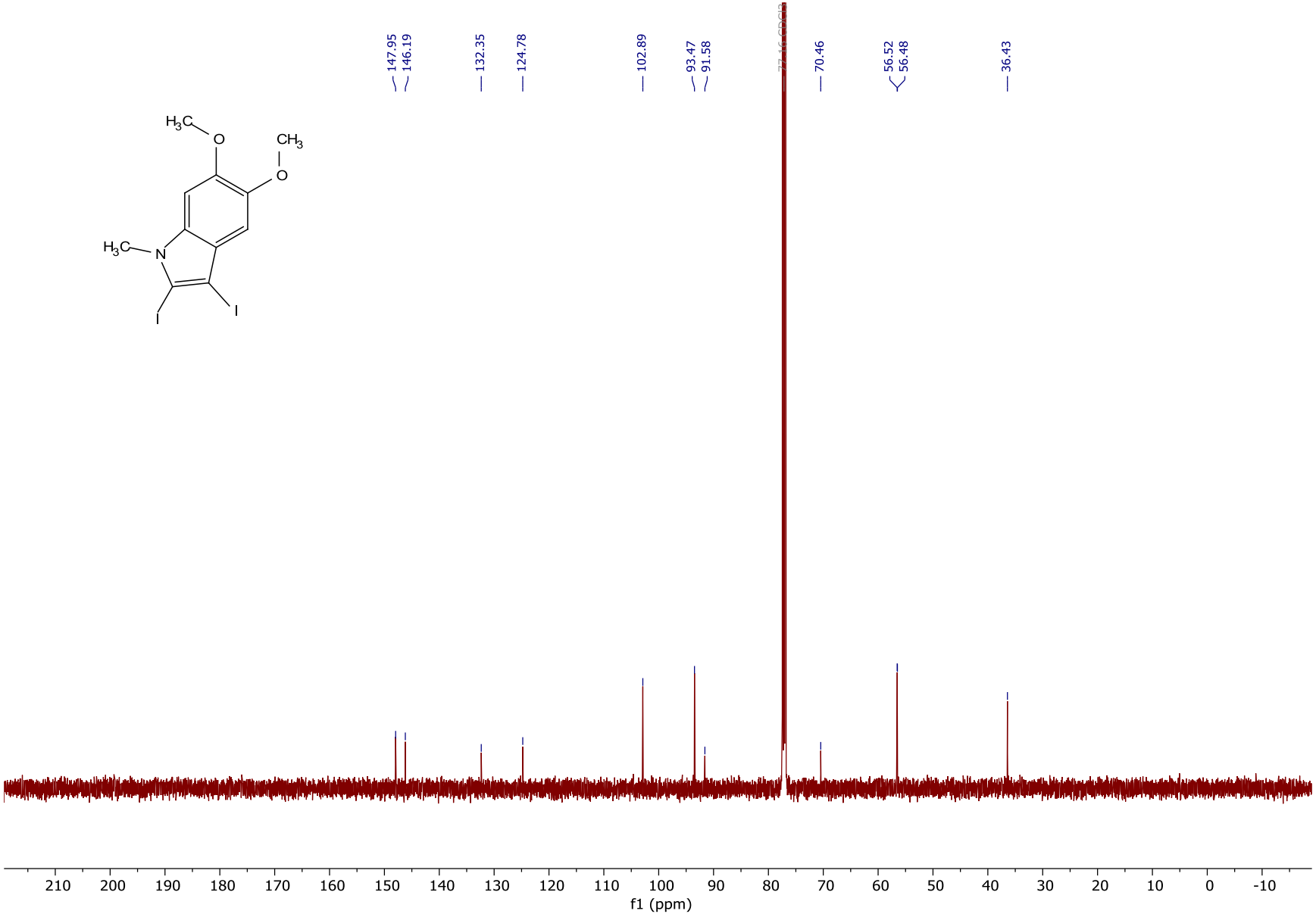
147.95
146.19
132.35
124.78
102.89
93.47
91.58
77.16
70.46
56.52
56.48
36.43
H3C
O
CH3
O
H3C
N
I
I
210 200 190 180 170 160 150 140 130 120 110 100 90 80 70 60 50 40 30 20 10 0 -10
f1 (ppm)

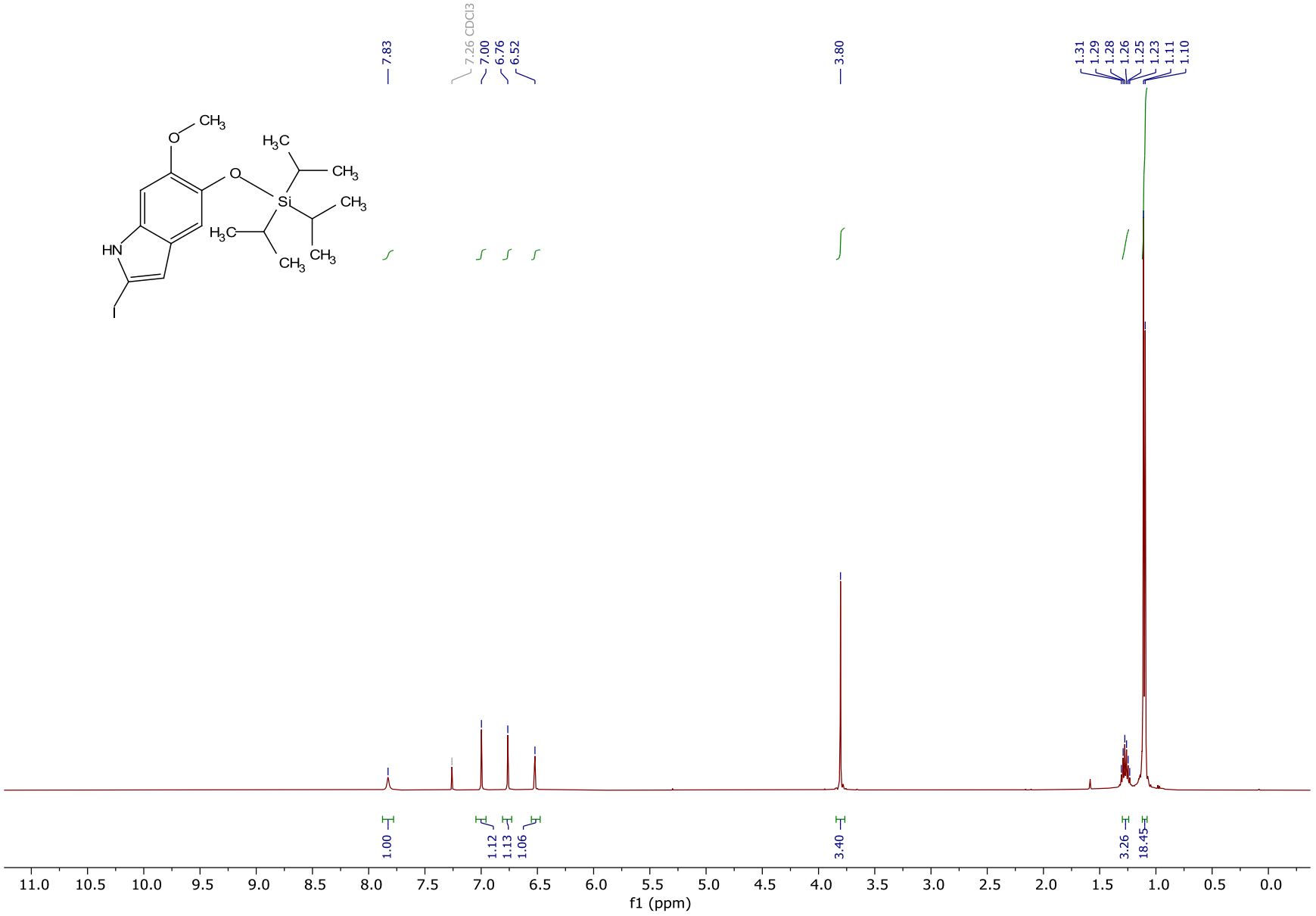
7.83
7.26 CDCl3
7.00
6.76
6.52
3.80
1.31
1.29
1.28
1.26
1.25
1.23
1.11
1.10
O
CH3
H3C
CH3
O
Si
CH3
H3C
CH3
CH3
HN
I
1.00
1.12
1.13
1.06
3.40
3.26
18.45
11.0
10.5
10.0
9.5
9.0
8.5
8.0
7.5
7.0
6.5
6.0
5.5
5.0
4.5
4.0
3.5
3.0
2.5
2.0
1.5
1.0
0.5
0.0
f1 (ppm)

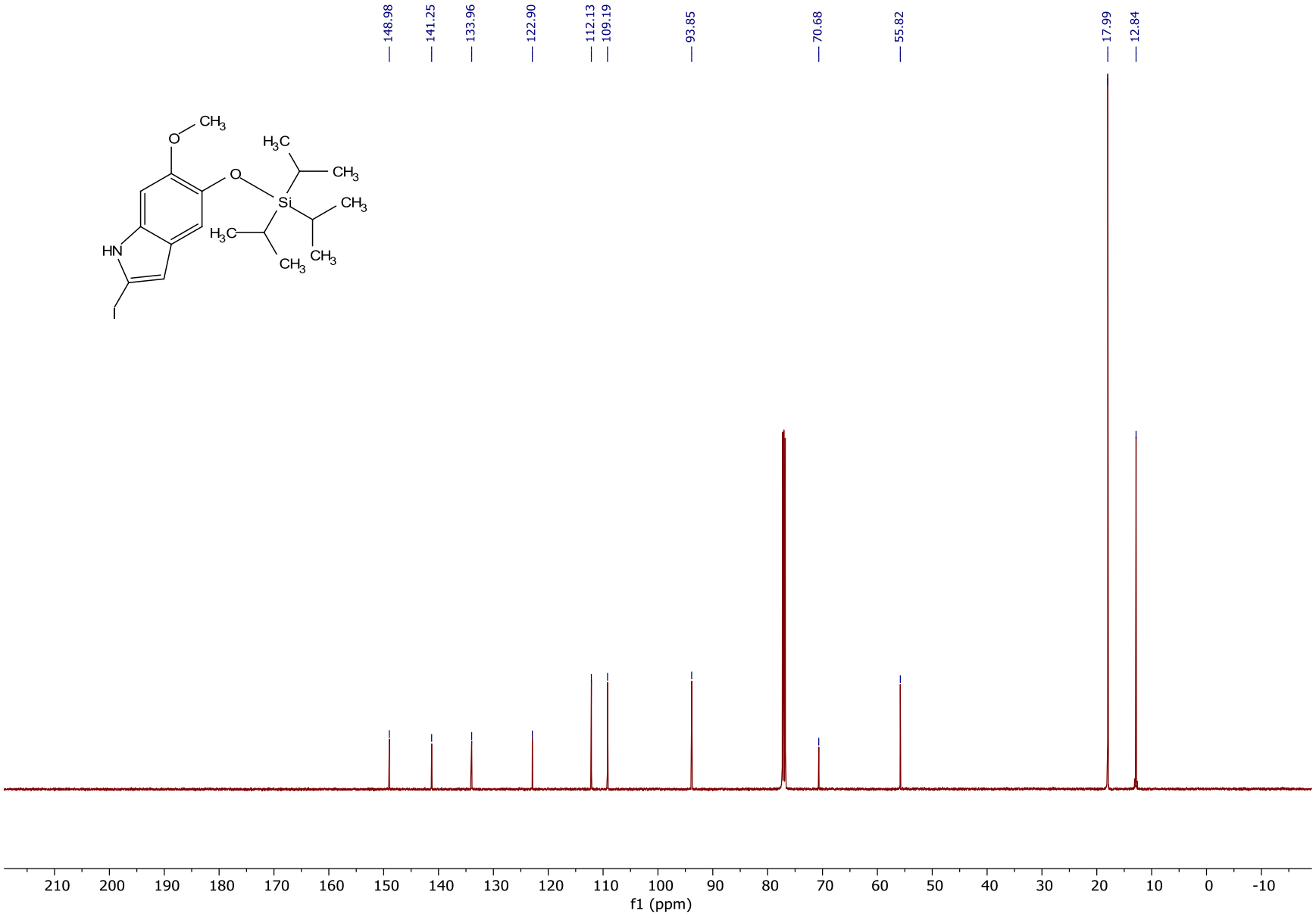
148.98
141.25
133.96
122.90
112.13
109.19
93.85
70.68
55.82
17.99
12.84
O
CH3
H3C
CH3
O
Si
CH3
H3C
CH3
CH3
HN
I
210 200 190 180 170 160 150 140 130 120 110 100 90 80 70 60 50 40 30 20 10 0 -10
f1 (ppm)

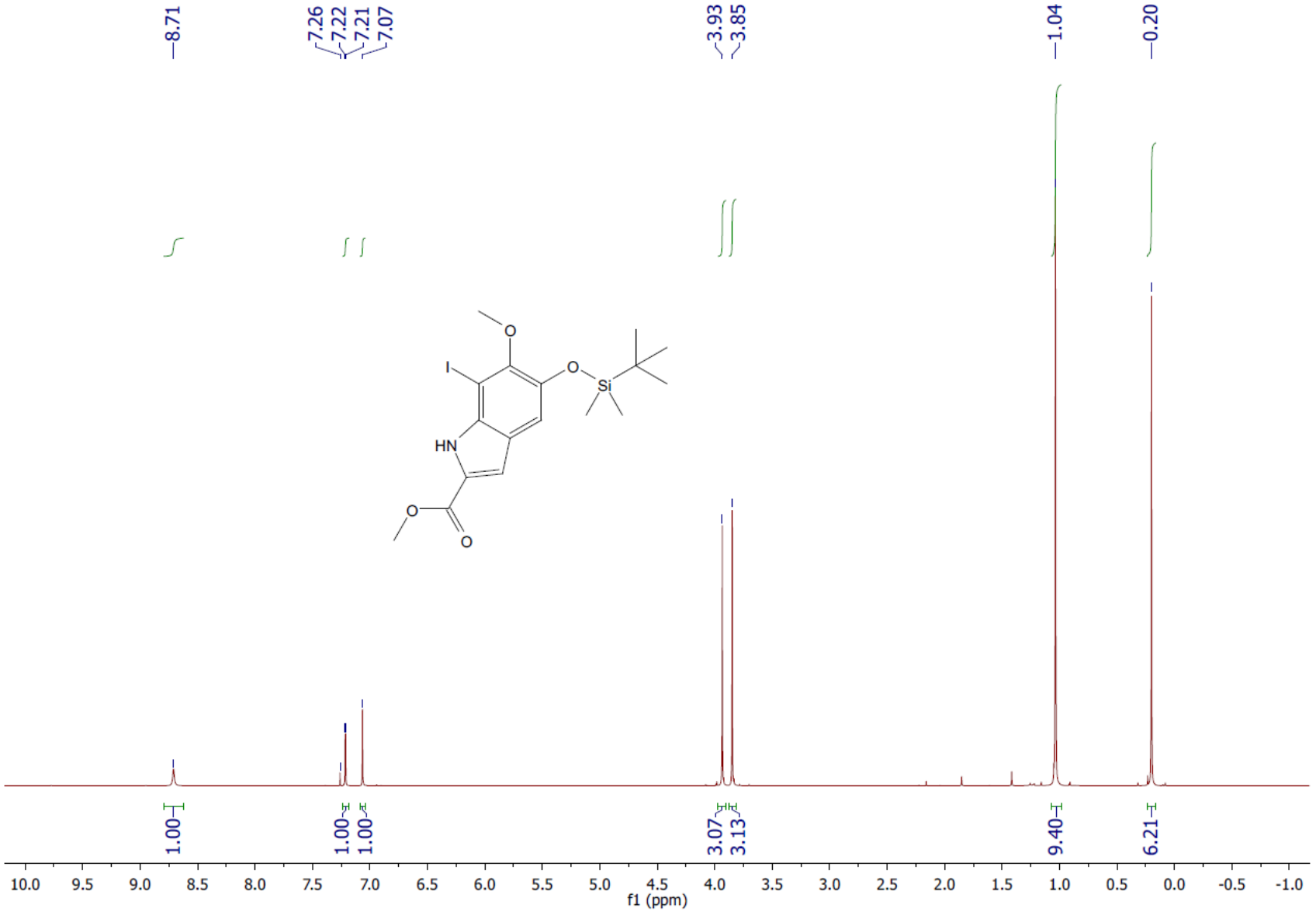
8.71
7.26
7.22
7.21
7.07
3.93
3.85
1.04
0.20
1.00
1.00
1.00
3.07
3.13
9.40
6.21
f1 (ppm)

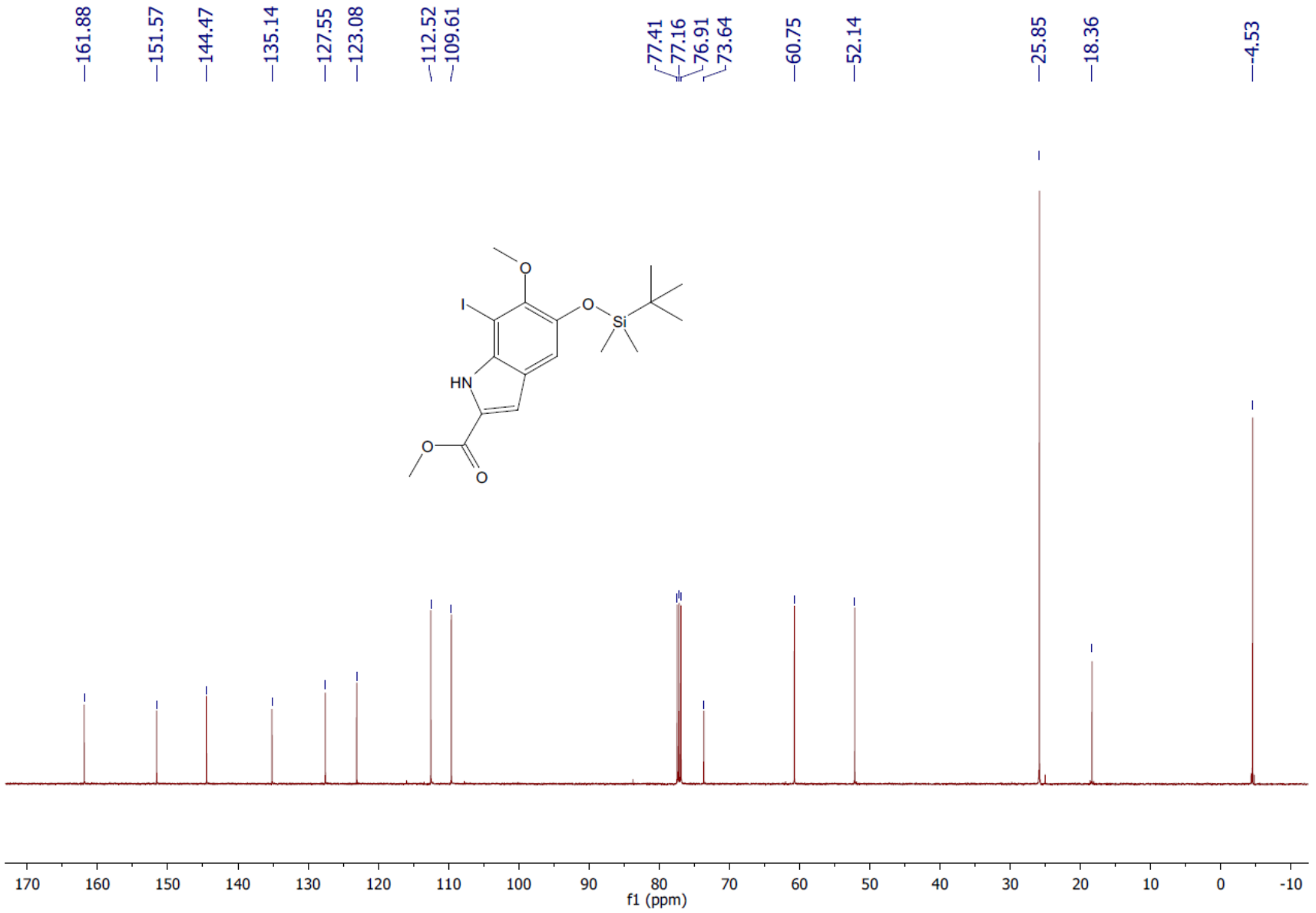
161.88
151.57
144.47
135.14
127.55
123.08
112.52
109.61
77.41
77.16
76.91
73.64
60.75
52.14
25.85
18.36
-4.53
O
I
O
Si
HN
O
O
170
160
150
140
130
120
110
100
90
80
70
60
50
40
30
20
10
0
-10
f1 (ppm)

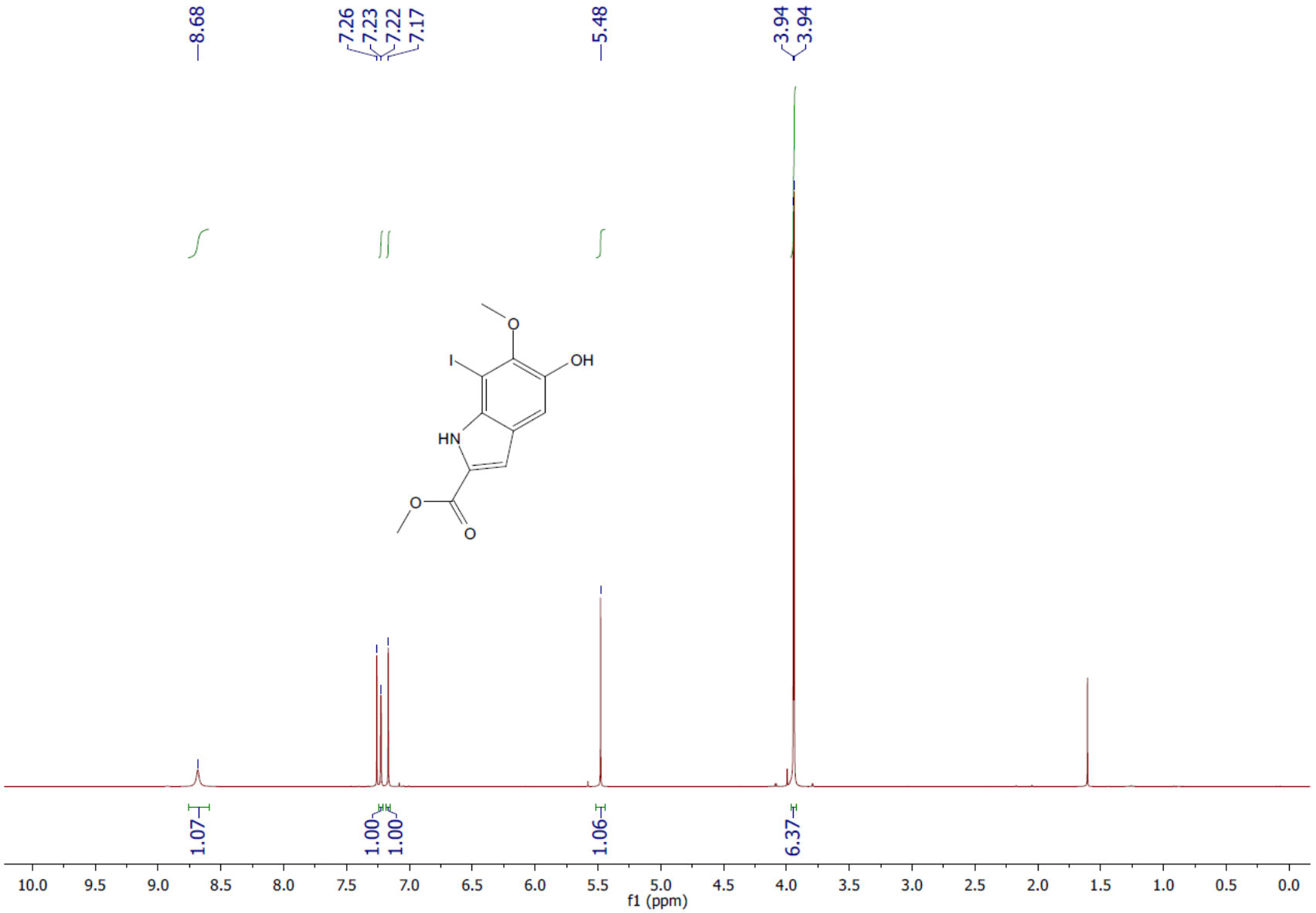
8.68
7.26
7.23
7.22
7.17
5.48
3.94
3.94
O
I
OH
HN
O
O
1.07
1.00
1.00
1.06
6.37
10.0
9.5
9.0
8.5
8.0
7.5
7.0
6.5
6.0
5.5
5.0
4.5
4.0
3.5
3.0
2.5
2.0
1.5
1.0
0.5
0.0
f1 (ppm)

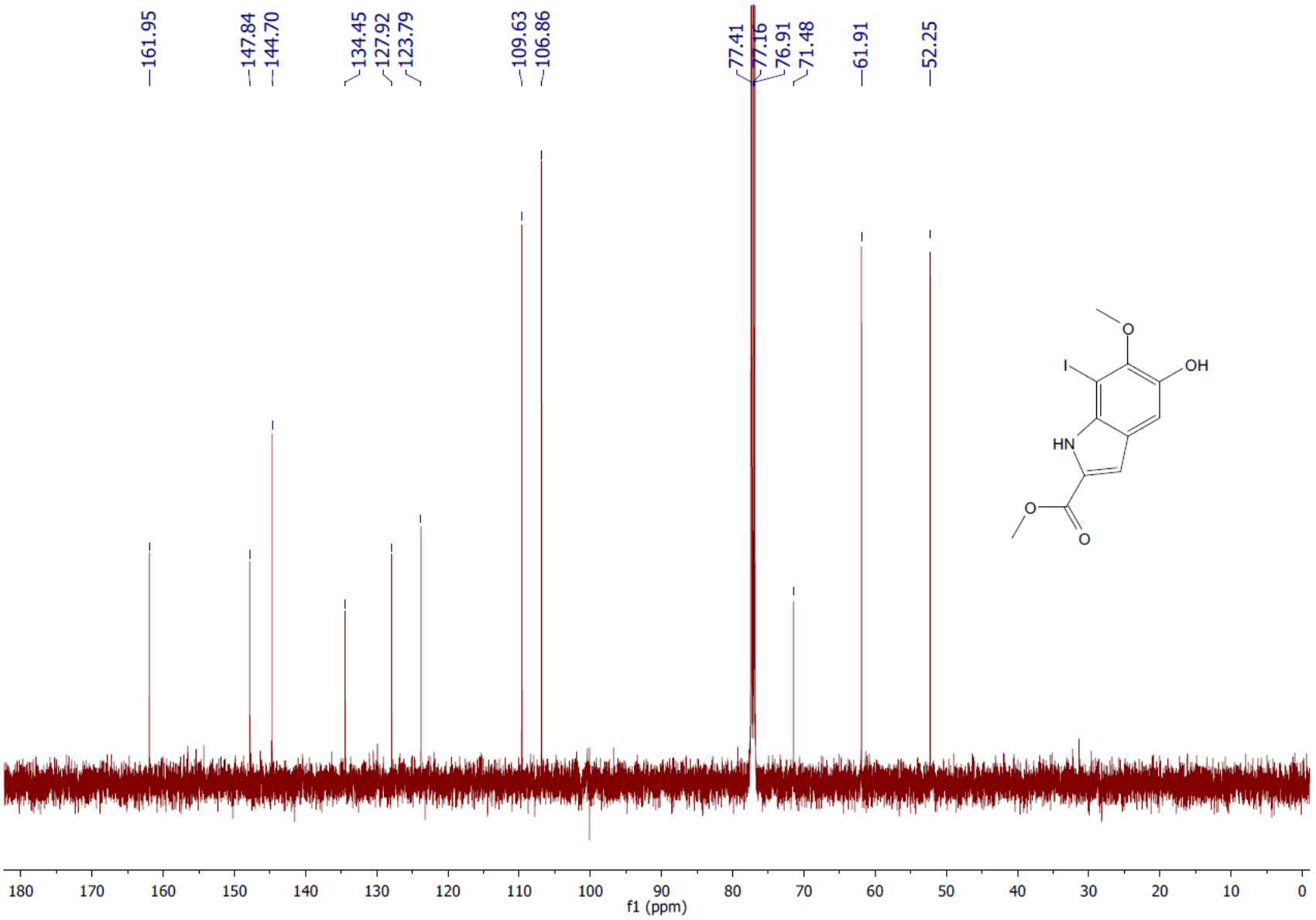
161.95
147.84
144.70
134.45
127.92
123.79
109.63
106.86
77.41
77.16
76.91
71.48
61.91
52.25
O
I
OH
HN
O
O
180
170
160
150
140
130
120
110
100
90
80
70
60
50
40
30
20
10
0
f1 (ppm)

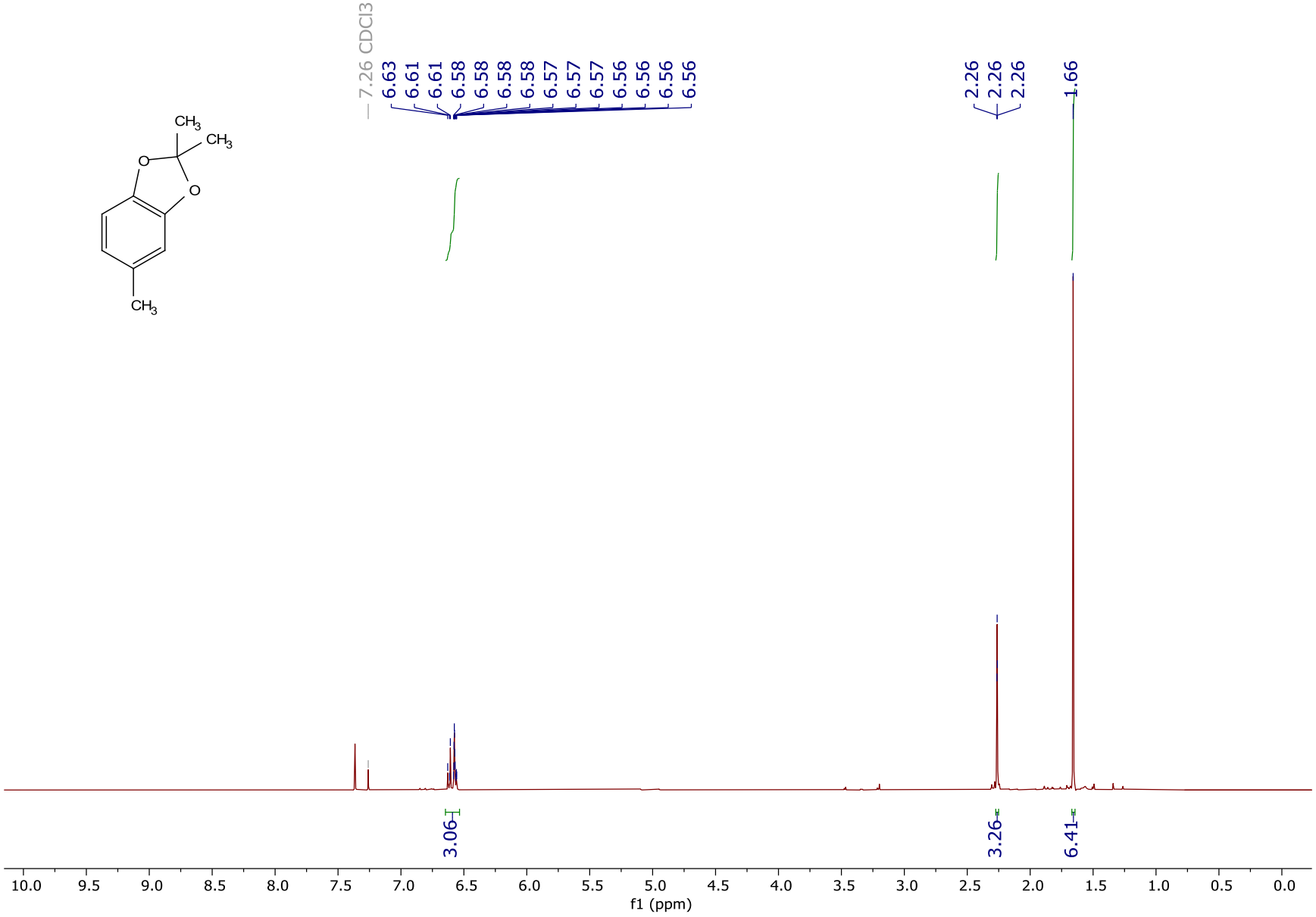
7.26 CDCl3
6.63
6.61
6.61
6.58
6.58
6.58
6.58
6.57
6.57
6.57
6.56
6.56
6.56
6.56
2.26
2.26
2.26
1.66
CH3
CH3
O
O
CH3
3.06
3.26
6.41
10.0
9.5
9.0
8.5
8.0
7.5
7.0
6.5
6.0
5.5
5.0
4.5
4.0
3.5
3.0
2.5
2.0
1.5
1.0
0.5
0.0
f1 (ppm)

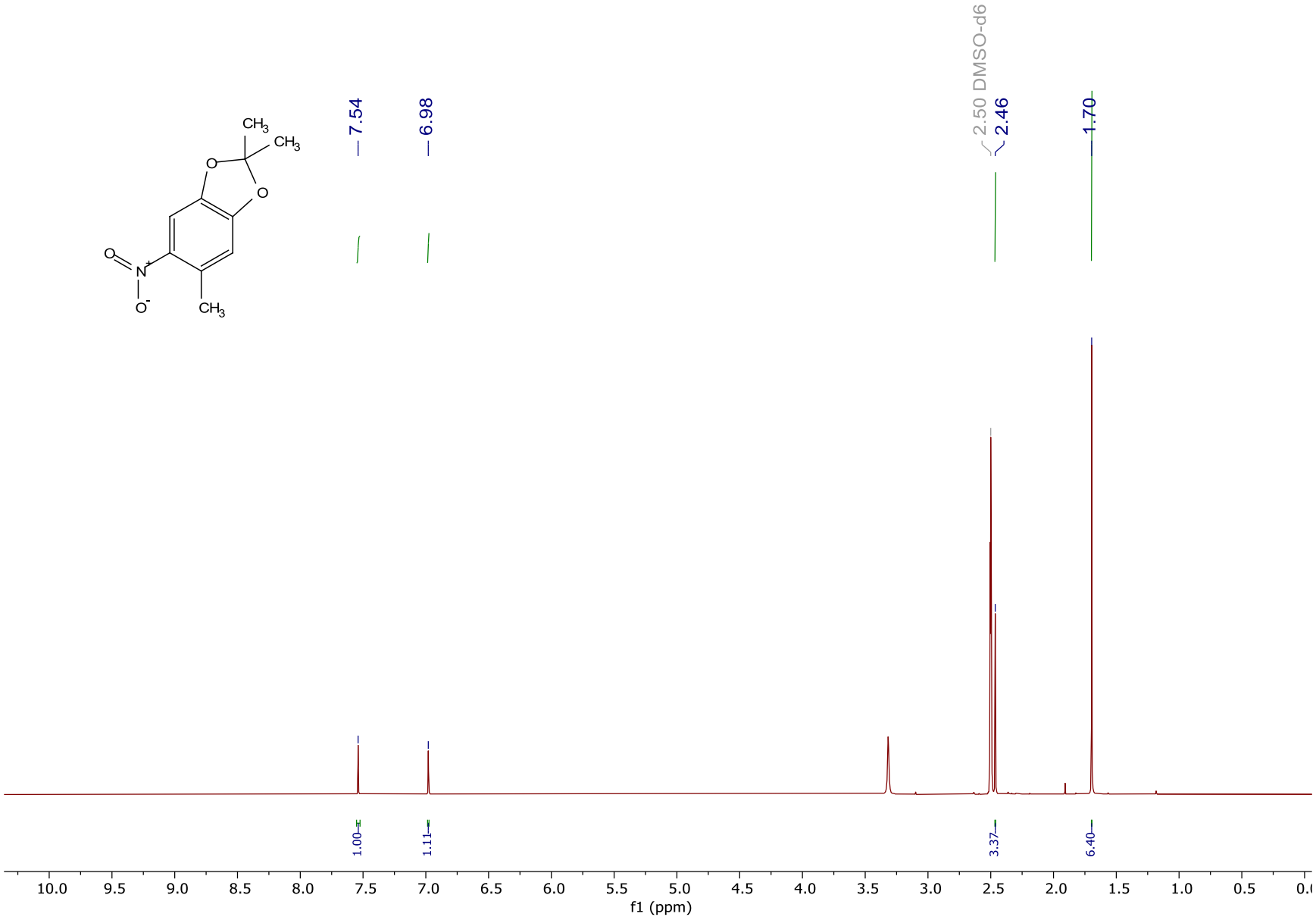
7.54
6.98
2.50 DMSO-d6
2.46
1.70
1.00
1.11
3.37
6.40
f1 (ppm)

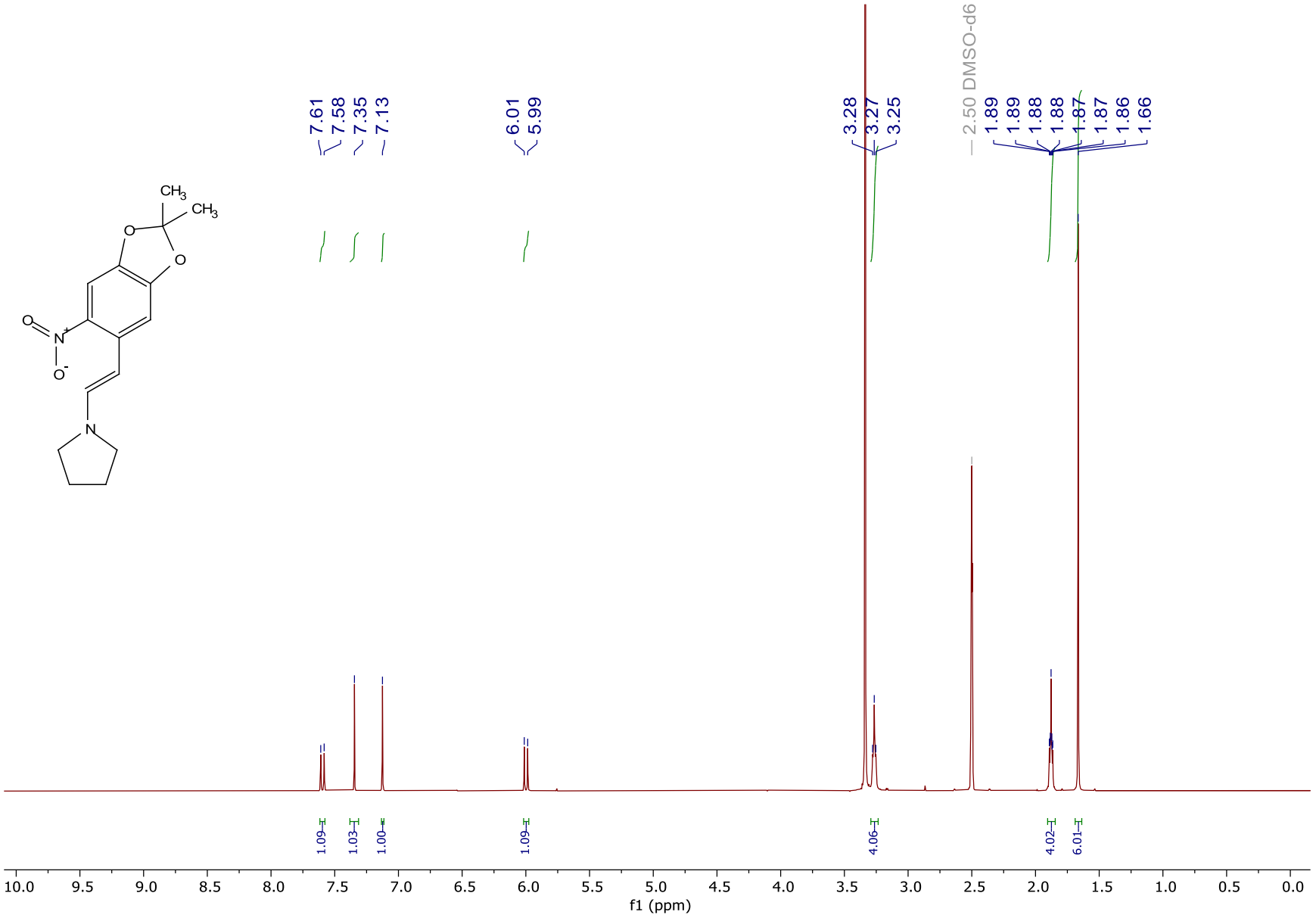
7.61
7.58
7.35
7.13
6.01
5.99
3.28
3.27
3.25
2.50 DMSO-d6
1.89
1.89
1.88
1.88
1.87
1.87
1.86
1.66
1.09
1.03
1.00
1.09
4.06
4.02
6.01
10.0
9.5
9.0
8.5
8.0
7.5
7.0
6.5
6.0
5.5
5.0
4.5
4.0
3.5
3.0
2.5
2.0
1.5
1.0
0.5
0.0
f1 (ppm)

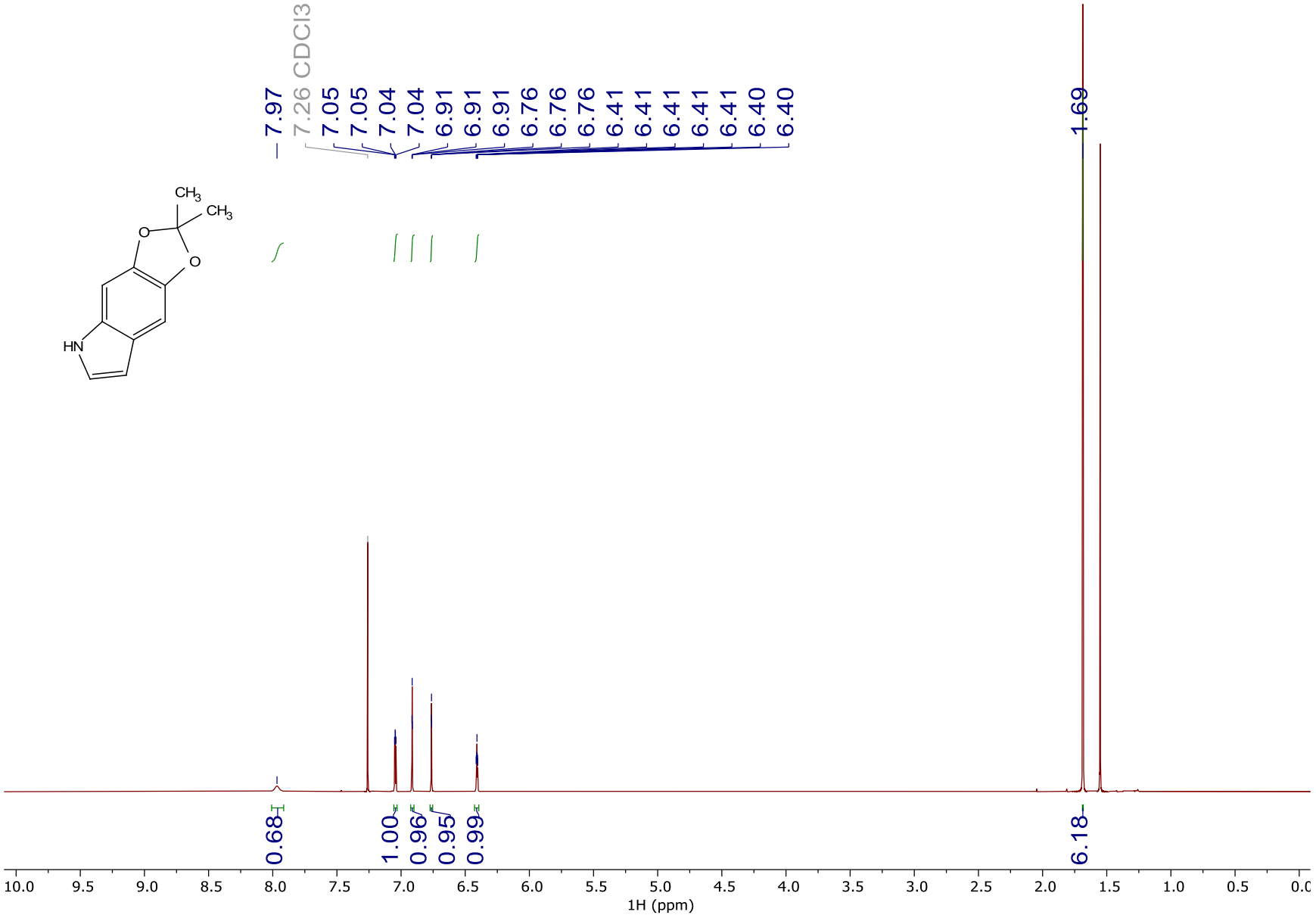
7.97
7.26 CDCl3
7.05
7.05
7.04
7.04
6.91
6.91
6.91
6.76
6.76
6.76
6.41
6.41
6.41
6.41
6.41
6.40
6.40
1.69
CH3
CH3
O
O
HN
0.68
1.00
0.96
0.95
0.99
6.18
10.0
9.5
9.0
8.5
8.0
7.5
7.0
6.5
6.0
5.5
5.0
4.5
4.0
3.5
3.0
2.5
2.0
1.5
1.0
0.5
0.0
1H (ppm)

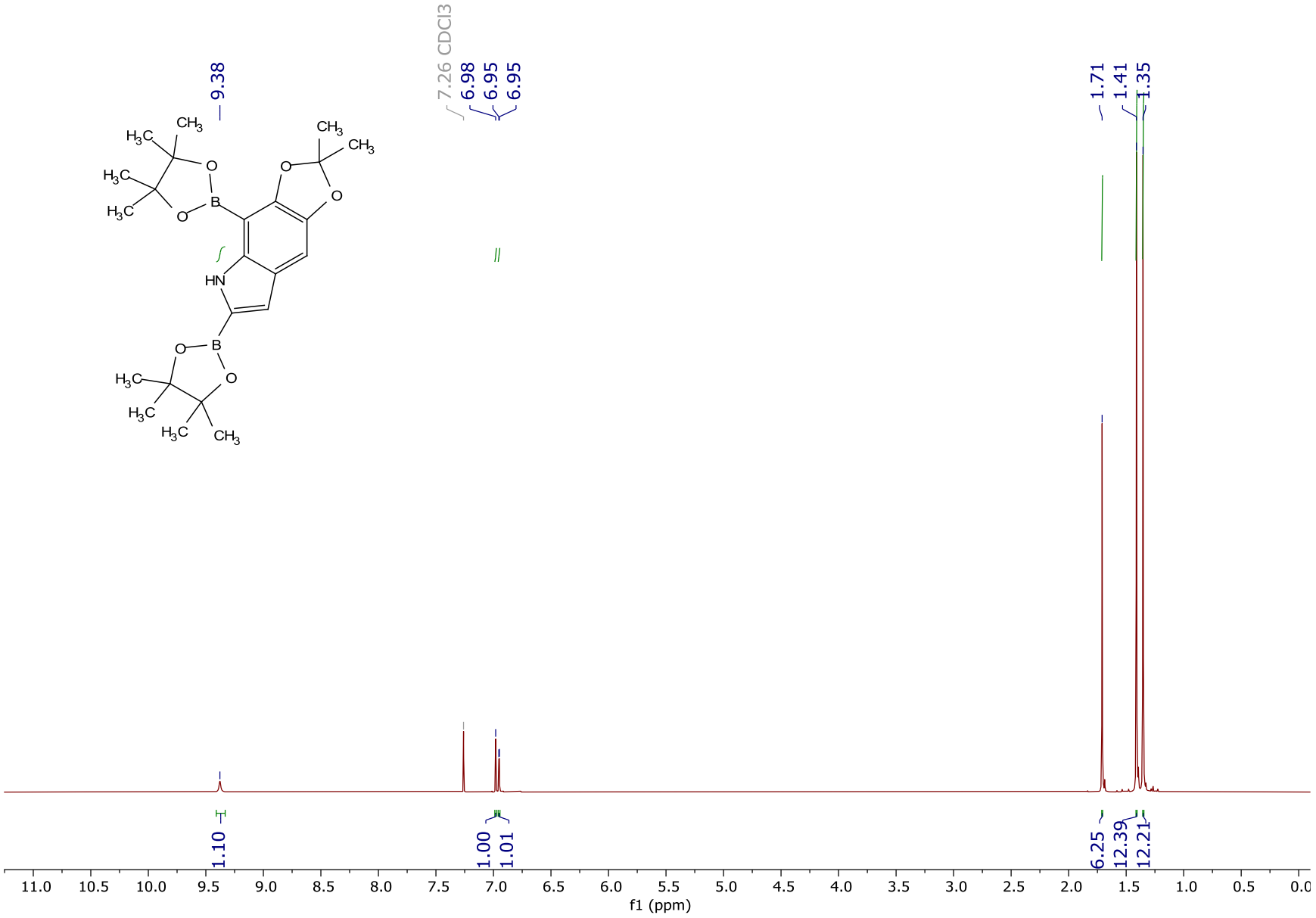
9.38
7.26 CDCl3
6.98
6.95
6.95
1.71
1.41
1.35
1.10
1.00
1.01
6.25
12.39
12.21
f1 (ppm)

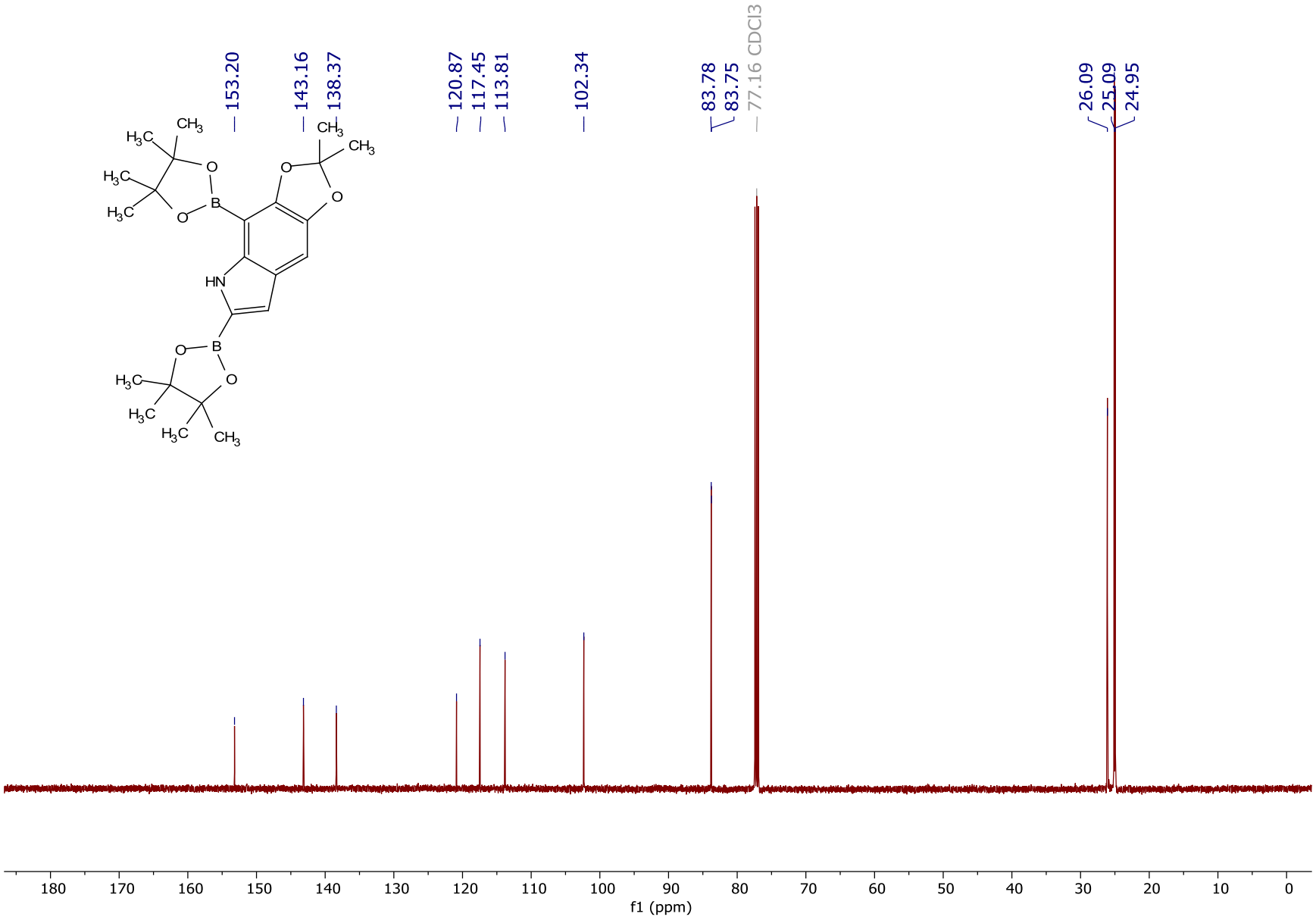
153.20
143.16
138.37
120.87
117.45
113.81
102.34
83.78
83.75
77.16 CDCl3
26.09
25.09
24.95
f1 (ppm)

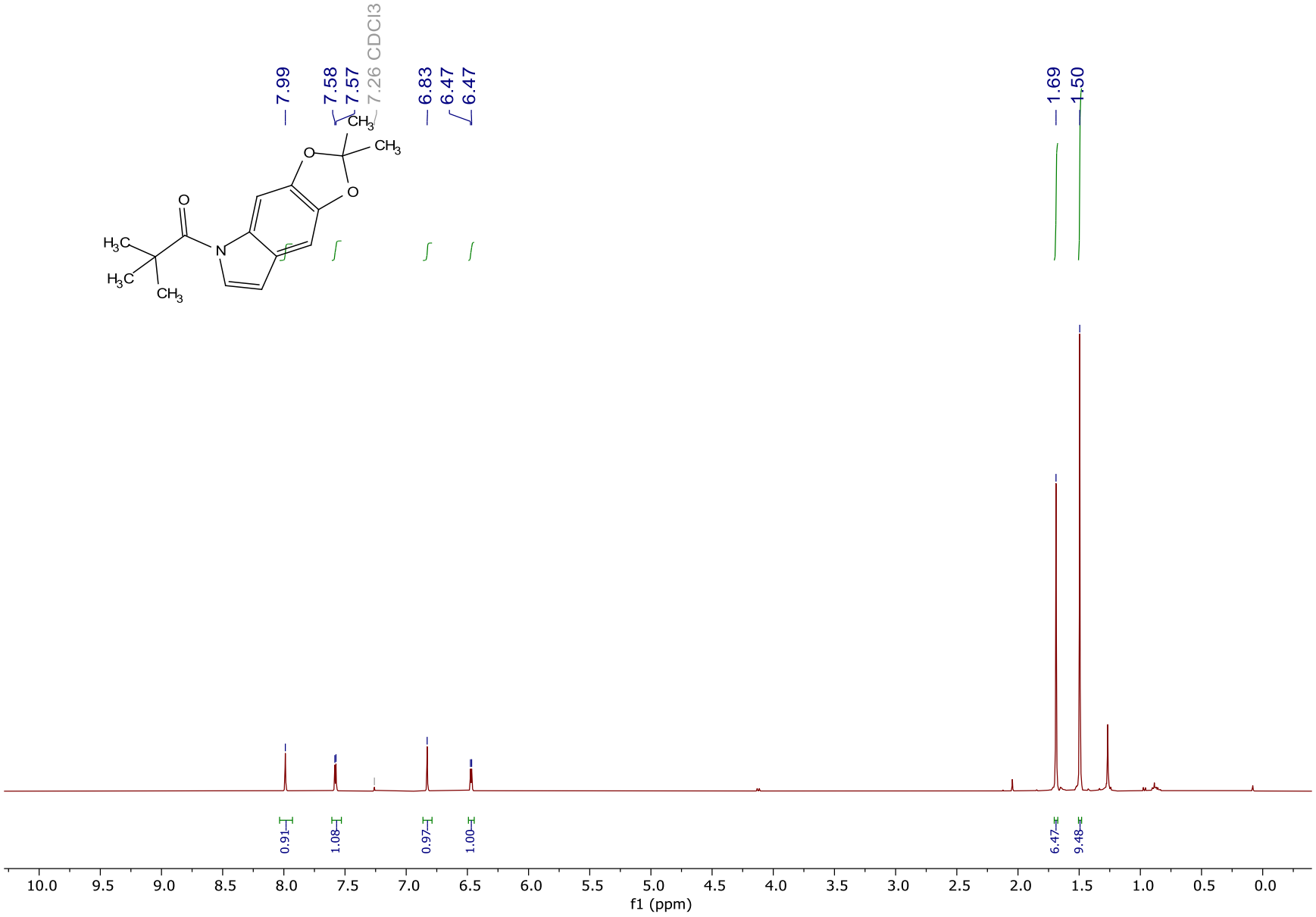
7.99
7.58
7.57
7.26 CDCl3
6.83
6.47
6.47
1.69
1.50
CH3
CH3
O
O
O
N
H3C
H3C
CH3
0.91
1.08
0.97
1.00
6.47
9.48
10.0
9.5
9.0
8.5
8.0
7.5
7.0
6.5
6.0
5.5
5.0
4.5
4.0
3.5
3.0
2.5
2.0
1.5
1.0
0.5
0.0
f1 (ppm)

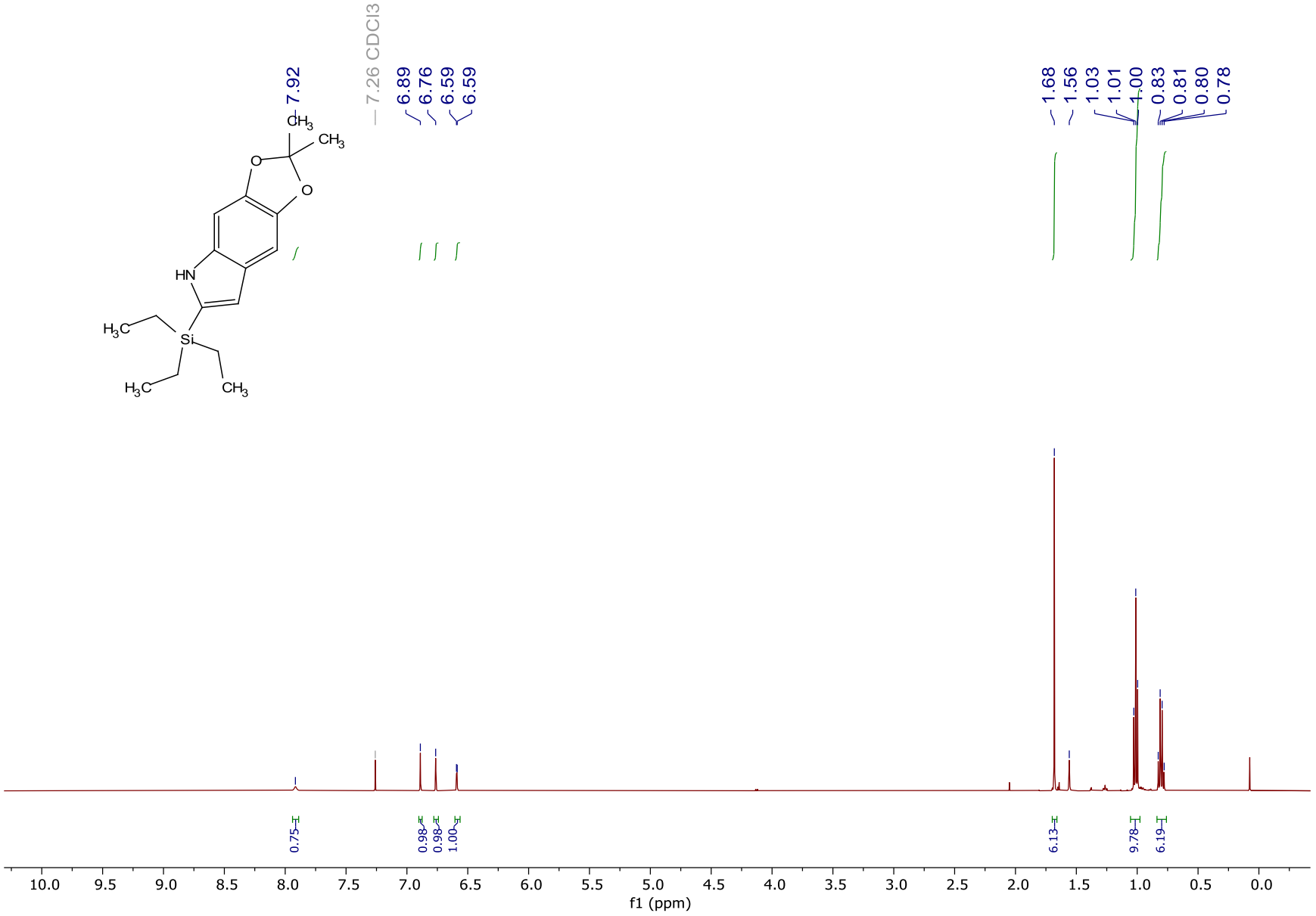
7.92
7.26 CDCl3
6.89
6.76
6.59
6.59
1.68
1.56
1.03
1.01
1.00
0.83
0.81
0.80
0.78
CH3
CH3
O
O
HN
H3C
Si
H3C
CH3
0.75
0.98
0.98
1.00
6.13
9.78
6.19
10.0 9.5 9.0 8.5 8.0 7.5 7.0 6.5 6.0 5.5 5.0 4.5 4.0 3.5 3.0 2.5 2.0 1.5 1.0 0.5 0.0
f1 (ppm)

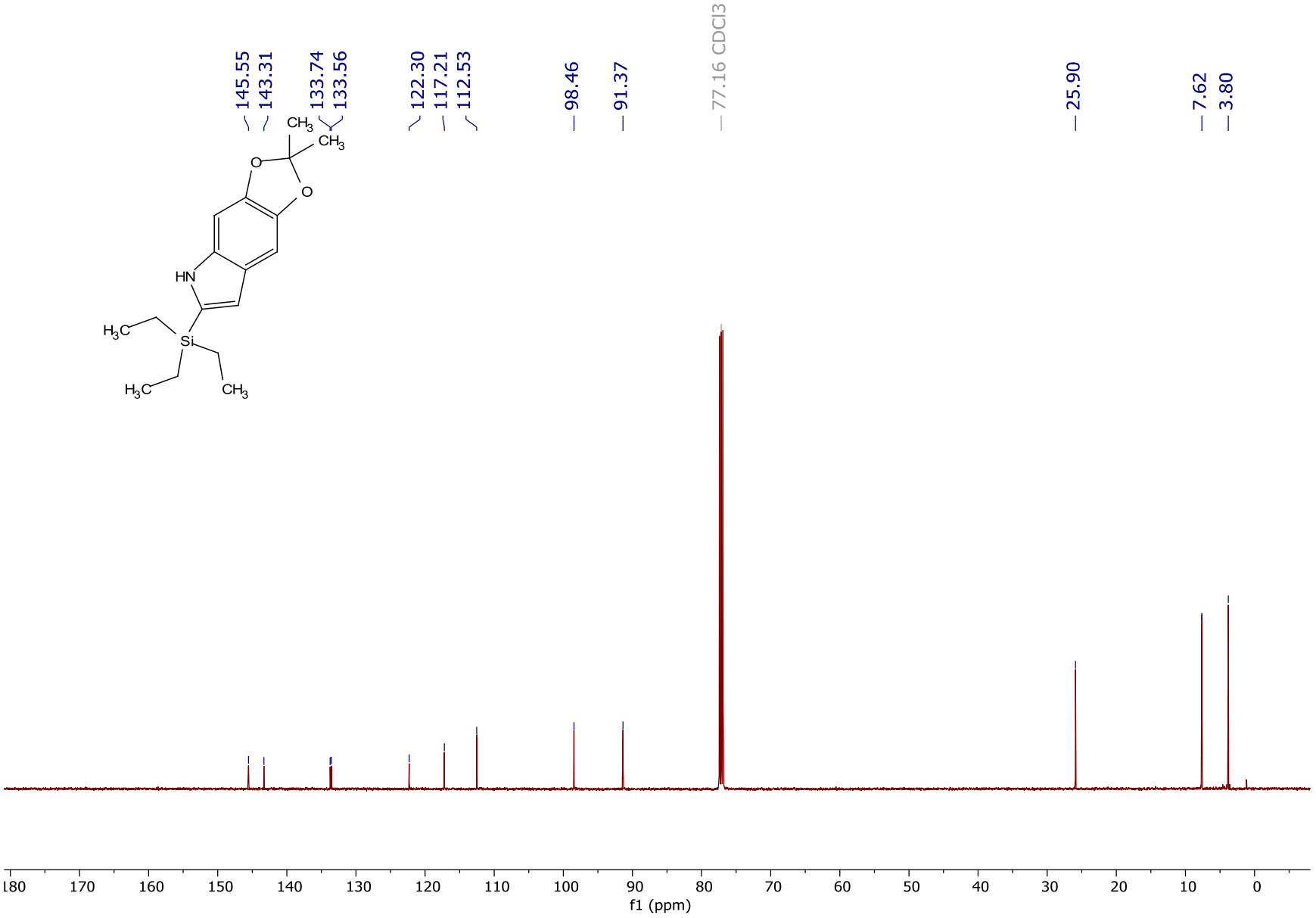
145.55
143.31
133.74
133.56
122.30
117.21
112.53
98.46
91.37
77.16 CDCl3
25.90
7.62
3.80
CH3
CH3
O
O
HN
H3C
Si
H3C
CH3
180
170
160
150
140
130
120
110
100
90
80
70
60
50
40
30
20
10
0
f1 (ppm)

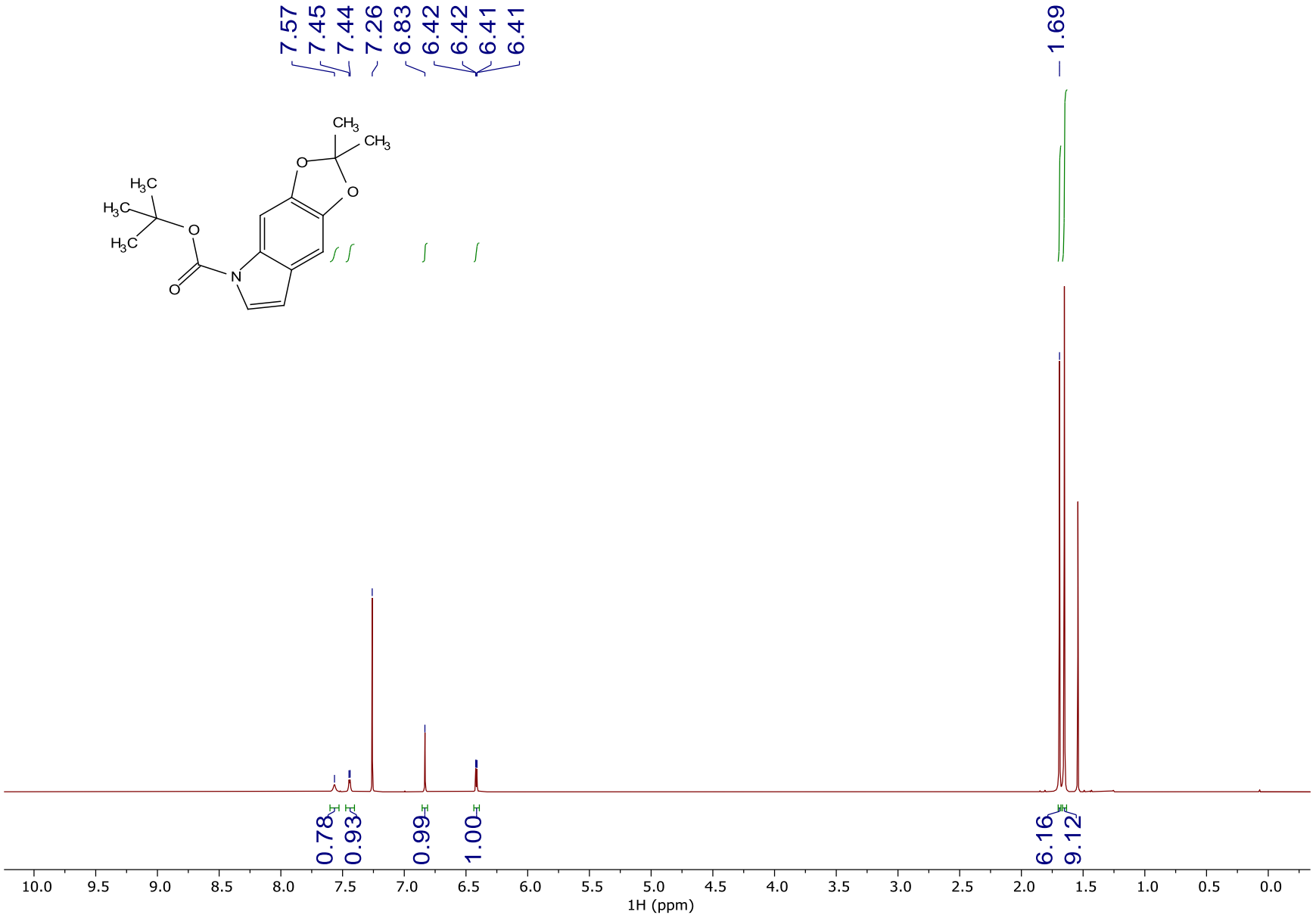
7.57
7.45
7.44
7.26
6.83
6.42
6.42
6.41
6.41
1.69
CH3
CH3
O
O
H3C
H3C
H3C
O
O
N
0.78
0.93
0.99
1.00
6.16
9.12
10.0
9.5
9.0
8.5
8.0
7.5
7.0
6.5
6.0
5.5
5.0
4.5
4.0
3.5
3.0
2.5
2.0
1.5
1.0
0.5
0.0
1H (ppm)

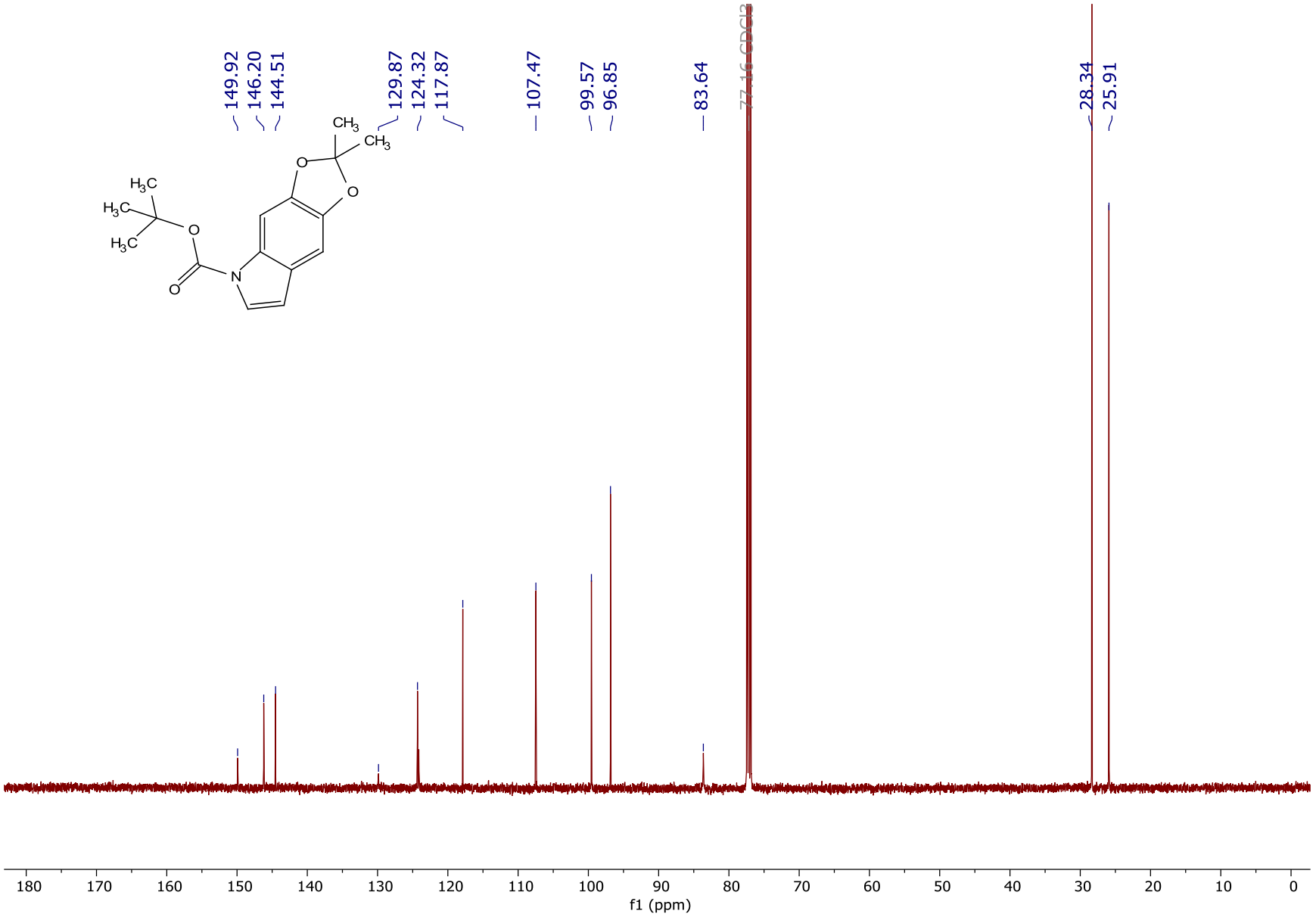
149.92
146.20
144.51
129.87
124.32
117.87
107.47
99.57
96.85
83.64
77.16 CDCl3
28.34
25.91
CH3
CH3
H3C
H3C
H3C
O
O
O
O
N
180
170
160
150
140
130
120
110
100
90
80
70
60
50
40
30
20
10
0
f1 (ppm)

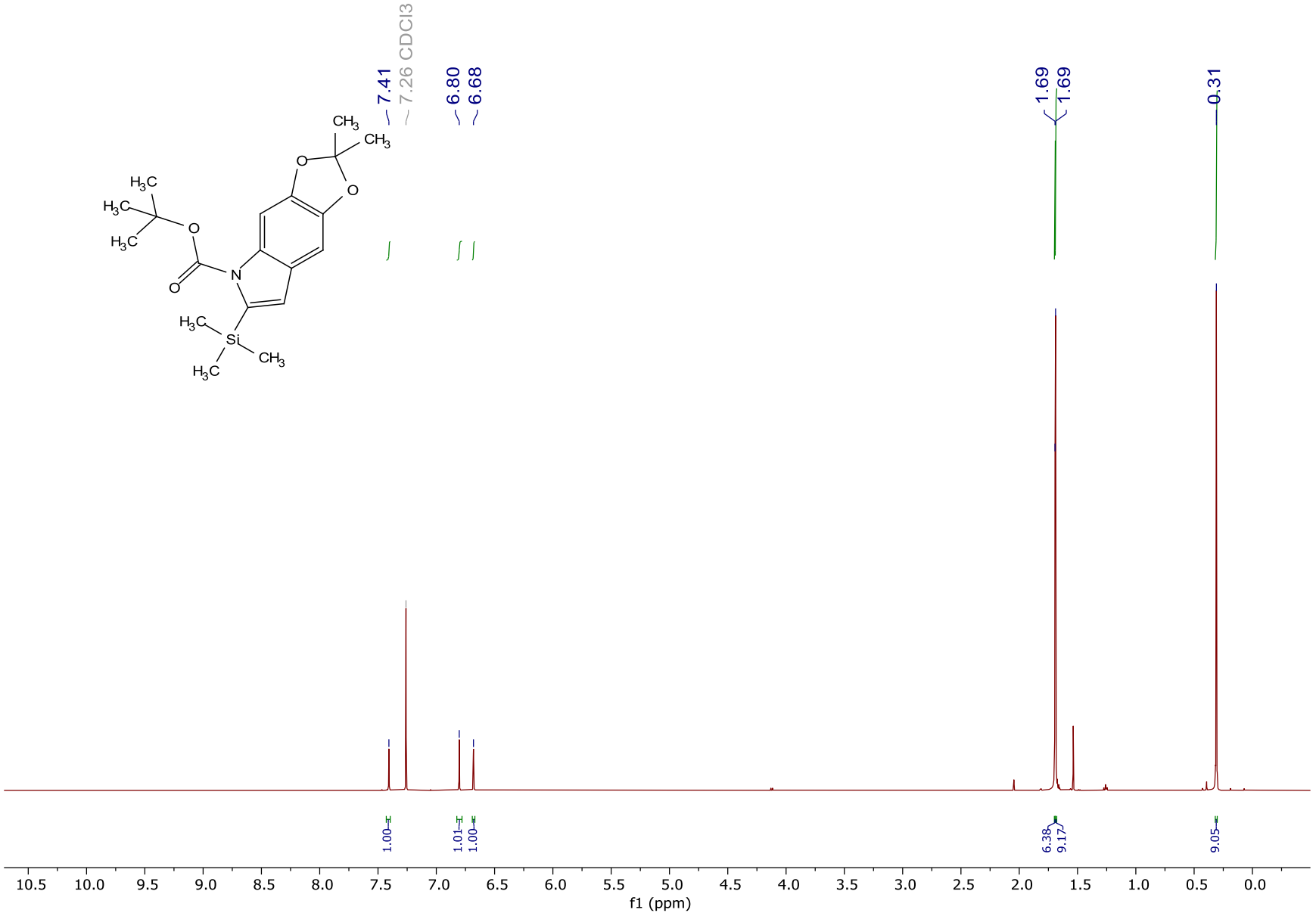
7.41
7.26 CDCl3
6.80
6.68
1.69
1.69
0.31
1.00
1.01
1.00
6.38
9.17
9.05
10.5 10.0 9.5 9.0 8.5 8.0 7.5 7.0 6.5 6.0 5.5 5.0 4.5 4.0 3.5 3.0 2.5 2.0 1.5 1.0 0.5 0.0
f1 (ppm)

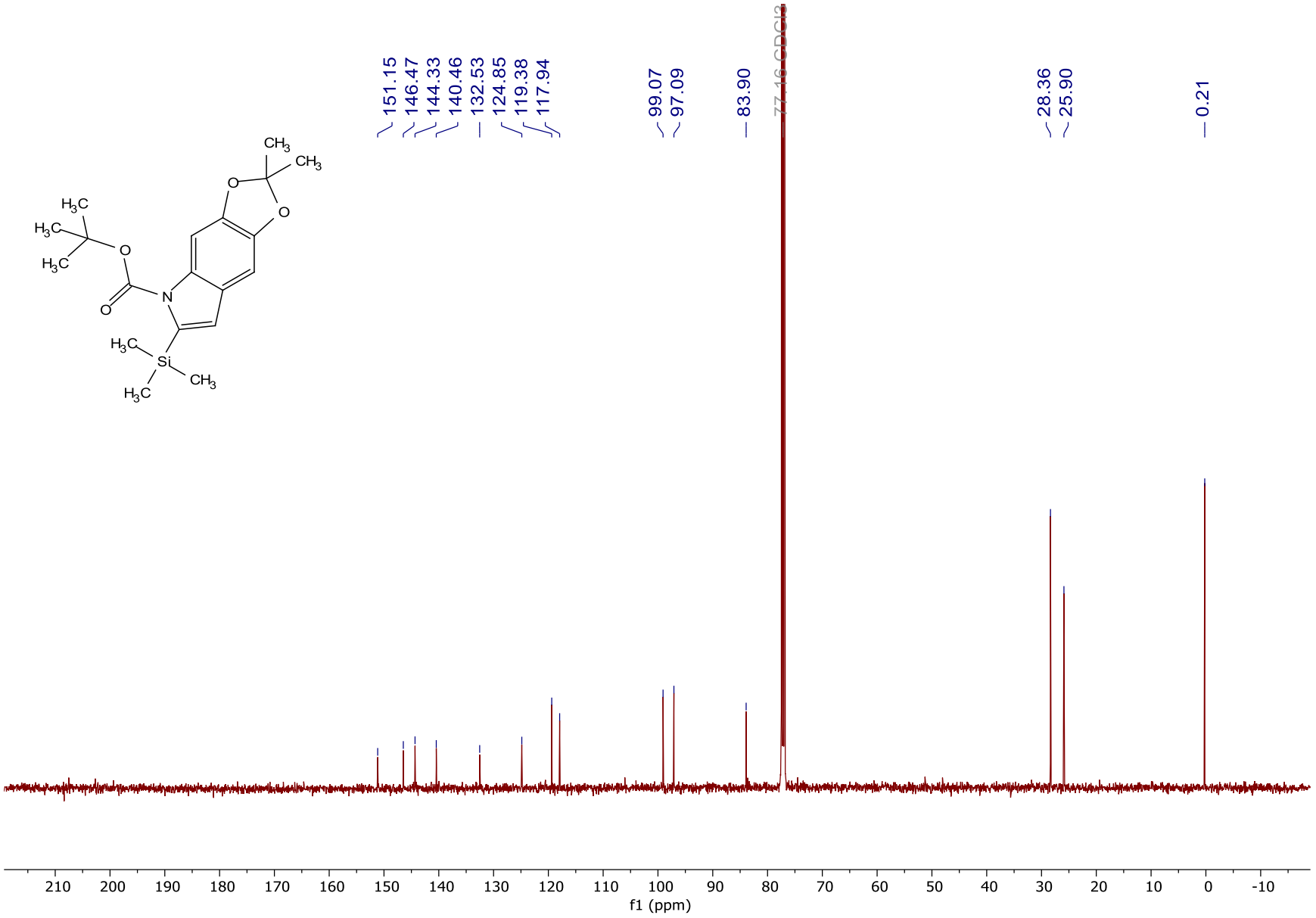
151.15
146.47
144.33
140.46
132.53
124.85
119.38
117.94
99.07
97.09
83.90
77.16 CDCl3
28.36
25.90
0.21
f1 (ppm)

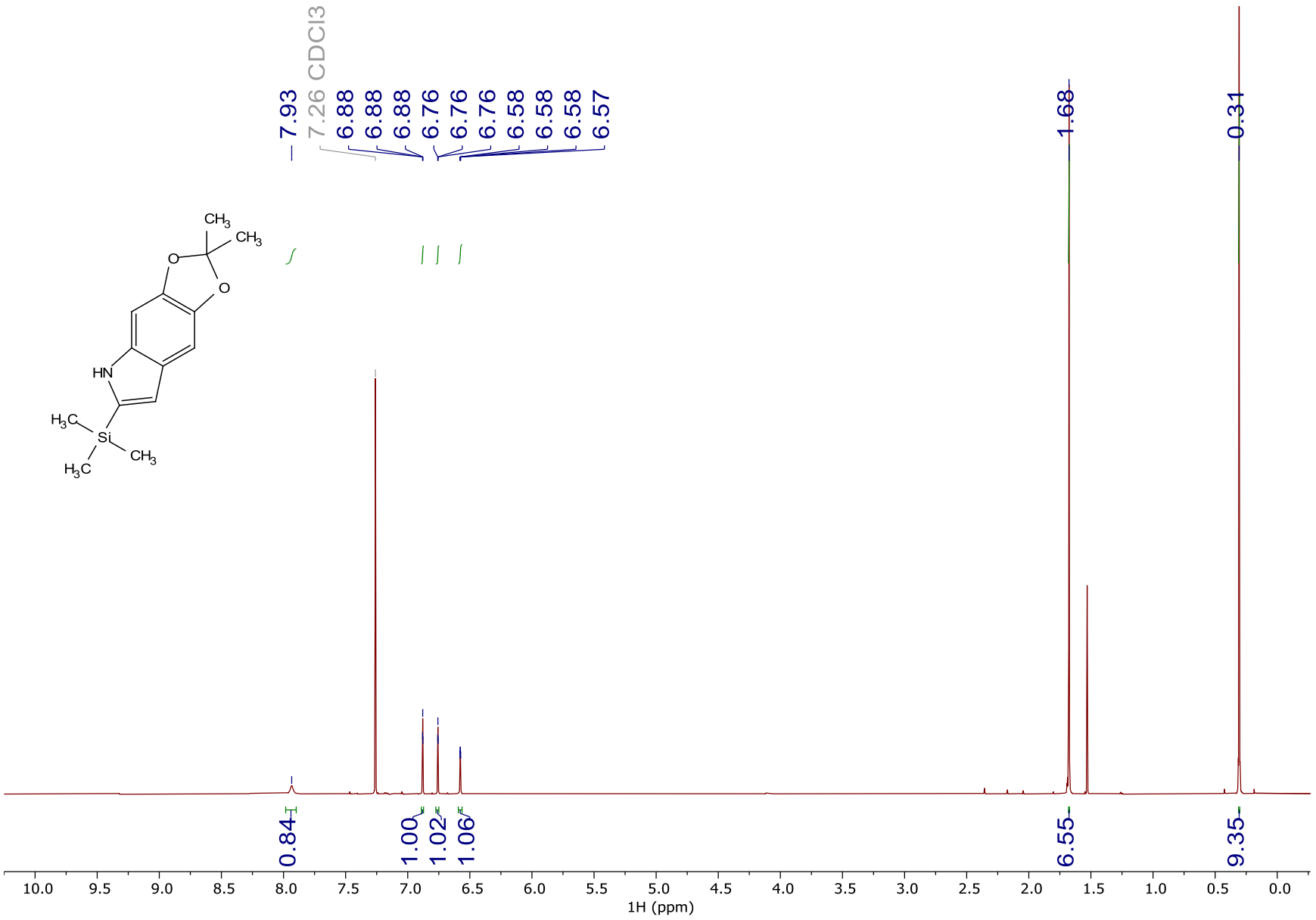
7.93
7.26 CDCl3
6.88
6.88
6.88
6.76
6.76
6.76
6.58
6.58
6.58
6.57
1.68
0.31
CH3
CH3
O
O
HN
H3C
Si
CH3
H3C
0.84
1.00
1.02
1.06
6.55
9.35
10.0 9.5 9.0 8.5 8.0 7.5 7.0 6.5 6.0 5.5 5.0 4.5 4.0 3.5 3.0 2.5 2.0 1.5 1.0 0.5 0.0
1H (ppm)

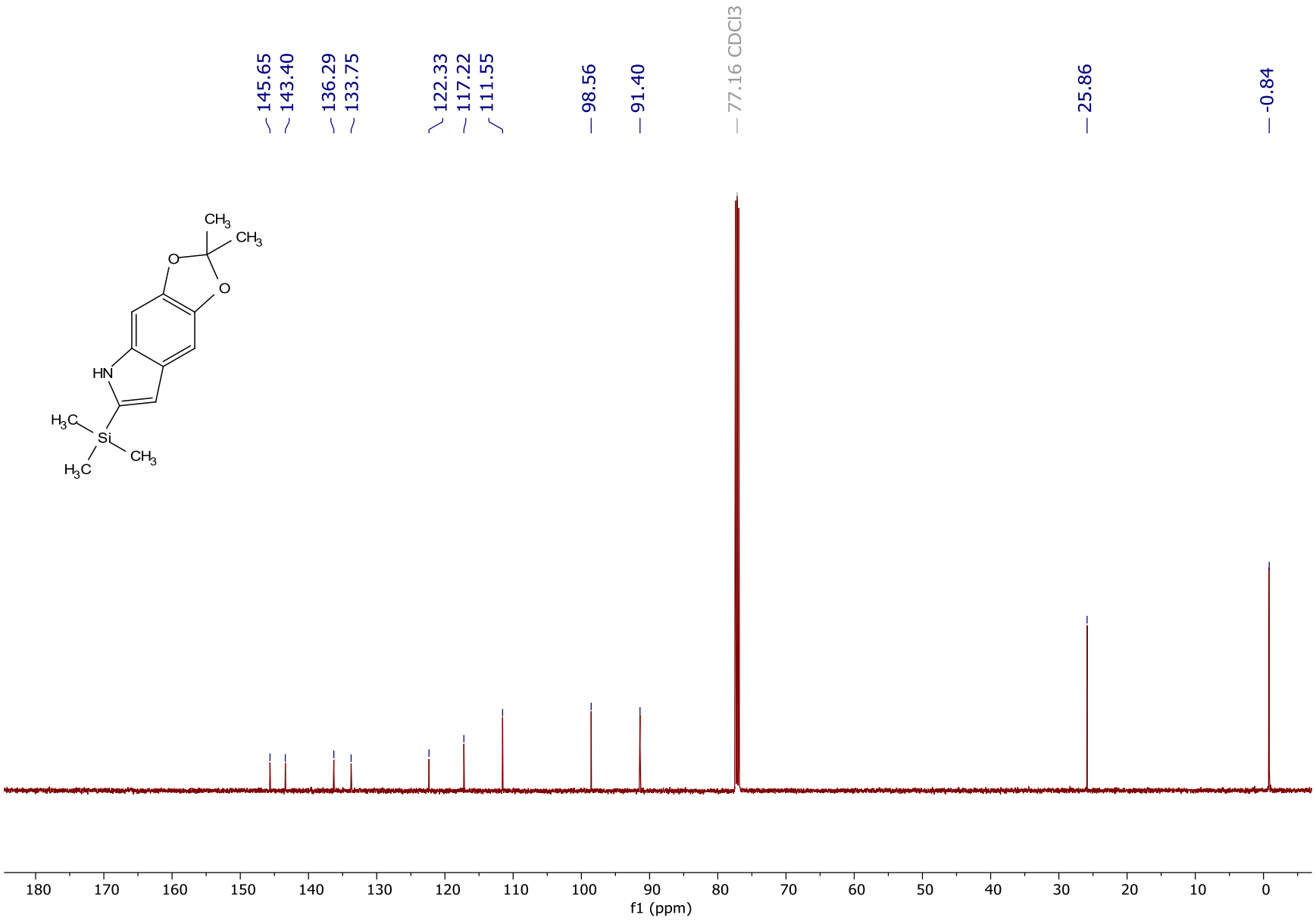
145.65
143.40
136.29
133.75
122.33
117.22
111.55
98.56
91.40
77.16 CDCl3
25.86
-0.84
CH3
CH3
O
O
HN
H3C
Si
CH3
H3C
180
170
160
150
140
130
120
110
100
90
80
70
60
50
40
30
20
10
0
f1 (ppm)

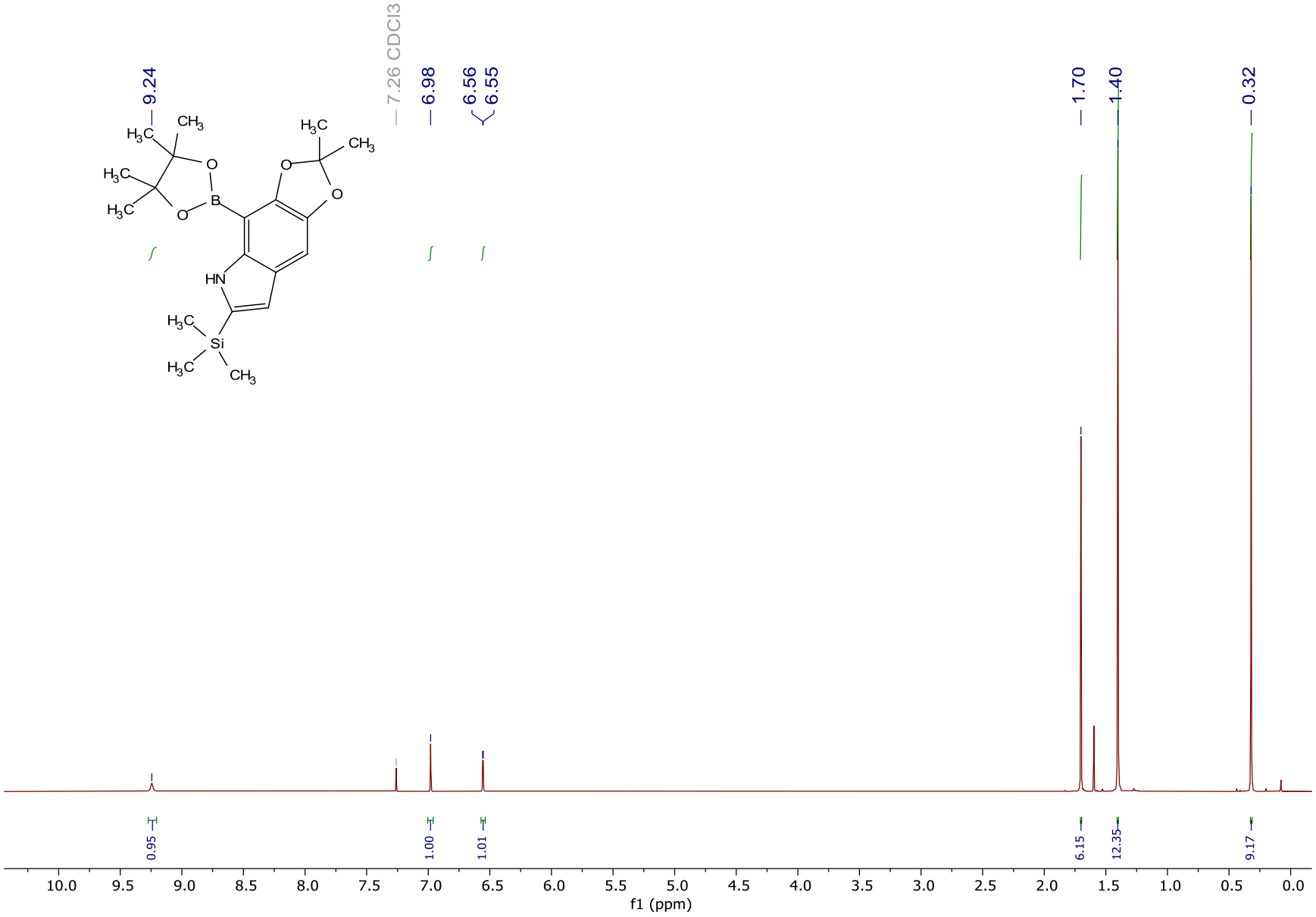
9.24
7.26 CDCl3
6.98
6.56
6.55
1.70
1.40
0.32
0.95
1.00
1.01
6.15
12.35
9.17
f1 (ppm)

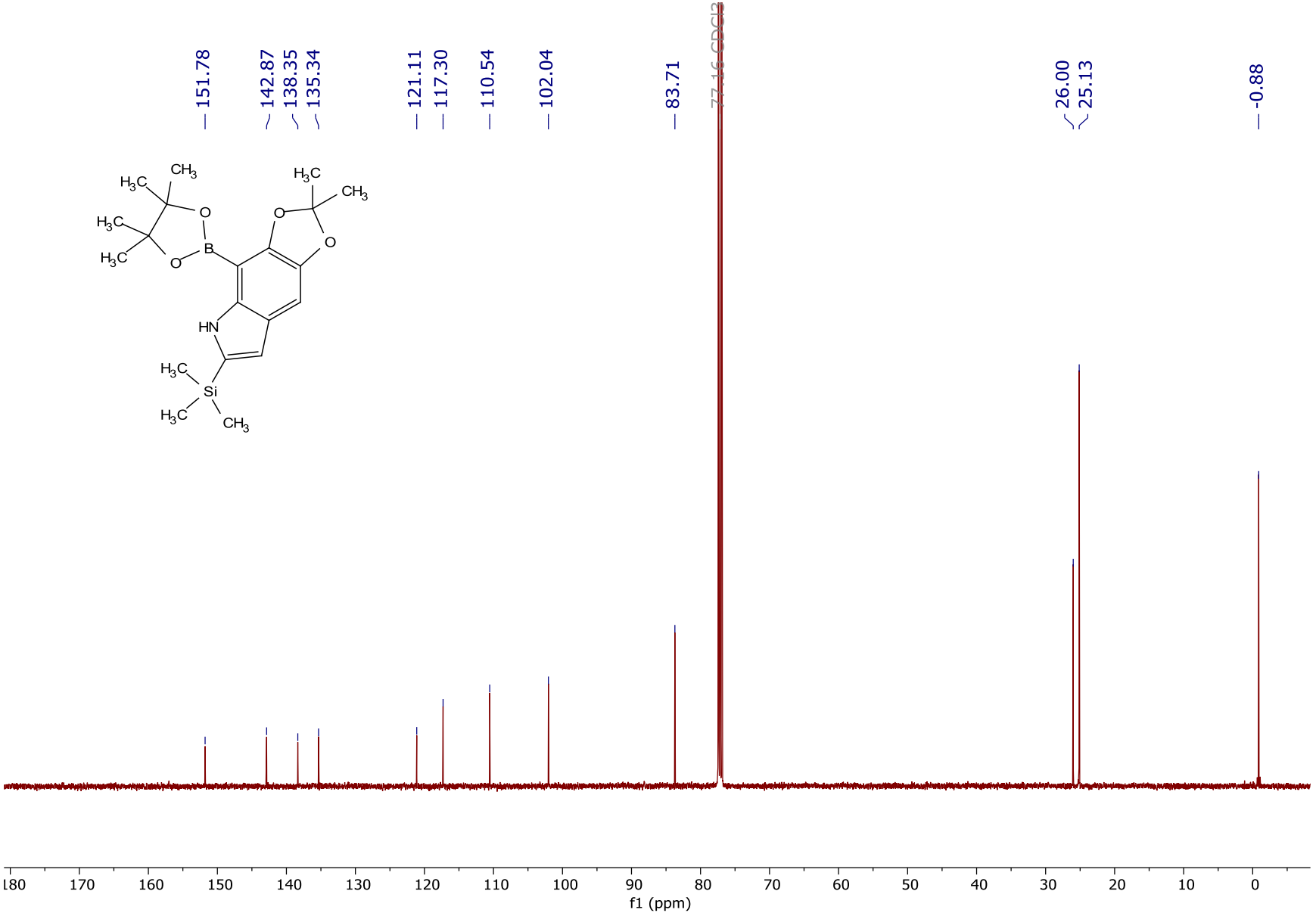
151.78
142.87
138.35
135.34
121.11
117.30
110.54
102.04
83.71
77.16 CDCl3
26.00
25.13
-0.88
f1 (ppm)

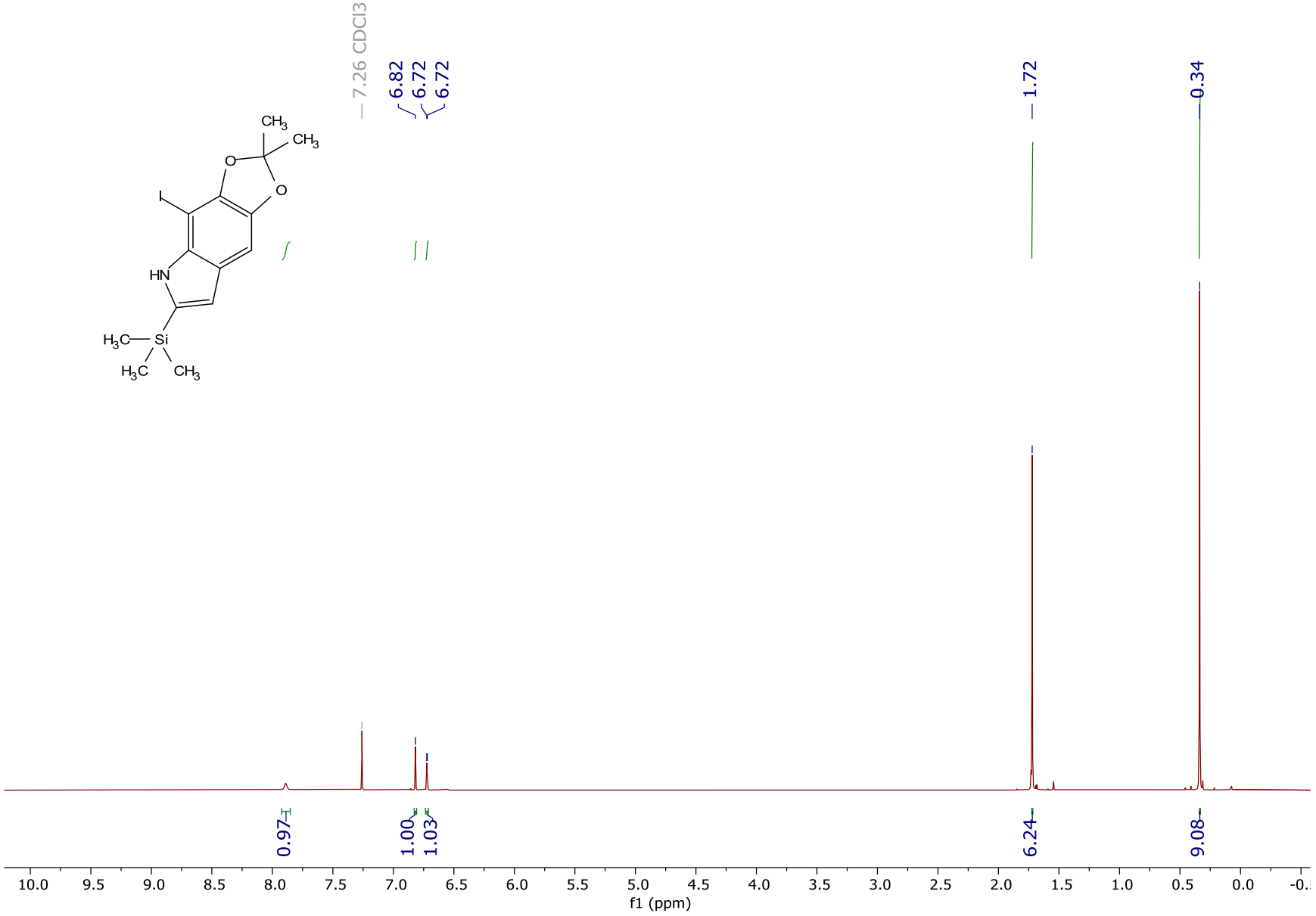
7.26 CDCl3
6.82
6.72
6.72
1.72
0.34
CH3
CH3
O
O
I
HN
H3C
Si
H3C
CH3
0.97
1.00
1.03
6.24
9.08
10.0
9.5
9.0
8.5
8.0
7.5
7.0
6.5
6.0
5.5
5.0
4.5
4.0
3.5
3.0
2.5
2.0
1.5
1.0
0.5
0.0
f1 (ppm)

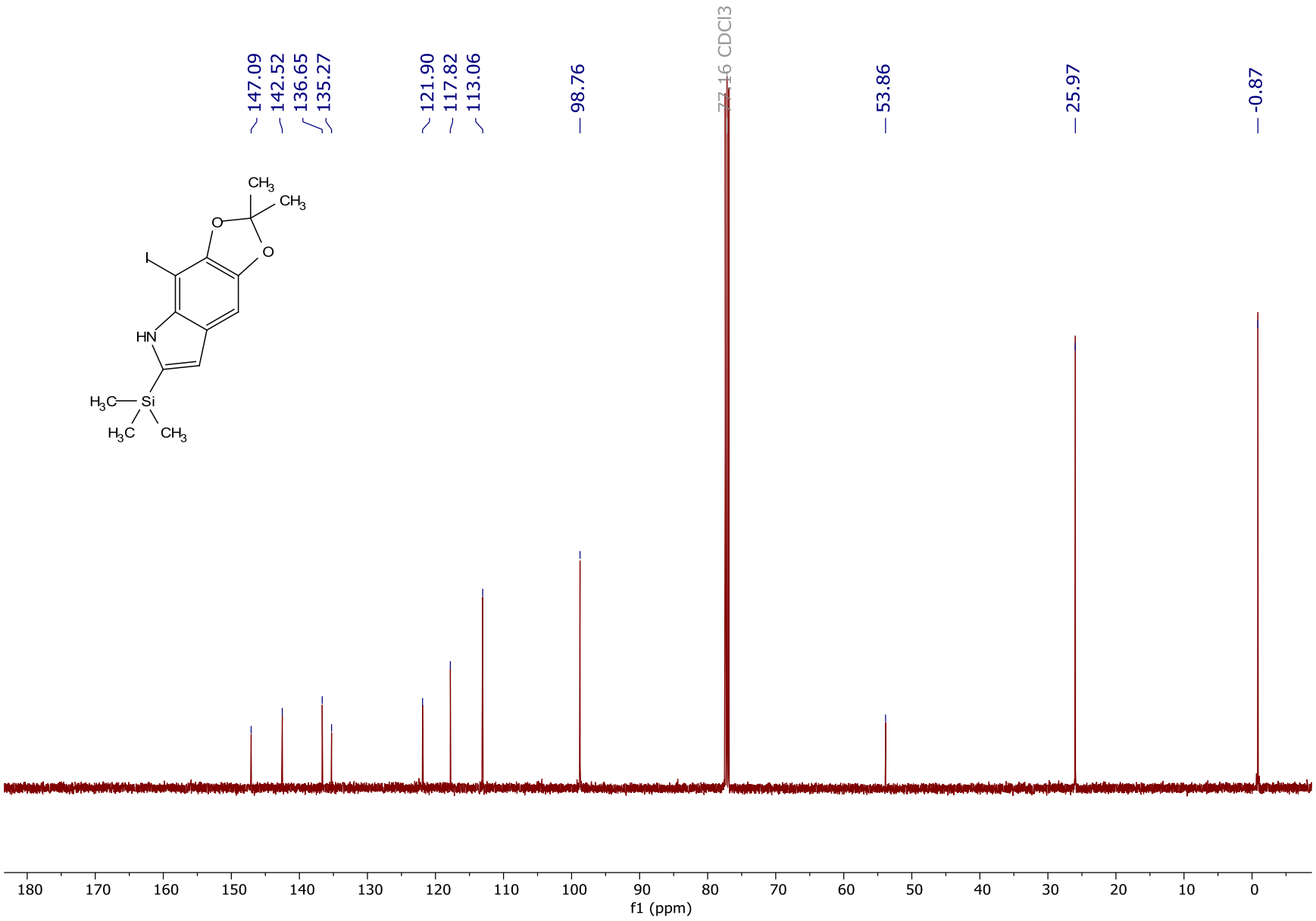
147.09
142.52
136.65
135.27
121.90
117.82
113.06
98.76
77.16 CDCl3
53.86
25.97
-0.87
CH3
CH3
O
O
I
HN
H3C
Si
H3C
CH3
180
170
160
150
140
130
120
110
100
90
80
70
60
50
40
30
20
10
0
f1 (ppm)

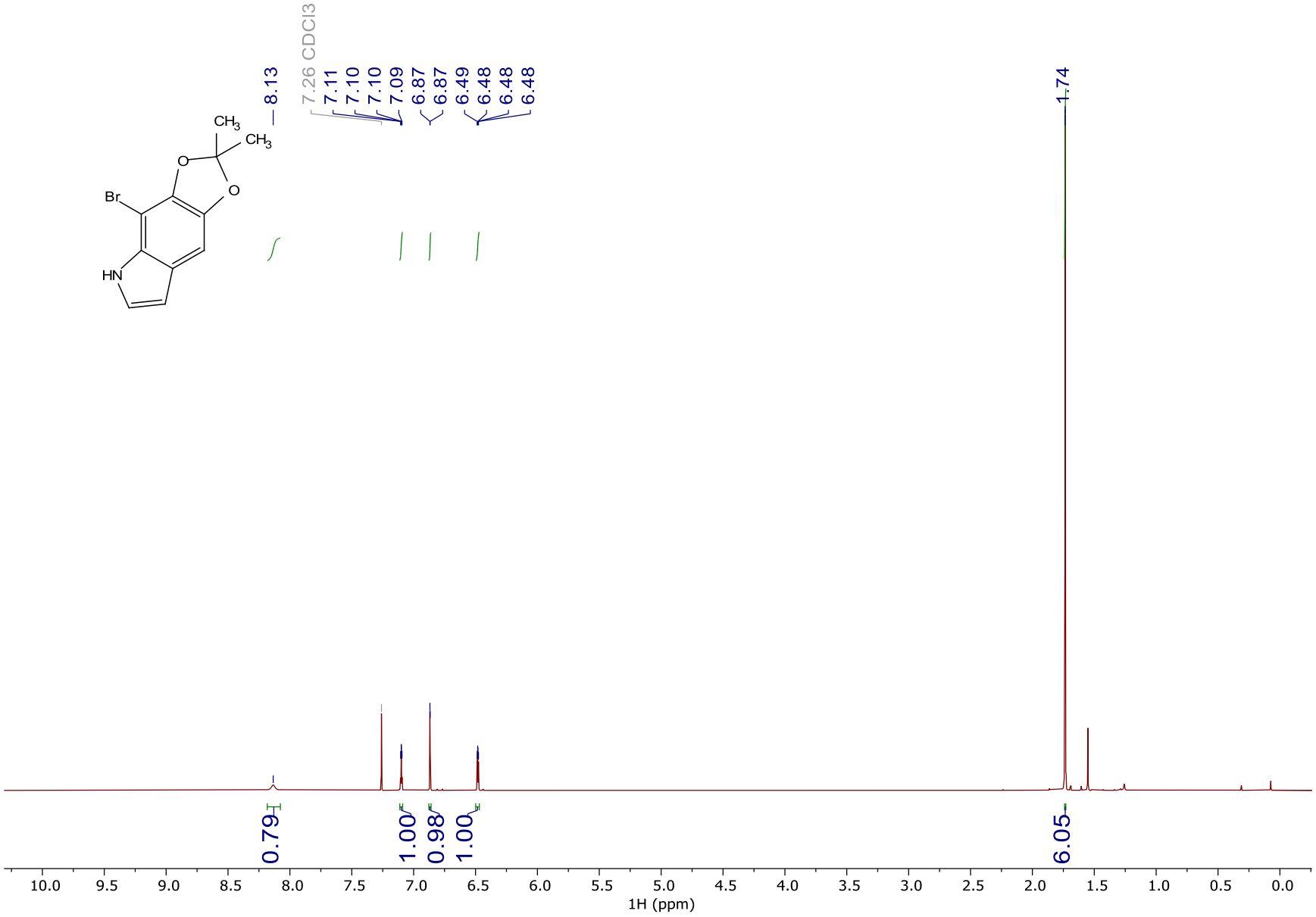
8.13
7.26 CDCl3
7.11
7.10
7.10
7.09
6.87
6.87
6.49
6.48
6.48
6.48
1.74
CH3
CH3
O
O
Br
HN
0.79
1.00
0.98
1.00
6.05
10.0
9.5
9.0
8.5
8.0
7.5
7.0
6.5
6.0
5.5
5.0
4.5
4.0
3.5
3.0
2.5
2.0
1.5
1.0
0.5
0.0
1H (ppm)

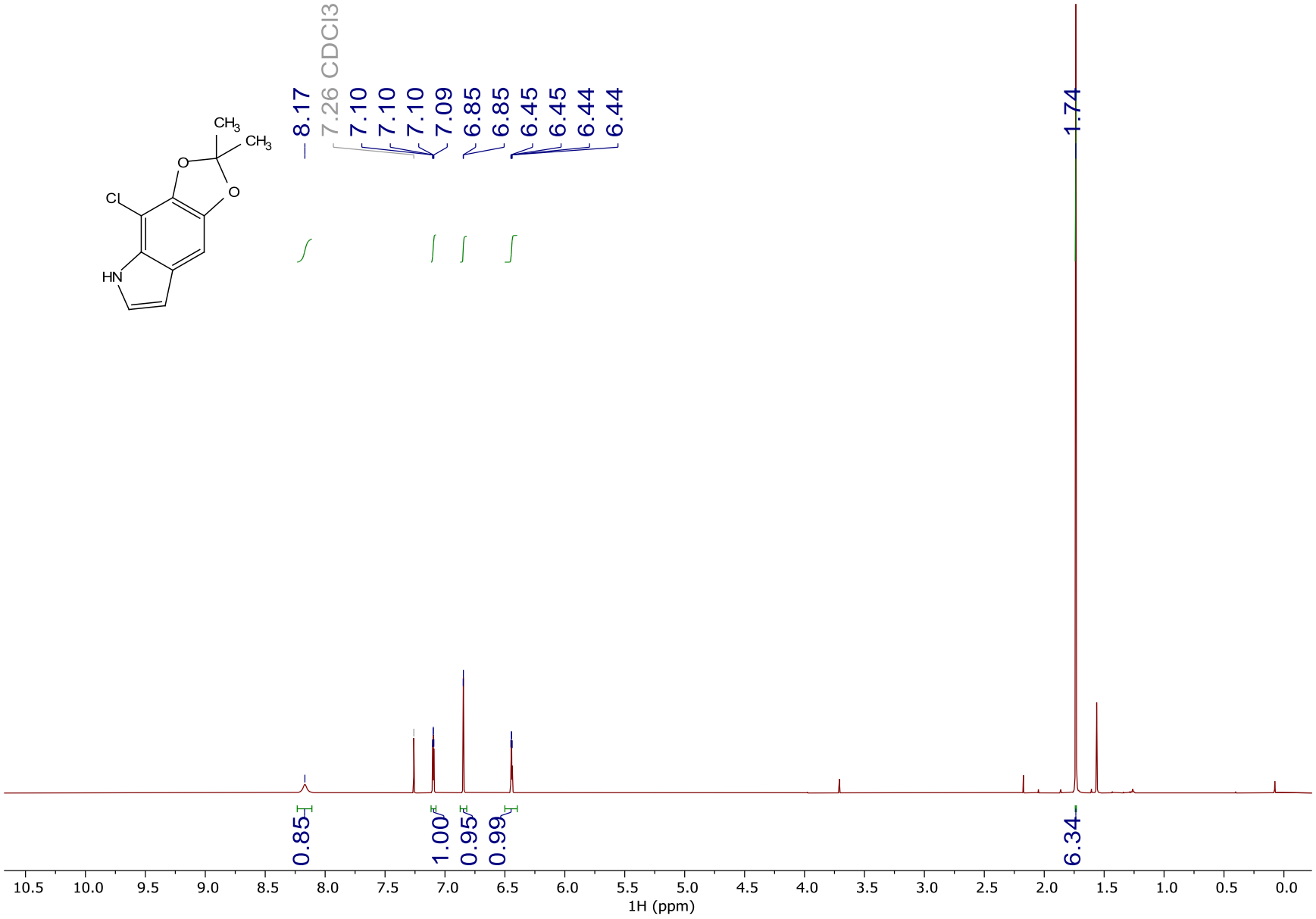
CH3
CH3
O
O
Cl
HN
8.17
7.26 CDCl3
7.10
7.10
7.10
7.09
6.85
6.85
6.45
6.45
6.44
6.44
1.74
0.85
1.00
0.95
0.99
6.34
10.5 10.0 9.5 9.0 8.5 8.0 7.5 7.0 6.5 6.0 5.5 5.0 4.5 4.0 3.5 3.0 2.5 2.0 1.5 1.0 0.5 0.0
1H (ppm)

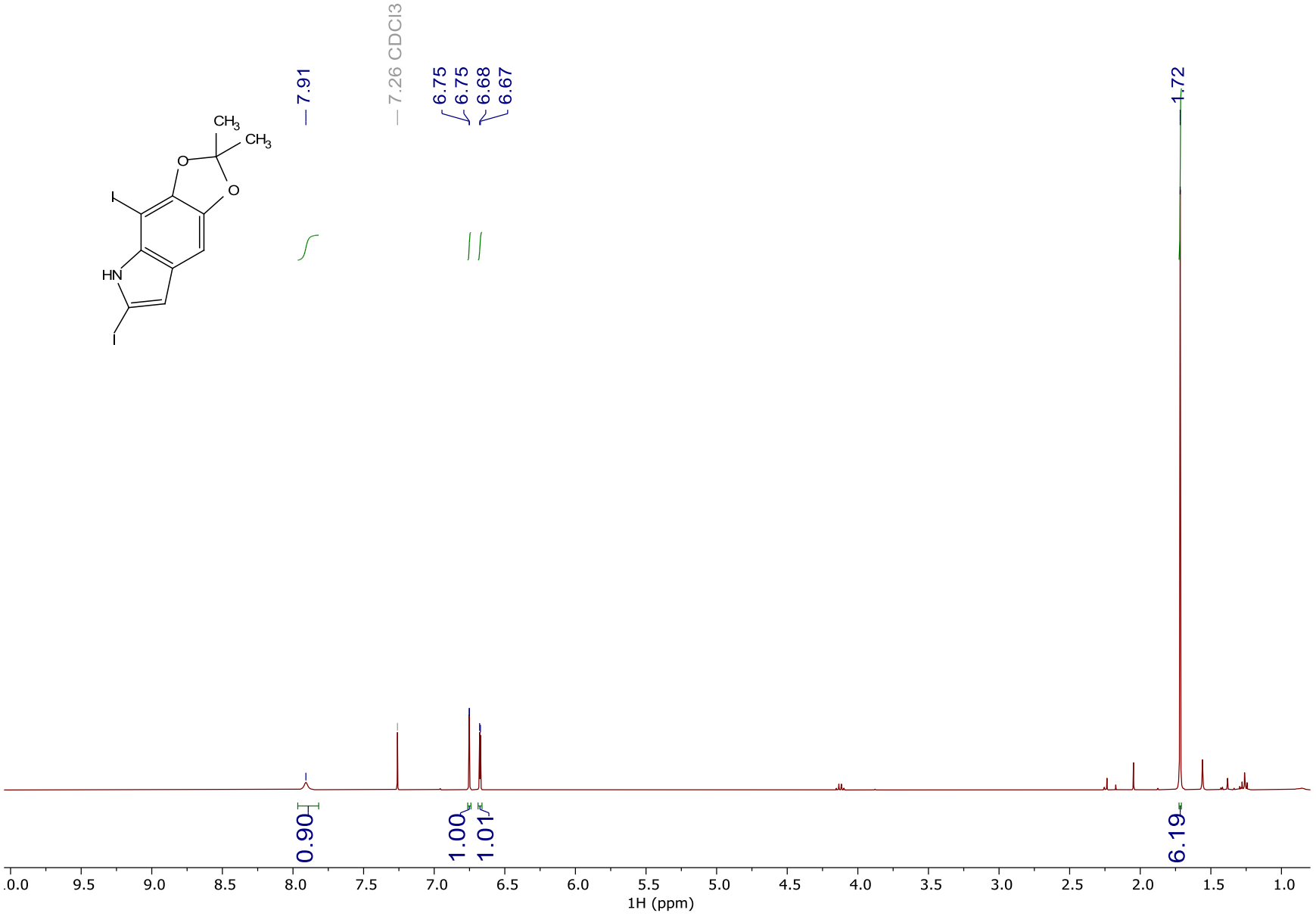
7.91
7.26 CDCl3
6.75
6.75
6.68
6.67
1.72
CH3
CH3
O
O
I
HN
I
0.90
1.00
1.01
6.19
1H (ppm)

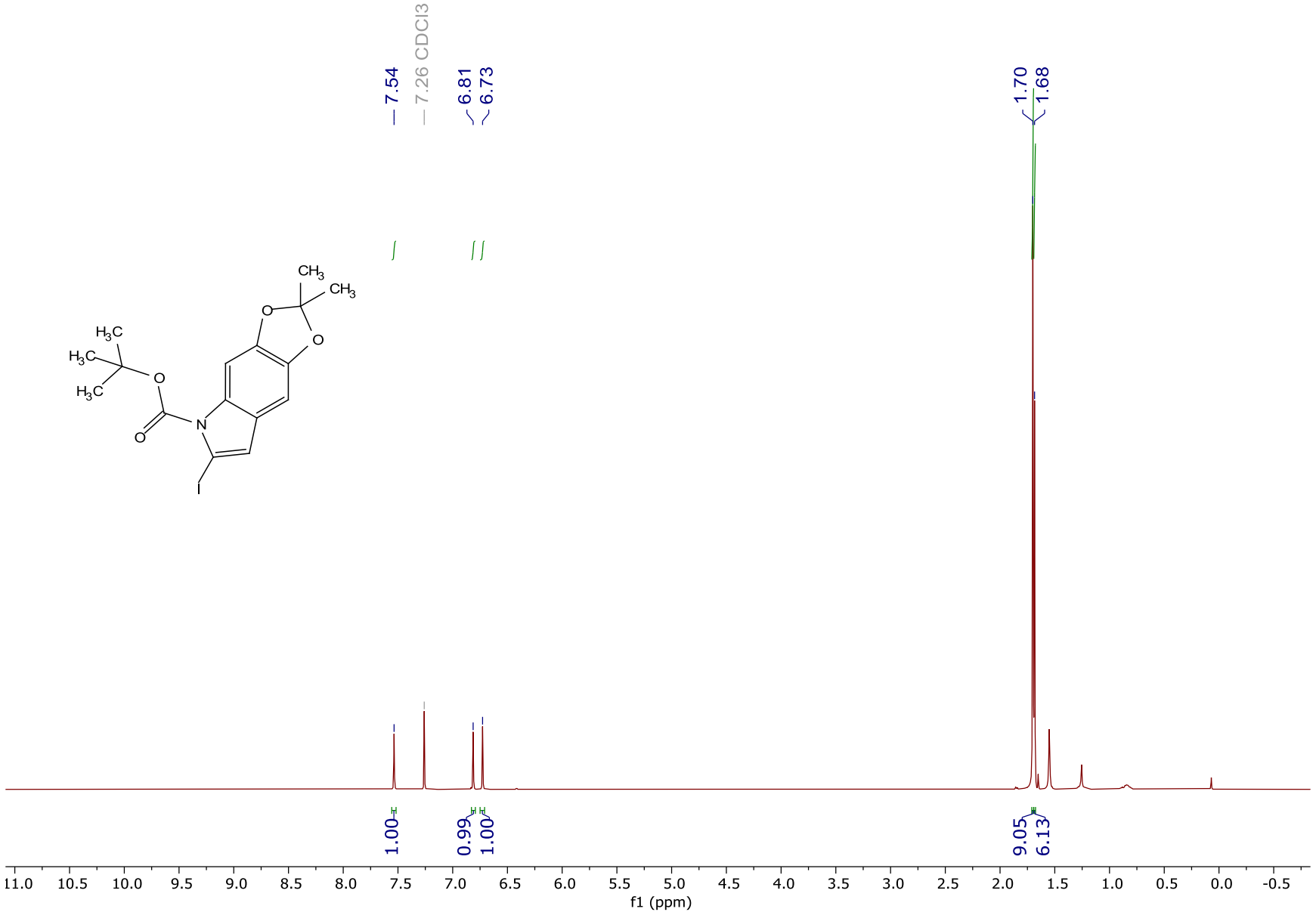
7.54
7.26 CDCl3
6.81
6.73
1.70
1.68
1.00
0.99
1.00
9.05
6.13
f1 (ppm)

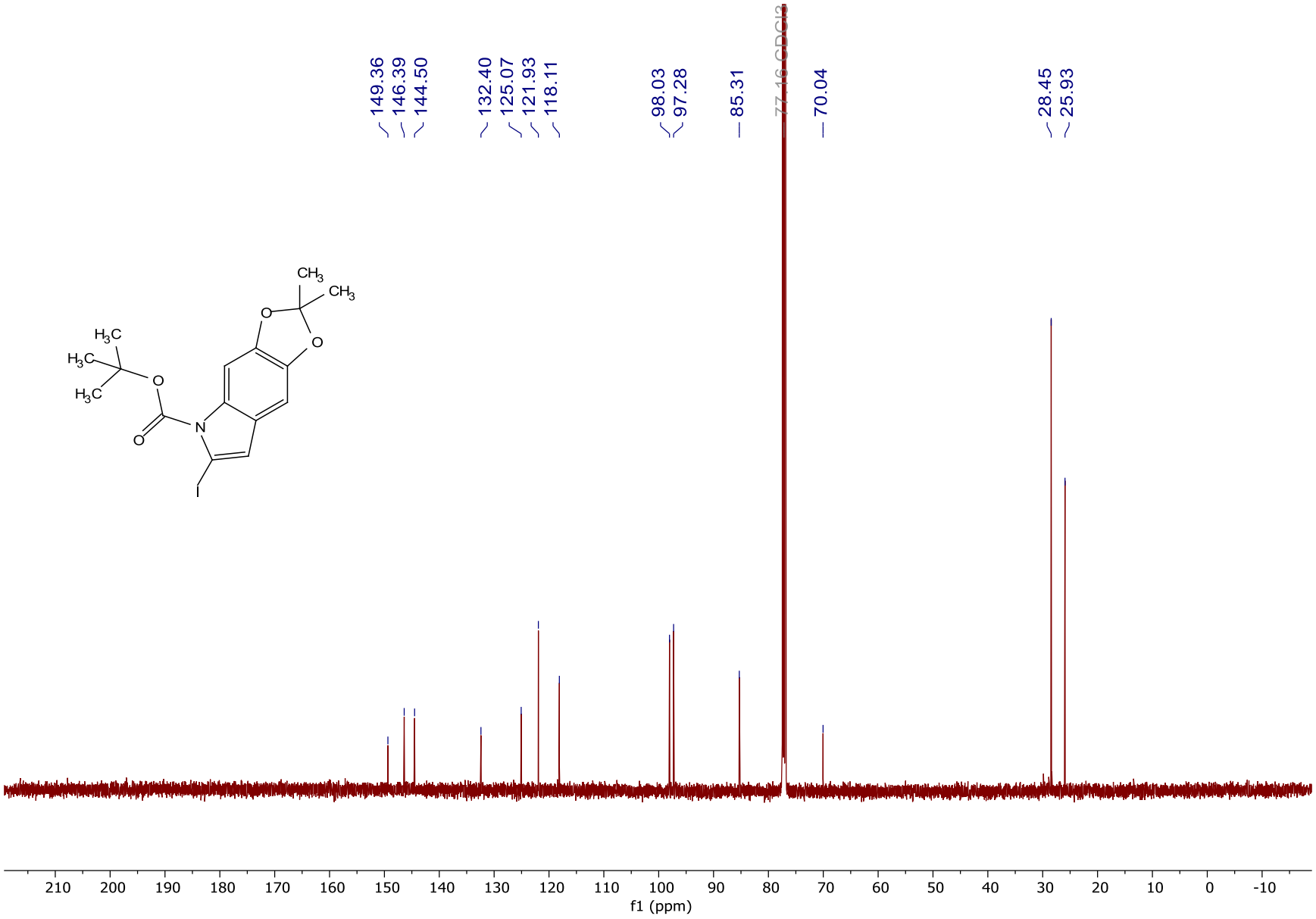
149.36
146.39
144.50
132.40
125.07
121.93
118.11
98.03
97.28
85.31
77.16 CDCl3
70.04
28.45
25.93
CH3
CH3
H3C
H3C
H3C
O
O
O
O
N
O
I
210
200
190
180
170
160
150
140
130
120
110
100
90
80
70
60
50
40
30
20
10
0
-10
f1 (ppm)

Appendix:

^{1}H and ^{13}C NMR Spectra Relevant to **Chapter 3**

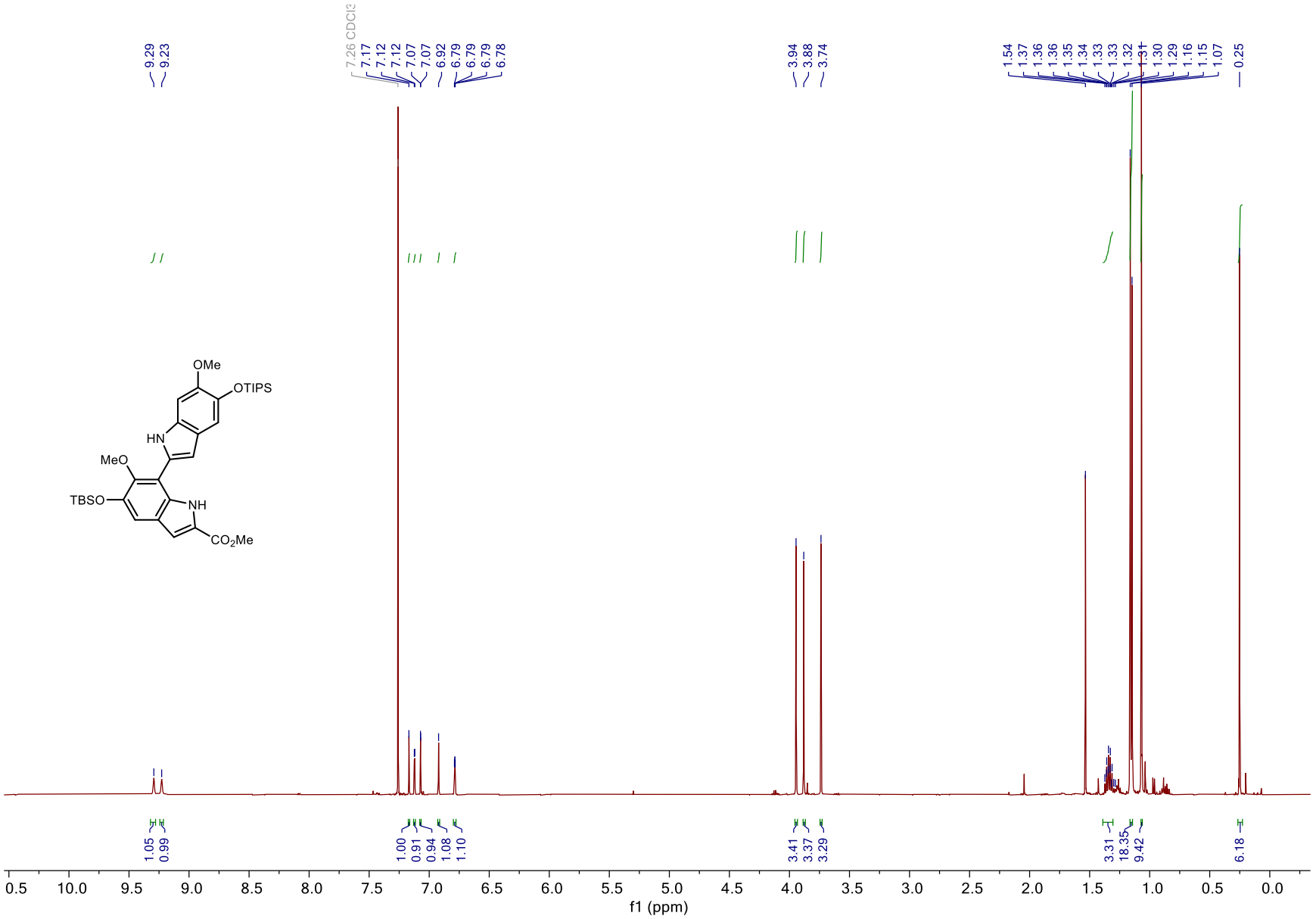
9.29
9.23
7.26 CDCl3
7.17
7.12
7.12
7.07
7.07
6.92
6.79
6.79
6.79
6.78
3.94
3.88
3.74
1.54
1.37
1.36
1.36
1.35
1.34
1.33
1.33
1.32
1.31
1.30
1.29
1.16
1.15
1.07
0.25
OMe
OTIPS
HN
MeO
TBSO
NH
CO2Me
1.05
0.99
1.00
0.91
0.94
1.08
1.10
3.41
3.37
3.29
3.31
18.35
9.42
6.18
f1 (ppm)

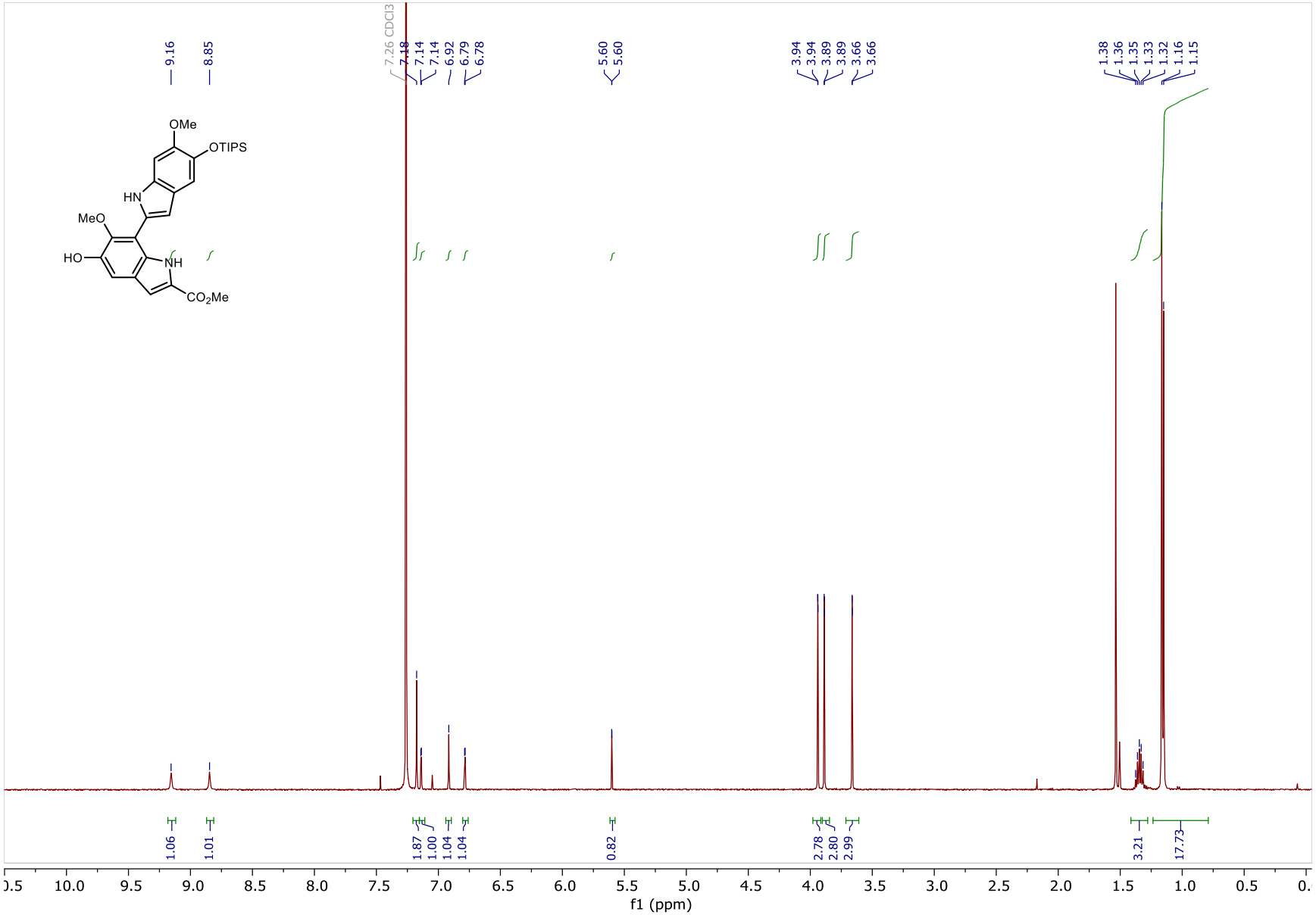
9.16
8.85
7.26 CDCl3
7.18
7.14
7.14
6.92
6.79
6.78
5.60
5.60
3.94
3.94
3.89
3.89
3.66
3.66
1.38
1.36
1.35
1.33
1.32
1.16
1.15
OMe
OTIPS
HN
MeO
HO
NH
CO2Me
1.06
1.01
1.87
1.00
1.04
1.04
0.82
2.78
2.80
2.99
3.21
17.73
f1 (ppm)

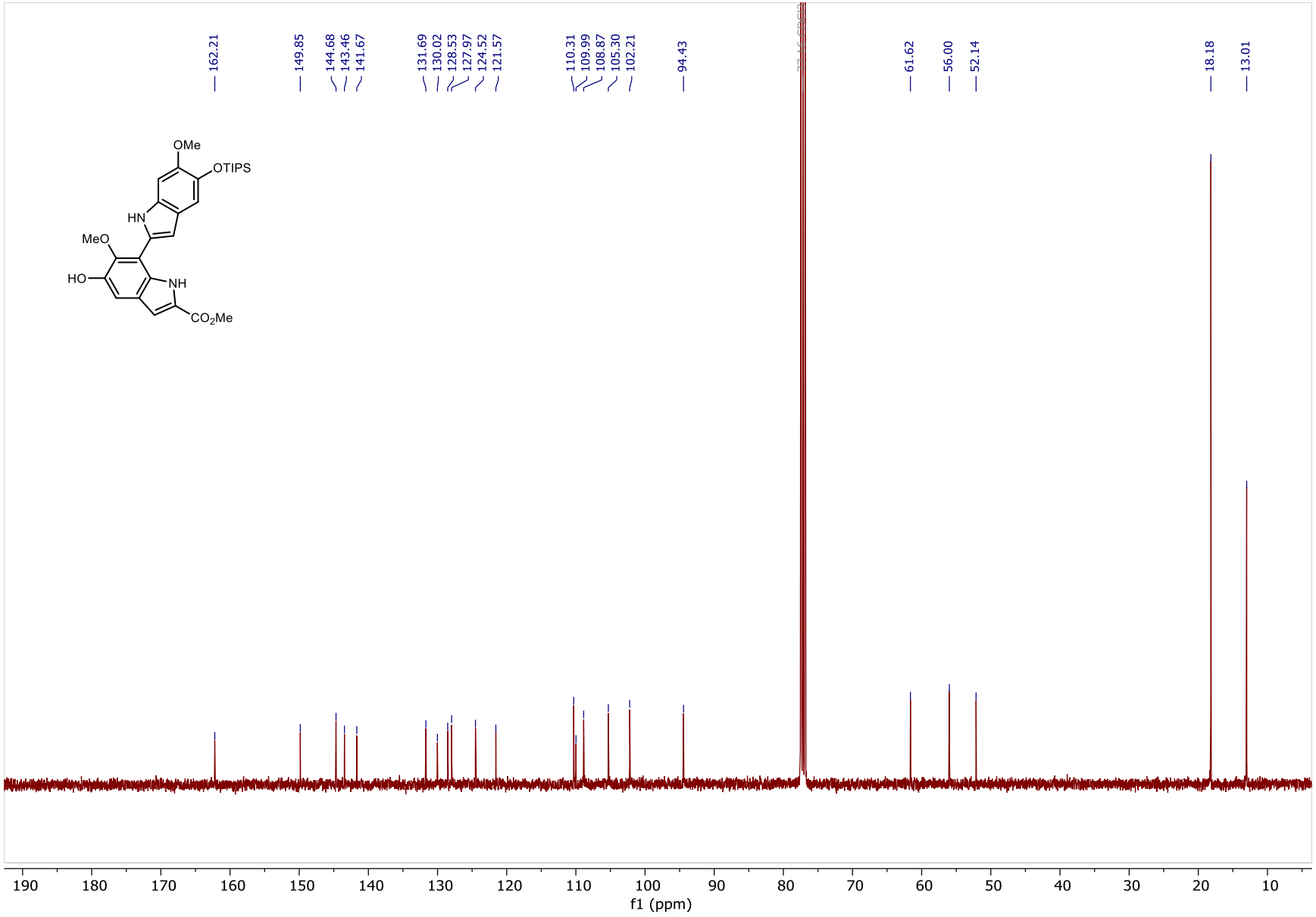
162.21
149.85
144.68
143.46
141.67
131.69
130.02
128.53
127.97
124.52
121.57
110.31
109.99
108.87
105.30
102.21
94.43
61.62
56.00
52.14
18.18
13.01
OMe
OTIPS
HN
MeO
HO
NH
CO2Me
190
180
170
160
150
140
130
120
110
100
90
80
70
60
50
40
30
20
10
f1 (ppm)

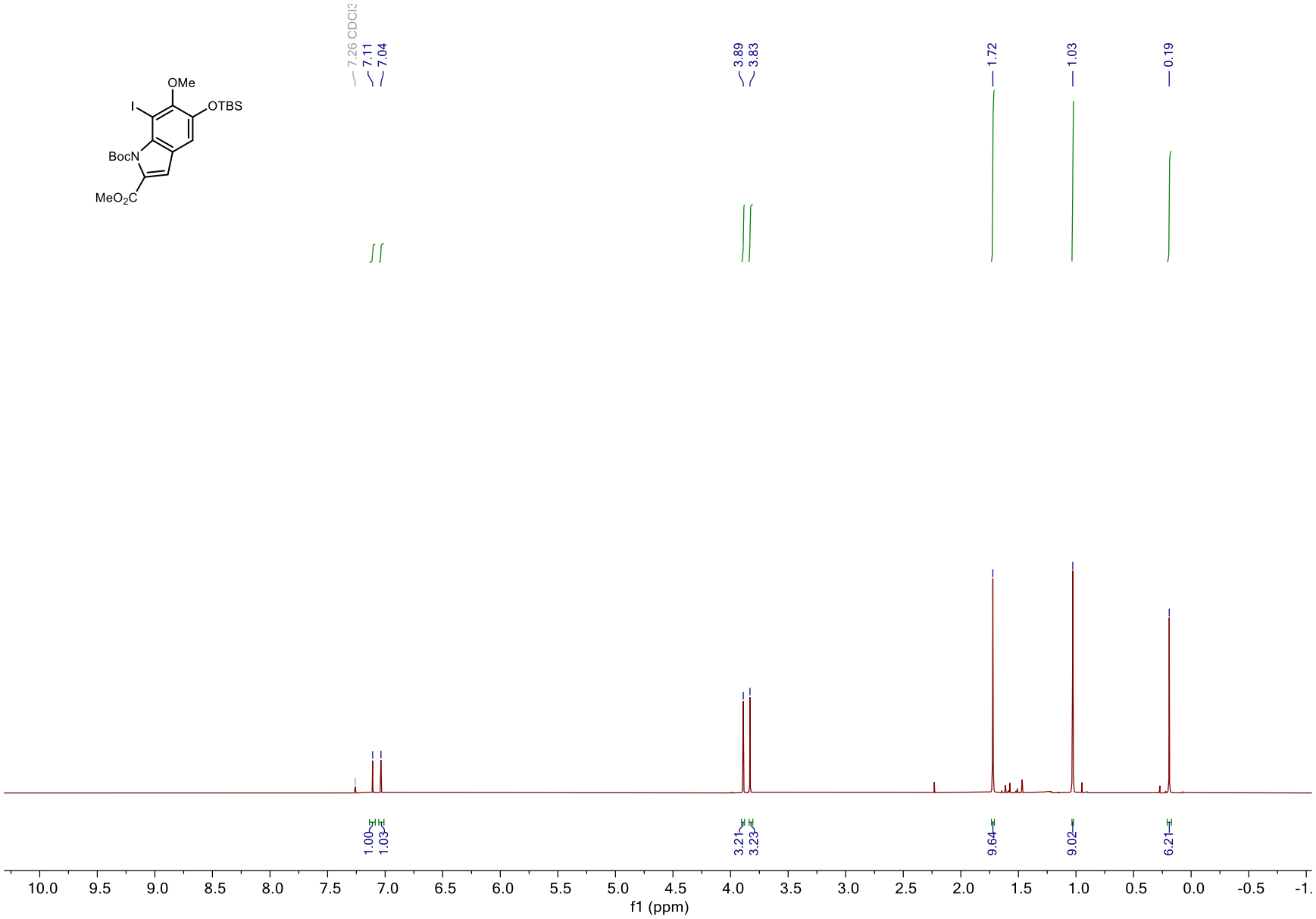
OMe
I
OTBS
BocN
MeO2C
7.26 CDCl3
7.11
7.04
3.89
3.83
1.72
1.03
0.19
1.00
1.03
3.21
3.23
9.64
9.02
6.21
10.0 9.5 9.0 8.5 8.0 7.5 7.0 6.5 6.0 5.5 5.0 4.5 4.0 3.5 3.0 2.5 2.0 1.5 1.0 0.5 0.0 -0.5 -1.
f1 (ppm)

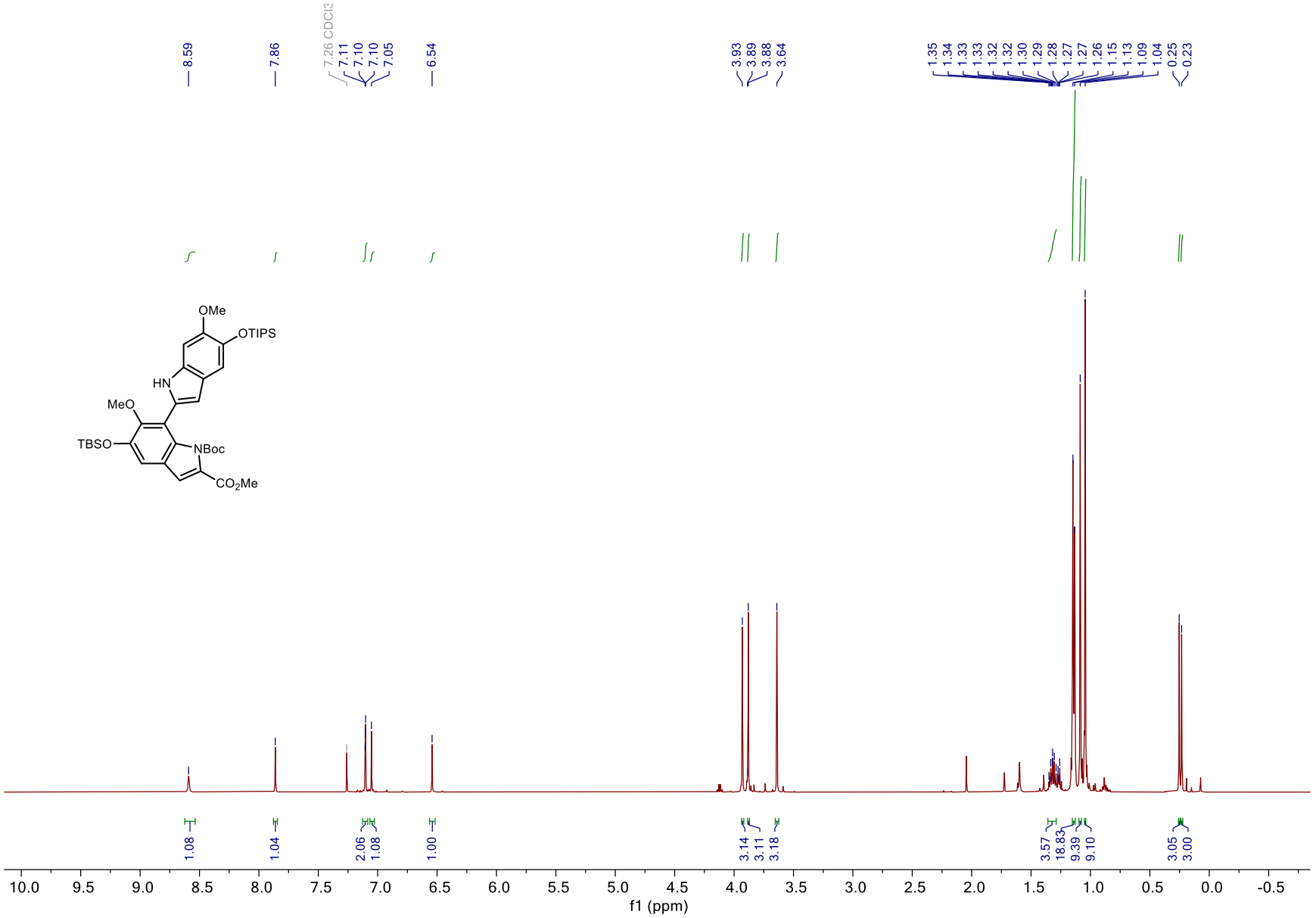
8.59
7.86
7.26 CDCl3
7.11
7.10
7.10
7.05
6.54
3.93
3.89
3.88
3.64
1.35
1.34
1.33
1.33
1.32
1.32
1.30
1.29
1.28
1.27
1.27
1.26
1.15
1.13
1.09
1.04
0.25
0.23
OMe
OTIPS
HN
MeO
TBSO
NBoc
CO2Me
1.08
1.04
2.06
1.08
1.00
3.14
3.11
3.18
3.57
18.83
9.39
9.10
3.05
3.00
10.0
9.5
9.0
8.5
8.0
7.5
7.0
6.5
6.0
5.5
5.0
4.5
4.0
3.5
3.0
2.5
2.0
1.5
1.0
0.5
0.0
-0.5
f1 (ppm)

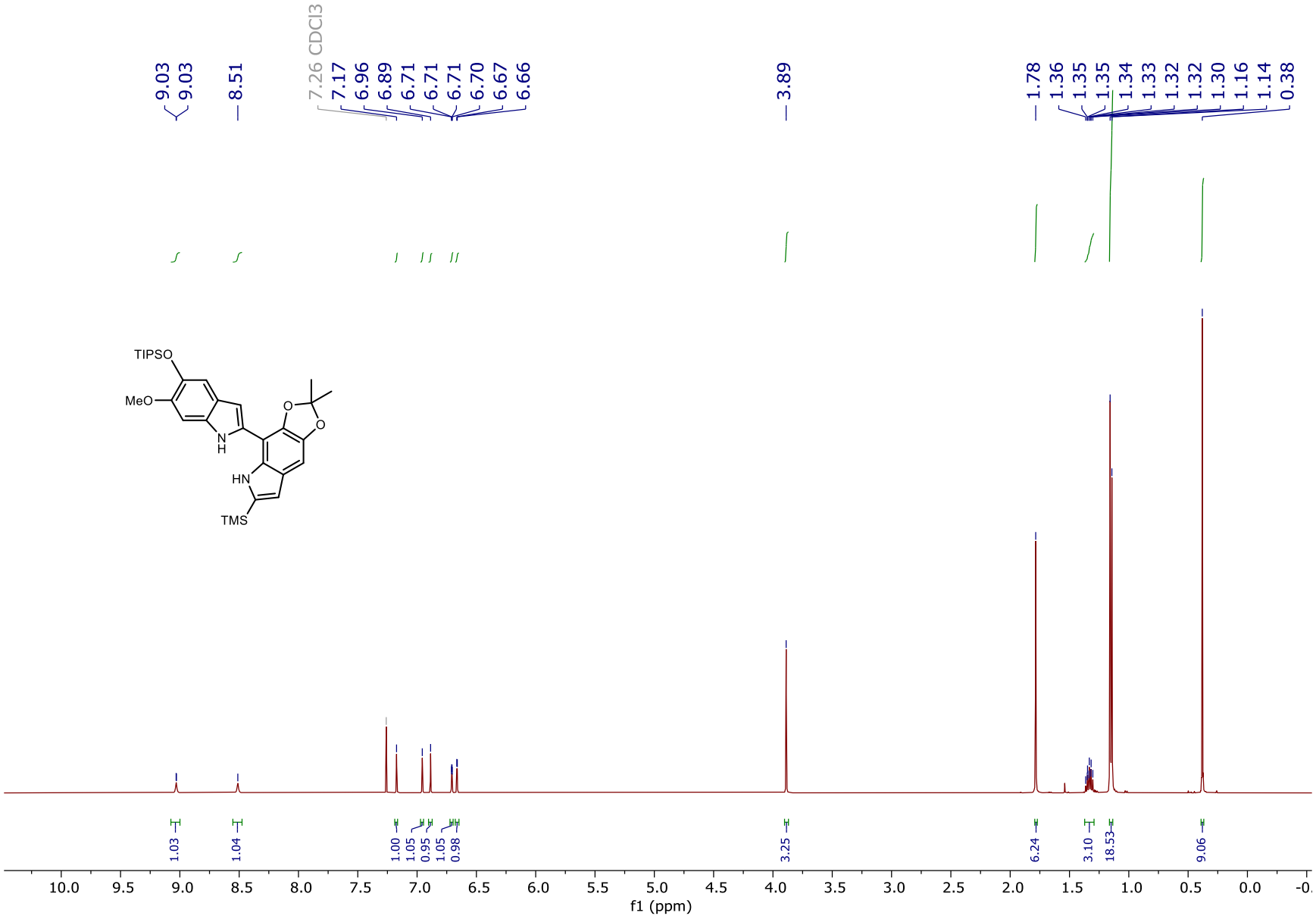
9.03
9.03
8.51
7.26 CDCl3
7.17
6.96
6.89
6.71
6.71
6.71
6.70
6.67
6.66
3.89
1.78
1.36
1.35
1.35
1.34
1.33
1.32
1.32
1.30
1.16
1.14
0.38
TIPSO
MeO
N
H
O
O
HN
TMS
1.03
1.04
1.00
1.05
0.95
1.05
0.98
3.25
6.24
3.10
18.53
9.06
10.0
9.5
9.0
8.5
8.0
7.5
7.0
6.5
6.0
5.5
5.0
4.5
4.0
3.5
3.0
2.5
2.0
1.5
1.0
0.5
0.0
f1 (ppm)

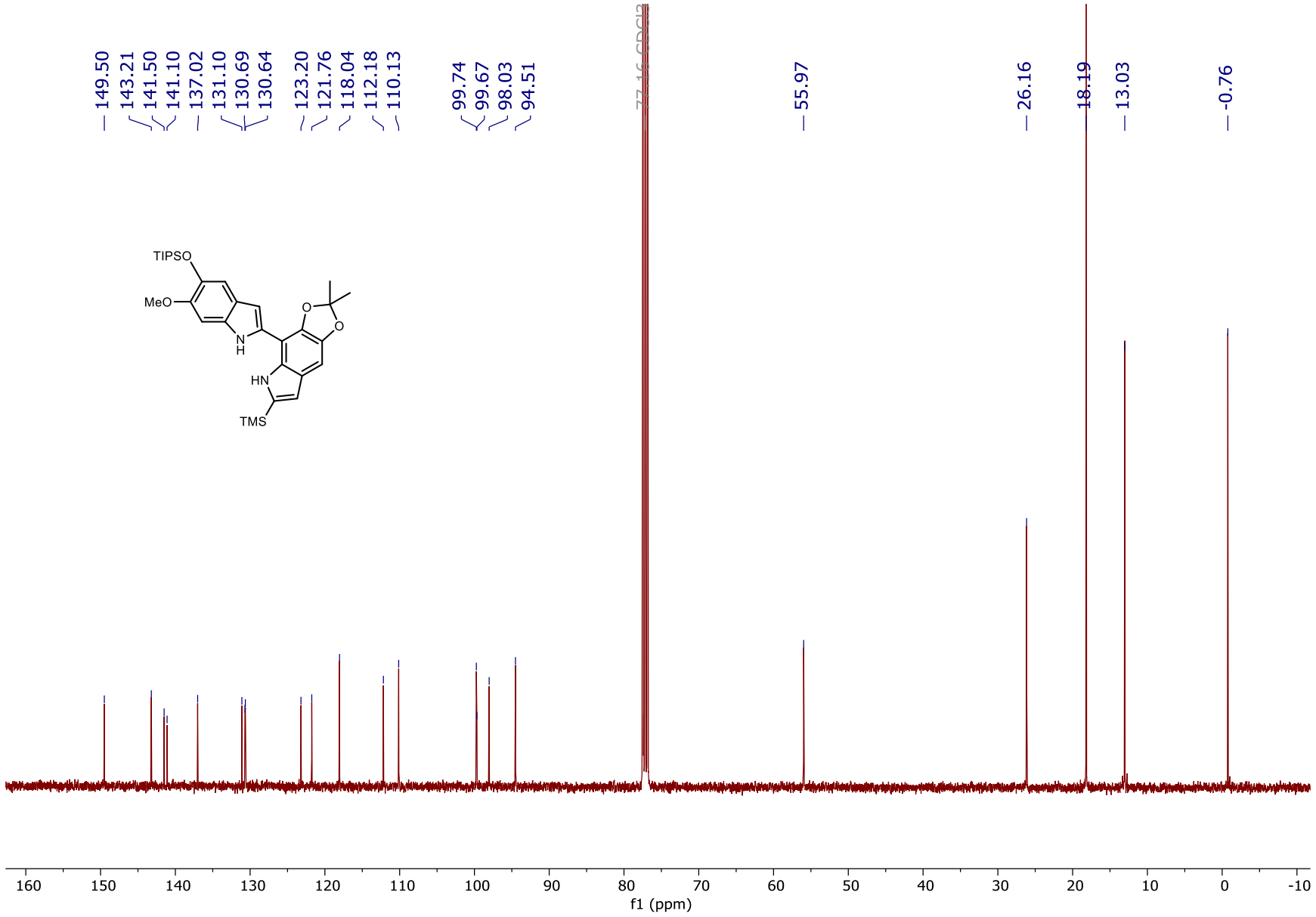
149.50
143.21
141.50
141.10
137.02
131.10
130.69
130.64
123.20
121.76
118.04
112.18
110.13
99.74
99.67
98.03
94.51
77.16 CDCl3
55.97
26.16
18.19
13.03
-0.76
TIPSO
MeO
N
H
O
O
HN
TMS
160
150
140
130
120
110
100
90
80
70
60
50
40
30
20
10
0
-10
f1 (ppm)

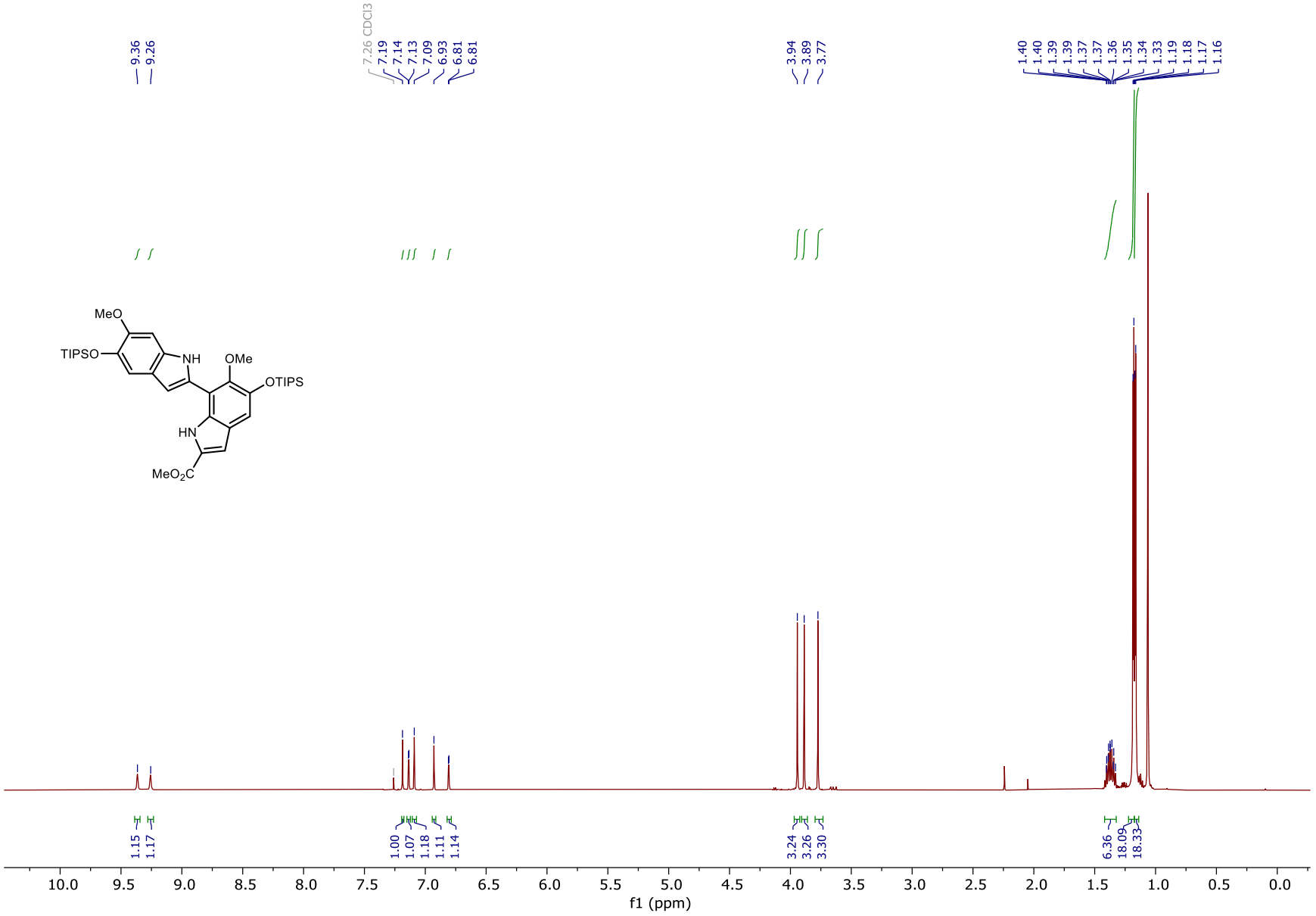
9.36
9.26
7.26 CDCl3
7.19
7.14
7.13
7.09
6.93
6.81
6.81
3.94
3.89
3.77
1.40
1.40
1.39
1.39
1.37
1.37
1.36
1.35
1.34
1.33
1.19
1.18
1.17
1.16
MeO
TIPSO
NH
OMe
OTIPS
HN
MeO2C
1.15
1.17
1.00
1.07
1.18
1.11
1.14
3.24
3.26
3.30
6.36
18.09
18.33
10.0
9.5
9.0
8.5
8.0
7.5
7.0
6.5
6.0
5.5
5.0
4.5
4.0
3.5
3.0
2.5
2.0
1.5
1.0
0.5
0.0
f1 (ppm)

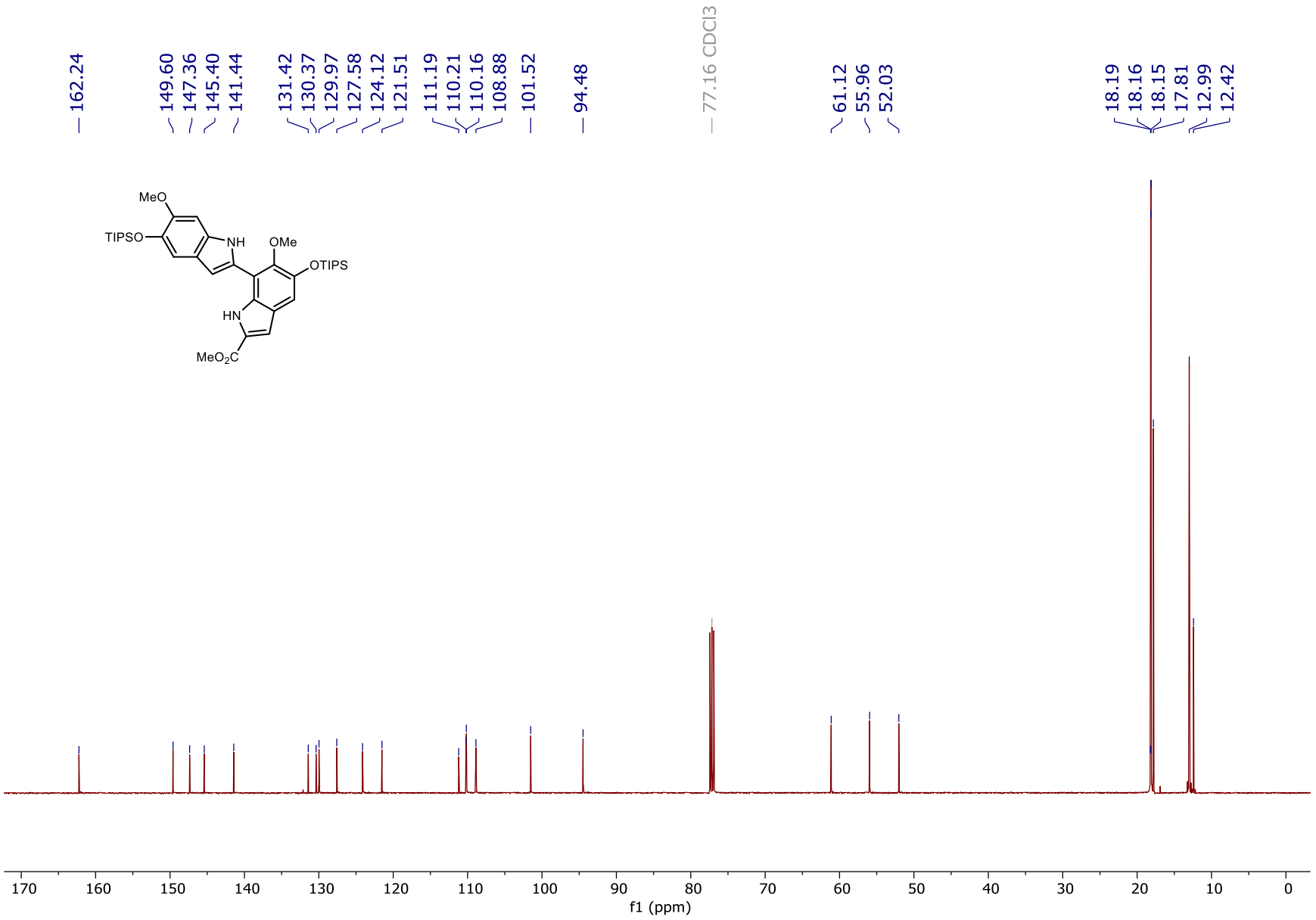
162.24
149.60
147.36
145.40
141.44
131.42
130.37
129.97
127.58
124.12
121.51
111.19
110.21
110.16
108.88
101.52
94.48
77.16 CDCl3
61.12
55.96
52.03
18.19
18.16
18.15
17.81
12.99
12.42
MeO
TIPSO
NH
OMe
OTIPS
HN
MeO2C
170
160
150
140
130
120
110
100
90
80
70
60
50
40
30
20
10
0
f1 (ppm)

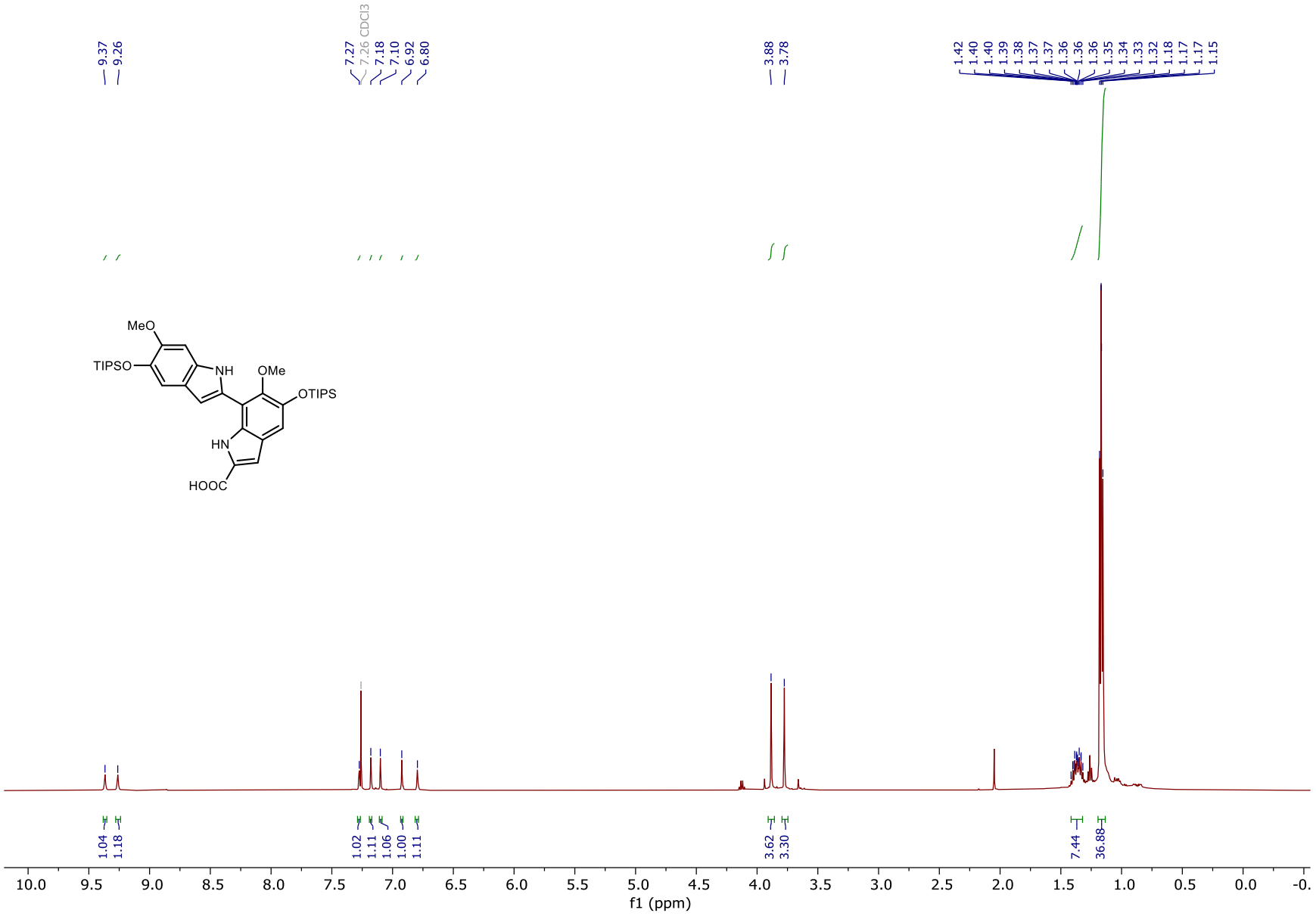
9.37
9.26
7.27
7.26 CDCl3
7.18
7.10
6.92
6.80
3.88
3.78
1.42
1.40
1.40
1.39
1.38
1.37
1.37
1.36
1.36
1.36
1.35
1.34
1.33
1.32
1.18
1.17
1.17
1.15
MeO
TIPSO
NH
OMe
OTIPS
HN
HOOC
1.04
1.18
1.02
1.11
1.06
1.00
1.11
3.62
3.30
7.44
36.88
10.0
9.5
9.0
8.5
8.0
7.5
7.0
6.5
6.0
5.5
5.0
4.5
4.0
3.5
3.0
2.5
2.0
1.5
1.0
0.5
0.0
f1 (ppm)

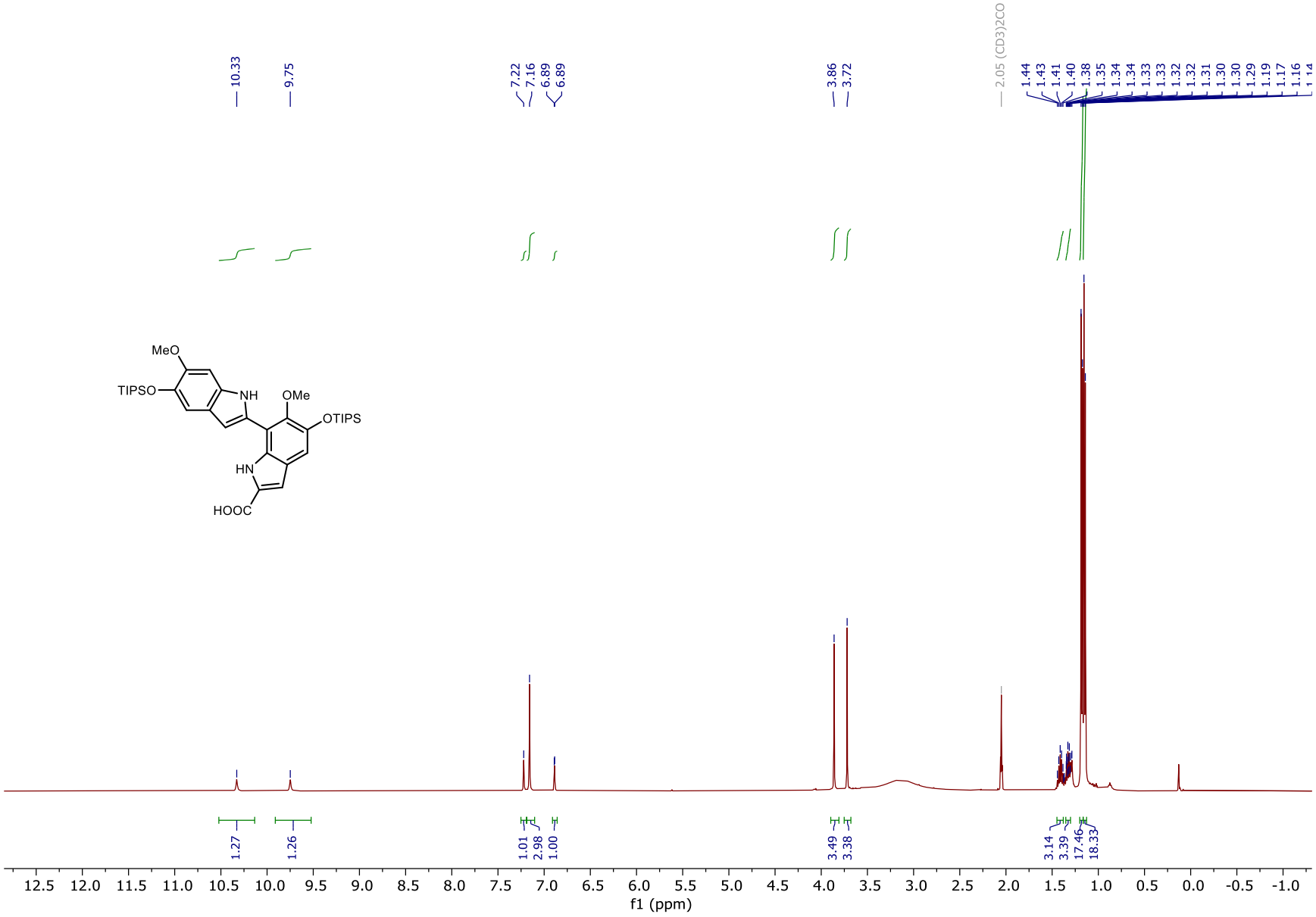
10.33
9.75
7.22
7.16
6.89
6.89
3.86
3.72
2.05 (CD3)2CO
1.44
1.43
1.41
1.40
1.38
1.35
1.34
1.34
1.33
1.33
1.32
1.32
1.31
1.30
1.30
1.29
1.19
1.17
1.16
MeO
TIPSO
NH
OMe
OTIPS
HN
HOOC
1.27
1.26
1.01
2.98
1.00
3.49
3.38
3.14
3.39
17.46
18.33
12.5 12.0 11.5 11.0 10.5 10.0 9.5 9.0 8.5 8.0 7.5 7.0 6.5 6.0 5.5 5.0 4.5 4.0 3.5 3.0 2.5 2.0 1.5 1.0 0.5 0.0 -0.5 -1.0
f1 (ppm)

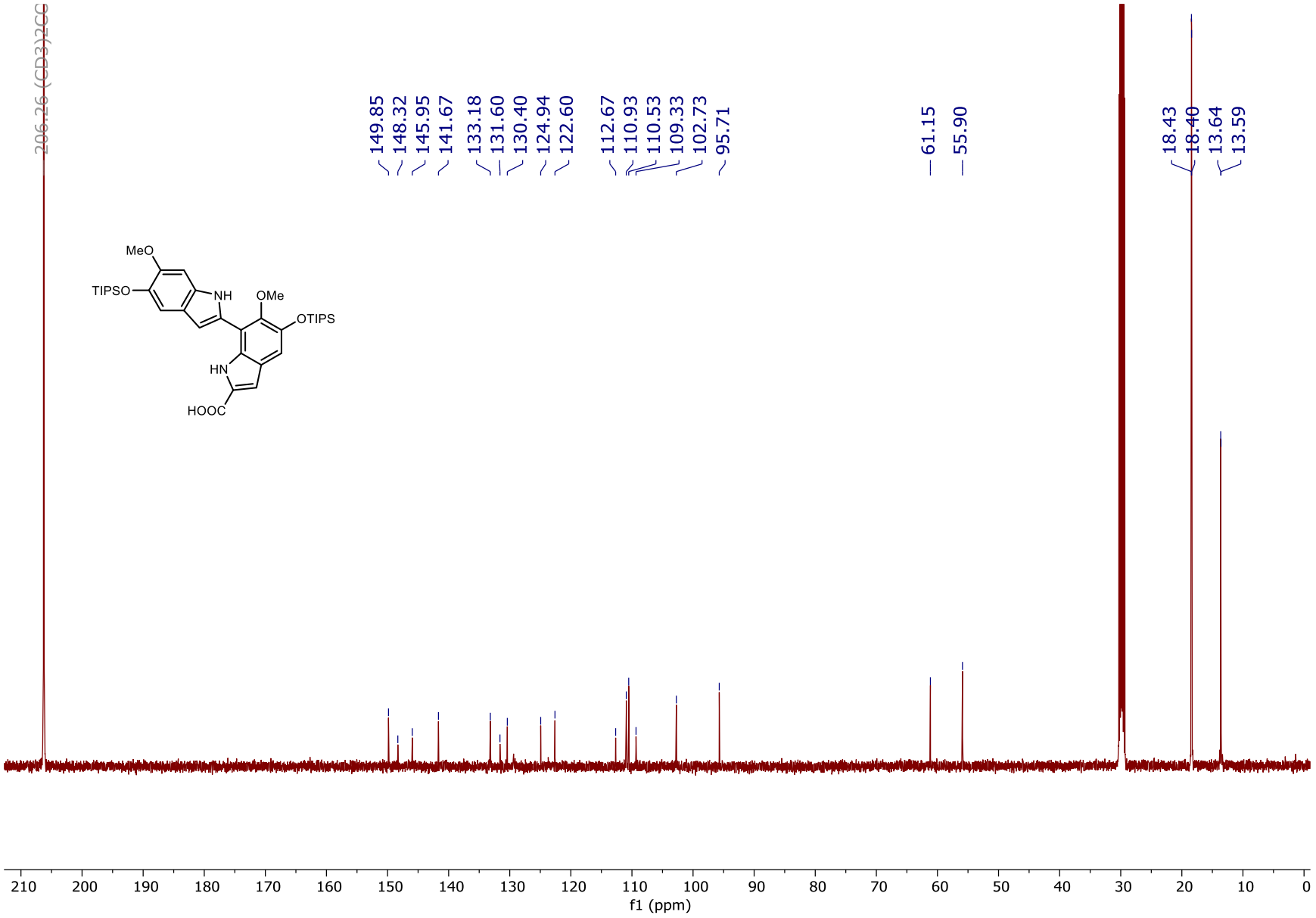
206.26 (CD3)2CO
149.85
148.32
145.95
141.67
133.18
131.60
130.40
124.94
122.60
112.67
110.93
110.53
109.33
102.73
95.71
61.15
55.90
18.43
18.40
13.64
13.59
MeO
TIPSO
NH
OMe
OTIPS
HN
HOOC
210 200 190 180 170 160 150 140 130 120 110 100 90 80 70 60 50 40 30 20 10 0
f1 (ppm)

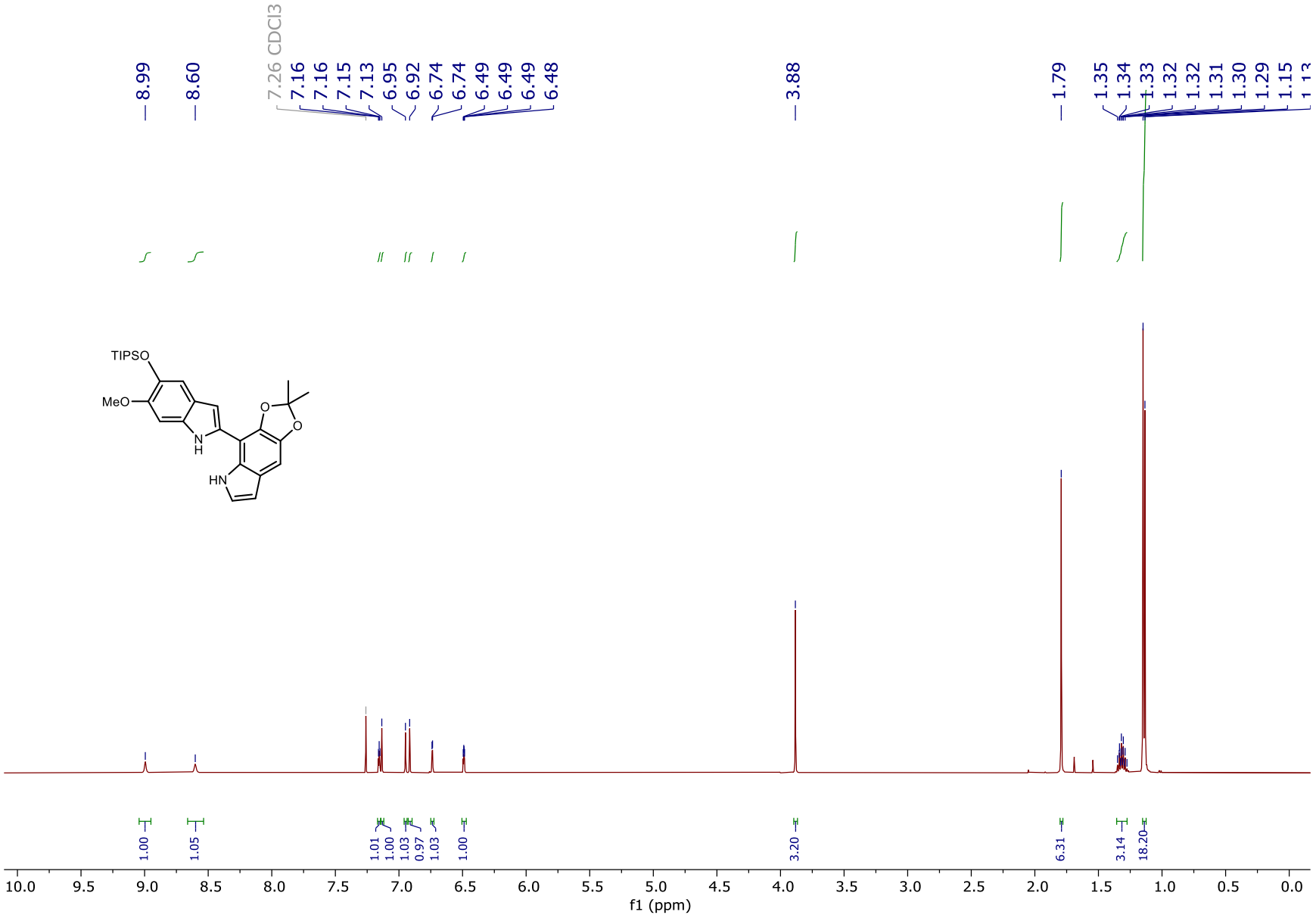
8.99
8.60
7.26 CDCl3
7.16
7.16
7.15
7.13
6.95
6.92
6.74
6.74
6.49
6.49
6.49
6.48
3.88
1.79
1.35
1.34
1.33
1.32
1.32
1.31
1.30
1.29
1.15
TIPSO
MeO
N
H
O
O
HN
1.00
1.05
1.01
1.00
1.03
0.97
1.03
1.00
3.20
6.31
3.14
18.20
10.0
9.5
9.0
8.5
8.0
7.5
7.0
6.5
6.0
5.5
5.0
4.5
4.0
3.5
3.0
2.5
2.0
1.5
1.0
0.5
0.0
f1 (ppm)

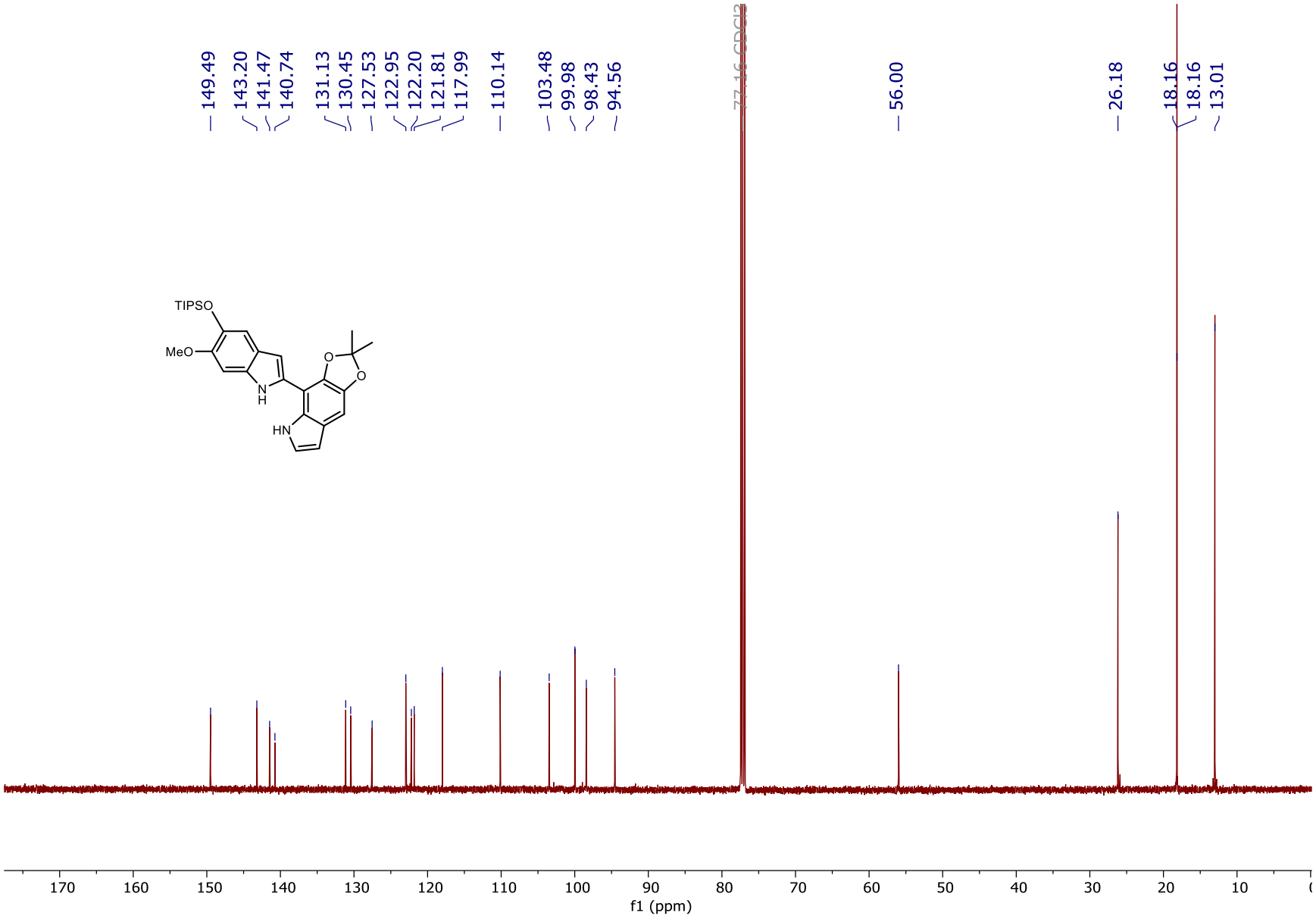
149.49
143.20
141.47
140.74
131.13
130.45
127.53
122.95
122.20
121.81
117.99
110.14
103.48
99.98
98.43
94.56
77.16 CDCl3
56.00
26.18
18.16
18.16
13.01
TIPSO
MeO
O
O
N
H
HN
170
160
150
140
130
120
110
100
90
80
70
60
50
40
30
20
10
f1 (ppm)

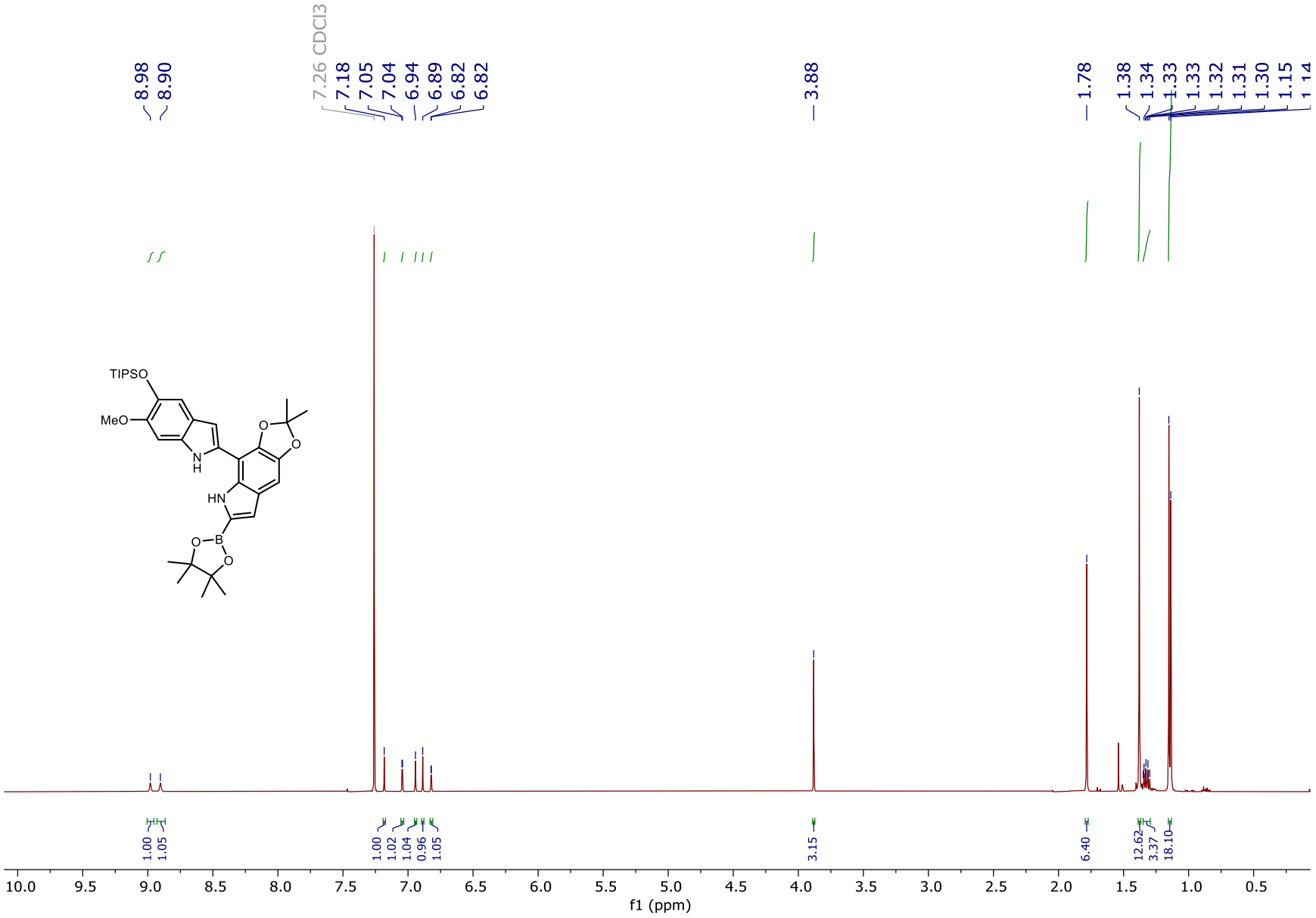
8.98
8.90
7.26 CDCl3
7.18
7.05
7.04
6.94
6.89
6.82
6.82
3.88
1.78
1.38
1.34
1.33
1.33
1.32
1.31
1.30
1.15
TIPSO
MeO
N
H
O
O
HN
O
B
O
1.00
1.05
1.00
1.02
1.04
0.96
1.05
3.15
6.40
12.62
3.37
18.10
10.0
9.5
9.0
8.5
8.0
7.5
7.0
6.5
6.0
5.5
5.0
4.5
4.0
3.5
3.0
2.5
2.0
1.5
1.0
0.5
f1 (ppm)

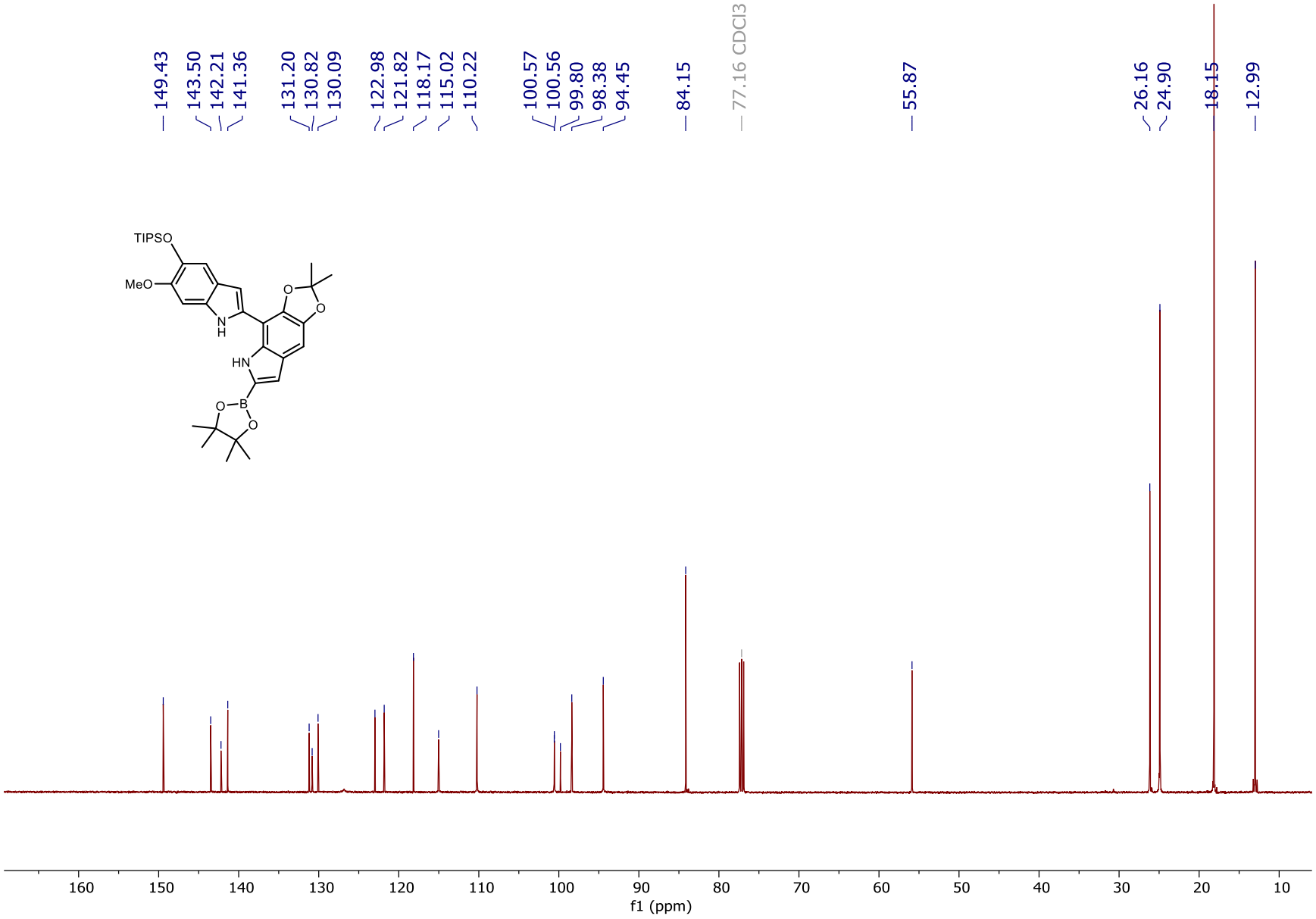
149.43
143.50
142.21
141.36
131.20
130.82
130.09
122.98
121.82
118.17
115.02
110.22
100.57
100.56
99.80
98.38
94.45
84.15
77.16 CDCl3
55.87
26.16
24.90
18.15
12.99
TIPSO
MeO
N
H
HN
O
O
O
O
B
O
160
150
140
130
120
110
100
90
80
70
60
50
40
30
20
10
f1 (ppm)

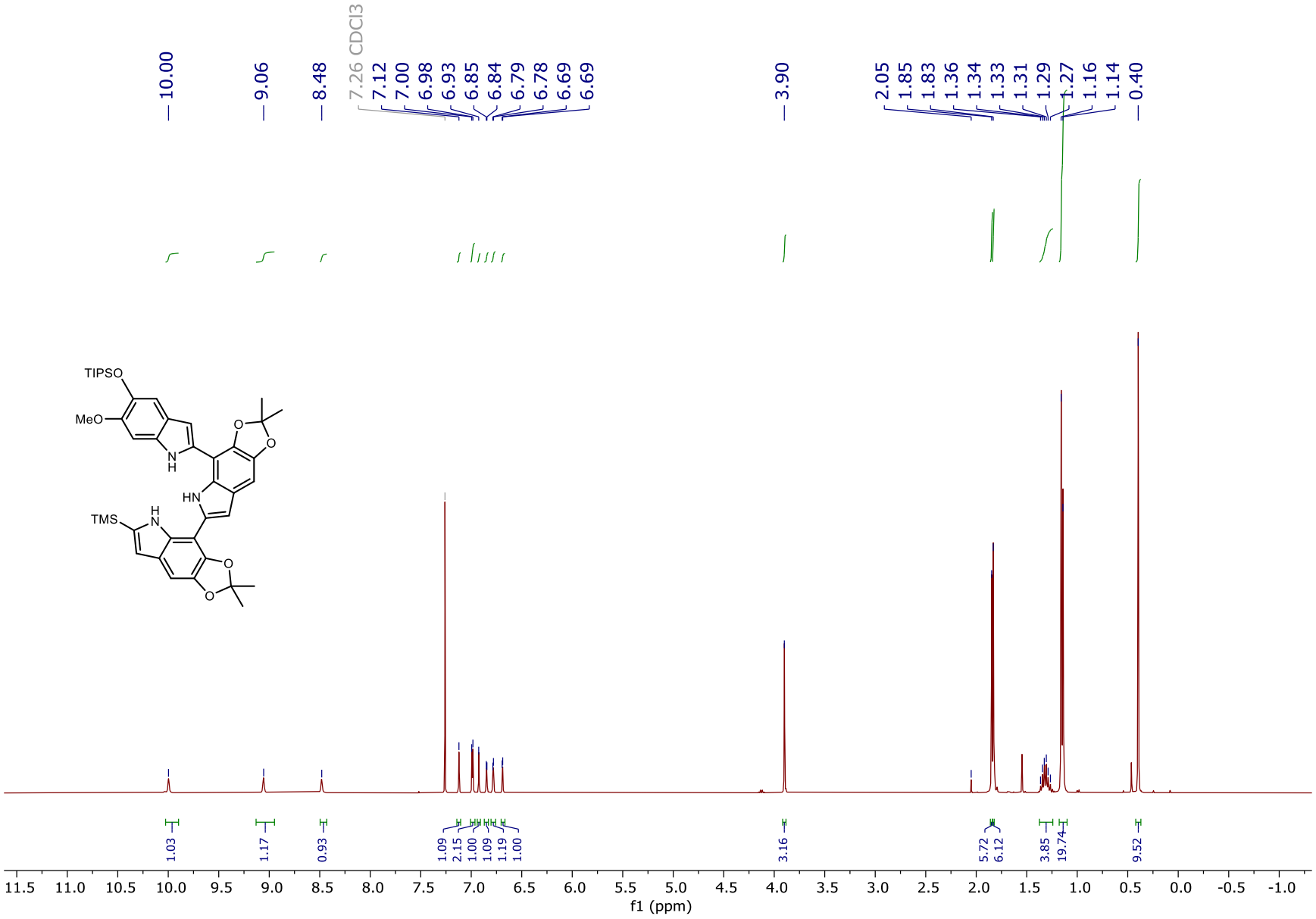
10.00
9.06
8.48
7.26 CDCl3
7.12
7.00
6.98
6.93
6.85
6.84
6.79
6.78
6.69
6.69
3.90
2.05
1.85
1.83
1.36
1.34
1.33
1.31
1.29
1.27
1.16
1.14
0.40
TIPSO
MeO
N
H
O
O
HN
H
N
TMS
O
O
1.03
1.17
0.93
1.09
2.15
1.00
1.09
1.19
1.00
3.16
5.72
6.12
3.85
19.74
9.52
11.5 11.0 10.5 10.0 9.5 9.0 8.5 8.0 7.5 7.0 6.5 6.0 5.5 5.0 4.5 4.0 3.5 3.0 2.5 2.0 1.5 1.0 0.5 0.0 -0.5 -1.0
f1 (ppm)

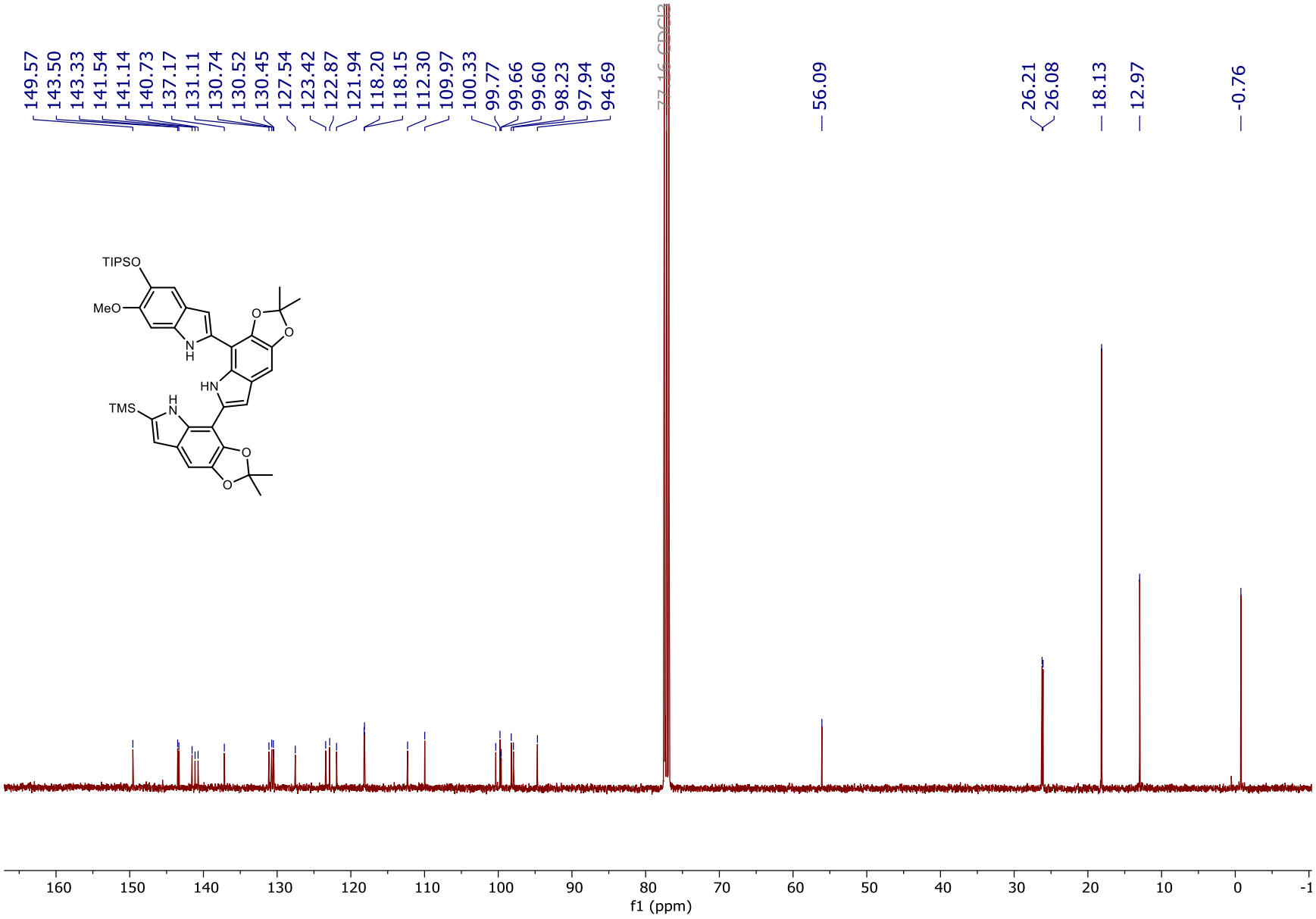
149.57
143.50
143.33
141.54
141.14
140.73
137.17
131.11
130.74
130.52
130.45
127.54
123.42
122.87
121.94
118.20
118.15
112.30
109.97
100.33
99.77
99.66
99.60
98.23
97.94
94.69
77.16 CDCl3
56.09
26.21
26.08
18.13
12.97
-0.76
TIPSO
MeO
N
H
O
O
HN
TMS
H
N
O
O
160
150
140
130
120
110
100
90
80
70
60
50
40
30
20
10
0
-1
f1 (ppm)

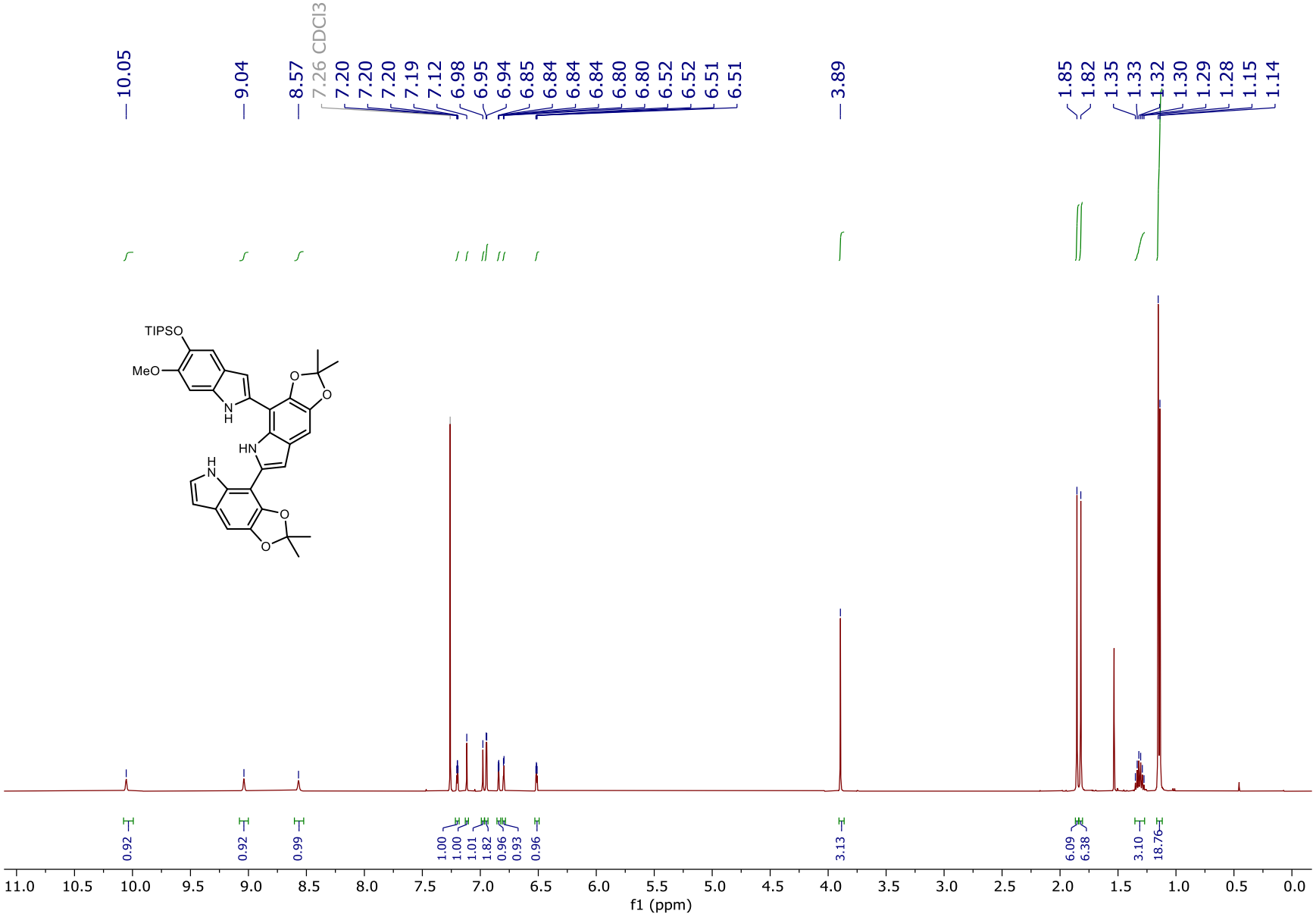
10.05
9.04
8.57
7.26 CDCl3
7.20
7.20
7.20
7.19
7.12
6.98
6.95
6.94
6.85
6.84
6.84
6.84
6.80
6.80
6.52
6.52
6.51
6.51
3.89
1.85
1.82
1.35
1.33
1.32
1.30
1.29
1.28
1.15
1.14
TIPSO
MeO
O
O
N
H
HN
N
H
O
O
0.92
0.92
0.99
1.00
1.00
1.01
1.82
0.96
0.93
0.96
3.13
6.09
6.38
3.10
18.76
11.0
10.5
10.0
9.5
9.0
8.5
8.0
7.5
7.0
6.5
6.0
5.5
5.0
4.5
4.0
3.5
3.0
2.5
2.0
1.5
1.0
0.5
0.0
f1 (ppm)

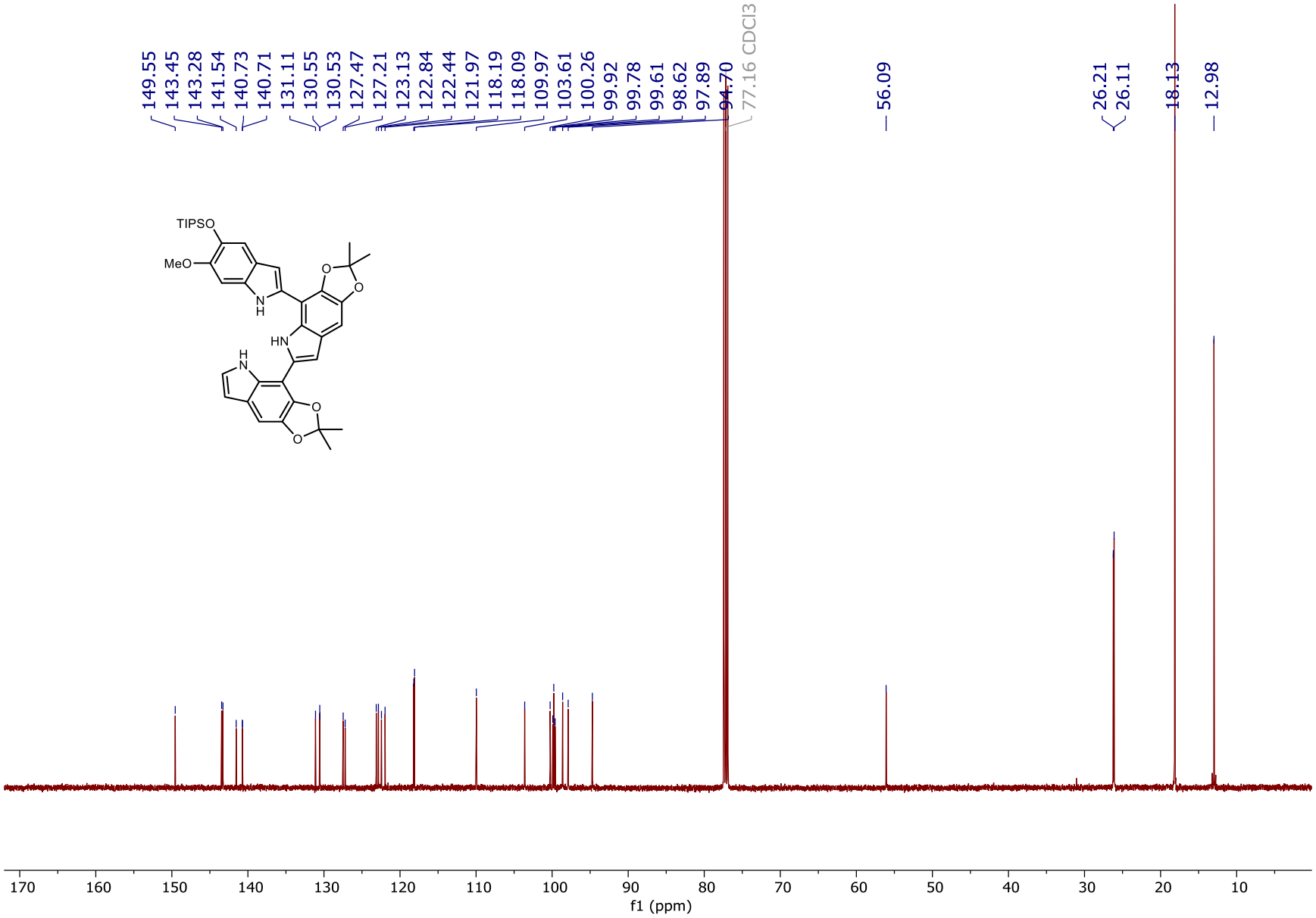
149.55
143.45
143.28
141.54
140.73
140.71
131.11
130.55
130.53
127.47
127.21
123.13
122.84
122.44
121.97
118.19
118.09
109.97
103.61
100.26
99.92
99.78
99.61
98.62
97.89
94.70
77.16 CDCl3
56.09
26.21
26.11
18.13
12.98
TIPSO
MeO
N
H
HN
O
O
O
O
170
160
150
140
130
120
110
100
90
80
70
60
50
40
30
20
10
f1 (ppm)

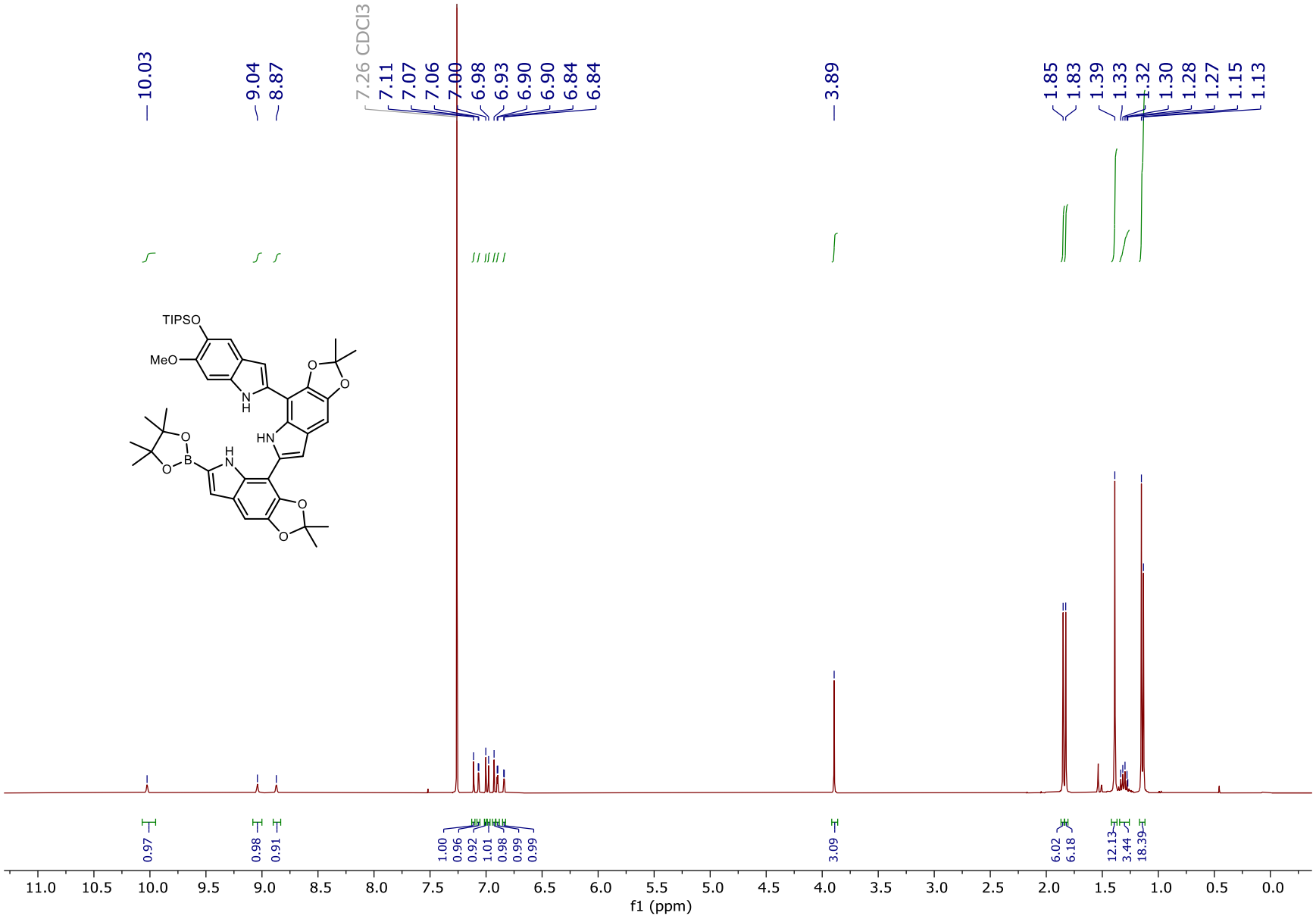
10.03
9.04
8.87
7.26 CDCl3
7.11
7.07
7.06
7.00
6.98
6.93
6.90
6.90
6.84
6.84
3.89
1.85
1.83
1.39
1.33
1.32
1.30
1.28
1.27
1.15
1.13
TIPSO
MeO
N
H
O
O
HN
H
N
O
B
O
O
O
O
0.97
0.98
0.91
1.00
0.96
0.92
1.01
0.98
0.99
0.99
3.09
6.02
6.18
12.13
3.44
18.39
11.0
10.5
10.0
9.5
9.0
8.5
8.0
7.5
7.0
6.5
6.0
5.5
5.0
4.5
4.0
3.5
3.0
2.5
2.0
1.5
1.0
0.5
0.0
f1 (ppm)

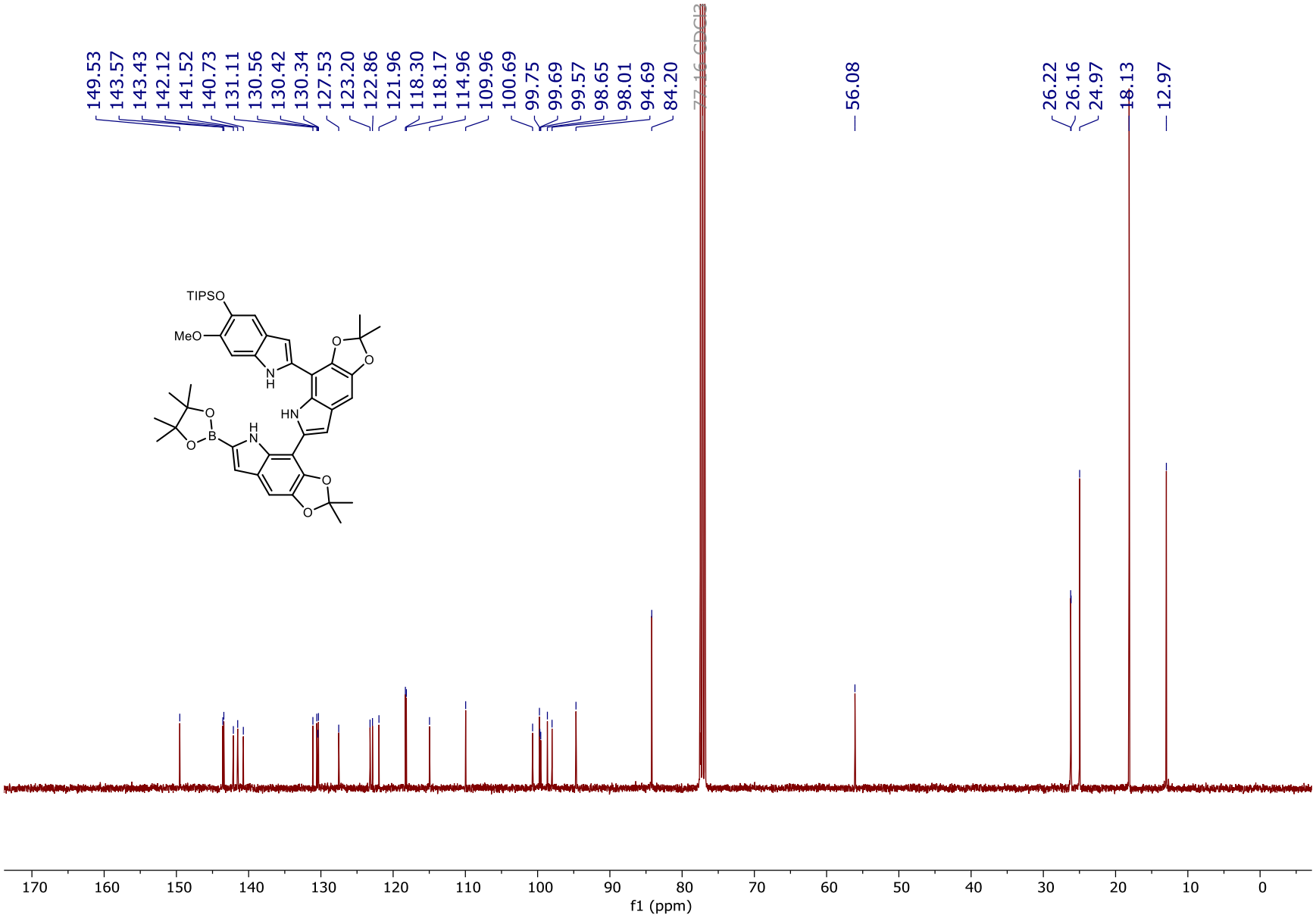
149.53
143.57
143.43
142.12
141.52
140.73
131.11
130.56
130.42
130.34
127.53
123.20
122.86
121.96
118.30
118.17
114.96
109.96
100.69
99.75
99.69
99.57
98.65
98.01
94.69
84.20
77.16 CDCl3
56.08
26.22
26.16
24.97
18.13
12.97
TIPSO
MeO
O
O
N
H
HN
H
N
O
B
O
O
O
170
160
150
140
130
120
110
100
90
80
70
60
50
40
30
20
10
0
f1 (ppm)

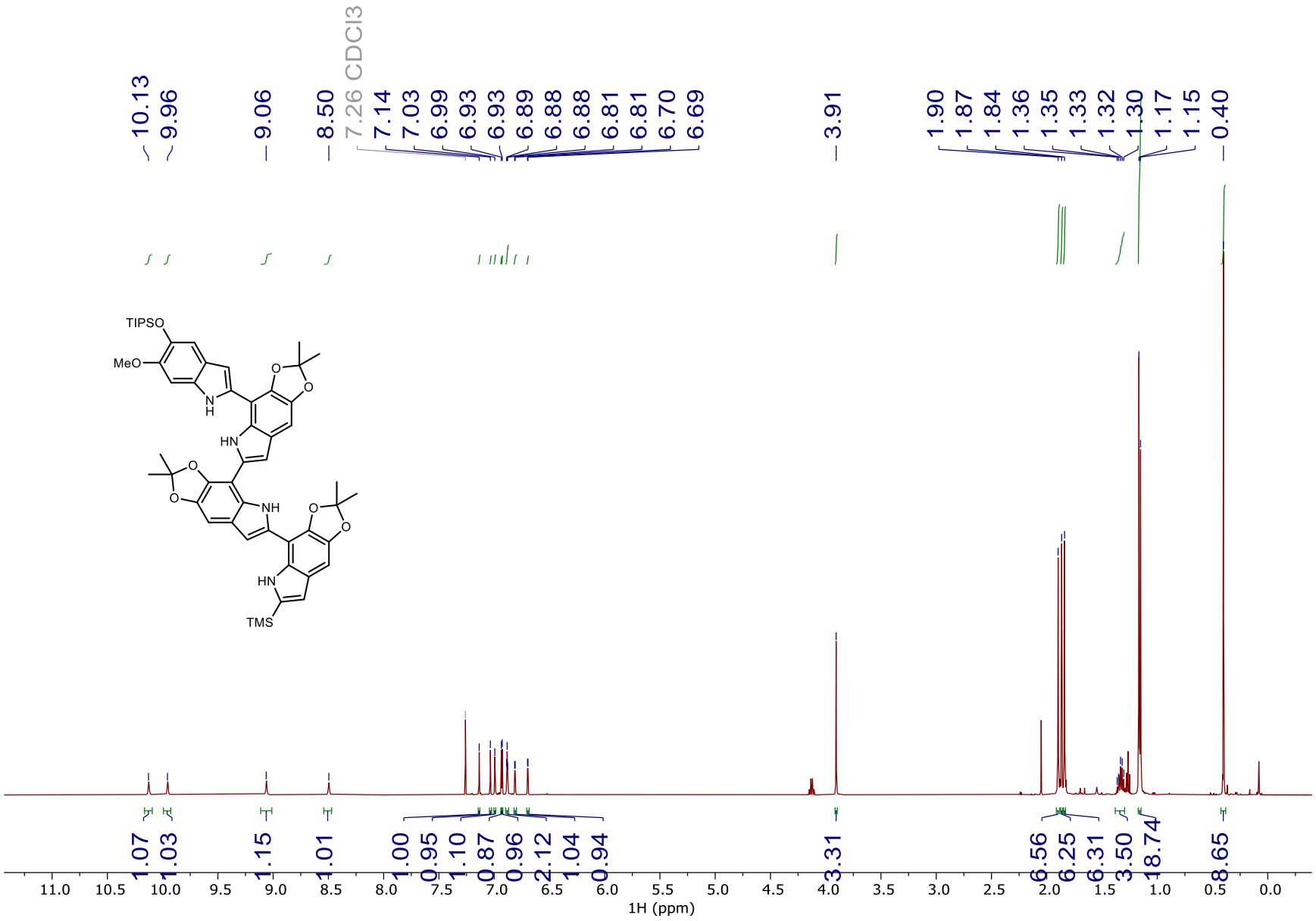
10.13
9.96
9.06
8.50
7.26 CDCl3
7.14
7.03
6.99
6.93
6.93
6.89
6.88
6.88
6.81
6.81
6.70
6.69
3.91
1.90
1.87
1.84
1.36
1.35
1.33
1.32
1.30
1.17
1.15
0.40
TIPSO
MeO
N
H
HN
O
O
O
O
NH
O
O
HN
TMS
1.07
1.03
1.15
1.01
1.00
0.95
1.10
0.87
0.96
2.12
1.04
0.94
3.31
6.56
6.25
6.31
3.50
18.74
8.65
11.0
10.5
10.0
9.5
9.0
8.5
8.0
7.5
7.0
6.5
6.0
5.5
5.0
4.5
4.0
3.5
3.0
2.5
2.0
1.5
1.0
0.5
0.0
1H (ppm)

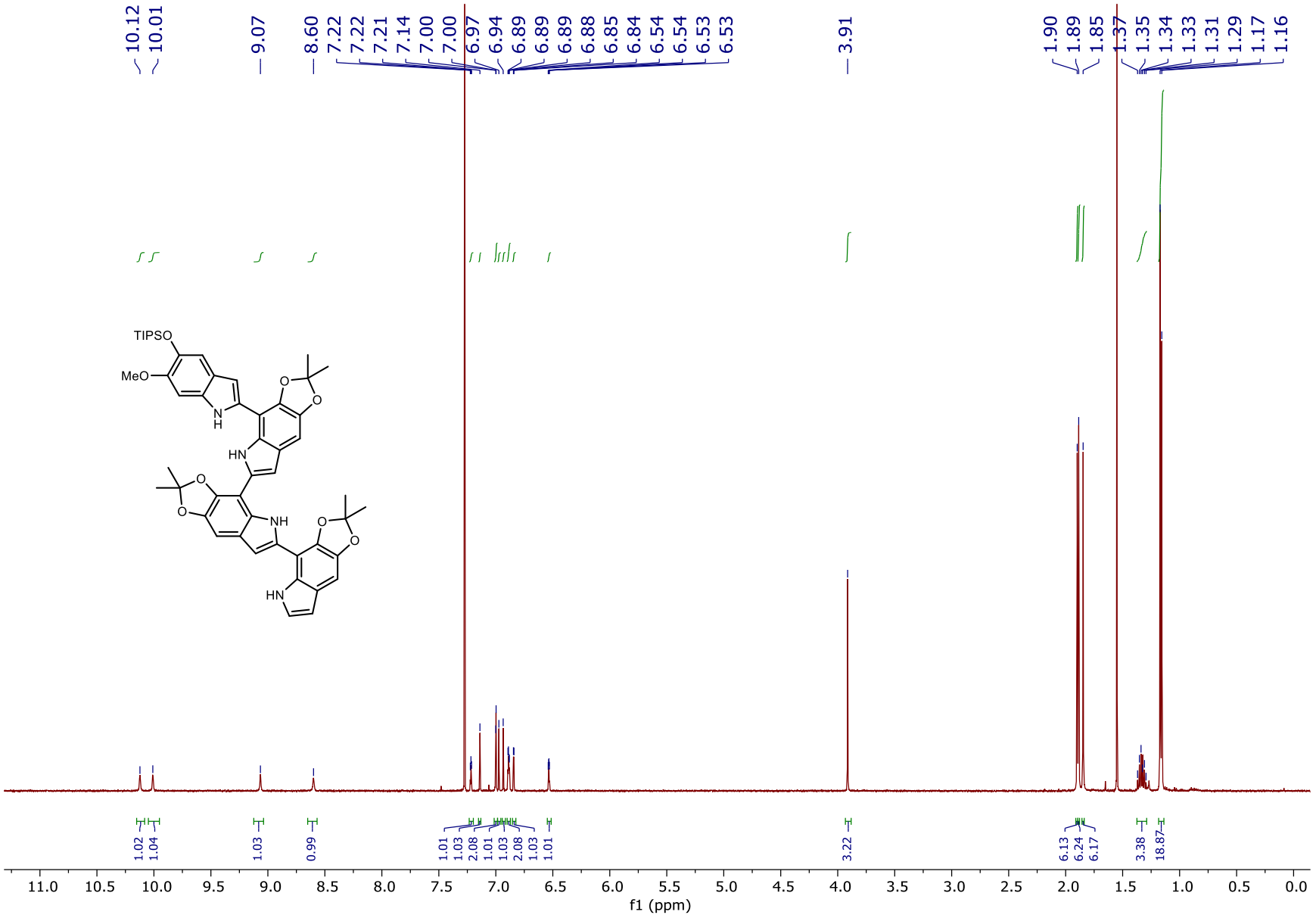
10.12
10.01
9.07
8.60
7.22
7.22
7.21
7.14
7.00
7.00
6.97
6.94
6.89
6.89
6.89
6.88
6.85
6.84
6.54
6.54
6.53
6.53
3.91
1.90
1.89
1.85
1.37
1.35
1.34
1.33
1.31
1.29
1.17
1.16
TIPSO
MeO
N
H
HN
O
O
O
O
NH
O
O
HN
1.02
1.04
1.03
0.99
1.01
1.03
2.08
1.01
1.03
2.08
1.03
1.01
3.22
6.13
6.24
6.17
3.38
18.87
11.0
10.5
10.0
9.5
9.0
8.5
8.0
7.5
7.0
6.5
6.0
5.5
5.0
4.5
4.0
3.5
3.0
2.5
2.0
1.5
1.0
0.5
0.0
f1 (ppm)

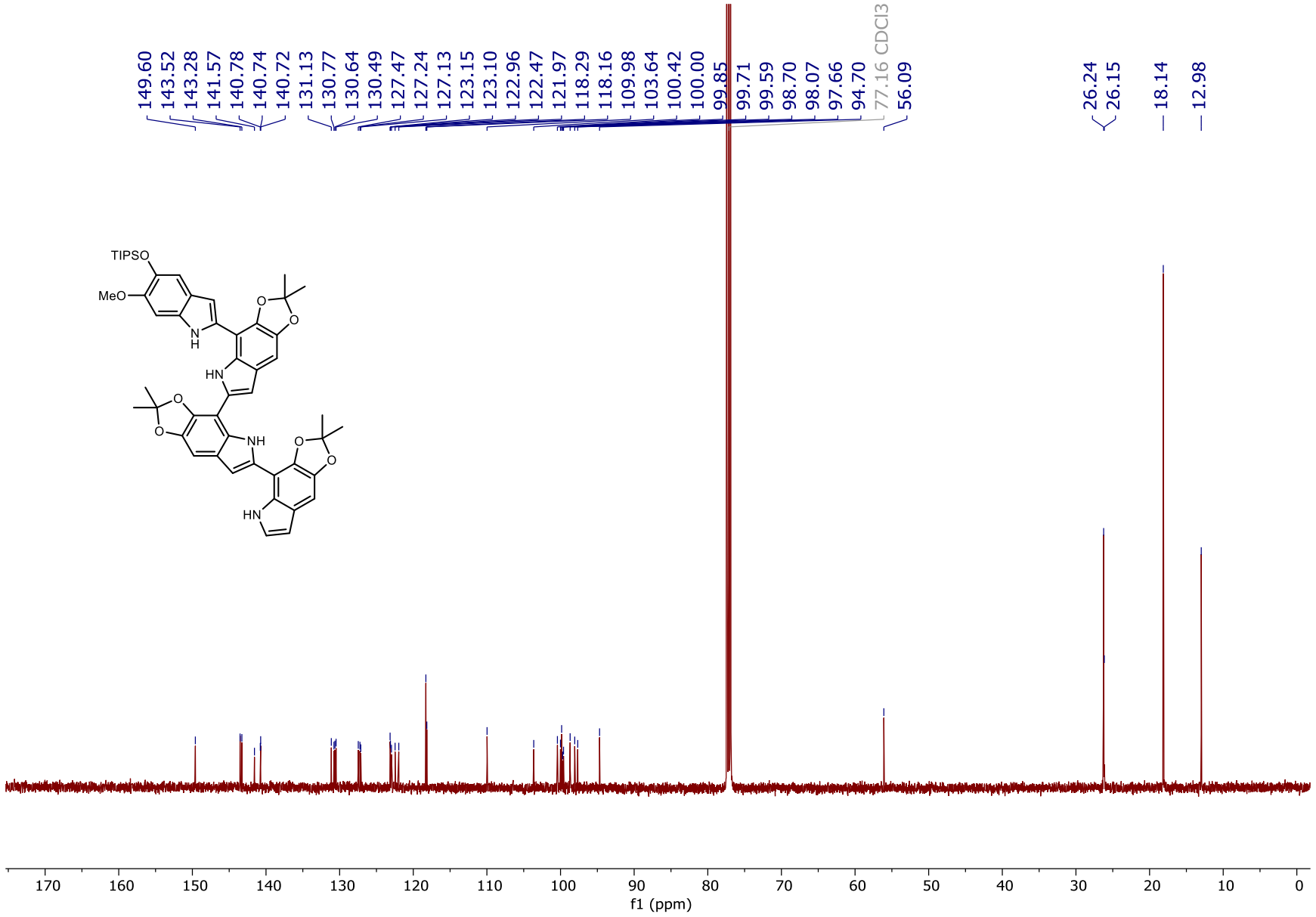
149.60
143.52
143.28
141.57
140.78
140.74
140.72
131.13
130.77
130.64
130.49
127.47
127.24
127.13
123.15
123.10
122.96
122.47
121.97
118.29
118.16
109.98
103.64
100.42
100.00
99.85
99.71
99.59
98.70
98.07
97.66
94.70
77.16 CDCl3
56.09
26.24
26.15
18.14
12.98
TIPSO
MeO
N
H
O
O
HN
O
O
NH
O
O
HN
170
160
150
140
130
120
110
100
90
80
70
60
50
40
30
20
10
0
f1 (ppm)

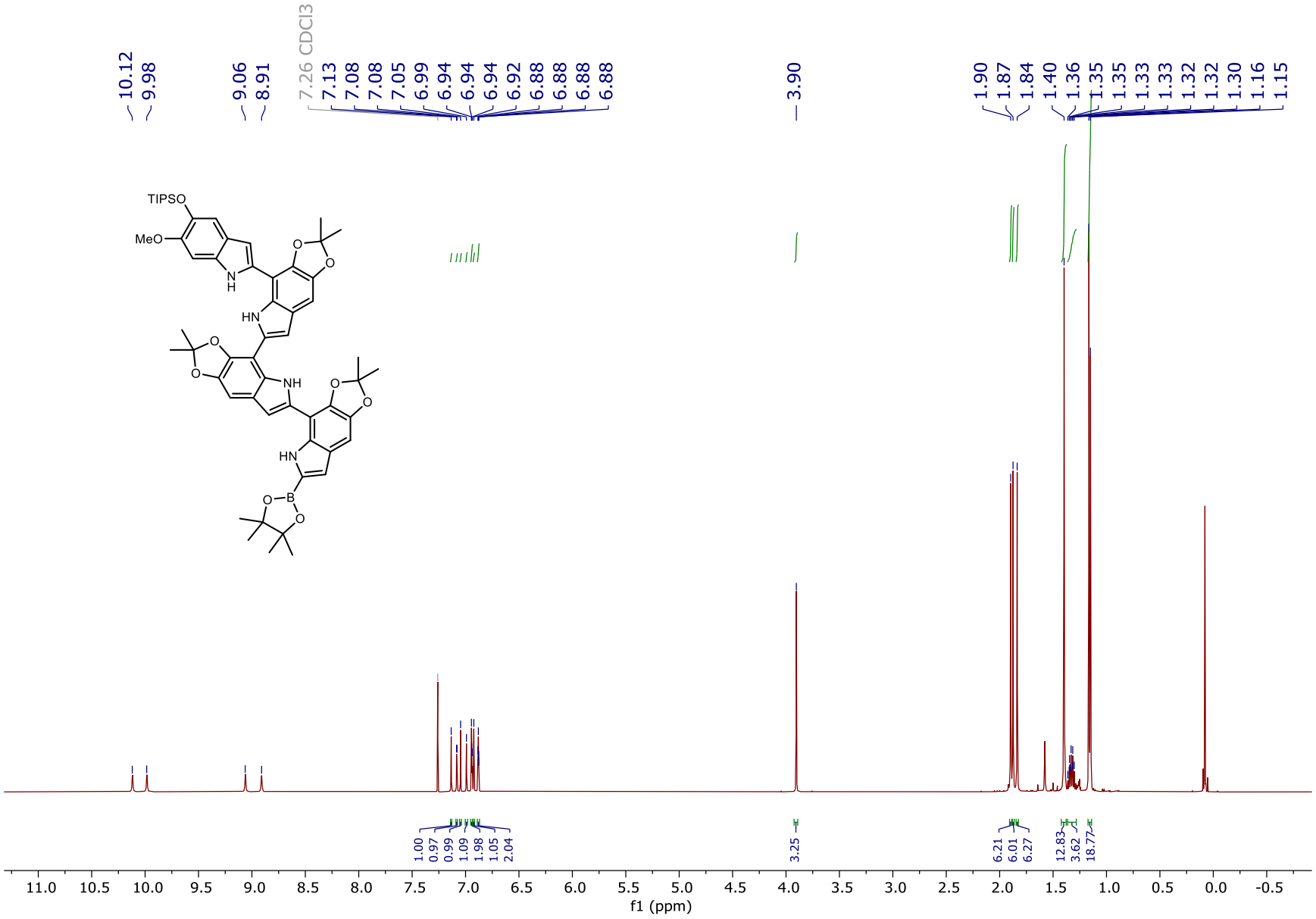
10.12
9.98
9.06
8.91
7.26 CDCl3
7.13
7.08
7.08
7.05
6.99
6.94
6.94
6.94
6.92
6.88
6.88
6.88
6.88
3.90
1.90
1.87
1.84
1.40
1.36
1.35
1.35
1.33
1.33
1.32
1.32
1.30
1.16
1.15
TIPSO
MeO
N
H
HN
O
O
O
O
NH
O
O
HN
O
B
O
1.00
0.97
0.99
1.09
1.98
1.05
2.04
3.25
6.21
6.01
6.27
12.83
3.62
18.77
11.0
10.5
10.0
9.5
9.0
8.5
8.0
7.5
7.0
6.5
6.0
5.5
5.0
4.5
4.0
3.5
3.0
2.5
2.0
1.5
1.0
0.5
0.0
-0.5
f1 (ppm)

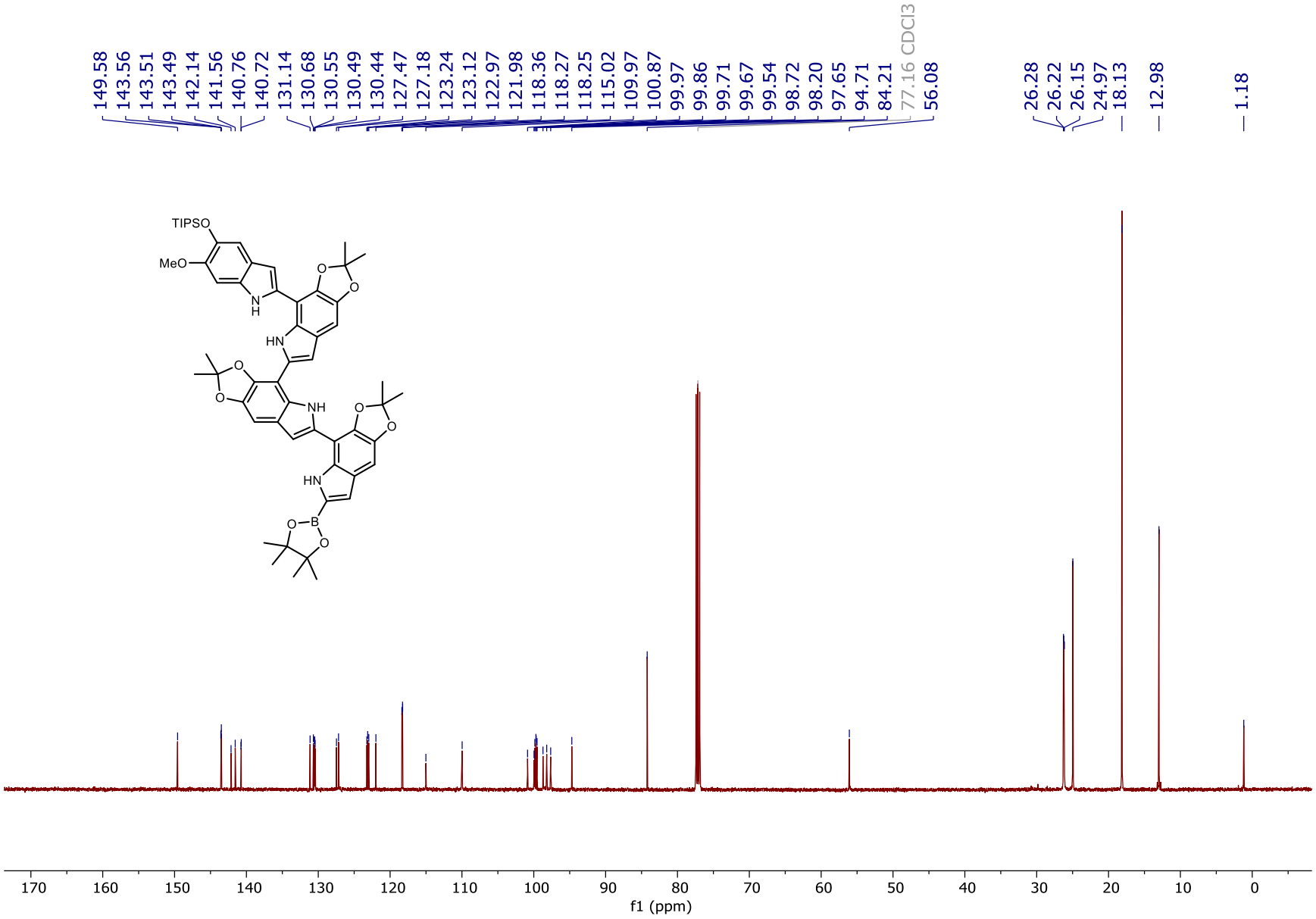
149.58
143.56
143.51
143.49
142.14
141.56
140.76
140.72
131.14
130.68
130.55
130.49
130.44
127.47
127.18
123.24
123.12
122.97
121.98
118.36
118.27
118.25
115.02
109.97
100.87
99.97
99.86
99.71
99.67
99.54
98.72
98.20
97.65
94.71
84.21
77.16 CDCl3
56.08
26.28
26.22
26.15
24.97
18.13
12.98
1.18
TIPSO
MeO
N
H
HN
O
O
O
O
NH
O
O
HN
O
B
O
O
170
160
150
140
130
120
110
100
90
80
70
60
50
40
30
20
10
0
f1 (ppm)

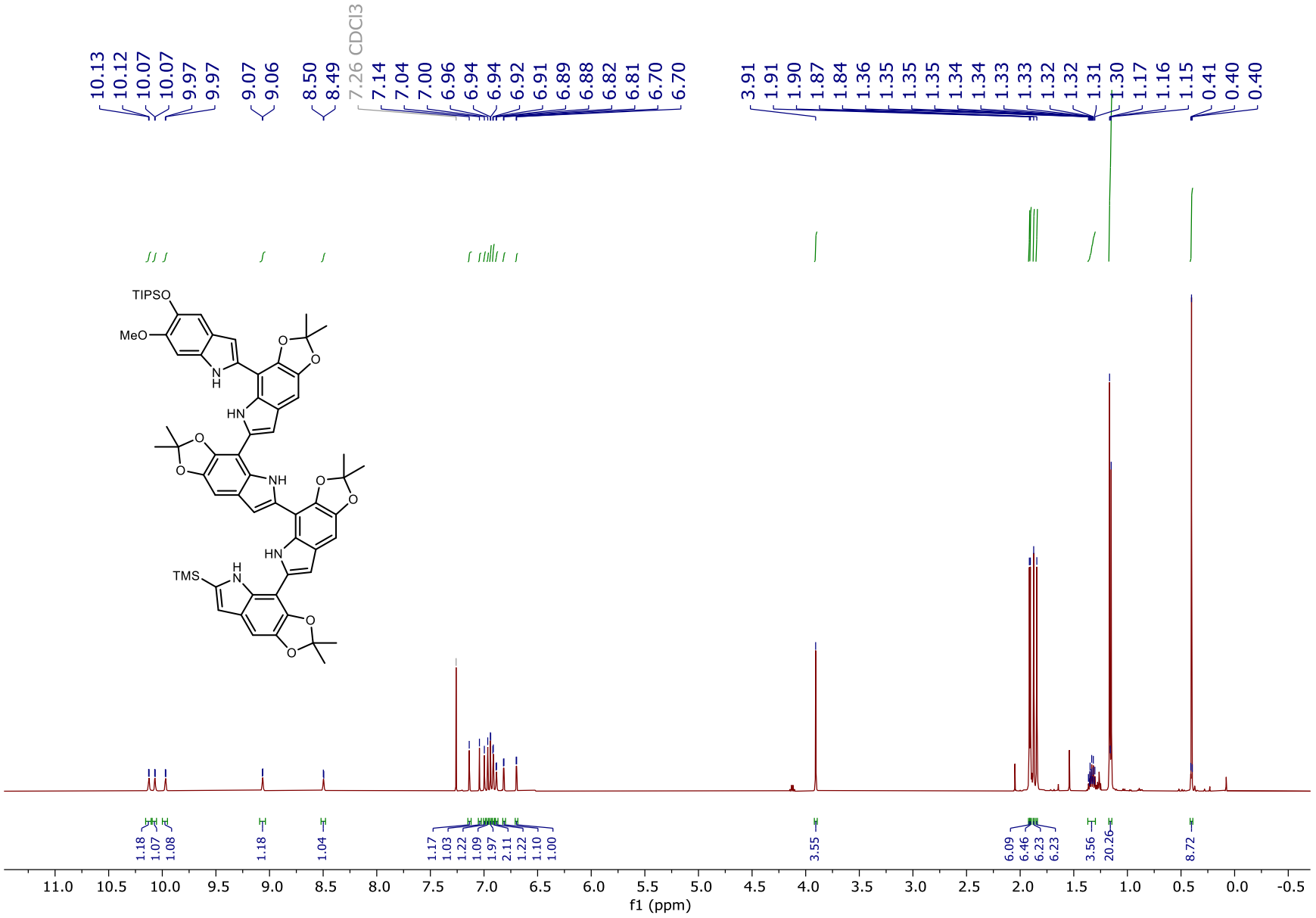
10.13
10.12
10.07
10.07
9.97
9.97
9.07
9.06
8.50
8.49
7.26 CDCl3
7.14
7.04
7.00
6.96
6.94
6.94
6.92
6.91
6.89
6.88
6.82
6.81
6.70
6.70
3.91
1.91
1.90
1.87
1.84
1.36
1.35
1.35
1.35
1.34
1.34
1.33
1.33
1.32
1.32
1.31
1.30
1.17
1.16
1.15
0.41
0.40
0.40
TIPSO
MeO
N
H
O
O
HN
O
O
NH
O
O
HN
TMS
N
H
O
O
1.18
1.07
1.08
1.18
1.04
1.17
1.03
1.22
1.09
1.97
2.11
1.22
1.10
1.00
3.55
6.09
6.46
6.23
6.23
3.56
20.26
8.72
11.0
10.5
10.0
9.5
9.0
8.5
8.0
7.5
7.0
6.5
6.0
5.5
5.0
4.5
4.0
3.5
3.0
2.5
2.0
1.5
1.0
0.5
0.0
-0.5
f1 (ppm)

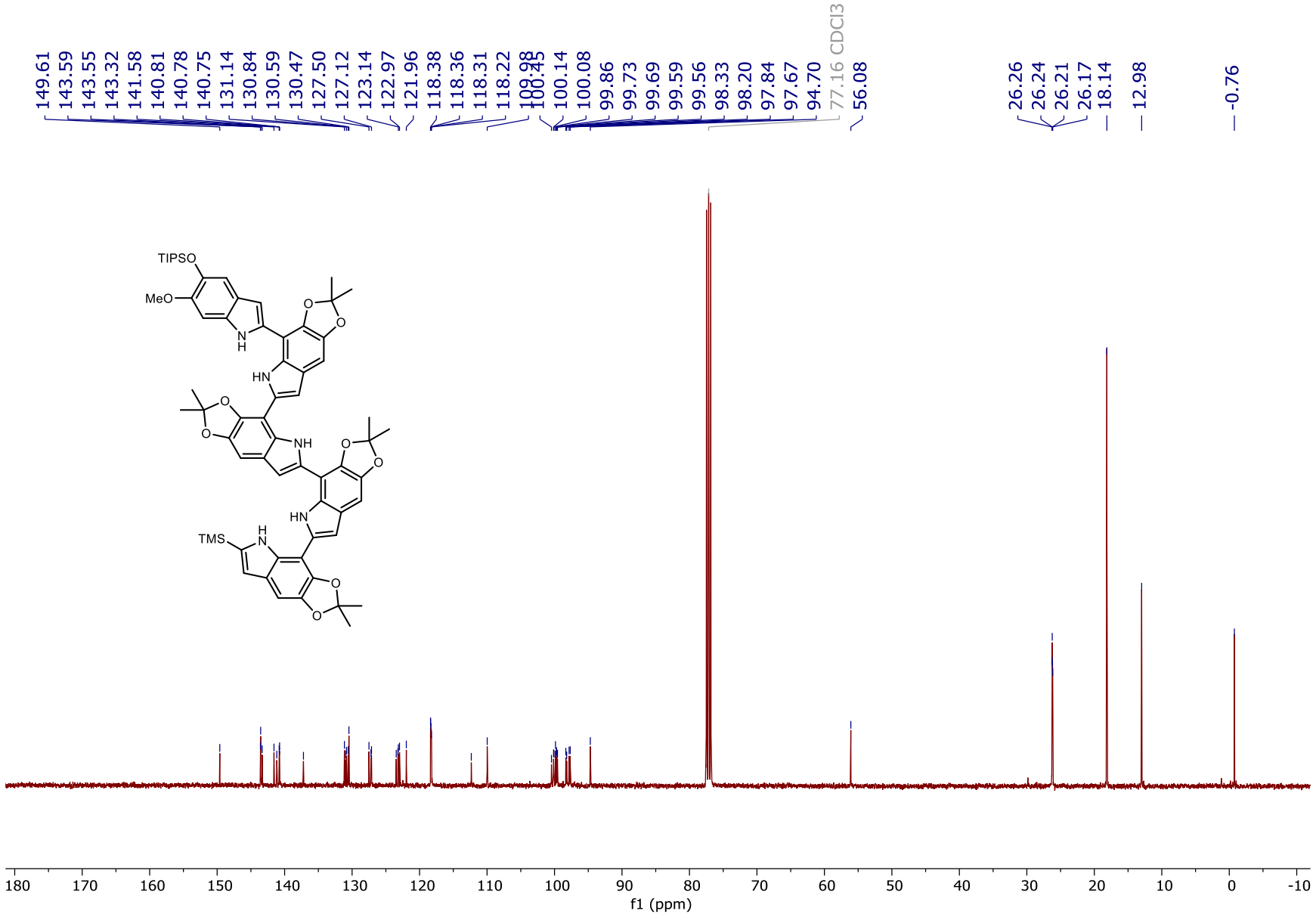
149.61
143.59
143.55
143.32
141.58
140.81
140.78
140.75
131.14
130.84
130.59
130.47
127.50
127.12
123.14
122.97
121.96
118.38
118.36
118.31
118.22
100.14
100.08
99.86
99.73
99.69
99.59
99.56
98.33
98.20
97.84
97.67
94.70
77.16 CDCl3
56.08
26.26
26.24
26.21
26.17
18.14
12.98
-0.76
TIPSO
MeO
TMS
f1 (ppm)

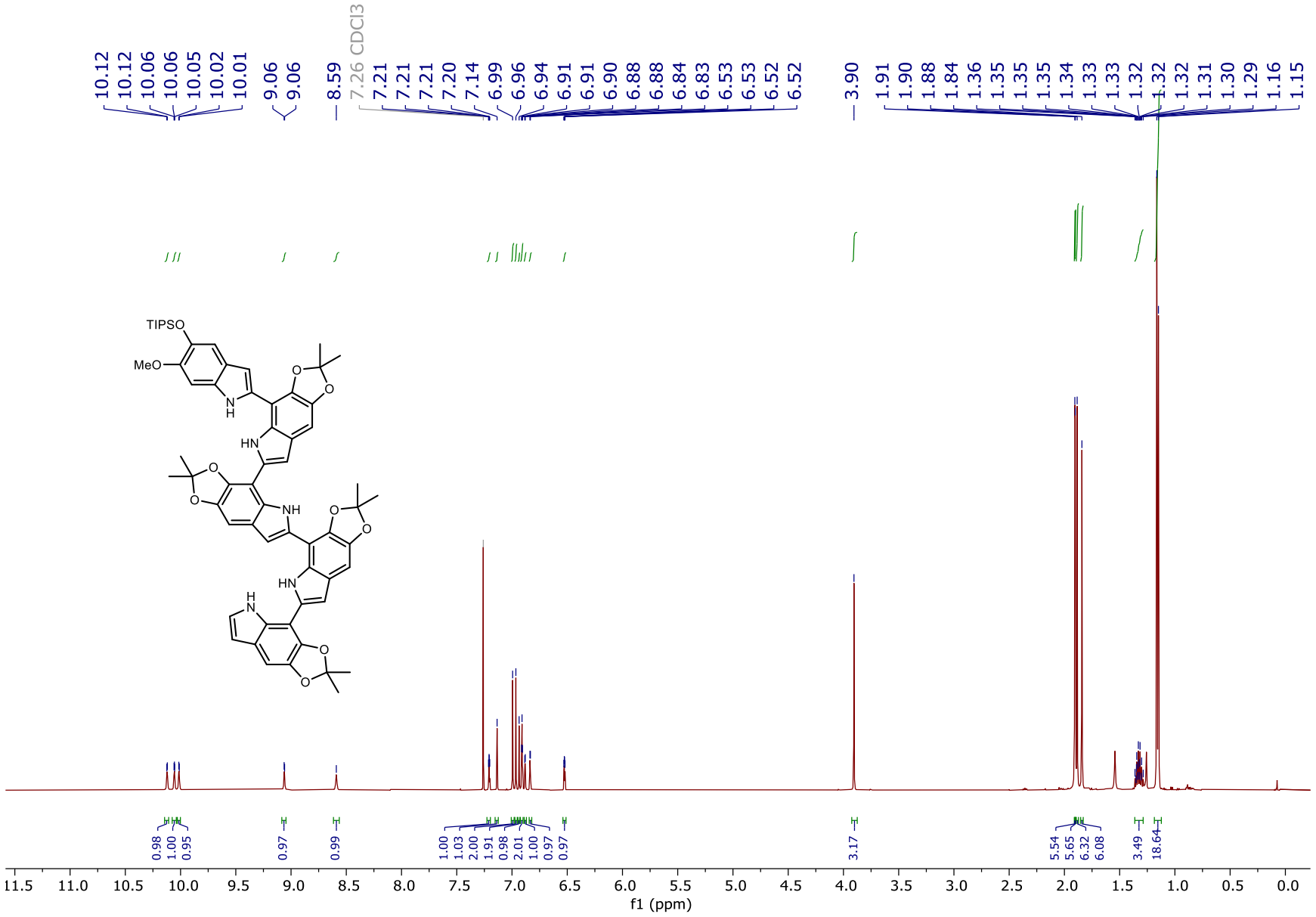
10.12
10.12
10.06
10.06
10.05
10.02
10.01
9.06
9.06
8.59
7.26 CDCl3
7.21
7.21
7.21
7.20
7.14
6.99
6.96
6.94
6.91
6.91
6.90
6.88
6.88
6.84
6.83
6.53
6.53
6.52
6.52
3.90
1.91
1.90
1.88
1.84
1.36
1.35
1.35
1.35
1.34
1.33
1.33
1.32
1.32
1.32
1.31
1.30
1.29
1.16
1.15
TIPSO
MeO
NH
HN
NH
HN
NH
0.98
1.00
0.95
0.97
0.99
1.00
1.03
2.00
1.91
0.98
2.01
1.00
0.97
0.97
3.17
5.54
5.65
6.32
6.08
3.49
18.64
11.5
11.0
10.5
10.0
9.5
9.0
8.5
8.0
7.5
7.0
6.5
6.0
5.5
5.0
4.5
4.0
3.5
3.0
2.5
2.0
1.5
1.0
0.5
0.0
f1 (ppm)

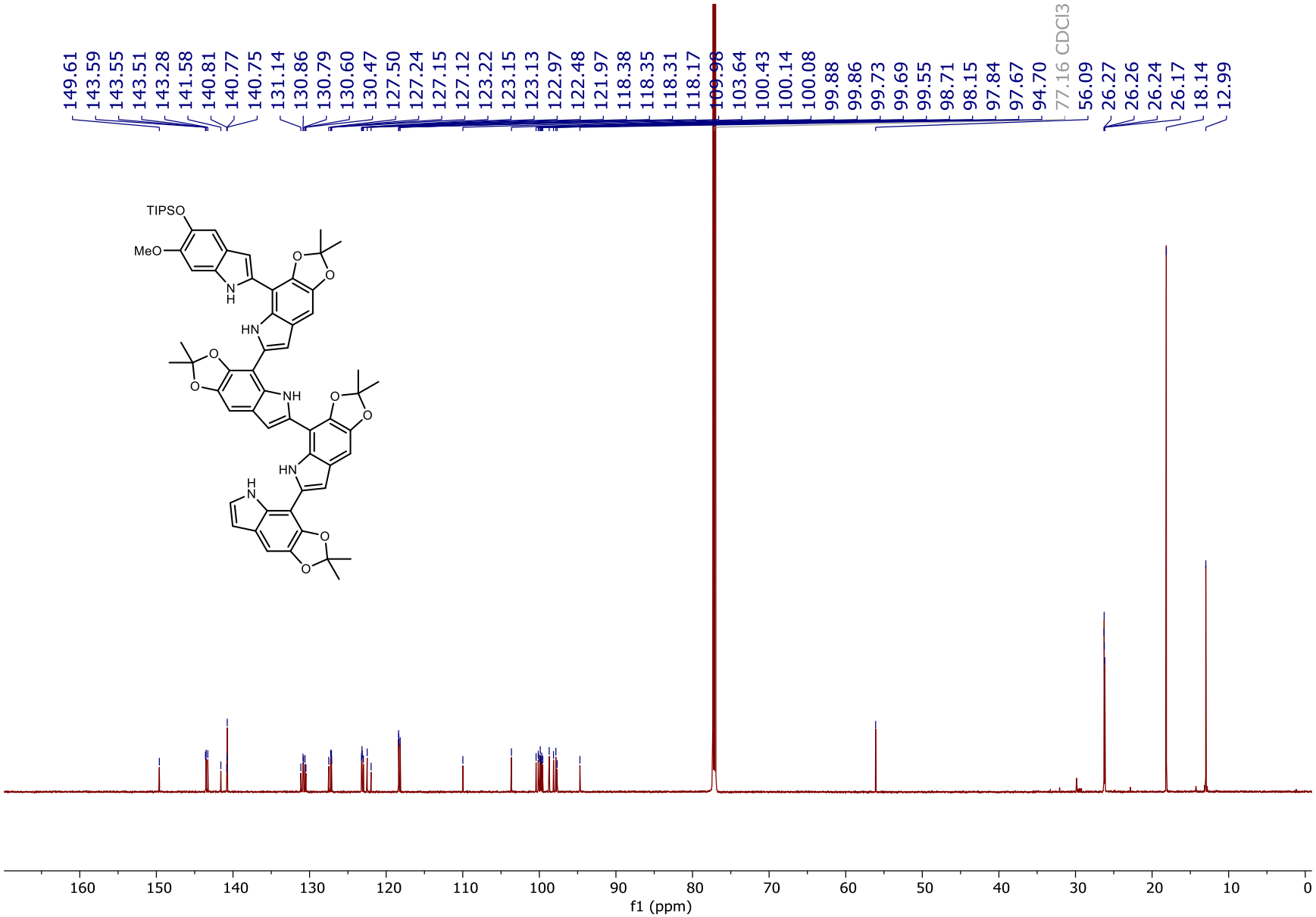
149.61
143.59
143.55
143.51
143.28
141.58
140.81
140.77
140.75
131.14
130.86
130.79
130.60
130.47
127.50
127.24
127.15
127.12
123.22
123.15
123.13
122.97
122.48
121.97
118.38
118.35
118.31
118.17
109.98
103.64
100.43
100.14
100.08
99.88
99.86
99.73
99.69
99.55
98.71
98.15
97.84
97.67
94.70
77.16 CDCl3
56.09
26.27
26.26
26.24
26.17
18.14
12.99
TIPSO
MeO
160
150
140
130
120
110
100
90
80
70
60
50
40
30
20
10
0
f1 (ppm)

Appendix:

^{1}H and ^{13}C NMR Spectra Relevant to **Chapter 4**

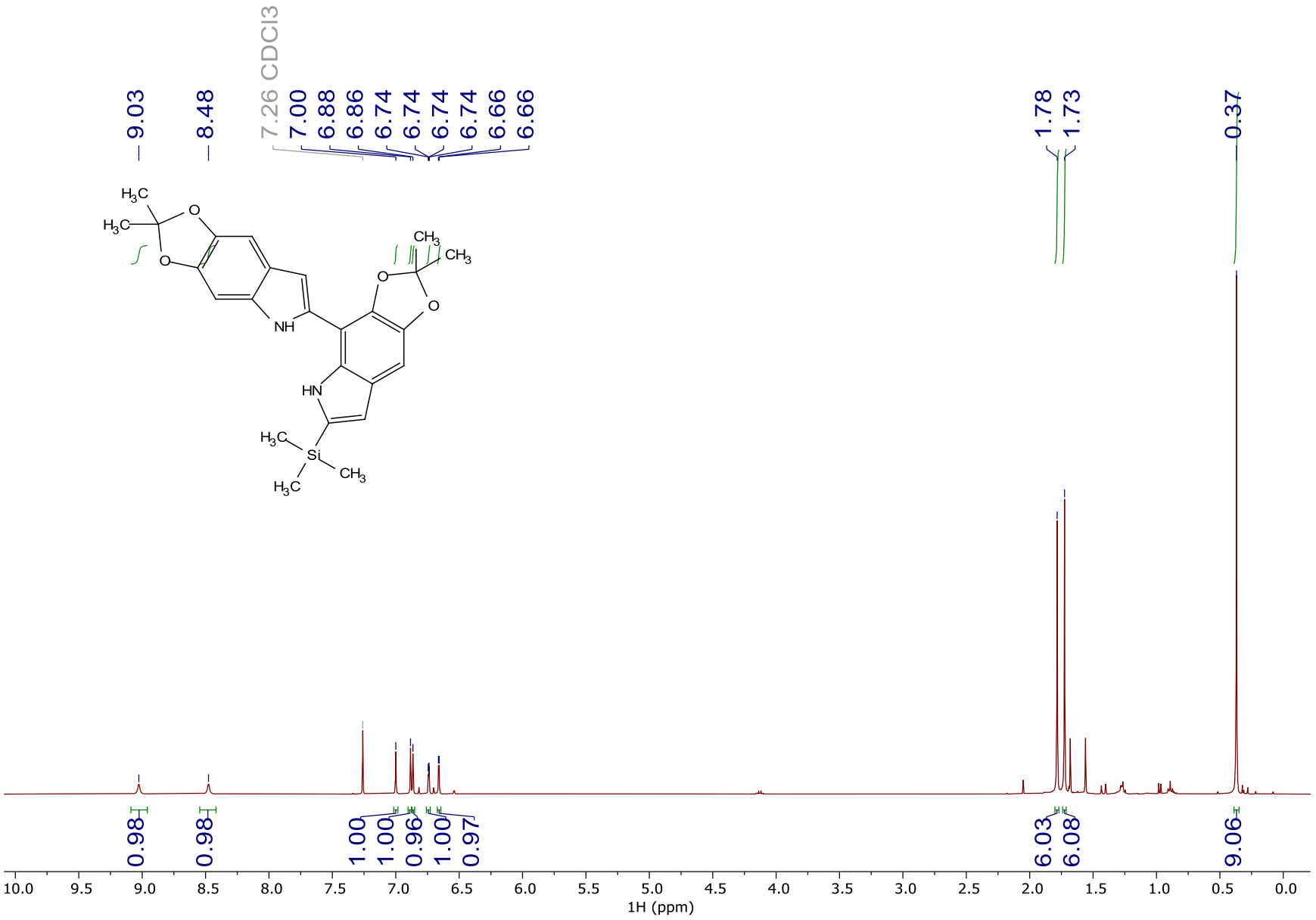
9.03
8.48
7.26 CDCl3
7.00
6.88
6.86
6.74
6.74
6.74
6.74
6.66
6.66
1.78
1.73
0.37
0.98
0.98
1.00
1.00
0.96
1.00
0.97
6.03
6.08
9.06
10.0
9.5
9.0
8.5
8.0
7.5
7.0
6.5
6.0
5.5
5.0
4.5
4.0
3.5
3.0
2.5
2.0
1.5
1.0
0.5
0.0
1H (ppm)

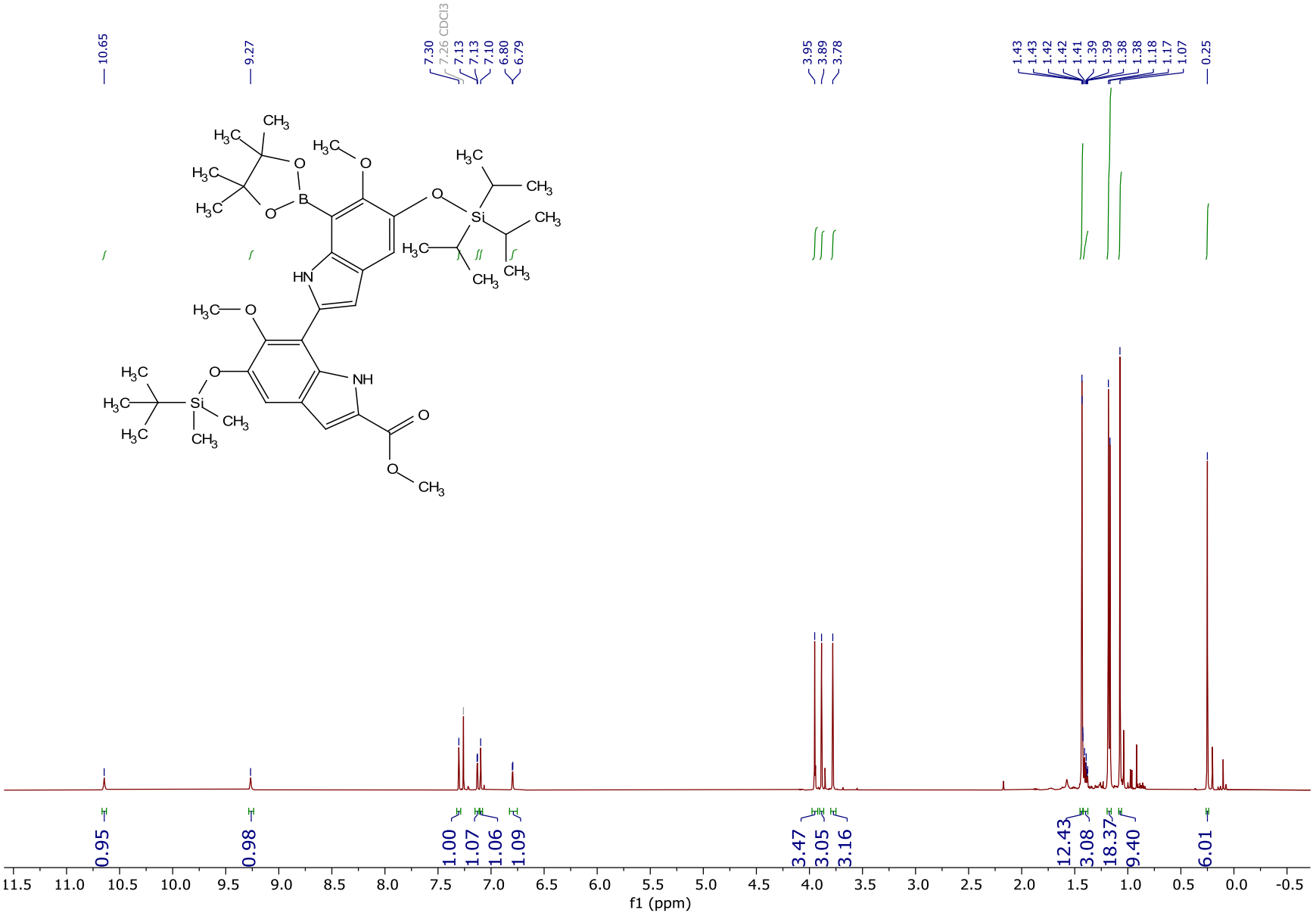
10.65
9.27
7.30
7.26 CDCl3
7.13
7.13
7.10
6.80
6.79
3.95
3.89
3.78
1.43
1.43
1.42
1.42
1.41
1.39
1.39
1.38
1.38
1.18
1.17
1.07
0.25
0.95
0.98
1.00
1.07
1.06
1.09
3.47
3.05
3.16
12.43
3.08
18.37
9.40
6.01
f1 (ppm)

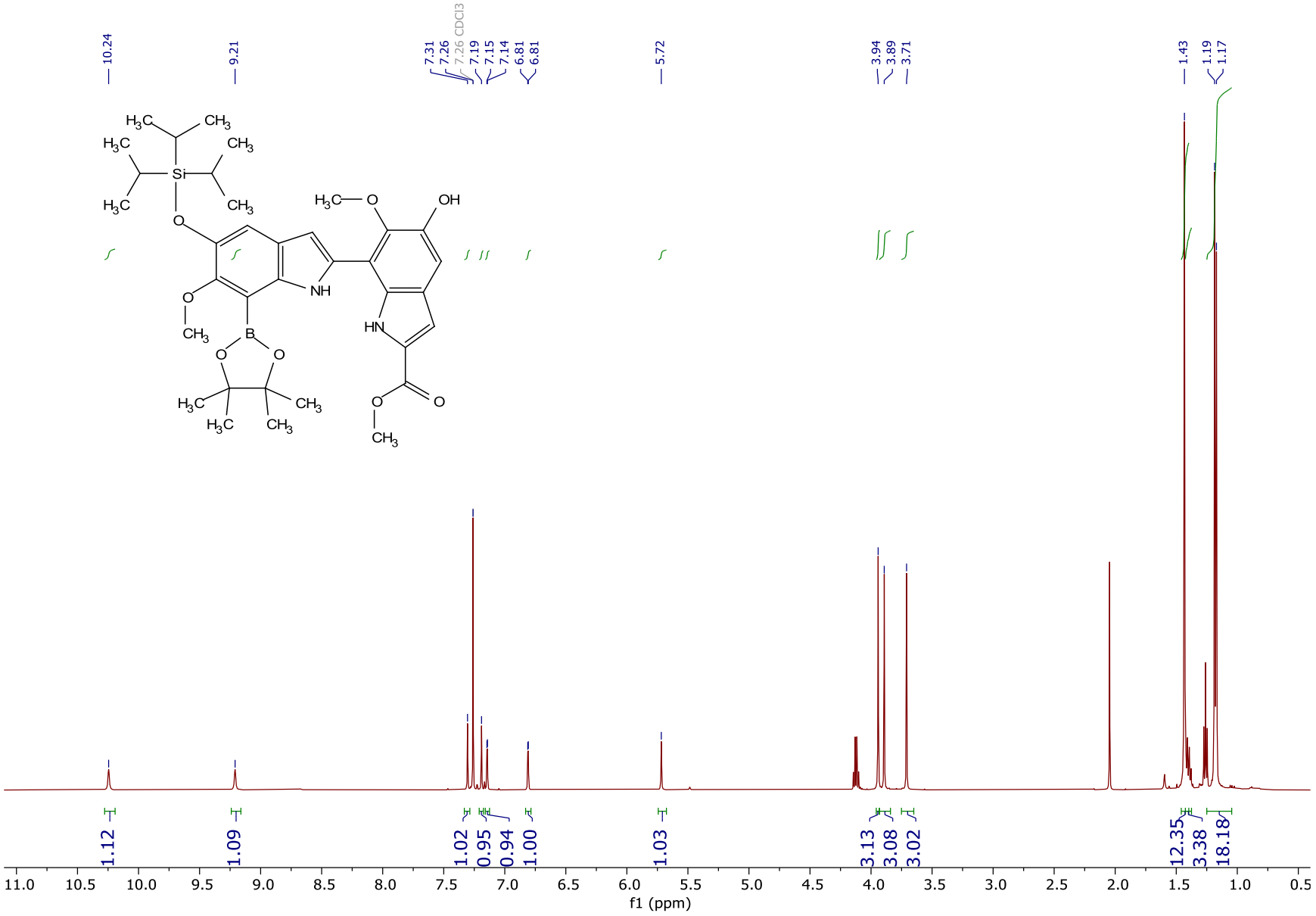
10.24
9.21
7.31
7.26
7.26 CDCl3
7.19
7.15
7.14
6.81
6.81
5.72
3.94
3.89
3.71
1.43
1.19
1.17
1.12
1.09
1.02
0.95
0.94
1.00
1.03
3.13
3.08
3.02
12.35
3.38
18.18
f1 (ppm)

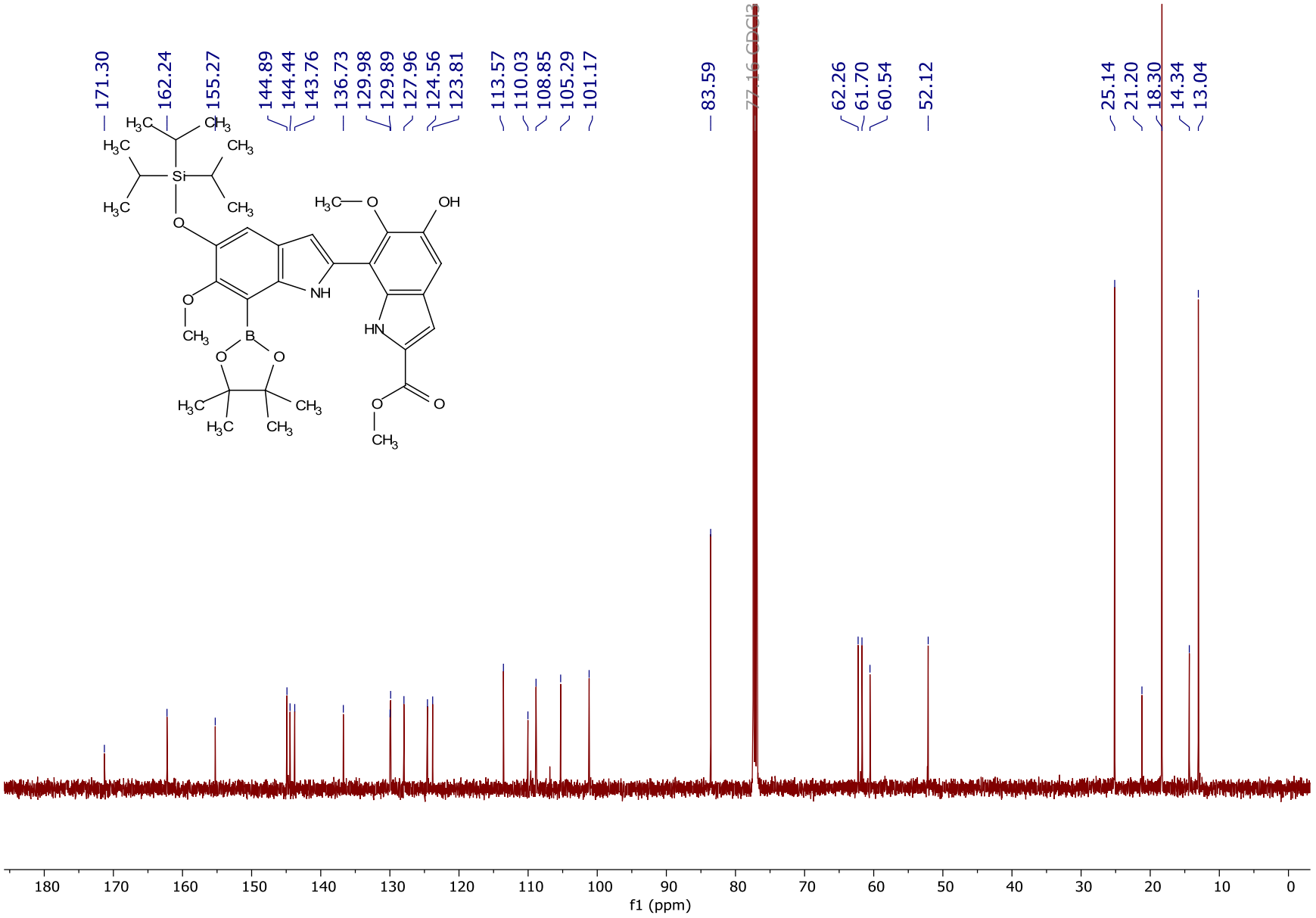
171.30
162.24
155.27
144.89
144.44
143.76
136.73
129.98
129.89
127.96
124.56
123.81
113.57
110.03
108.85
105.29
101.17
83.59
77.16 CDCl3
62.26
61.70
60.54
52.12
25.14
21.20
18.30
14.34
13.04
f1 (ppm)

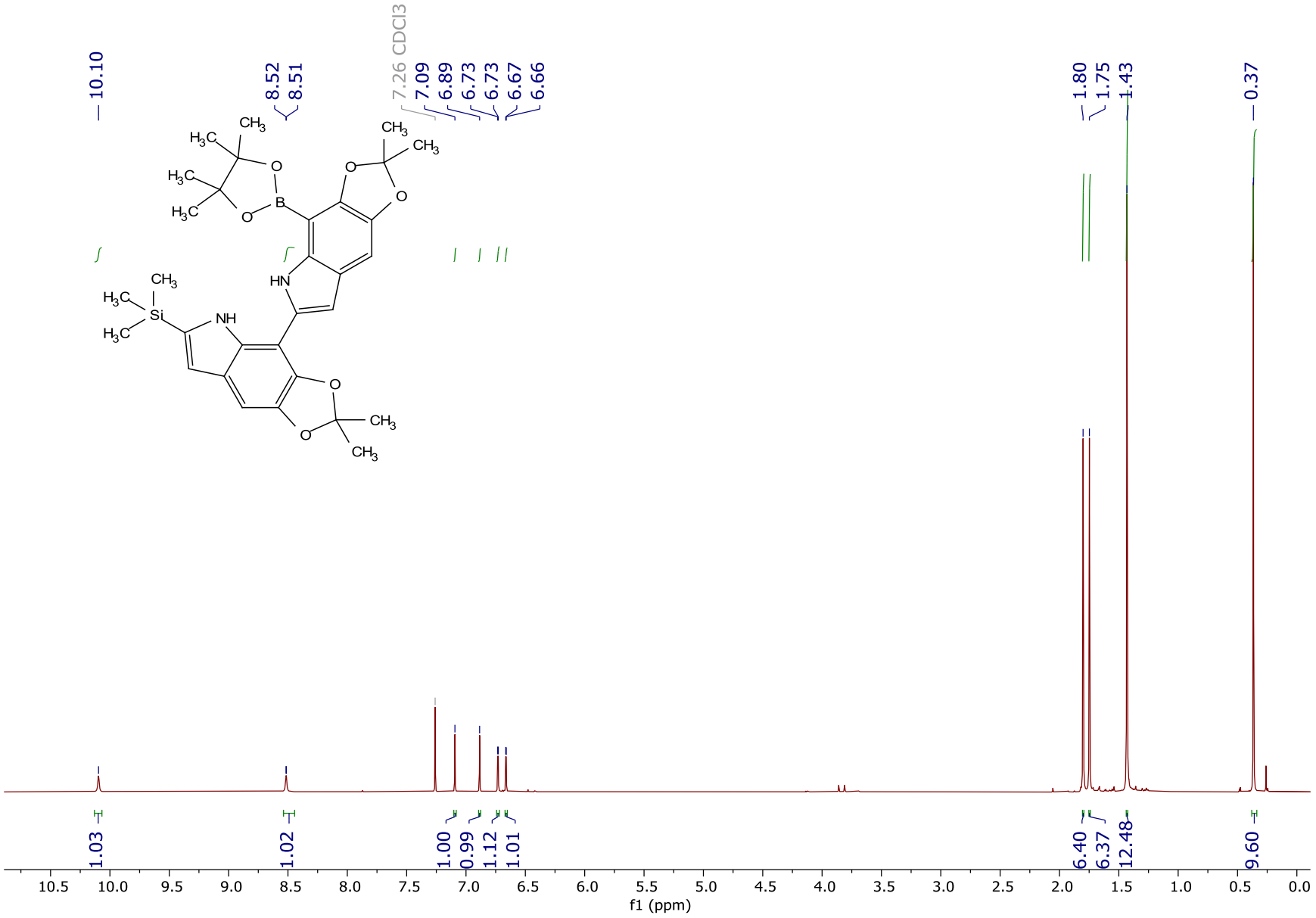
10.10
8.52
8.51
7.26 CDCl3
7.09
6.89
6.73
6.73
6.67
6.66
1.80
1.75
1.43
0.37
1.03
1.02
1.00
0.99
1.12
1.01
6.40
6.37
12.48
9.60
f1 (ppm)

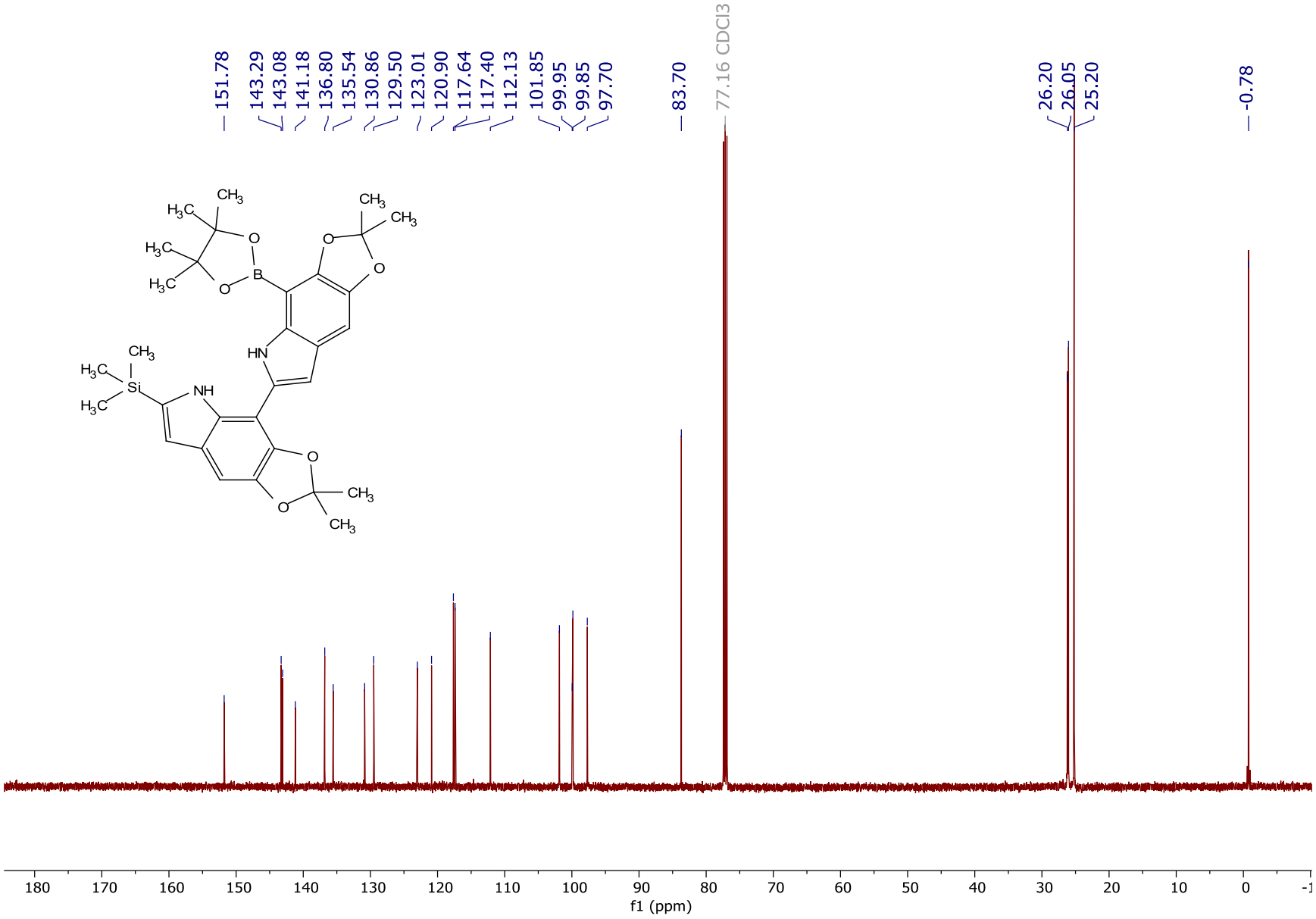
151.78
143.29
143.08
141.18
136.80
135.54
130.86
129.50
123.01
120.90
117.64
117.40
112.13
101.85
99.95
99.85
97.70
83.70
77.16 CDCl3
26.20
26.05
25.20
-0.78
f1 (ppm)

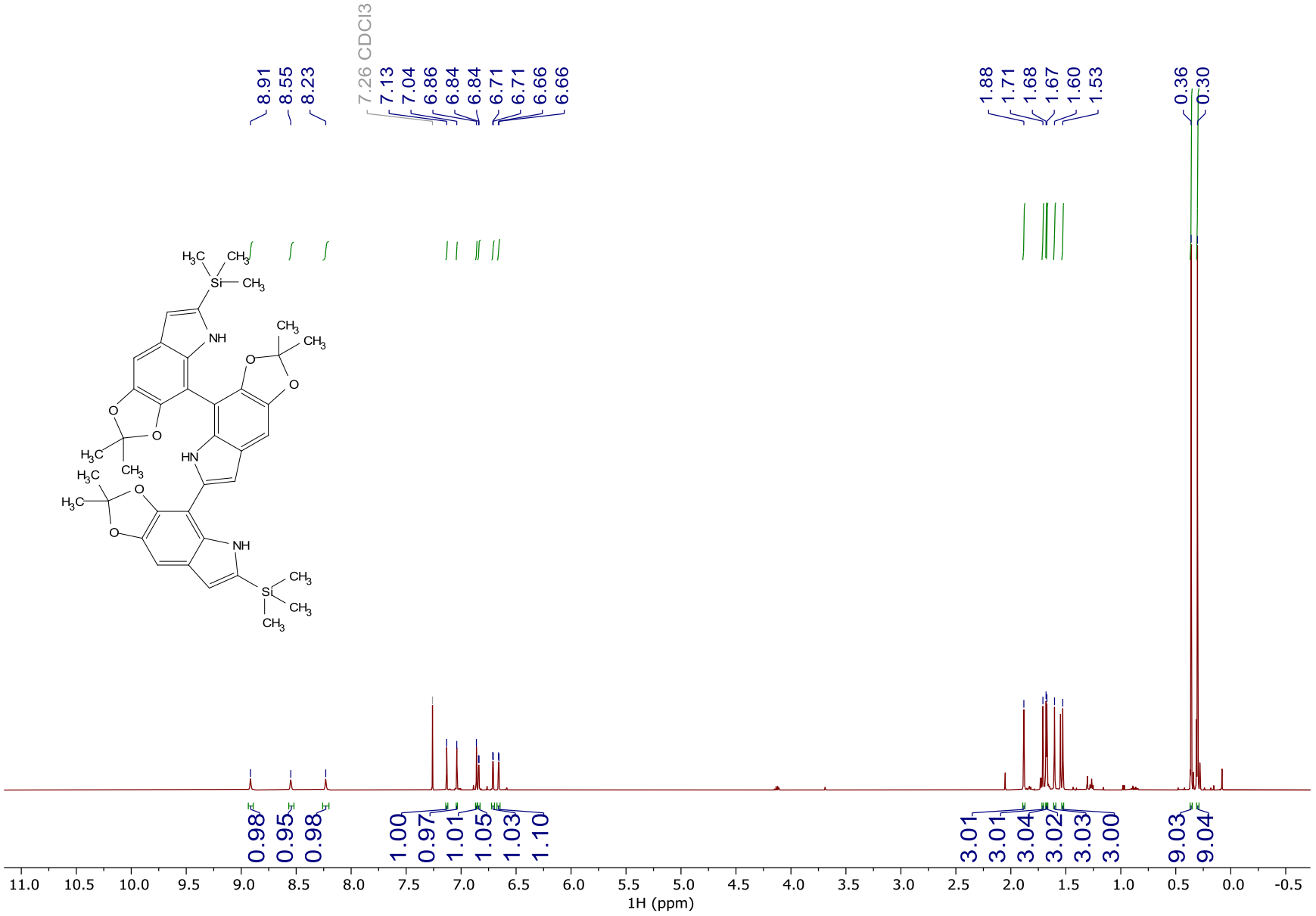
8.91
8.55
8.23
7.26 CDCl3
7.13
7.04
6.86
6.84
6.84
6.71
6.71
6.66
6.66
1.88
1.71
1.68
1.67
1.60
1.53
0.36
0.30
0.98
0.95
0.98
1.00
0.97
1.01
1.05
1.03
1.10
3.01
3.01
3.04
3.02
3.03
3.00
9.03
9.04
11.0 10.5 10.0 9.5 9.0 8.5 8.0 7.5 7.0 6.5 6.0 5.5 5.0 4.5 4.0 3.5 3.0 2.5 2.0 1.5 1.0 0.5 0.0 -0.5
1H (ppm)

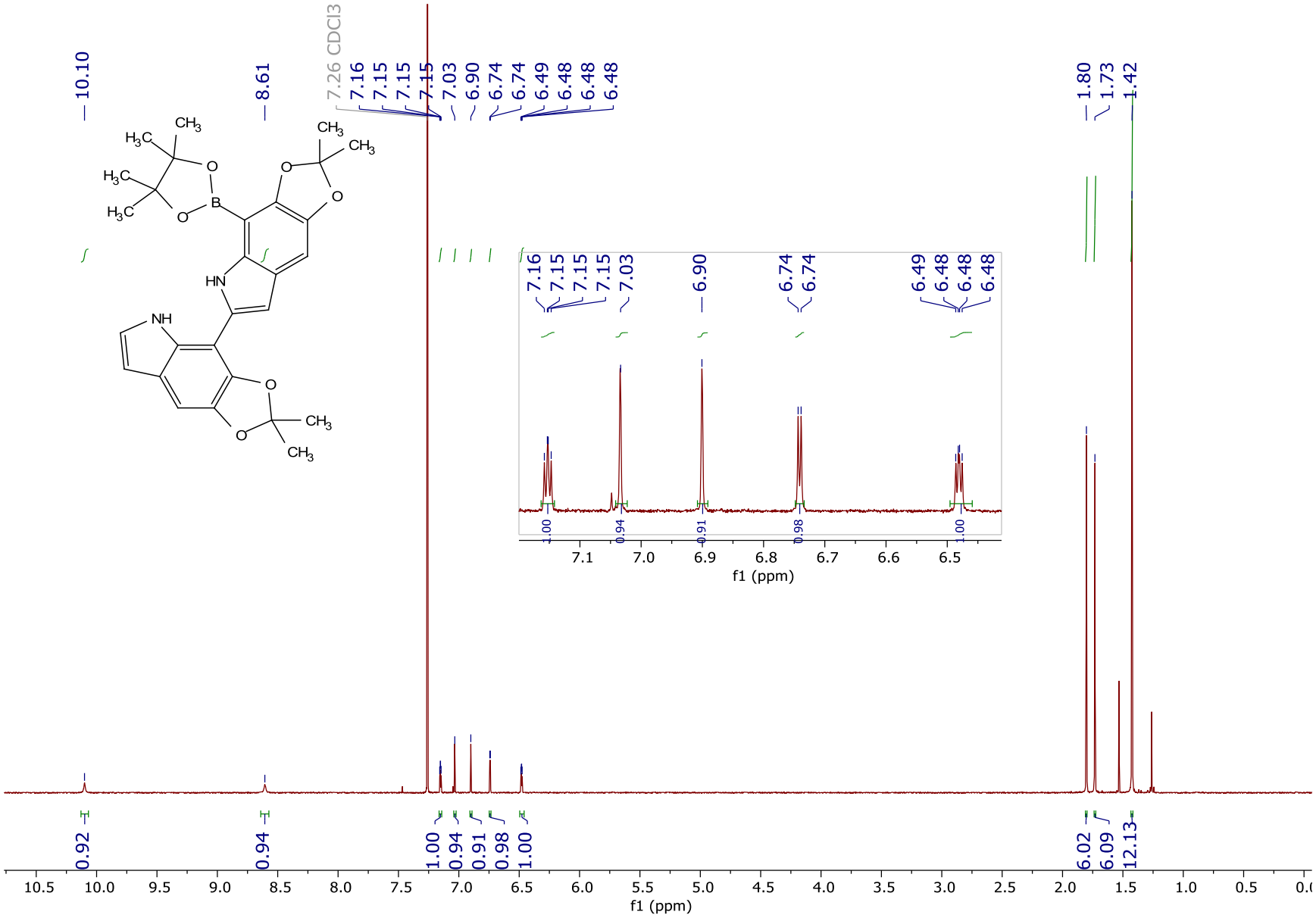
10.10
8.61
7.26 CDCl3
7.16
7.15
7.15
7.15
7.03
6.90
6.74
6.74
6.49
6.48
6.48
6.48
1.80
1.73
1.42
HN
NH
f1 (ppm)
0.92
0.94
1.00
0.94
0.91
0.98
1.00
6.02
6.09
12.13

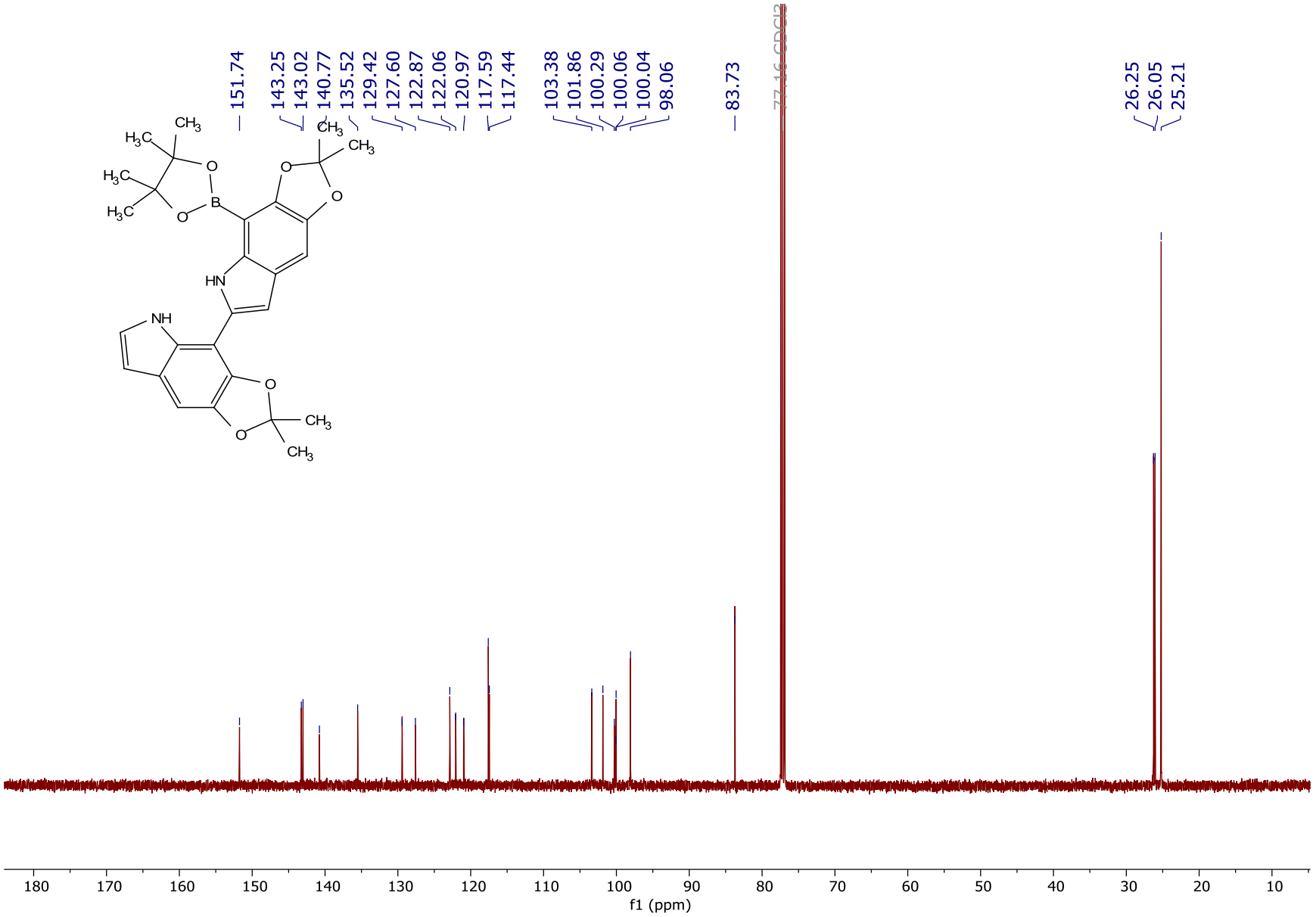
151.74
143.25
143.02
140.77
135.52
129.42
127.60
122.87
122.06
120.97
117.59
117.44
103.38
101.86
100.29
100.06
100.04
98.06
83.73
77.16 CDCl3
26.25
26.05
25.21
f1 (ppm)

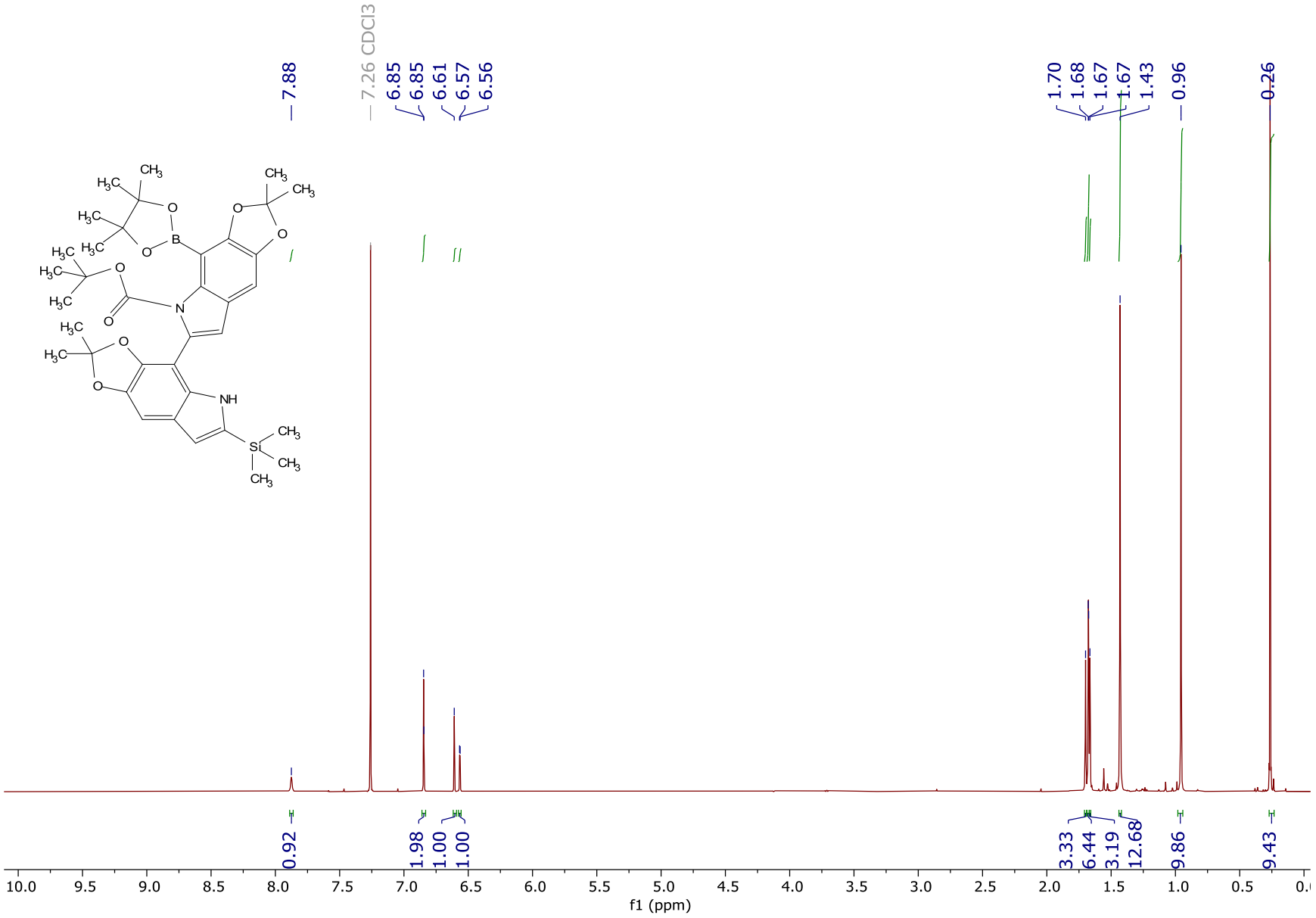
7.88
7.26 CDCl3
6.85
6.85
6.61
6.57
6.56
1.70
1.68
1.67
1.67
1.43
0.96
0.26
0.92
1.98
1.00
1.00
3.33
6.44
3.19
12.68
9.86
9.43
f1 (ppm)

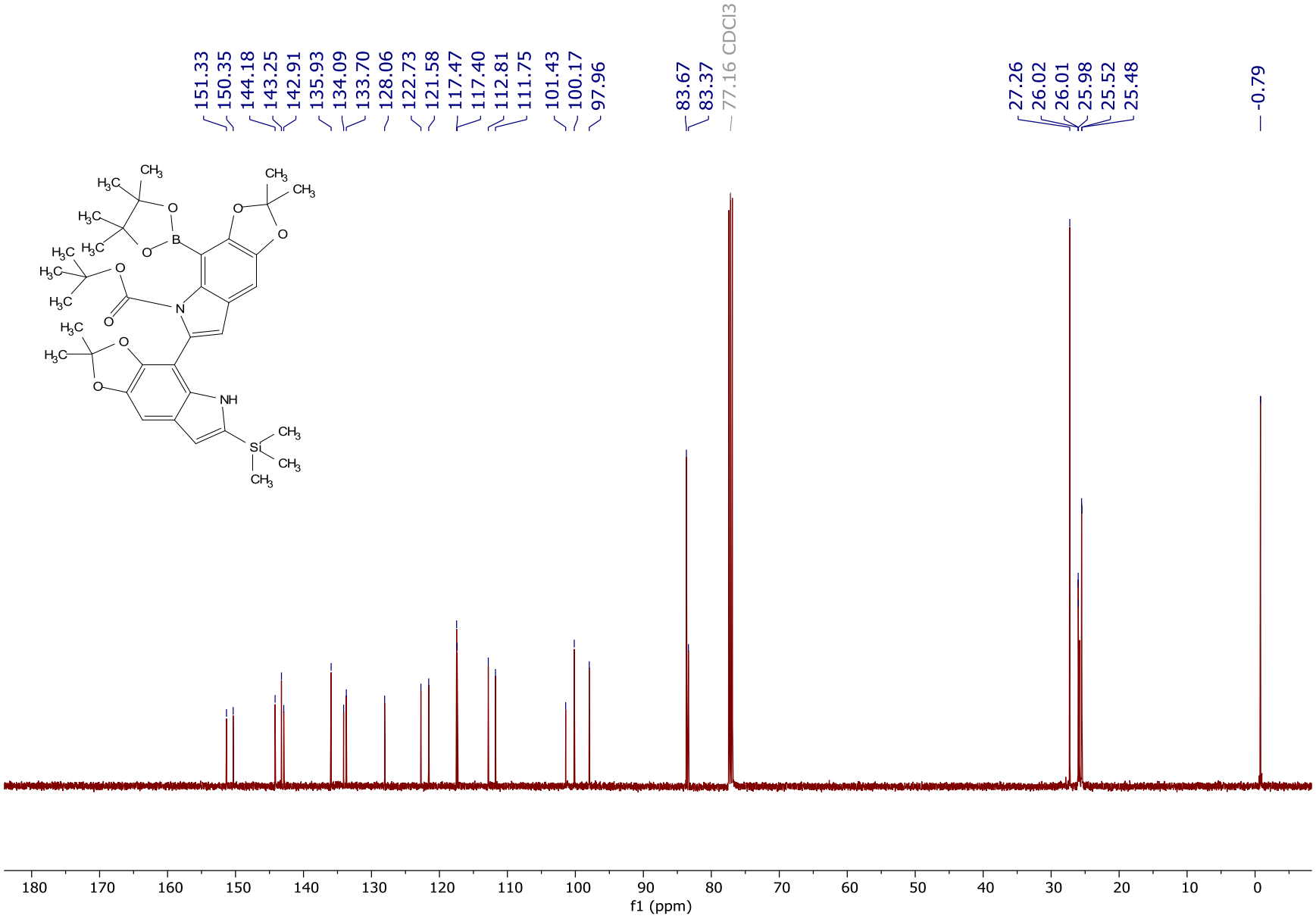
151.33
150.35
144.18
143.25
142.91
135.93
134.09
133.70
128.06
122.73
121.58
117.47
117.40
112.81
111.75
101.43
100.17
97.96
83.67
83.37
77.16 CDCl3
27.26
26.02
26.01
25.98
25.52
25.48
-0.79
f1 (ppm)

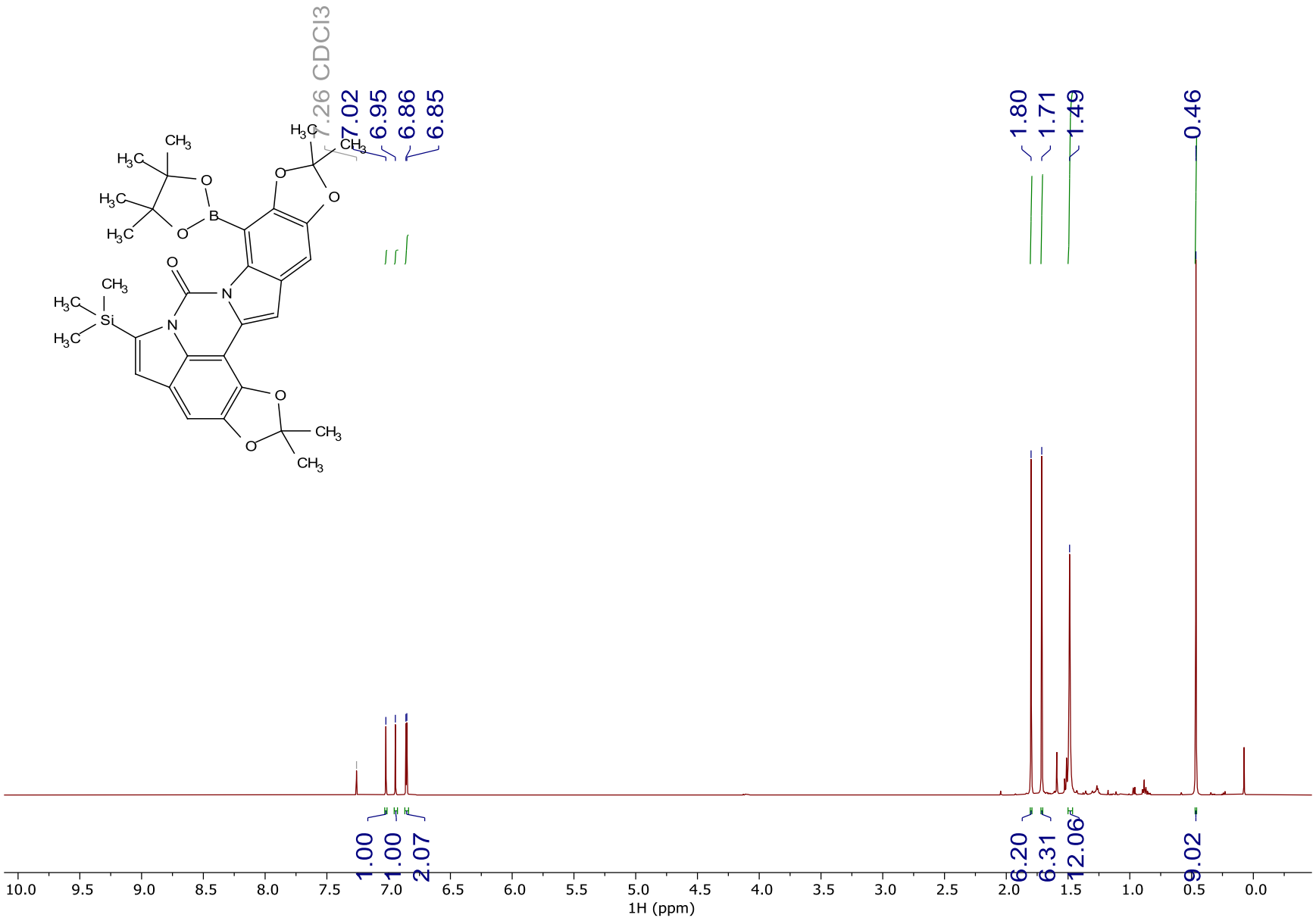
7.26 CDCl3
7.02
6.95
6.86
6.85
1.80
1.71
1.49
0.46
1.00
1.00
2.07
6.20
6.31
12.06
9.02
1H (ppm)

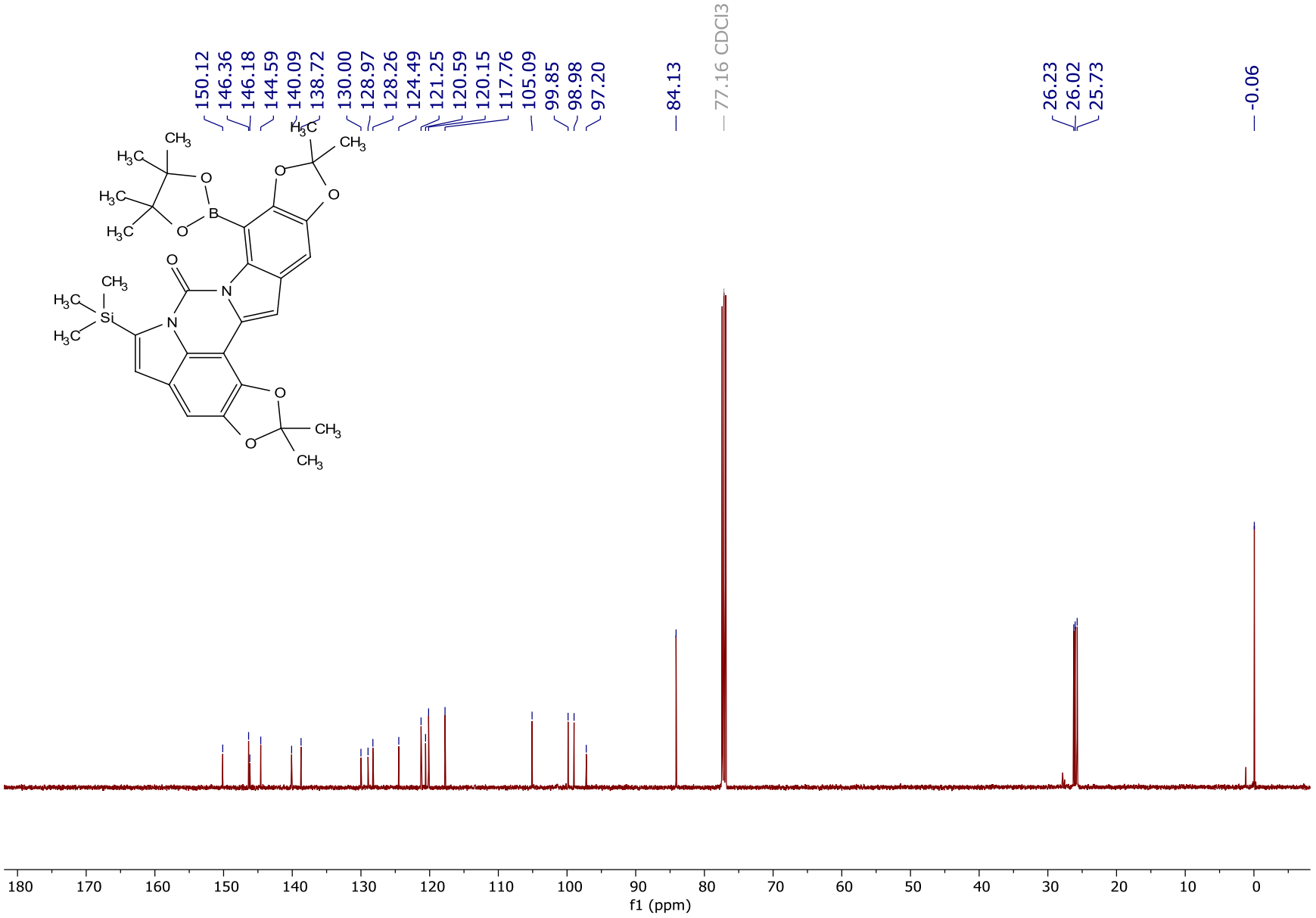
150.12
146.36
146.18
144.59
140.09
138.72
130.00
128.97
128.26
124.49
121.25
120.59
120.15
117.76
105.09
99.85
98.98
97.20
84.13
77.16 CDCl3
26.23
26.02
25.73
-0.06
f1 (ppm)

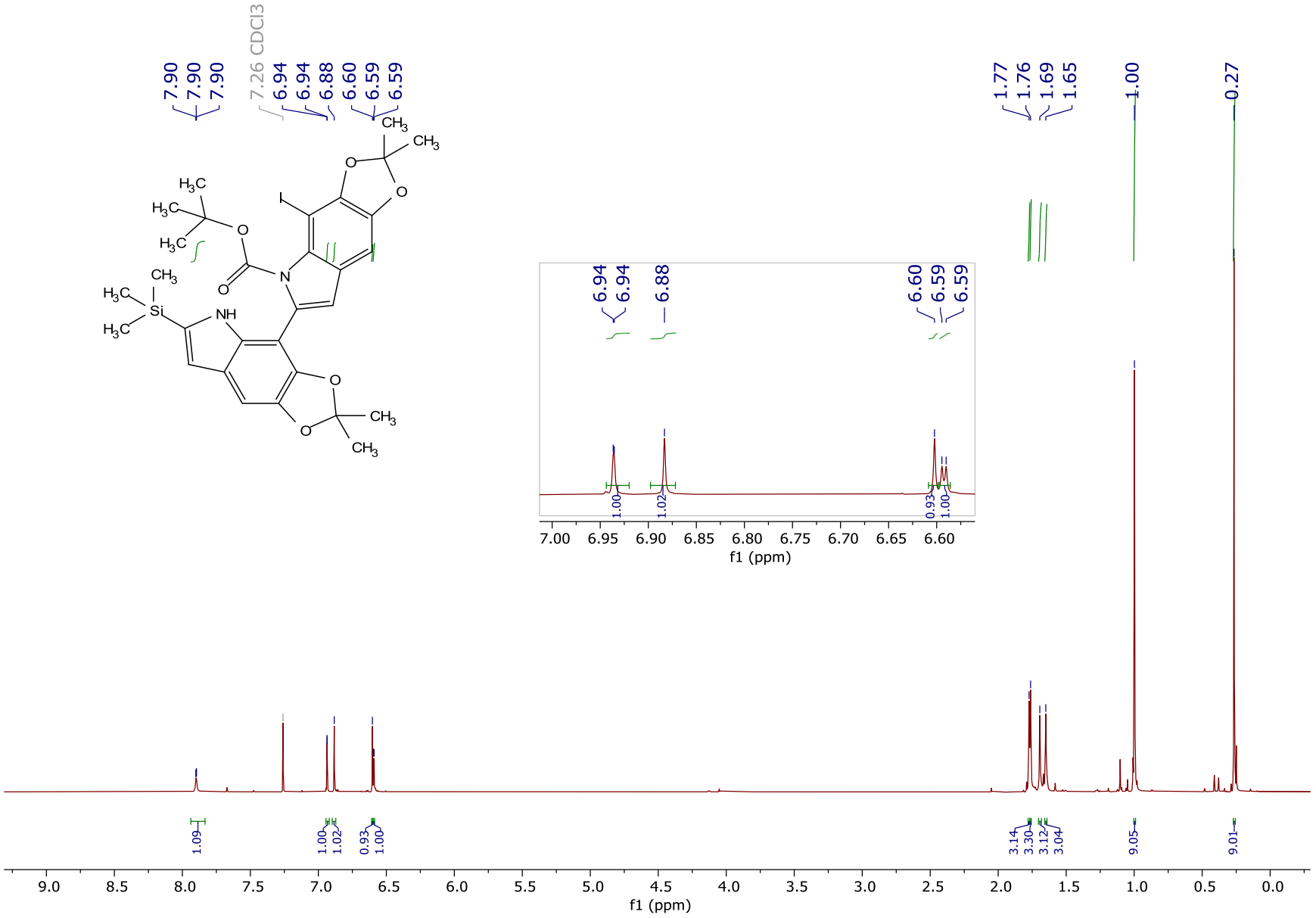
7.90
7.90
7.90
7.26 CDCl3
6.94
6.94
6.88
6.60
6.59
6.59
1.77
1.76
1.69
1.65
1.00
0.27
CH3
CH3
H3C
H3C
H3C
O
O
I
O
N
CH3
H3C
Si
H3C
NH
O
O
CH3
O
CH3
6.94
6.94
6.88
6.60
6.59
6.59
1.00
1.02
0.93
1.00
7.00 6.95 6.90 6.85 6.80 6.75 6.70 6.65 6.60
f1 (ppm)
1.09
1.00
1.02
0.93
1.00
3.14
3.30
3.12
3.04
9.05
9.01
9.0 8.5 8.0 7.5 7.0 6.5 6.0 5.5 5.0 4.5 4.0 3.5 3.0 2.5 2.0 1.5 1.0 0.5 0.0
f1 (ppm)

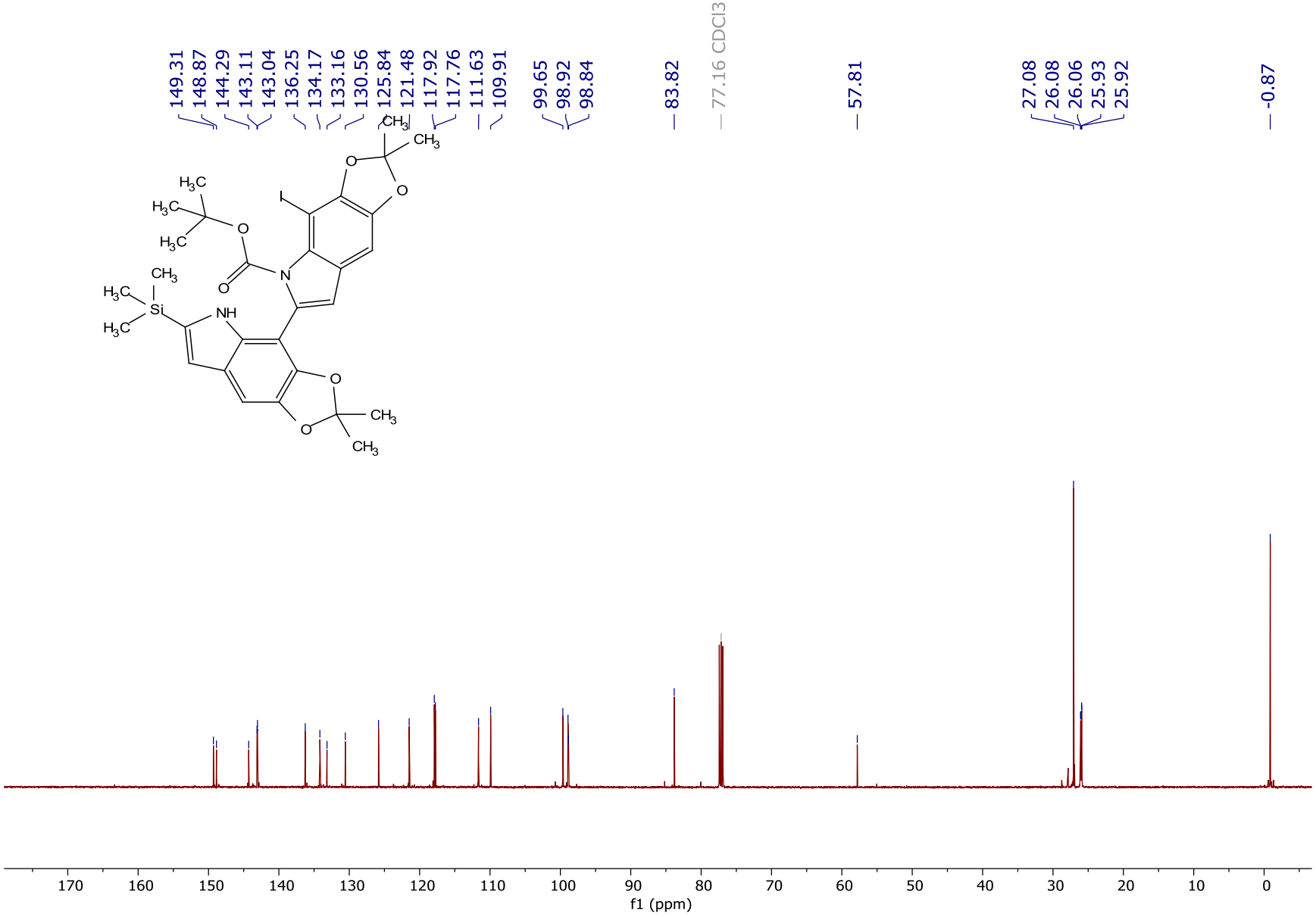
149.31
148.87
144.29
143.11
143.04
136.25
134.17
133.16
130.56
125.84
121.48
117.92
117.76
111.63
109.91
99.65
98.92
98.84
83.82
77.16 CDCl3
57.81
27.08
26.08
26.06
25.93
25.92
-0.87
f1 (ppm)

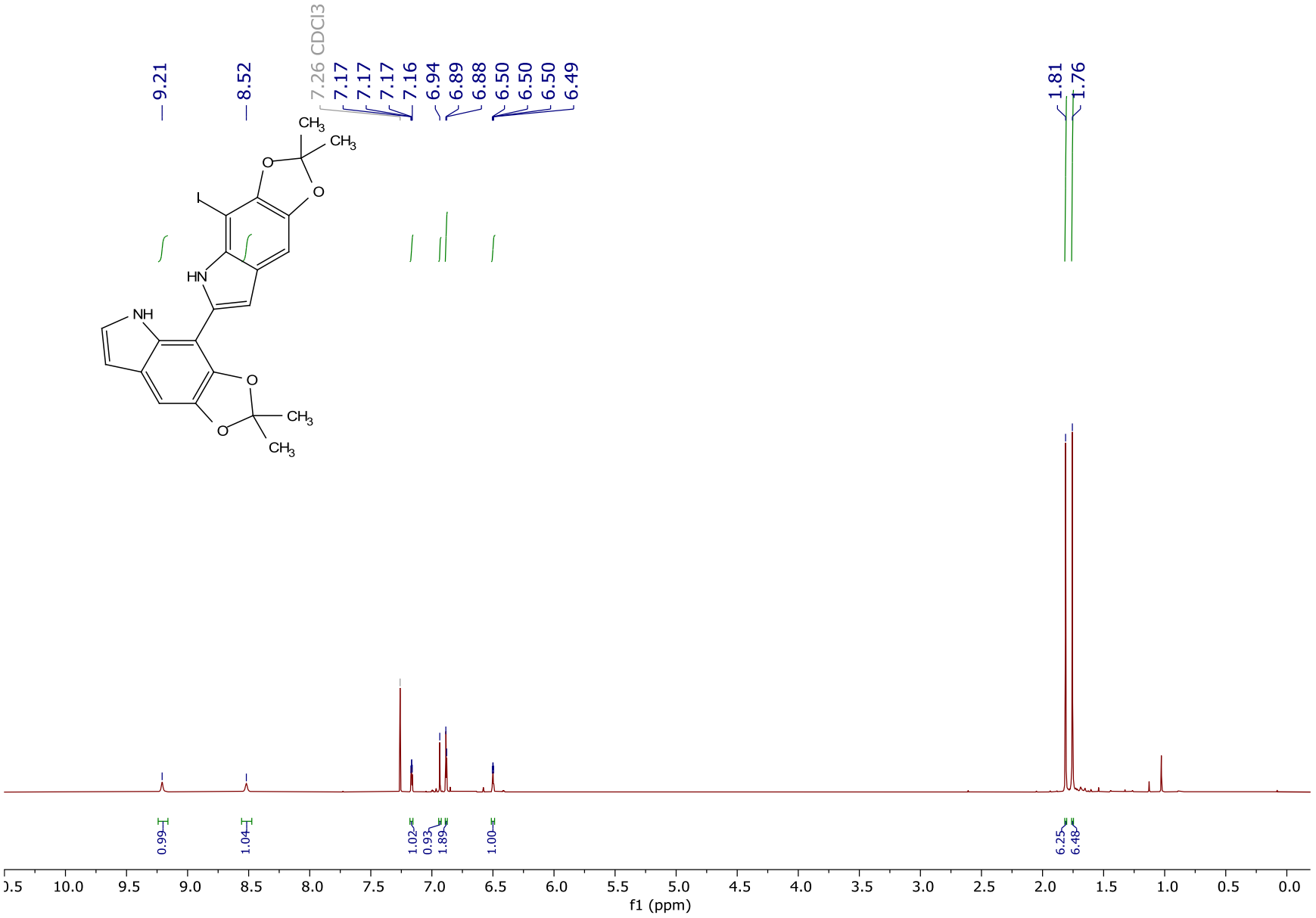
9.21
8.52
7.26 CDCl3
7.17
7.17
7.17
7.16
6.94
6.89
6.88
6.50
6.50
6.50
6.49
1.81
1.76
CH3
CH3
O
O
I
HN
NH
O
O
CH3
CH3
0.99
1.04
1.02
0.93
1.89
1.00
6.25
6.48
f1 (ppm)

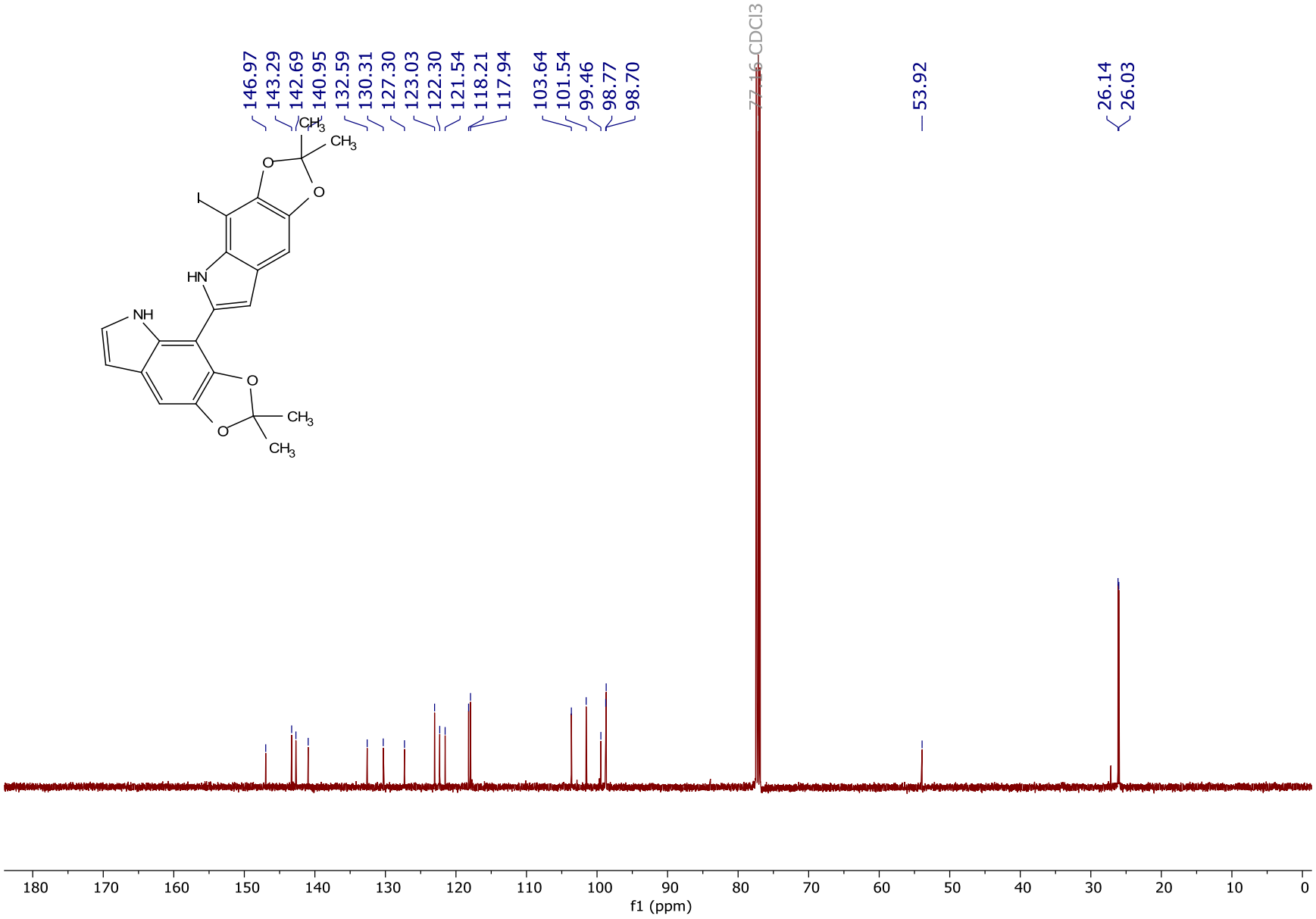
146.97
143.29
142.69
140.95
132.59
130.31
127.30
123.03
122.30
121.54
118.21
117.94
103.64
101.54
99.46
98.77
98.70
77.16 CDCl3
53.92
26.14
26.03
CH3
CH3
O
O
I
HN
NH
O
O
CH3
CH3
180
170
160
150
140
130
120
110
100
90
80
70
60
50
40
30
20
10
0
f1 (ppm)

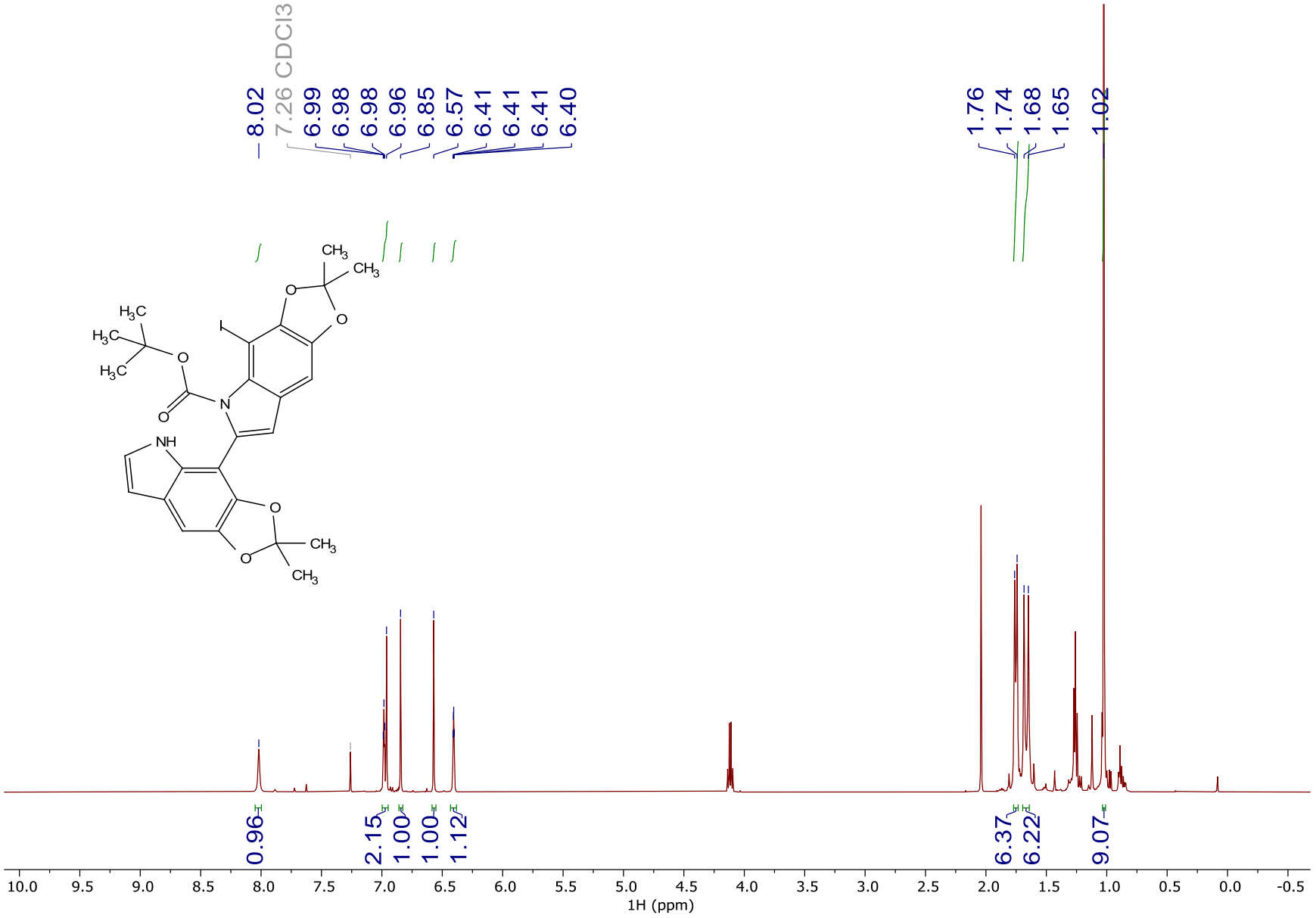
8.02
7.26 CDCl3
6.99
6.98
6.98
6.96
6.85
6.57
6.41
6.41
6.41
6.40
1.76
1.74
1.68
1.65
1.02
0.96
2.15
1.00
1.00
1.12
6.37
6.22
9.07
1H (ppm)

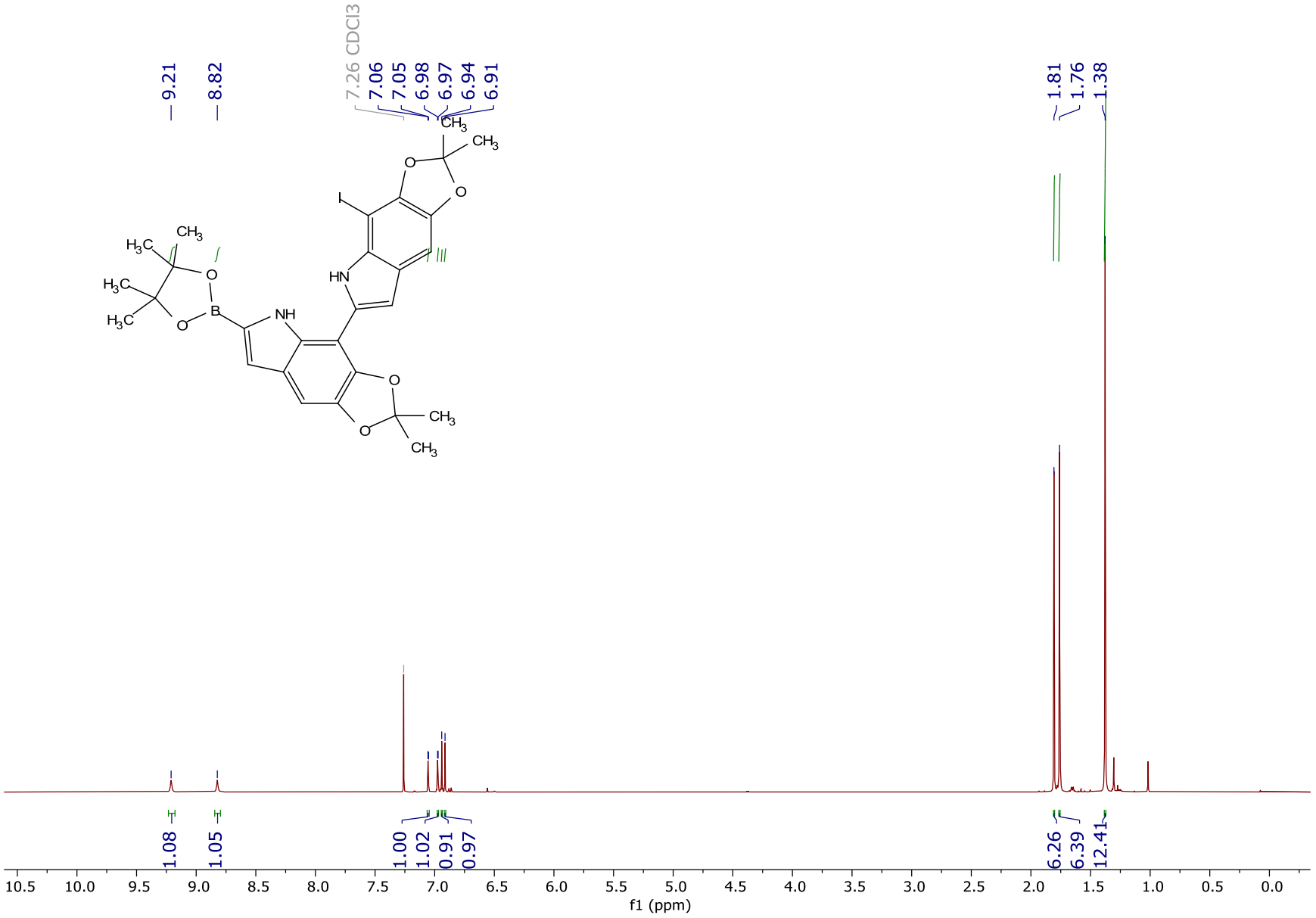
9.21
8.82
7.26 CDCl3
7.06
7.05
6.98
6.97
6.94
6.91
1.81
1.76
1.38
1.08
1.05
1.00
1.02
0.91
0.97
6.26
6.39
12.41
f1 (ppm)

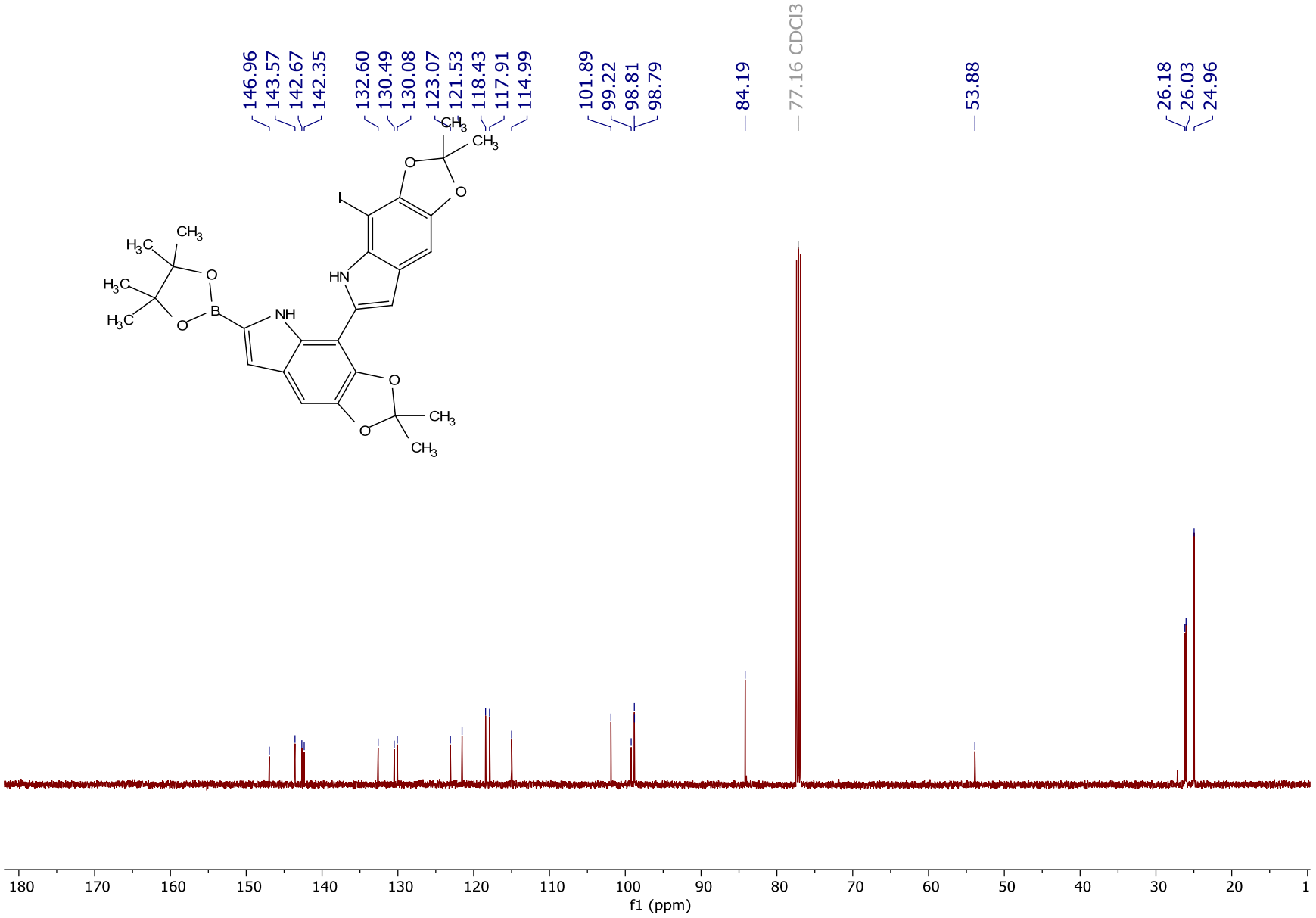
146.96
143.57
142.67
142.35
132.60
130.49
130.08
123.07
121.53
118.43
117.91
114.99
101.89
99.22
98.81
98.79
84.19
77.16 CDCl3
53.88
26.18
26.03
24.96
CH3
CH3
O
O
I
HN
H3C
CH3
H3C
O
B
H3C
O
NH
O
O
CH3
CH3
180
170
160
150
140
130
120
110
100
90
80
70
60
50
40
30
20
1
f1 (ppm)

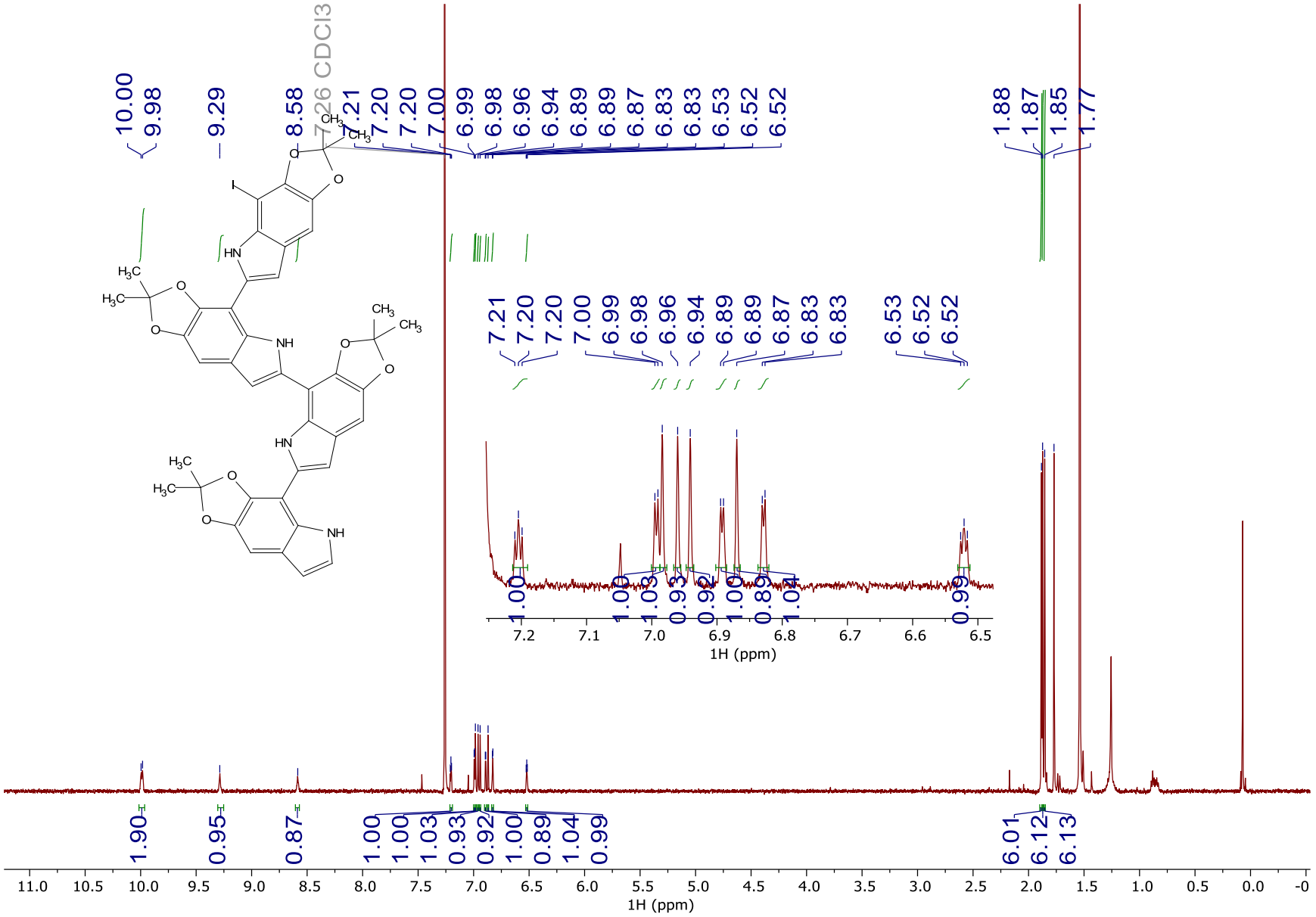
10.00
9.98
9.29
8.58
7.26 CDCl3
7.21
7.20
7.20
7.00
6.99
6.98
6.96
6.94
6.89
6.89
6.87
6.83
6.83
6.53
6.52
6.52
1.88
1.87
1.85
1.77
1.90
0.95
0.87
1.00
1.00
1.03
0.93
0.92
1.00
0.89
1.04
0.99
6.01
6.12
6.13
1H (ppm)

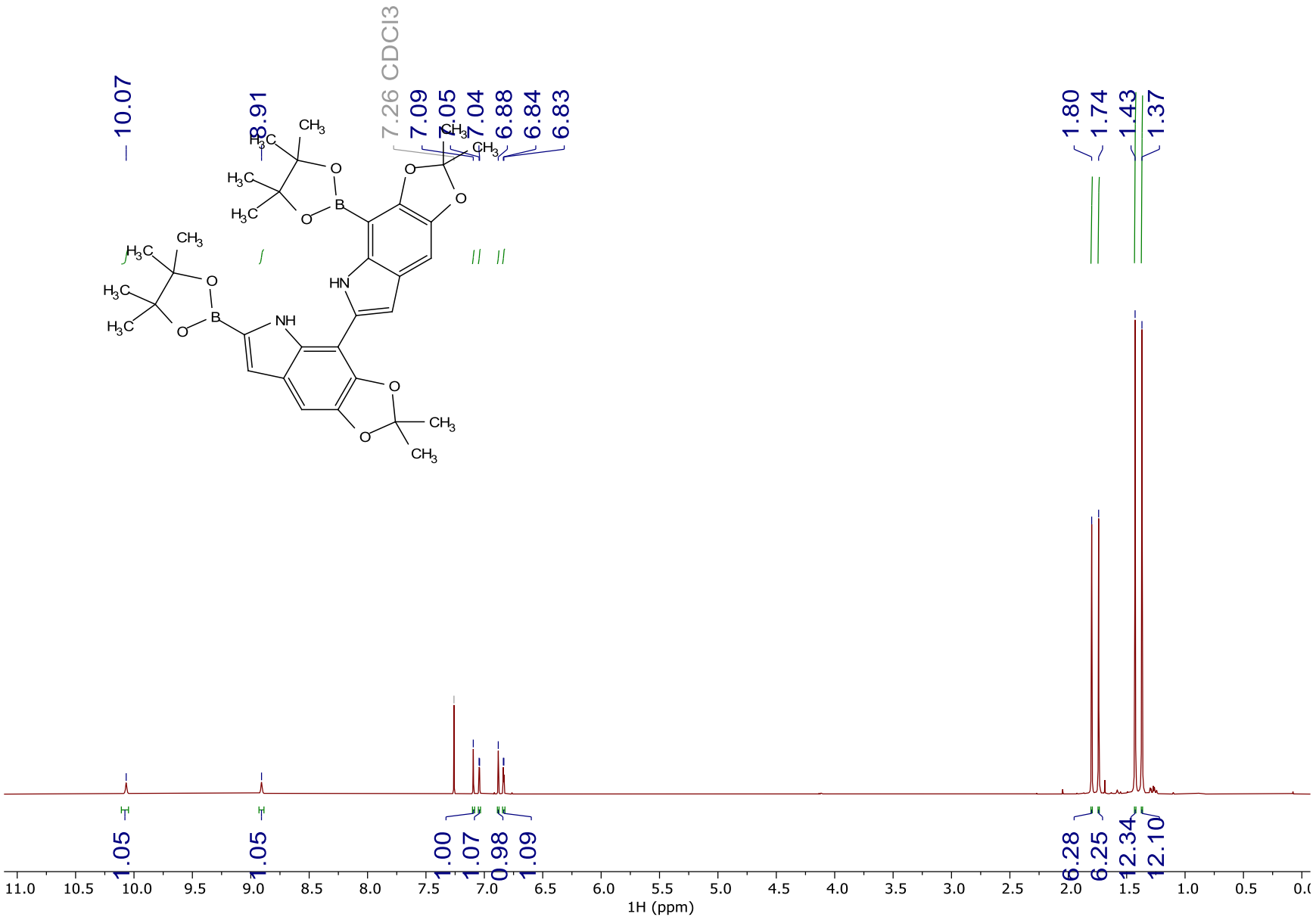
10.07
8.91
7.26 CDCl3
7.09
7.05
7.04
6.88
6.84
6.83
1.80
1.74
1.43
1.37
1.05
1.05
1.00
1.07
0.98
1.09
6.28
6.25
12.34
12.10
1H (ppm)

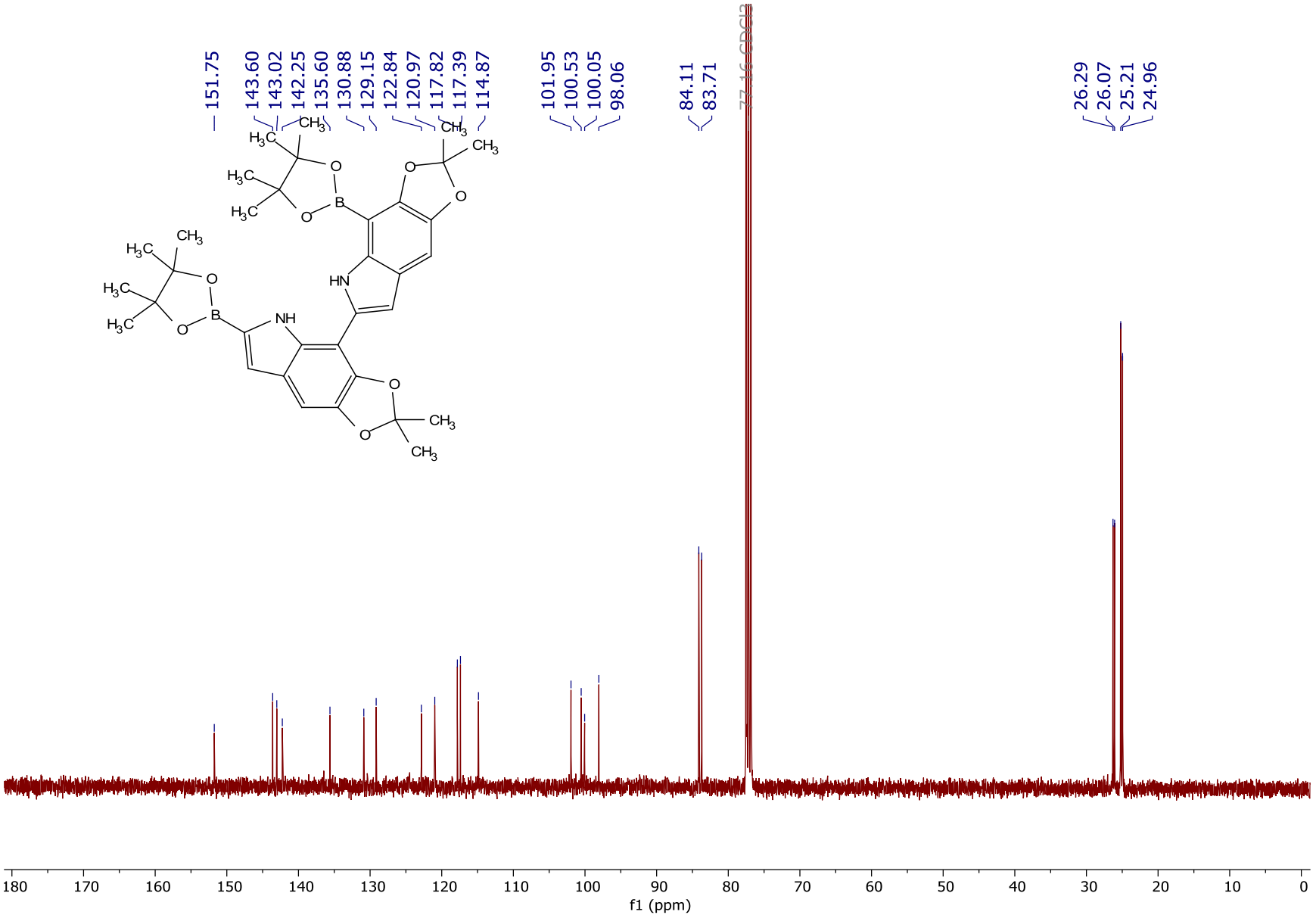
151.75
143.60
143.02
142.25
135.60
130.88
129.15
122.84
120.97
117.82
117.39
114.87
101.95
100.53
100.05
98.06
84.11
83.71
77.16 CDCl3
26.29
26.07
25.21
24.96
f1 (ppm)

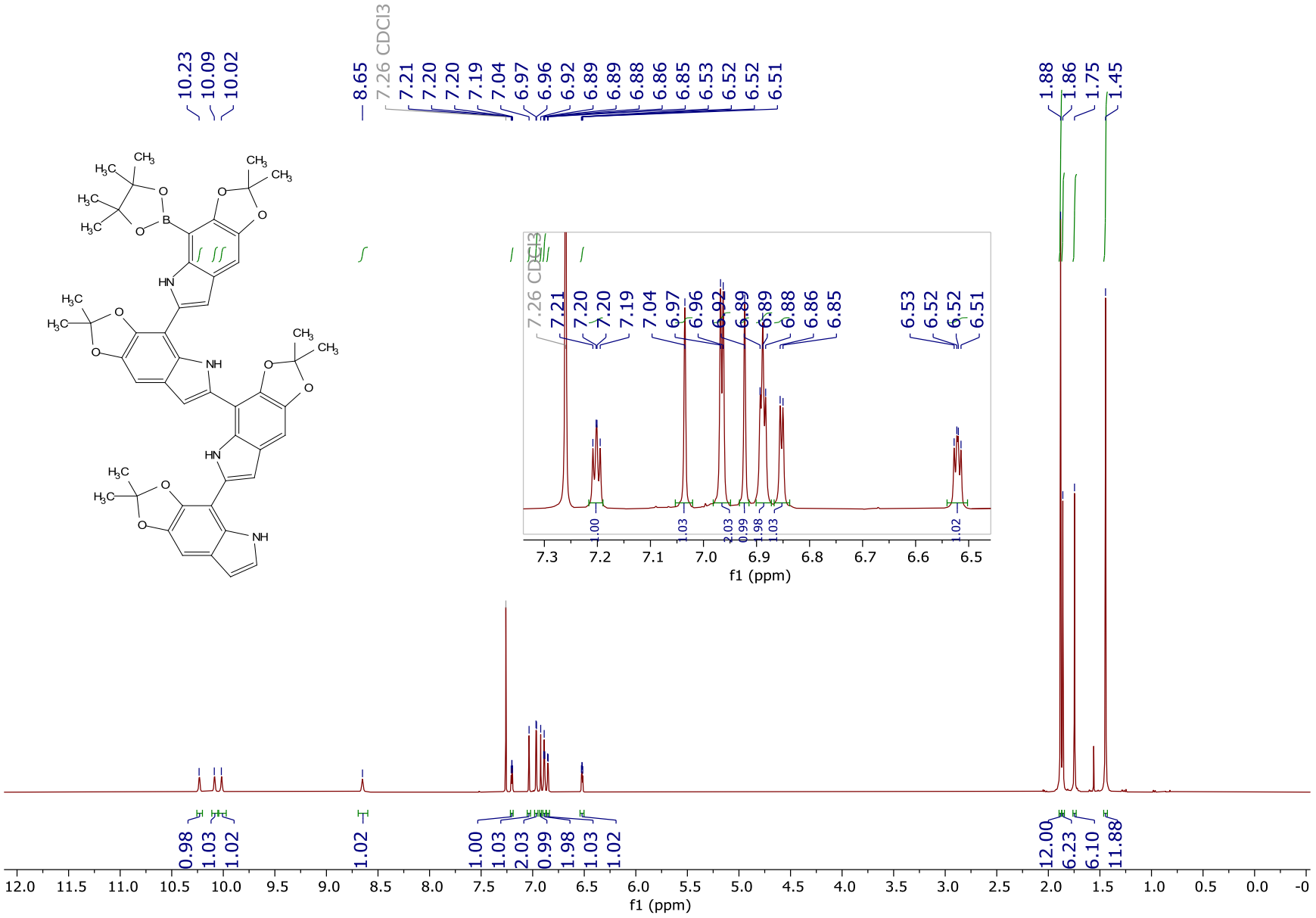
10.23
10.09
10.02
8.65
7.26 CDCl3
7.21
7.20
7.20
7.19
7.04
6.97
6.96
6.92
6.89
6.89
6.88
6.86
6.85
6.53
6.52
6.52
6.51
1.88
1.86
1.75
1.45
HN
NH
HN
NH
f1 (ppm)
0.98
1.03
1.02
1.02
1.00
1.03
2.03
0.99
1.98
1.03
1.02
12.00
6.23
6.10
11.88

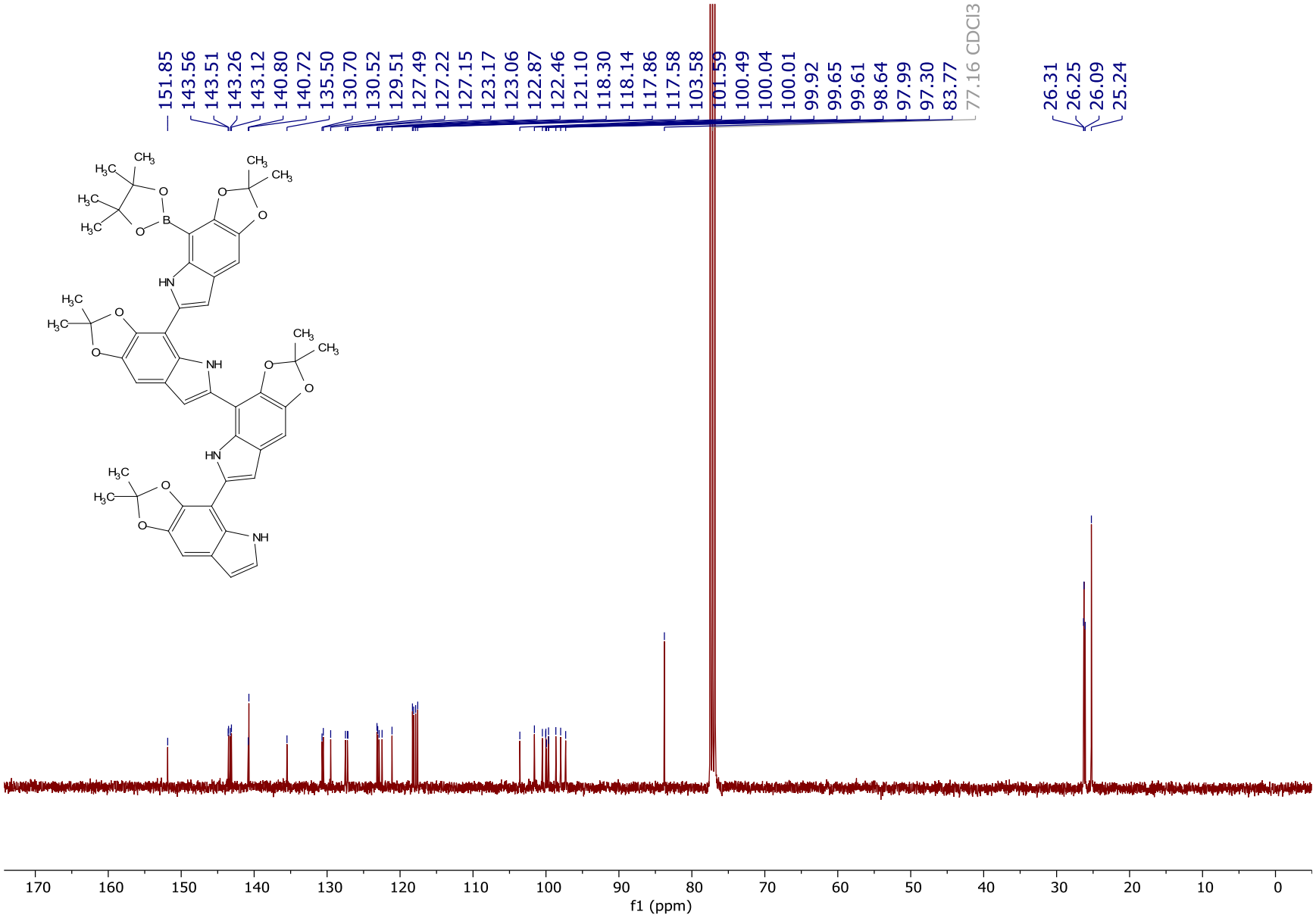
151.85
143.56
143.51
143.26
143.12
140.80
140.72
135.50
130.70
130.52
129.51
127.49
127.22
127.15
123.17
123.06
122.87
122.46
121.10
118.30
118.14
117.86
117.58
103.58
101.59
100.49
100.04
100.01
99.92
99.65
99.61
98.64
97.99
97.30
83.77
77.16 CDCl3
26.31
26.25
26.09
25.24
170
160
150
140
130
120
110
100
90
80
70
60
50
40
30
20
10
0
f1 (ppm)

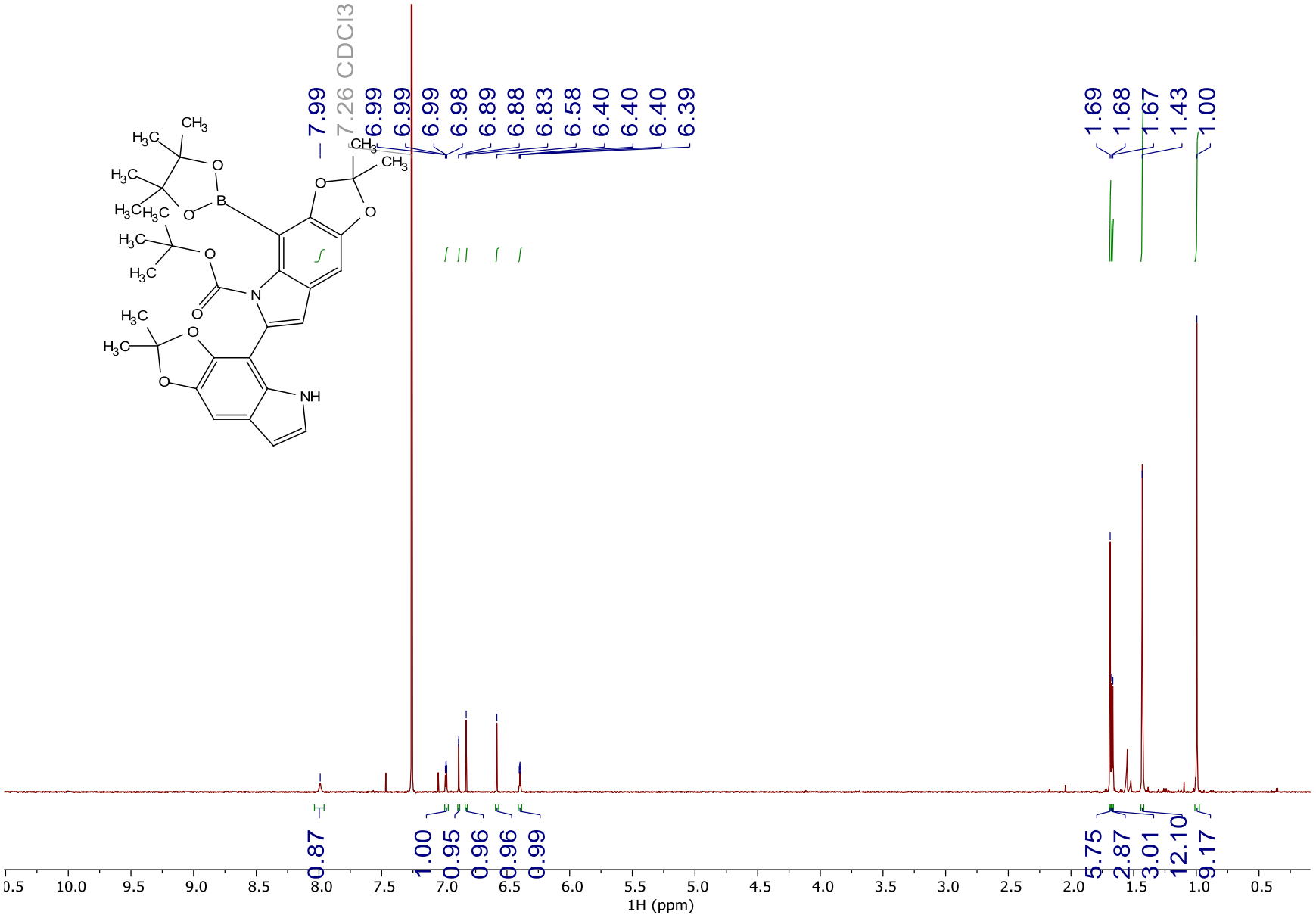
7.99
7.26 CDCl3
6.99
6.99
6.99
6.98
6.89
6.88
6.83
6.58
6.40
6.40
6.40
6.39
1.69
1.68
1.67
1.43
1.00
0.87
1.00
0.95
0.96
0.96
0.99
5.75
2.87
3.01
12.10
9.17
1H (ppm)

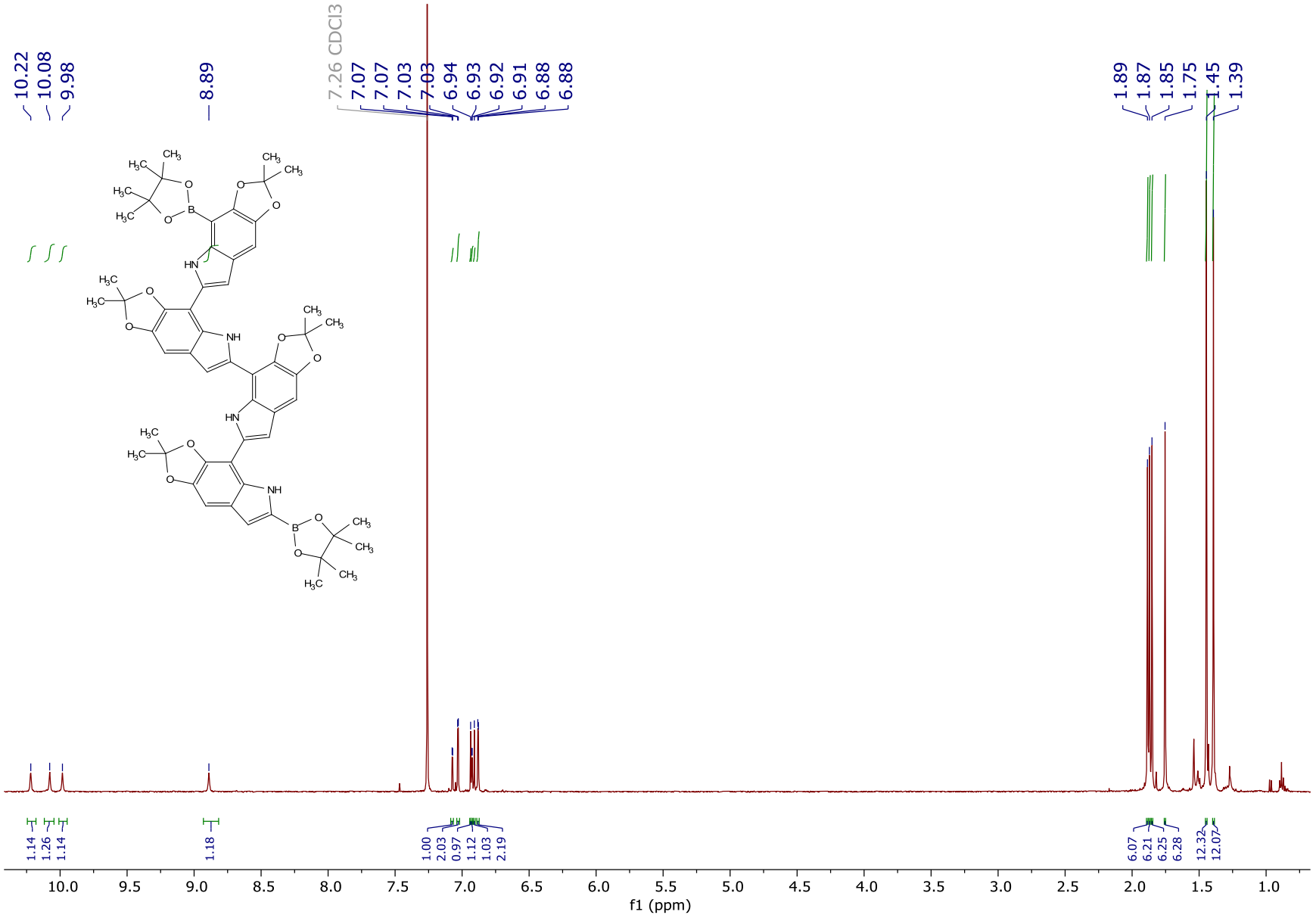
10.22
10.08
9.98
8.89
7.26 CDCl3
7.07
7.07
7.03
7.03
6.94
6.93
6.92
6.91
6.88
6.88
1.89
1.87
1.85
1.75
1.45
1.39
1.14
1.26
1.14
1.18
1.00
2.03
0.97
1.12
1.03
2.19
6.07
6.21
6.25
6.28
12.32
12.07
10.0
9.5
9.0
8.5
8.0
7.5
7.0
6.5
6.0
5.5
5.0
4.5
4.0
3.5
3.0
2.5
2.0
1.5
1.0
f1 (ppm)

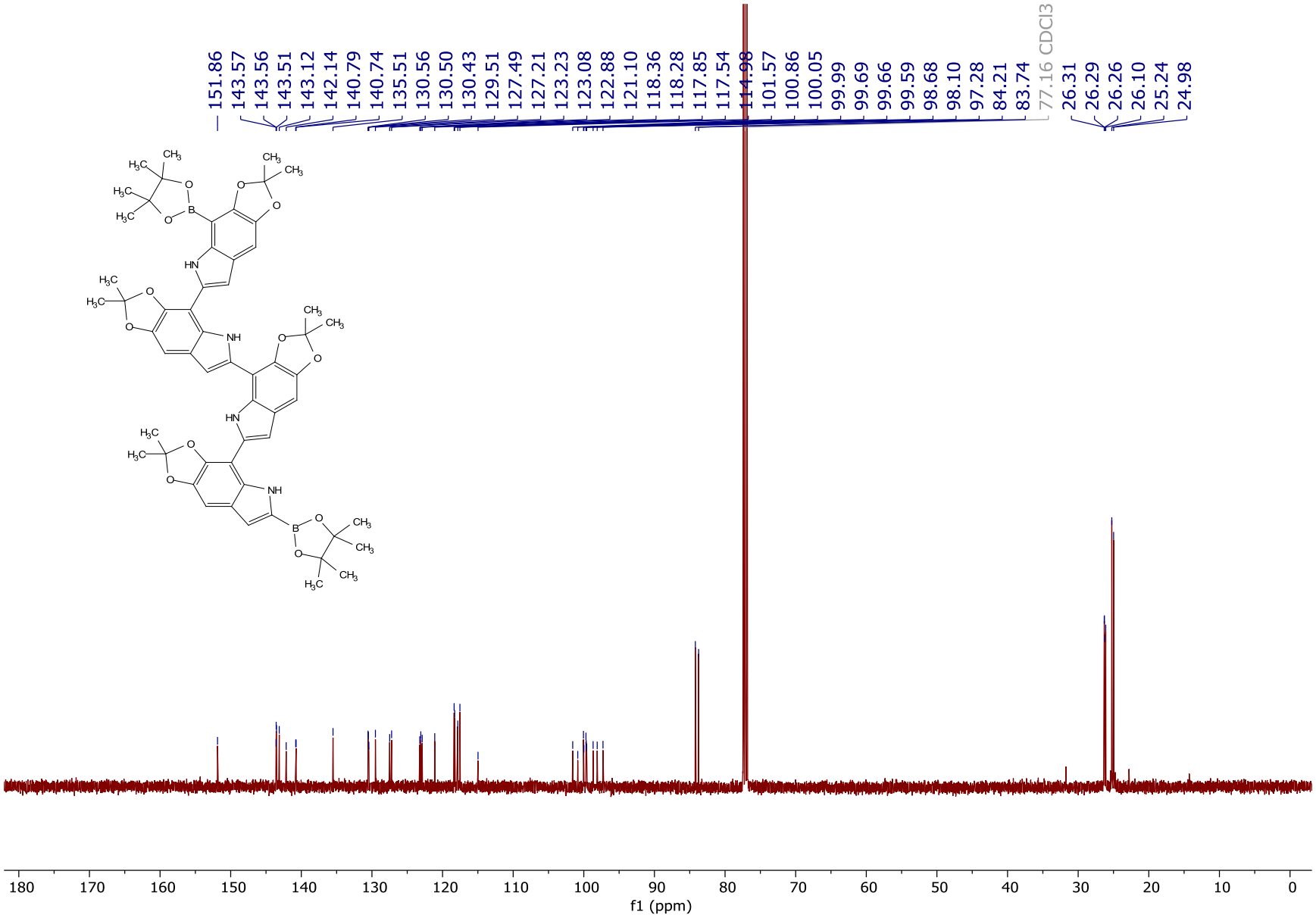
151.86
143.57
143.56
143.51
143.12
142.14
140.79
140.74
135.51
130.56
130.50
130.43
129.51
127.49
127.21
123.23
123.08
122.88
121.10
118.36
118.28
117.85
117.54
114.98
101.57
100.86
100.05
99.99
99.69
99.66
99.59
98.68
98.10
97.28
84.21
83.74
77.16 CDCl3
26.31
26.29
26.26
26.10
25.24
24.98
HN
NH
HN
NH
B
B
180
170
160
150
140
130
120
110
100
90
80
70
60
50
40
30
20
10
0
f1 (ppm)

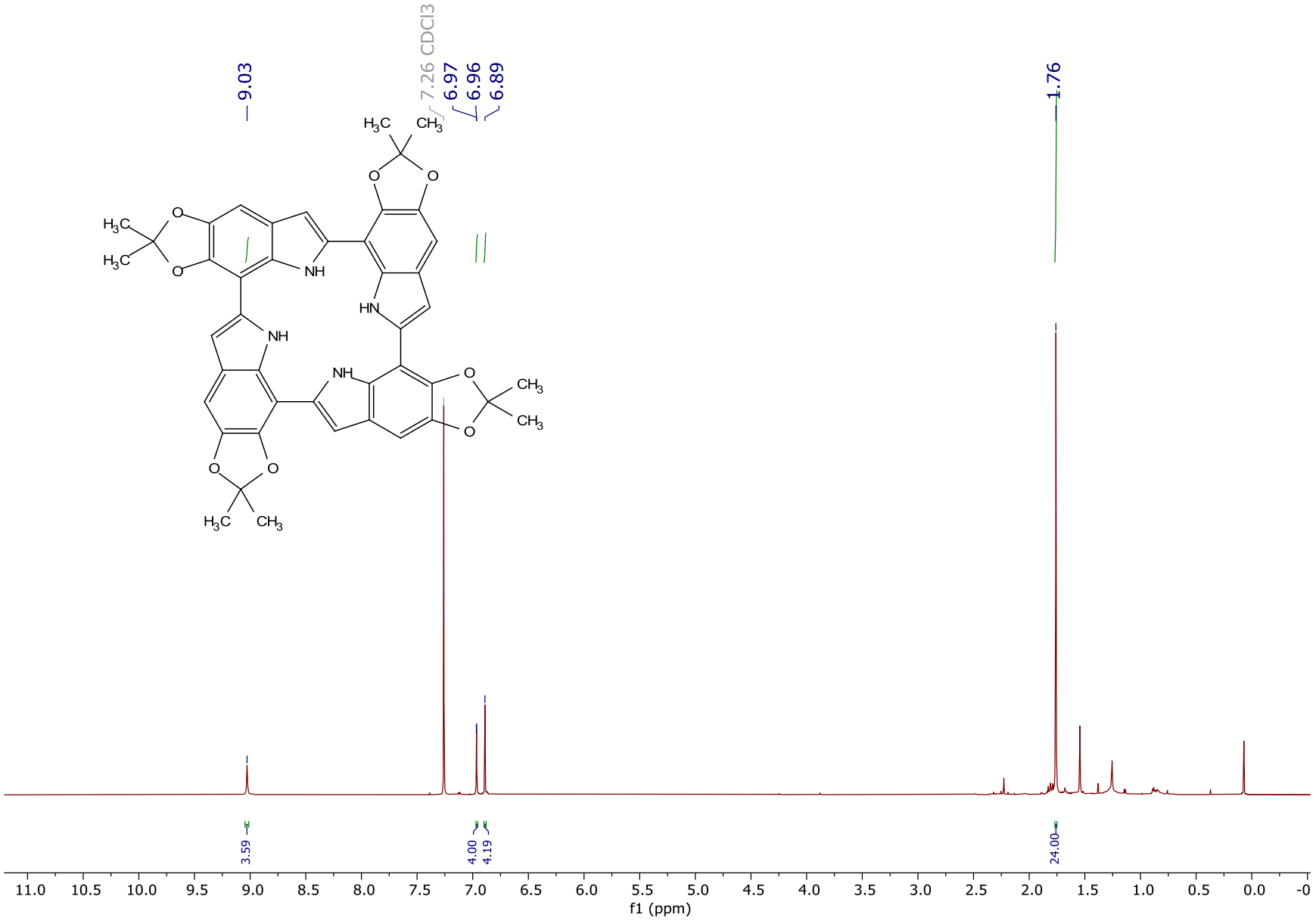
9.03
7.26 CDCl3
6.97
6.96
6.89
1.76
3.59
4.00
4.19
24.00
f1 (ppm)

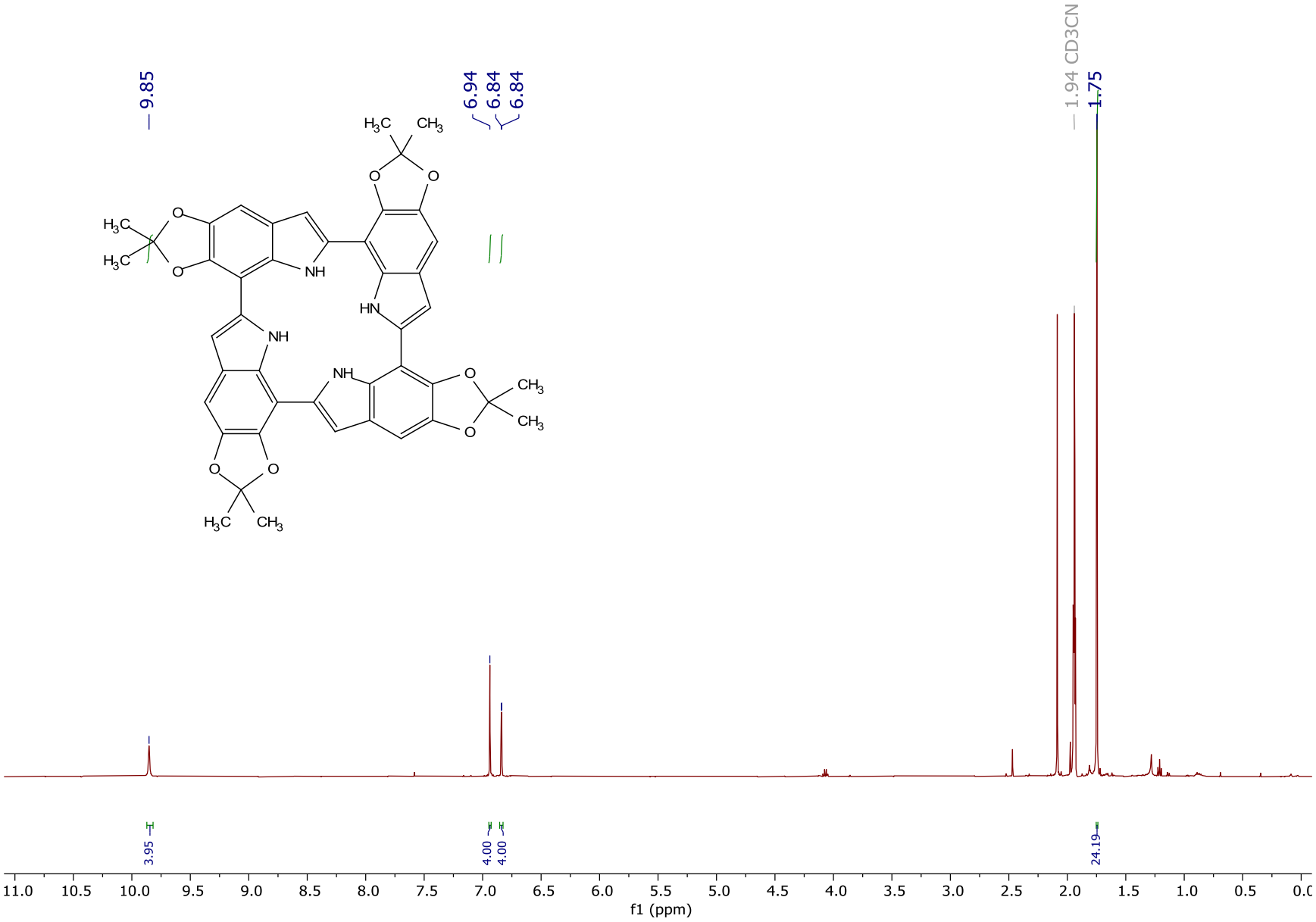
9.85
6.94
6.84
6.84
1.94 CD3CN
1.75
3.95
4.00
4.00
24.19
f1 (ppm)

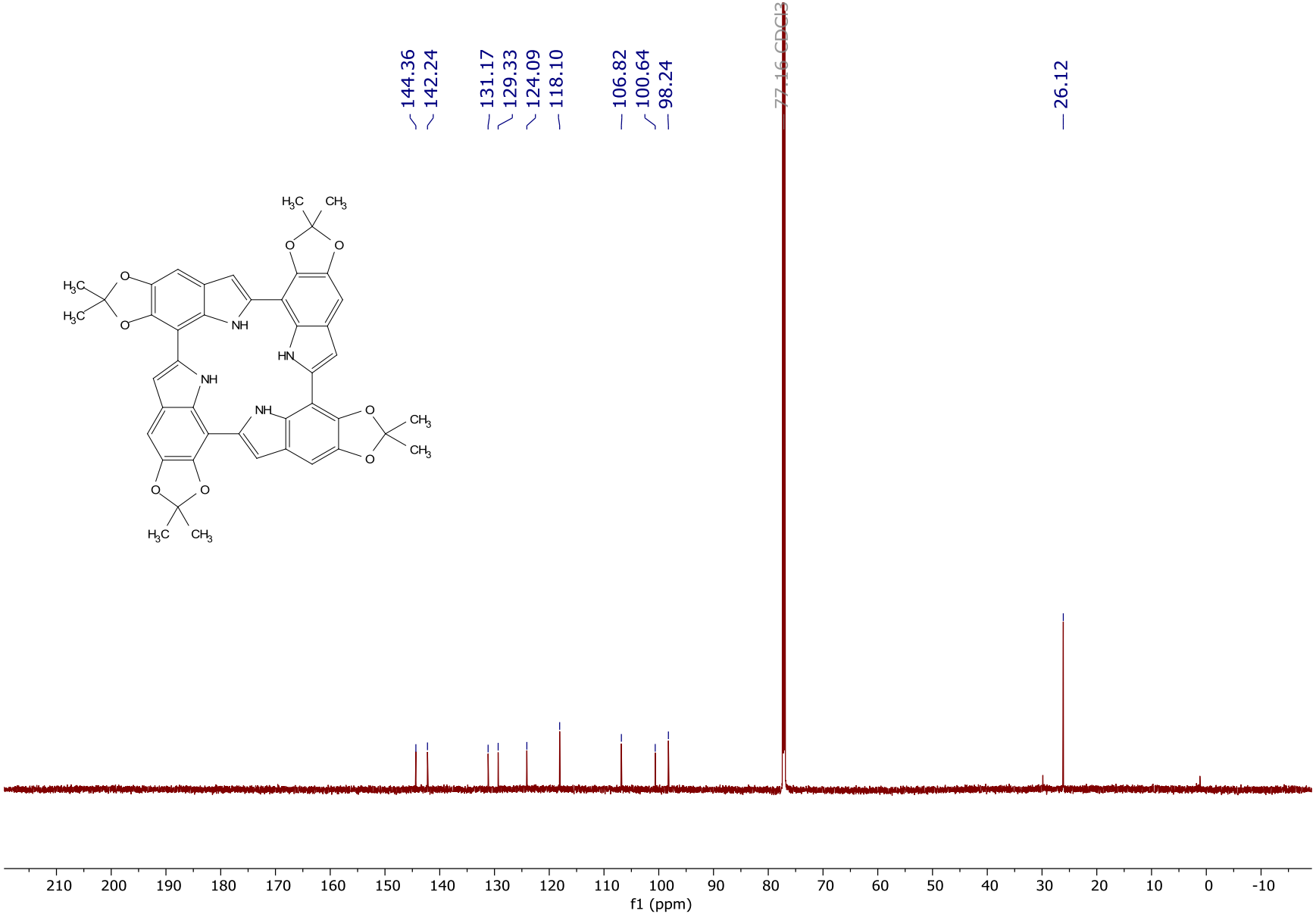
144.36
142.24
131.17
129.33
124.09
118.10
106.82
100.64
98.24
77.16 CDCl3
26.12
f1 (ppm)

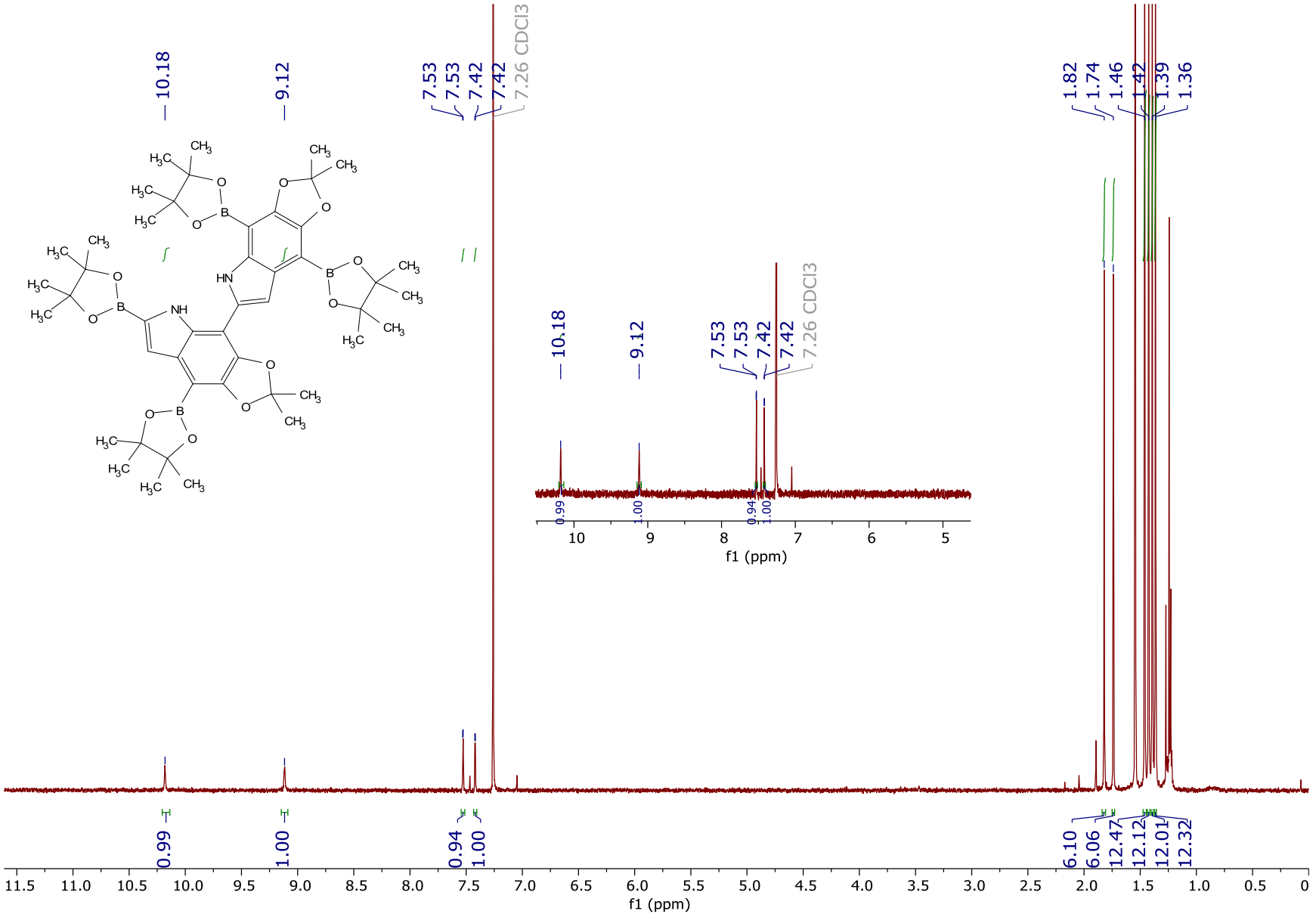
10.18
9.12
7.53
7.53
7.42
7.42
7.26 CDCl3
1.82
1.74
1.46
1.42
1.39
1.36
0.99
1.00
0.94
1.00
6.10
6.06
12.47
12.12
12.01
12.32
f1 (ppm)

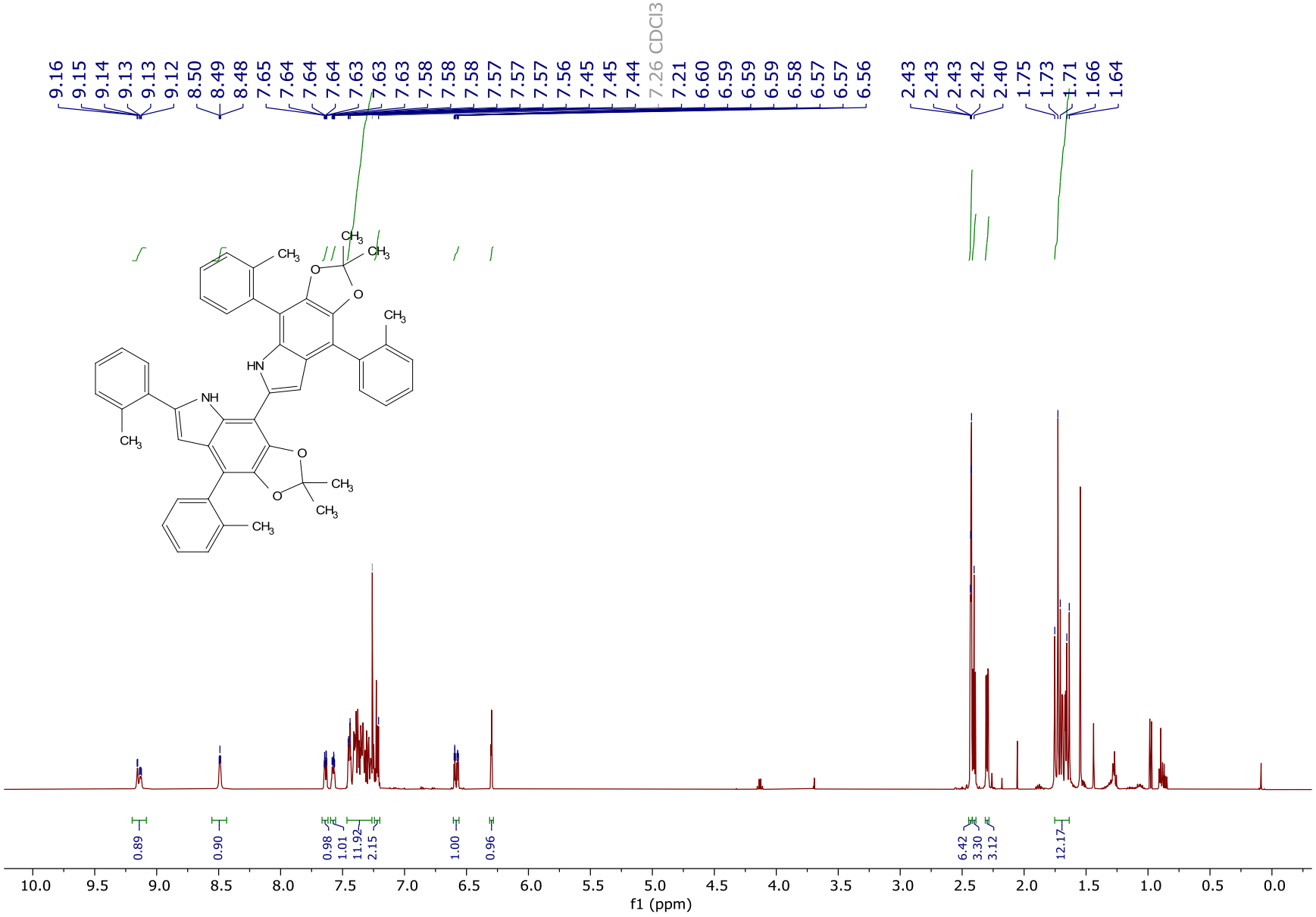
9.16 9.15 9.14 9.13 9.13 9.12 8.50 8.49 8.48 7.65 7.64 7.64 7.64 7.63 7.63 7.63 7.58 7.58 7.58 7.57 7.57 7.57 7.56 7.45 7.45 7.44 7.26 CDCl3 7.21 6.60 6.59 6.59 6.59 6.58 6.57 6.57 6.56 2.43 2.43 2.43 2.42 2.40 1.75 1.73 1.71 1.66 1.64
CH3
CH3
CH3
O
O
HN
NH
CH3
O
O
CH3
CH3
CH3
0.89 0.90 0.98 1.01 11.92 2.15 1.00 0.96 6.42 3.30 3.12 12.17
10.0 9.5 9.0 8.5 8.0 7.5 7.0 6.5 6.0 5.5 5.0 4.5 4.0 3.5 3.0 2.5 2.0 1.5 1.0 0.5 0.0
f1 (ppm)

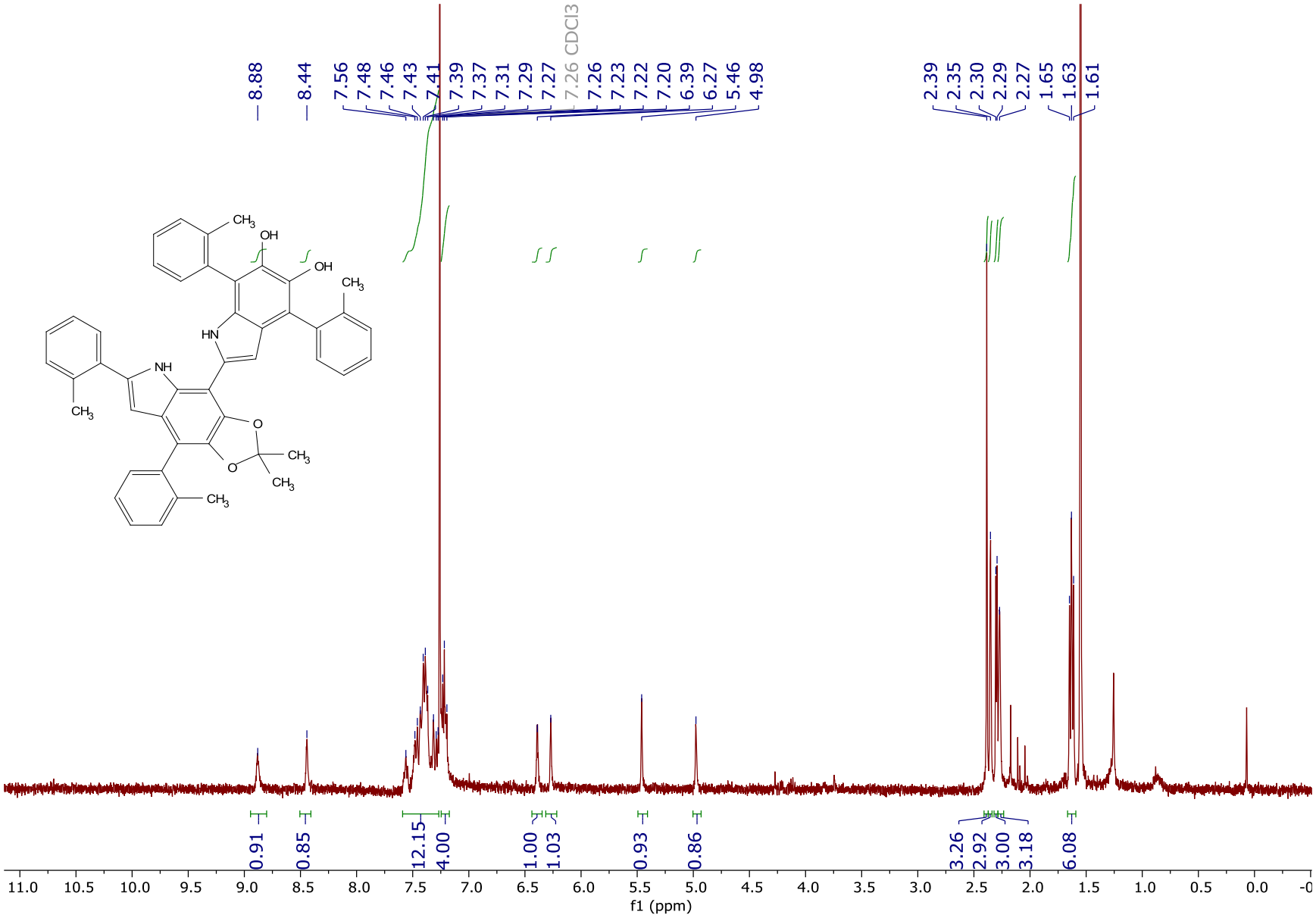
8.88
8.44
7.56
7.48
7.46
7.43
7.41
7.39
7.37
7.31
7.29
7.27
7.26 CDCl3
7.26
7.23
7.22
7.20
6.39
6.27
5.46
4.98
2.39
2.35
2.30
2.29
2.27
1.65
1.63
1.61
CH3
OH
OH
CH3
HN
NH
CH3
O
O
CH3
CH3
CH3
0.91
0.85
12.15
4.00
1.00
1.03
0.93
0.86
3.26
2.92
3.00
3.18
6.08
11.0
10.5
10.0
9.5
9.0
8.5
8.0
7.5
7.0
6.5
6.0
5.5
5.0
4.5
4.0
3.5
3.0
2.5
2.0
1.5
1.0
0.5
0.0
f1 (ppm)

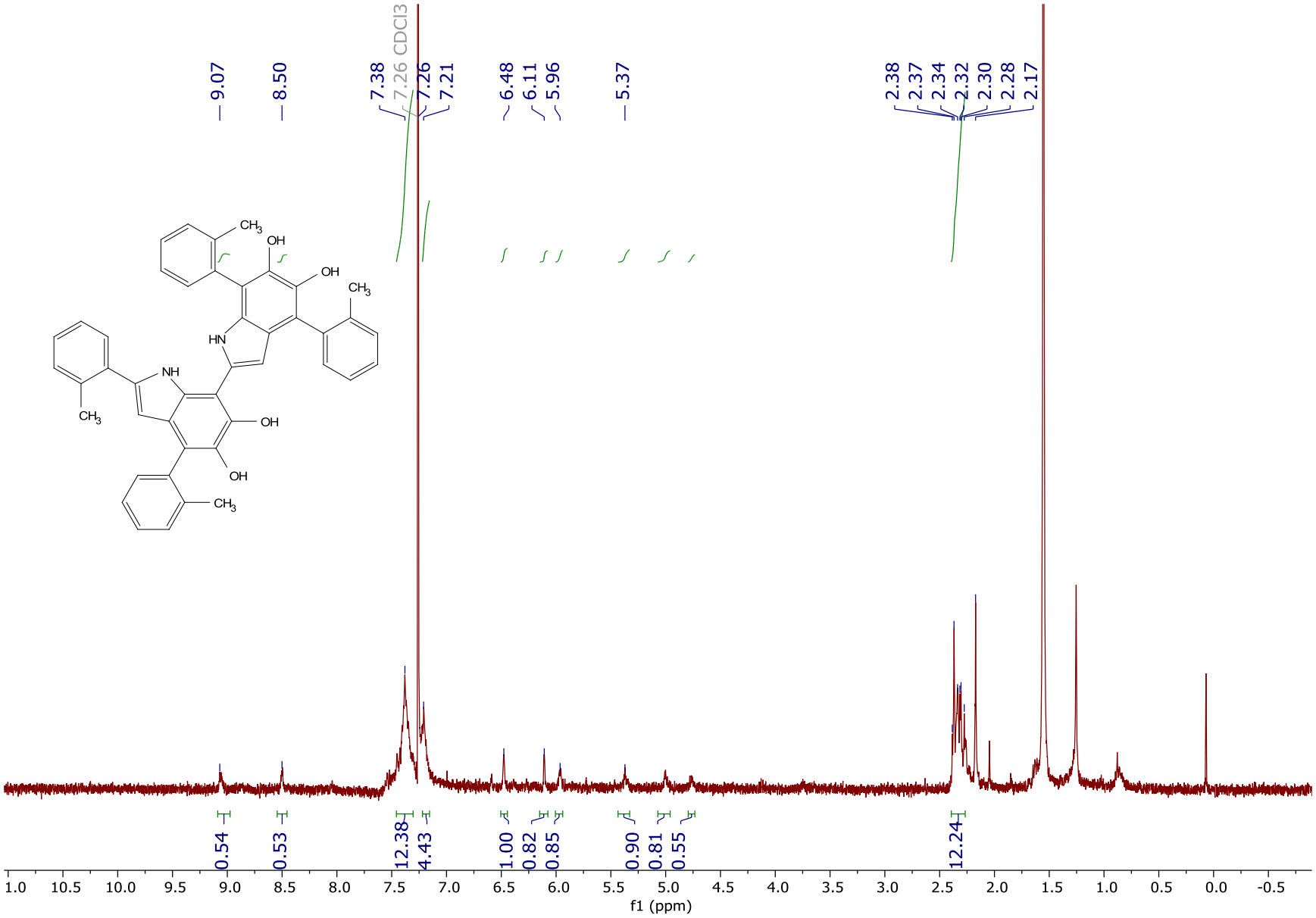
9.07
8.50
7.38
7.26 CDCl3
7.26
7.21
6.48
6.11
5.96
5.37
2.38
2.37
2.34
2.32
2.30
2.28
2.17
0.54
0.53
12.38
4.43
1.00
0.82
0.85
0.90
0.81
0.55
12.24
f1 (ppm)

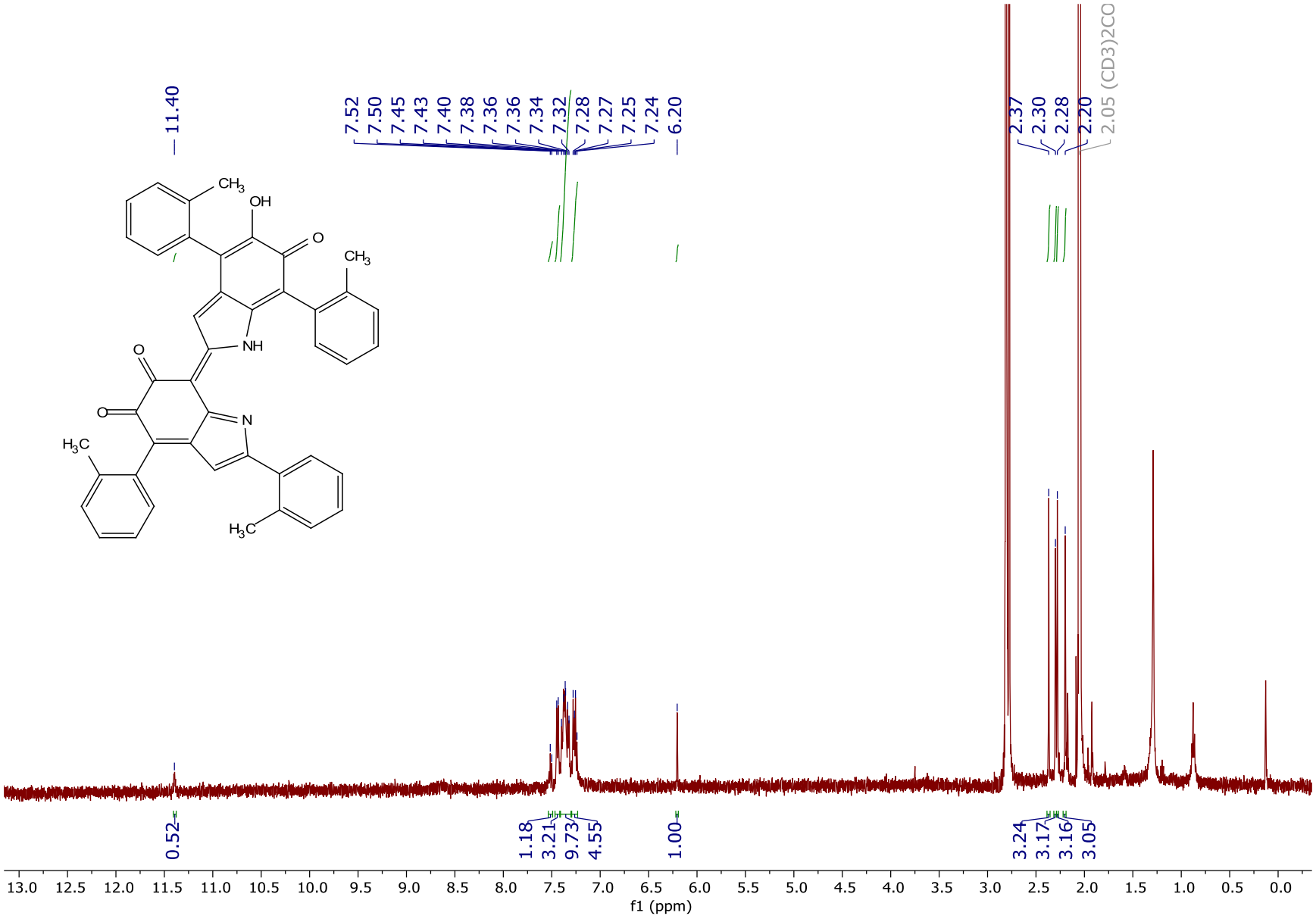
11.40
7.52
7.50
7.45
7.43
7.40
7.38
7.36
7.36
7.34
7.32
7.28
7.27
7.25
7.24
6.20
2.37
2.30
2.28
2.20
2.05 (CD3)2CO
CH3
OH
O
CH3
NH
O
O
N
H3C
H3C
0.52
1.18
3.21
9.73
4.55
1.00
3.24
3.17
3.16
3.05
13.0 12.5 12.0 11.5 11.0 10.5 10.0 9.5 9.0 8.5 8.0 7.5 7.0 6.5 6.0 5.5 5.0 4.5 4.0 3.5 3.0 2.5 2.0 1.5 1.0 0.5 0.0
f1 (ppm)

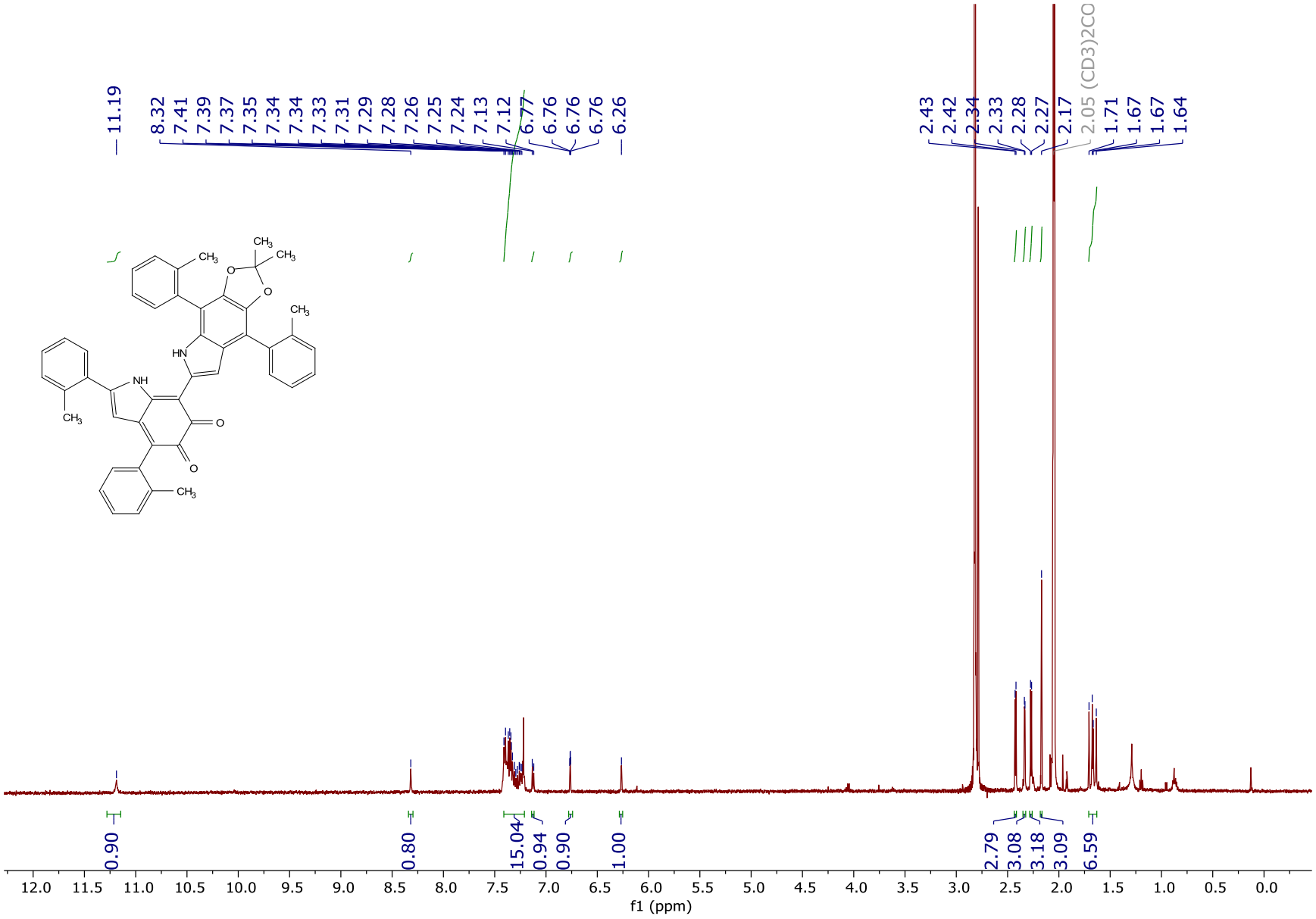
11.19
8.32
7.41
7.39
7.37
7.35
7.34
7.34
7.33
7.31
7.29
7.28
7.26
7.25
7.24
7.13
7.12
6.77
6.76
6.76
6.76
6.26
2.43
2.42
2.34
2.33
2.28
2.27
2.17
2.05 (CD3)2CO
1.71
1.67
1.67
1.64
CH3
CH3
CH3
O
O
HN
NH
O
O
CH3
CH3
CH3
0.90
0.80
15.04
0.94
0.90
1.00
2.79
3.08
3.18
3.09
6.59
12.0
11.5
11.0
10.5
10.0
9.5
9.0
8.5
8.0
7.5
7.0
6.5
6.0
5.5
5.0
4.5
4.0
3.5
3.0
2.5
2.0
1.5
1.0
0.5
0.0
f1 (ppm)

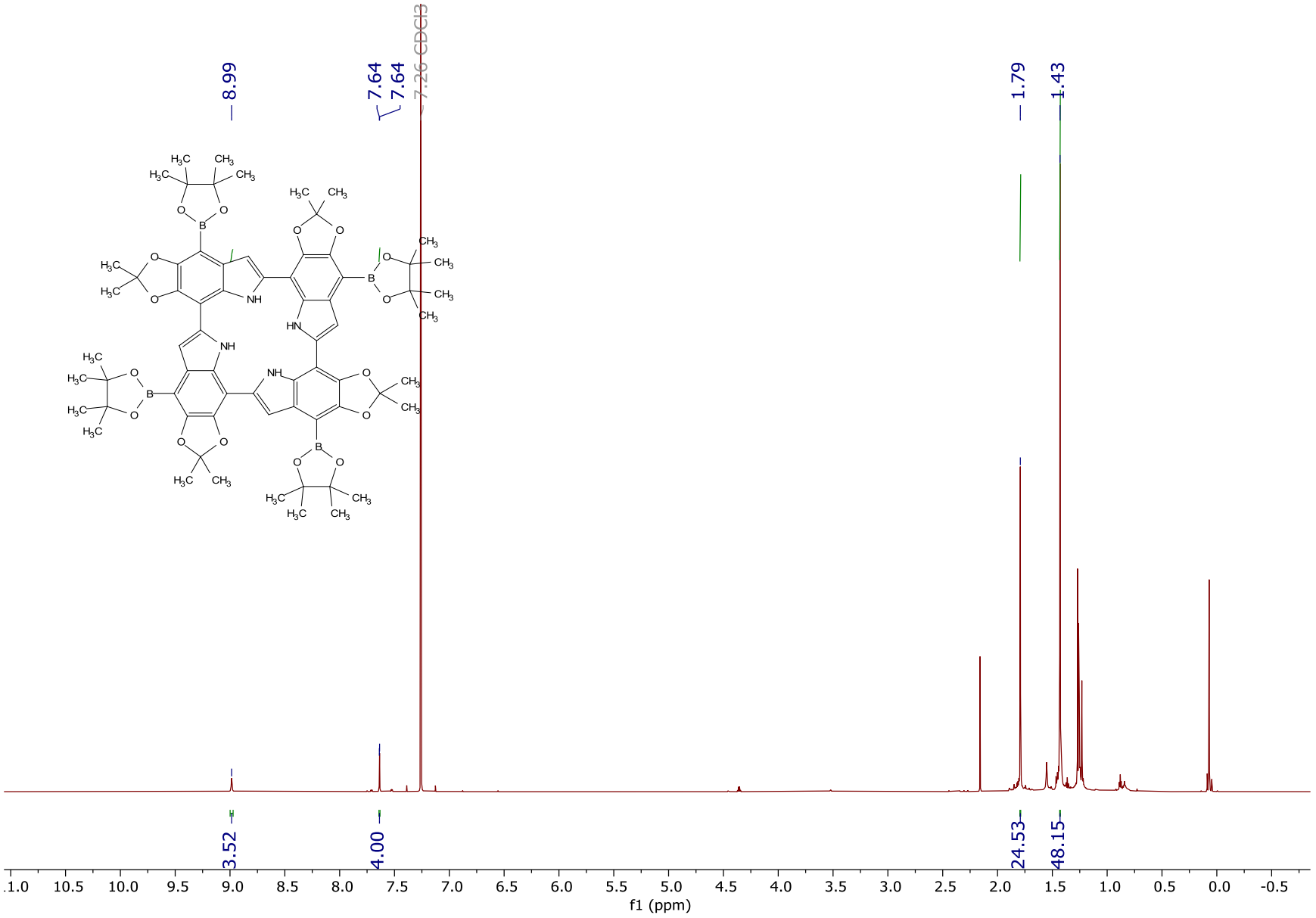
8.99
7.64
7.64
7.26 CDCl3
1.79
1.43
3.52
4.00
24.53
48.15
f1 (ppm)

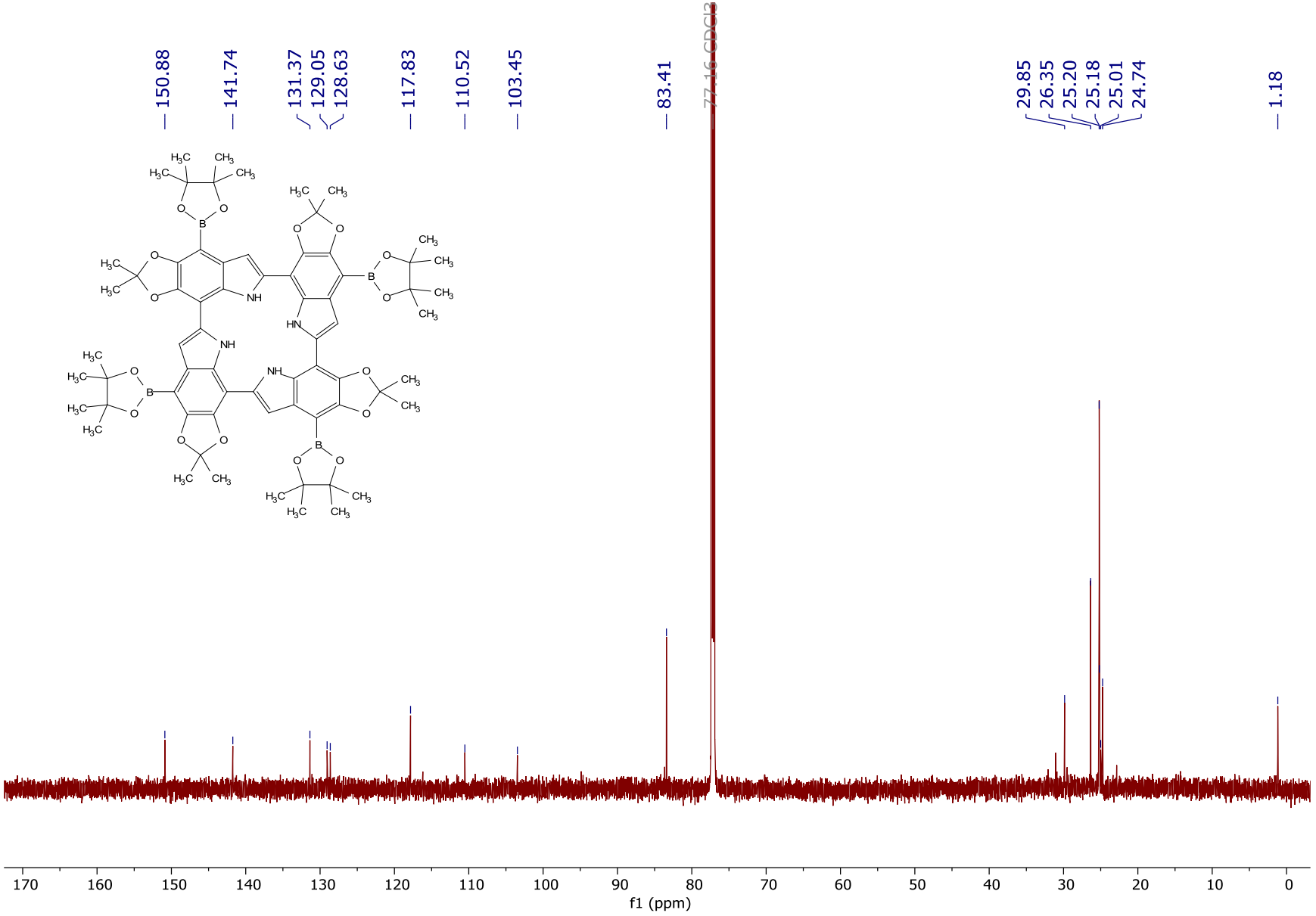
150.88
141.74
131.37
129.05
128.63
117.83
110.52
103.45
83.41
77.16 CDCl3
29.85
26.35
25.20
25.18
25.01
24.74
1.18
170
160
150
140
130
120
110
100
90
80
70
60
50
40
30
20
10
0
f1 (ppm)

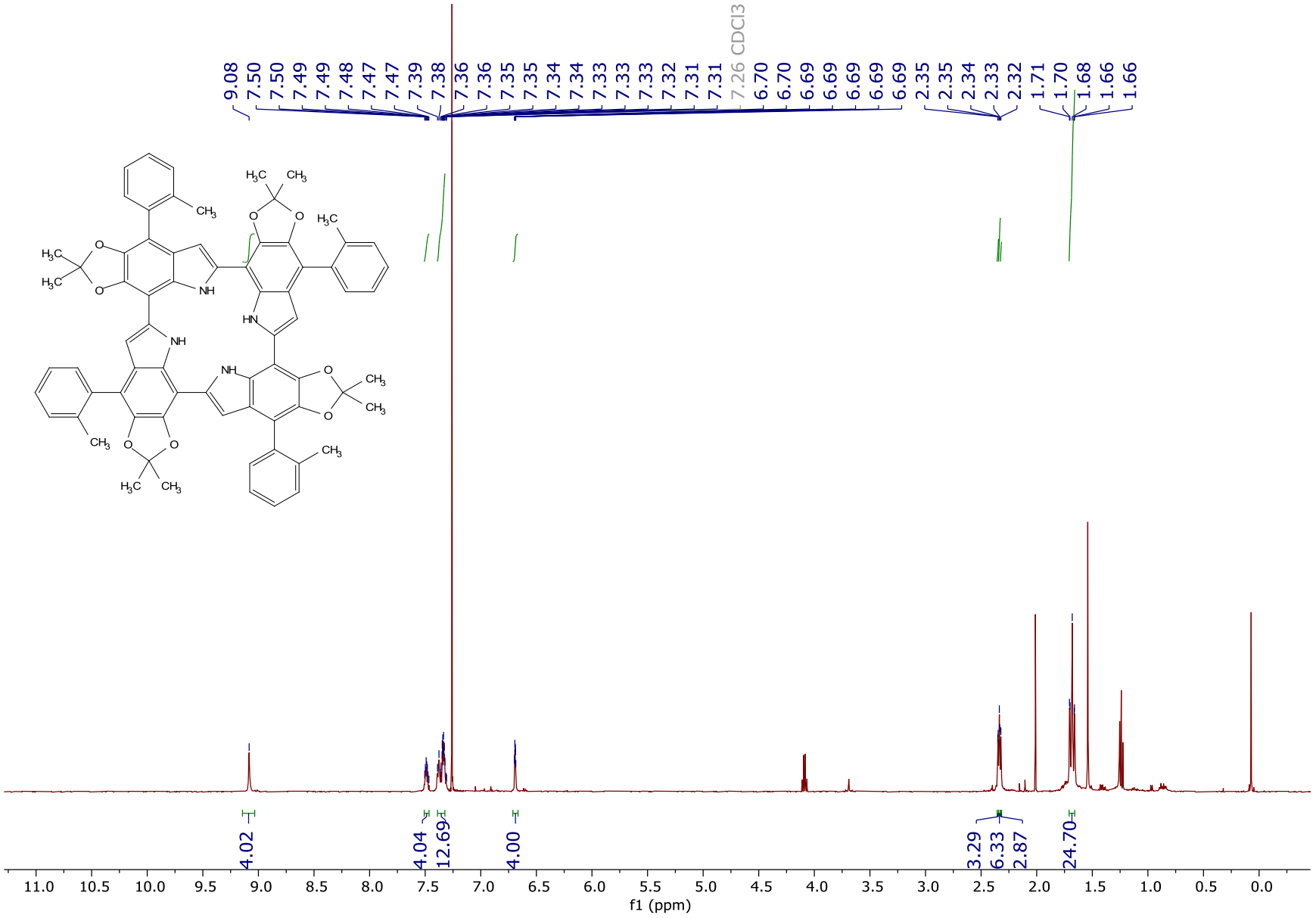
9.08
7.50
7.50
7.49
7.49
7.48
7.47
7.47
7.39
7.38
7.36
7.36
7.35
7.35
7.34
7.34
7.33
7.33
7.33
7.32
7.31
7.31
7.26 CDCl3
6.70
6.70
6.69
6.69
6.69
6.69
6.69
2.35
2.35
2.34
2.33
2.32
1.71
1.70
1.68
1.66
1.66
4.02
4.04
12.69
4.00
3.29
6.33
2.87
24.70
11.0
10.5
10.0
9.5
9.0
8.5
8.0
7.5
7.0
6.5
6.0
5.5
5.0
4.5
4.0
3.5
3.0
2.5
2.0
1.5
1.0
0.5
0.0
f1 (ppm)